The University of Nottingham

DEVELOPING A MODEL SYSTEM TO INVESTIGATE THE EPIGENETIC MECHANISMS UNDERLYING PLURIPOTENCY IN HUMAN CELLS

Submitted by

Elena Matsa MSc, BSc

School of Clinical Sciences
Department of Obstetrics and Gynaecology
The University of Nottingham

June 2010

Thesis submitted to The University of Nottingham for the degree of Doctor of Philosophy

ACKNOWLEDGEMENTS

I would like to thank Dr. Christine Mummery for her donation of the hESC line HOGN, Dr. Ramiro Alberio for the BJ human newborn fibroblast line, Dr. David Brook for the adult fibroblast line SUKE, Dr. David Darling for the BL15 line, and Dr. Virginie Sottile for the mouse mesenchymal and neural stem cells. I would also like to thank Mr. Nigel Smith for his kind help with karyotype analysis of HUES7 and iPS cells, Dr. Adrian Robins and Mrs. Nina Lane for their help with flow cytometry analysis, Dr. Michalis Talias for his help with statistical analysis, and William Steele for his input in primer design for bisulfite PCR analysis.

Big thank you should also go to Mr. Jayson Bispham for his help with real-time PCR and bisulfite sequencing, to Miss Maria Barbadillo-Mũnoz for her help with manual dissection cultures, and also to Dr. Alexandra Thurston and Dr. Roger McGilvray for their help with real-time PCR and bisulfite sequencing, Dr. Kee-Pyo Kim for his help with MSP-PCR and COBRA analysis, and Dr. Emily Dick for sharing her expertise on western blotting and lentiviral transduction. I am also grateful to Dr. David Anderson who trained me in hESC culture and Dr. Emma Lucas who trained me in molecular techniques in my first year as a PhD student.

My greatest appreciation goes to my supervisors Prof. Lorraine Young and Dr. Chris Denning for their constant guidance and support, and for always believing in me.

Finally, I would like to thank my housemates Vivian, Maria and Andy for their patience during the three years of my PhD, my sister Ioanna, my brother Andreas and my friend Kiril for their ethical support, and my parents for their love and selfless devotion.

I would like to dedicate this thesis to my aunt Maria, who always encouraged my dream of becoming a researcher

DECLARATION

I hereby declare that this thesis has been composed by myself and has not been submitted for any other degree previously. Acknowledgements of specific procedures not performed by myself are stated; otherwise, the work described is my own.

Elena Matsa 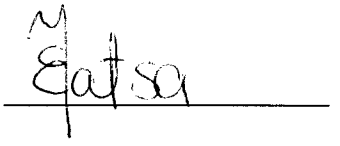

Date: 01/06/2010

ABSTRACT

Pluripotent human embryonic stem cells (hESCs) are a valuable tool for clinical therapies, drug testing and investigation of developmental pathways. Recently, over-expression of four pluripotency-associated genes (*OCT4*, *NANOG*, *SOX2*, and *LIN28*) has proven sufficient to reprogram differentiated cells into pluripotent stem cells, potentially alleviating the need for human embryos to isolate hESCs and opening new avenues for the investigation of pluripotency.

This project aimed to generate an *in vitro* model system to study the epigenetic mechanisms regulating pluripotency transcription factors. hESCs were differentiated into fibroblasts (hESC-Fib) and subsequently reprogrammed to induced pluripotency stem cells (iPSCs) by lentiviral over-expression of human *OCT4*, *NANOG*, *SOX2* and *LIN28*. iPSC colonies were positively identified by live staining with the surface marker TRA-1-81 and expanded in culture. They were then further differentiated into a fibroblast line to allow comparison with hESC-Fib. All cells in the model system shared the same genotype and were cultured under similar conditions, enabling unbiased analysis of epigenetic characteristics.

DNA methylation analysis of key pluripotency-genes such as *OCT4, SOX2, NANOG,* and *REX1* by bisulfite sequencing, revealed that these were hypomethylated in hESCs and iPSCs, and hypermethylated in their fibroblast derivatives. A gradual increase in the number of CpGs gaining DNA methylation was observed when hESCs and iPSCs were differentiated into fibroblasts, while TaqMan real-time PCR and fluorescence staining revealed that expression of these genes was inversely related to the levels of DNA methylation in their promoters. The master pluripotency regulators *OCT4*, *SOX2* and *NANOG* all showed differential methylation in their OCT/SOX binding regions, suggesting a common regulatory mechanism between them. This is, to our knowledge, the first report for SOX2 differential methylation in human non-cancerous cells. Reactivation of *REX1* was not found to be necessary for the reprogramming of hESC-Fib to iPSCs, calling for re-evaluation of its role in human pluripotency.

Based on the observation that the DNA methylation levels of pluripotency genes were higher in fibroblast cell lines compared to hESCs and iPSCs, we hypothesised that reduction in DNA methylation could render differentiated cells more permissive to reprogramming. Stable knock-downs of the DNA methyltransferases (DNMTs) DNMT1 and DNMT3A were, thus, performed in hESC-Fib. Knock-down of DNMT1, the most abundant DNMT in hESC-Fib, resulted in global reduction of DNA methylation levels as determined by restriction digests with methylation specific enzymes. Reprogramming of hESC-Fib carrying a DNMT1 knock-down showed a 40% reduction in generation of iPSC colonies compared to untreated controls, perhaps owing to the delay in progression of S phase in the cell cycle caused by DNMT1 knock-down. In contrast, knock-down of DNMT3A resulted in a >80% increase in iPSC colony formation, potentially indicating differences in mechanism of action and specificity between the two DNMT enzymes.

Through this study, we have gained new insights into the epigenetic mechanisms underlying cell phenotype and provided the foundation for further improving reprogramming efficiency.

TABLE OF CONTENTS

LIST OF FIGURES

LIST OF TABLES

ABBREVIATIONS

Abbreviation	Description
%	Per cent
AP	Alkaline phosphatase
ATP	Adenosine triphosphate
BL15	Biotin-lenti clone 15
bp	Base pairs
BSA	Bovine serum albumin
BSC	Biological safety cabinet
ChIP	Chromatin immunoprecipitation
COBRA	Combined bisulfite restriction analysis
DAPI	Di-amino phenyl-indole
DMEM	Dublecco's (Modified Eagle's) minimal essential medium
DMR	Differentially methylated region
DMSO	Dimethyl sulfoxide
DNA	Deoxyribonucleic acid
DNMT	DNA methyltransferase
dNTP	Deoxyribonucleotide triphosphate
DTT	Di-thio-threitol
EB	Embryoid body
EDTA	Ethylenediaminetetraacetic acid
ESC	Embryonic stem cell
FBS	Foetal bovine serum
FC	Flow cytometry
FGF	Fibroblast growth factors
FITC	Fluorescein iso-thiocyanate
FSA	Fibroblast surface antigen
GFP	Green fluorescence protein
HAT	Histone acetyltransferase
HDAC	Histone de-acetylase
HEK	Human embryonic kidney
hESC	Human embryonic stem cell
ICM	Inner cell mass
ICR	Imprinting control region
IMS	Industrial methylated spirit
iPSC	Induced pluripotency stem cell
IRES	Internal ribosome entry side
KD	Knock-down
KSR	Knock-out serum replacement
LTR	Long terminal repeat
MEF	Mouse embryonic fibroblast
mESC	Mouse embryonic stem cell
miRNA	Micro-RNA
mMSC	Mouse mesenchymal stem cell
mNSC	Mouse neural stem cell

mRNA	Messenger RNA
MSP	Methylation-specific PCR
NEAA	Non essential amino acids
NT	Non-targeting
NuRD	Nucleosome remodelling and de-acetylase
NV	No virus
°C	Degrees Celsius
PBS	Phosphate buffered saline
PcG	Polycomb Group complex
PCR	Polymerase chain reaction
PD	Population doubling
PE	Phycoerythrin
PFA	Paraformaldehyde
PMSF	Phenyl-methyl-sulphonyl fluoride
PTD	Post-transduction
PTF	Post-transfection
RISC	RNA-Induced Silencing Complex
RNA	Ribonucleic acid
RNAi	RNA interference
RQ	Relative quantification
RT	Reverse transcriptase
RT-PCR	Reverse transcriptase PCR
SCNT	Somatic cell nuclear transfer
SDS	Sodium dodecyl sulfate
SDW	Sterile distilled water
shRNA	Short hairpin RNA
siRNA	Small interfering RNA
TBE	Tris-borate-EDTA
TF	Transcription factor
T-DMR	Tissue-specific differentially methylated region
TSS	Transcriptional start site
UV	Ultra-violet
XCI	X-chromosome inactivation

GENE SYMBOLS

Abbreviation	Full name
AFP	Alpha-fetoprotein
Bmi1	B lymphoma Mo-MLV insertion region 1
BMP4	Bone morphogenic protein 4
BRG1	Brahma-related gene 1
CARM1	Co-activator associated arginine methyltransferase 1
CD	Cluster of differentiation
CDH1	Cadherin 1
CDKN1C	Cyclin-dependent kinase inhibitor 1C
Chd1	Chromodomain helicase DNA-binding protein 1
Coup-tf I & II	Chicken ovalbumin upstream promoter transcription factor *I* & *II*
DAPK1	Death-associated protein kinase 1
Dmap1	DNA methyltransferase-associate protein 1
DNMT1, 3A, 3B & 3L	DNA methyltransferase 1, 3A, 3B & 3L
Dot1L	Disruptor of telomeric silencing
Eed	Embryonic ectoderm development
EHMT1	Euchromatic histone methyltransferase 1
EHOX	ESC- paired-like homeobox-containing
ESR1	Estrogen receptor1
Esrrb	*Estrogen-related receptor beta*
Ezh2	Enhancer of zeste homologue 2
FBX15	F-box containing protein 15
FGF4	Fibroblast growth factor 4
FOXD3	Forkhead box D3
FSA	Fibroblast surface antigen
GABRB3	Gamma aminobutyric acid receptor sub-unit beta 3
GATA4, 5& 6	Recognise GATA motif in gene promoters
Gcn5	General control of amino-acid synthesis protein 5
GCNF	Germ cell nuclear factor
GNAS1 XLαs	Guanine alphas protein 1 complex locus
GTL2	Gene trap locus 2
HDAC1	Histone de-acetylase 1
hGDF3	Human growth-differentiation factor 3
HIC1	Hypermethylated in cancer 1
HMG2A	High mobility group 2A
HP1	Heterochromatin protein 1
HPRT	Hypoxanthine-guanine phosphoribosyltransferase
IGF2	Insulin-like growth factor 2
Jmjd1a, 2c & 3	Jumonji domain-containing protein 1a, 2c and 3
KLF4	Kruppel-like factor 4
Kv	Voltage-gated potassium channel
LEFTB	Left-right determination factor B
LIF	Leukaemia inhibitory factor
Lrh1	Liver receptor homolog 1
MBP3	Methyl-binding protein 3
MGMT	Methyl-guanine DNA methyltransferase
MLL	Myeloid/lymphoid leukaemia
Mta1	Metastasis-associated 1
MYOG	Myogenin

NANOG	From Tir Na Nog (=land of the ever young)
NESP55	Neuroendocrine secretory protein 55
OCT4	Octamer 4 (aka POU5F1 for POU class 5 forkhead box 1)
P4HB	Prolyl-4-hydroxylase B
PEG 1 & 10	Paternally expressed gene 1 & 10
PODXL	Podocalyxin-like
PTPN6	Protein tyrosine phosphatase non-receptor type 6
RASSF1	Ras association domain-containing protein 1
Rbp2	Retinol binding protein 2 (aka Jarid1a for Jumonji AT-rich interactive domain 1a)
REX1	Reduced expression 1
Ring1b	Really interesting new gene (RING)-finger protein
Rxbr	Retinoid x receptor beta
Sf1	Steroidogenic factor 1 (aka Nr5a1)
SLC22A18	Solute carrier family 22 member 18
SNRPN	Small nuclear ribonucleiprotein polypeptide N
SOX2	Sex-determining region Y (SRY)-related high mobility group (HMG) box 2
SSEA	Stage-specific embryonic antigen
Suz12	Suppressor of zeste homologue 12
TBN	Taube nuss (=deaf nut)
TDGF1	Teratocarcinoma-derived growth factor 1 (aka crypto-1)
TERT	Telomere reverse transcriptase
TIMP3	Tissue inhibitor of metalloproteinases 3
TP73	Tumour protein 73
UTF1	Undifferentiated ESC transcription factor 1
UTX	Ubiquitously transcribed tetratricopeptide repeat, X chromosome
VCAM-1	Vascular cell adhesion molecule 1
TGF5	Transforming growth factor
Pax6	Paired box gene 6

GENE NOMENCLATURE

According to current guidelines from the Human Genome Nomenclature Committee (http://www.gene.ucl.ac.uk/nomenclature/), abbreviations for human genes are capitalized and italicized, while their respective proteins are capitalized but not italicized. Mouse gene and protein nomenclature follows guidelines from the current Mouse Genome Nomenclature Committee (http://www.informatics.jax.org/mgihome/nomen/), based on which gene abbreviations are written with a capitalized first letter and subsequent lower case letters, all italicized. Abbreviations for mouse proteins have the same gene symbol but are not italicized.

1. INTRODUCTION

1.1 THESIS RATIONALE & OBJECTIVES

Pluripotent human embryonic stem cells (hESCs) were first derived from the inner cell mass (ICM) of human blastocysts (Thomson *et al.* 1998). hESCs have the remarkable potential to self-renew indefinitely and differentiate into the three embryonic germ layers, which can potentially give rise to all types of cells in the adult body (Reubinoff *et al.* 2000). More recently, over-expression of four pluripotency-associated genes (*OCT4*, *SOX2*, and *KLF4* & *c-MYC* or *NANOG* & *LIN28*) in differentiated somatic cells was proven sufficient to induce reprogramming towards pluripotent ESC-like cells (induced-pluripotency stem cells, iPSCs; Takahashi *et al.* 2007; Yu *et al.* 2007b), and has opened new avenues for investigation of the pluripotent cell state.

The pluripotent state is largely dependent on the actions of transcription factors such as *OCT4*, *NANOG*, *SOX2* and *KLF4*. These genes are considered as "master regulators" that hold pivotal roles in maintaining pluripotent characteristics, and are at the top of a transcriptional hierarchy that regulates the expression of over 300 genes in hESCs (Boyer *et al.* 2005; Babaie *et al.* 2007). The activation and silencing of pluripotency-related genes in undifferentiated and differentiated cell lineages also involves a range of epigenetic mechanisms that act in concert to maintain local chromatin in an open or closed conformation (reviewed by Minard *et al.* 2009).

Limited studies in mouse ESCs (mESCs) have shown that key pluripotency transcription factors, such as *Oct4*, can be themselves subject to epigenetic regulation (Azuara *et al.* 2006; Feldman *et al.* 2006). However, the epigenetic factors that determine whether pluripotency-associated genes are expressed or silenced in differentiated cell types are almost unknown in human cells. Moreover, the exact epigenetic processes associated with activating or repressing/silencing the human pluripotent state are poorly understood.

This thesis aimed to investigate some of the epigenetic mechanisms associated with the transcriptional activity of key pluripotency genes in hESCs and iPSCs, as well as during transition of cell phenotype from a pluripotent to a differentiated state and during reprogramming to iPSCs. Chapter 3 of this thesis created a model cell system where hESCs were differentiated into a fibroblast cell line, which was subsequently reprogrammed to iPSCs by lentiviral over-expression of human *OCT4*, *NANOG*, *SOX2* and *LIN28*. The iPSCs were then further differentiated into fibroblasts, so that undifferentiated hESCs and iPSCs, and derived-fibroblast cells originated from one hESC line, shared the same genotype and were cultured under similar conditions, to minimise experimental variation that could affect the analysis of epigenetic gene regulation (Figure 1.1).

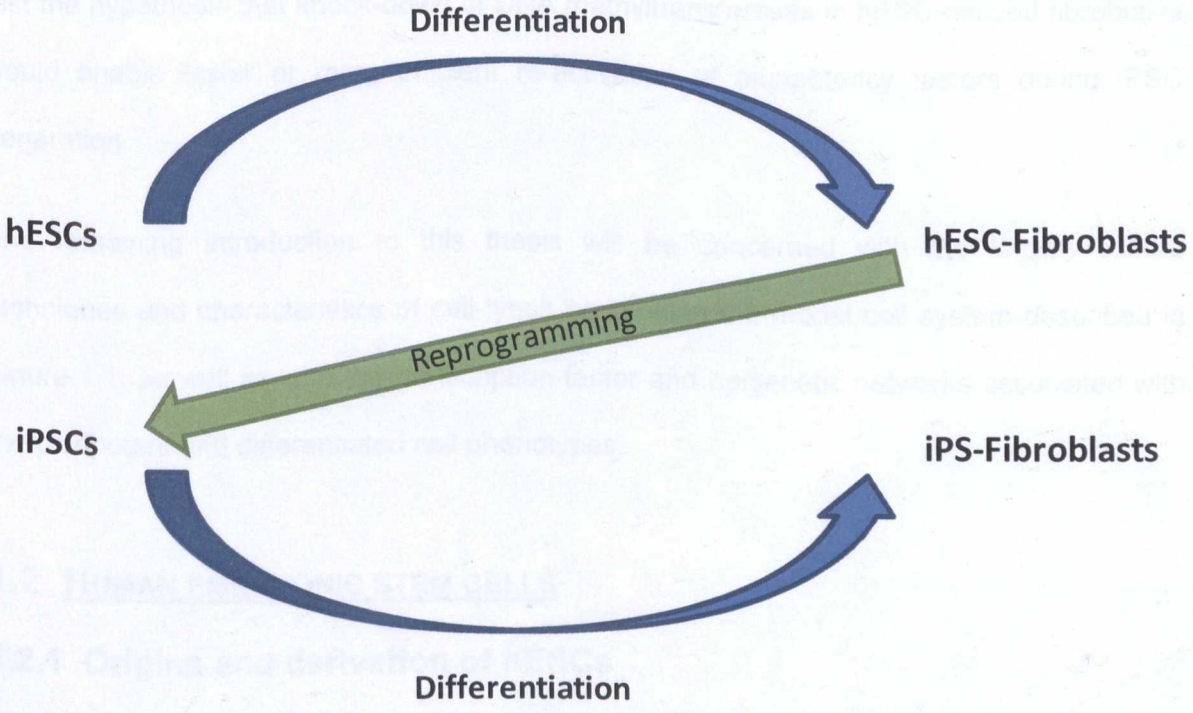

Figure 1.1- Model system for studying the epigenetic mechanisms of pluripotency in hESCs and iPSCs
Model system of cells having the same genotype, but different phenotypes. This system was generated from HUES7 hESCs in order to study the epigenetic mechanisms associated with pluripotency maintenance, differentiation and reprogramming.

In chapter 4, this model cell system was used to characterise gene and protein expression profiles of the key pluripotency factors OCT4, NANOG, SOX2, KLF4, LIN28, DNMT3B and REX1 during differentiation and reprogramming, and in the pluripotent and fibroblast-differentiated states. The epigenetic mechanisms associated with expression, repression and re-activation of key pluripotency factors were also investigated, by analysing the DNA methylation profiles and histone modifications associated with regulatory regions of each gene.

Through the generation of hESC and hESC-derived fibroblast lines carrying shRNA-mediated knock-down of the DNA methyltransferases DNMT1 and DNMT3A, chapter 5 of this thesis aimed to investigate the effects of epigenetic manipulation on cell phenotype, cell cycle progression, DNA methylation of imprinted and tumour suppressor genes, and finally, test the hypothesis that knock-down of DNA methyltransferases in hESC-derived fibroblasts would enable faster or more efficient re-activation of pluripotency factors during iPSC generation.

The remaining introduction to this thesis will be concerned with the known culture techniques and characteristics of cell-types comprising the model cell system described in Figure 1.1, as well as with the transcription-factor and epigenetic networks associated with the pluripotent and differentiated cell phenotypes.

1.2 HUMAN EMBRYONIC STEM CELLS

1.2.1 Origins and derivation of hESCs

Pluripotent hESCs were first isolated *via* immunosurgical procedures from the ICM of pre-implantation embryos, at the blastocyst stage (Thomson *et al.* 1998). hESCs have the capacity to remain in an undifferentiated state and self-renew indefinitely or, in the presence of appropriate stimulating factors, differentiate into cell types derived from endoderm, mesoderm and ectoderm (Reubinoff *et al.* 2000). This potential, known as pluripotency,

makes hESCs a powerful tool for regenerative medicine, drug screening and investigation of early human developmental pathways (Odorico *et al.* 2001; Smith 2001; Anke *et al.* 2006; Cervera and Stojkovic 2007).

It is estimated that, since 1998, over 400 hESC lines have been generated, mostly from embryos derived from *in vitro* fertilized oocytes, using whole blastocysts, isolated ICM, morula stage or developmentally arrested embryos (reviewed by Brimble *et al.* 2004; Zhang *et al.* 2006). Blastomere biopsy technologies also enabled hESC isolation from a single blastomere (Klimanskaya *et al.* 2006). While most laboratories fail to detail the number or quality of oocytes/embryos needed to generate a hESC line, Cowan *et al.* (2004) reported that 286 cleaved embryos (6 to 12 cell stage) and 58 blastocysts were used to derive 17 new hESC lines, demonstrating a 5% success rate in the derivation process.

1.2.2 Characterisation of hESCs

In order to standardise the characterisation of independently derived hESCs lines, a set of minimum criteria have been proposed (reviewed by Hoffman and Carpenter 2005) which include the expression of hESC-specific surface markers and transcription factors. The proposed minimum criteria of what defines a hESC line are outlined below:

* Expression of factors associated with the pluripotent state (e.g. *OCT4*, *NANOG*)
* Expression of surface markers associated with the pluripotent state (e.g. TRA-1-81/TRA-1-60, SSEA4/SSEA3)
* Karyotype stability over extended undifferentiated culture
* Functional telomerase expression
* Ability to differentiate into lineages from all three embryonic germ layers, either by teratoma formation after injection into immunodeficient mice or by *in vitro* differentiation *via* embryoid body formation (see sections 1.2.4 and 3.1.2).

Even though fulfilment of these criteria is important for determining whether hESCs possess self-renewal and differentiation capacities, some hESC lines lack extensive characterisation, especially in terms of teratoma formation, telomerase activity and karyotype stability (Chung *et al.* 2008). This problem is being addressed by the International Stem Cell Initiative (ISCI) which has launched an extensive study comparing 59 hESC lines, in order to further define hESC characteristics (Adewumi *et al.* 2007).

1.2.3 *In vitro* culture of human hESCs

1.2.3.1 Feeder cells

hESCs were originally cultured on mouse embryonic fibroblast (MEF) feeders, in medium containing 20% foetal bovine serum (FBS), and passaged by manual dissection (Thomson *et al.* 1998). This method remains widely used to date and allows undifferentiated culture of hESCs, as assessed by morphology and phenotype (Reubinoff *et al.* 2000; Heins *et al.* 2004). The colony-like growth of hESCs on MEFs offers the advantage of positively-selecting undifferentiated colonies to expand by manual dissection at each passage (Bigdeli *et al.* 2008). However, this culture method is particularly laborious, requiring specialised skills and time (Bigdeli *et al.* 2008). Automated dissection of hESC colonies, achieved using Laser Microdissection and Pressure Catapulting (LMPC; Terstegge *et al.* 2009), has alleviated some of the manual labour requirements, but still involves the use of specialised equipment and is considered to be a subjective process since only a few colonies are propagated at each passage, based only on their morphological characteristics. Propagating whole populations of hESCs to the next passage has been achieved *via* enzymatic dissociation of hESC colonies (e.g. using collagenase IV, trypsin or dispase), which however yields variable-sized colonies and leads to increased karyotype instability (reviewed by Grandela and Wolvetang 2007; Heng *et al.* 2007).

Moreover, the use of animal feeder cells (i.e. MEFs) for hESC culture increases the risk of infection by retroviruses or other animal pathogens (Amit *et al.* 2004; Martin *et al.* 2005). Immunogenic epitopes such as N-glycolylneuraminic acid non-human sialic acid can be transferred from MEFs or FBS to hESCs, increasing the possibility of an immune reaction upon potential hESC transplantation to humans, and hindering reliable and reproducible hESC research (Skottman and Hovatta 2006). Human fibroblast cells, derived from foreskin, placenta, adult marrow stroma and hESCs have been used as feeders for hESCs to replace animal feeders (Richards *et al.* 2002; Richards *et al.* 2003; Xu *et al.* 2004; Genbacev *et al.* 2005; Inzunza *et al.* 2005; Skottman *et al.* 2006). Despite their human origin, human feeder cells are still often cultured in FBS-containing media prior to their use in hESC culture and therefore carry a slight risk for hESC xeno-infection.

1.2.3.2 Culture media

Culture of hESCs in 20% FBS is subject to inconsistencies due to batch-to-batch variations in commercially available FBS (reviewed in Skottman and Hovatta 2006). This contributed towards the use of defined serum replacement (KnockOut Serum Replacement, KSR: Invitrogen; Richards *et al.* 2002; Koivisto *et al.* 2004) which could sustain undifferentiated culture of hESCs when supplemented with 4ng/ml of the paracrine signalling molecule, basic-FGF (bFGF or FGF2; Amit *et al.* 2000; Inzunza *et al.* 2005). However, KSR still contained some products of animal origin, such as AlbuMAX (lipid enriched bovine serum albumin; Unger *et al.* 2008). Treatment with bFGF and Activin A, Nodal, or Noggin, (members of the TGF-β signalling pathway) was able to support undifferentiated *in vitro* culture of hESCs in serum-free and feeder-free conditions (Vallier *et al.* 2005; Xu *et al.* 2005), through inactivation of SMAD1 and 5, which are responsible for hESCs differentiation towards mesoderm, stabilisation of *NANOG* expression and inhibition of apoptosis (James *et al.* 2005; Li *et al.* 2007b; Vallier *et al.* 2009a). These observations formed the foundation of formulating chemically-defined media that could sustain and potentially-standardize hESC

cultures. Examples of chemically defined media include; mTeSR™1 Maintenance Medium from StemCell Technologies and STEMPRO® ESCs culture medium from Invitrogen (Ludwig *et al.* 2006a; Ludwig *et al.* 2006b; Wang *et al.* 2007; Swistowski *et al.* 2009). However, chemically-defined, commercially available media are very costly, a feature that can limit their use for everyday research. Also, they rely on the use of artificial Matrigel™ surfaces (see section 1.2.3.3) which are derived from animal sources (Kleinman and Martin 2005).

1.2.3.3 Feeder-free culture surfaces

In order to alleviate the need for feeder cells, hESCs have been cultured on natural or artificial matrices that are synthesised by extra-cellular matrix components (e.g. Matrigel™ and human laminin). Matrigel™ is the most commonly used surface for feeder-free hESC culture. It supports the growth of numerous hESC lines passaged either by trypsin, dispase or collagenase IV enzymes, and cultured either in MEF-conditioned medium with KSR and bFGF, or in defined media (Xu *et al.* 2001; Ludwig *et al.* 2006b; Braam *et al.* 2008a). However, Matrigel™ is expensive and has limited shelf-life. Cheaper, more stable, easy-to-handle and defined surfaces for hESC culture have been developed recently, and include oxygen plasma etched tissue culture polystyrene (PE-TCPS) or thermo-responsive co-polymer coated surfaces (Loh *et al.* 2009; Mahlstedt *et al.* 2010). Nevertheless, these surfaces could only support hESC culture in MEF-conditioned medium with KSR and bFGF, and failed to support undifferentiated culture in defined media. Also, defined surfaces are still not commercially available (Loh *et al.* 2009; Mahlstedt *et al.* 2010).

1.2.4 *In vitro* differentiation of hESCs

1.2.4.1 Differentiation *via* embryoid body formation

hESCs can differentiate *in vitro* into cell types representative of the three embryonic germ layers *via* formation of three-dimensional 3D aggregates, known as embryoid bodies (EBs; reviewed by Andrés *et al.* 2009).

One method by which EBs can be generated is the manual dissection or enzymatic treatment of hESC colonies with collagenase IV, trypsin or dispase, followed by suspension culture in non-adhesive surfaces, using 15-20% FBS (Itskovitz-Eldor *et al.* 2000; Kehat *et al.* 2001). However, suspension cultures generate EBs with significant size variation (3 to 1000 cells) due to variable size and dissociation of starting hESC colonies, thus introducing considerable inconsistency to differentiation towards desired lineages (Kehat *et al.* 2001; Ng *et al.* 2005b; Pal and Khanna 2007). Moreover, contaminating MEFs have the potential to interfere with the differentiation process by competing for cell-cell interactions as well as insulating communication between hESCs (Weitzer 2006).

Other methods, such as the formation of hanging drops with a defined numbers of cells, allow more uniform formation of EBs, but are not amenable to scale-up and have been more successful in mESCs than hESCs (Reubinoff *et al.* 2000; Baharvand *et al.* 2006; Burridge *et al.* 2007). Large-scale production of EBs has been achieved *via* the use of spinner flasks and bioreactors (Schroeder *et al.* 2005), but often results in agglomeration of EBs (Cameron *et al.* 2006). Forced aggregation of a defined number of hESCs by centrifugation in ultralow-attachment U96-well plates or silicon etched 384-well plates enables formation of EBs with a controllable size (Ng *et al.* 2005a; Ungrin *et al.* 2008), but is excessively costly. Forced aggregation in untreated V-96 plates (Burridge *et al.* 2007) is a cost effective method for the generation of EBs with uniform and controllable size, following simple and reproducible procedures (Burridge *et al.* 2007).

1.2.4.2 Differentiation *via* non-embryoid body methods

hESCs can also be induced to differentiate in monolayer cultures with defined growth factors added to the medium or by co-culture with differentiated cell types of a relevant lineage (reviewed by Andrés *et al.* 2009). For example, treatment of monolayer hESC cultures with Activin A and BMP4, or co-culture with END-2 mouse visceral endoderm cells have been shown to induce differentiation and facilitate formation of cardiomyotes (Mummery *et al.* 2003; Yao *et al.* 2006). Equally, co-culture with mouse foetal liver-derived stromal cells facilitated differentiation towards haematopoietic lineages (Ma *et al.* 2007). Even though monolayer differentiation uniformly exposes cells to components of the culture medium, it is believed that differentiation towards some lineages might require the cell-cell or cell to extra-cellular matrix interactions that are provided by the formation of 3D EB aggregates (Andrés *et al.* 2009).

1.2.4.3 Small molecules and paracrine factors affecting hESC differentiation

Small soluble molecules such as 5-aza-2'-deoxycytidine and ascorbic acid have been shown to influence differentiation of hESCs towards cardiomyocytes or haematopoietic lineages (Passier *et al.* 2005; Yoon *et al.* 2006; Ma *et al.* 2007). Moreover, Activin A in combination to Wnt3a signalling have been associated with differentiation of hESCs towards hepatic lineages (Hay *et al.* 2008; Sadhana *et al.* 2008), while Activin A and BMP4 can promote formation of cardiac lineages (Laflamme *et al.* 2007). An elaborate study by Vallier *et al.* (2009c) has determined that BMP4 signalling induces hESCs to differentiate towards primitive endoderm and trophectoderm, BMP4 in combination to Activin and bFGF induce mesoderm differentiation, and finally inhibition of Activin/nodal signalling leads to the formation of neuroectoderm.

1.2.4.4 Culture system used in this thesis

Since hESCs cultured for this thesis were used only for research purposes, refraining from animal products was of a lesser significance. Therefore, chemically defined medium was not used, to reduce the cost of experimentation. In this thesis, hESCs were cultured on Matrigel™-coated plastic surfaces, using KSR and bFGF-containing medium that had been conditioned on MEF feeders. Cells were passaged enzymatically using trypsin. This culture system has been shown to sustain a stable karyotype in hESCs following prolonged passaging (Denning *et al.* 2006) and also provided several advantages for the work carried out in this thesis; 1) it permitted the use of defined numbers of hESCs for forced aggregation, which was the selected differentiation system used in this thesis as it enabled standardisation of differentiation procedures (Burridge *et al.* 2007) and direct comparison between fibroblast cells derived from hESCs and iPSCs (see section 3.1.1). This culture system also enabled precise cell counts for 2) the formation of growth curves and 3) for efficient genetic modification by shRNA-mediated gene knock-down experiments performed in chapter 5 (Braam *et al.* 2008a).

1.3 TRANSCRIPTION FACTOR NETWORKS ASSOCIATED WITH PLURIPOTENCY

The pluripotent phenotype of hESCs is sustained by a complex network of transcription factors (TFs; Boyer *et al.* 2005), that can act either to repress differentiation-specific genes or stimulate factors which actively maintain pluripotency. This section will discuss the mechanisms of TF-regulation over gene expression and pluripotency maintenance.

1.3.1 Regulation of gene expression by transcription factors

Initiation of transcriptional activity in eukaryotic genes is dependent on the accessibility of regulatory regions in gene promoters to the RNA Polymerase II (Pol II) transcriptional machinery (Ptashne and Gann 1997). Regulatory regions in gene promoters fall within three categories; the core promoter, the proximal enhancer and the distal enhancer (Figure 1.2).

Elements of the core promoter sequence attract binding of transcriptional pre-initiation complexes (PIC) and general transcription factors (GTFs, e.g. TATA binding proteins TFIIA, B, D), whereas the proximal and distal enhancers attract "activator" or repressor" TFs. Transcriptional "activator" or "repressor" TFs affect gene expression either by direct interaction with components of the core promoter or with co-regulators (also known as transcription-associated factors, TAFs) which in turn interact directly with Pol II, GTFs or nucleosome remodelling and histone modifying enzymes (section 1.5.1) that can change the chromatin compaction of the promoter and improve the accessibility of Pol II to the core promoters (reviewed by Fuda *et al.* 2009). Transcriptional enhancer elements can be located upstream or downstream the transcription start site (TSS) and can modulate gene expression independently of their orientation (Visel *et al.* 2009).

Activator or repressor TF-proteins contain conserved DNA binding motifs (e.g. forkhead, OCT/SOX, zing-finger, helix-loop-helix, and POU motifs) that enable association with promoter regulatory regions based on compatibility to the DNA sequence (Reid *et al.* 2010). Transcription factors are stimulated to bind DNA based on developmental or environmental signalling, transmitted by hormones or morphogenic molecules (e.g. thyroxin, retinoic acid; reviewed by Cosma 2002).

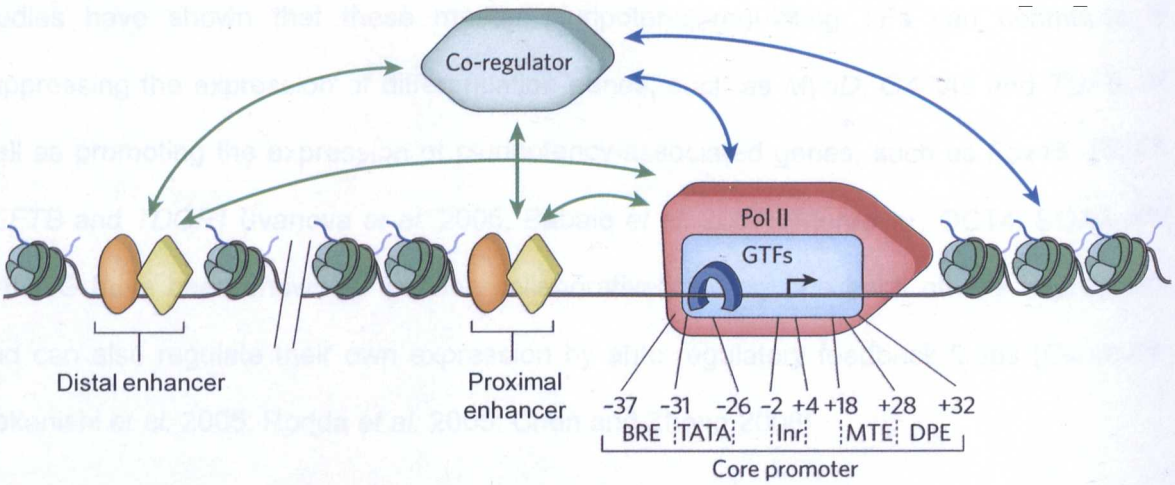

Figure 1.2- Transcription regulatory interactions
General transcription factors (GTFs, light blue) bind to specific sequences in gene promoters (B recognition element (BRE), TATA box (TATA), initiator (Inr), motif ten element (MTE) or downstream promoter element (DPE)), located within close proximity to the transcription start site (TSS, black arrow). Activator or repressor

transcription factors (orange and yellow) bind the proximal and distal enhancers, and can interact with GTFs (green arrows), TATA binding protein (TBP, dark blue) or RNA polymerase II (Pol II, red) to enhance or repress gene transcription. Activator or repressor transcription factors also interact with co-regulators which in turn either interact with the general transcription machinery or chromatin-modifying factors (blue arrows; Fuda *et al.* 2009)

1.3.2 Master regulators of pluripotency

The establishment and maintenance of pluripotency in mouse and human ESCs is regulated by a complex network of transcription factors, in which over 300 different genes are involved (Boyer *et al.* 2005; Orkin 2005; Kim *et al.* 2008a). In this network, the transcription factors OCT4 (also known as POU5F1), NANOG and SOX2 stand out for the significance of their contribution to pluripotency establishment and maintenance, and are considered to be master regulators at the top of the pluripotency network (Boyer *et al.* 2006; Wang *et al.* 2006; Babaie *et al.* 2007; Masui *et al.* 2007). Chromatin immuno-precipitation studies have revealed that OCT4, SOX2, and NANOG TFs occupy hundreds of gene promoters in mouse and human ESCs (Boyer *et al.* 2005; Chen *et al.* 2008b) and mostly bind within ±2kb of the TSS in mESCs (Liu *et al.* 2008b). In some cases, these TFs co-localise on promoter regions, suggesting that they might act in protein complexes to regulate gene expression (Kim *et al.* 2008a). Binding of Oct4, Sox2 and Nanog TFs is enriched in genes involved in developmental processes (Kim *et al.* 2008a). RNA interference (RNAi, see section 5.1.2) studies have shown that these master pluripotency-regulating TFs can contribute to suppressing the expression of differentiation genes, such as *MyoD*, *GATA6* and *TGF5*, as well as promoting the expression of pluripotency-associated genes, such as *Fbx15, REX1, LEFTB* and *TDGF1* (Ivanova *et al.* 2006; Babaie *et al.* 2007). Moreover, OCT4, SOX2 and NANOG have been shown to function collaboratively to regulate each other's expression, and can also regulate their own expression by auto regulatory feedback loops (Okumura-Nakanishi *et al.* 2005; Rodda *et al.* 2005; Chen and Zhong 2008).

Another factor that is considered to be at the top of the ESC transcriptional hierarchy, at least in mESCs, is Klf4 (Li *et al.* 2005; Jiang *et al.* 2008). Klf4 also exhibits auto regulatory

abilities, making this a common feature between key ESC genes (Figure 1.3). Klf4 co-occupies numerous gene promoters in mESCs, together with Oct4, Nanog and Sox2 (Loh *et al.* 2006; Chen and Zhong 2008), but shares the majority of its targets with Nanog (Loh *et al.* 2006; Jiang *et al.* 2008) and acts as an enhancer of Oct4 and Sox2 in the regulation of developmental processes (Liu *et al.* 2008b).

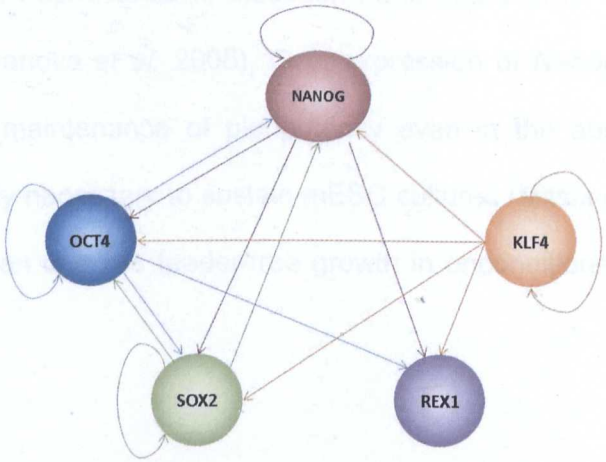

Figure 1.3- Transcriptional regulatory circuit between master pluripotency regulators
Transcription factors at the top of mouse and human ESC transcriptional hierarchy (OCT4, NANOG, SOX2 and KLF4) exhibit auto-regulatory abilities, unlike downstream regulators of pluripotency, such as REX1. Arrows point to the factor being transcriptionally regulated (modified from Chen and Zhong 2008).

1.3.3 Expression and roles of master pluripotency regulators in determining cell phenotype

1.3.3.1 OCT4

OCT4 is expressed in mouse and human totipotent and pluripotent cells in the ICM, ESCs and embryonic carcinoma cells (ECs; reviewed by Koestenbauer *et al.* 2006). Deletion of *Oct4* in mouse embryos has been shown to prevent normal formation of the ICM (Nichols *et al.* 1998), while its knock-down in mESCs leads to trophectoderm differentiation through up-regulation of *Cdx2* (Niwa *et al.* 2000; Niwa *et al.* 2005). *Oct4* over-expression in mESCs results in differentiation towards primitive endoderm and mesoderm (Niwa *et al.* 2000). In hESCs, *OCT4* down-regulation was shown to promote differentiation towards endoderm and mesoderm lineages, while its up-regulation resulted in differentiation towards endoderm (Rodriguez *et al.* 2007).

1.3.3.2 NANOG

NANOG is expressed in mouse and human ICM, ESCs and ECs, while in the mouse, expression is also detected in morula-stage embryos (reviewed by Koestenbauer *et al.* 2006). Loss of *Nanog* is lethal in mouse embryos at the blastocyst stage (Mitsui *et al.* 2003), and its down-regulation in mouse and human ESCs results in loss of pluripotency and induction of endoderm, trophectoderm, mesoderm and neural crest cell marker expression (Hyslop *et al.* 2005; Ivanova *et al.* 2006). Over-expression of *Nanog* in mESCs has been shown to enable the maintenance of pluripotency even in the absence of extrinsic LIF treatment that is usually necessary to sustain mESC cultures (Mitsui *et al.* 2003). In hESCs, *NANOG* over-expression enables feeder-free growth in unconditioned medium (Darr *et al.* 2006).

1.3.3.3 SOX2

SOX2 is expressed in the mouse and human morula, ICM, ESCs and ECs (reviewed by Koestenbauer *et al.* 2006). This TF is also expressed in the neural plate during embryogenesis (Zappone *et al.* 2000; Miyagi *et al.* 2004) and in neural stem cells in the adult organism, albeit from an alternative regulatory region (Miyagi *et al.* 2006). Despite its somewhat widespread expression and role in neurogenesis (Graham *et al.* 2003; Ferri *et al.* 2004) SOX2 plays a major role in pluripotency maintenance; its deletion is lethal for mouse embryos which do not develop an epiblast, while knock-down in mouse and human ESCs leads to loss of self-renewal capacity and differentiation towards trophectoderm (Avilion *et al.* 2003; Ivanova *et al.* 2006; Li *et al.* 2007a; Fong *et al.* 2008).

1.3.3.4 KLF4

KLF4 expression has a more widespread tissue distribution as it has been detected in the gut, epithelial cells, keratinocytes as well as mouse and human ESCs (Garrett-Sinha *et al.* 1996; Shields *et al.* 1996; Aasen *et al.* 2008). Klf4 has a major role in chromatin remodelling

and interacts with Klf2 and Klf5 to maintain mESC identity by supporting their self-renewal capacity (Li *et al.* 2005). Klf4 also co-operates with Oct4 and Sox2 to induce activation of Lefty1, which in turn promotes Oct4 and Sox2 expression (Nakatake *et al.* 2006). Klf4 depletion in mESCs leads to differentiation and up-regulation of lineage commitment genes such as *Brachyury* (*T*) and *Cdx2* (Jiang *et al.* 2008).

1.3.4 Downstream regulators of pluripotency

Despite the hierarchical significance of OCT4, NANOG, SOX2 and KLF4 TFs in the establishment and maintenance of pluripotency, other factors such as LIN28, DNMT3B and REX1 have been implicated in the transcriptional network of mouse and human ESCs (Adewumi *et al.* 2007; Kim *et al.* 2008a). These factors, often referred to as "downstream regulators" of pluripotency, are among the most highly expressed transcripts in ESCs, and are expressed at almost undetectable levels in differentiated cell types (Richards *et al.* 2004; Enver *et al.* 2005; Adewumi *et al.* 2007; Viswanathan *et al.* 2008). Some down-steam regulators of pluripotency, such as *Rex1*, assist in the maintenance of pluripotency by suppressing lineage commitment genes (e.g. Pax6; Darr and Benvenisty 2009; Scotland *et al.* 2009), while others, such as TDGF1 can actively maintain pluripotency by promoting self-renewal (Babaie *et al.* 2007; Xu *et al.* 2009a; Table 1.1).

1.4 MICRO RNAS AND THEIR ROLE IN PLURIPOTENCY AND DIFFERENTIATION

Micro-RNAs (miRNAs) are non-coding 21-nucleotide RNA molecules capable of binding to and causing the degradation of endogenous mRNAs *via* the RNAi pathway (see section 5.1.2; Valencia-Sanchez *et al.* 2006; Kim *et al.* 2009d). miRNAs of the *miR-290*, *miR-302* and *miR-17-95* families have been detected at elevated levels in mESCs and are believed to promote rapid proliferation and maintenance of self-renewal (Wang *et al.* 2008b). Other miRNAs have been implicated in differentiation (reviewed in Bosnali *et al.* 2009), including miRNAs of the *let-7* family, which are suppressed in ESCs by the pluripotency factor LIN28

(Newman *et al.* 2008). *Let-7* miRNAs are up-regulated upon differentiation, repressing cell-cycle regulators, such as *CDC25A* and *CDK6* (Johnson *et al.* 2007), and growth promoting factors, such as *RAS*, *HMG2A* and *c-MYC* (Johnson *et al.* 2005). Moreover, miRNA-145 represses the 3' untranslated region (UTR) of *OCT4*, *SOX2* and *KLF4*, leading to translational inhibition of these genes and to differentiation (Xu *et al.* 2009c).

Table 1.1- Roles of downstream pluripotency TFs in the maintenance of self-renewal and differentiation
ESCs= embryonic stem cells, ECs= embryonic carcinoma cells, EGs= embryonic germ cells, ICM= Inner cell mass

Gene		Expression	Function	References
LIN28	mouse and human	ESCs, ECs	Stimulates production of histone H2a mRNA involved in co-ordinating ESC proliferation, stimulates post-transcriptional OCT4 expression, blocks processing of let-7 miRNAs which promote differentiation	Yu *et al.* 2007a; Newman *et al.* 2008; Darr and Benvenisty 2009; Qiu *et al.* 2009; Xu and Huang 2009
REX1		ESCs, ECs, EGs	Regulated by Nanog and Sox2. Dispensable for self-renewal in ESCs, prevents differentiation to endoderm	Thompson and Gudas 2002; Shi *et al.* 2006; Scotland *et al.* 2009
DNMT3B		ICM, ESCs, ECs	Dispensable for self-renewal in ESCs, necessary for differentiation and silencing of *Oct4* & *Nanog*	Jackson *et al.* 2004; Tsumura *et al.* 2006
c-MYC		ESCs, ECs	Promotes self renewal in ESCs	Cartwright *et al.* 2005
TERT		ESCs, ECs	Highly expressed in ESCs & ECs, regulated by c-Myc, supports self-renewal	Armstrong *et al.* 2000; Armstrong *et al.* 2005
TDGF1		ESCs, ECs	Regulated by Oct4, co-receptor of Nodal, stimulates self-renewal in ESCs	Babaie *et al.* 2007
UTF1		Blastocyst, ESCs, ECs, EGs	Regulated by Oct4 and Sox2, delays or blocks differentiation	Okuda *et al.* 1998; Nishimoto *et al.* 2005
FOXD3		Blastocyst, ESCs, ECs	Interacts with Oct4, necessary for generation of pluripotent cell populations in embryos	Hanna *et al.* 2002; Laslett *et al.* 2003
TBN		ICM, ESCs, ECs,	Essential for survival of ICM cells in mouse	Voss *et al.* 2000
FBX15		ICM, ESCs, ECs	Interacts with Oct4 and Sox2. Dispensable for self-renewal in ESCs	Tokuzawa *et al.* 2003
hGDF3		ESCs, ECs	High expression levels in ESCs & ECs	Adewumi *et al.* 2007
EHOX		ESCs	Prevents differentiation to haematopoietic, endothelial and cardiac markers upon differentiation in ESCs	Jackson *et al.* 2002
GABRB3		ESCs, ECs	High expression levels in ESCs & ECs	Adewumi *et al.* 2007
LEFTB	hESCs		Regulated by Oct4, high expression levels in ESCs	Babaie *et al.* 2007; Sun *et al.* 2007
Esrrb	mESCs		Interacts with *Oct4* and *Nanog*, promotes establishment of self-renewal and pluripotency	Zhang *et al.* 2008
Ronin			Supports self-renewal & inhibits differentiation upon LIF removal in mESCs, through epigenetic silencing of lineage commitment factors	Dejosez *et al.* 2008

1.5 EPIGENETIC CONTROL OF GENE EXPRESSION

Complex organisms, such as humans, contain a variety of cell-types that are all derived from a single genome (Holliday 1994; Lynch 2004). Divergent cell phenotypes are determined by expression of unique sets of genes in each cell-type, a trait that is to some extent dependent on a range of heritable covalent modifications of the DNA and associated histone proteins, known as epigenetic modifications (Hemberger *et al.* 2009; Ho and Crabtree 2010; Law and Jacobsen 2010). Epigenetic modifications can affect the expression of individual genes by altering chromatin architecture, and thus changing the accessibility of Pol II to gene promoters (reviewed by Cairns 2009).

1.5.1 Chromatin remodelling and histone modifications

1.5.1.1 Chromatin organisation

In order to fit within a nucleus, eukaryotic genomic DNA is compacted more than 10,000 times by histone proteins (Figure 1.4.A). 147bp of super helical DNA are wrapped around a histone octamer, composed of two H2A-H2B dimers and two molecules of each H3 and H4, to form a nucleosome (Luger 2003). The point at which DNA enters and exits a nucleosome is occupied by "linker" H1 molecules. Nucleosomes line up to form 11nm fibres, which are further compacted into 30nm fibres that give rise to the highly ordered structure known as chromatin (Sparmann and van Lohuizen 2006).

Chromatin condensation varies at different areas of the genome, in a manner that is related to gene activity; actively transcribed genes are usually located within chromatin with an open conformation, known as euchromatin, whereas silenced genes are found within densely compacted chromatin, known as heterochromatin (Gilbert *et al.* 2004). Repetitive sequences, such as centromeres and telomeres, are permanently associated with heterochromatic regions (constitutive heterochromatin) whereas developmentally regulated genes become associated with heterochromatin depending on cell type or stage of the cell cycle (facultative heterochromatin; Woodcock and Dimitrov 2001). Heterochromatic regions

tend to assemble at the nuclear lamina (Figure 1.4.B), while transcriptionally active euchromatic regions are clustered towards the interior of the nucleus and interact *via* chromosome loops (*cis*) or bridges (*trans*; Lanctot *et al.* 2007a; Guelen *et al.* 2008). This 3D chromatin topography forms "transcriptional factories", which regulate gene expression by facilitating interactions between distal regulatory elements and target genes (reviewed by Gondor and Ohlsson 2009).

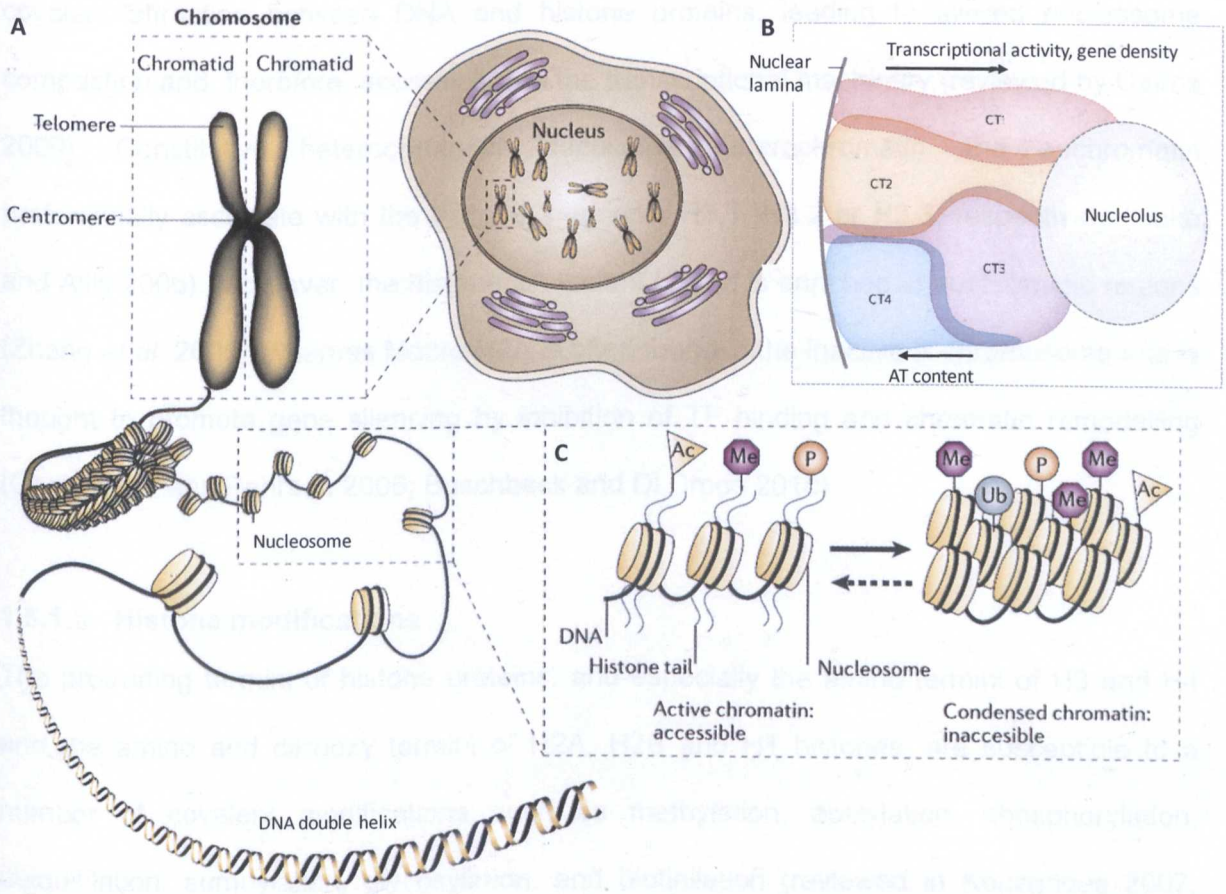

Figure 1.4- Chromatin organisation and regulation of gene expression
A. Genetic information within eukaryotic nuclei is assembled into chromosomes, in which the DNA double helix is wrapped around nucleosomes forming a "beads on string" structure that is subsequently folded into higher order chromatin (Sparmann and van Lohuizen 2006). **B.** Radial organisation of chromosome territories (CT) within nuclei that facilitates chromatin cross-talk. The relative positions of chromosomes in the interphase nucleus depend on the proportion of genes and A+T content (Gondor and Ohlsson 2009). **C.** Histone proteins within the nucleosome have long, flexible amino-terminal domains (tails) in which a number of amino-acids are targets of covalent modification, such as acetylation (Ac), methylation (Me), phosphorylation (P), and ubiquitilation (Ub). Histone modifications affect the dynamic chromatin structure and are associated with alterations in gene transcriptional activity (Sparmann and van Lohuizen 2006).

1.5.1.2 Chromatin remodelling

Chromatin remodelling enzymes facilitate nucleosome re-positioning or ejection in order to "cover" or uncover" regulatory elements located in gene promoters (Cairns 2005). Such chromatin remodelling enzymes include the ATP-dependent SWI/SNF complex (usually associated with gene activation) and the ISWI complex (associated with gene silencing), which catalyse nucleosome disassembly or sliding along the DNA (Fazzio and Tsukiyama 2003). Also, incorporation of different histone isoforms into the nucleosome affects the covalent attraction between DNA and histone proteins, leading to altered nucleosome compaction and, therefore, accessibility to the transcriptional machinery (reviewed by Cairns 2009). Constitutive heterochromatin, facultative heterochromatin and euchromatin preferentially associate with the histone 3 variants H3.1, H3.2 or H3.3, respectively (Hake and Allis 2006). Moreover, the histone 2A variant H2A.Z is enriched in euchromatic regions (Zhang *et al.* 2005), whereas Macro-H2A is often found in the inactive X chromosome and is thought to promote gene silencing by inhibition of TF binding and chromatin remodelling (Changolkar and Pehrson 2006; Buschbeck and Di Croce 2010).

1.5.1.3 Histone modifications

The protruding termini of histone proteins, and especially the amino termini of H3 and H4 and the amino and carboxy termini of H2A, H2B and H1 histones, are susceptible to a number of covalent modifications such as methylation, acetylation, phosphorylation, ubiquitilation, sumoylation, glycosylation, and biotinilation (reviewed in Kouzarides 2007; Table 1.2). Histone modifications have important roles in the regulation of gene activation or repression by maintaining the dynamic equilibrium of chromatin structure (Li 2002; Margueron *et al.* 2005; Turek-Plewa and Jagodzinski 2005). For example, lack of acetylation on histone 4 lysine 16 (H4K16Ac) attracts binding of the ISWI complex to gene promoters, which in turn facilitates gene silencing (Corona *et al.* 2002). Also, histone 3 lysine 9 methylation (H3K9me), catalyzed by G9a methyltransferase (Tachibana *et al.* 2001)

is believed to be important in the recruitment of heterochromatin protein 1 (HP1), which compacts chromatin structure and establishes long term transcriptional repression (Boulias and Talianidis 2004). Histone acetylation is typically associated with active transcription and open chromatin architecture (Kurdistani and Grunstein 2003; Margueron *et al.* 2005; Table 1.2; Figure 1.4.C), whereas histone methylation has a more diverse effect on transcriptional activity. For example, H3K9 methylation is associated with repressed gene activity (tri-methylation of this residue found in heterochromatic regions and di- & mono- methylation found in silent euchromatic regions), whereas H3K4 methylation is exclusively associated with transcriptionally active genes (reviewed by Martin and Zhang 2005; Shilatifard 2008). Ubiquitilation can be associated with transcriptional activation or repression, dependent on its interaction with other histone modifications. This is exemplified by co-operation of H3K9me, H3K27me and H2AK199 ubiquitilation (H2AK199Ub) in silencing of the inactive X-chromosome (Senner and Brockdorff 2009), in contrast to H2BK120Ub which interacts with transcriptional activators, and H3K4me and H3K79me, to promote early steps of transcriptional initiation (Weake and Workman 2008).

Table 1.2- Classes of histone modifications and examples of enzymes catalysing each modification
Red= repressive mark, associated with gene silencing, green= activating mark, associated with gene expression. List not exhaustive (modified from Berger 2007; Kouzarides 2007).

Modification	Histone	Amino-acid		Enzyme	Function
Acetylation	H2A	K5	Histone acetyl-transferases (HATs)	CBP/P300	Transcription, DNA repair, replication, condensation
	H2B	K12, K15			
	H3	K4, K18			
		K9, K14, K18		PCAF/GCN5	
		K14		TIP60	
		K14, K23		ScSAS3	
		K56		ScRTT109	
	H4	K5, K12		HAT1	
		K5, K8		CBP/P300	
		K5, K8, K12, K16		PCAF/GCN5	
		K5, K8, K12		HB01	
		K16		ScSAS3	
De-acetylation	H4	K16		SirT2	
	-	K		**Histone de-acetylases (HDAC)** class I, II and III	

Methylation	H3	K4	Histone methyltransferases	**Trithorax (Trx) group** proteins; MLL1, MLL2, MLL3, MLL4, MLL5,		Transcription, DNA repair
				SET1A, SET1B, ASH1, Sc/Sp SET1		
		K9		Suv39H1, Suv39H2, G9a, ESET/SETDB1, Riz1, EuHTMase/GLP, CLL8, SpClr4		
		K20		Pr-SET 7/8, SUV4 20H1, SUV420H2, SpSet9		
		K27		**Polycomb group (PcG)** proteins; EZH2, SUZ12, EED		
		K36		SET2, NSD1, SYMD2		
		K79		DOT1, Sc/Sp DOT1		
		R2, R17, R26		CARM1		Transcription
	H4	R3		PRMT4, PRMT5		
De-methylation	H3	K4	Histone Demethylases	LSD1, Rbp2		Transcription
		K9		Jumonji (JMJ) domain	JMJD1A, JHDM2a, JHDM2b, JMJD2A/JMJDM3A, JMJD2B, JMJD2C/GASC1, JMJD2D	
		K36			JHDM1a, JHDM1b, JMJD2A/JMJDM3A, JMJD2C/GASC1	
Phosphorylation	H2B	S14	MST1			Transcription, DNA repair, chromosome condensation
	H3	T3	Haspin			
		S28	MSK1, MSK2			
	H4	S1	CKII			
Ubiquitilation	H2A	K119	Bmi/Ring1A			Transcription, DNA repair
	H2B	K120	RNF20/RNF40			
Sumoylation	H2A	K126	UBC9			Transcription
	H2B	K6, K7				

1.5.1.4 Regulation of pluripotency and differentiation by chromatin remodelling

Regulation of the pluripotent cell phenotype by chromatin remodelling and histone modifications has mostly been studied in mESCs, whereas information from hESCs is scarce. mESCs are actively dividing cells, with a uniquely high transcriptional activity (Efroni *et al.* 2008) that correlates to increased formation of open chromatin structures compared to differentiated cells (Azuara *et al.* 2006). Formation of euchromatic regions is associated with high expression of the chromatin remodelling enzyme, Chd1, which is believed to promote transcriptional activity by incorporation of the histone 3 variant H3.3 (section 1.5.1.2) into nucleosomes (McKittrick *et al.* 2004). Chd1 associates with the pluripotency regulators *Oct4*, *Nanog* and *Sox2* and promotes their transcriptional activity, and thus the maintenance of self-renewal in mESCs (Sims *et al.* 2007; Chen *et al.* 2008a; Gaspar-Maia *et al.* 2009).

mESCs also have a unique embryonic isoform of the SWI/SNF-related chromatin remodelling complex, Baf (esBAF), whose ATPase-subunit, Brg1, shares common gene targets with the key ESC TFs Oct4, Sox2 and Nanog (Ho *et al.* 2009b). esBAF is believed to be necessary for the maintenance of pluripotency and self-renewal in mESCs by suppressing lineage commitment genes, such as *Fgf5* and *EphrinB4* (Ho *et al.* 2009a). Upon differentiation of mouse and human ESCs, chromatin compaction increases (Meshorer and Misteli 2006), and is associated with increased expression of HP1 (Bartova *et al.* 2008).

1.5.1.5 Regulation of pluripotency and differentiation by histone modifications

mESCs have been characterised with elevated levels of histone acetylation, which also facilitate the high transcriptional activity observed in mESCs (Efroni *et al.* 2008). The histone acetyltransferase Tip60/p400 is believed to be recruited to the promoters of active genes in mESCs, and have an essential role in the maintenance of mESC identity (Fazzio *et al.* 2008). p300 and Gcn5 HATs also have important roles in embryonic development, demonstrated by their co-localisation with the master pluripotency regulators Oct4, Sox2 and Nanog in mESCs (Chen *et al.* 2008b). Further histone modifications implicated in the maintenance of pluripotency and transition of cell phenotype from a pluripotent to a differentiated state are outlined in Table 1.3.

Table 1.3– Histone modifying enzymes associated with pluripotency and differentiation
Red= repressive mark, associated with gene silencing, green= activating mark, associated with gene expression. * PRC = Polycomb repressive complex

Class		Enzyme	Function	References
Polycomb Group (PcG)	**PRC2***	Suz12, Eed, Ezh2	Catalyse H3K27me3, interact with *Oct4* and *Sox2*, essential for early embryogenesis and ESC differentiation	Faust *et al.* 1998; O'Carroll *et al.* 2001; Pasini *et al.* 2007
	PRC1*	Ring1b	Essential for early embryogenesis & proper maintenance of self-renewal in ESCs	de Napoles *et al.* 2004; Stock *et al.* 2007; van der Stoop *et al.* 2008
Trithorax Group (Trx)		MLL complex	Catalyses H3K4me3. Essential for neuronal (Mll1) & haematopoietic differentiation (Mll5)	Ayton and Cleary 2001; Lim *et al.* 2009; Madan *et al.* 2009

Methylation	G9a	H3K9 methylation. Required for repression of key pluripotency genes during mESC differentiation	Tachibana *et al.* 2002; Feldman *et al.* 2006; Epsztejn-Litman *et al.* 2008
	Rbp2 (Jarid1a)	H3K4me3 de-methylation. Represses developmental regulators in mESCs	Pasini *et al.* 2007; Lopez-Bigas *et al.* 2008
	Dot1L	H3K79 methylation. Dispensable for self-renewal in mESCs. Necessary for early differentiation, where its deficiency leads to proliferative arrest in G2/M-phase	Barry *et al.* 2009; Jacinto *et al.* 2009
	Jarid2	Associates with and inhibits PCR2	Shen *et al.* 2009
	Jmjd1a, Jmjd2c	H3K9 de-methylation. Deletion leads to loss of pluripotency. Prevent H3K9me in *Nanog*	Loh *et al.* 2007
	Jmjd3, UTX	H3K27me3 de-methylation. Repression in mESCs leads to differentiation towards neural lineages. Needed for resolution of bivalent domains in differentiation	Agger *et al.* 2007; Hong *et al.* 2007; Lan *et al.* 2007; Lee *et al.* 2007; Xiang *et al.* 2007; Burgold *et al.* 2008; Sen *et al.* 2008
	CARM1	Catalyses H3R26me2, H3R17me2. Required for self renewal & pluripotency. Deletion down-regulates *Oct4* & *Sox2*, over expression up-regulates *Nanog* & resists differentiation	Torres-Padilla *et al.* 2007; Wu *et al.* 2009a
	Paf1C	Maintains H3K4me3 in promoters of *Oct4* and *Nanog*	Ding *et al.* 2009
Acetylation	HDAC1	Associated with transcriptional repression and heterochromatin formation during differentiation	Ma and Schultz 2008; Weichert *et al.* 2008
	Mta1	Part of the alternative NuRD complex, NODE, which associates with *Oct4* and *Nanog* in ESCs. Deletion in mESCs leads to reactivation of differentiation factors	Liang *et al.* 2008
	Tip60/p400 complex	Associated with transcriptional activity & maintenance of mESC identity	Fazzio *et al.* 2008
	p300, Gcn5	Essential roles during development. p300 associated with *Oct4*, *Sox2* and *Nanog*	Chen *et al.* 2008b

Worth noting is that mouse and human ESCs are enriched in "bivalent" chromatin domains, which are promoter regions associated with both the activating mark, H3K4me3, and the silencing mark, H3K27me3 (Pan *et al.* 2007; Kim *et al.* 2008a). Genes associated with bivalent domains in ESCs are inactive, but poised for quick reactivation upon differentiation (Figure 1.5). A poised epigenetic state in ESCs is found in genes necessary for lineage commitment, such as TFs of the *Sox*, *Fox*, *Pax*, *Irx*, and *Pou* gene families and developmental regulators, such as *Ikaros*, *Math1*, *Npas3*, *Meis2*, and *Pax2* (Bernstein *et al.* 2006). Upon differentiation, lineage commitment genes lose one of the two epigenetic marks, and either become activated or stably repressed, depending on the lineage of

differentiation (Mikkelsen *et al.* 2007; Pan *et al.* 2007). Gene promoters that lack bivalent domains can be associated with one or none of the two epigenetic marks, while those promoters that lack both H3K4me3 and H3K27me3 have a tendency to be regulated by DNA methylation (Fouse *et al.* 2008).

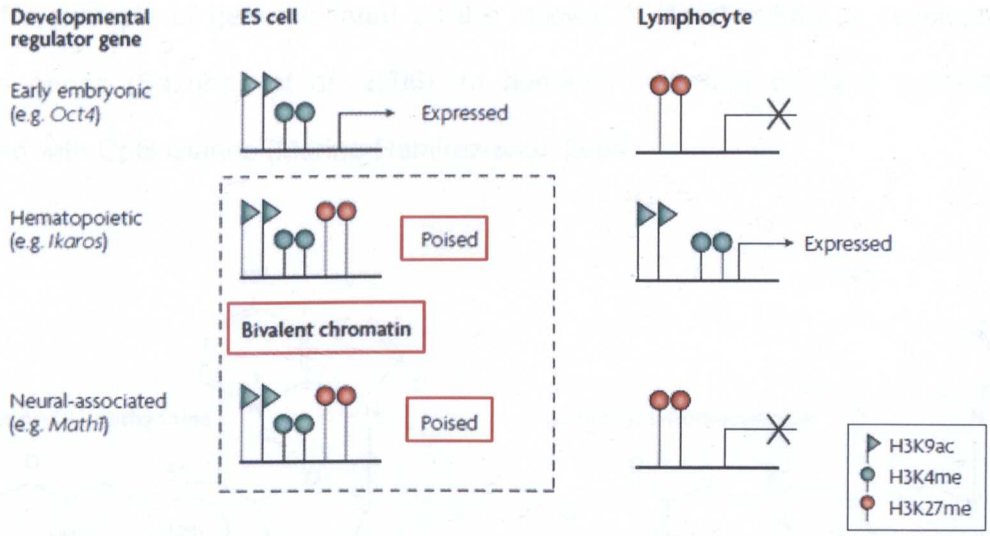

Figure 1.5- Bivalent domains in ESCs
In human and mouse ESCs the promoters of a range of transcriptionally inactive genes are associated with the opposing histone marks, H3K27me3 (associated with gene silencing) and H3K4me3 (associated with gene activation). Bivalent histone conformation denotes silenced genes that are poised for quick activation upon differentiation. During differentiation, bivalent domains are resolved, leading to transcriptional activation of tissue-specific genes (e.g. activation of *Ikaros* upon differentiation towards lymphocytes) and silencing of loci associated with alternative developmental pathways (e.g. *Math1* in this example). Pluripotency-associated genes such as *Oct4* also become repressed upon differentiation (adapted from Spivakov and Fisher 2007).

1.5.2 DNA methylation

DNA methylation is a reaction that involves the addition of methyl groups to 5' cytosine residues of CpG dinucleotides on DNA strands, using S-adenosyl-L-methionine (AdoMet) as a donor for the methyl groups (Gruenbaum *et al.* 1981; Figure 1.6). This epigenetic modification is catalysed by the DNA methyltransferase (DNMT; section 1.5.2.2) family of enzymes and has been associated with transcriptional silencing (section 1.5.2.1).

CpG dinucleotides represent 0.83-0.99% of the human and mouse genomes. Depending on cell-type, ~60-90% of cytosine residues in CpG sites are methylated (Zhao and Zhang

2006), with the majority of methylated cytosines being located within heterochromatic regions, such as repetitive and transposable elements (reviewed by Brenner and Fuks 2006). Non-methylated CpG sites are usually clustered in CpG islands, which are regions of ≥500bp in length with CpG content ≥55%, often located in gene promoters and exons (Takai and Jones 2002). DNA methylation changes at CpG islands can impact on transcriptional activity, for example of genes located on the inactive X-chromosome or developmentally regulated genes (Saxonov *et al.* 2006). In humans, ~50-70% of gene promoters are associated with CpG islands (Marino-Ramirez *et al.* 2004).

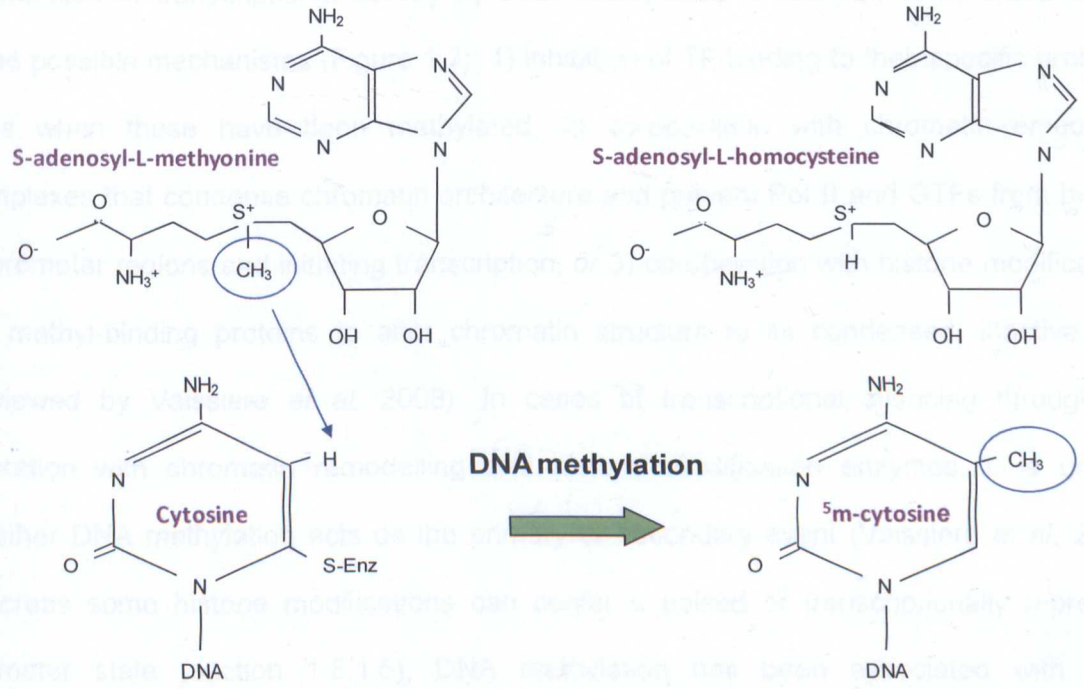

Figure 1.6– Addition of methyl groups to DNA cytosine residues
Methyl groups are added to 5' cytosine residues of CpG dinucleotides on DNA strands, using S-adenosyl-L-methionine as a donor for the methyl groups. Following donation of a methyl group, S-adenosyl-L-methionine is converted to S-adenosyl-L-homocysteine (modified from Gruenbaum *et al.* 1981).

1.5.2.1 Gene silencing by DNA methylation

DNA methylation is associated with silencing of transposable elements, as a defence mechanism against disruption of surrounding genes, as well as silencing of repetitive DNA sequences at pericentromeric and telomeric regions that is required to maintain genomic stability (reviewed by Wilson *et al.* 2007). Gene silencing by DNA methylation has also been

implicated in X-chromosome inactivation (Yen *et al.* 2007), genomic imprinting (Hore *et al.* 2007; see section 1.5.2.5), DNA replication timing (Ting *et al.* 2004; Unterberger *et al.* 2006), global shaping and maintenance of developmental patterning (Ehrlich 2003; Cavalli 2006), and tissue-specific gene expression (reviewed by Brena *et al.* 2006). Each cell type is thought to have a unique DNA methylation "fingerprint" or tissue-specific differential DNA methylation (T-DMR) that extends from imprinting and X-chromosome inactivation, to gene promoters, exons, introns, transposons and repetitive elements (Yang *et al.* ; Illingworth *et al.* 2008).

Repression of transcriptional activity by DNA methylation is believed to be achieved *via* three possible mechanisms (Figure 1.7); 1) inhibition of TF binding to their specific promoter sites when these have been methylated, 2) co-operation with chromatin-remodelling complexes that condense chromatin architecture and prevent Pol II and GTFs from binding to promoter regions and initiating transcription, or 3) co-operation with histone modifications *via* methyl-binding proteins to alter chromatin structure to its condensed, inactive form (reviewed by Vaissiere *et al.* 2008). In cases of transcriptional silencing through co-operation with chromatin remodelling and histone modification enzymes, it is unclear whether DNA methylation acts as the primary or secondary event (Vaissiere *et al.* 2008). Whereas some histone modifications can confer a poised or transcriptionally repressed promoter state (section 1.5.1.5), DNA methylation has been associated with more permanent silencing of gene expression (Feldman *et al.* 2006; Fouse *et al.* 2008; Mohn *et al.* 2008).

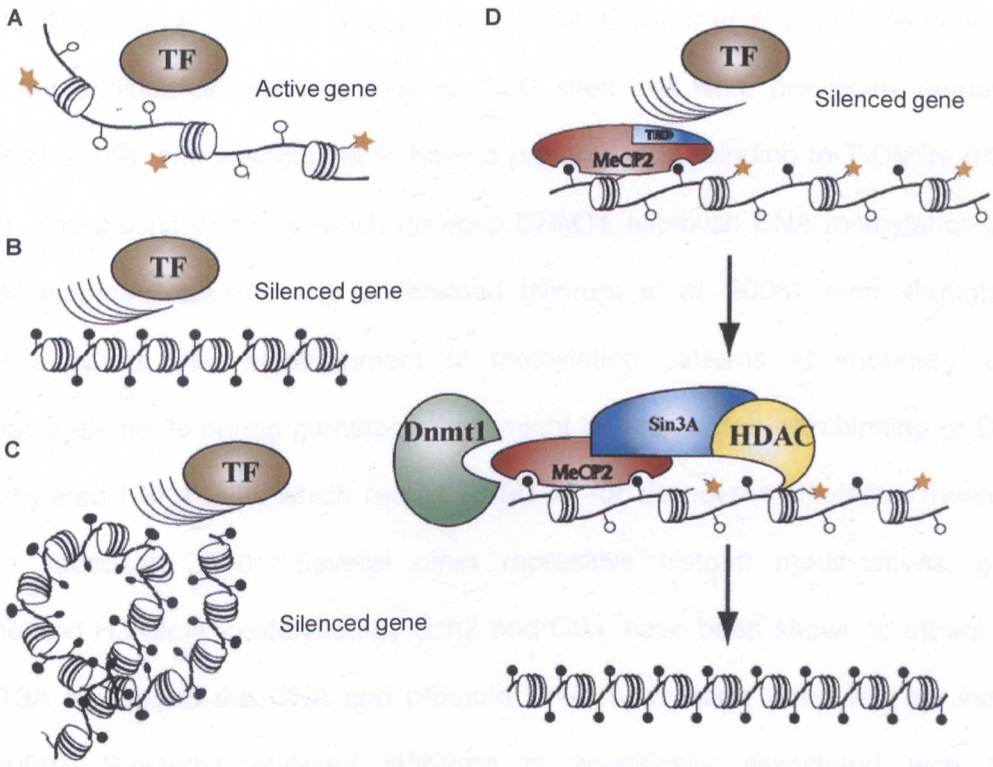

Figure 1.7- Regulation of gene silencing by DNA methylation
A. Active gene promoters can be associated with unmethylated CpG sites, acetylation of histone tails and an open chromatin conformation that allow transcription factor (TF) binding to regulatory elements. Promoters containing methylated CpGs can inhibit gene transcription by **B.** blocking TF binding to promoter regions, **C.** promoting heterochromatin formation through histone de-acetylation and chromatin remodelling complexes, or **D.** association of methyl-binding proteins (such as MeCP2/MBP2) with methylated cytosines, that in turn recruit histone de-acetylases (HDAC) that create a non-permissive chromatin state for TFs. Black and white circles represent methylated and unmethylated CpGs, respectively. Yellow stars represent histone acetylation (modified from Vaissiere *et al.* 2008).

1.5.2.2 *De novo* and maintenance DNA methylation

The global levels of DNA methylation undergo cycles of methylation and de-methylation events (Figure 1.8), during gametogenesis from primordial germ cells (PGCs) and during embryonic development (reviewed by Li 2002). Global de-methylation during embryogenesis occurs at the 4-8 cell stage in human embryos (Fulka *et al.* 2004) and at the 2-8 cell stage in mouse and sheep embryos (Young and Beaujean 2004; Yang *et al.* 2007). By the blastocyst stage, global DNA methylation levels increase (Fulka *et al.* 2004), mostly due to *de novo* DNA methylation (Figure 1.9) catalysed by the DNA methyltransferase (DNMT) enzymes DNMT3A and DNMT3B. Another enzyme of the DNMT3 family; DNMT3L, interacts with and stimulates the action of DNMT3A and 3B, but has no methyltransferase

activity itself (Chedin *et al.* 2002; Suetake *et al.* 2004; Gowher *et al.* 2005). *De novo* DNMTs catalyse the addition of methyl groups on CpG sites that were previously unmethylated (Chen *et al.* 2003), and are thought to have a preference for binding to T-DMRs (Hattori *et al.* 2004). The mechanisms by which *de novo* DNMTs establish DNA methylation patterns during development are not well understood (Nimura *et al.* 2006), even though recent evidence suggests that establishment of methylation patterns at imprinted loci and transposable elements during gametogenesis might be associated with binding of DNMT3L to unmethylated H3K4 tails, which recruit DNMT3A for *de novo* methylation (reviewed by Law and Jacobsen 2010). Several other repressive histone modifications, such as H3K27me and H3K9me - catalysed by Ezh2 and G9a, have been shown to attract binding of DNMT3A and 3B to the DNA and promote DNA methylation (reviewed by Jones and Liang 2009). Suv39/h1-catalysed H3K9me is specifically associated with Dnmt3b recruitment to pericentromeric repeats (Lehnertz *et al.* 2003).

Once established, DNA methylation patterns are maintained at every cycle of DNA replication by the "maintenance" methyltransferase, DNMT1 (Figure 1.9). DNMT1 catalyses the addition of methyl groups to CpG sites on newly synthesised DNA strands (Leonhardt *et al.* 1992; Pradhan *et al.* 1999) after being recruited to the replication fork by the proliferating cell nuclear antigen (PCNA) and the ubiquitin-like homeodomain & ring-finger domain 1 protein (UHRF1), an enzyme that has a high affinity for binding hemi-methylated DNA (Bostick *et al.* 2007).

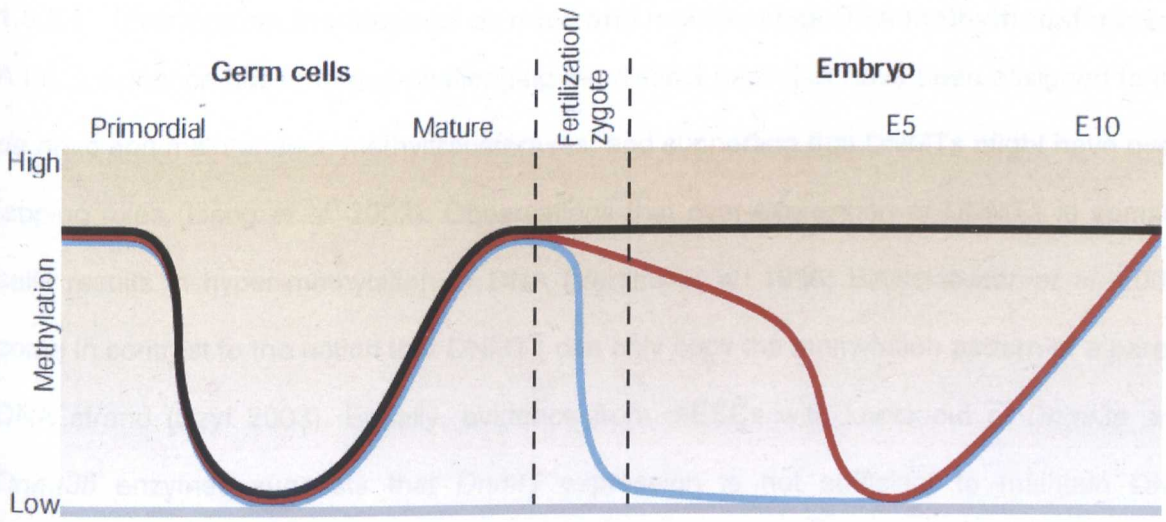

Figure 1.8- Cycles of DNA methylation and de-methylation during early embryonic development
DNA methylation levels during germ-cell and early embryonic development in methylated imprinted genes (black), unmethylated imprinted genes (grey), and non-imprinted DNA sequences of the maternally (red) and paternally (blue) inherited alleles. The horizontal and vertical axes, and the relative levels of DNA methylation are not drawn to scale (Reik and Walter 2001).

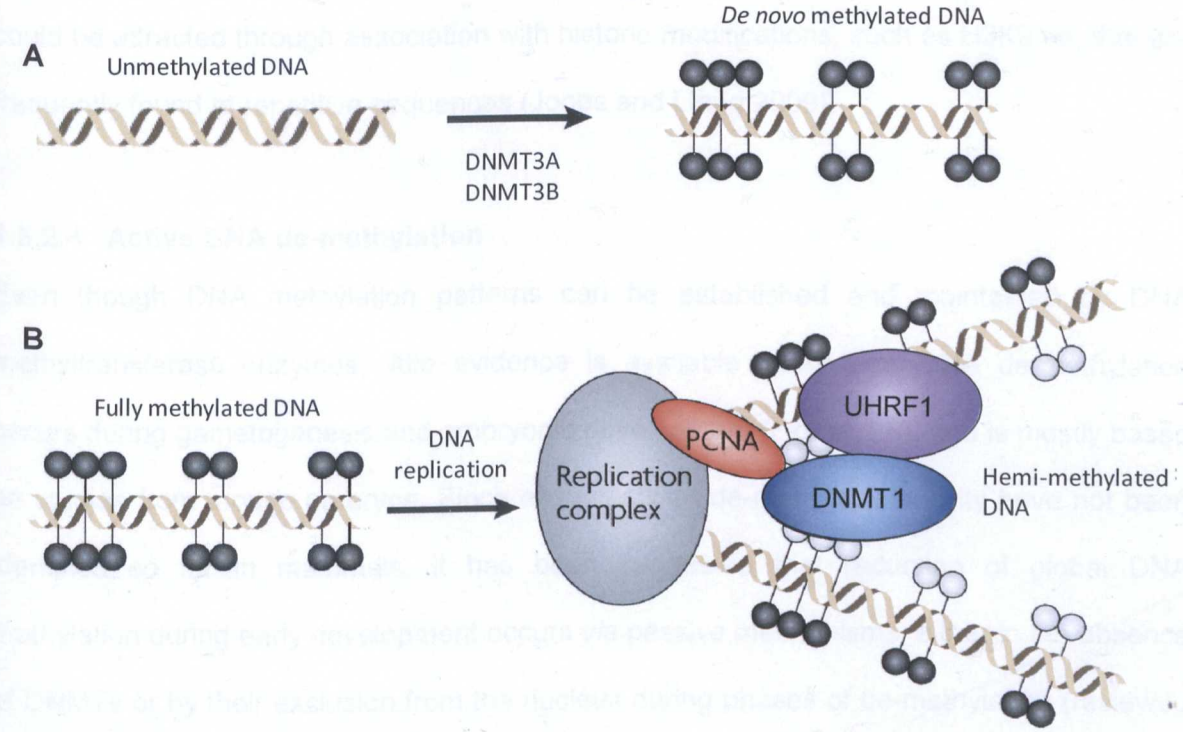

Figure 1.9– *De novo* and maintenance DNA methylation
A. *De novo* DNA methylation is carried out by the DNA methyltransferase enzymes DNMT3A and DNMT3B, and it is responsible for establishing DNA methylation patterns during early development. **B.** Model depicting maintenance DNA methylation during DNA replication. DNMT1 is proposed to be recruited to the replication fork through interactions with the proliferating cell nuclear antigen (PCNA) and ubiquitin-like homeodomain & ring-finger domain 1 protein (UHRF1), which specifically interacts with hemimethylated DNA. DNMT1 acts to maintain DNA methylation patterns by restoring hemimethylated DNA to a fully methylated state. Black and white circles represent methylated and unmethylated DNA, respectively (Law and Jacobsen 2010).

1.5.2.3 Overlapping functions of *de novo* and maintenance DNA methyltransferases

A lot of evidence has emerged challenging the distinct roles that have been assigned to the *de novo* and maintenance methyltransferases, and supporting that DNMTs might have over-lapping roles (Liang *et al.* 2002). Observations that over-expression of DNMT1 in somatic cells results in hyper-methylation of DNA (Vertino *et al.* 1996; Biniszkiewicz *et al.* 2002) come in contrast to the notion that DNMT1 can only copy the methylation pattern of a parent DNA strand (Szyf 2003). Equally, evidence from mESCs with knock-out of *Dnmt3a* and *Dnmt3b* enzymes suggests that *Dnmt1* expression is not sufficient to maintain DNA methylation at repetitive sequences such as intracisternal A-particle (IAP) repeats, major and minor satellite elements, transposons, and centromeric and pericentromeric regions (Table 1.5). It is, therefore, proposed that *de novo* DNMTs might be necessary to maintain DNA methylation at highly methylated regions of DNA (i.e. repeat sequences), to which they could be attracted through association with histone modifications, such as H3K9me, that are frequently found at repetitive sequences (Jones and Liang 2009).

1.5.2.4 Active DNA de-methylation

Even though DNA methylation patterns can be established and maintained by DNA methyltransferase enzymes, little evidence is available about how DNA de-methylation occurs during gametogenesis and embryonic development (Figure 1.8), and is mostly based on studies from mouse embryos. Since enzymes with de-methylase activity have not been identified so far in mammals, it has been suggested that reduction of global DNA methylation during early development occurs *via* passive mechanisms, either in the absence of DNMTs or by their exclusion from the nucleus during phases of de-methylation (reviewed by Ooi and Bestor 2008). However, the speed by which some de-methylation events occur, such as the de-methylation of the paternal genome within hours of fertilisation (Oswald *et al.* 2000), suggests that de-methylation takes place *via* active mechanisms that occur independently to DNA replication (Szyf 2003).

It has been proposed that active de-methylation might occur through glycosylation of methyl-cytosine residues, catalysed by ^{me}CG glycosylase enzymes (Zhu *et al.* 2000). However, this mechanism is not favourable at early stages of embryonic development since it introduces damage to the DNA, which would constantly need to be repaired. Other groups have shown that the methylated-DNA binding protein, MBD2, possesses DNA de-methylase activity *in vitro* (Hendrich and Bird 1998; Bhattacharya *et al.* 1999; Ramchandani *et al.* 1999), but *in vivo* evidence for this remains controversial (Hendrich *et al.* 2001; Detich *et al.* 2002). Even more controversially, the *de novo* methyltransferases DNMT3A and DNMT3B have been shown to possess de-methylase activities through their ability to de-aminate ^{me}C residues to T, and C residues to U during transcription of DNA (Kangaspeska *et al.* 2008; Metivier *et al.* 2008), though it remains unclear whether the efficiency of de-amination is compatible with the timing of reported de-methylation events (Ooi and Bestor 2008).

1.5.2.5 Genomic imprinting

Expression of genes located on autosomal chromosomes occurs from both the maternally and paternally inherited alleles (bi-allelic expression), except in "imprinted" genes, that are only expressed from one of the two alleles (mono-allelic expression; Ferguson-Smith and Surani 2001). Over 50 imprinted genes have been identified in the human genome, most of which are clustered in chromosomes 7, 11, 15 and 20 (Morison *et al.* 2005; Table 1.4). Mono-allelic expression at these genes can be established following global genomic de-methylation either during gametogenesis (germline imprints) or during embryogenesis (somatic imprints; Reik and Walter 2001; Surani 2001). Even though the exact mechanism of imprint establishment is poorly understood, silencing of the inactive allele has been associated with increased DNA methylation at imprinting control regions (ICR) and differentially methylated regions (DMR) located within the promoter regions of imprinted genes (Reik and Walter 2001; Constancia *et al.* 2004). Increased DNA methylation at the silenced allele has also been associated with enrichment of the repressive histone marks

H3K9me & K27me, while H3 & H4 acetylation have been associated with the unmethylated, active alleles (Hu *et al.* 2000; Grandjean *et al.* 2001; Fournier *et al.* 2002; Lewis *et al.* 2004).

Table 1.4- Human imprinted genes
ARR= antisense regulatory region (Thorvaldsen *et al.* 1998; Yang *et al.* 1998; Buiting *et al.* 1999; Fitzpatrick *et al.* 2002; Lin *et al.* 2003; Williamson *et al.* 2004; Morison *et al.* 2005; Williamson *et al.* 2006).

Imprinted gene/cluster	Chromosome locus	Transcripts	Expressed allele	Imprint establishment	Imprint locus
ARHI	1p31	-	paternal	-	-
DIRAS3		-	paternal	germline	promoter
TP73	1p36	-	maternal	germline	promoter
NAP1L5	4q22	-	paternal	germline	promoter
ZAC1	6q24	*Isoform 1*	paternal	germline	promoter
IGF2R	6q25	-	maternal	-	-
GRB10	7p11	-	paternal	germline	intron CGI2
PEG10	7q21	*PEG10*	paternal	germline	PEG10 promoter
		SGCE			
DLX5		-	maternal	-	-
MEST/PEG1	7q32	*CPA4*	maternal	-	-
		KLF14		germline	promoter
		MESTIT1	paternal	germline	MEST promoter
		MEST isoform 1			
		MEST isoform 2			
CTNNA3	10q22	-	maternal	-	-
INPP5F_V2	10q26	-	paternal	germline	promoter
WT1	11p13	-	paternal	germline	ARR DMR
KCNQ1	11p15	*PHLDA2*	maternal	germline	KCNQ10T1 promoter (KvDMR)
		SLC22A18			
		SLC22A1LS			
		CDKN1C			
		KCNQ1			
		KCNQ10T1	paternal		
IGF2/H19		*H19*	maternal	germline	intergenic DMR
		IGF2	paternal	somatic	promoter DMR0
					intron DMR2
		IGF2AS		-	-
DKL1/DIO3	14q32	*GTL2/MEG3*	maternal	somatic	GTL2 promoter
		DLK1	paternal	germline	intergenic DMR
		DOI3			
SNURF/SNRPN	15q11	*NDN*	paternal	-	promoter
		SNRPN		germline	-
		IPW			
		ATP10C	maternal	-	-
PEG3	19q13	-	paternal	germline	promoter
GNAS	20q13	*NESP*	maternal	somatic	NESP55
		GNAS		germline	1A promoter
		Exon 1A	paternal		
		GNAS XLas		germline	XL/NESPAS promoter
		NESPAS			

1.5.2.6 DNA methylation defects during mammalian development and human disease

DNA methylation is an essential process for mammalian development, demonstrated by observations that *Dnmt3a* defects result in underdeveloped offspring and lead to death by four weeks after birth, while *Dnmt1* or *3b* defects are lethal in mouse embryos at E14.5-18.5 (Kaneda *et al.* 2004; Ueda *et al.* 2006). *Dnmt3b*$^{-/-}$ mouse embryos also exhibit defects in neural tube development (Okano *et al.* 1999). Disruption of the *de novo* methyltransferase, *Dnmt3l*, results in global hypo-methylation and developmental arrest by E8.5, as well as defective spermatogenesis and failure to establish maternal DNA methylation imprints in oocytes (reviewed by Gopalakrishnan *et al.* 2008). In humans, mutations in *DNMT3B* have been associated with ICF (immunodeficiency, centromere instability, facial disruption) syndrome, mental retardation, and developmental delay (Hansen *et al.* 1999; Jin *et al.* 2008).

Global genomic hypo-methylation (especially at repetitive regions and transposable elements) and tissue-specific hyper-methylation (e.g. in tumour-suppressor genes) are regarded as hallmarks of cancer, whereas loss of mono-allelic expression at imprinted loci has also been to linked disorders such as the Prader-Willi/ Angelman syndromes, Beckwith-Wiedermann syndrome, Albrights hereditary osteodystrophy, Pseudohypothyroidism type 1a and 1b, and cancer (Robertson 2005; Feinberg 2007; Jelinic and Shaw 2007).

1.5.2.7 Regulation of pluripotency and differentiation by DNA methylation

As development and differentiation proceed, the global DNA methylation signatures of pluripotent and differentiated cells become distinctively different (Bibikova *et al.* 2006; Fouse *et al.* 2008; Ball *et al.* 2009). Using Illumina® universal bead arrays, Bibikova *et al.* (2006) demonstrated that the DNA methylation profiles of 14 independently isolated hESC lines were clearly distinguished from those of somatic and cancer cells. They produced a list of

49 CpG sites from 40 genes, including imprinted and differentially methylated genes, tumour suppressor genes, oncogenes, and genes involved in cell cycle regulation, differentiation, apoptosis and DNA damage repair, which contributed the most to the unique hESC DNA methylation signature. More recently, genome-wide DNA methylation analysis by next generation bisulfite sequencing demonstrated that 286 regions, mostly in promoter clusters and CpG islands, were hypomethylated in hESCs compared to differentiated cells, whereas the overall level of DNA methylation (mostly in repeat sequences and transposons) was higher in hESCs (Laurent *et al.* 2010). Closer examination revealed that pluripotency associated TFs, such as *OCT4* and *KLF4*, were hypo-methylated in hESCs (see section 4.1.1), in contrast to several lineage-commitment genes, such as *TCF3*, that were hyper-methylated in hESCs (Meissner *et al.* 2008; Brunner *et al.* 2009; Laurent *et al.* 2010).

DNMT knock-out studies in mESCs have shown that loss of *Dnmt1* expression and/or combined knock-out *Dnmt3a* & *Dnmt3b* resulted in reduced global DNA methylation, especially evident at repeat elements (summarised in Table 1.5). Overall, knock-down of DNMTs in mESCs did not affect self-renewal or other undifferentiated characteristics (e.g. expression of *Oct4*), but did impair differentiation, especially in cases of combined knock-out (Shen *et al.* 2006). Dnmt3a and Dnmt3b were shown to co-operate in the methylation of *Oct4* and *Nanog* in differentiating mESCs, since knock-out of these two enzymes resulted in abnormal differentiation and failure to silence *Oct4* and *Nanog* (Jackson *et al.* 2004).

Interestingly, hESCs also have uniquely high cytosine methylation at CpA residues of the DNA. CpA methylation is found at similar patterns to CpG methylation (across the genome and gene regions, but reduced at gene promoters; Laurent *et al.* 2010). However, the functional significance of this type of methylation in ESCs is not well understood.

Table 1.5- Roles of DNA methyltransferase enzymes in mouse and human ESCs
KO= knock-out, DKO= double knock-out, TKD= triple knock-out

Cell type	Gene	Treatment	Effect	Papers
mESCs	*Dnmt1*	KO	Hypo-methylation in 236 methylation sites, 52-84% reduction in global methylation, hypo-methylation at repetitive elements & imprinted loci, telomere elongation, reduced differentiation ability	Chen *et al.* 2003; Hattori *et al.* 2004; Jackson *et al.* 2004; Li *et al.* 2007c
			Reduced differentiation ability. Initial establishment of *Oct4* and *Nanog* methylation gradually lost	Hattori *et al.* 2004; Gonzalo *et al.* 2006; Li *et al.* 2007c
		Over-expression	Hyper-methylation at repetitive sequences (IAP, centromeres), loss if imprinting (*Igf2* & *H19*)	Jackson *et al.* 2004
	Dnmt3a	KO	Partial methylation of *Oct4* & *Nanog* upon differentiation. No effect on other processes studied	Biniszkiewicz *et al.* 2002
	Dnmt3b	KO	Partial methylation of *Oct4* & *Nanog* upon differentiation. No effect on other processes studied	
	Dnmt3a-3b	DKO	Hypo-methylation in 236 methylation sites (same as in D*nmt1* KO), near loss in global methylation	Chen *et al.* 2003; Hattori *et al.* 2004; Jackson *et al.* 2004
			Viable cells with normal alkaline phosphatase and *Oct4* expression. Progressive DNA hypo-methylation between passages 5 to75 at repeat sequences (IAP, major and minor satellite repeats at centromeric and pericentromeric regions) and individual genes (*H19*, *Igf2*, *Peg1*, *Snrpn*). Increased histone acetylation	Hattori *et al.* 2004
			Abnormal differentiation and failure to methylate/ silence *Oct4* & *Nanog*. Increased histone acetylation	Chen *et al.* 2003; Jackson *et al.* 2004; Gonzalo *et al.* 2006
	Dnmt1, 3a & 3b	TKO	No change in undifferentiated characteristics. Maintenance of normal chromosome numbers, pericentromeric heterochromatin domains marked with H3K9me & HP1. Severe global DNA hypo-methylation at repeat sequences (IAP, pericentromeric major satellite repeats, retroelements) and individual genes (*Igf2*, *Snrpn*),	Li *et al.* 2007c
hESC	*DNMT3A*	Differentiation to neural progenitors	*OCT4*, *CPT1A* & *SPAG6* gene promoters associated with DNMT3A during differentiation	Shen et al., 2006 HMG

1.5.2.8 Regulation of pluripotency-associated TFs by epigenetic modifications

Transcription factors that are key for the maintenance of a pluripotent phenotype in ESCs (section 1.3) are themselves regulated by epigenetic modifications. As mentioned earlier, *OCT4* and *KLF4*, but also *NANOG*, are hypo-methylated in their transcriptionally active

states in ESCs, and hyper-methylated in differentiated cell types, indicating that transcriptional activity of pluripotency-regulators is inversely related to enrichment of DNA methylation in their promoters (Meissner *et al.* 2008; Brunner *et al.* 2009; Laurent *et al.* 2010). Also, it has been suggested that silencing of *Oct4* during differentiation of mESCs occurs *via* a carefully orchestrated step-wise process that involves G9a-mediated H3K9 methylation (Feldman *et al.* 2006; Epsztejn-Litman *et al.* 2008). Further details about the regulation of pluripotency genes by epigenetic modifications will be discussed later, in section 4.1.1.

1.6 DIFFERENCES BETWEEN HUMAN AND MOUSE ESCs

Animal models have been the backbone of biological research for several years. Their extensive use has enabled the investigation and understanding of human disease, and has lead to the development of novel therapeutic drugs for human conditions (Tsumura *et al.* 2006). Nevertheless, due to divergent evolution, several dissimilarities exist between humans and model organisms, including differences in gene regulation and gene expression, protein structure and activity, protein interactions, and consequently, differences in their response towards toxins and drugs (reviewed in Olson *et al.* 2000; Chakraborty *et al.* 2009; Shively and Clarkson 2009).

Substantial differences have also been observed between human and mouse ESCs, regarding their transcriptional profiles, culture conditions and expression of surface markers. For example, the genome-wide transcriptional profile of mESCs is only 13-55% similar to that of hESCs (reviewed in Pound *et al.* 2004; Dixit and Boelsterli 2007; Shanks *et al.* 2009). Moreover, mESCs require exogenous treatment with LIF and BMP4 molecules to maintain their pluripotency *in vitro*, and express the surface antigen SSEA1 in their pluripotent state (Sato *et al.* 2003; Abeyta *et al.* 2004; Wei *et al.* 2005). In contrast, hESC *in vitro* culture is independent of LIF and BMP4 signalling, and SSEA1 is expressed only when cells are

differentiated. In their pluripotent state, hESCs express the surface antigens SSEA4, SSEA3, TRA-1-81 and TRA-1-60 (Chambers 2004; Rao 2004). mESCs and hESCs also exhibit considerably different sensitivities to treatment with chemicals or drugs, such as 5-aza-cytidine, which is toxic to hESCs even at small doses, but is tolerable in mESCs and promotes their differentiation towards endothelial cells (Pera *et al.* 2000; Boiani and Scholer 2005; Adewumi *et al.* 2007).

Mouse ESCs derived from the epiblast instead of the ICM (known as epiblast stem cells, EpiSCs; Brons *et al.* 2007) show more similarity to hESCs in terms of morphology, and do not require extrinsic LIF or BMP signalling to self-renew *in vitro* (Tesar *et al.* 2007). Instead, similar to hESCs, the maintenance of self-renewal in EpiSCs is associated with Activin A/Nodal signalling, while early differentiation stages are associated with BMP4 signalling (Vallier *et al.* 2009c). EpiSCs also show increased similarity to hESCs in the regulation of gene expression by pluripotency-associated TFs, such as Oct4 (Tesar *et al.* 2007).

Even though mESC-based studies have provided valuable information about the epigenetic regulation of the pluripotent cell state (sections 1.5.1.4, 1.5.1.5 and 1.5.2.7), limited information is available for hESCs or EpiSCs. Also, despite the increased similarity between hESCs and EpiSCs, divergent evolution might still have contributed to yet uncharacterised differences between these two cell types. Developing human models to study the regulation of pluripotency and differentiation is of paramount significance towards understanding human development and disease. Therefore, this study has developed a hESC-based model cell system (Figure 1.1) in order to investigate the epigenetic mechanisms that regulate key pluripotency-associated genes and affect the transition of cell phenotype from a pluripotent to a differentiated state and vice-versa.

1.7 DIFFERENCES BETWEEN hESC LINES

1.7.1 Variation in transcriptional profiles

Since the initial isolation of hESCs from human blastocysts in 1998 (Thomson *et al.* 1998), well over 400 additional hESC lines have been derived (Brimble *et al.* 2004). hESC lines share a range of characteristics, such as morphology, and expression of the pluripotency-associated factors OCT4, NANOG, and SOX2 (reviewed by Allegrucci and Young 2007). However, they also exhibit a number of dissimilarities concerning their proliferation rate, which has been shown to range between 24-48 hours (Hoffman and Carpenter 2005), and the relative expression levels of pluripotency-associated factors (Amit *et al.* 2000; Cowan *et al.* 2004; Zeng *et al.* 2004; Sjogren-Jansson *et al.* 2005). It is suggested that a range of "pluripotency states" might exist which could allow differentiation towards the three embryonic germ layers (Carpenter *et al.* 2003; Rho *et al.* 2006; Adewumi *et al.* 2007), but confer some differentiation bias, since even a two-fold change in the levels of *OCT4* can favour differentiation towards endoderm or mesoderm in hESCs (Rodriguez *et al.* 2007). Indeed, an extensive study by Osafune *et al.* (2008) demonstrated that certain hESC lines preferentially differentiate towards ectodermal (HUES6), endodermal (HUES8) or mesodermal lineages (HUES3). Some of the differences observed between hESC lines have been accounted by genotype variation (reviewed by Allegrucci and Young 2007). However, transcriptional diversity among different passages of the same hESC line suggests that culture-related effects and methodological differences can also affect hESC phenotype (Cowan *et al.* 2004; Skottman *et al.* 2005).

1.7.2 Variation in epigenetic profiles

Current methods used for ESCs culture can induce stable and heritable changes in the epigenome of hESCs. Such evidence has been provided by Allegrucci *et al.* (2007), who showed that the global DNA methylation levels in hESCs differ considerably between independently derived cell lines. Even though some differences might be due to genetic

variation (Richards *et al.* 2004), Allegrucci *et al.* were able to show that the greatest alterations in the DNA methylome, at least under the conditions tested, occurred during the earliest passages of hESC *in vitro* culture, with further changes being introduced upon prolonged culture or when cells were transferred from MEF feeders to feeder-free culture on Matrigel™. The epigenetic alterations introduced to hESCs due to *in vitro* manipulations were stably inherited to their differentiated derivatives (Allegrucci *et al.* 2007).

Further differences in the epigenetic characteristics of hESCs have been demonstrated by Kim *et al.* (2007), who showed variation in the allele-specific expression of imprinted genes in 22 different hESC lines and associated these differences to changes in DNA methylation. Similar results were published by the International Stem Cell Initiative (Adewumi *et al.* 2007), Rugg-Gunn *et al.* (2007), and Sun *et al.* (2006), who also reported imprinting variation between samples of the same hESC line, analysed at different passages. Tumour suppressor genes, such as RASSF1 and PTPN6, have also exhibited accumulation of aberrant DNA methylation in hESC cultures (Maitra *et al.* 2005). Moreover, epigenetic characteristics associated with differentiation, such as the % DNA methylation of *OCT4* and *NANOG*, were shown to vary when hESCs were differentiated either by retinoic acid or cell clumps (Yeo *et al.* 2007).

X-chromosome inactivation (XCI) is another epigenetic trait exhibiting variation among hESC lines. XCI is one of the first measurable epigenetic changes that occur in the early mammalian embryo, and is thought to take place during the same time as differentiation into the three germ layers (Monk and Harper 1979). Some hESC lines (HUES1, HUES9 and HUES14) show the ability to carry out XCI upon *in vitro* differentiation, when others seem to have already inactivated one X-chromosome in their pluripotent states (HUES5 and HES-3) or to be completely incapable of XCI (HUES6, HUES12, HES-2, H7 and H9; Silva *et al.* 2008). Considering the importance of XCI in embryogenesis, adult physiology, brain function and social skill development, as well as in cancer, correct dosage of X-chromosome genes

is vital for cellular integrity and human development (Tomkins *et al.* 2002; Ganesan *et al.* 2005; Skuse 2005; Cutter *et al.* 2006).

Together, these findings challenge current culture techniques as well as the overall ability of hESCs to serve as a model for developmental epigenetic studies without careful prior characterisation (Allegrucci *et al.* 2007). By generating a single-genotype model cell system (Figure 1.1), maintaining the same culture conditions between pluripotent cell lines (hESCs & iPSCs, section 1.2.4.4) and using the same protocols to generate and culture fibroblast differentiated cells from hESCs and iPSCs (section 3.1.1), this study aimed to eliminate the factor of genetic variation and limit any changes in cell phenotype due to culture-induced effects, in order to enable unbiased analysis of the epigenetic regulation mechanisms associated with key pluripotency-genes.

1.8 REPROGRAMMING SOMATIC CELLS INTO A PLURIPOTENT STATE

The limited supply of human oocytes/embryos for the derivation of hESCs, as well as ethical considerations surrounding the need for human embryos to isolate hESCs have, thus far, limited the use of hESCs or their differentiated derivatives in research and in the clinic (Cervera and Stojkovic 2007). Alternative sources of pluripotent cells have, therefore, been sought after, mostly relying on reprogramming somatic cells to an ESC-like state. Techniques such as somatic cell nuclear transfer (SCNT), fusion of somatic cells with ESCs, or treatment of somatic cells with ESC or amphibian oocyte and egg extracts were able to reprogram differentiated cells to an ESC-like state (reviewed by Alberio *et al.* 2006), but suffered from dependence on animal products, need for oocytes or generation of tetraploid cells, which would still be controversial if used in humans (reviewed by Hochedlinger and Jaenisch 2006; Figure 1.10).

1.8.1 Generation of induced-pluripotency stem cells

Extensive characterisation of the transcription factor networks that regulate pluripotency enabled, in 2006, the reprogramming of differentiated mouse fibroblasts to an ESC-like state (Takahashi and Yamanaka 2006). Initially, twenty-four candidate TFs were tested for their ability to induce pluripotency when they were retrovirally over-expressed in mouse fibroblasts. Four of these factors; *Oct4*, *Sox2*, *Klf4* and *c-myc*, were found to be necessary and sufficient for inducing pluripotency in differentiated cells. Soon after this discovery, it emerged that the same four factors, as well as combination of the TFs *OCT4*, *SOX2*, *NANOG* and *LIN28* could induce pluripotency in human differentiated fibroblasts (Okita *et al.* 2007; Yu *et al.* 2007b). Reprogramming somatic cells by over-expression of defined TFs can potentially alleviate the need for human embryos to isolate ESCs. It also opens new possibilities for treatments in regenerative medicine using autologous patient cells that could be isolated from tissues such as the skin, using non-invasive procedures (Amabile and Meissner 2009).

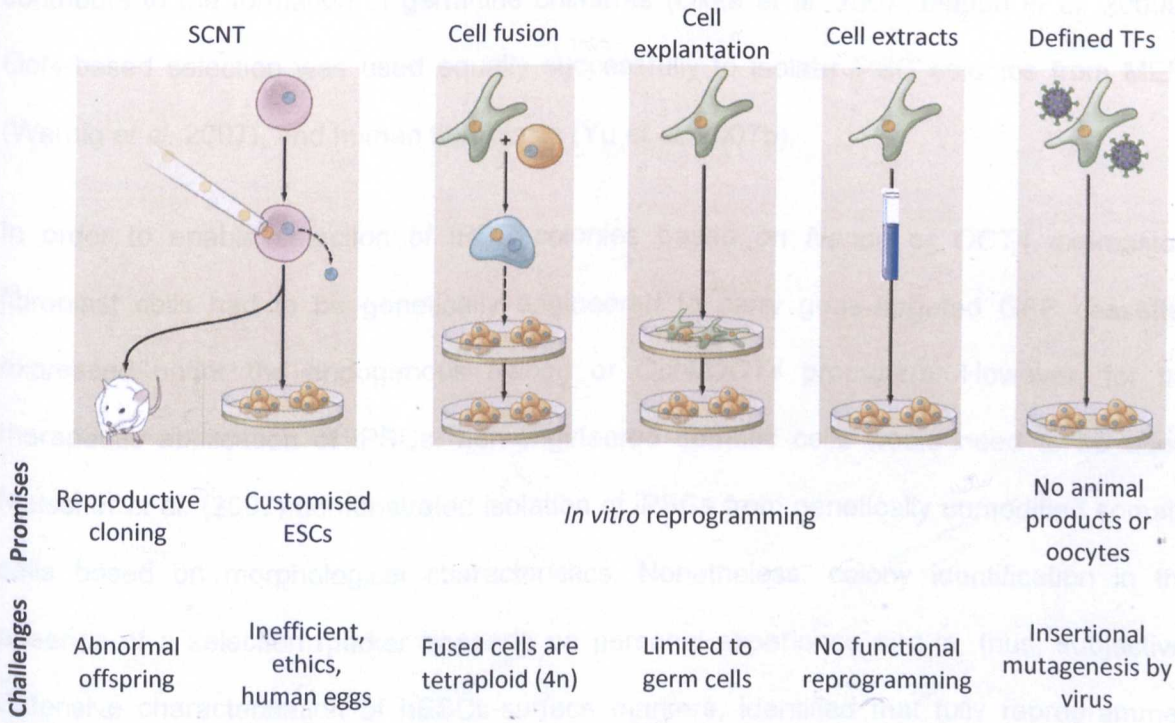

Figure 1.10- Strategies used to induce reprogramming of somatic cells
Somatic cell nuclear transfer (SCNT) involves the injection of a somatic-cell nucleus into an enucleated egg, which upon transfer to a surrogate mother can give rise to offspring, or upon explantation in culture can give

rise to genetically matched ESCs. Cell fusion of somatic cells with ESCs results in the generation of hybrids that show all features of pluripotent ESCs. Explantation of somatic cells in culture selects for immortal cell lines that may be pluripotent or multipotent, but has so far only given rise to spermatogonial stem cells. Treatment with cell extracts from ESCs or animal oocytes induces reactivation of some pluripotency-associated transcription factors (TFs) but does not induce complete reprogramming. Over-expression of defined TFs in somatic cells enables complete reprogramming to iPSCs (modified from Jaenisch and Young 2008).

1.8.1.1 Identification and characterisation of reprogrammed iPSCs

In the first experiments performed to generate iPSCs, potentially reprogrammed cells were selected based on re-activation of the pluripotency-associated factor *Fbx15* (Takahashi and Yamanaka 2006). Despite having an ESC-like morphology, cells selected based on *Fbx15* expression had notably different transcriptional and epigenetic profiles to mESCs, and could not contribute to the formation of chimeras (Takahashi and Yamanaka 2006). In subsequent experiments, selection of putative iPSC colonies was based on *Nanog* reactivation (Okita *et al.* 2007), and resulted in the formation of cell colonies that were morphologically indistinguishable from mESCs, demonstrated ESC-like proliferation rates and telomere length, had similar transcriptional and DNA methylation profiles to ESCs, and could contribute to the formation of germ-line chimeras (Okita *et al.* 2007; Marion *et al.* 2009b). *Oct4*-based selection was used equally successfully to isolate iPSC colonies from MEFs (Wernig *et al.* 2007), and human fibroblasts (Yu *et al.* 2007b).

In order to enable selection of iPSC colonies based on *Nanog* or *OCT4* expression, fibroblast cells had to be genetically engineered to carry gene-targeted GFP cassettes expressed under the endogenous *Nanog* or *Oct4/OCT4* promoters. However, for the therapeutic application of iPSCs, non-engineered somatic cells would need to be used. Meissner *et al.* (2007) demonstrated isolation of iPSCs from genetically unmodified somatic cells based on morphological characteristics. Nonetheless, colony identification in the absence of a selection marker depends on personal experience and is, thus, subjective. Extensive characterisation of hESCs-surface markers, identified that fully reprogrammed iPSCs could be selected based on reactivation of TRA-1-81 (Figure 1.11; Chan *et al.* 2009). Non-reprogrammed somatic cells and "partially reprogrammed" cell colonies emerging

during iPSC generation (see section 1.8.1.2) did not express TRA-1-81, but some did express the hESC-surface marker SSEA4, therefore rendering this marker as inappropriate for the identification of fully reprogrammed iPSCs. Even though early *in vitro* identification of putative iPSCs could be performed based on colony morphology, size and TRA-1-81 expression (Chan *et al.* 2009), these were not enough to confirm full reprogramming. Further criteria that are necessary for the selection of *bona fide* iPSCs have been reviewed by Maherali and Hochedlinger (2008), and are outlined below:

* Morphological similarity to ESCs
* Reactivation of endogenous pluripotency factors (e.g. OCT4, NANOG, SOX2)
* Reactivation of ESC-specific surface antigens (e.g. TRA-1-81)
* Functional telomerase expression
* Repression of viral transgene expression
* Epigenetic similarity to ESCs in the promoters of pluripotency factors, X-chromosome reactivation in female lines, and formation of bivalent histone domains (see section 1.8.3)
* Ability to differentiate into lineages from all three embryonic germ layers

Maherali and Hochedlinger (2008) suggested that the differentiation potential of iPSCs should be assessed by the highest stringency test possible, which in mice means; germ-line transmission following blastocyst chimerism, and in humans; teratoma formation (reviewed by Daley *et al.* 2009).

1.8.1.2 Partially reprogrammed colonies formed during iPSC generation

Partially reprogrammed colonies represent an intermediate state between iPSCs and the somatic cell type used for reprogramming (Figure 1.11). They are considered to originate from somatic cells that either do not incorporate all four iPSC factors, incorporate all factors but do not express some of them or expressed them at the wrong levels (Papapetrou *et al.* 2009). Some partially reprogrammed colonies generated from mouse fibroblasts express

the mESC-surface marker, SSEA1, but not *Oct4* or *Nanog*, and down-regulate fibroblast-specific genes more readily than they activate mESC-specific genes (Sridharan *et al.* 2009). Partially reprogrammed colonies generated from human differentiated cells can express the hESC-surface marker SSEA4, but lack TRA-1-81 expression and show persistent expression of viral transgenes (Subramanyam and Blelloch 2009). Overall, partially reprogrammed colonies show incomplete re-activation of endogenous pluripotency genes as well as incomplete silencing of differentiation genes and viral transgenes. Also, the DNA methylation and histone modification characteristics of partially reprogrammed colonies are in an intermediate state between iPSCs and the somatic cell-type used for reprogramming (section 1.8.3; Takahashi and Yamanaka 2006; Mikkelsen *et al.* 2008).

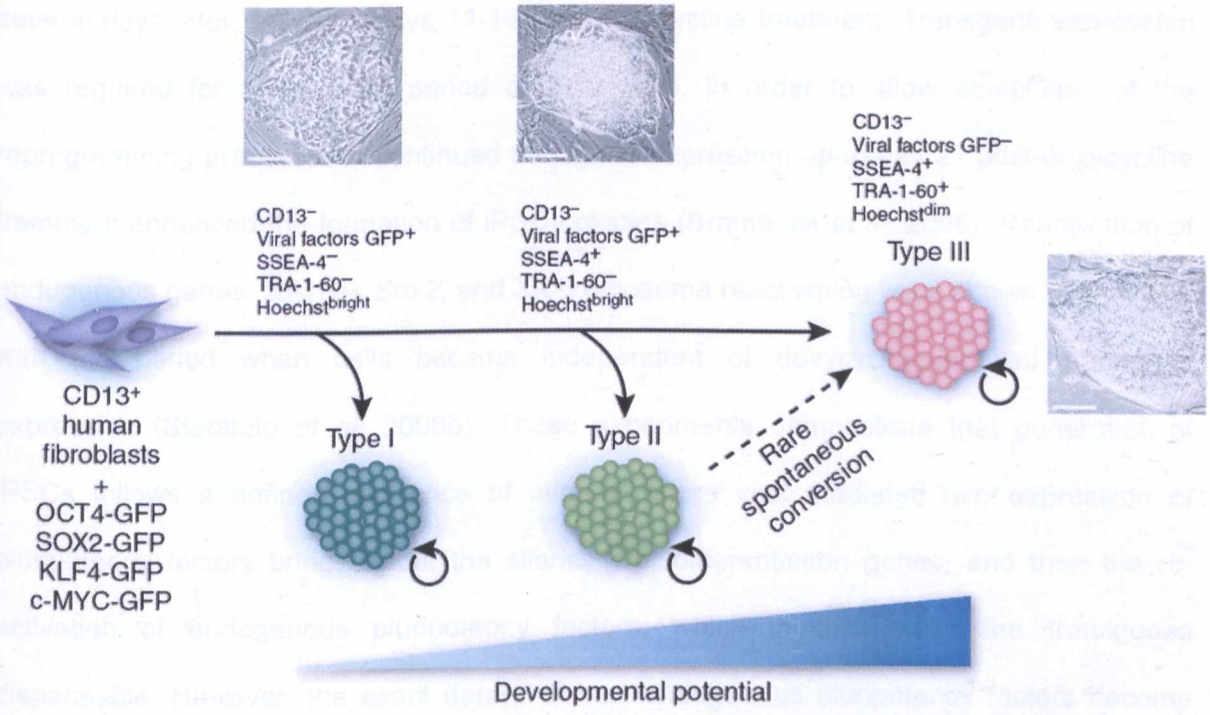

Figure 1.11- Distinguishing fully reprogrammed iPSCs from partially reprogrammed cells
Phase images (20x magnification) and marker expression of fully reprogrammed (Type III) and partially reprogrammed (Type I & II) cell colonies generated from hESC-derived fibroblasts following transduction with retroviruses over-expressing OCT4, SOX2, KLF4 and c-MYC. Fully reprogrammed *bona fide* iPSCs reactivate both the TRA-1-81/TRA-1-60 and SSEA4 hESC-surface markers, and silence viral transgenes and differentiation genes (CD13; modified from Chan *et al.* 2009; Subramanyam and Blelloch 2009).

1.8.1.3 Molecular events during iPSC generation

Two studies have attempted to investigate the molecular mechanisms that underline reprogramming of somatic cells to iPSCs, by using doxycycline-inducible viral vectors to perform time-course analysis of pluripotency gene re-activation in mouse fibroblasts (Brambrink *et al.* 2008; Stadtfeld *et al.* 2008b). Flow cytometry analysis showed that down-regulation of Thy1, a surface antigen expressed in fibroblasts and other differentiated cell types (Rege and Hagood 2006), was one of the first events to occur during reprogramming (Stadtfeld *et al.* 2008b; Figure1.12). Alkaline phosphatase (AP) was the first mESC marker to be reactivated upon iPSC formation (day 3 post doxycycline treatment; Brambrink *et al.* 2008). Expression of the mESC-surface marker, SSEA1, was observed on day 9 post-doxycycline treatment, whereas *Oct4*- and *Nanog*-driven GFP expression were expressed several days later, between days 11-16 post-doxycycline treatment. Transgene expression was required for a minimum period of 8-12 days, in order to allow completion of the reprogramming process, but continued transgene expression up to day 21 post-doxycycline treatment enhanced the formation of iPSC colonies (Brambrink *et al.* 2008). Reactivation of endogenous genes, such as *Sox2*, and X-chromosome reactivation were shown to correlate with the period when cells became independent of doxycycline-induced transgene expression (Stadtfeld *et al.* 2008b). These experiments demonstrate that generation of iPSCs follows a defined sequence of events, where viral mediated over-expression of pluripotency factors brings about the silencing of differentiation genes, and then the re-activation of endogenous pluripotency factors, which in turn make the transgenes dispensable. However, the exact details of how endogenous pluripotency factors become reactivated during iPSC generation remain undefined.

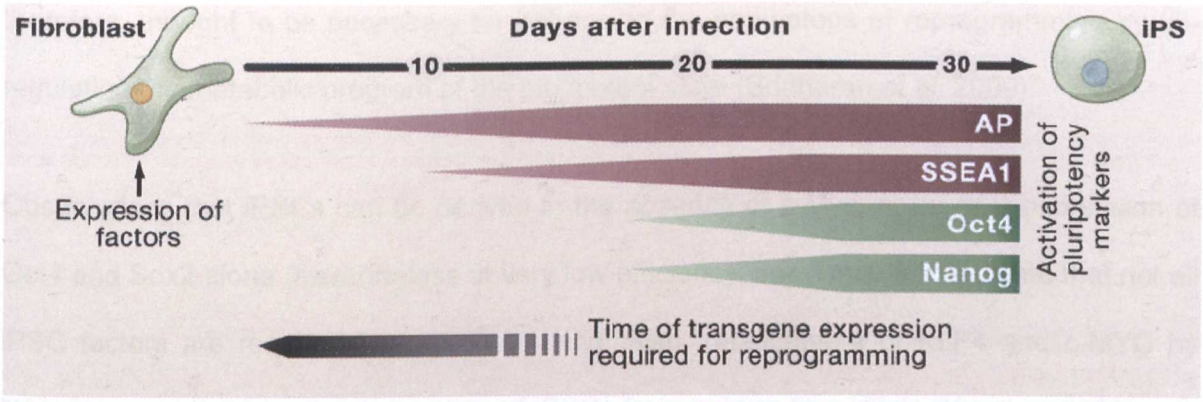

Figure1.12- Sequential activation of pluripotency markers during reprogramming to iPSCs
Kinetics of pluripotency marker reactivation during reprogramming of mouse fibroblasts to iPSCs, by lentiviral over-expression of Oct4, Sox2, Klf4 and c-myc. Alkaline phosphatase and SSEA1 are reactivated 3-9 days post lentiviral transduction (PTD), whereas endogenous Oct4 and Nanog protein reactivation was detected 2 weeks PTD. Expression of lentiviral transgenes was necessary for approximately 2 weeks to initiate iPSC formation (Jaenisch and Young 2008).

1.8.2 The role of reprogramming TFs in the induction of pluripotency

ChIP and microarray analysis performed by Sridharan *et al.* (2009) revealed that the iPSC TFs; Oct4, Sox2, Klf4 and c-Myc, occupy similar gene promoters in mESCs and mouse iPSCs (~87% similarity). Some gene promoters are occupied by all four iPSC factors, while others are bound by combinations of three or two, or just one factor. Genes associated with Oct4, Sox2 and Klf4 in the absence of c-Myc are mostly involved in transcriptional control of development (e.g. *Lefty2*, *Foxh1*) and show the highest increase in expression upon reprogramming of mouse fibroblasts to iPSCs, which correlates with loss of the repressive mark H3K27me3 and enrichment of the activating mark H3K4me3 (Wei *et al.* 2009), as well as a decrease in DNA methylation (Doi *et al.* 2009). However, genes bound individually by Oct4, Sox2, or Klf4 are not activated as strongly or become repressed (e.g. lineage commitment genes), indicating that transcriptional activation might be achieved by co-operation of the three master pluripotency regulators (Figure 1.13). Genes associated with c-Myc alone or in combination with other factors are mostly involved in metabolic processes (e.g. control of translation, RNA splicing, cell cycle, and energy production). c-Myc is,

therefore, thought to be necessary for enhancing the early steps of reprogramming by up-regulating the metabolic program of the pluripotent state (Sridharan *et al.* 2009).

Observations that iPSCs can be derived in the absence of c-Myc, or by over-expression of Oct4 and Sox2 alone (nevertheless at very low efficiency, see Table 3.2) indicate that not all iPSC factors are required for reprogramming. Also, replacement of KLF4 and c-MYC by NANOG and LIN28 for the generation of iPSCs from human fibroblasts (Yu *et al.* 2007b; Jia *et al.* 2010) indicates that different molecular pathways can lead to reprogramming or that the functions of KLF4 and c-MYC overlap with those of NANOG and LIN28 (reviewed by Hochedlinger and Plath 2009). Indeed, LIN28 appears to positively regulate c-MYC though inhibition of let-7 miRNAs that can target c-MYC for degradation, suggesting that the two TFs might induce iPSC generation *via* similar mechanisms (Kumar *et al.* 2007; Viswanathan *et al.* 2008). Also, LIN28 might promote reprogramming by directly activating translation of *OCT4* mRNA (Qiu *et al.* 2009).

Nonetheless, the exact pathway of somatic cell reprogramming by defined TFs is largely unknown. It is suggested that exogenous TFs might down-regulate lineage commitment genes and "jump-start" the re-activation of endogenous pluripotency-TFs by triggering the auto-regulatory feed-back loops that control their expression (section 1.3.2). Equally, exogenous TFs could induce iPSC formation by triggering the activation of differentiation antagonists, or altering chromatin architecture to an open conformation that would be permissive to reactivation of the ESC-transcriptional machinery (reviewed by Hochedlinger and Plath 2009).

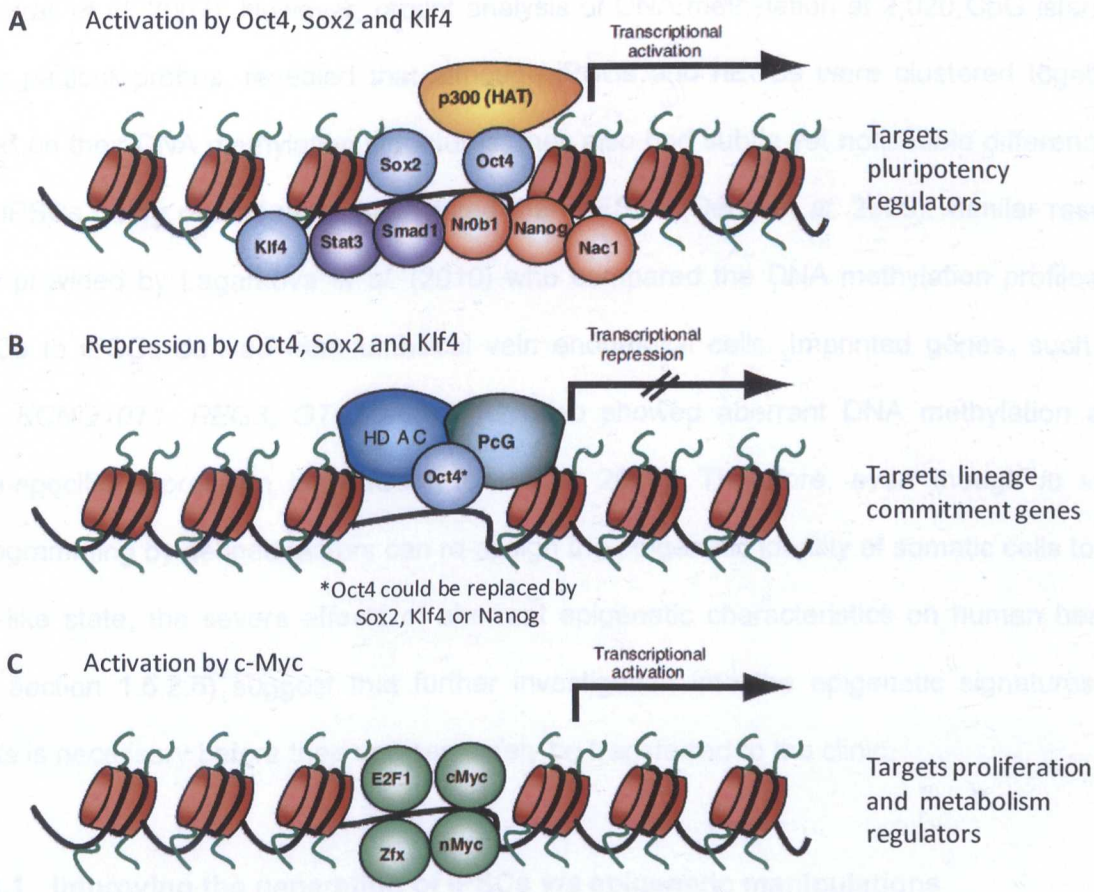

Figure 1.13- Possible roles of key pluripotency-regulators in the generation of iPSCs
A. Co-binding of Oct4, Sox2 and Klf4 to gene promoters together with other transcription factors (TFs), including Nanog and Esrrb, recruit co-activators such as the histone acetyltransferase (HAT) p300, thus promoting transcriptional activity in genes necessary for self-renewal. **B.** Genes bound be either Oct4, Sox2 or Klf4 are often repressed through recruitment of histone de-acetylases (HDAC) and histone methyltransferases of the Polycomb complex group (PcG). **C.** In collaboration with other TFs, c-Myc is suggested to activate the basic energy, proliferation and metabolism program of the mESC-state (adapted from Hochedlinger and Plath 2009)

1.8.3 Epigenetic characteristics of iPSCs

Both mouse and human iPSCs show hypo-methylation in the promoter regions of pluripotency regulators such as *OCT4*, *NANOG* and *REX1*, compared to the somatic cells they were derived from (Takahashi *et al.* 2007; Mikkelsen *et al.* 2008; Park *et al.* 2008c; Doi *et al.* 2009). mESCs also show re-establishment of histone protein "bivalent domains" (section 1.5.1.5) in the promoter regions of lineage-specific genes, such as *Pax5*, *Sox1* and *Nkx2.2* (Mikkelsen *et al.* 2007; Wernig *et al.* 2007) and reactivation of the silent X-chromosome in female lines, which is associated with reduced Ezh2-catalysed H3K27me3

(Maherali *et al.* 2007). However, recent analysis of DNA methylation at 2,020 CpG islands, using padlock-probes, revealed that although iPSCs and hESCs were clustered together based on their DNA methylation signatures, they also had subtle yet noticeable differences, with iPSCs being overall more methylated than hESCs (Deng *et al.* 2009). Similar results were provided by Lagarkova *et al.* (2010) who compared the DNA methylation profiles of hESCs to iPSCs derived from umbilical vein endothelial cells. Imprinted genes, such as *H19*, *KCNQ10T1*, *PEG3*, *GTL2* and *IGF2*, also showed aberrant DNA methylation and allele-specific expression in iPSCs (Pick *et al.* 2009). Therefore, even though *in vitro* reprogramming by defined factors can re-assign the epigenetic identity of somatic cells to an ESC-like state, the severe effects of aberrant epigenetic characteristics on human health (see section 1.5.2.6) suggest that further investigation into the epigenetic signatures of iPSCs is necessary before their use can safely be transferred to the clinic.

1.8.3.1 Improving the generation of iPSCs *via* epigenetic manipulations

The efficiency of iPSC generation has been manipulated by treatment of somatic cells with small molecules capable of affecting DNA methylation or histone modifications (Table 1.6). Treatment of MEFs with 5-azacytidine, a DNA methyltransferase inhibitor molecule, was shown to enhance reprogramming efficiency by 10-fold (Huangfu *et al.* 2008a), while treatment of the same cells with the HDAC inhibitors; valporic acid (VPA), suberoylanilide hydroxamic acid (SAHA), or trichostatin A (TSA) was also shown to improve the efficiency of iPSC generation (Huangfu *et al.* 2008a). VPA had the most profound effect, as it enabled a 100-fold improvement of the reprogramming process (Huangfu *et al.* 2008a). Treatment of human fibroblasts with this molecule enabled a 10 to 20-fold increase in iPSC production, and also allowed iPSCs to be generated when fibroblasts were transduced with *OCT4* and *SOX2* alone (Huangfu *et al.* 2008b). Treatment with the small molecule BIX-01294, a G9a inhibitor capable of significantly reducing H3K9 methylation (Kubicek *et al.* 2007) enabled reprogramming of mouse neural progenitor cells by infection with *Oct4* and *Klf4* alone (Shi

et al. 2008). Moreover, treatment of partially reprogrammed granular colonies generated during reprogramming of MEFs, with siRNAs or shRNAs against the DNA methyltransferase DNMT1 was shown to enable full reprogramming of these colonies into iPSCs (Mikkelsen *et al.* 2008). Despite their success in improving the efficiency of iPSC generation, most chemical compounds used to date to improve iPSC-generation efficiency have a broad specificity, affecting all types of DNA methylation or all histone de-acetylation enzymes, therefore providing little information about the exact mechanism by which they impact on reprogramming efficiency.

Table 1.6– Small molecules used to manipulate iPSC generation
O= OCT4, S= SOX2, K= KLF4, C= c-MYC

Treatment	Function	Vector & transgenes	Cell type	Effect	References
5-azacytidine (5-aza)	DNMT inhibitor	Retrovirus OSKC	MEFs	Increased iPSC generation by 10-fold. Combination with the glucocorticoid Dexamethasone improved 5-aza effect by a further 2.6-fold	Huangfu *et al.* 2008a
Valporic acid (VPA)	HDAC inhibitor			Increased iPSC generation by >100-fold	
		Retrovirus OSK		Improved iPSC generation by 50-fold	
Suberoylanilide Hydroxamic acid (SAHA)		Retrovirus OSKC		Increased iPSC generation efficiency	
Trichostatin A (TSA)					
5-azacytidine (5-aza)	DNMT inhibitor	Dox-inducible lentivirus OSKC	2nd generation MEFs	Partially reprogrammed iPSC become fully reprogrammed	Mikkelsen *et al.* 2008
Dnmt1	DNMT enzyme	siRNA/shRNA			
Chd1	Chromatin remodelling	shRNA	MEFs	Inhibits iPSC generation	Gaspar-Maia *et al.* 2009
BIX-01294	G9a inhibitor	Retrovirus SKC	Mouse Neural Progenitors	Increased iPSC generation efficiency	Shi *et al.* 2008
		Retrovirus OK			
		Retrovirus KC			
BayK8644 or RG108	L-channel calcium agonist	Retrovirus OK	MEFs	Combination of RG108 or BayK8644 with BIX-01294 further improved iPSC generation efficiency	
Valporic acid (VPA)	HDAC inhibitor	Retrovirus OSK	Human Fibroblasts (BJ, HDF)	Increased iPSC generation by 10-20 fold	Huangfu *et al.* 2008b
		Retrovirus OS			

1.8.4 Differentiation of iPSCs

iPSCs generated form mouse and human fibroblasts have been differentiated to a variety of cell types, including cardiomyocytes, neurons, macrophages, T-cells, neurospheres, B-cells, adipocytes, osteoblasts and retina cells (Maherali *et al.* 2007; Hirami *et al.* 2009; Katsuhisa *et al.* 2009). Haematopoietic progenitors generated from iPSCs have so far been used in mouse models to rescue sickle cell anaemia symptoms (Hanna *et al.* 2007), while neural iPSC-derivatives have been used in rat models to improve symptoms of Parkinson's disease (Wernig *et al.* 2008b). Human iPSC-derived cardiomyocytes as well as hepatocytes and vascular cells have been extensively characterised and were found to have similar properties to their ESC-derived equivalents (Gai *et al.* 2009; Song *et al.* 2009; Taura *et al.* 2009; Yokoo *et al.* 2009), demonstrating that hESCs and iPSCs share common differentiation potentials. hESCs and iPSCs were also shown to rely on the same signalling pathways for differentiation into extra-embryonic tissues, neuroectoderm and mesendoderm (Vallier *et al.* 2009b). In this thesis, iPSCs were differentiated into fibroblasts (see section 3.1.1) in order to determine whether they could "circle" back to the same cell phenotype that they were derived from (Figure 1.1) or whether the "parent" hESC-derived fibroblasts would have different gene expression and epigenetic regulation of pluripotency-associated TFs compared to iPSC-derived fibroblasts.

1.9 THESIS PERSPECTIVE

Gene expression is regulated by complex interactions between transcription factors and epigenetic modifications, which ultimately lead to gene activation or repression/silencing by changing the availability of gene promoter regions to binding of the Pol II transcriptional machinery (section 1.3.1). Over-expression of a defined set of transcription factors in differentiated cells is sufficient to trigger reactivation of endogenous pluripotency genes and transition the differentiated cell phenotype to an ESC-like state (section 1.8.1). However, the mechanisms of endogenous TF reactivation are not well understood, and it is unknown

whether a change in cell phenotype is induced by the viral transgenes or if it occurs as a consequence of endogenous TF reactivation. Repression/ silencing of the same TFs can lead to differentiation of pluripotent hESCs and iPSCs, therefore raising the question of how key pluripotency-associated TFs become activated or repressed to enable a change in cell phenotype. The mechanisms of endogenous pluripotency-associated TF activation and repression/ silencing were subject to investigation in chapters 4 and 5 of this thesis. Chapter 4 also investigated whether TFs in iPSCs reach the same epigenetic state as hESCs and whether they use the same mechanisms to repress pluripotency-associated TFs upon phenotype transition to fibroblasts. Chapter 5 was concerned with demonstrating that altering the epigenetic modifications associated with pluripotency genes in differentiated cells to a more ESC-like state can facilitate gene reactivation and improve the overall reprogramming to iPSCs.

2 MATERIALS AND METHODS

2.1 CELL CULTURE

All cell culture experiments were performed in a type II Biological Safety Cabinet, and cells were incubated at 37°C, 5% CO2, in a humidified atmosphere. Bright field and fluorescence images of live cells were captured using a Nikon ECLIPSE TE2000-S inverted microscope.

2.1.1 Media

All media were filter sterilized though a 0.2µm filter (Sartorius: 16532K) and were warmed-up to 37°C before use.

Table 2.1– Composition of media used for cell culture

Medium	Component	% volume / concentration	Supplier	Product number
MEF/HEK293	1x DMEM	88%	GIBCO Invitrogen	21969
	FBS	10%	HyClone	SH30070.03
	L-glutamine	1%	GIBCO Invitrogen	25030-024
	NEAA	1%	GIBCO Invitrogen	11140
BGK	1x DMEM-F12	83%	GIBCO Invitrogen	11320
	KSR	15%	GIBCO Invitrogen	10828
	GlutaMAX	1%	GIBCO Invitrogen	35050
	NEAA	1%	GIBCO Invitrogen	11140
	β-mercaptoethanol	100µM	SIGMA	M-7522
	bFGF	4ng/ml	R & D Systems	4114-TC-01M
DIFF	1x DMEM	78%	GIBCO Invitrogen	21969
	FBS	20%	HyClone	SH30070.03
	GlutaMAX	1%	GIBCO Invitrogen	35050
	NEAA	1%	GIBCO Invitrogen	11140
	β-mercaptoethanol	100µM	SIGMA	M-7522

2.1.2 Isolation of mouse embryonic fibroblasts (MEFs)

MEFs were isolated from mouse embryos and used either to condition BGK medium for feeding hESCs or as feeder cells for manual passaging of hESCs.

Pregnant female CD1 mice (Charles River Laboratories), at day 13.5 of gestation, were sacrificed by cervical dislocation and placed in a type I Biological Safety Cabinet. An initial horizontal incision was made on the abdomen skin and, using forceps and scissors, and a cut was made on the peritoneum to expose the uterine horns, which were removed and dipped in IMS. The horns were then placed in a Petri dish containing PBS (GIBCO

Invitrogen: 14190), where each embryo was dissected out and decapitated, and visceral tissue was removed. The embryos from each pregnant mouse were placed in a 50ml Universal tube containing fresh PBS and were transferred from the dissection room to a stem cell culture suite. There, the embryos were placed in a 90mm Petri dish containing 1.5ml of 0.25% Trypsin (GIBCO Invitrogen: 25200-072) and were thoroughly sliced using a scalpel. The embryos were transferred to a 250ml container, where the volume of trypsin was topped up to 2ml per embryo. They were then vortexed and incubated in a 37°C water bath for 5 minutes. This was repeated until the embryos appeared to be homogenized. Following homogenization, 4ml of MEF medium, supplemented with 1x penicillin and streptomycin (GIBCO Invitrogen: 15870-063), were added per embryo. The suspension was shaken vigorously and vortexed again, and then allowed to stand at room temperature for 1 minute. The cells were transferred to a fresh container, leaving any sedimented tissue behind, and were aliquoted to 175cm^2 tissue culture flasks (NUNC: 156502) at a density equivalent to 2 embryos per flask. The volume in the flasks was topped up to 30ml using MEF medium, supplemented with penicillin and streptomycin. The flasks were stored in a humidified 37°C, 5% CO_2 incubator (Heraeus HERAcell 150). The next day, the medium was replaced with fresh MEF medium without penicillin or streptomycin, and cells were cultured until confluent. Cells were then cryopreserved in Dimethyl Sulfoxide (DMSO; SIGMA: D2650), at a density of 3 vials per 175cm^2 flask.

2.1.3 Growth and passage of MEFs

A cryopreserved vial (Nunc CryoTube Vials; NUNC: 343958) of MEFs was removed from the liquid nitrogen storage tank and was mixed with 10ml of MEF medium. The cell suspension was centrifuged (SIGMA 3-16 Mid-bench centrifuge; SIGMA: 10270) at 200xg for 5 minutes to remove DMSO. Following centrifugation, the supernatant was removed, and the cells were re-suspended in 15ml of MEF medium and transferred to a 75cm^2 culture flask (NUNC: 153732). They were then placed in a 37°C incubator for 1-3 days or until

confluent, depending on the MEF batch. Once the flask was confluent, the MEF medium was aspirated. The cells were washed with 15ml of PBS and treated with 1.5ml of 0.05% trypsin (GIBCO: 25300) for 1 minute, at 37°C. The trypsin was inactivated with 13.5ml of MEF medium, and 5ml were transferred to a 75cm^2 flask. The medium was toped-up to 15ml and the flask was placed in a 37°C incubator for 1-3 days or until confluent.

2.1.4 Inactivation of MEFs

Inactivation of MEFs was performed by treating ~80% confluent 75cm^2 flasks with 5ml of 10µg/ml mitomycin-c (SIGMA: M4287) dissolved in MEF medium, for 2.5h. After that, mitomycin-c was aspirated and the cells were washed 3 times in 15ml of PBS. They were then treated with 1.5ml 0.05% trypsin for 3-5 minutes, at 37°C. The trypsin was inactivated with 8.5ml of MEF medium, and the cell suspension was centrifuged at 200xg for 5 minutes. Following centrifugation, the supernatant was aspirated and the cells were re-suspended in 10ml of fresh MEF medium. 20µl were removed to perform a cell count, and the cells were centrifuged again at 200xg for 5 minutes. Cells were then seeded in 75cm^2 flasks coated with 0.1% gelatin (SIGMA: G9391), at a density of 4.8 x 10^6 cells per flask, and placed in a 37°C incubator.

2.1.5 Harvesting conditioned medium from MEFs

After inactivation with mitomycin-c, MEFs were allowed at least 4 hours to attach to the surface of the flasks. The MEF medium was then aspirated and replaced with 25ml of BGK medium. The flasks were placed in a 37°C incubator to allow conditioning of the medium. 24 hours later, the medium was collected and replaced with 25ml of fresh BGK. The harvested conditioned medium was supplemented with FGF (1µl/ml) and was used to maintain hESC cultures. Conditioned medium collection was repeated every 24 hours, for 7 days.

2.1.6 Growth and passage of hESCs on Matrigel coated surfaces

Growth and culture of hESCs on Matrigel™ coated flasks was performed as described in Denning *et al.* (2006). Coating was performed by adding 5ml of Matrigel™ (BD Biosciences: 354234), diluted by 1:100 in DMEM medium, per 25cm^2 flask and treating for 1 hour, at r.t. Coated flasks were stored at 4°C for up to 2 weeks.

Vials of hESCs, of the cell line HUES7 (HUES Facility, Harvard University, Cambridge; Cowan *et al.* 2004), were removed from liquid nitrogen and mixed with 10ml of BGK medium. The cell suspension was centrifuged at 160xg for 4 minutes. Following centrifugation, the supernatant was removed, and the cells were re-suspended in 5ml of MEF conditioned medium and transferred to a Matrigel™ coated 25cm^2 culture flask (NUNC: 163371). Cells were then placed in a 37°C incubator until confluent, with daily changes of MEF conditioned medium. Once the flask was confluent, the MEF conditioned medium was aspirated, the cells were washed with 5ml of PBS, and then treated with 0.5ml of 0.05% trypsin for 1 minute, at 37°C. The trypsin was inactivated with 5.5ml of BGK medium, and 2ml were transferred to a 20ml Universal tube for a 1 in 3 passage. The cells were centrifuged at 160xg for 4 minutes. The supernatant was then aspirated, the cells were re-suspended in 5ml of MEF conditioned medium, and transferred to a Matrigel™ coated 25cm^2 flask. The flask was stored in a 37°C incubator, with daily changes of MEF conditioned medium. hESCs were passaged routinely every 48h.

The genetically modified hESC line, HOGN, (gifted by Dr. Christine Mummery, Leiden University Medical Centre, The Netherlands) was cultured as described above for HUES7 cells. This line carried a gene targeted insertion of an *IRES-GFP-IRES-Neo* cassette immediately after the endogenous *OCT4* gene. The cassette was able to support expression of *GFP* protein and provide resistance Neomycin under the control of the endogenous *OCT4* promoter (Braam *et al.* 2008b).

2.1.7 hESC differentiation through embryoid body (EB) formation by forced aggregation

The protocol used for hESC differentiation was adapted from Burridge *et al.* (2007). In a 70% confluent 25cm^2 culture flask, the MEF conditioned medium was aspirated and the cells were washed with 5ml of PBS. The cells were then treated with 0.5ml of 0.05% trypsin for 1 minute, at 37°C. The trypsin was inactivated with 4.5ml of BGK medium, and the cell suspension was transferred to a 20ml Universal tube. 20µl were removed to perform a cell count, and the cells were centrifuged at 160xg for 4 minutes. The cells were then re-suspended in MEF conditioned medium and seeded in 96-well V-bottom plates (NUNC: 249662) at a density of 10,000 cells per well. The plate was centrifuged at 950xg for 5 minutes, and placed in a 37°C incubator for 2 days, after which a medium change was performed with fresh MEF conditioned medium.

A further two days later (i.e. on day 4 of differentiation), the EBs formed were transferred from the V-bottom plates to 20ml Universal tubes, where the MEF conditioned medium was replaced with DIFF medium. EBs were then transferred to untreated 90mm Petri dishes and stored in a 37°C incubator for 8 days (i.e. up to 12 of differentiation). The EBs were detached from the bottom of the Petri dishes daily, by pipetting, while the medium was replaced with fresh DIFF medium every 3-4 days. Following this treatment, EBs were transferred to untreated 96-well U-bottom plates (NUNC: 262162), at a density of one EB per well. The plates were stored in a 37°C incubator for up to 10 days. The medium was replaced by 150µl of fresh DIFF medium every 3-4 days.

The EBs were finally transferred to 20ml Universal tubes and frozen at -80°C to be used for molecular biology analyses, or cultured further to derive cell lines of differentiated cells. For analysis of differentiation into the three embryonic germ layers, EBs were seeded onto glass chamber slides on day 21 of differentiation, and fixed using 4% PFA in order to be used for immunofluorescence staining.

2.1.8 Derivation of human fibroblast cell-lines from hESCs

After culture of EBs in 96-well U-bottom plates for ~10 days (i.e. day 22 of differentiation), EBs were transferred to a 20ml Universal tube and centrifuged at 200xg for 5 minutes. Following centrifugation, the supernatant was aspirated and the EBs were treated with 2ml of 0.05% trypsin for 3 minutes, in a 37°C water bath. The EBs were then vortexed and trypsin was inactivated with 18ml of DIFF medium. The EBs were centrifuged again as before, the supernatant was aspirated, the EBs were re-suspended in 10ml of DIFF medium, and were transferred to a 90mm culture dish (NUNC: 150350) which was placed in a 37°C incubator for 2 days to allow EB attachment to the plates. The medium was then replaced with 10ml of fresh DIFF medium and the EBs were allowed to grow for a further 2 days. After this, the EBs were washed with 10ml PBS and visible cell clumps were removed by aspiration. Remaining cells were treated with 1.5ml 0.05% trypsin for 3 minutes. The trypsin was inactivated with 8.5ml of differentiation medium, and the cells were transferred to a 20ml Universal tube to be centrifuged for 5 minutes, at 200xg. The pellet was re-suspended in 5ml differentiation medium and the cells were seeded in a 25cm^2 culture flask. Once the cells were confluent, they were passaged in a 1:3 split, while a portion was cryopreserved in DMSO for future use.

2.1.9 Generation of clonal cell lines from hESC-derived fibroblasts

A confluent flask of hESC-derived fibroblasts grown in DIFF medium was trypsinised by treatment with 1ml of 0.05% trypsin for 3 minutes, at 37°C. The trypsin was inactivated with 4ml of DIFF medium, and cells were transferred to a 20ml Universal tube for centrifugation at 200xg for 5 minutes. The supernatant was then aspirated, and the cells were re-suspended in 5ml of DIFF medium. Cells were then seeded in 96-well flat-bottom plates (NUNC: 167008) at a density of 20 cells per plate, and a total volume of 100µl per plate. The plate was placed in a 37°C incubator for 4 days, after which a medium change was performed with fresh DIFF medium. The medium was replaced every 48h for a further 10

days, after which the plates were scanned to identify wells containing proliferating fibroblasts. The cells in each well were considered to represent clonal lines originating from single cells. Each clonal line was expanded in culture and cryopreserved in DMSO for future experiments.

2.1.10 Growth and culture of primary fibroblast lines

The BJ neonatal foreskin fibroblast line (kind gift by Dr. Ramiro Alberio, The University of Nottingham) and the adult skin fibroblast line SUKE (gift by Dr. David Brook, The University of Nottingham) were used in this thesis for comparison to hESC-derived fibroblasts. BJ fibroblasts were originally derived by the group of Dr. J.R. Smith (Baylor College Medical School, Houston) and are now available from the American Type Culture Collection (Product no.: CRL-2522). SUKE fibroblasts were isolated by the lab of Dr. D. Brook. Both lines had a normal diploid karyotype.

BJ and SUKE fibroblasts were cultured in differentiation (DIFF) medium, as described previously for hESC-derived fibroblasts (Section 2.1.8). Once a 25cm^2 flask of cells was confluent, the DIFF medium was aspirated and the cells were washed with 5ml of PBS. They were then treated with 1ml of 0.05% trypsin for 3 minutes, at 37°C. The trypsin was inactivated with 5ml of DIFF medium, and 2ml were transferred to a 20ml Universal tube for a 1 in 3 passage. The cells were centrifuged at 200xg for 5 minutes. The supernatant was then aspirated, cells were re-suspended in 5ml of DIFF medium, and transferred to a 25cm^2 flask which was stored in a 37°C incubator. The medium was replaced every 48h and the cells were passaged every 3-4 days.

2.1.11 Growth and passage of Human Embryonic Kidney cells

Human Embryonic Kidney (HEK) cells of the cell line HEK293/T17 (American Type Culture Collection: CRL-11268; Graham *et al.* 1977; Harrison *et al.* 1977) and the clonal HEK293

line BL15 (kindly gifted by Dr. David Darling, King's College London; Nesbeth *et al.* 2006) were removed from liquid nitrogen and were mixed with 10ml of HEK293 medium. The cell suspension was centrifuged at 200xg for 5 minutes. Following centrifugation, the supernatant was removed, and the cells were re-suspended in 5ml of HEK293 medium and transferred to a 25cm^2 culture flask. They were then placed in a 37°C incubator for 2 days or until confluent. Once the flask was confluent, the medium was aspirated and the cells were washed with 5ml of PBS. They were then treated with 1ml of 0.05% trypsin for 1 minute, at 37°C. The trypsin was inactivated with 4ml of HEK293T medium, and 1ml was transferred to a clean 25cm^2 flask, for a 1 in 5 passage. The flask was placed in a 37°C incubator for 2 days or until confluent.

The culture medium for BL15 cells was supplemented with 2.5µg/ml Puromycin and Blasticidin (SIGMA; P8833 and 15205, respectively) to maintain clonal selection.

2.1.12 Toxicity testing for the antibiotic G418

hESCs and hESC-derived fibroblasts were seeded in 6-well plates (NUNC: 152795) at a density of 40,000 cells per well, and were grown in 2.5ml of conditioned or DIFF medium, respectively. Wells were coated with Matrigel™ (section 2.1.6) prior to seeding of hESCs. 24 hours following cell seeding, the medium was replaced with fresh conditioned or DIFF medium, which was supplemented with the antibiotic G148 (SIGMA; A1720), at concentrations varying from 0 to 800 µg/ml. This was repeated daily for 5 days, and the percentage cell survival at each G418 concentration was calculated on the final day based on total cell counts.

2.1.13 Calculation of population doubling time

hESCs and hESC-derived fibroblasts were seeded in 6-well plates at a density of 200,000 cells per well, and were grown in 2.5ml of conditioned or DIFF medium, respectively. Wells

were coated with Matrigel™ (section 2.1.6) prior to seeding of hESCs. When confluent, the cells were passaged as described in section 2.1.6 for hESCs and section 2.1.8 for hESC-derived fibroblasts. The number of cells per well was calculated by total cell counts, and the cells were re-seeded in fresh 6-well plates at a density of 200,000 cells per well. This was repeated for a total of 6 passages, after which population doubling times were estimated based on Denning *et al.* (2006). The equations used to calculate population doubling times were based on cumulative population doubling and cumulative time in culture, as shown below.

$$\text{Cumulative population doubling} = \text{Sum} \frac{\text{Log}_{10}(\text{fold increase in cell number per passage})}{\text{Log}_{10}(2)}$$

$$\text{Population doubling time (hours)} = \frac{\text{Cumulative time in culture}}{\text{Cumulative population doubling}}$$

2.1.14 Live cell staining for the surface antigen TRA-1-81

Immunofluorescence staining for the hESC surface marker TRA-1-81 was performed based on Lowry *et al.* (2008), using live cells that were attached to culture surfaces. A phycoerythrin (PE) conjugated anti-human TRA-1-81 antibody (eBioscience; 12-8883-80) was diluted by 1:100 in MEF conditioned medium and filtered-sterilised through a Millex-GV_4 0.22µm/4mm filter unit (Millipore: SLGV004SL). Cells were then incubated with the diluted antibody for 20 minutes, in a 37°C incubator, in the dark. Following incubation, the antibody was removed and cells were washed twice with MEF conditioned medium. Fluorescence staining with TRA-1-81 antibody was assessed within 1 hour of antibody removal, under a Nikon ECLIPSE TE2000-S inverted microscope.

2.1.15 Oil red-O staining

Oil-red O staining for adipocyte detection was performed with help from Dr. David Anderson using cells fixed in 4% paraformaldehyde, for 20 minutes. Following fixation, the cells were washed in 60% isopropanol and then treated with 0.2% Oil-red O (SIGMA; O-0625; diluted in 60% isopropanol) for 10min, at room temperature. Oil-red O was washed off with distilled water and images were captured under a Nikon ECLIPSE TE2000-S bright field inverted microscope.

2.2 CELL MANIPULATION BY LIPOFECTION AND VIRAL TRANSDUCTION

2.2.1 Buffers and solutions

All buffers and solutions were autoclaved before use.

Table 2.2– Buffers and solutions used for lipofection and viral transduction

Buffer	Component	w/v or v/v	Supplier	Product number
2x HBS pH7.5	NaCl	1.6g	SIGMA	S5886
	KCl	0.076g	SIGMA	P5405
	Na_2HPO_4	0.02g	SIGMA	S5136
	Glucose	0.2g	SIGMA	G7021
	HEPES	1.0g	SIGMA	H1016
	SDW	to 100ml	SIGMA	W3500
2.5M $CaCl_2$ pH7.5	HEPES	0.119g	SIGMA	H1016
	$CaCl_2$	13.88g	SIGMA	C4901
	SDW	to 50ml	SIGMA	W3500

2.2.2 hESC lipofection with siRNAs

In a confluent 25cm^2 culture flask of hESCs, MEF conditioned medium was aspirated and the cells were washed with 5ml of PBS. They were then treated with 0.5ml of 0.05% trypsin for 1 minute, at 37°C. The trypsin was inactivated with 4.5ml of BGK medium, and the cell suspension was transferred to a 20ml Universal tube. 20µl were removed to perform a cell count, and the cells were centrifuged at 160xg for 4 minutes. The cells were then re-suspended in MEF conditioned medium and seeded in 24-well plates (NUNC: 143982) at a density of 10,000 cells per well. Cells were placed in a 37°C incubator for 24 hours, after

which MEF conditioned medium was replaced by 0.5ml of OptiMEM I (GIBCO: 31985) containing 1.5µl of the cationic lipid reagent Lipofectamine-2000 (Invitrogen: 11668-027), and 2.5µl of 20µM stock siRNA against the gene of interest. The transfection was allowed to occur for 4 hours, in a 37°C incubator, after which OptiMEM was replaced by 0.5ml of fresh MEF conditioned medium. The cells were further incubated at 37°C and were collected in 1.5ml Eppendorf tubes at 24, 48 and 72 hours after transfection, by lysis with 350µl RLT buffer (QIAGEN RNeasy Kit: 74014). The cells were snap-frozen immediately on dry ice and were stored at -80°C. All lipofections included a negative control sample which received no treatment (Untreated), as well as a sample which was treated with lipid but no siRNA (Lipid control).

Table 2.3- Invitrogen Stealth Select siRNAs used for lipofection of hESCs

Gene	Target sequences	Invitrogen Oligo ID		Oligo sequence (5'→3')
DNMT1	NM_001379.1	HSS102859	F	GACAAAUGAGAAGCUGUCCAUCUUU
			R	AAAGAUGGACAGCUUCUCAUUUGUC
		HSS102860	F	GGAAACAAAGGGAAGGGCAAGGGA
			R	UUCCCUUGCCCUUCCCUUUGUUUC
		HSS10286	F	CAAAUCGGAUGAGUCCAUCAAGGAA
			R	UUCCUUGAUGGACUCAUCCGAUUUG
DNMT3A	NM_153759.2 NM_175629.1 NM_022552.3	HSS141868	F	AGCGCACAAGAGAGCGGCUGGUGUA
			R	UACACCAGCCGCUCUCUUGUGCGCU
		HSS141869	F	CCACGACCAGGAAUUUGACCCUCCA
			R	UGGAGGGUCAAAUUCCUGGUCGUGG
		HSS141870	F	CCCUGUGAUGAUUGAUGCCAAAGA
			R	UUCUUUGGCAUCAAUCAUCACAGGG

2.2.3 HEK293 cell lipofection with plasmid DNA

In a confluent 25cm^2 culture flask, the HEK293 medium was aspirated and cells were washed with 5ml of PBS. They were then treated with 1ml of 0.05% trypsin for 2 minutes, at 37°C. The trypsin was inactivated with 4ml of HEK293 medium, and the cell suspension was transferred to a 20ml Universal tube. 20µl were removed to perform a cell count, and the cells were centrifuged at 200xg for 5 minutes. Cells were then re-suspended in HEK293 medium and seeded in 6-well plates at a density of 5,000 or 10,000 cells per well. Plates were placed in a 37°C incubator for 24 hours, after which HEK293 medium was replaced by

2ml of OptiMEM I containing a cationic lipid reagent (Lipofectamine-2000, Lipofectamine-LTX; Invitrogen: 15338-100, GeneJammer; STRATAGENE: 204130, or FuGENE HD; Roche: 04709691001) and plasmid DNA. The transfection was allowed to occur for 4 hours, at 37°C, after which OptiMEM was replaced by 2ml of fresh HEK293 medium. The cells were grown for 24 hours at 37°C, they were photographed under bright-field and fluorescence light, and were finally prepared for FACS analysis. All lipofections included a negative control sample which received no treatment (Untreated), as well as a sample treated with lipid but no DNA (DNA control).

2.2.4 Transduction with lentivirus produced in HEK293/T17 cells

HEK293 cells were seeded in a 175cm^2 flask at a density of 5 million cells per flask, in a total of 20ml of HEK293 medium. 24 hours later, the HEK293 cells were transfected as described in section 2.2.3, using Lipofectamine-2000, 66.7μg of a lentiviral transfer plasmid, (e.g. pLVTHM; Addgene: 12247), 50μg of the lentiviral packaging plasmid psPAX2 (Addgene: 12260) and 20μg of the envelope plasmid pMD2.G (Addgene: 12259). Formation of lentiviral particles in HEK293 cells was allowed to occur for 48 hours, after which the culture medium was collected and filtered through a 0.2μm filter unit. The virus-containing medium was then concentrated by approximately 75-fold using centrifugation at 4000xg, for 20 minutes, in Amicon Ultra-15 Centrifugal Filter Units 100NMWL (Millipore; UCF910008). 200μl of fresh concentrated virus was used to transduce 50,000 target cells, seeded in 6-well plates 4-6 hours prior to lentiviral transduction. Transduction was carried out in a total of 2ml of appropriate medium for each cell type, in the presence of 8μg/ml hexadimethrine bromide (Polybrene) solution (SIGMA: H9268). The medium was replaced with fresh culture medium 24 hours later, and the cells were maintained as described before until needed for further analysis.

2.2.5 Transduction with lentivirus produced in BL15 cells

BL15 cells were cultured in antibiotic-free medium supplemented with 100μM of Biotin (SIGMA; P2165), for 48 hours prior to their use for generation of lentiviral particles. BL15 cells were seeded on gelatine coated 90mm culture dishes at a density of 6 million cells per dish, in Biotin-supplemented HEK293 medium. 24 hours later, BL15 cells placed in 7ml of OptiMEM medium supplemented with 10% FBS and 100μM Biotin, for 1 hour at 37°C, and were then transfected as described in section 2.2.3, using 60μl of Lipofectamine-2000, 10μg of a lentiviral transfer plasmid (e.g. pLVTHM), 7.5μg of the lentiviral packaging plasmid psPAX2, and 3μg of the envelope plasmid pMD2.G. After 5-6 hours, BL15 cells were carefully washed three times with serum-free HEK293 medium, supplemented with 1mM sodium pyruvate (SIGMA; S8636), and were stored in this medium, at 37°C. Virus-containing culture media were collected in 50ml Universal tubes at 12 and 24 hours following transfection and were stored at -80°C until a final collection at 48 hours following transfection was performed.

All virus-containing media where then thawed in cold water and were filter-sterilised through a 0.2μm filter unit. They were then pH adjusted to a pH of 7.7, using 100mM NaOH (SIGMA; S8045), and were precipitated by incubation with 60mM $CaCl_2$ (SIGMA; C4901) for 30 minutes, in a 37°C water bath. Following formation of white precipitates, the tubes were centrifuged at 4000xg for 5 minutes, and the pellet was re-suspended in virus buffer (50mM NaCl, 100mM EDTA in SDW), at $1/10^{th}$ of the original volume prior to precipitation. The virus was then concentrated further using streptavidin paramagnetic beads (Promega; Z5481), which were mixed with the precipitated virus at a 1:1 ratio and incubated on a roller for 2.5 hours, at r.t. Following incubation, the bead-bound virus was washed twice in DIFF medium and was finally re-suspended in DIFF medium, at ½ the original volume. The virus was used to transduce cells at a multiplicity of infection (MOI) of 5 units, in the presence of 8μg/ml Polybrene solution.

2.2.6 Formation of iPSCs from hESC-derived fibroblasts

hESC-derived fibroblasts grown in DIFF medium were seeded in 6-well plates, at a density of 50,000 cells per well, and were transduced with lentiviral particles 4-6 hours later. For virus produced in HEK293T cells (section 2.2.4), 200µl of viral particles prepared with each transfer plasmid; pSin-EF2-OCT4-Pur (Addgene: 16579), pSin-EF2-NANOG-Pur (Addgene: 16578), pSin-EF2-SOX2-Pur (Addgene: 16577), and pSin-EF2-LIN28-Pur (Addgene: 16580; Yu *et al.* 2007b) were added to each well, in a total volume of 3ml. For virus produced in BL15 cells (section 2.2.5), cells were transduced at an MOI of 5 for each of the viruses mentioned above.

hESC-derived fibroblasts were trypsinised (section 2.1.8) at 48 hours following lentiviral transduction and were seeded onto inactivated MEF feeder cells. From then on, they were cultured in BGK medium, supplemented with 10ng/ml FGF, with daily medium changes. Seven days later, the BGK medium was replaced with MEF conditioned medium, supplemented with 10ng/ml FGF. Daily medium changes were performed with fresh MEF conditioned medium, supplemented with 10ng/ml FGF, until day 18-23 post-transduction, when emerging iPSC colonies where expanded in culture using manual dissection procedures (section 2.2.7) and were finally adapted to culture on Matrigel (section 2.1.6).

2.2.7 Growth and passage of iPSCs by manual dissection

iPSCs were derived as colonies on mitotically inactivated MEFs (see section 2.1.4) and were maintained in BGK medium, with daily medium changes. Colonies were dissected under a Leica MZ12.5 stereomicroscope, using a 0.190-0.210mm micro-dissecting glass knife (STEM CELL CUTTING TOOL: Vitrolife;14601). Colony pieces of 100-200µm in diameter were transferred to a fresh culture dish seeded with mitotically inactive MEFs, and were incubated in a 37°C incubator with daily medium changes for a further 2-5 days, until they were ready for the next passage.

2.3 KARYOTYPE ANALYSIS

To prepare cells for karyotype analysis, sub-confluent exponentially growing cultures of hESCs or iPSCs were treated for 60 minutes, at 37°C, with the anti-mitotic agent KaryoMAX® Colcemid™ (Invitrogen; 15212012) diluted to a final concentration of 100ng/ml in MEF conditioned medium. The KaryoMAX containing medium, together with any floating cells, was collected in a 20ml Universal tube. Attached cells were harvested by treatment with 0.05% trypsin, as described in section 2.1.6, and were added to the same 20ml Universal tube as before. Following centrifugation at 300xg for 5 minutes, the cell pellet was re-suspended by slow drop-wise addition of hypotonic 0.6% sodium citrate solution (Fisher Scientific; S/3320), while vortexing at 1800rpm. Incubation in hypotonic solution was then carried out for 20 minutes, at r.t., after which the cells were pelleted by centrifugation at 300xg for 5 minutes. The cells were fixed by drop-wise addition of fixative solution (methanol acetic acid mix at a 5:1 ratio), while vortexing at 1800rpm. Cells were then stored at -20°C, ready for G-banding analysis. G-banding was performed by Mr. Nigel Smith (Nottingham City Hospital, UK), based on guidelines from the International System for Human Cytogenetic Nomenclature (ISCN, 2005). 30 metaphase spreads were analysed for each sample.

2.4 FLOW CYTOMETRY

2.4.1 Analysis of GFP expression

Cells grown in 6-well plates were washed in 2ml PBS and then trypsinised for 5-6 minutes, at 37°C. Trypsin was inactivated with 5ml of 10% FBS in PBS per well, and the suspended cells were transferred to 15ml Universal tubes to be centrifuged at 200xg for 5 minutes. The supernatant was then aspirated and the cell pellet was re-suspended in 1ml of 10% FBS in PBS. The cells were mixed well by pipetting and transferred to glass test tubes (SARSTEDT; 55.476.005) for flow cytometry analysis which was performed by staff of the Flow Cytometry Facility in Queen's Medical Centre, Nottingham.

2.4.2 Analysis of protein expression

Cells were harvested by treatment with 0.05% trypsin, and were fixed by incubation in 600µl of 4% PFA in PBS (SIGMA; P-6148) for 15 minutes, at r.t. For staining of non-surface antigens, the cells were treated with 200µl of 0.5% Triton X-100 in PBS (SIGMA; T-8532) for 15 minutes, at r.t. They were then centrifuged at 300xg for 5 minutes and the pellet was re-suspended in primary antibody, diluted at an appropriate concentration in 5% FBS in PBS (Table 2.13). Following a 20 minute treatment in primary antibody, at r.t., the cells were washed with 10ml of 5% FBS and centrifuged as before. The samples were wrapped in aluminium foil and the pellet was re-suspended in AlexaFluor488 secondary antibody (Invitrogen; A11001), diluted at a 1:200 ratio in 5% FBS. The cells were incubated in secondary antibody for 20 minutes, at r.t., and were then washed in 10ml of 5% FBS. Cells were centrifuged for a final time at 300xg, for 5 minutes, and the pellet was re-suspended in 0.5ml of 5% FBS, ready for flow cytometry analysis.

2.4.3 Cell cycle analysis

Cells were harvested by treatment with 0.05% trypsin, and were re-suspended in 10 ml PBS. They were then centrifuged at 160xg for 4 minutes, and the pellet was re-suspended by drop-wise addition of ice-cold PBS. The cells were centrifuged as before and fixed by drop-wise addition of ice-cold 70% ethanol, while vortexing at 1800rpm. Cells were stored in fixative solution at 4°C for 24 hours, and were then centrifuged at 160xg for 4 minutes. The pellet was re-suspended in staining solution, which consisted of 0.2% Tween-20 (SIGMA; P5927), 250µg/ml RNase A (SIGMA; R4642) and 10µg/ml propidium iodide (SIGMA; P4170) in PBS. Following a 30-minute incubation in staining solution, at r.t., the samples were transferred to glass test tubes which were wrapped in aluminium foil to avoid bleaching of propidium iodide. Cell cycle analysis was performed using an FC500 Flow Cytometer (Beckmen Coulter). Propidium Iodide was excited at 488nm and emission data was collected at 620nm. The data was analysed using Cylchred software, version 1.0.2.

2.4.4 Analysis of flow cytometry results

Flow cytometry analysis was performed using a Coulter Altra Flow Sorter, unless otherwise stated. The cytometer was set to count 50,000 cells per sample, and results were evaluated on WinMDI software, version 2.9. To analyse the results, the linear functions of the cells' forward scatter (FS Lin) were initially plotted against those of the side scatter (SS Lin) as shown in Figure 2.1.i. Healthy cells were selected (coloured red in Figure 2.1.ii) on these plots, and cell debris (coloured black in Figure 2.1.ii) was excluded from further analysis of marker expression (Figure 2.1.iii). Analysis of marker expression was performed by plotting the Log_{10} function of its expression levels against the events/cells counted by the flow cytometer. Quantification of % expression was performed relative to a negative control sample (Untreated or GFP negative), whose expression level was set to 1%, in order to account for cell auto-fluorescence.

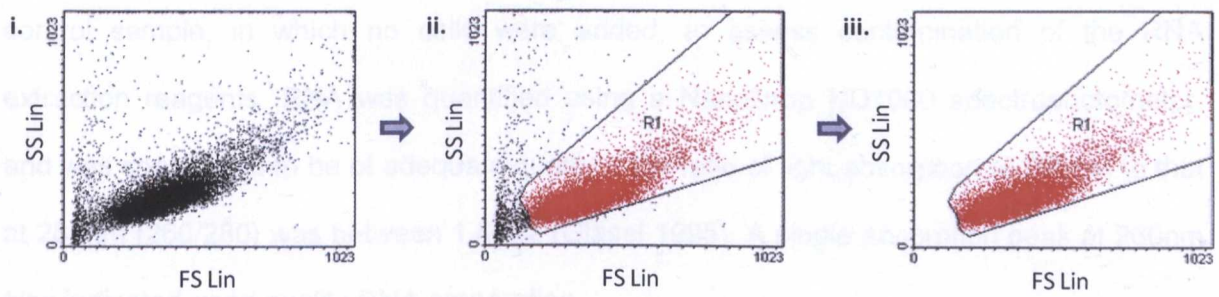

Figure 2.1– Scatter plots for flow cytometry analysis
Following collection of data from a flow cytometer, analysis was performed using WinMDI 2.9 software, where **i.** the linear functions of the forward scatter (FS Lin) and side scatter (SS Lin) were plotted against each other. **ii.** Healthy cells were selected (region highlighted in red) and **iii.** cell debris was excluded from further analysis.

2.5 MOLECULAR BIOLOGY ANALYSIS

2.5.1 Buffers and solutions

All buffers and solutions were autoclaved before use.

Table 2.4– Buffers and solutions used in protocols for molecular analysis

Buffer	Component	w/v or v/v	Supplier	Product number
3M sodium acetate pH5	Sodium acetate	61.52g	SIGMA	S2889
	SDW	to 250ml	N/A	N/A
10x TBE pH8	Tris Base	108g	Fisher Scientific	BPE152-1
	Boric acid	55g	SIGMA	B1934
	EDTA	7.44g	SIGMA	E5134
	SDW	to1L	N/A	N/A
Agarose gel loading buffer	Bromophenol Blue	125mg	SIGMA	B6126
	Glycerol	60ml	SIGMA	G6376
	Water	to 100ml	SIGMA	W4502

2.5.2 Total RNA extraction from animal cells

Total RNA was extracted from animal cells using the QIAGEN RNeasy Mini kit (QIAGEN: 74104), according to the manufacturer's instructions, on pg25-30 of the RNeasy Mini Handbook. Optional steps 3b, 9 and DNase (QIAGEN: 79254) digestion were performed. RNA was eluted in 30µl of sterile distilled water, precipitated using glycogen precipitation (Invitrogen: 10814-010), and stored at -80°C. All experiments included an RNA negative control sample, in which no cells were added, to assess contamination of the RNA extraction reagents. RNA was quantified using a NanoDrop ND1000 spectrophotometer, and was considered to be of adequate quality if the ratio of light absorption at 260nm to that at 280nm (260/280) was between 1.8-2.2 (Glasel 1995). A single absorption peak at 260nm also indicated good quality RNA preparation.

2.5.3 cDNA synthesis

cDNA was synthesised using the First Strand cDNA Synthesis kit (GE Healthcare: 279261-01). 100ng mRNA were mixed with RNase-free water in a final volume of 8µl, and were heated to 65°C for 10 minutes. Samples were then placed on ice and mixed with 1µl of random hexamer primers pd$(N)_6$, 1µl DTT solution, and 5µl Bulk First-Strand cDNA reaction mix (all supplied in the First Strand cDNA Synthesis kit). Samples were heated to 37°C for 1 hour, after which they were placed on ice and mixed with 85µl of RNase-free water. All experiments included a Reverse Transcriptase (RT) negative control, in which the 5µl of

Bulk First-Strand cDNA reaction mix were substituted by 5µl of water, and a cDNA negative control in which the RNA template was replaced by water.

2.5.4 Real-time PCR

2µl of cDNA synthesised using the First Strand cDNA synthesis kit (section 2.5.3) were mixed with 10µl of 2x TaqMan Universal PCR Mastermix (Applied Biosystems: 4324018) and 1µl of the appropriate TaqMan Gene Expression Assay, in a final volume of 20µl. The reactions were set-up in ABI-PRISM® 96-well Optical Reaction Plates (Applied Biosystems: 4306737), which were sealed with Optical Adhesive Covers (Applied Biosystems: 43609954) after sample addition. The plates were centrifuged at 300xg for 2 minutes, and the PCR was run in an Applied Biosystems 7500 Fast Real-Time PCR System. The results were analysed based on the ΔΔCt method of relative quantification (Livak and Schmittgen 2001), using 7500 Fast System SDS V2.0 software (Applied Biosystems).

Table 2.5- TaqMan Gene Expression Assays used for Real-Time PCR

Gene	Ref. Seq.	ABI cat. no./Ref	Primer	Primer sequence (5'→3')
OCT4	NM_002701	Liedtke *et al.* 2007	F	GAAGGTATTCAGCCAAAC
			R	CTTAATCCCAAAAACCCTGG
NANOG	NM_024865	-	F	GCAATGGTGTGACGCAGAAG
			R	GGCATCCCTGGTGGTAGGA
			Probe	CCCAGCCTTTACTC
SOX2	NM_003106.2	Hs01053049_s1	-	-
LIN28	NM_024674.4	Hs00702808_s1	-	-
KLF4	NM_004235.4	Hs00358836_m1	-	-
REX1	NM_174900.3	Hs00399279_m1	-	-
P4HB	NM_000918.3	Hs00168586_m1	-	-
DNMT3B	NM_175848.1 NM_175849.1 NM_175850.1 NM_006892.3	Hs01003405_m1	-	-
DNMT1	NM_001379.2 NM_001130823.1	Hs00945900_g1	-	-
DNMT3A	NM_153759.2 NM_175629.1 NM_022552.3	Hs01027166_m1	-	-
DNMT3L	NM_175867.1 NM_013369.2	Hs00203536_m1	-	-
HPRT	NM_000194.1	Hs99999909_m1	-	-
18S	-	Hs99999901_s1	-	-

2.5.5 Gene expression analysis by RT-PCR

PCR reactions were set in a final volume of 25µl. Each sample contained 2.5µl of 10µM primers, 2.5µl of 10x PCR buffer containing 1.5mM $MgCl_2$ (QIAGEN: 1005479), 2.5µl of 2.5mM dNTPs (Invitrogen: R725-01), 0.125µl of Hot Start Taq Polymerase (QIAGEN: 1007837), and 2µl of cDNA. Additional $MgCl_2$ (QIAGEN: 1005482) was added according to the primers used (Table 2.6). The reactions were set up in a thermal cycler (TECHNE TC-412), with initial denaturation occurring at 95°C for 5 minutes, followed by repeated cycles with denaturation at 95°C for 1 minute, annealing at a primer depended temperature for 30 seconds, and synthesis at 72°C for 1 minute. The cycle number varied according to the primers used (Table 2.6). A final synthesis step was set at 72°C for 5 minutes. All reactions included a negative control where cDNA was substituted by 2µl of water. 10µl of amplified PCR products were analysed by agarose gel electrophoresis (section 2.5.6) and the rest were stored at -20°C.

2.5.6 Agarose Gel Electrophoresis

Molecular grade agarose (Invitrogen: 15510-027) was mixed with 1x TBE buffer to give the percentage gel of choice. The suspension was heated in a microwave oven to dissolve the agarose and, once cooled to ~60°C, 0.4µg/ml ethidium bromide (SIGMA: E1510) was added. The agarose was then poured into a clean gel-casting tray and was allowed to set for 30-45 minutes. Once set, it was placed in an electrophoresis trough containing 1x TBE buffer with 0.4µg/ml ethidium bromide. 10µl of sample, together with 2µl of gel loading buffer, were loaded in each well. Gels were run at 100V for ~60min, after which they were visualised using a UV transilluminator (Fujifilm; LAS4000). Band sizes were estimated using appropriate DNA ladders that were run along with the samples, and were quantified using AIDA V.4.15 2D densitometry software (Raytek Scientific Ltd).

Table 2.6- Primers and PCR conditions used for gene expression analysis by RT-PCR
Primers were purchased from Invitrogen, at a 0.05µmol quality and Desalt purity

Gene	GenBank ID	Primer name	Primer sequence (5'→3')	Amplicon size (bp)	Mg^{2+} Conc. (mM)	Annealing Temp. (°C)	Cycle number
DNMT1	NM_001379.2 NM_001130823.1	F	CCCCATAAATGAATGGTGGA	195	1.5	55	40
		R	TAGGTCGAGTCGGAATTGCT				
DNMT3A	NM_153759.2 NM_175629.1 NM_022552.3	F	ACAAAACCAAGCTCCCTTCC	198	1.5	55	40
		R	TCCTCTCTCCCACCTTTCCT				
DNMT3B	NM_175848.1 NM_175849.1 NM_175850.1 NM_006892.3	F	CATTTTTAAGGGCCCAGGAT	184	1.5	55	40
		R	CCCTGAATGTGATGATGACG				
DNMT3L	NM_175867.1 NM_013369.2	F	AGATTCTTTGCCCCCATAGC	166	1.5	55	40
		R	GTGGGTTCAAGGTTCCAGTG				
OCT4	NM_002701	tF	TGCACAACGAGAGGATTTTG	184	1.5	55	35 or 40
		tR	CAGAGTGGTGACGGAGACAG				
		eR	GGCACAAACTCCAGGTTTTC	281	1.5	55	35 or 40
NANOG	NM_024865	tF	CAGTTCCAGCCAAATTCTCC	159	1.5	55	35 or 40
		tR	CACGTCTTCAGGTTGCATGT				
		eR	AGGATTCAGCCAGTGTCCAG	215	1.5	55	35 or 40
SOX2	NM_003106	tF	CCCCTGTGGTTACCTCTTCC	198	1.5	55	35 or 40
		tR	ACATGTGTGAGAGGGGCAGT				
		eR	AGTCCCCCAAAAAGAAGTCC	463	1.5	55	35 or 40
LIN28	NM_024674.4	tF	GTCTGGAATCCATCCGTGTC	262	1.5	55	35 or 40
		tR	GTAGGTTGGCTTTCCCTGTG				
		eR	CTCTGCCTGCTCCTCAAAAC	380	1.5	55	35 or 40
IRES-OCT4	-	pR-OCT4	CCCTAGGAATGCTCGTCAAG	468	1.5	55	35 or 40
IRES-NANOG	-	pR-NANOG		403	1.5	55	35 or 40
IRES-SOX2	-	pR-SOX2		413	1.5	55	35 or 40
IRES-LIN28	-	pR-LIN28		536	1.5	55	35 or 40

2.5.7 DNA gel extraction and purification

PCR amplification products were extracted using the QIAquick Gel Extraction kit (QIAGEN: 28704) according to the manufacturer's instructions, pg25-26 of the QIAquick Spin Handbook. DNA was eluted in 30µl of elution buffer or sterile distilled water, quantified using a NanoDrop spectrophotometer (NanoDrop ND-1000), if necessary, and stored at -20°C.

2.5.8 DNA extraction from animal cells

DNA was extracted from animal cells using the QIAGEN DNeasy Blood and Tissue kit (QIAGEN; 69504), according to the manufacturer's instructions, pg25-27 of the DNeasy kit Handbook. Optional steps 1c, and RNase A (QIAGEN: 19101) treatment were performed. DNA was eluted in 100µl of AE Buffer, and step 8 was omitted. If necessary, DNA was precipitated using ethanol and Pellet Paint co-precipitant (Novagen; 69-049-3). DNA was quantified using a NanoDrop ND1000 spectrophotometer, and stored at -20°C for future use.

2.6 DNA METHYLATION ANALYSIS

2.6.1 Bisulfite conversion of DNA

Bisulfite conversion of DNA was performed according to Kim *et al.* (2007). 1µg of genomic DNA, extracted as described in section 2.5.8, was digested in a total volume of 25µl for 16 hours, in a 37°C oven, with an appropriate restriction enzyme according to the gene analysed (Table 2.7). The digested DNA was denatured by incubation at 100°C, for 5 minutes and then immediately placed on ice to avoid re-annealing of the DNA. The DNA was then mixed with 2.5µl of freshly prepared 3M NaOH (SIGMA; S8045) and incubated at 37°C for 20 minutes. During this incubation period, 3.8g of sodium bisulphite (BDH Chemicals: 103564D) were eluted in 5.5 ml of water (SIGMA; W4502) and 1.5ml of 2M NaOH, all the while being kept in dark conditions. 110mg of hydroquinone (SIGMA: H9003) were also dissolved in 1ml of water by heating at 55°C, for 10 min. The dissolved

hydroquinone and bisulphite solutions were mixed together, and each DNA sample was treated with 270µl of the freshly prepared mixture. The samples were kept in the dark, layered with 200µl of mineral oil (SIGMA; M5310) and placed on a 55°C heat clock for 5 hours, to allow bisulfite conversion of the DNA. Following incubation, the mineral oil was carefully removed, and the bisulphite treated DNA was added to 2ml sterile tubes (Eppendorf; 0030 120.094) containing 600µl of water, 90µl of 3M sodium acetate pH5 (SIGMA; S2889) and 2.5µl of Pellet Paint co-precipitant. 900µl of isopropanol were then added to each tube, and mixed well by pipetting. The samples were centrifuged in a desk-top centrifuge, at maximum speed for 20 minutes. The resulting DNA pellets were washed in 800µl of 70% ethanol and centrifuged as before, for 5 minutes. The supernatants were carefully removed, and pellets were air-dried for 10 minutes. The pellets were then re-suspended in 50µl of water, and the samples were desulfonated by addition of 5µl fresh 3M NaOH. The reaction was completed by incubation at 37°C for 15 minutes, and the DNA was purified using the QIAquick PCR purification kit (QIAGEN; 28104) according to the manufacturer's instructions, pg19-20 of the QIAquick Spin Handbook. The DNA was eluted in 33µl of water, and stored at -20°C for future use.

2.6.2 Bisulfite PCR

Bisulfite PCR was performed in a final volume of 25µl, consisting of 0.125µl Platinum Taq (Invitrogen; 10966), 6µl of 5µM forward and reverse primers (Invitrogen), 2.5µl of 10x Reaction buffer (Invitrogen; 10966), 1.25µl of 2.5mM dNTPs (Invitrogen; R72501), Xoptimal $MgCl_2$ (Invitrogen), and 1µl of bisulfite converted DNA (section 2.6.1). The PCR cycling conditions were 95°C for 10 min followed by 40 cycles of; 95°C for 1min, Xoptimal °C for 1min, 72°C for 1min) and a final extension step at 72°C for 10min. Optimal conditions for each primer set are shown in Table 2.7. Bisulfite PCR primers were designed using MethPrimer software (Li and Dahiya 2002) or were previously published as described in Table 2.7.

Table 2.7– Conditions used for bisulfite PCR

Gene	Primer	Primer sequence (5'→3')	gDNA digest	Amplicon size (bp)	Mg^{2+} Conc. (mM)	Annealing Temp. (°C)	Reference
OCT4	F*	TTAGGAAAATGGGTAGTAGGGATTT	PacI	295	1.5	63	Deb-Rinker *et al.* 2005b
	R*	TACCCAAAAAACAAATAAATTATAAAACCT					
NANOG	F*	TGGTTAGGTTGGTTTTAAATTTTTG	PacI	336	1.5	63	-
	R	AACCCACCCTTATAAATTCTCAATTA					
SOX2	F-OS*	TTTGGGTTGAATTGAGGATATTTTA	PacI	344	1.5	63	-
	R-OS	CCCCCAAAATAATCATTTAAATCTT					
SOX2	F-P*	TTTTAGAAAATTGAGTTATTAAGGTAGTAA	PacI	374	1.5	59	-
	R-P	AATAAAAACTAACCAAACATCTTACTATTA					
SOX2	F-TSS*	AAAGGGAGAGAAGTTTGAGTTTTAG	PacI	455	1.5	59	-
	R-TSS*	CCACACCATAAAAACATTCATAAAC					
REX1	F*	GGTTTAAAAGGGTAAATGTGATTATATTTA	PacI	361	1.5	63	Takahashi *et al.* 2007
	R	CAAACTACAACCACCCATCAAC					
LIN28	F	GGGGGAAGATGTAGTAGTTTTTTTT	PacI	310	1.5	63	-
	R*	CCACTAAAACACCAAAATTCCTAAC					
KLF4	F	GGGGATTGGTTAGGTAGGAAGTAT	PacI	493	1.5	63	-
	R*	ACCTTAAAATCACCAAAAACCACTA					
DNMT3B	F	GGGAGAGATTTTTTTTAGGGATTT	PacI	343	1.5	63	-
	R*	CCCAAAACAAAAACCAAATAATTAC					
P4HB	F	TTTTTTTTGTTTTGGTTTTTAATTG	PacI	170	1.5	59	-
	R*	TAAACTAAAAACTCCTCCCCACTAC					
GTL2 CpG2	F	GTAAGTTTTATAGGTTGTAAAGGGGGTGTT	EcoRI	216	2.5	55	Kawakami *et al.* 2006
	R*	CCACAACTAATAACTAAAAAAATAAACATT					
KvDMR1	F*	TGATGTGTTTATTATTTYGGGG	BamHI	304	2.5	55	Monk *et al.* 2006b
	R	CCCTAAAATCCCAAATCCTC					
GNAS XLas	F	GTTGGTTTTAGAGGAGGTTATAGTT	EcoRI	442	2.5	55	-
	R	CCTCCTCAACTAAAAATCTCTCTAC					
	*	GTTATTTGAGTTTGATGGAGAAGG		-	-	-	

= primer used for direct sequencing

2.6.3 Bisulfite sequencing

PCR products from bisulfite PCR (section 2.6.2) were separated by agarose gel electrophoresis and purified using the QIAquick gel extraction kit (QIAGEN; 28704), according to the manufacturer's instructions, pg25-26 of the QIAquick Spin handbook. Sequencing analysis was performed using primers depicted by an asterix (*) in Table 2.7, by staff of the DNA sequencing Lab, Queen's Medical Centre, The University of Nottingham. Sequencing results were analysed as shown in Figure 2.2.

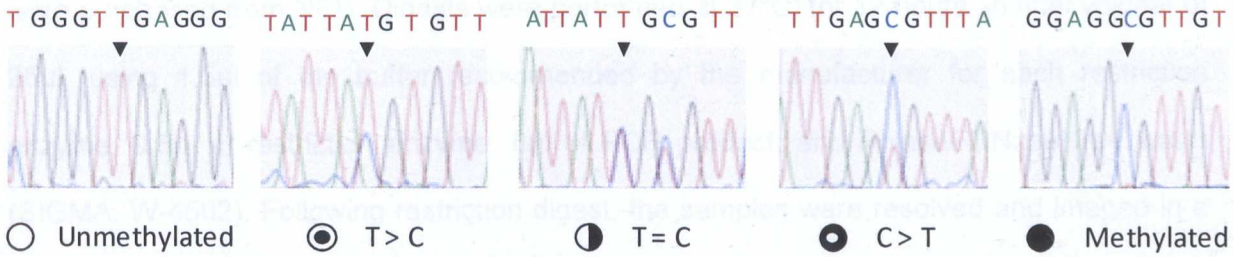

Figure 2.2- Key for determining the methylation state of CpG sites in direct bisulfite sequencing
Thymidine (T) peaks in CpG dinucleotides indicated unmethylated DNA, cytosine (C) peaks indicated methylated DNA. Overlapping T and C peaks in individual CpG sites were regarded as preferentially unmethylated if T>C, semi-methylated if T=C, and preferentially methylated if C>T.

2.6.4 Methylation-specific PCR (MSP)

MSP (Herman *et al.* 1996) was performed as described in section 2.5.5, for 40 cycles, using 2µl of bisulfite converted genomic DNA (sections 2.5.8 and 2.6.1). DNA was amplified using primers specific to both methylated and un-methylated DNA for each gene, as shown in table Table 2.9. As positive control, a reference sample was methylated *in vitro* using SssI methylase enzyme (NEB: M0226S). For this, 1µl of S-adenosy-L-methionine (SAM) was added into 19µl of RNase/DNase free water, to a final concentration of 1600µM. The reaction was performed in a total volume of 20µl, with 1µg of genomic DNA, 2µl of 10X buffer, 1µl of SssI methylase, 2µl of diluted SAM and 10µl of RNase/DNase free water. *In vitro* methylation was performed at 37°C for 2 hours, at the end of which the enzyme was inactivated at 60°C for 20 minutes. Methylated DNA was purified using the QIAquick PCR

purification kit according to the manufacturer's instructions. Following PCR amplification, the samples were resolved and imaged in a 2% agarose gel, as described before (section 2.5.6)

2.6.5 Combined bisulfite restriction analysis (COBRA)

PCR for COBRA (Xiong and Laird 1997) was performed as described in section 2.5.5, for 40 cycles, using 2µl of bisulfite converted genomic DNA (sections 2.5.8 and 2.6.1). Primers and conditions used for PCR amplification are shown in Table 2.10. Following PCR, the products were digested with appropriate restriction enzymes, as described in Table 2.8. All enzymes were purchased from NEB. Digests were performed at 37°C, for 12 hours, in final volume of 25µl, using 1.5µl of the buffer recommended by the manufacturer for each restriction enzyme, 0.5µl of restriction enzyme, 8µl of PCR product, and RNase/ DNase free water (SIGMA: W-4502). Following restriction digest, the samples were resolved and imaged in a 3% agarose gel, as described before (section 2.5.6)

Table 2.8– Restriction enzymes used for digestion of PCR products in COBRA analysis

Gene	Restriction enzyme	NEB Catalogue Number
TP73 promoter	*Acl*I	R0598S
PEG10	*Bst*UI	R0518S
	*Aci*I	R0551S
PEG1	*Acl*I	R0598S
	*Hpy*CH4IV	R0619S
SLC22A18	*Bst*UI	R0518S
CDKN1C	*Hpy*CH4IV	R0619S
KvDMR1	*Bst*UI	R0518S
	*Hpy*CH4IV	R0619S
IGF2 DMR0	*Hpy*CH4IV	R0619S
	*Aci*I	R0551S
GTL2 CpG2	*Acl*I	R0598S
	*Hpy*CH4IV	R0619S
SNRPN	*Aci*I	R0551S
NESP55 DMR	*Acl*I	R0598S
GNAS1 XLαs	*Aci*I	R0551S
	*Bst*UI	R0518S

Table 2.9– Conditions used for Methylation Specific PCR (MSP)
M= methylated, U= um-methylated

Gene	Primer	Primer sequence (5'→3')	gDNA digest	Amplicon size (bp)	Mg^{2+} Conc. (mM)	Annealing Temp. (°C)	Reference
CDH1	F-M	TTAGGTTAGAGGGTTATCGCGT	EcoRI or BamHI	116	2.5	60	Herman *et al.* 1996
	R-M	TAACTAAAAATTCACCTACCGAC					
	F-U	TAATTTTAGGTTAGAGGGTTATTGT		97			
	R-U	CACAACCAATCAACAACACA					
TIMP3	F-M	CGTTTCGTTATTTTTTGTTTTCGGTTTC	EcoRI or BamHI	116	2.5	60	Zochbauer-Muller *et al.* 2001
	R-M	CCGAAAACCCCGCCTCG					
	F-U	TTTTGTTTTGTTATTTTTTGTTTTTGGTTTT		119			
	R-U	CCCCCAAAAACCCCACCTCA					
DAPK1	F-M	GGATAGTCGGATCGAGTTAACGTC	EcoRI or BamHI	98	2.5	60	
	R-M	CCCTCCCAAACGCCGA					
	F-U	GGATAGTTGGATTGAGTTAATGTC		103			
	R-U	CAAATCCCTCCCAAACACCAA					
GATA4	F-M	GTATAGTTTCGTAGTTTGCGTTTAGC	EcoRI or BamHI	102	2.5	60	Akiyama *et al.* 2003
	R-M	AACTCGCGACTCGAATCCCCG					
	F-U	TTTGTATAGTTTTGTAGTTTGTGTTTAGT		101			
	R-U	CCCAACTCACAACTCAAATCCCCA					
GATA5	F-M	AGTTCGTTTTTAGGTTAGTTTTCGGC	EcoRI or BamHI	103	1.5	60	
	R-M	CCAATACAACTAAACGAACGAACCG					
	F-U	TGGAGTTTGTTTTTAGGTTAGTTTTTGGT		101			
	R-U	CAAACCAATACAACTAAACAAACAAACCA					

Gene	Primer	Primer sequence (5'→3')	gDNA digest	Amplicon size (bp)	Mg^{2+} Conc. (mM)	Annealing Temp. (°C)	Reference
HIC1	F-M	TCGGTTTTCGCGTTTTGTTCGT	EcoRI or BamHI	95	2.5	60	Dong *et al.* 2001
	R-M	AACCGAAAACTATCAACCCTCG					
	F-U	TTGGGTTTGGTTTTTGTGTTTTG		118			
	R-U	CACCCTAACACCACCCTAAC					
CCND1	F-M	TACGTGTTAGGGTCGATCG	EcoRI or BamHI	276	2.5	55	Evron *et al.* 2001
	R-M	CGAAATATCTACGCTAAACG					
	F-U	GTTATGTTATGTTTGTTGTATG		222			
	R-U	TAAAATCCACCAACACAATCA					
ESR1	F-M	ATTTGTTTTCGTCGGGTC	EcoRI or BamHI	107	2.5	55	Imura *et al.* 2006
	R-M	ATTAAAAACGACGCAACG					
	F-U	GTATTTGTTTTTGTTGGGTT		114			
	R-U	CCAAAATTAAAAACAACACA					
p16	F-M	TTATTAGAGGGTGGGGCGGATCGC	EcoRI or BamHI	150	1.5	58	Zochbauer-Muller *et al.* 2001
	R-M	GACCCCGAACCGCGACCGTAA					
	F-U	TTATTAGAGGGTGGGGTGGATTGT		151			
	R-U	CAACCCCAAACCACAACCATAA					
MGMT	F-M	TTTCGACGTTCGTAGGTTTTCGC	EcoRI or BamHI	81	2.5	60	Zochbauer-Muller *et al.* 2001
	R-M	GCACTCTTCCGAAAACGAAACG					
	F-U	TTTGTGTTTTGATGTTTGTAGGTTTTTGT		93			
	R-U	AACTCCACACTCTTCCAAAAACAAAACA					

Table 2.10– Conditions used for Combined Bisulfite Restriction analysis (COBRA)

Gene	Primer	Primer sequence (5'→3')	gDNA digest	Amplicon size (bp)	Mg^{2+} Conc. (mM)	Annealing Temp. (°C)	Reference
TP73 promoter	F	GTTTGGGGGATAGTAGGGAGTT	EcoRI	552	1.5	55	Dong *et al.* 2002
	R	ACCCTAAACCTCCTACCTACAACC					
PEG10	F	GGTGTAATTTATATAAGGTTTATAGTTTG	EcoRI	234	2.5	55	Kim *et al.* 2007
	R	AACAAAAAAAAATAAAATCCCACAC					
PEG1	F	TYGTTGTTGGTTAGTTTTGTAYGGTT	EcoRI	209	1.5	55	Kerjean *et al.* 2000
	R	AAAAATAACACCCCCTCCTCAAAT					
SLC22A18	F	GGGTAGGATTTAAGTTGGAGG	BamHI	427	1.5	55	Monk *et al.* 2006a
	R	CAACAAACACRTCAAAAACACC					
CDKN1C	F	GTTTTAAATTGYGAGGAGAGGGG	EcoRI	284	2.5	55	Monk *et al.* 2006a
	R	CCTCTCRAATCTCCRAAC					
KvDMR1	F	TGATGTGTTTATTATTTYGGGG	BamHI	304	2.5	55	Monk *et al.* 2006a
	R	CCCTAAAATCCCAAATCCTC					
IGF2 DMR0	F	TTGGTGTTGGAAAGTGTTTG	EcoRI	305	2.5	55	Kim *et al.* 2007
	R	CTATAACRTCCAAACCCTCTA					
GTL2 CpG2	F	GTAAGTTTTATAGGTTGTAAAGGGGGTGTT	EcoRI	216	2.5	55	Kawakami *et al.* 2006
	R	CCACAACTAATAACTAAAAAAATAAACATT					
SNRPN	F	TAGGTTGTTTTTTGAGAGAAGTTAT	EcoRI	236	2.5	57	Kim *et al.* 2007
	R	AAAAAAACTAAAACCCCTACACTAC					
NESP55 DMR	F	TTTTTGTAGAGTTAGAGGGTAGGT	EcoRI	344	2.5	55	Judson *et al.* 2002
	R	AAAAAAAACAACTCAAAATCTACC					
GNAS1 XLαs	F	GTTGGTTTTAGAGGAGGTTATAGTT	EcoRI	442	2.5	55	-
	R	CCTCCTCAACTAAAAATCTCTCTAC					

2.6.6 Genomic DNA digestion with methylation specific enzymes

Digests with the methylation specific enzyme McrBC (NEB; M0272S) were performed in a final volume of 25µl, using 1.5µl of NEBuffer 2, 0.15µl 10mg/ml BSA, 0.15µl of 100mM GTP, and RNase/ DNase free water (SIGMA: W-4502). 1µl of restriction enzyme was used to catalyse the digestion of 0.4µg of genomic DNA (section 2.5.8). The digests were performed at 37°C, for 12 hours. The enzyme was then heat-inactivated at 65°C, for 5 minutes, and samples were run on a 1% agarose gel, as described in section 2.5.6.

2.7 CARRIER CHROMATIN IMMUNOPRECIPITATION (cChIP)

Cell pellets for cChIP analysis were collected and sent to The University of Birmingham, UK, where cChIP was performed with help from Dr. Laura O'Neil. cChIP was carried out as described in O'Neill *et al.* (2006), with *D.melanogaster* SL2 cells being used as co-precipitants for human cells. Nuclei were released by homogenization in a Dounce all-glass homogenizer with a 'tight' pestle using two strokes. Chromatin of satisfactory quality (predominantly but not exclusively mononucleosomal with minimal subnucleosomal fragments), was used for ChIP with antibodies against H3K27me3, H3K9me2, H3K4Ac and H3K4me3. DNA fractions precipitated with each antibody were analyzed using radioactive-PCR (O'Neill L *et al.* 2006). Primers and conditions for PCR are in shown in Table 2.11.

Table 2.11– Primers and PCR conditions used for radioactive-PCR

Gene	Accession number	Primer name	Primer sequence (5'→3')	Annealing temp. °C
OCT4	NM_002701	F	TTCCCCTTCCACA	58
		R	GGGAGAGAGGGGTTGAGT	
NANOG	NM_024865	F	TGTCTTCAGGTTCTGTTGCTCGGT	58
		R	CGTCTACCAGTCTCACCAAGGCCA	
SOX2	NM_003106	F	TTAAGTACCCTGCACCAAAAA	58
		R	GGGGATACAAAGGTTTCTCA	
REX1	NM_174900.3	F	CACCATGCCTGGCTAATTTT	58
		R	CTGTCGTCCCAGCACTTTG	

2.8 IMMUNOHISTOCHEMISTRY

2.8.1 Solutions

All solutions, apart from 4% PFA which was stored at -20°C, were made fresh for each experiment and were dissolved by placing on a roller for at least 20 minutes, at room temperature.

Table 2.12– Buffers and solutions used for immunofluorescence staining

Buffer	Component	w/v or v/v	Supplier	Product number
4% PFA	PFA	4g	SIGMA	P-6148
	PBS	100ml	GIBCO	14190
8% goat serum	Goat serum	8ml	SIGMA	G9023
	PBS	92ml	GIBCO	14190
8% rabbit serum	Rabbit serum	8ml	SIGMA	R9133
	PBS	92ml	GIBCO	14190
0.1% Triton X-100	Triton X-100	10µl	SIGMA	T-8532
	PBS	990µl	GIBCO	14190
1% serum wash buffer	Goat serum	0.5ml	SIGMA	G9023
	Tween-20	50µl	SIGMA	P-5927
	PBS	49.5ml	GIBCO	14190

2.8.2 Cell preparation for immunofluorescence staining

Cells from confluent culture flasks were washed with PBS, trypsinised and centrifuged to obtain a cell pellet. The pellets were re-suspended in an appropriate medium, and cells were seeded in 8-chamber glass slides (NUNC: 177402) at a density of $1.7x10^4$ cells/chamber. The slides were placed in a 37°C incubator for 2-3 days. Once they were 70-80% confluent, the cells were fixed by treatment with 200µl of 4% PFA per chamber, for 20 minutes at room temperature. The PFA was aspirated, cells were washed twice in 200µl PBS per chamber and were then stored at 4°C until needed for staining. To ensure good quality staining, the slides were used within one week of cell fixation.

2.8.3 Immunofluorescence staining

Cells fixed in 4% PFA were removed from 4°C and were washed twice in PBS, for 5 minutes at room temperature. Cells were then incubated in 100µl of permeabilisation solution (0.1% TritonX-100 in PBS), for 15 minutes at room temperature, and were washed again in PBS

as before. Following permeabilisation, the cells were incubated in blocking solution (8% goat serum in PBS for antibodies raised in mouse or rabbit, 8% rabbit serum for antibodies raised in goat; Table 2.13), for 1 hour at room temperature, and were then washed once in PBS, for 5 minutes, at r. t. After this, cells were incubated in primary antibody diluted in 2% goat or rabbit serum, overnight at 4°C. The following day, cells were washed 4 times in 1% serum wash buffer, for 10 minutes at r.t., incubated in 100µl secondary antibody diluted in 2% goat or rabbit serum (Table 2.13), for 1 hour at r.t, and washed again in 1% serum wash buffer as before. The chambers were finally removed from the glass slides, a small amount of Vectashield Mounting Medium with DAPI (Vector Laboratories: H-1200) was placed over the area where each chamber used to be, and a glass coverslip was placed over the glass slides. The slides were sealed with nail varnish and were stored at 4°C, in the dark. Image acquisition was carried out using a Nikon ECLIPE 90i Fluorescence Microscope, a Hamamatsu 1394 ORCA-285 Digital Camera and Volocity 5 Improvision software.

Table 2.13- Antibodies used for immunofluorescence staining

Primary antibody	Supplier	Dilution	Secondary antibody	Supplier	Dilution
OCT4	Santa Cruz; SC-5279	1:200	goat anti-mouse AlexaFluor® 633	Invitrogen; A21052	1:400
SSEA4	Millipore; MAB4304	1:50			
TRA-1-81	Millipore; MAB4381	1:50			
FSA	Abcam; ab11333	1:750			
P4HB	Abcam; ab44971	1:50			
β-III-tubulin	COVANCE; MMS-435P	1:1000			
AFP	SIGMA; A8452	1:1000			
Cardiac α-actinin	SIGMA; A7811	1:800			
DNMT1	NEB; M0231S	1:100	goat anti-rabbit AlexaFluor® 633	Invitrogen; A21071	1:400
DNMT3A	Abcam; ab4897	1:400			
DNMT3L	Abcam; ab3493	1:200			
LIN28	Abcam; ab462020	1:1500			
REX1	Abcam; ab50828	1:50			1:200
Cardiac Troponin-I	Spectral Diagnostics; PA-1010	1:1000			
SOX2	R&D Systems; AF2018	1:200	rabbit anti-goat AlexaFluor® 568	Invitrogen; A11079	1:400
NANOG	R&D Systems; AF1997	1:50			
DNMT3B	Santa Cruz; SC-10236	1:250			
KLF4	R&D Systems; AF3640	1:100			1:200

2.8.4 Haematoxylin staining

Immunohistochemical analysis by haematoxylin staining was performed as described previously (Burridge *et al.*, 2007), with kind help from Miss Maria Barbadillo-Mũnoz. EBs were pelleted, fixed with 4% PFA for 15 minutes, washed twice in PBS, and set in 1% agarose. EBs were then processed overnight, in a Shandon Excelsior tissue processor (Thermo scientific), and embedded in paraffin wax (Tissue-Tek II embedding wax). Wax blocks were sliced in 5µm sections, using a microtome, and slices were affixed to clean glass slides (SuperFrost Plus, Menzel-Glaser: J1800AMNZ). The slices were de-waxed by treatment with Bond Dewax solution (Leica: AR9222), rehydrated through an ethanol/water gradient, stained with Harri's-Haematoxylin (VWR: 95057-858), and finally mounted with DePEX mounting medium (VWR: 10140-638). Staining was performed using BOND-MAX system and reagents (Leica). Image acquisition was carried out using a Nikon ECLIPE 90i Microscope and Volocity 5 Improvision software.

Table 2.14- Antibodies used for EB haematoxylin staining

Primary antibody	Supplier	Dilution	Secondary antibody	Supplier	Dilution
NANOG	R&D Systems; AF1997	1:100	Bond Polymer Refine Detection	Leica; DS9800	1:200
SOX2	R&D Systems; AF2018	1:600			
Brachyury (T)	R&D Systems; AF2085	1:200			
KLF4	R&D Systems; AF3640	1:100			
DNMT3B	Santa Cruz; SC-10236	1:1000			
OCT4	Santa Cruz; SC-5279	1:200	HRP anti-goat IgG	Vision BioSystems; DS9800	
TRA-1-81	Millipore; MAB4381	1:200			
REX1	Abcam; ab50828	1:50			

2.9 WESTERN BLOTTING

2.9.1 Buffers and solutions

Table 2.15– Sample Lysis buffer for protein extraction from animal cells

Reagent	Supplier	Final conc.	Mass / volume
Tris Base pH 7.5	Fisher Scientific; BP152-1	50mM	5ml of 500mM
NaF	SIGMA; 57920	50mM	5ml of 500mM
B-glycerophosphate	SIGMA; G6376	50mM	2.5ml of 1M
Sodium orthovanadate	SIGMA; S6508	10mM	500ul of 1M

Triton X-100	SIGMA; T8532	1% (v/v)	500ul
Water	SIGMA; W4502	-	36.5ml

Table 2.16- 2x SDS sample buffer for protein loading onto acrylamide gels

Reagent	Supplier	Final conc.	Mass / volume
Tris Base pH 6.8	Fisher Scientific; BP152-1	100mM	1ml of 1M
DTT	Fisher Scientific; BP172-5	200mM	2ml of 1M
SDS	SIGMA; L4390	4% w/v	2ml of 20%
Glycerol	SIGMA; G6376	20% w/v	2ml of 100%
Bromophenol Blue	SIGMA; B6126	0.2% w/v	1ml of 2%
Water	SIGMA; W4502	-	10ml

Table 2.17– Resolving and Stocking gels for polyacrylamide gel electrophoresis

Reagent	Supplier	6% Resolving gel	5% Stocking gel
SDW	SIGMA; W4502	7.9ml	3.425ml
30% acrylamide	Severn Biotechnology; 202100-05	3ml	830µl
1.5M Tris pH 8.8	Fisher Scientific; BP152-1	3.8ml	-
1M Tris pH 6.8	Fisher Scientific; BP152-1	-	630µl
10% SDS	SIGMA; L4390	150µl	50µl
10% APS	Fisher Scientific; BP179-100	150µl	50µl
TEMED	Fluka Biochemika; 87689	12µl	5µl

Table 2.18– 10x Electrophoresis buffer for western blotting

Reagent	Supplier	Final conc.	Mass / volume
Tris Base	Fisher Scientific; BP152-1	0.2M	30.3g
Glycine	SIGMA; 241261	1.92M	144g
SDS	SIGMA; L4390	50mM	10g
SWD	-	-	to 1L

Table 2.19– 10x Transfer buffer for western blotting

Reagent	Supplier	Final conc.	Mass / volume
Tris Base	Fisher Scientific; BP152-1	0.25M	36.3g
Glycine	SIGMA; 241261	2.4M	181.25g
SWD	-	-	to 1L

2.9.2 Protein extraction from animal cells

Cell lysates were prepared from animal cells by treatment with sample Lysis buffer (Table 2.15), which was supplemented with 1mM PMSF (SIGMA; 93482) and Protease Inhibitors (Roche; 11873 580 001) immediately before use. 10µl of Lysis buffer were used per 1 million cells, and incubation was allowed to occur for 5 minutes, on ice. The samples were then centrifuged at 800xg for 5 minutes, at 4°C, and the supernatants were transferred to

clean Eppendorf tubes. Pelleted insoluble membranes and genomic material were discarded. Protein samples were quantified *via* the Bradford assay using an Eppendorf Bio Photometer, and were then mixed with 1x volume of 2x SDS sample buffer (Table 2.16), which had previously been heated to 95°C on a heating block. The samples were placed on a 95°C heating block for 5 minutes to denature proteins for polyacrylamide gel electrophoresis, and were finally stored at -20°C.

2.9.3 Polyacrylamide gel electrophoresis

6% polyacrylamide resolving gels were prepared as described in Table 2.17, in an omniPAGE Mini vertical gel electrophoresis system (Cleaver Scientific; VS10D). TEMED was added to the gel immediately before casting into the tank. The gel was layered with isopropanol so that it set evenly. After 15 minutes, the isopropanol was washed away. An appropriate comb was placed on top of the resolving gel, and stacking gel was used to form the wells. The stacking gel was allowed to set for 15 minutes, after which the combs were removed and the gels were assembled in the tank. 750ml of 1x electrophoresis buffer were added to the tank and the gels were loaded with 30µg of protein per well. 6µl of pre-stained protein marker (NEB; P7708) were added to one of the wells to determine protein size. The gels were run at 125V for 90 minutes, or until the dye front reached the bottom.

2.9.4 Protein transfer to nitrocellulose membrane and immunoblotting

10x Transfer buffer (Table 2.19) was diluted 1:10 and supplemented with 20% methanol, to make 1x Transfer buffer. 0.45µm Hybond-ECL Nitrocellulose membrane (Amersham Biosciences; 7040096), as well as 3M blotting paper were cut in 8x8cm pieces and were soaked in 1x Transfer buffer for 15 minutes. The polyacrylamide gels were removed from the electrophoresis tanks and disassembled. The electrophoretically separated proteins were transferred to the nitrocellulose membrane by a wet transfer system, in 2L of 1x Transfer buffer. The transfer was allowed to occur for 70 minutes, at 110V.

Following transfer, the membranes were incubated in blocking solution (5% skimmed milk in PBS) for 1 hour, at r.t., and were then treated with primary antibody diluted to the appropriate concentration (Table 2.20) in 0.02% Tween-20 in PBS (PBS-T), for 12 hours, at 4°C, on a rocking platform. The primary antibody was removed and the membranes were washed 3x in PBS-T for 5 minutes per wash, at r.t. They were then incubated in secondary antibody (Table 2.20) diluted in PBS-T, for 1 hour at r.t., on a rocking surface. The membranes were washed as before, and developed using the EZ-ECL™ chemiluminescence detection kit for HPR (Biological Industries; 20-500-120), according to the manufacturer's instructions. Imaging was performed using a LAS4000 system (Fujifilm), and protein expression was quantified using AIDA V.4.15 2D densitometry software.

Table 2.20– Antibodies used for western blotting

Primary antibody	Supplier	Dilution	Secondary antibody	Supplier	Dilution
α-Tubulin	Calbiochem; CP06	1:2000	HPR anti-mouse	Cell Signalling; 7076	1:200
DNMT1	NEB; M0231S	1:2000	HPR anti-rabbit	Cell Signalling; 7074	1:200
DNMT3A	Abcam; ab4897	1:200			

2.10 BACTERIAL CLONING

2.10.1 Buffers and Media

All buffers and media were autoclaved before use

Table 2.21– Composition of buffers media used for bacterial cloning

Buffer / Medium	Component	w/v or v/v	Supplier	Product number
LB broth	LB broth powder	6.25g	Fisher Scientific	BPE1426
	SDW	250ml	N/A	N/A
LB agar	LB broth powder	6.25g	Fisher Scientific	BPE1426
	Agar	3.75g	Fisher Scientific	BPE1423
	SDW	250ml	N/A	N/A
Oligo annealing buffer	Potassium acetate	100mM	Fluka BioChemika	60035
	HEPES pH 7.4	30mM	SIGMA	H-1016
	Magnesium acetate	2mM	Fluka BioChemika	63052

SOC medium	Tryptone	20g	Fisher Scientific	BPE1421
	Yeast extract	5g	Fisher Scientific	BP1422
	5M NaCl	2ml	Fisher Scientific	S/3160/63
	1M KCl	2.5ml	BDH	101985M
	1M $MgCl_2$	10ml	Fisher Scientific	M/0600/53
	1M $MgSO_4$	10ml	SIGMA	M7506
	1M glucose	20ml	Fisher Scientific	G/0500/53
	SDW	to 1L	N/A	N/A

2.10.2 Restriction Enzyme Digestion

All digests were performed in a final volume of 25µl, using the buffer recommended by the manufacturer for each restriction enzyme and RNase/ DNase free water (SIGMA: W-4502). 0.5µl of restriction enzyme were used to catalyse the digestion of 1µg DNA. The digests were performed at 37°C, for 2 hours. All digest products were passed through QIAquick Gel Extraction columns, even if not electrophoresed on an agarose gel. This was done to ensure separation of fragments excised by restriction digestion form the remaining plasmid.

2.10.3 Oligo cloning into plasmids

Single stranded complementary oligos were mixed at a 1:1 concentration (2µl each) and were added to 48µl of annealing buffer. In order to anneal to each other, the oligos were heated to 95°C for 4 minutes, then to 70°C for 10 minutes, and were finally left to cool down to room temperature. 1 or 3µl of annealed oligos were then mixed with 1µg plasmid DNA, which had been digested with restriction enzymes compatible to the oligo ends. Following this, oligos were ligated into the plasmid using 0.5µl ligase enzyme (Quick Ligation Kit; NEB: M2200S). Ligation was allowed to occur for 5 minutes at room temperature and was followed by transformation of competent *E. coli* bacterial cells.

2.10.4 Transformation of *E.coli* DH5α competent cells

LB agar was melted in a microwave oven and left to cool down to 50°C. 50mg/ml ampicillin were added to the agar which was then aliquoted to 90mm Petri dishes. The agar was left to

set for ~20 minutes at room temperature, and was then placed in a 37°C oven for 1 hour. 50µl *E.coli* Subcloning Efficiency DH5α Competent Cells (Invitrogen: 18265-017) were thawed on ice, and mixed with 1µg plasmid DNA. The cells were incubated on ice for 30 minutes, heat-shocked at 42°C for 45 seconds and finally placed on ice for 3 minutes. They were then mixed with 200µl SOC medium and placed in a 37°C shaking incubator for 1 hour. When the cells were removed from the shaking incubator, they were spread on LB agar which was set in 90mm Petri dishes, using a sterile technique. The dishes were inverted and placed in a 37°C oven for at least 16 hours.

The following day, single bacterial colonies were picked from the Petri dishes, added to 2ml SOC medium (supplemented with 50mg/ml ampicillin) in 20ml Universal tubes, and placed in a 37°C shaking incubator for up to 12 hours. A mini-prep of the amplified DNA was performed after this (section 2.10.5). If a DNA midi-prep was required (section 2.10.5), single bacterial colonies were added to 1ml SOC medium in 20ml Universal tubes, and placed in a 37°C shaking incubator for 5-6 hours. Following this, the cell suspension was added to a further 40ml of SOC medium, and placed in the shaking incubator overnight.

2.10.5 Plasmid purification by Mini, Midi and maxi preps

Plasmid Midi and Maxi-preps were performed using the QIAfilter Plasmid Midi or Maxi Kit (QIAGEN: 12243 and 12262 respectively), according to the manufacturer's instructions, pg16-20 of the QIAfilter Plasmid Purification Handbook, onwards from step 4. After precipitation (step 14), samples were eluted in 100µl of sterile distilled water for midi-preps and 330µl for maxi-preps, and placed on a 65°C heat-block for 15 minutes. They were then quantified using a NanoDrop spectrophotometer and stored at -20°C.

Mini-preps were performed using the QIAprep Spin Mini Prep Kit (QIAGEN: 27104), according to the manufacturer's instructions, pg22-23 of the QIAprep Miniprep Handbook. Samples were eluted in 50µl of sterile distilled water in the final step.

2.11 STATISTICAL ANALYSIS

Numerical results are presented as mean values of experimental replicates, ± the standard error of the mean, as calculated using Microsoft Excel 2007. Statistical analysis was performed using NCSS 2007 software for Windows v7.1.15. Initially, the Kolmogorov-Smirnov test was performed on all data to determine whether the datasets were normally distributed. Since none of the data presented here were normally distributed ($p>0.05$), non-parametric analysis was used to statistically compare the data. The Kruskal-Wallis H test was used for analysis of non-parametric independent data-groups, with the null hypothesis (H_0) that there was no significant difference between the median values of the samples analysed, and alternative hypothesis (H_a) that the median values differed between samples. Tests were performed at a significance level of 0.05. Where a statistically significant result ($p<0.05$) was returned, the H_0 was rejected and pair-wise comparisons using the Mann-Whitney's U test were performed to identify the samples that caused rejection of H_0. Differences between sample distributions in each experiment were also demonstrated using non-parametric box plots (Figure 2.3; Appendix IV; Williamson *et al.* 1989; Donnelly 1992).

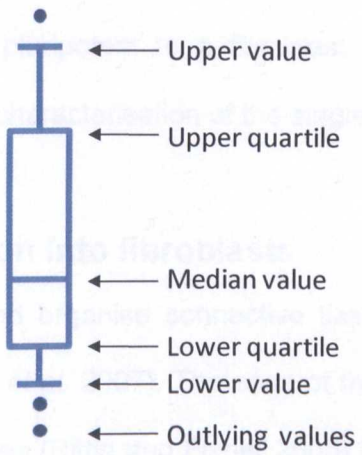

Figure 2.3– Box plot graph
A box plot graph shows the lowest and highest observations/values in a sample, the median value, the lowest 25% and highest 25% of observations (lower and upper quartiles), outlying observations, as well as the dispersion and skewness of the data. The box plot makes no assumption about the distribution of the data and is, therefore, a non-parametric plot.

3 GENERATION OF A SINGLE-GENOTYPE MODEL CELL SYSTEM FOR THE INVESTIGATION OF PHENOTYPE TRANSITION MECHANISMS

3.1 INTRODUCTION

To achieve the aims of this project, a model cell system was generated, by using cultures of the HUES7 hESC line as the starting point from where fibroblast and iPSC lines were derived. All cell lines in the model system shared the same genotype, hESCs and iPSCs were cultured using the same method, and fibroblast cells were derived and cultured using the same protocol. This was performed in order to eliminate genotype and culture-induced variation among cell lines of the model system and enable unbiased characterisation of the epigenetic mechanisms associated with transcription factors that are key in regulating phenotype transition from a pluripotent to a fibroblast differentiated state. This chapter describes the generation and characterisation of the single-genotype model cell system.

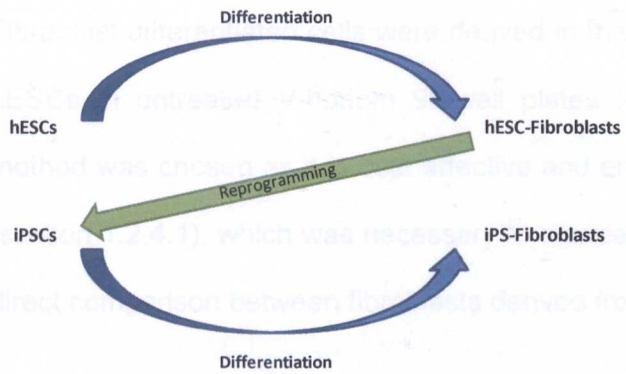

3.1.1 hESC differentiation into fibroblasts

Fibroblast cells synthesise and organise connective tissue in a number of adult organs, including the skin (dermis; He *et al.* 2007). The ease of their isolation from the human body using non-invasive skin biopsies (Rittie and Fisher 2005) has made fibroblasts an attractive differentiated lineage for reprogramming by over-expression of defined TFs (see Table 3.2). Using *in vitro*-derived fibroblasts as a reprogramming starting point represents an appropriate model for patient-derived primary cells, which would ease the transfer of

experimental findings to potential clinical application. hESCs were, thus, differentiated to fibroblasts in this thesis.

3.1.1.1 Method used for fibroblast derivation

Fibroblasts are a very diverse cell type and can arise either from the mesenchyme tissue or the ectoderm through epithelial to mesenchymal transition (Dennis and Charbord 2002; Kalluri and Neilson 2003). *In vitro*, cells with a fibroblast-like morphology (spindle-like long, flat cells with elongated nucleus) can be derived from hESCs by 1-3 passages following differentiation *via* EB formation, in the absence of a specific growth factor (Xu *et al.* 2004). Fibroblast differentiated cells were derived in this thesis using forced aggregation of 10,000 hESCs in untreated V-bottom 96-well plates (Burridge *et al.* 2007). This differentiation method was chosen as it is cost effective and enables formation of EBs with a defined size (section 1.2.4.1), which was necessary to standardise differentiation procedures and enable direct comparison between fibroblasts derived from hESCs and iPSCs.

3.1.1.2 Characterisation of hESC-derived fibroblasts

In order to confirm the identity of hESC and iPSC-derived fibroblasts, appropriate fibroblast-specific markers had to be used. However, since fibroblasts are a very diverse cell-type, showing slightly different characteristics in each organ they reside (e.g. skin, liver, muscle, kidney, lungs) identification of appropriate fibroblast-specific markers is a difficult task (Annunen *et al.* 1997; Oh *et al.* 2004; He *et al.* 2007).

Phenotype characterisation of hESC-derived fibroblasts has included staining with a range of human mesenchymal stem cell (hMSC) surface markers, such as CD29 (integrin-β1), CD44 (surface glycoprotein), CD71 (transferring receptor), CD90 (Thy-1) and CD106 (VCAM-1; Pittenger *et al.* 1999; Xu *et al.* 2004; Stojkovic *et al.* 2005). Vimentin and prolyl-4-hydroxylase B (P4HB) have also been used to characterise hESC-derived fibroblasts (Wang *et al.* 2005); vimentin is a marker detected in a number of cells with mesenchymal origin,

and can also be found in astrocytes, Sertoli cells, and vascular smooth muscle (Moll *et al.* 1982), while P4HB is a cytoplasmic marker involved in collagen formation (Kivirikko *et al.* 1989) that has only been detected, thus far, in fibroblast cells (Annunen *et al.* 1997; Oh *et al.* 2004; He *et al.* 2007). Therefore, aside from P4HB, the markers used to characterise ESC-derived fibroblast cells have a broad specificity.

Surface markers, such as 1B10 (also known as fibroblast surface antigen, FSA) and AS02, have been used to characterise primary fibroblast cells and eliminate contaminating fibroblasts from other thymic epithelial and thyrocyte cell cultures (Esterre *et al.* 1992; Saalbach *et al.* 1996; Saalbach *et al.* 1997; Saalbach *et al.* 1998). Of these, only FSA is commercially available, but has not been studied in hESC-derived fibroblasts. Therefore, the most appropriate fibroblast-specific markers for use in this thesis were P4HB and, possibly, FSA.

3.1.2 Differentiation of hESCs and iPSCs to the three embryonic germ layers

The ability of hESCs and TRA-1-81 positive iPSCs to differentiate to the three embryonic germ layers; endoderm, mesoderm and ectoderm, was assessed by *in vitro* differentiation in this thesis. *In vitro* differentiation has been used in several studies to confirm pluripotency of hESCs (Shamblott *et al.* 1998; Reubinoff *et al.* 2000; Odorico *et al.* 2001), but has a disputed stringency because it does not demonstrate *in vivo* differentiation (Maherali and Hochedlinger 2008). Formation of tissue representative of the three germ layers in teratomas (Thomson *et al.* 1998; Reubinoff *et al.* 2000) is thought to be a more stringent test, because differentiation is demonstrated *in vivo* (see Table 3.1). However, teratoma formation does not test the ability of cells to promote normal development (Jaenisch and Young 2008). It is also a non-quantitative test, that requires expert skills (Daley *et al.* 2009), whose stringency has somewhat been challenged from evidence that teratoma

characteristics vary greatly according to the type of tissue used to drive them (Miura *et al.* 2009). On the other hand, *in vitro* differentiation is simpler and allows quantification of germ layer formation by real-time PCR (Mahlstedt *et al.* 2009). The ability to demonstrate formation of beating cardiomyocytes by *in vitro* differentiation also contradicts the argument that this method does not show formation of functional cell types (Jaenisch and Young 2008). For these reasons, *in vitro* differentiation was the method of choice in this study for demonstrating formation of the three embryonic germ layers from hESCs and iPSCs.

Table 3.1- Methods used to test the developmental potential of mouse and human pluripotent cells (adapted from Jaenisch and Young 2008)

Species	Assay	Experimental approach	Limitations
Human & mouse	*In vitro* differentiation	Differentiation of cultured cells followed by assay for the expression of cell-type specific markers	Differentiation not *in vivo*
	Teratoma formation	Injection into immunodeficient mice results in tumour formation that demonstrates differentiation into various cell types and lineages	Does not demonstrate the ability for normal development
Mouse	Chimera formation	Injection into host blastocyst demonstrates ability to support normal development	Autologous cells in chimera may complement for defects in injected cells
	Germline contribution	Ability to generate functional germ cells	Does not account for epigenetic defects that could affect development
	Tetraploid complementation	Injection into a 4n blastocyst which cannot contribute to somatic lineages results to embryo composed exclusively by injected cells	Most stringent test, but does not assess ability to form trophectoderm

3.1.3 Methods and cell types used to generate iPSCs

Since 2006, several methods other than retroviral transduction have been employed to achieve over-expression of the four "iPSC factors" (*OCT4*, *SOX2* and either *KLF4* and *c-MYC* or *NANOG* and *LIN28*, summarised in Table 3.2). These methods either aimed in improving the efficiency of iPSC generation (lentiviral transduction) or eliminate the risk of insertional mutagenesis due to retroviral or lentiviral DNA integration into the host-genome (adenoviral transduction, use of plasmids, transposons, episomal vectors and recombinant proteins). However, integration-free techniques have suffered from very low reprogramming efficiencies, or limited success in hESCs compared to mESCs (Table 3.2).

Several differentiated cell types, other than fibroblasts, have been used to generate iPSCs, including stomach, liver, cord blood, and mature B cells (Aoi *et al.* 2008; Hanna *et al.* 2008; Haase *et al.* 2009). Nevertheless, iPSCs generated from different cell-types show differences in their transcriptional profiles, mostly due to residual expression of donor cell-type specific genes (Ghosh *et al.* 2010). Transcription factor-induced reprogramming has also crossed the human and mouse species barriers, as it was used successfully to generate iPSCs from swine, rat and monkey fibroblasts (Liu *et al.* 2008a; Liao *et al.* 2009a; Roberts *et al.* 2009; Wu *et al.* 2009b), opening further possibilities for disease modelling (Esteban *et al.* 2010).

3.1.3.1 iPSC-generation system used in this thesis

One of the aims of this thesis was to investigate the mechanisms associated with reactivation of key pluripotency genes during the formation of iPSCs. Early reprogramming time-points had to be analysed, in order to study the epigenetic changes associated with the transition of cell phenotype from a differentiated to a pluripotent state. To increase the possibility of detecting these changes, the most efficient method available for the generation of iPSCs from fibroblast cells, i.e. lentiviral transduction, (Table 3.2) was used in this study. Since the use of iPSCs generated in this study was restricted to research purposes, avoiding integration of viral DNA into the host genome was of a lesser significance. At the point when this method was selected, lentivirus-mediated generation of iPSCs had only been achieved using over-expression of the TFs *OCT4*, *NANOG*, *SOX2* and *LIN28* (Yu *et al.* 2007b). Therefore, these four factors were used instead of the *OCT4*, *SOX2*, *KLF4* and *c-MYC* TF combination (Okita *et al.* 2007). A protocol for efficient genetic modification using lentiviral vectors had to be established before generating iPSCs, since neither lentiviral transduction nor iPSC formation had been performed in our lab previous to this thesis.

Table 3.2– Strategies used for iPSC generation
O= OCT4, S= SOX2, K= KLF4, C= c-MYC, N= NANOG, L= LIN28, E= embryonic, F= foetal, NB= newborn, A= adult

	Vector	Transgenes	Cell type	Efficiency (%)	References
Mouse	Retrovirus	OSKC	MEFs	0.01-0.5	Meissner *et al.* 2007; Wernig *et al.* 2007; Huangfu *et al.* 2008a; Okita *et al.* 2008
			Hepatocytes	1-3	Aoi *et al.* 2008
			Gastric epithelia	1-3	
			B cells	0.01-0.1	Hanna *et al.* 2008
			β-cells	0.1-0.2	Stadtfeld *et al.* 2008a
			Neural stem cells	3-5	Eminli *et al.* 2008; Kim *et al.* 2008b
		OSK	MEFs	0.001-0.01	Huangfu *et al.* 2008a; Nakagawa *et al.* 2008; Wernig *et al.* 2008a
			Hepatocytes	0.5-1	Aoi *et al.* 2008
			Neural stem cells	0.1-1	Kim *et al.* 2008b
		OKC or OSC		0.1-1	Eminli *et al.* 2008; Kim *et al.* 2008b
		OK or OS		0.1-0.2	Kim *et al.* 2008b
		O		0.014	Kim *et al.* 2009c
	Lentivirus	OSKC	MEFs	0.03-1	Brambrink *et al.* 2008; Stadtfeld *et al.* 2008b; Shao *et al.* 2009
	Adenovirus	OSKC	MEFs	0	Stadtfeld *et al.* 2008c
			Hepatocytes	0.001-0.0001	
	Plasmid	OSKC	MEFs	0.001-0.0001	Okita *et al.* 2008
	Lentivirus + Cre	OSKC	Dermal fibroblasts (A)	N/A	Chang *et al.* 2009a
	Plasmids + Cre	OSKC	MEFs	0.001-0.0001	Kaji *et al.* 2009
	piggyBac transposon	OSKCL		0.01	Woltjen *et al.* 2009; Yusa *et al.* 2009
		OSKC		0.005	
	Transient transfection	OSKC		N/A	Okita *et al.* 2008; Gonzalez *et al.* 2009; Okita *et al.* 2010
	Protein	OSKC		0.00006	Zhou *et al.* 2009
Human	Retrovirus	OSKC	Dermal fibroblasts (F, NB, A)	0.001-0.01	Takahashi *et al.* 2007; Dimos *et al.* 2008; Park *et al.* 2008a
			Bone marrow MSCs	N/A	
		OSK	Fibroblasts (NB, A)	0.001-0.01	Huangfu *et al.* 2008b; Nakagawa *et al.* 2008
		OS	Fibroblasts (NB)	0.001-0.004	
		OK	Neural stem cells	0.01	Hester *et al.* 2009
		O		0.004	Kim *et al.* 2009b
	Lentivirus	OSNL	Dermal fibroblasts (E, NB, A)	0.01-0.1	Yu *et al.* 2007b; Ebert *et al.* 2009
		OSN or OSL		0.0001-0.001	
		OSNL	Cord blood	0.0003-0.03	Haase *et al.* 2009
		OSKC	Keratinocytes	0.00001	Carey *et al.* 2009
	Lentivirus + Cre	OSKC	Fibroblasts (A)	0.01	Soldner *et al.* 2009
		OSK		0.005	
	Episomal vectors	OSCKNL & SV40LT	Foreskin fibroblasts (NB)	N/A	Yu *et al.* 2009
	Protein	OSKC	Fibroblasts (NB)	0.001	Kim *et al.* 2009a
	Minicircle-DNA	OSNL	Adult adipose stem cells	0.005	Jia *et al.* 2010

3.1.3.2 Genetic modification of human cells by lentiviral transduction

Viruses are parasitic organisms, highly evolved in their ability to transduce host cells, and can therefore efficiently deliver target DNA within them (Patil *et al.* 2005). Adenoviruses, retroviruses, and adeno-associated viruses have been used both in research and clinical

trials to transduce host cells (reviewed in Somia and Verma 2000; Patil *et al.* 2005). However, retroviral-based vectors are one of the most desirable tools for transgene delivery as they enable transduction of some of the most resistant cell lines (Garton *et al.* 2002; Merten 2004). Retroviruses are single-stranded RNA viruses which replicate by transducing host cells and reverse transcribing their genome into double-stranded DNA that becomes integrated into the host genome in a random location (Nisole and Saib 2004). Viral RNA is transcribed along with the host genome during the lifetime of the cell, thus enabling new viral particles to be assembled within host cells in a capsid and membranous envelope (Blesch 2004). The basic retroviral genomic organisation consists of a packaging signal (ψ), 3' and 5' long terminal repeats (LTRs) that contain promoter, enhancer and viral integration sequences, and the poly-proteins *gag*, *pol* and *env* which are required for viral replication and packing (Figure 3.1; Somia and Verma 2000).

A subfamily of retroviral vectors, known as lentiviruses, has been shown to possess several advantages over other family members. Lentiviruses are capable of infecting both dividing and non-dividing cells, their genome shows high resistance to transcriptional silencing once integrated into the host genome, they have low immunogenicity (reviewed by Park 2007) and can accommodate the use of many ubiquitous or tissue-specific promoters (Follenzi and Naldini 2002; Georgiades *et al.* 2007). Their basic genomic organisation is similar to that of other retroviruses, but they also possess several accessory genes, such as *vif*, *vpr*, *vpu*, *nef*, *tat* and *rev*, some of which are crucial for replication and pathogenesis (Buchschacher and Wong-Staal 2000). Lentiviruses can be engineered to avoid an immune response by the host genome through removal of their non-essential regulatory genes (Blesch 2004), something that also allows for safer experimentation with lentiviruses. Based on the number of non-essential genes removed from their genome, lentiviral vectors are categorised to 1st, 2nd, and 3rd generation systems, with increasing safety being introduced at each generation (Blesch 2004).

Lentiviral particles can be assembled *in vitro* by transfection of HEK293 cells (known as a "viral-packaging cell line") with three plasmids; a packaging, a transfer, and an envelope-coding plasmid (Figure 3.1.B; Naldini *et al.* 1996). Essential viral genes are divided among these three plasmids so that the viral particles generated in HEK293 cells are replication defective (Somia and Verma 2000). This measure improves the safety of experimentation with lentiviruses further. Once packaged, the viral particles are titered form HEK293 cells and used for transduction experiments, to generate stable transgenic cell lines (Suter *et al.* 2006; Xia *et al.* 2008).

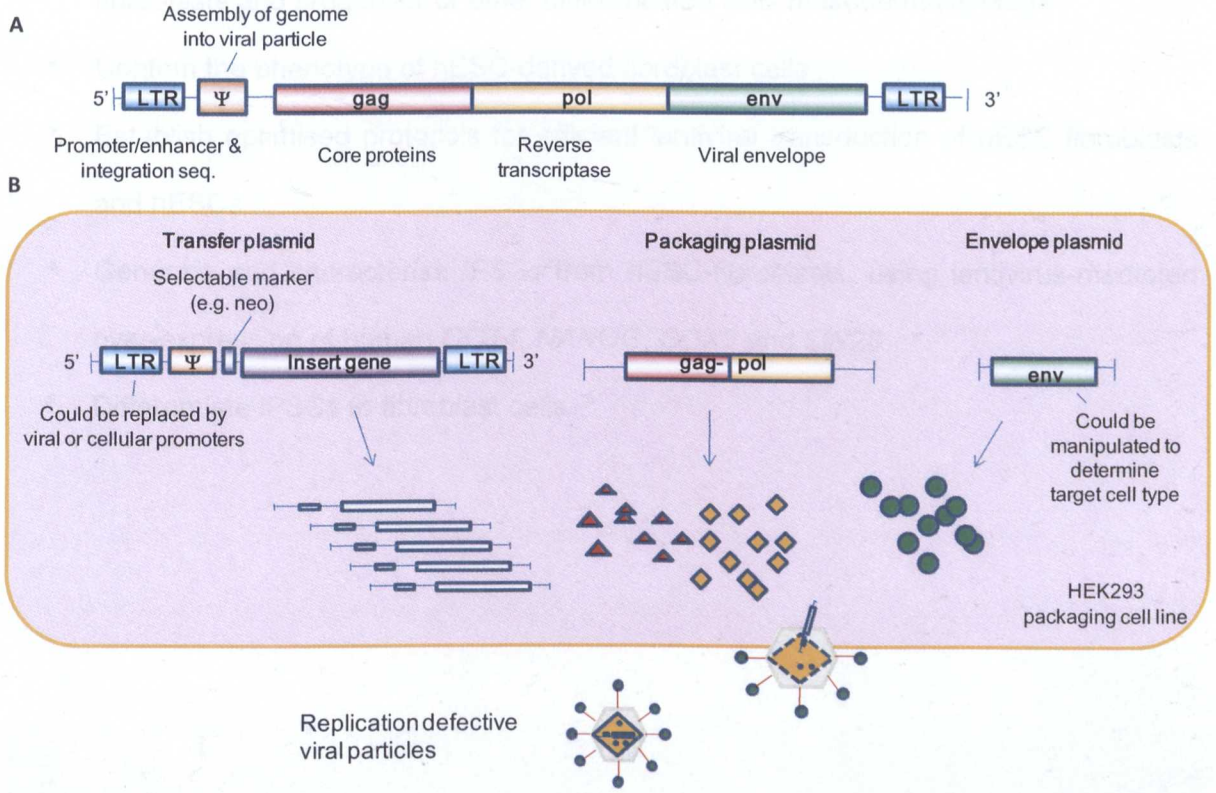

Figure 3.1– *In vitro* assembly of lentiviral particles
A. Basic genome organisation of retroviral and lentiviral vectors, consisting of two long terminal repeats (LTR) on either end of the genome, a ψ (psi) sequence; necessary for genome assembly into viral particles, and gag, pol and env genes; required for viral replication and packaging. **B.** Construction and packaging of viral particles in a HEK293 "packaging cell line". The viral genes are divided in separate vectors in order to enable the generation of replication defective viral particles (Adapted from Somia and Verma 2000).

3.1.4 Chapter Aims and Objectives

The aim of this chapter was to generate the cell types involved in the model system described in Figure 1.1. For this purpose, the following objectives had to be met:

* Establish and characterise cultures of two hESC lines; HUES7 and the clonal variant HOGN, which carried an *OCT4*-targeted *IRES-GFP-IRES-Neo* cassette and would enable identification of endogenous *OCT4* reactivation during iPSC formation
* Differentiate the two hESC lines into fibroblast-like cells
* Assess for the ability of putative fibroblast-specific markers to distinguish between fibroblasts and progenitor or other differentiated cells mesodermal lineage
* Confirm the phenotype of hESC-derived fibroblast cells
* Establish optimised protocols for efficient lentiviral transduction of hESC-fibroblasts and hESCs
* Generate and characterise iPSCs from hESC-fibroblasts, using lentivirus-mediated over-expression of human *OCT4*, *NANOG*, *SOX2* and *LIN28*
* Differentiate iPSCs to fibroblast cells

3.2 RESULTS

3.2.1 Culture and phenotype assessment of HUES7 hESCs

HUES7 hESCs (Cowan *et al.* 2004) were adapted, in our to lab, to feeder-free Matrigel™ culture in MEF conditioned medium (Denning *et al.* 2006). Cells were typically maintained in culture at low passages (passages 20 to 32) following their derivation from human embryos, in order to minimise karyotype instability and accumulation of mutations in the DNA, observed upon extended culture of many hESC lines (Draper *et al.* 2004; Baker *et al.* 2007; Spits *et al.* 2008). During this period, HUES7 cells appeared healthy (densely packed cells with angular cell walls, low cell death; Figure 3.2.C), and were typically passaged by 1:3 splits every 48 hours. The karyotype of HUES7 cells was normal (46,XY) at passage 22, according to analysis performed by Mr Nigel Smith, Nottingham City Hospital. In order to assess the ability of HUES7 to form derivatives of the three embryonic germ layers, cells were differentiated *via* EB formation by forced aggregation. EBs were seeded onto glass chamber slides on day 21 of differentiation, and fixed using 4% PFA in order to be used for immunofluorescence staining. Figure 3.3 demonstrates differentiation into ectoderm (expression the neural marker β-III-tubulin), endoderm (expression of the foetal kidney marker alpha-feto protein, AFP), and mesoderm (presence of α-actinin positive, beating cardiomyocytes; Carpenter *et al.* 2003; Zeng *et al.* 2004).

Figure 3.2- Culture of HUES7 hESCs
Bright field images of passage 22 HUES7 cells grown on a feeder-free Matrigel™ surface in MEF-conditioned medium, **A.** 8h, **B.** 24h and **C.** 48h following a 1:3 split. Scale bar represents 100μm.

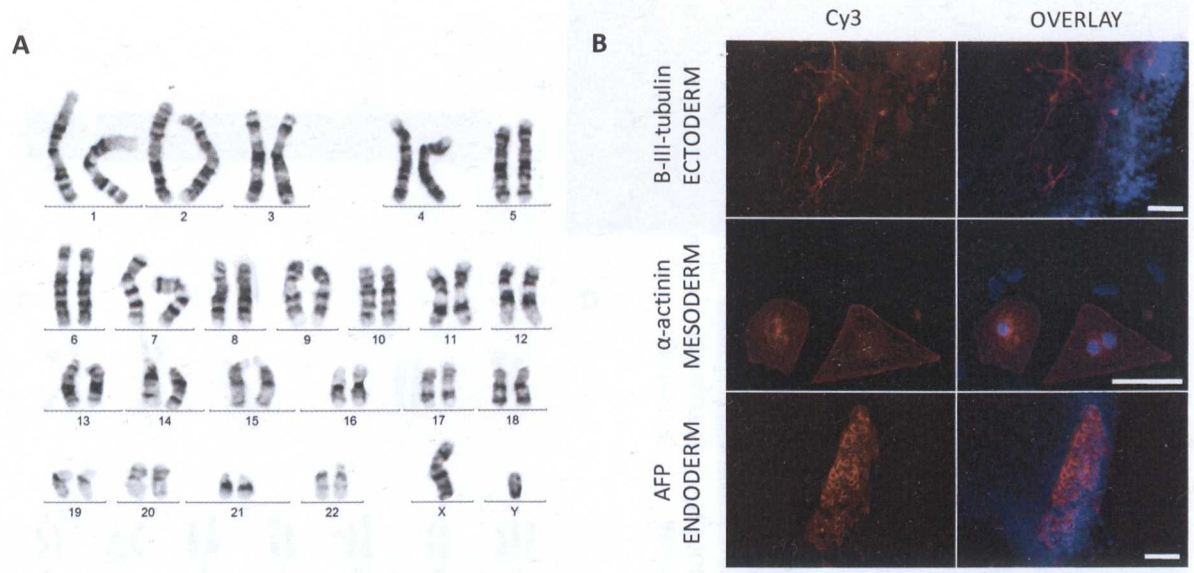

Figure 3.3– Karyotype and pluripotency of HUES7 hESCs
A. HUES7 cells grown on Matrigel had a normal 46,XY karyotype at passage 22. **B.** Differentiation of HUES7 cells to cell types representative of the three germ layers; ectoderm, mesoderm and endoderm indicated their pluripotent potential. Protein expression was captured using the Cy3 channel, while the overlay represents a merge of the DAPI (nuclear staining) and Cy3 channels. Scale bars represent 64μm.

3.2.2 Culture and phenotype assessment of HOGN hESCs

A transgenic HUES7 line, modified to carry gene targeted insertion of an *IRES-GFP-IRES-Neo* cassette immediately after the endogenous *OCT4* gene (Figure 3.4.A), was kindly provided for this study by Dr. Christine Mummery, Leiden University Medical Centre, The Netherlands (Braam *et al.* 2008b). In their undifferentiated state, the genetically modified cells, referred to as HOGN for HUES7-OCT4-GFP-Neomycin, were GFP positive (Figure 3.4.B) and showed resistance to neomycin (Figure 3.7; Braam *et al.* 2008b). HOGN were reported to have a normal karyotype after transfection and clonal growth (Braam *et al.* 2008b), but during culture scale-up, cells showed trisomy 12 and addition of chromosomal material to the small arm of chromosome 21, believed to have originated from chromosome 17 (Figure 3.4, Figure 3.6.C). Nevertheless, cells could differentiate to the three embryonic germ layers (Figure 3.4, Figure 3.6.D) and were used for further experiments as they comprised a good control system to monitor the expression of endogenous *OCT4* during differentiation and iPSCs generation.

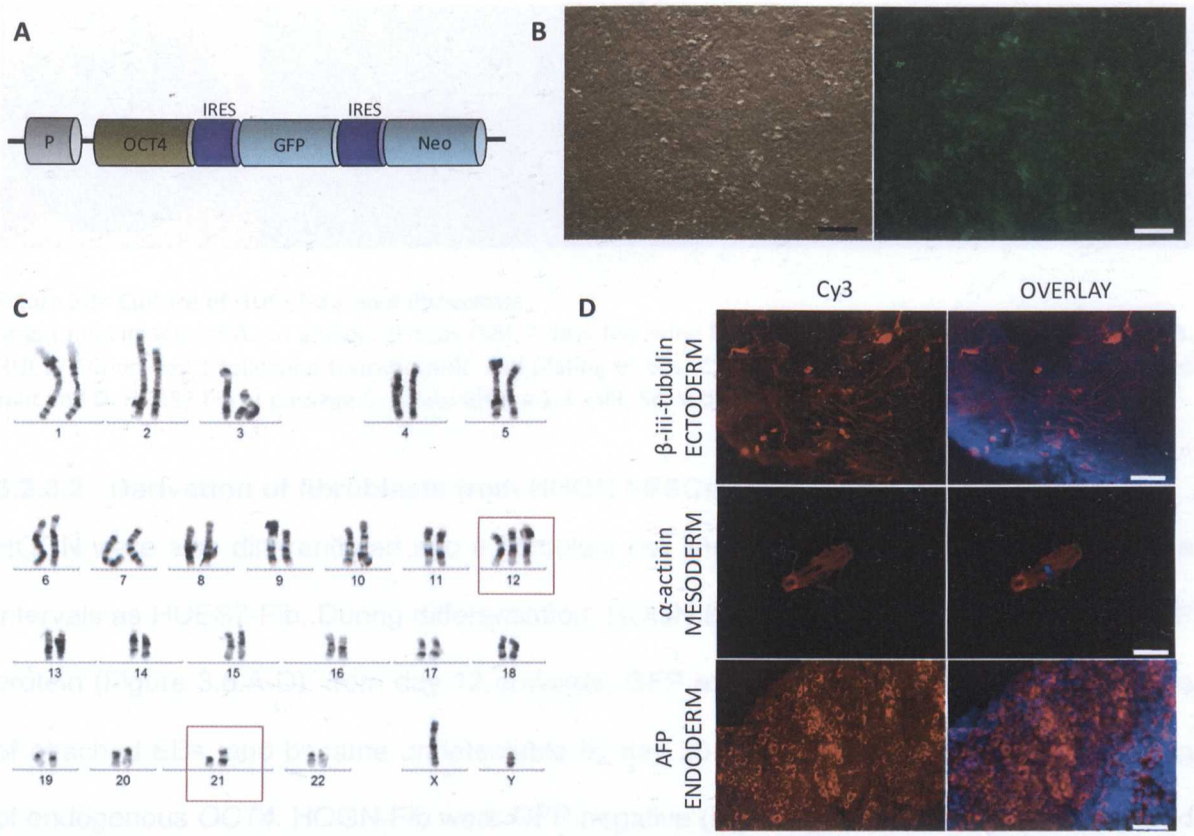

Figure 3.4– Culture, karyotype and pluripotency assessment of HOGN hESCs
A. Representation of the *IRES-GFP-IRES-Neo* cassette inserted downstream of the endogenous *OCT4* locus in HUES7 cells, to create the HOGN cell line (Braam *et al.* 2008b) P= promoter. **B.** Bright field and fluorescence images of HOGN cells at passage p+8, on day 2 following a 1:3 split. Scale bars represent 100μm. **C.** Differentiation of HOGN to cell types representative of the three germ layers; ectoderm, endoderm and mesoderm. Protein expression was captured using the Cy3 channel, while the overlay represents a merge of the DAPI (nuclear staining) and Cy3 channels. Scale bars represent 64μm. **D.** HOGN carried an abnormal 47,XY,+12,add(21)(p1) karyotype. Red boxes highlight the karyotype abnormalities.

3.2.3 Derivation and characterisation of hESC-fibroblast lines

3.2.3.1 Derivation of fibroblasts from HUES7 hESCs

Fibroblast-like cells were derived from HUES7 cells, as described in sections 2.1.7 and 2.1.8. As shown in Figure 3.5, EBs trypsinised and plated onto 90mm culture dishes appeared to have the characteristic spindle-like morphology of fibroblasts (Stojkovic *et al.* 2005) by passage 2. The formed line was named HUES7-Fib. HUES7-Fib cells were cultured in DIFF medium, and passaged by 1:3 splits every 72 hours. They maintained this regular split interval for 20 passages following their derivation, after which their growth rate became slower. For this reason, HUES7-Fib were only used for characterisation or iPSC experiments within 15 passages following their derivation.

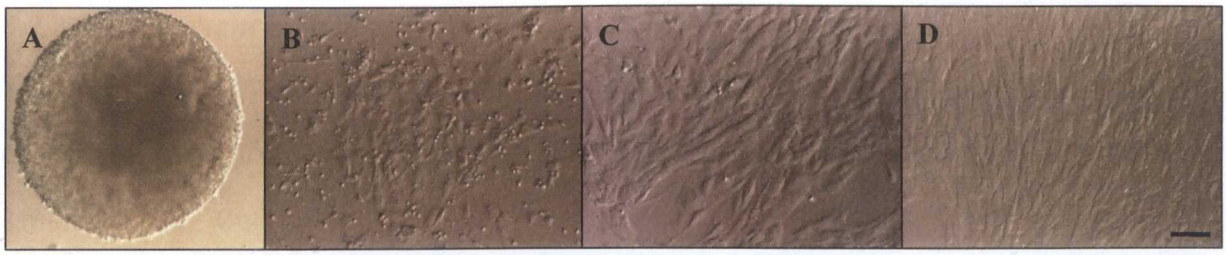

Figure 3.5- Culture of HUES7-derived fibroblasts
Bright field images of **A.** an embryoid body (EB), 4 days following forced aggregation of 10,000 HUES7 cells, **B.** HUES7-Fib on day 1 following trypsinisation and plating of EBs, **C.** HUES7-Fib at passage 2, 2 days after a 1:3 split and **D.** HUES7-Fib at passage 2, 3 days after a 1:3 split. Scale bar represents 100μm.

3.2.3.2 Derivation of fibroblasts from HOGN hESCs

HOGN were also differentiated into a fibroblast cell line, which was passaged at the same intervals as HUES7-Fib. During differentiation, HOGN EBs gradually lost expression of GFP protein (Figure 3.6.A-D); from day 12 onwards, GFP expression was lost in the outgrowths of attached EBs, and became undetectable by day 20 of differentiation, depicting silencing of endogenous *OCT4*. HOGN-Fib were GFP negative (Figure 3.6.E) and showed decreased resistance to neomycin compared to undifferentiated HOGN cells (Figure 3.7).

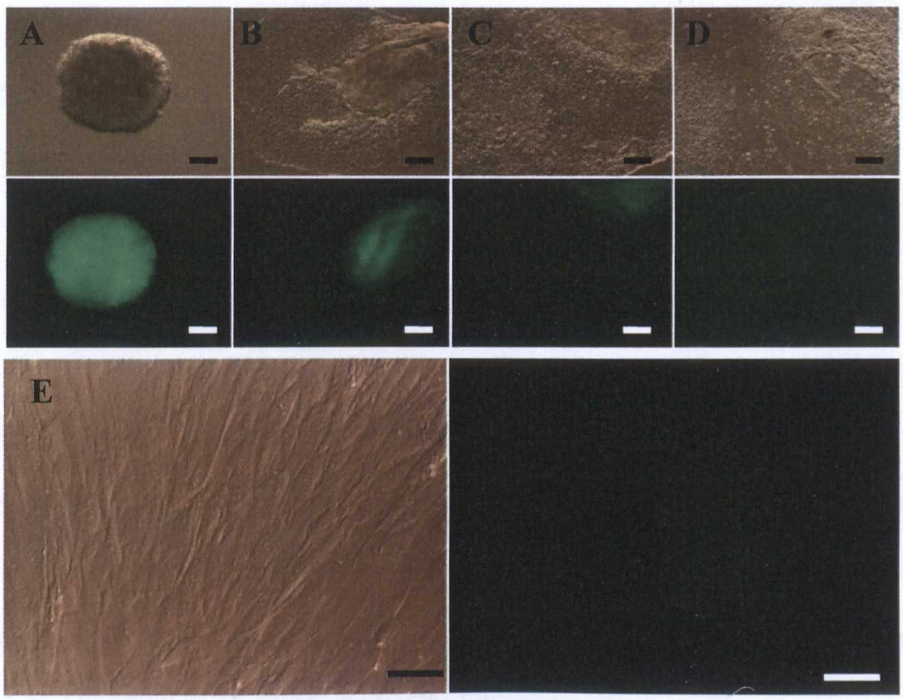

Figure 3.6- Culture of HOGN hESCs and HOGN-derived fibroblasts (HOGN-Fib)
Bright field and fluorescence images of **A.** EBs on day 4, **B.** day 10, **C.** day 14 and **D.** day 20 following forced aggregation of HOGN cells . **E.** HOGN-Fib cells at passage 2, 3 days after a 1:3 split. Scale bars represent 100μm.

3.2.3.3 Neomycin resistance of HOGN and HOGN-Fib cells

To assess neomycin resistance in HOGN and HOGN-Fib cells, a sensitivity test was performed using the neomycin analogue G418, also known as Geneticin (Davies and Jimenez 1980). Cells were treated with the antibiotic reagent for 6 days, at concentrations varying from 0 to 800μg/ml. At the end of this treatment, total cell counts were performed for each sample, and the percentage of surviving cells at each G418 concentration was calculated relative to the untreated control (0μg/ml) for each cell type. The genetically unmodified HUES7 and HUES7-Fib cells were sensitive to G418 at all concentrations tested (Figure 3.7). HOGN cells treated with 50μg/ml, 100μg/ml and 200μg/ml of G418 showed survival at 100%, 78.3% and 77.5%. In contrast, HOGN-Fib treated with 50-200μg/ml showed survival at less than 60%. Since pluripotent HOGN cells could tolerate G418 treatment at concentrations up to 200μg/ml, while differentiated HOGN-Fib cells were sensitive to G418 at concentrations of 50μg/ml or higher, it was decided that 50μg/ml of G418 could be used in future experiments for the generation of iPSCs from HOGN-Fib. This way, emerging iPSC colonies reactivating endogenous *OCT4* and the *IRES-GFP-IRES-Neo* cassette, would be selected against non-reprogrammed or incompletely reprogrammed cells lacking *OCT4* expression and Neomycin resistance.

3.2.3.4 Expression of pluripotency markers in HUES7-Fib and HOGN-Fib

In order to confirm that HUES7-Fib and HOGN-Fib had down-regulated the expression of hESC-specific markers, such as OCT4, NANOG, SSEA4 and TRA-1-81 (Kannagi *et al.* 1983; Andrews *et al.* 1984; Adewumi *et al.* 2007; Lanctot *et al.* 2007b), immunofluorescence staining was performed using antibodies raised against these markers. As shown in Figure 3.8, the pluripotent HUES7 and HOGN lines expressed all four markers tested, in contrast to the differentiated lines HUES7-Fib and HOGN-Fib.

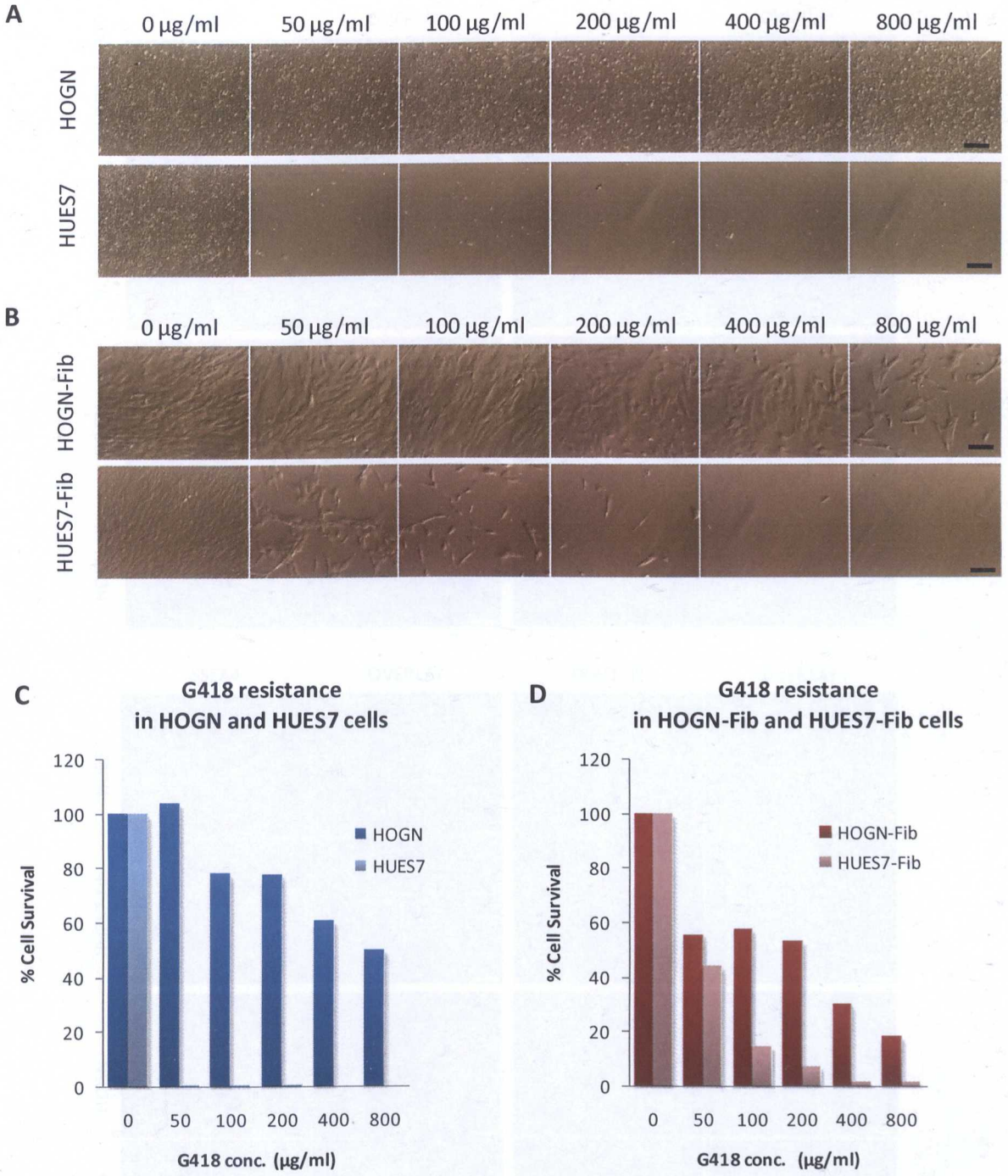

Figure 3.7– Effect of G418 treatment on the survival of HOGN, HUES7, HOGN-Fib and HUES7-Fib
Bright field images of **A.** HOGN and HUES7, and **B.** HOGN-Fib and HUES7-Fib cells treated with varying concentrations of G418, ranging from 0 to 800 µg/ml. Histograms of % cell survival in **C.** HOGN and HUES7, and **D.** HOGN-Fib and HUES7-Fib cells treated with varying concentrations of G418, as shown in A. and B. Scale bars represent 100µm.

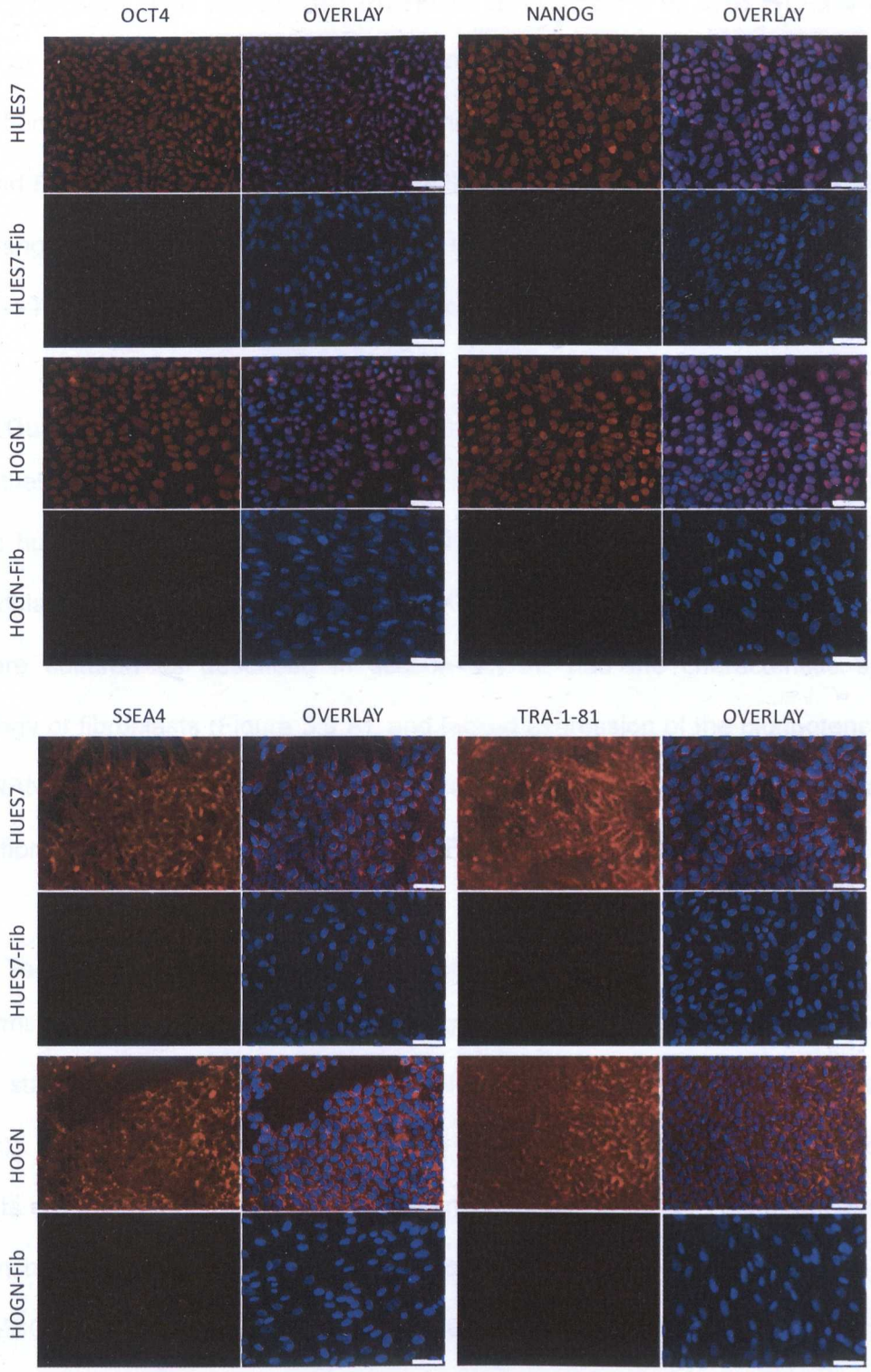

Figure 3.8- Expression of pluripotency-associated markers in hESC-derived fibroblasts
Expression of OCT4, NANOG, SSEA4 and TRA-181 in HUES7, HUES7-Fib, HOGN and HOGN-Fib cells, as determined by immunofluorescence staining. Marker expression was captured using the Cy3 channel (red), while the overlay represents a merge of the DAPI (nuclear staining) and Cy3 channels. Scale bars represent 64μm.

3.2.4 Expression of fibroblast markers in HUES7-Fib and HOGN-Fib

In order to confirm the fibroblast phenotype of HUES7-Fib and HOGN-Fib, expression of putative fibroblast markers was assessed in these lines. A survey of the literature indicated P4HB and FSA to be possible fibroblast-specific markers (Singer *et al.* 1989; Esterre *et al.* 1992; Wang *et al.* 2005; He *et al.* 2007) since most other markers used to identify fibroblast cells cross-react with additional types of cells, or fibroblast precursors (section 3.1.1).

3.2.4.1 Culture and characterisation of primary fibroblast lines

To test these antibodies for their specificity in staining fibroblast cells, the commercially available human newborn foreskin fibroblast line BJ (referred to as BJ-Fib) and the adult skin fibroblast line SUKE (referred to as SUKE-Fib) were used as positive controls. Both lines were cultured as described in section 2.1.11, had the characteristic spindle-like morphology of fibroblasts (Figure 3.9.A), and lacked expression of the pluripotency markers OCT4, NANOG, SSEA4 and TRA-1-81 (Figure 3.9.D). Both lines stained uniformly for the putative fibroblast specific markers P4HB and FSA (Figure 3.9.B&C).

3.2.4.2 Testing the specificity of putative fibroblast-specific markers

To determine cross-reactivity with other lineages, the anti-P4HB and FSA antibodies were used to stain mouse neural stem cells (mNSCs) and mouse mesenchymal stem cells (mMSCs). These cells were considered to be appropriate "negative" controls, since fibroblasts are thought to arise from the mesenchyme tissue or from ectoderm *via* epithelial to mesenchymal transition (Dennis and Charbord 2002; Kalluri and Neilson 2003). Slides of fixed mMSCs and mNSCs were kindly provided for this experiment by Dr. Virginie Sottile, School of Clinical Sciences, The University of Nottingham. Mouse embryonic fibroblasts (MEFs) were also included in the analysis, to determine whether the antibodies cross reacted with mouse cells. As a further control, beating clusters (heterogeneous populations comprising of cardiomyocytes and fibroblasts, Figure 3.10.A) derived from HUES7 cells

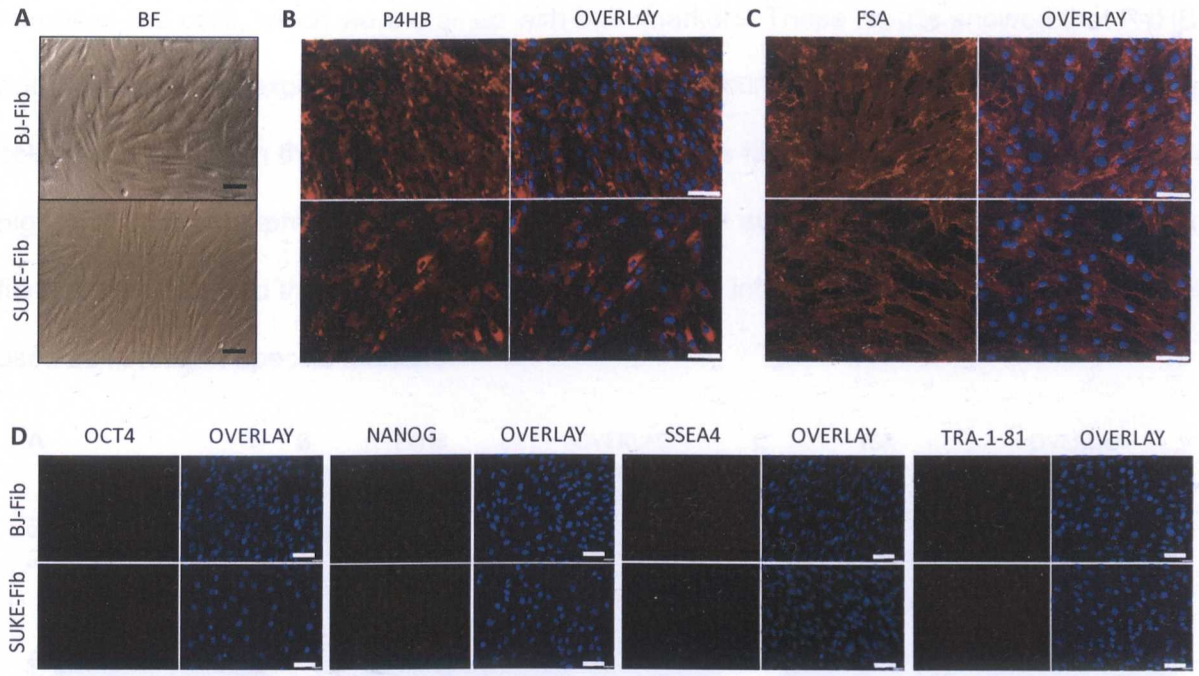

Figure 3.9- Culture and characterisation of the patient fibroblast lines BJ and SUKE
A. Bright field (BF) images of the fibroblast lines BJ (passage33, 3 days following a 1:3 split) and SUKE (passage 14, 3 days following a 1:3 split). Immunofluorescence analysis of **B.** P4HB, **C.** FSA and **D.** pluripotency-associated marker expression in BJ and SUKE fibroblasts. Target protein expression was captured using the Cy3 channel, while the overlay represents a merge of the DAPI (nuclear staining) and Cy3 channels. Scale bars represent 64μm.

were dissociated (Burridge *et al.* 2007) and attached to glass slides (section 2.8.2.); since cardiomyocytes originate from the mesoderm (Beqqali *et al.* 2006), the same germ layer that gives rise to mesenchyme tissue and fibroblasts, they acted as a stringent negative control and should not react with fibroblast antibodies. The cardiac-specific marker troponin-I was used to confirm the identity of cardiomyocytes (Figure 3.10, FITC staining).

Both the BJ and SUKE primary fibroblast lines stained uniformly for P4HB and FSA (Figure 3.10). No staining was observed in HUES7, or potential fibroblast precursors (mMSCs and mNSCs). MEFs did show staining for both markers, confirming species cross reactivity of the antibodies. However, many cells in the MEF population lacked expression of P4HB and FSA, perhaps not unexpectedly, since these heterogeneous cell lines were prepared from whole mouse embryos (section 2.1.2.). Furthermore, the mesoderm-originating human cardiomyocytes did not stain for either P4HB or FSA, in contrast to the surrounding

fibroblast-like cells, which were stained with both markers. These results showed that P4HB and FSA were not expressed in potential fibroblast precursors (mMSCs and mNSCs) or in cells originating from the same embryonic germ layer as fibroblasts (cardiomyocytes). Their high and uniform expression levels in the commercially available human newborn foreskin fibroblast line BJ and the adult skin fibroblast line SUKE inferred that P4HB and FSA can be used as fibroblast-specific markers.

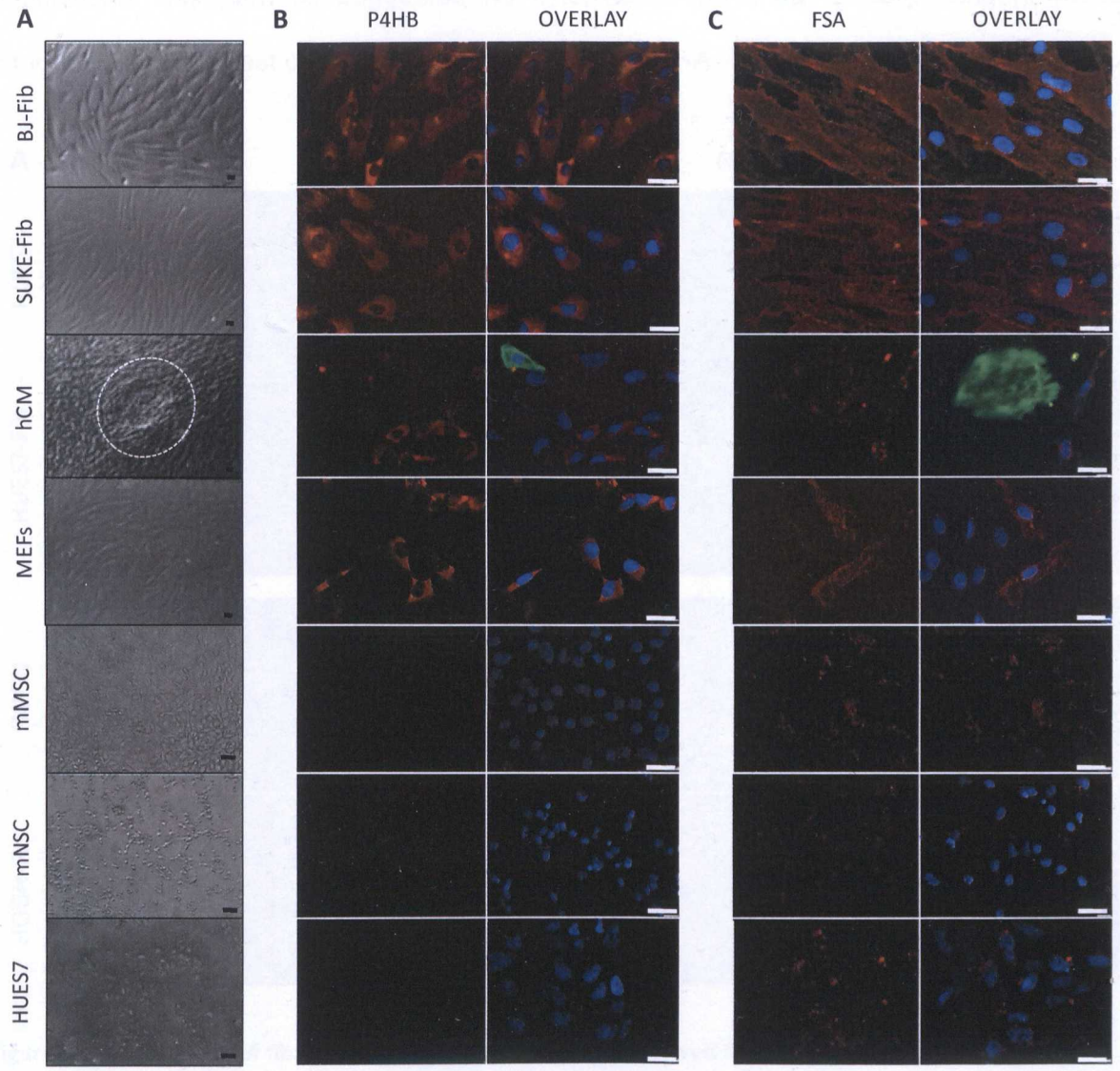

Figure 3.10- Determining the specificity of putative fibroblast-specific antibodies
A. Phase contrast images of human BJ and SUKE fibroblasts (BJ-Fib and SUKE-Fib), a beating cluster (circled in dotted line) containing human cardiomyocytes, mouse embryonic fibroblasts (MEFs), mouse mesenchymal and neural stem cells (mMSC and mNSC), and HUES7 hESCs. Expression of the fibroblast-specific markers **B.** P4HB and **C.** FSA in the cell populations shown in A., as determined by immuno-fluorescence staining. Target protein expression was captured using the Cy3 channel (red), while the overlay represents a merge of the DAPI (nuclear staining), FITC (cardiac troponin-I) and Cy3 channels. Scale bars represent 32μm.

3.2.4.3 Expression of fibroblast markers in hESCs and their fibroblast derivatives

HUES7, HOGN, HUES7-Fib and HOGN-Fib were then assessed for the expression of P4HB and FSA antigens. The pluripotent lines HUES7 and HOGN lacked both these markers, whereas expression was detected in HUES7-Fib and HOGN-Fib (Figure 3.11). Expression of FSA was uniform across the population of the two fibroblast lines, but a proportion of cells lacked expression of P4HB, both in the HUES7-Fib and HOGN-Fib populations. This, perhaps, suggested that cytoplasmic P4HB was a more stringent marker for identifying fibroblast cells than the surface antigen FSA.

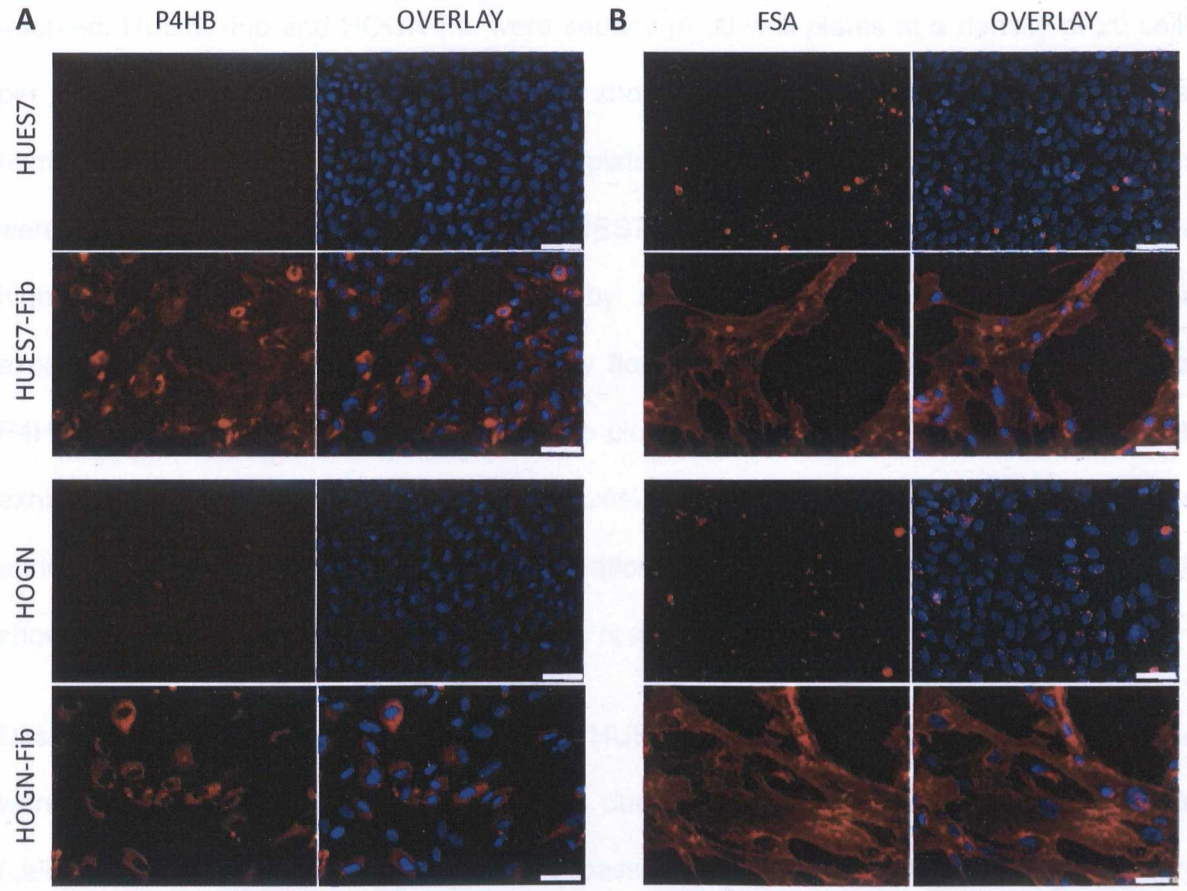

Figure 3.11- Expression of fibroblast-specific markers in hESC-derived fibroblasts
Expression of the fibroblast-specific markers **A.** P4HB and **B.** FSA in HUES7, HUES7-Fib, HOGN and HOGN-Fib cells, as determined by immuno-fluorescence staining. Marker expression was captured using the Cy3 channel (red), while the overlay represents a merge of the DAPI (nuclear staining) and Cy3 channels. Scale bars represent 64μm.

3.2.5 Generation of clonal hESC-fibroblast lines expressing P4HB

Having shown that the HUES7-Fib and HOGN-Fib lines did not consist of uniform cell populations, attempts were made to produce pure fibroblast lines that could be used for reprogramming experiments. This was considered necessary in order to eliminate the possibility that reprogrammed cells in future experiments would originate from undifferentiated or precursor cells residing in the HUES7-Fib and HOGN-Fib lines.

After unsuccessful attempts to sort live HUES7-Fib cells based on FSA expression, using FACS and magnetic-bead separation (data not shown), a single-cell cloning strategy was adopted. HUES7-Fib and HOGN-Fib were seeded in 96-well plates at a density of 20 cells per plate, since this density was previously shown mathematically to provide the highest number of single vs. mixed cell clones per plate (Ma and Wells 2004). Eight clonal lines were expanded and analysed for both HUES7-Fib and HOGN-Fib. Lines showing the highest enrichment in P4HB expression by immunofluorescence (Figure 3.12) were expanded further in culture and analysed by flow cytometry to confirm the percentage of P4HB positive cells in their populations. Two clonal lines from HUES7-Fib and HOGN-Fib exhibited P4HB expression of between 90-96%, (Figure 3.12). This was a considerable enrichment compared to the starting populations of HUES7-Fib and HOGN-Fib, which showed a 41% and 27% expression of P4HB, respectively.

Despite having generated clonal lines of the HUES7-Fib and HOGN-Fib populations, these were not used to generate iPSCs. This was due to their extremely slow proliferation rate (cells reached proliferative arrest after 2-3 passages), which did not allow the necessary scale-up of cultures prior to their use for iPSC generation. Clone 4 of HUES7-Fib (referred to as HUES7-Fib Cl4), remained proliferative until passage 4 and was pelleted in order to be used in comparison to HUES7-Fib in molecular biology analyses (chapter 4).

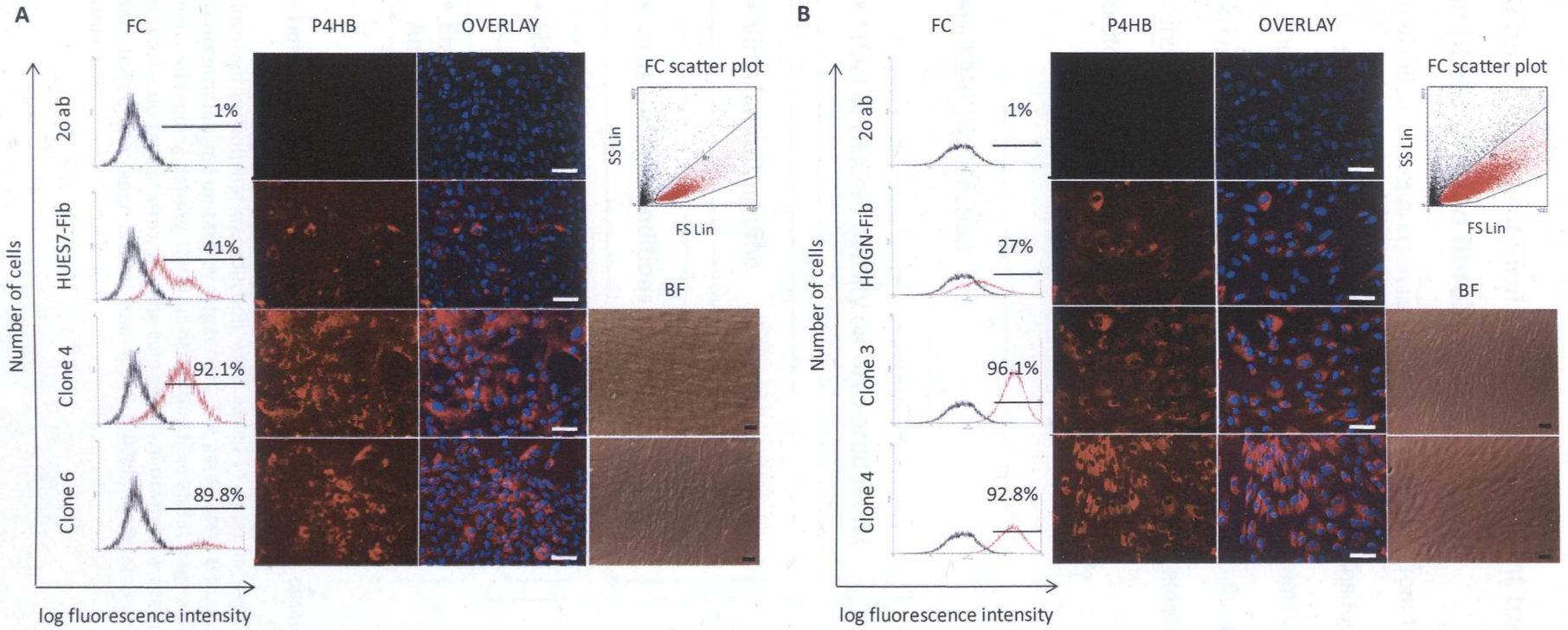

Figure 3.12– Generation and characterisation of clonal cell lines from HUES7-Fib and HOGN-Fib
Flow cytometry and immunofluorescence analysis of P4HB protein expression in **A.** HUES7-Fib and **B.** HOGN-Fib clonal lines. For flow cytometry analysis, gating of the total cells examined (FC scatter plot) as well as gating of the positive populations (FC) are shown. For immunofluorescence analysis, target protein expression was captured using the Cy3 channel (red), while the overlay represents a merge of the DAPI (nuclear staining) and Cy3 channels. Bright field (BF) images of the clonal lines show the spindle-like morphology of the cells, which is characteristic of fibroblasts. Scale bars represent 64μm.

3.2.6 Establishing a lentiviral system for efficient transduction of hESCs and hESC-derived fibroblasts

Following derivation and characterisation of fibroblast lines from HUES7 and HOGN, it was necessary to establish an efficient protocol for lentiviral transduction of these cells in our laboratory. The protocol would be used to enable reprogramming of fibroblasts into iPSCs (section 3.2.7), and to introduce shRNAs for the manipulation of epigenetic characteristics in fibroblasts and hESCs (chapter 5). A flow chart of the parameters tested to establish an optimised protocol is presented in Figure 3.13.

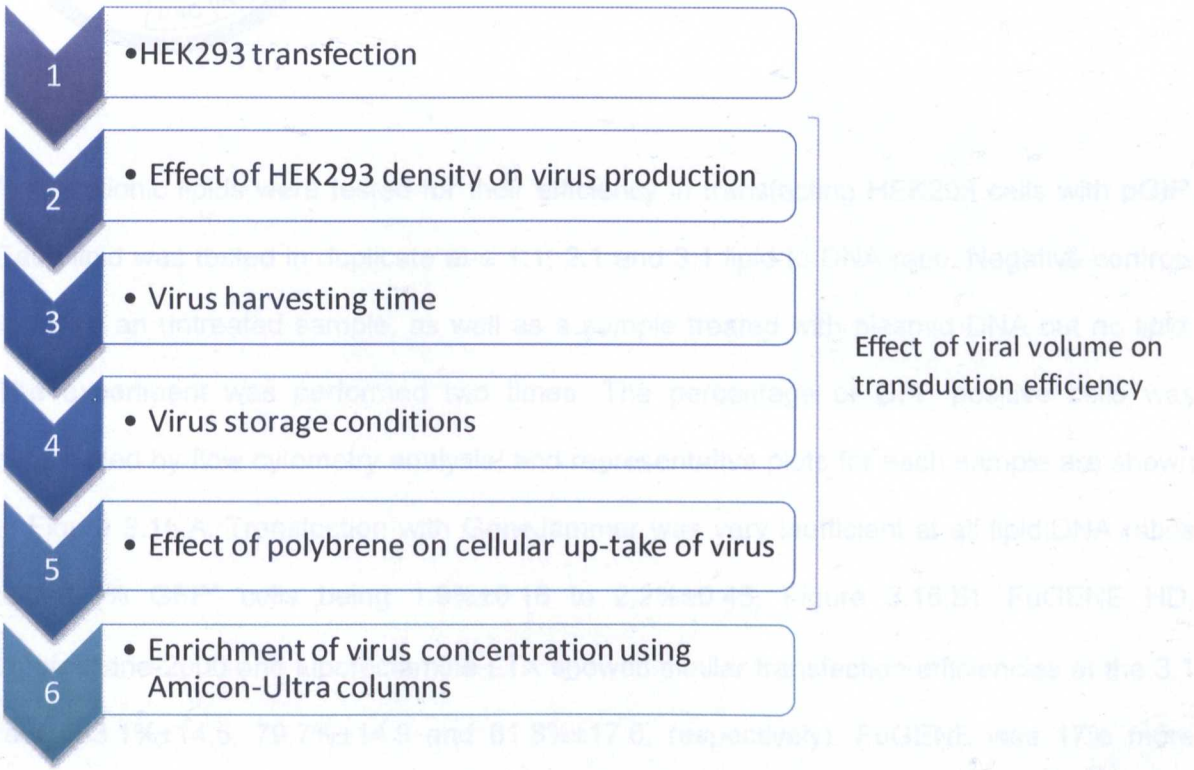

Figure 3.13– Flow chart representation of experiments performed to optimise the lentiviral transduction system

Parameters involved in lentiviral transduction were varied in order to derive a protocol for efficient virus production, concentration and up-take by target cells. The parameters tested included the method of HEK293 cell transfection and seeding density, the virus harvesting time and storage conditions, the effect of polybrene treatment on cellular up-take of virus, and the concentration of viral particles using Amicon-Ultra columns. All conditions were tested at a range of viral volumes (0-1200µl), to determine the most efficient protocol for lentiviral transduction.

3.2.6.1 Assessing different methods to achieve efficient transfection of HEK293 cells

To optimise HEK293 transfection, the fluorescence reporter plasmid p*GFP-IRES-Puromycin* (pGIP) was used as a positive control (kindly gifted by Dr. Austin Smith, The University of Cambridge, UK) (Figure 3.14).

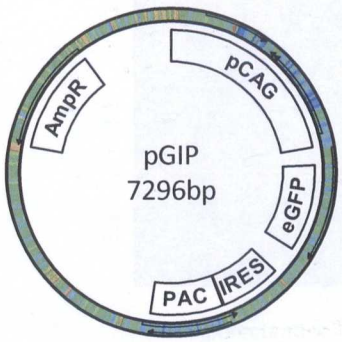

Figure 3.14– Map of the pGIP plasmid
The fluorescence plasmid pGIP, used to optimise lentiviral transduction. This plasmid supports expression of enhanced GFP (eGFP) protein from the potent pCAG promoter.

Four cationic lipids were tested for their efficiency in transfecting HEK293 cells with pGIP. Each lipid was tested in duplicate at a 1:1, 2:1 and 3:1 lipid to DNA ratio. Negative controls included an untreated sample, as well as a sample treated with plasmid DNA but no lipid. The experiment was performed two times. The percentage of GFP positive cells was determined by flow cytometry analysis, and representative plots for each sample are shown in Figure 3.15.A. Transfection with GeneJammer was very inefficient at all lipid:DNA ratios tested (% GFP^+ cells being 1.9%±0.16 to 2.2%±0.45, Figure 3.15.B). FuGENE HD, Lipofectiane-2000 and Lipofectamine-LTX showed similar transfection efficiencies at the 3:1 ratio (83.1%±14.5, 79.7%±14.9 and 81.8%±17.6, respectively). FuGENE was 17% more efficient than Lipofectamine-2000 (75.1%±11.3) and 29% more efficient than Lipofectamine-LTX (66.0%±33) at the 2:1 ratio. Less efficient transfection was observed at the 1:1 ratio (Lipofectamine-2000; 60%±0.5, Lipofectamine-LTX; 29.3%±18.9 and FuGENE; 9.6%±4.3).

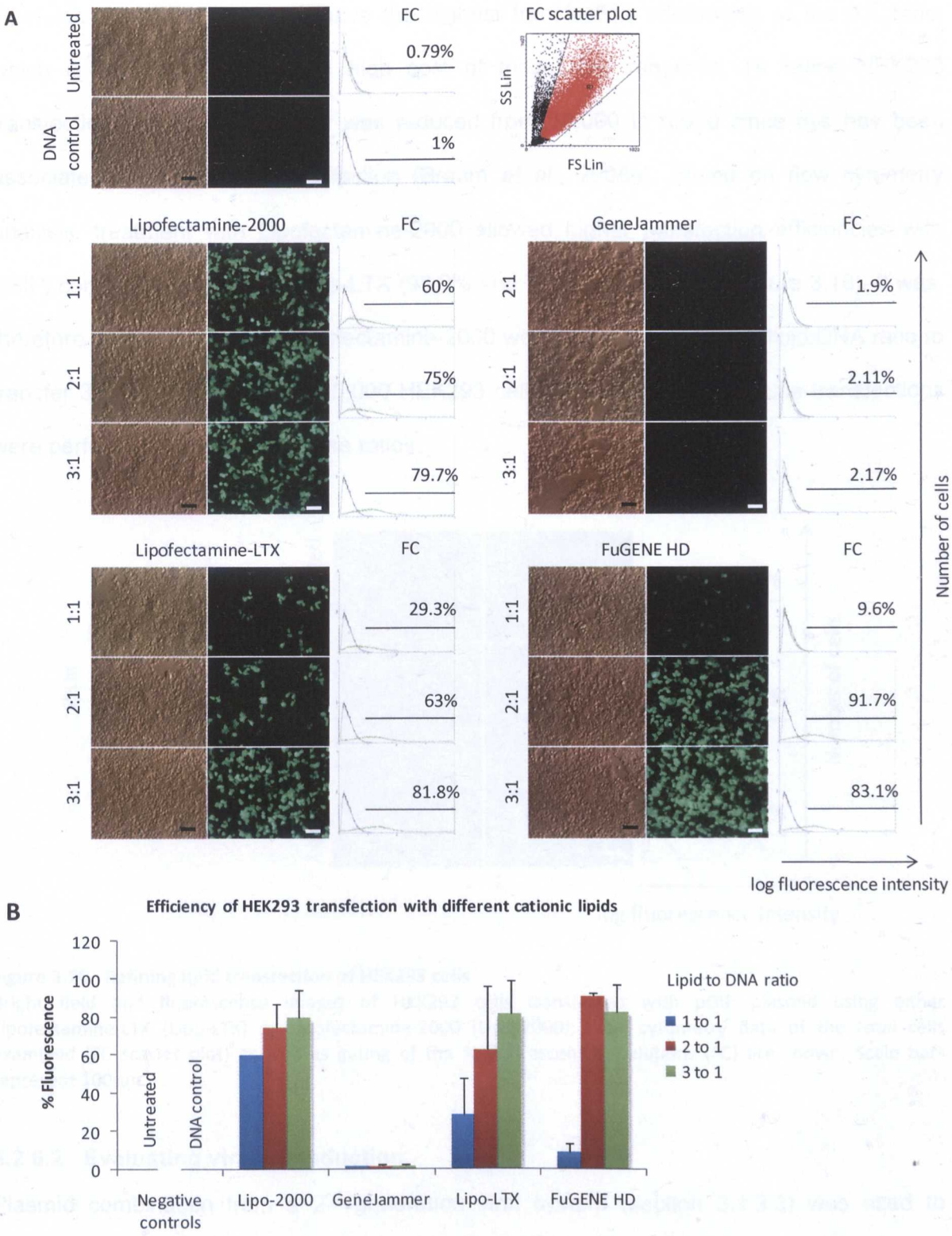

Figure 3.15– Testing the ability of different lipid vectors to transfect HEK293 cells

A. Bright field and fluorescence images of HEK293 cells transfected with pGIP plasmid, using either Lipofectamine-2000 (Lipo-2000), GeneJammer, Lipofectamine-LTX (Lipo-LTX) or FuGENE HD as a cationic lipid transfection vehicle. Flow cytometry data of the total cells examined (FC scatter plot) as well as gating of the positive fluorescent populations (FC) are shown. **B.** Histogram representing the % fluorescence in HEK293 cells shown in A., as determined by flow cytometry. Error bars represent standard error. Scale bars represent 100μm.

Lipofectamine-2000 and -LTX gave the highest transfection efficiencies at the 1:1 ratio, which is important due to the high cost of these lipid reagents. To refine HEK293 transfection further, cell number was reduced from 10,000 to 5,000 since this has been associated with improved transfection (Braam *et al.*, 2008a). Based on flow cytometry analysis, treatment with Lipofectamine-2000 allowed higher transfection efficiencies with pGIP, compared to Lipofectamine-LTX (98.9% and 76.9% respectively; Figure 3.16). It was, therefore decided that 3µl of Lipofectamine-2000 would be used at the 1:1 lipid:DNA ratio to transfer 3µg of plasmid DNA to 5,000 HEK293 cells. Smaller or bigger scale transfections were performed according to these ratios.

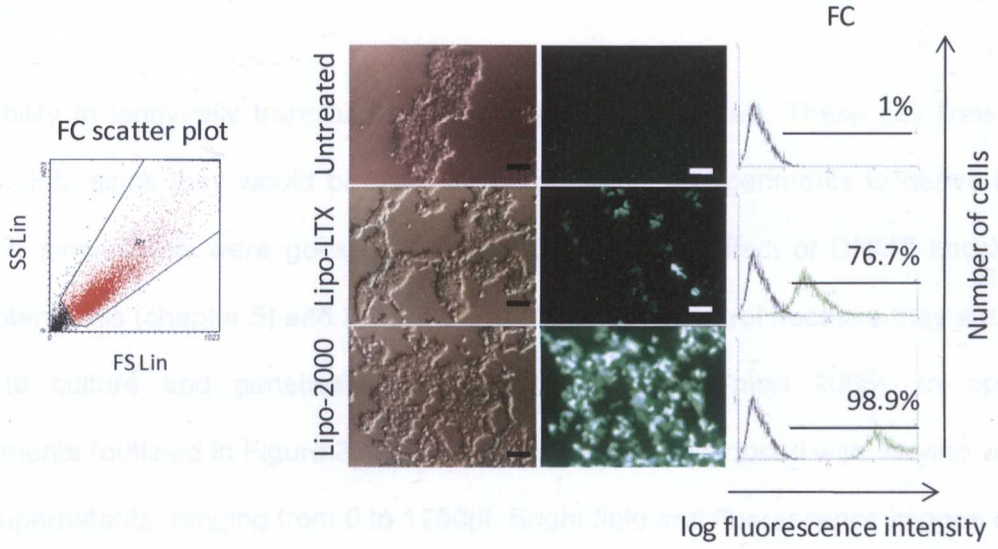

Figure 3.16– Refining lipid transfection of HEK293 cells
Bright field and fluorescence images of HEK293 cells transfected with pGIP plasmid using either Lipofectamine-LTX (Lipo-LTX) or Lipofectamine-2000 (Lipo-2000). Flow cytometry data of the total cells examined (FC scatter plot) as well as gating of the % fluorescent populations (FC) are shown. Scale bars represent 100µm.

3.2.6.2 Evaluating viral transduction

Plasmid combination from a 2nd generation viral system (section 3.1.3.2) was used to generate lentiviral particles. The plasmids used were; the GFP reporter-transfer plasmid pLVTHM, the packaging plasmid psPAX2 and the envelope plasmid pMD2.G (Figure 3.17).

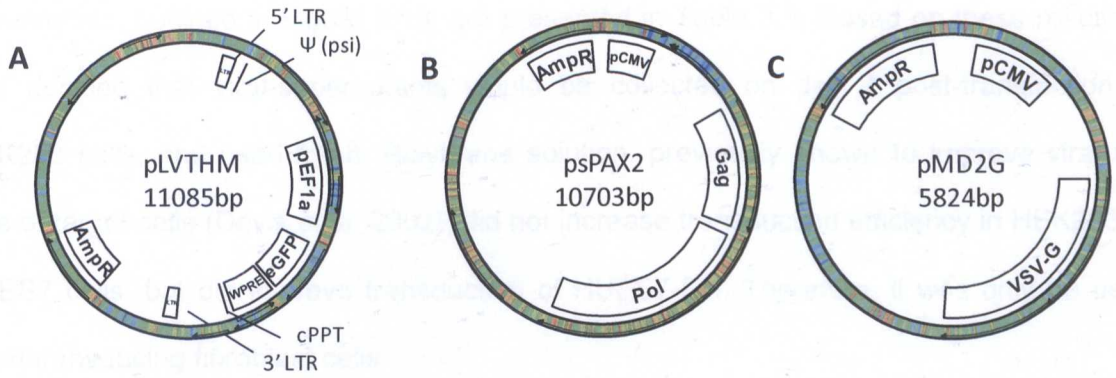

Figure 3.17- Maps of plasmids used to optimise lentiviral transduction
A. The fluorescence reporter lentiviral plasmid pLVTHM. **B.** The lentiviral packaging plasmid psPAX2. **C.** The lentiviral envelope plasmid pMD2G. pLVTHM supports expression of eGFP protein under the eukaryotic elongation factor 1α (EF1α). This plasmid also carries HIV-1 long terminal repeats (LTRs), an HIV-1 psi (ψ) pack, a central polypurine tract (cPPT) sequence responsible for HIV nuclear import, and a woodchuck hepatitis post-translational regulatory element (WPRE), shown to improve transgene expression and viral titres (Klein *et al.* 2006). psPAX2 and pMD2.G carry the viral genes g*ag*, *pol* and *VGV-G*, which are essential packaging of viral particles.

The ability to lentivirally transduce three cell types was tested. These cell lines were; 1) HUES7-Fib, since they would be used in reprogramming experiments to derive iPSCs, 2) HUES7, since these were going to be used to study the effect of DNMT knock-down in pluripotent cells (chapter 5) and 3) HEK293, as a positive control because they are relatively easy to culture and genetically modify (Thomas and Smart 2005). In optimisation experiments (outlined in Figure 3.13), each cell line was transduced with varying volumes of viral supernatants, ranging from 0 to 1200µl. Bright field and fluorescence images of all cells were captured at 72 hours post transduction (PTD), after which the cells were trypsinised and prepared for analysis of GFP expression by flow cytometry. The percentage of GFP positive cells was calculated relative to the untreated control sample (0µl of virus) for each cell type.

Treatment with increasing volumes of viral supernatant resulted in higher percentage cell transduction, with HEK293 proving to be the most easy to transduce cell line (Figure 3.18). Doubling the number of HEK293 cells used to generate viral particles (1.5 million instead of 0.75 million cells) increased transduction efficiency (Figure 3.18), indicating an increased overall production of virus from HEK293 cells. The results for subsequent optimisation

experiments, outlined in Figure 3.13, are presented in Table 3.3. Based on these results, it was decided that viral-supernatants would be collected on day 2 post-transfection of HEK293 cells, and used fresh. Polybrene solution, previously shown to improve viral up-take of target cells (Davis *et al.* 2002), did not increase transduction efficiency in HEK293 or HUES7 cells, but did improve transduction of HUES7-Fib. Therefore, it was only be used when transducing fibroblast cells.

Table 3.3– Experiments performed to improve lentiviral transduction of HEK293, HUES7 and HUES7-Fib

Parameter	Variables	% Transduction (1200µl of virus)		
		HEK293	HUES7	HUES7-Fib
HEK293 density	0.75 million	71.0	17.3	19.1
	1.5 million	79.7	19.6	39.0
Virus harvesting time	day 2 PTF	69.0	25.1	49.0
	day 4 PTF	26.8	5.5	17.1
	day 6 PTF	11.5	1.5	1.2
Virus storage conditions	Fresh	69.0	25.1	49.0
	Fridge (4°C)	51.0	6.9	15.1
	Frozen (-80°C)	42.2	4.6	9.1
Polybrene	0µg/ml	90.8	61.3	63.5
	8µg/ml	81	49.7	81.5

3.2.6.3 Viral concentration with Amicon-Ultra centrifugal filter units

With 1200µl approaching the highest volume physically possible to use for viral transduction of 5,000 target cells seeded in 24-well plates, it was necessary to concentrate viral supernatants to enable transduction with higher volumes. Amicon-Ultra centrifugal filter units with a 100kDa nominal molecular weight limit (NMWL; Sena-Esteves *et al.* 2004) were used to concentrate 15ml of viral supernatants by approximately 75-fold, to a final volume of 200µl. The centrifugation process did not result in loss of viral particles, since corresponding volumes of non-concentrated (1.5ml) and concentrated virus (20µl) were shown to transduce cells with the same efficiency, which was close to 100% for all cell lines tested (Figure 3.19). The use of Amicon-Ultra units opened the possibility of infecting a larger number of cells, and improving experimental through-put.

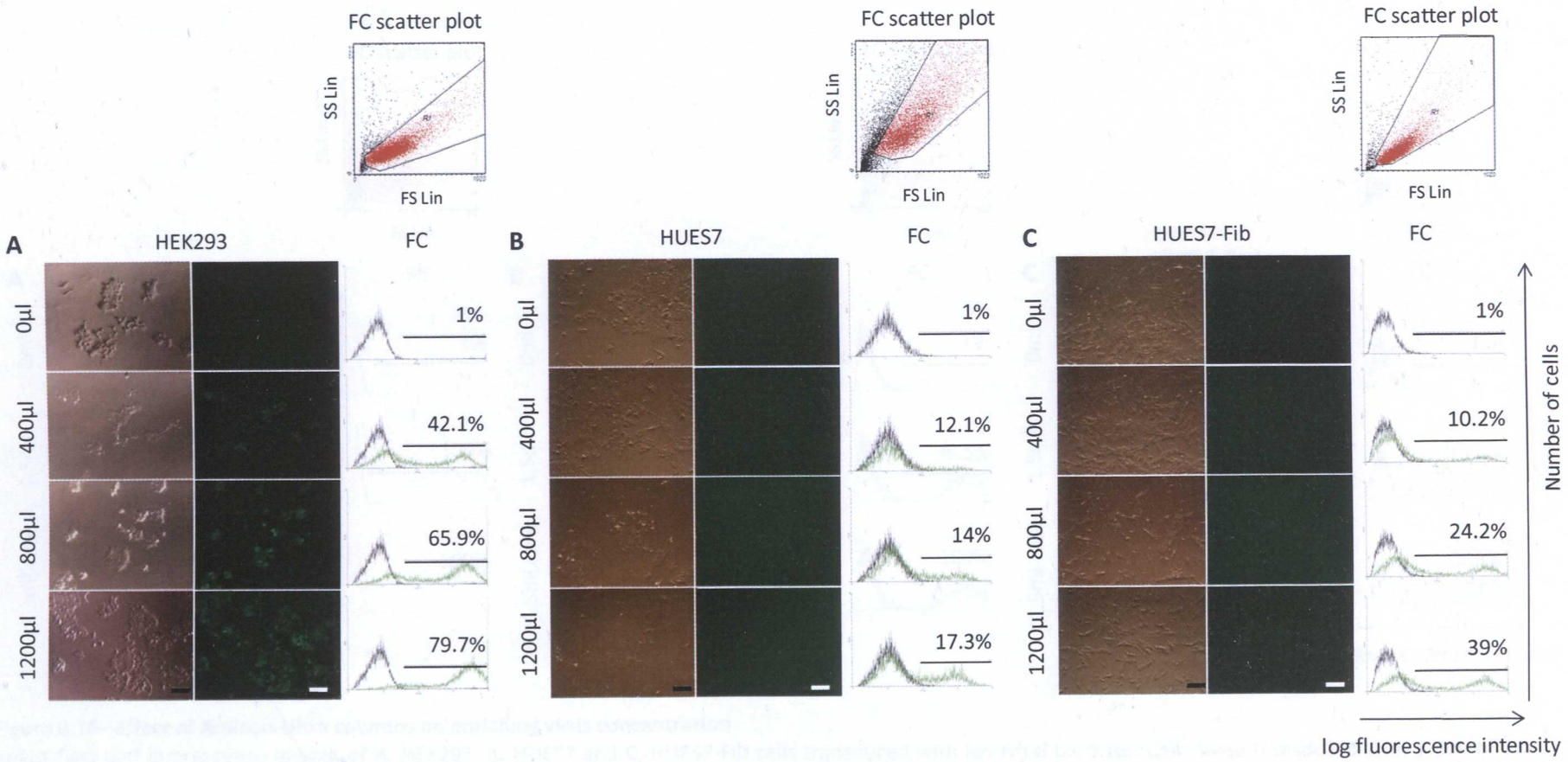

Figure 3.18- Lentiviral transduction: example of cell culture and flow cytometry analysis
Bright field and fluorescence images of **A.** HEK293, **B.** HUES7 and **C.** HUES7-Fib cells transduced with lentiviral particles, produced using HEK293 cells seeded at 1.5 million cells per 10cm dish. Cells were transduced with varying volumes of virus containing medium, ranging from 0 to 1200µl in total. Flow cytometry data of the total cells examined (FC scatter plot) as well as gating of the positive fluorescent populations (FC) are shown. Scale bars represent 100µm.

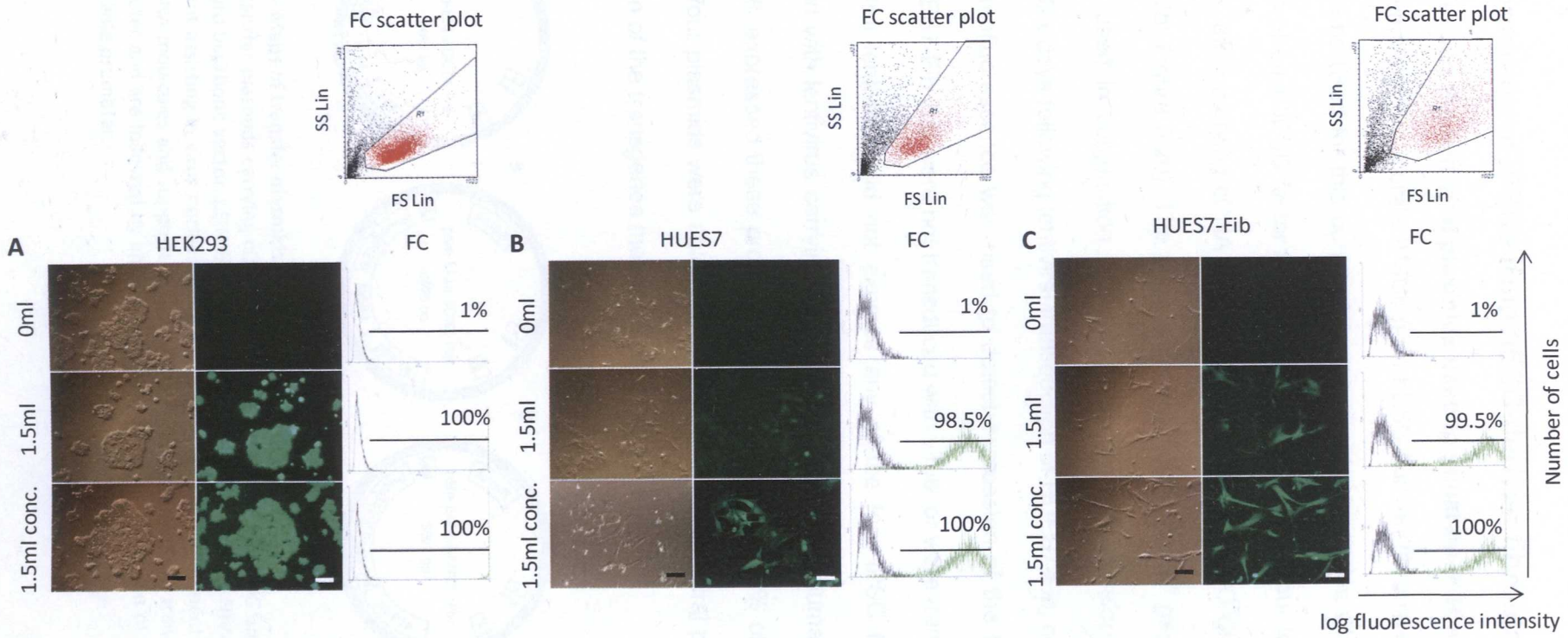

Figure 3.19– Effect of Amicon-Ultra columns on enriching virus concentration
Bright field and fluorescence images of **A.** HEK293, **B.** HUES7 and **C.** HUES7-Fib cells transduced with lentiviral particles. Cells were transduced with 1.5ml of virus containing medium which was either not concentrated or concentrated by ~70-fold using Amicon-Ultra columns. Flow cytometry data of the total cells examined (FC scatter plot) as well as gating of the positive fluorescent populations (FC) are shown. Scale bars represent 100µm.

3.2.7 Formation of iPSCs from hESC-derived fibroblasts

3.2.7.1 Testing the lentiviral plasmids used to generate iPSCs

Before attempting to generate iPSCs from hESC-derived fibroblasts, the lentiviral plasmids intended to be used for this purpose were tested to determine whether they could support expression of each iPSC factor individually, in HUES7-Fib. Four lentiviral transfer plasmids were used, each carrying cDNA of human *OCT4*, *NANOG*, *SOX2* or *LIN28* (Addegene; Yu *et al.* 2007b; Figure 3.20). The plasmids formed part of a 2nd generation lentiviral system, and were used in conjunction with the packaging and envelope plasmids psPAX2 and pMD2.G. Six days following lentiviral transduction of HUES7-Fib, cells were fixed in 4% PFA and immunofluorescence was used to detect expression of the four iPSC factors (Figure 3.21). HUES7-Fib that were not transduced with virus, or were transduced with the pLVTHM GFP control lentivirus, did not express any of the four iPSC factors. In contrast, cells transduced with lentivirus carrying transgene sequences of human *OCT4*, *NANOG*, *SOX2* and *LIN28*, expressed these proteins in approximately 60-80% of cells (visual estimation). Thus, all four plasmids were able to produce functional lentiviral particles, which supported expression of the transgenes they were carrying.

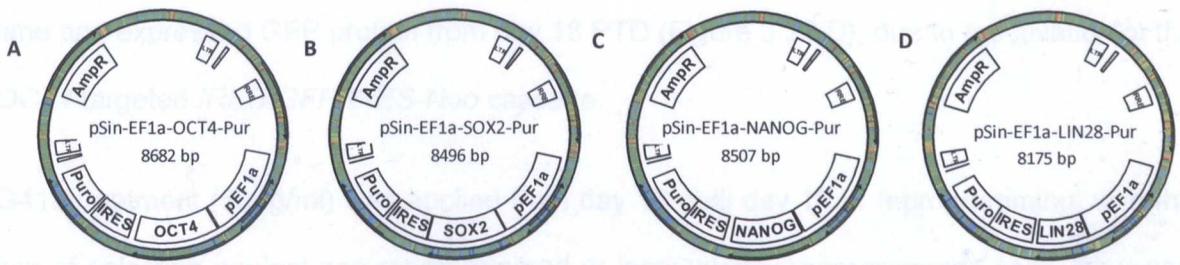

Figure 3.20- Maps of transfer plasmids used to generate iPSCs
Lentiviral transfer plasmids carrying cDNA for **A.** *OCT4*, **B.** *SOX2*, **C.** *NANOG* and **D.** *LIN28,* based on the pSin-EF2-IRES-Puro backbone vector. pSIN-EF2-IRES-Puro has HIV-1 LTRs and an HIV-1 ψ packing signal. It also has a cPPT element assisting in virus nuclear import, and a Rev-responsive element (RRE) which facilitates nuclear export of RNA molecules and supports their stability and translation. The transgenes are expressed under an EF1α promoter and are followed by an IRES sequence, allowing expression of the puromycin resistance gene under the same promoter.

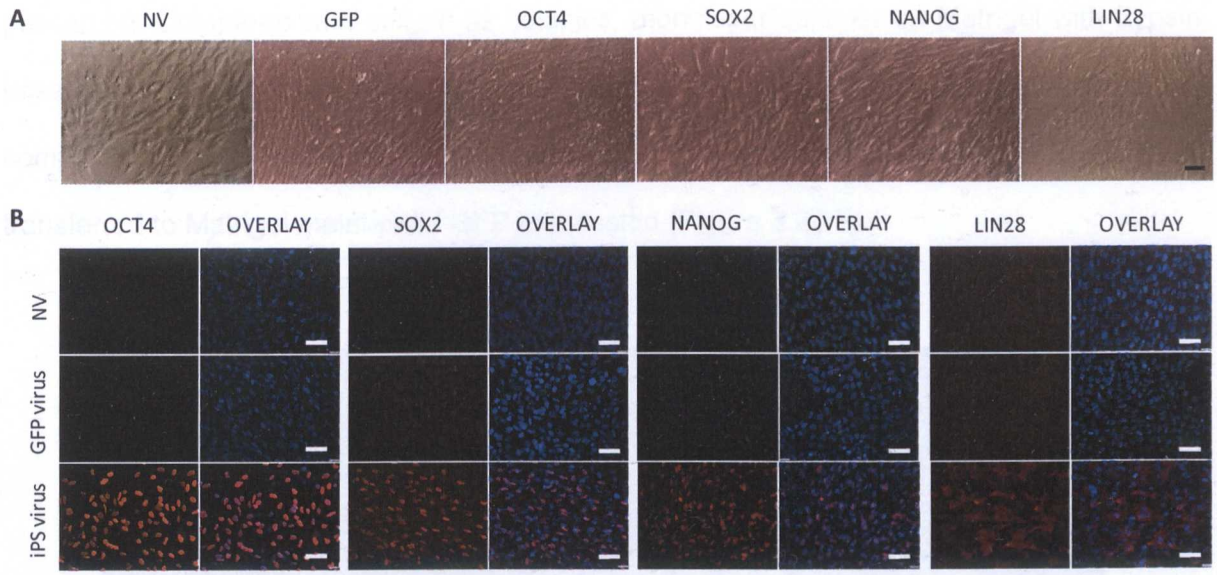

Figure 3.21– Protein expression of the four iPSC factors lentivirally transduced into HUES7-Fibroblasts
A. Bright field images and **B.** immunofluorescence analysis of HUES7-Fib cells transduced with lentivirus over-expressing *GFP*, *OCT4*, *SOX2*, *NANOG* or *LIN28*. For immunofluorescence analysis target protein expression was captured using the Cy3 channel, while the overlay represents a merge of the DAPI (nuclear staining), and Cy3 channels. NV = no virus. Scale bars represent 64μm.

3.2.7.2 Generation of iPSCs using fibroblasts derived from HOGN cells

Initially, the HOGN-Fib line was used to generate iPSCs, as described in section 2.2.6. On day 8 post-transduction (PTD), the first ESC-like colonies were detected in culture (Figure 3.22.B). Colonies considered to represent putative iPSCs had defined borders, and consisted of densely packed cells with angular cell walls. These colonies grew bigger over time and expressed GFP protein from day 18 PTD (Figure 3.22.D), due to reactivation of the *OCT4* targeted *IRES-GFP-IRES-Neo* cassette.

G418 treatment (50μg/ml) was applied from day 12 until day 16 of reprogramming, with the aim of selecting against non-reprogrammed or incompletely reprogrammed cells. However, this did not prove very effective, perhaps due to the low level resistance of HOGN-Fib cells to the antibiotic G418 (Figure 3.7), or due to reactivation of endogenous *OCT4* in some incompletely reprogrammed colonies. On day 21 PTD, putative iPSC colonies were selected based on hESC-like morphology and expression of GFP. They were manually dissected and expanded in culture, and were finally adapted to feeder-free culture on Matrigel with trypsin

passaging. Compared with culture as colonies, monolayer cultures on Matrigel with trypsin passaging facilitate downstream molecular analysis, homogeneous EB formation, and direct comparison to the HOGN hESC line which was also cultured on Matrigel. HOGN-iPSCs transferred to Matrigel maintained GFP expression (Figure 3.22.F).

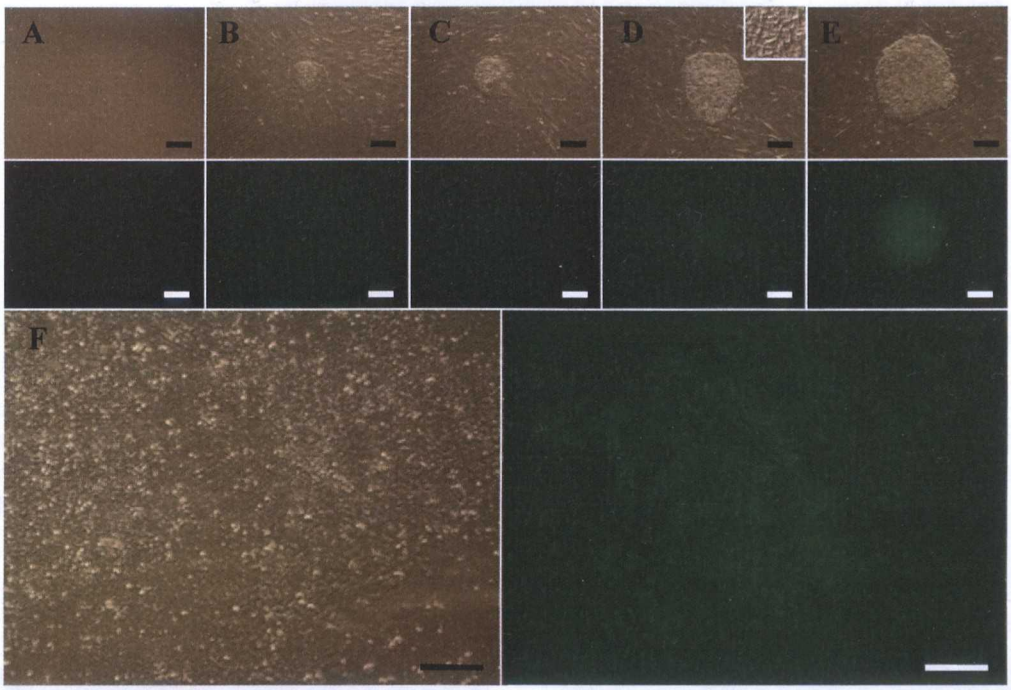

Figure 3.22- Generation of HOGN-iPSCs
Bright field and fluorescence images of iPSC colonies on **A.** day 0 **B.** day 8 **C.** day 10 **D.** day 18 and **E.** day 20 after transduction with lentiviruses over expressing *OCT4*, *NANOG*, *SOX2*, and *LIN28*. **F.** Bright field and fluorescence images of HOGN-iPSCs cultured on Matrigel at passage 2, 2 days after a 1:3 split. Scale bars represent 100μm.

3.2.7.3 Characterisation of HOGN-iPSCs

In order to assess the ability of HOGN-iPSCs to form derivatives of the three embryonic germ layers, cells were differentiated *via* EB formation. On day 21 of differentiation, EBs were seeded onto glass chamber slides, fixed using 4% PFA and analysed by immunofluorescence staining as described in section 3.2.1. Figure 3.23 demonstrates differentiation into ectoderm, endoderm, and mesoderm derivatives. Cells expressed the hESC markers OCT4, NANOG, SSEA4 and TRA-1-81, as determined by

immunofluorescence, and lacked expression of the fibroblast markers P4HB and FSA (Figure 3.24).

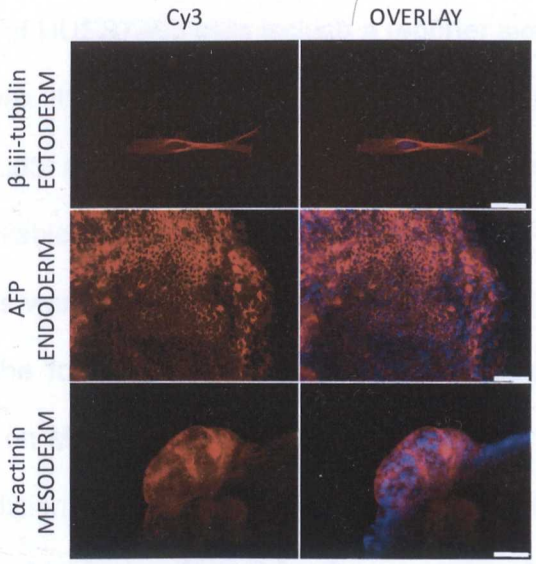

Figure 3.23- Germ layer formation in HOGN-iPSCs
Differentiation of HOGN-iPSCs to cell types representative of the three germ layers; ectoderm, endoderm and mesoderm. Protein expression was captured using the Cy3 channel, while the overlay represents a merge of the DAPI (nuclear staining) and Cy3 channels. Scale bars represent 64μm.

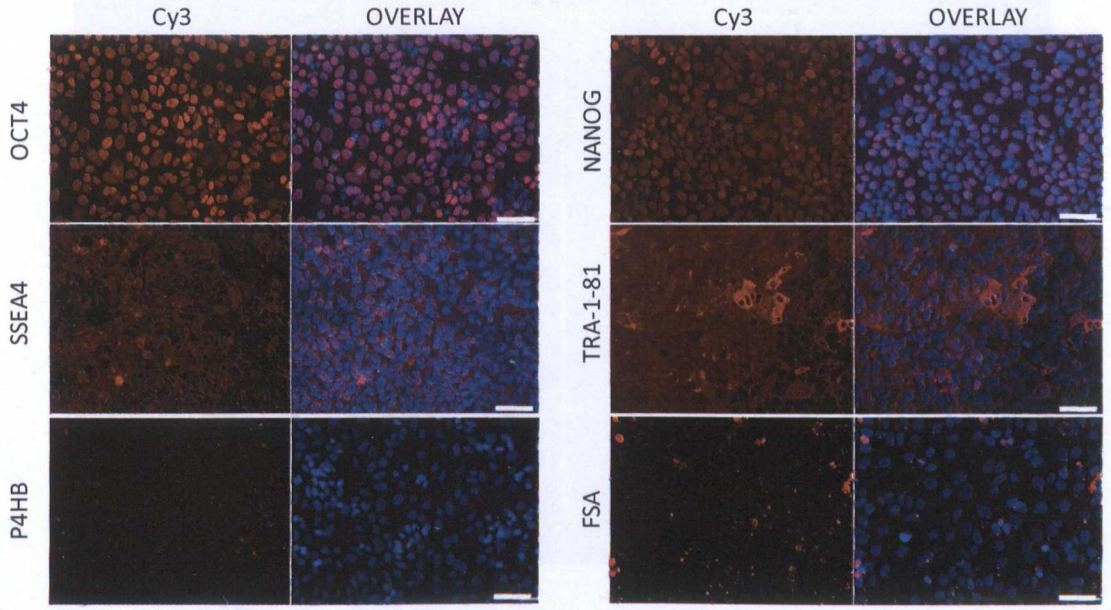

Figure 3.24- Expression of pluripotency-associated and fibroblast-specific markers in HOGN-iPSCs
Immunofluorescence analysis of OCT4, NANOG, SSEA4, TRA-1-81, P4HB and FSA expression in HOGN-iPSCs. Marker expression was captured using the Cy3 channel, while the overlay represents a merge of the DAPI (nuclear staining) and Cy3 channels. Scale bars represent 64μm.

3.2.7.4 Generation of iPSCs from fibroblasts derived from HUES7 cells

Having validated the reprogramming process and seen the morphology of putative iPSC colonies, reprogramming of HUES7-Fib cells lacking a reporter system to detect reactivation of endogenous genes was then attempted. Live staining with the hESC-surface marker TRA-1-81 (Lowry *et al.* 2008) was used to identify emerging colonies, since this was shown to be one of the most reliable markers for identification of true iPSCs *in vitro* (Chan *et al.* 2009). hESC-like colonies were identified from day 11 PTD (Figure 3.25.B), and increased in size and number in the following days until, on day 21 post-transduction, they were dissected and expanded on MEF-feeders. Colony counts on day 21 PTD revealed that the overall reprogramming efficiency of HUES7-Fib cells was 0.1±%0.01. HUES7-iPSC colonies were adapted to culture on Matrigel surfaces after 7 passages on MEF feeders.

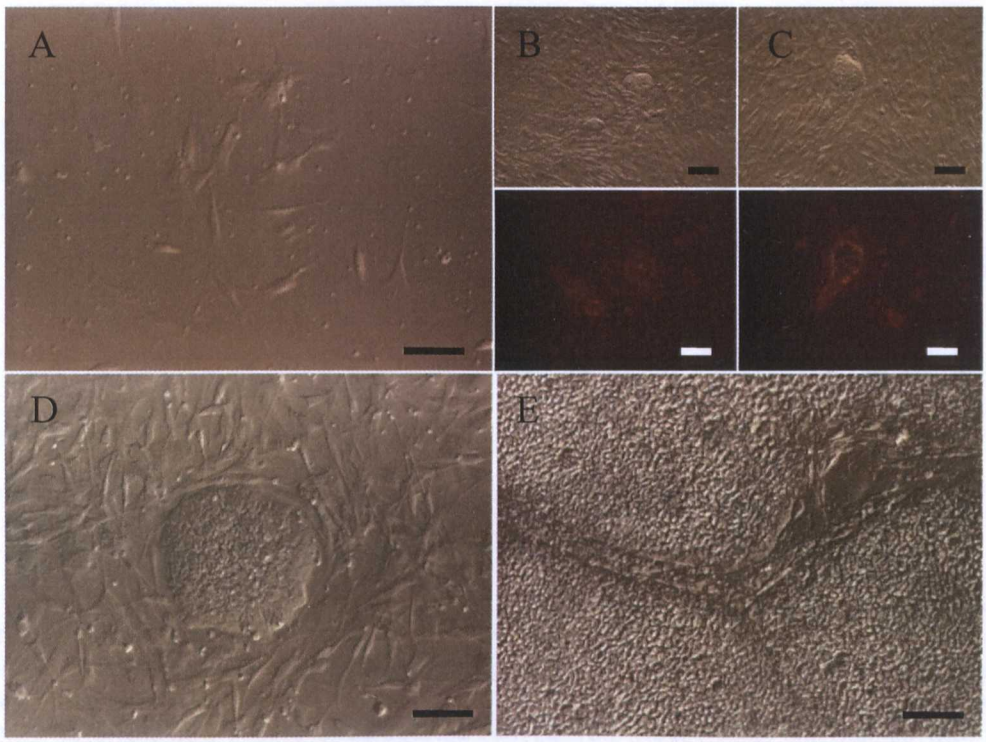

Figure 3.25- Generation of HUES7-iPSCs
Bright filed images of iPSC colonies on **A.** day 0 **B.** day 11 **C.** day 13 and **D.** day 20 after transduction with lentiviruses over-expressing the four iPSC factors. On **B.** day 11 and **C.** day 13 post-transduction, in vitro staining of iPSC colonies for the hESC-specific surface antigen TRA-1-81 was performed and visualised in the Cy3 channel (red). **E.** HUES7-iPSCs cultured on Matrigel at passage 2, 3 days after a 1:3 split. Scale bars represent 100μm.

3.2.7.5 Characterisation of HUES7-iPSCs

Differentiation of HUES7-iPSCs to endoderm and ectoderm derivatives was shown by immunofluorescence staining, as described in section 3.2.7.3 (Figure 3.26.A). Formation of mesoderm derivatives was shown by adipocyte Oil-red O staining (Figure 3.26.B), since beating cardiomyocytes were not detected in differentiated HUES7-iPSCs. Mesoderm formation from HUES7-iPSCs was also confirmed by expression of the early mesoderm marker Brachyury (Vidricaire *et al.* 1994), through immuno-histochemical and real-time PCR analysis of d10 EBs (data not shown). HUES7-iPSCs had a normal 46,XY karyotype (Figure 3.26.C), and expressed the pluripotency markers OCT4, NANOG, SSEA4 and TRA-1-81 (Figure 3.27). Cells lacked expression of the fibroblast markers P4HB and FSA. (Figure 3.27)

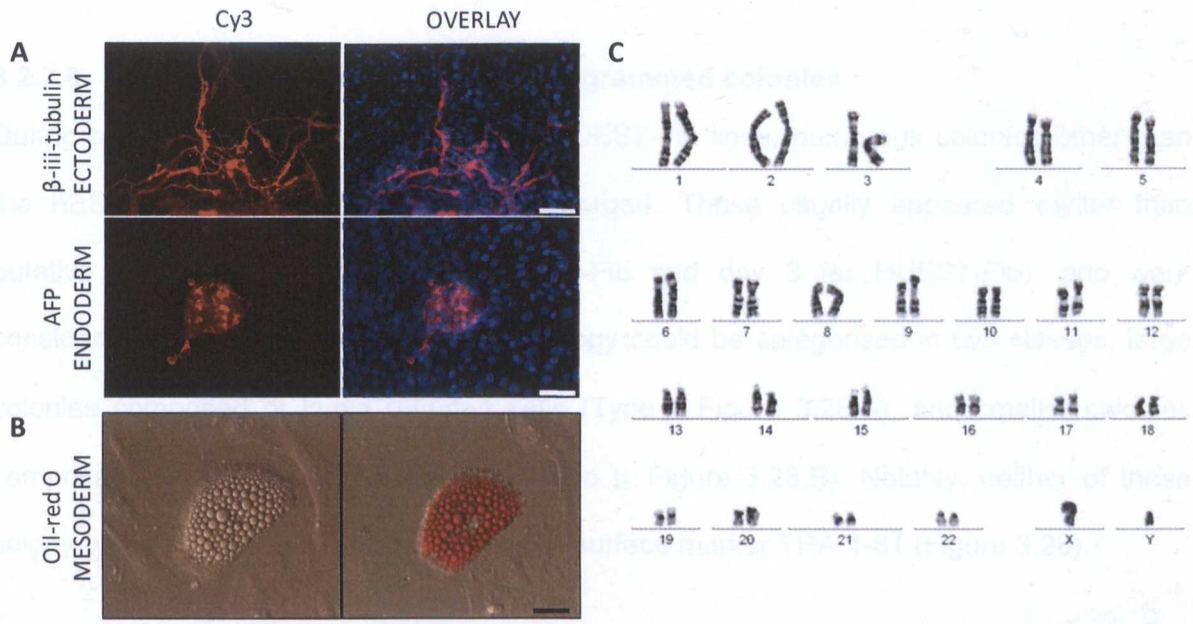

Figure 3.26- Germ layer formation and karyotype analysis in HUES7-iPSCs
A. Differentiation of HUES7-iPSCs to cell types representative of ectoderm and endoderm. Protein expression was captured using the Cy3 channel, while the overlay represents a merge of the DAPI (nuclear staining) and Cy3 channels. **B.** Bright field images of adipocytes derived from HUES7-iPSCs and stained with Oil-red O. Adipocyte generation is representative of mesoderm formation. **C.** HUES7-iPSCs carried an abnormal 46,XY karyotype. Scale bars represent 64μm.

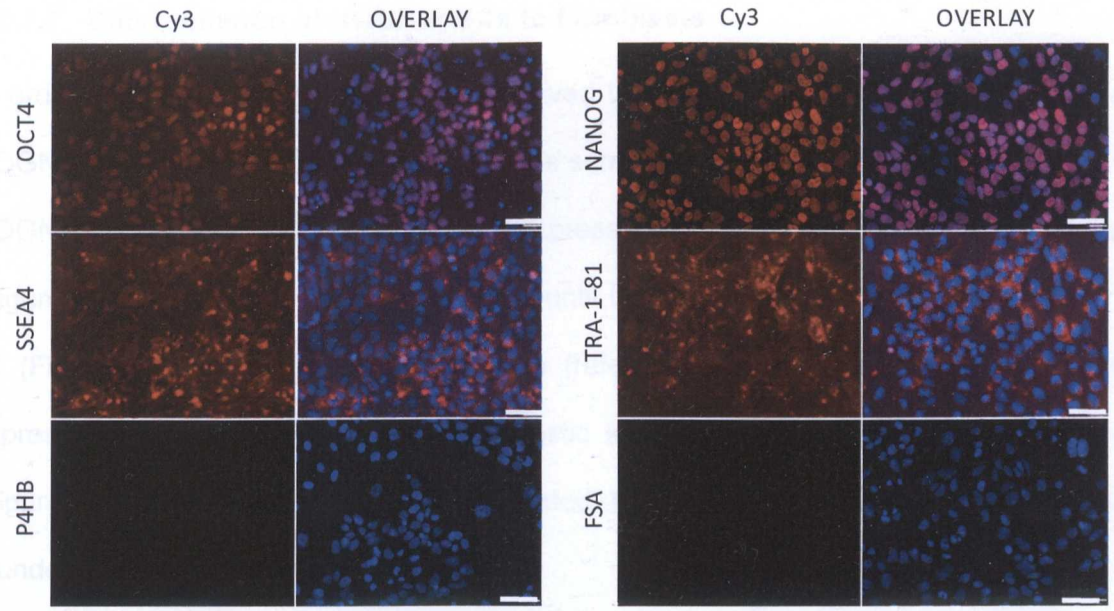

Figure 3.27- Expression of pluripotency-associated and fibroblast-specific markers in HUES7-iPSCs
Immunofluorescence analysis of OCT4, NANOG, SSEA4, TRA-1-81, P4HB and FSA expression in HUES7-iPSCs. Marker expression was captured using the Cy3 channel, while the overlay represents a merge of the DAPI (nuclear staining) and Cy3 channels. Scale bars represent 64μm.

3.2.7.6 Morphology of incompletely reprogrammed colonies

During reprogramming of HOGN-Fib and HUES7-Fib lines, numerous colonies other than the hESC-like putative iPSC colonies emerged. These usually appeared earlier than putative iPSC colonies (day 6 for HOGN-Fib and day 8 for HUES7-Fib), and were considerably more abundant. Their morphology could be categorised in two classes; large colonies composed of loose rounded cells (Type I, Figure 3.28.A), and smaller colonies composed of compacted granular cells (Type II, Figure 3.28.B). Notably, neither of these colony-types stained positively for the hESC-surface marker TRA-1-81 (Figure 3.28).

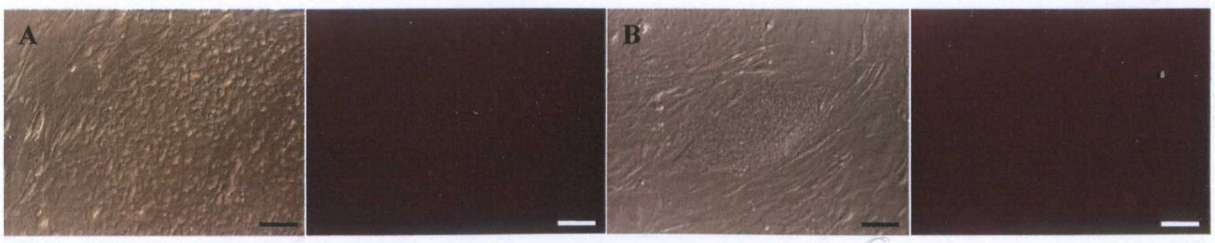

Figure 3.28– Incompletely reprogrammed colonies observed during reprogramming of HUES7-Fib
Incompletely reprogrammed colonies emerging during induction of HUES7-Fib to form iPSCs. Incompletely reprogrammed colonies were either **A.** large in size and composed of loose cells (Type I), or **B.** smaller in size and composed of granular cells (Type II). Both colony types appeared more frequently and earlier than iPSC colonies, but lacked expression of the TRA-1-81 hESC-surface marker. Scale bars represent 100μm.

3.2.7.7 Differentiation of HOGN-iPSCs to fibroblasts

In order to evaluate whether fibroblast-derived iPSCs could re-differentiate to fibroblasts, HOGN-iPSCs were differentiated through the same method previously used for HUES7 and HOGN cells (section 3.2.3). EBs strongly expressed GFP protein on day 4 of differentiation (Figure 3.29.A), but this was gradually lost until it became completely undetectable by day 18 (Figure 3.29.E). The resulting cell line (referred to as HOGN-iPS Fib) lacked GFP expression, but also lacked the characteristic spindle-like morphology of fibroblast cells (Figure 3.29.F). Differentiation was repeated twice, with fibroblasts having the same rounded morphology both times.

HOGN-iPS Fib did not express the hESC markers NANOG, SSEA4 and TRA-1-81, but did express OCT4. Lack of GFP expression in HOGN-iPS Fib (Figure 3.29) suggested that the OCT4 expression detected by immunofluorescence staining was driven by the lentiviral transgene, which failed to become silenced. Cells also lacked expression of the fibroblast marker, P4HB. Together with the rounded morphology of HOGN-iPS Fib cells (Figure 3.29), these observations suggested that the HOGN-iPS Fib line did not consist of fibroblasts.

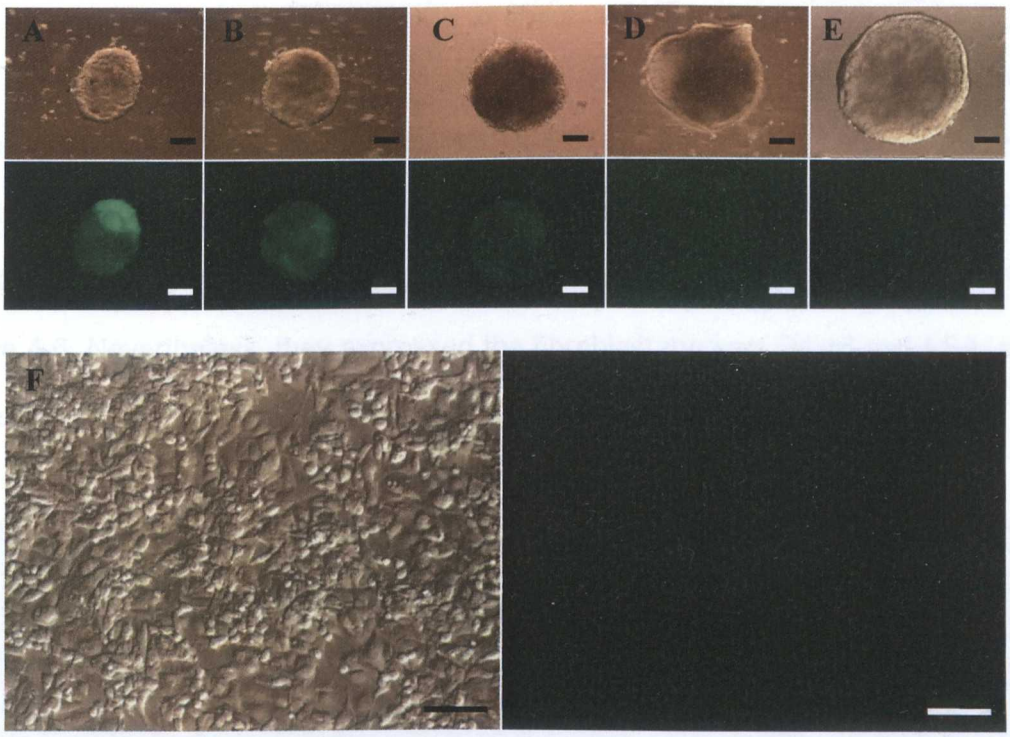

Figure 3.29- Differentiation of HOGN-iPSCs to fibroblasts
Bright field and fluorescence images of EBs on **A.** day 4 **B.** day 8 **C.** day 10 **D.** day 16 and **E.** day 18 of differentiation. **F.** Bright filed and fluorescence images of HOGN-iPS Fib at passage 3, 2 days following a 1:3 split. Scale bars represent 100μm.

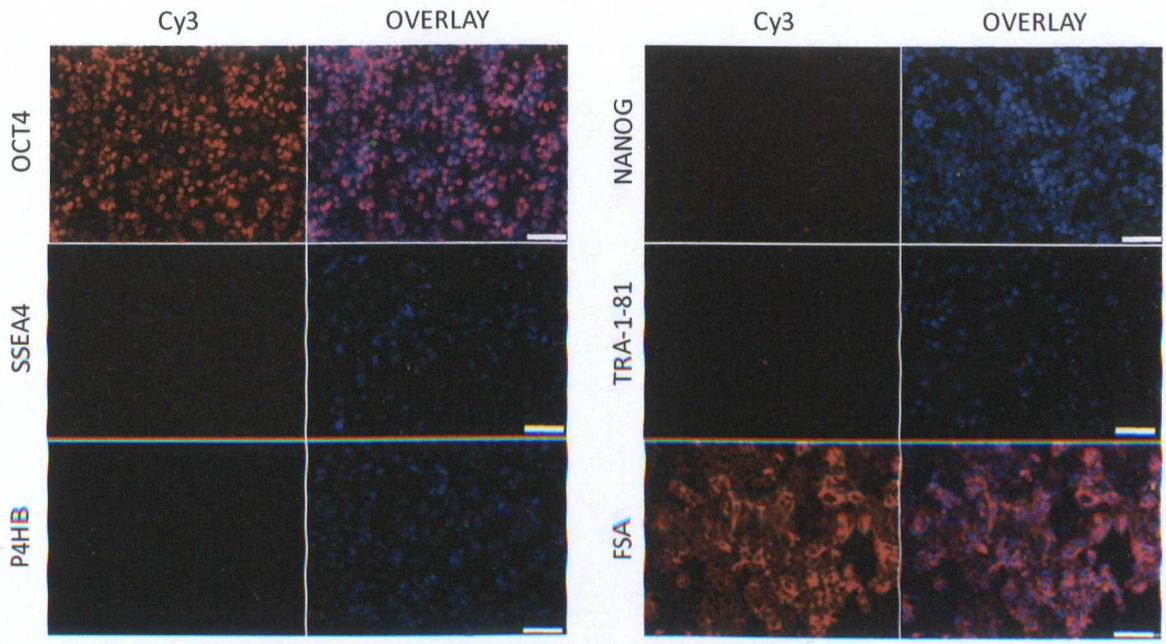

Figure 3.30- Expression of pluripotency-associated and fibroblast-specific markers in HOGN-iPS Fib
Immunofluorescence analysis of OCT4, NANOG, SSEA4, TRA-1-81, P4HB and FSA expression in HOGN-iPS Fib. Marker expression was captured using the Cy3 channel, while the overlay represents a merge of the DAPI (nuclear staining) and Cy3 channels. Scale bars represent 64μm.

3.2.7.8 Differentiation of HUES7-iPSCs to fibroblasts

HUES7-iPSCs were also differentiated into a fibroblast cell line, with the same method previously used for HUES7, HOGN and HOGN-iPSCs. The resulting cell line did show the characteristic spindle-like morphology of fibroblasts (Figure 3.31), but had reduced proliferation rates compared to HUES7-Fib. The cells reached proliferative arrest by passage 4-6. Nevertheless, they expressed the fibroblast markers P4HB and FSA, and had down-regulated expression of OCT4, NANOG, SSEA4 and TRA-1-81 (Figure 3.32).

Figure 3.31- Differentiation of HUES7-iPS to fibroblasts
Bright filed images of EBs on **A.** day 8 and **B.** day 18 of differentiation. **C.** HUES7-iPS fibroblasts (HUES7-iPS Fib) at passage 1, 3 days following trypsinisation and plating of EBs. Scale bar represents 100μm.

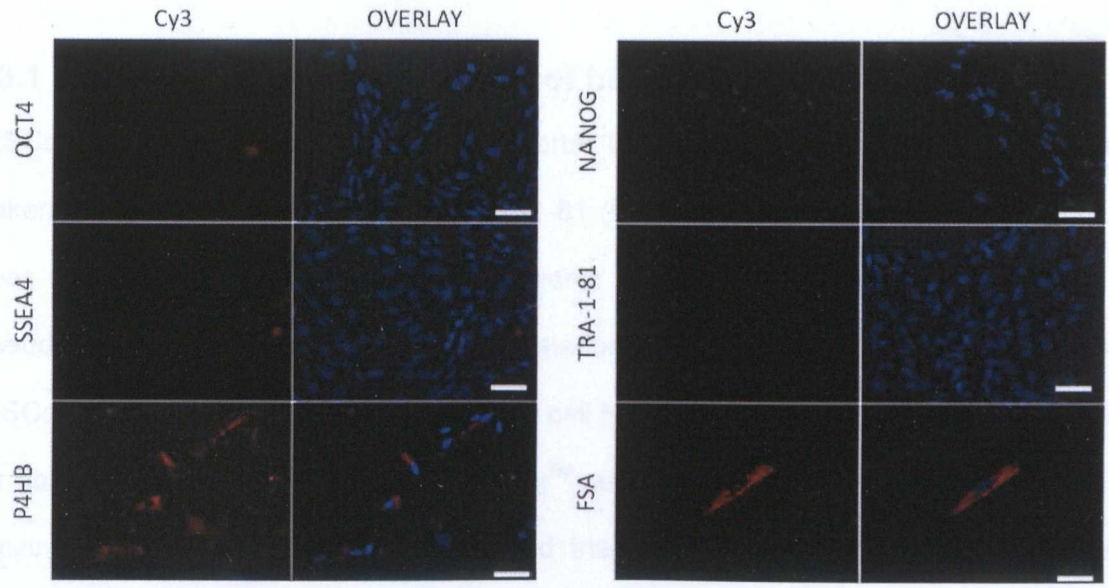

Figure 3.32- Expression of pluripotency-associated and fibroblast-specific markers in HUES7-iPS Fib
Immunofluorescence analysis of OCT4, NANOG, SSEA4, TRA-1-81, P4HB and FSA expression in HUES7-iPS Fib. Marker expression was captured using the Cy3 channel, while the overlay represents a merge of the DAPI (nuclear staining) and Cy3 channels. Scale bars represent 64μm.

3.3 DISCUSSION

In this chapter, hESC cultures of the HUES7 and *OCT4-GFP* targeted HOGN lines were characterised and differentiated *in vitro* to generate fibroblast-like cells. The fibroblasts lacked expression of pluripotency markers, but did express P4HB and FSA; two markers shown to specifically detect fibroblasts in this study. P4HB was only expressed in a subset of hESC-derived fibroblasts, in contrast to clonal lines derived from these cells that showed 90-96% expression of P4HB. Unfortunately, due to proliferative arrest, the clonal lines were not used in reprogramming experiments. Instead, they were pelleted for use in gene expression and epigenetic analyses (chapter 4). Since lentiviral transduction had not been performed previously in our lab, a protocol for efficient genetic manipulation by lentiviral transduction was established and then used to reprogram hESC-derived fibroblasts to iPSCs. Reprogrammed cells were successfully differentiated to all three embryonic germ layers, and showed silencing of fibroblast-specific markers as well as reactivation of hESC-specific markers. iPSCs were further differentiated to fibroblasts to complete generation of the model cell system, described in Figure 1.1.

3.3.1 Culture and characterisation of hESCs

hESCs of the HUES7 and *OCT4-GFP* reporter line, HOGN, expressed the hESC-specific makers OCT4, NANOG, SSEA4 and TRA-1-81 (Figure 3.8), and could differentiate to cell-types representative of the three embryonic germ-layers; endoderm, ectoderm and mesoderm (Figure 3.3 and Figure 3.4). Formation of beating cardiomyocytes indicated that hESCs could derive functional differentiated cell types (section 3.1.2). HUES7 hESCs had a normal karyotype when cultured on Matrigel™ surfaces with MEF conditioned medium and trypsin passaging (Figure 3.3). HOGN had trisomy of chromosome 12 and addition of chromosome 17 material to the small arm of chromosome 21 (Figure 3.4). When the HOGN cell line was generated by (Braam *et al.* 2008b) cells were reported to have normal karyotype after transfection with the *OCT4-GFP* targeting plasmid and clonal growth.

However, trisomy of chromosome 12 was detected in a sub-set of cells during culture scale-up (Braam *et al.* 2008b), and as a result, HOGN cultures used for this thesis also had an abnormal karyotype. Karyotype abnormalities involving chromosomes 12, 17q and 20q11, accumulate frequently in cultures of hESCs (Draper *et al.* 2004; Spits *et al.* 2008) and are speculated to confer a proliferative advantage to hESCs by increasing the dosage of pluripotency-associated genes such as NANOG, which is located on chromosome 12 (Clark *et al.* 2004; Draper *et al.* 2004). Despite their abnormal karyotype, HOGN were used to derive fibroblasts, and subsequently iPSCs, since their *OCT4-GFP* reporter system was valuable for distinguishing between fully and partially reprogrammed iPSC colonies, which were being derived for the first time in our lab.

3.3.2 Derivation and characterisation of hESC-fibroblast lines

In this project, fibroblast-like cells were generated from the *OCT4-GFP* reporter line, HOGN, and the genetically unmodified line, HUES7 (section 3.2.3.). Fibroblasts from both lines were cultured by regular split intervals for approximately 15 passages (45-60 days), after which they begun to senesce. Senescence is not uncommon for *in vitro* cultured primary fibroblasts (Hayflick and Moorhead 1961; Goldstein 1990), which show limited proliferative capacity related to telomere shortening (Allsopp and Harley 1995). It is also not uncommon for ESC-derived cells since telomere shortening due to reduced human telomerase reverse transcriptase (*hTERT*) expression begins upon differentiation of hESCs (Lebkowski *et al.* 2001; Xu *et al.* 2001). hESC-derived fibroblasts were previously shown to proliferate in culture for 40-55 days (Xu *et al.* 2004), in line to results from this study. Genetic modification involving *hTERT* over-expression could extend the life-span of hESC-derived fibroblasts by at least twice (Xu *et al.* 2004).

Fibroblasts derived from the *OCT4-GFP* reporter line, HOGN, were sensitive to treatment with G418 at concentrations of 50μg/ml or higher (Figure 3.7). Since 50μg/ml were not toxic

to undifferentiated cells, it was decided that this concentration would be used in reprogramming experiments using HOGN-Fib as a "parent cell-line", in order to select against partially reprogrammed cells that had not reactivated the expression endogenous *OCT4*. This was in agreement with the concentration of G418 used in Yu *et al.* (2007b), who employed the same lentiviral system used here for iPSC generation. Worth noting is that HOGN-Fib did not show detectable expression of OCT4 or GFP proteins (Figure 3.6), but had increased resistance to G418 compared to HUES7-Fib (Figure 3.7). This suggested that HOGN-Fib expressed OCT4 at residual levels or that some cells within the HOGN-Fib population remained undifferentiated. Latent undifferentiated cells have previously been observed in populations of differentiated mESCs, and are increasingly common in lines with karyotype abnormalities (Enseat-Waser *et al.* 2009), such as the HOGN line. Staining with the fibroblast-specific marker P4HB confirmed that both the HUES7-Fib and HOGN-Fib populations consisted of cells other than fibroblasts, while the percentage of non-fibroblast cells was ~15% higher in HOGN-Fib compared to HUES7-Fib (Figure 3.12). In contrast to P4HB, FSA expression was detected in most cells within the HOGN-Fib and HUES7-Fib populations (Figure 3.11), suggesting that P4HB was a more stringent fibroblast-specific marker than FSA. This is in accordance to studies that have reported FSA expression in other mesodermal lineages (e.g. macrophages and peripheral monocytes; Singer *et al.* 1989).

3.3.3 Lentiviral transduction of hESCs and hESC-fibroblasts

One of the aims of this chapter was to generate a protocol for efficient lentiviral transduction of hESCs and hESC-derived fibroblasts, since this had not been performed previously in our lab. Despite the availability of lentiviral transduction protocols in the literature (Kutner *et al.* 2009), it was important to determine the parameters that allowed efficient transduction with the type of second generation plasmids used in this thesis (VSV-G pseudotype; Burns *et al.* 1993; Zhou *et al.* 2003). Also, it was important to improve the efficiency of available

transduction protocols, which often result in the generation of low titre viral supernatants (D'Costa *et al.* 2001). After testing a number of parameters involved in the process (Figure 3.13), an optimised protocol was established that allowed close to 100% transduction of target cell lines (section 3.2.6). This protocol was published in Braam *et al.* (2008a), a paper describing methods for efficient genetic modification of hESCs. The protocol used centrifugal Amicon-Ultra filter units for the concentration of viral supernatants (Figure 3.19), which have been shown to result in higher lentiviral particle titres and recovery efficiencies compared to other techniques, such as ultra-centrifugation or anion exchange chromatography (Sena-Esteves *et al.* 2004), which are more elaborate and time-consuming processes (Tiscornia *et al.* 2006; Kutner *et al.* 2009). Also, the virus was used fresh to transduce target cells, since storage at 4 or -80°C decreased transduction efficiency by ~20-40% (Table 3.3). This is often ignored by other studies who recommend freezing the virus despite observing up to 50% losses in viral transduction due to repeated freeze-thaw cycles (Beyer *et al.* 2002). Collection of virus-containing medium from HEK293 cells at time-points after day 2 post transfection (i.e. day 4 and 6 post-transfection) resulted in a 20-58% decrease in transduction efficiency. This effect was consistent with findings from previous papers (Geraerts *et al.* 2006) and was likely to be related to the short life-time of lentiviral particles (19h±0.2; Chilton and Le Doux 2008), or to increasing deficiency in metabolic energy of the virus-producing cell-line HEK293 (Cynthia *et al.* 2003; Elias *et al.* 2003) and loss of plasmid expression following cell divisions of HEK293 cells (Geraerts *et al.* 2006).

3.3.4 Formation of iPSCs from hESC-fibroblast lines

Lentiviral-mediated over-expression of the four pluripotency-associated genes, *OCT4*, *NANOG*, *SOX2* and *LIN28,* was used in this study to induce reprogramming of hESC-derived fibroblasts to iPSCs (section 3.2.7). This method was originally described by the group of Dr. James Thomson (Yu *et al.* 2007b), who also pioneered the isolation of hESCs from blastocyst embryos (Thomson *et al.* 1998).

Fully reprogrammed HOGN-iPSCs were identified based on expression of GFP protein, which indicated reactivation of endogenous *OCT4* (Figure 3.22). HUES7-iPSCs were identified by live cell staining with the surface marker TRA-1-81 (Figure 3.25), previously shown to be the most reliable marker for early *in vitro* selection of *bona fide* iPSCs from genetically unmodified "parent" cells (section 1.8.1.1, Figure 1.11). Incompletely reprogrammed type I and type II colonies lacked TRA-1-81 expression (Figure 3.28), supporting the notion that TRA-1-81 is a powerful marker for early *in vitro* identification of *bona fide* iPSC colonies (Chan *et al.* 2009).

During reprogramming of HOGN-Fib, putative iPSC/ hESC-like colonies were first observed on day 8 PTD, which was 3 days earlier to colony detection during HUES7-Fib reprogramming (day 11 PTD). It is possible that the karyotypically abnormal HOGN-Fib cells, carrying an extra copy of the pluripotency gene NANOG, had a "reprogramming advantage" relative to HUES7-Fib that had a normal karyotype. Appearance of HUES7-iPSC colonies was detected on day 11 PTD. This was similar to reprogramming of IMR90 human foetal fibroblasts by lentiviral transduction of "iPSC factors", where iPSC colonies were detected on day 12 PTD (Yu *et al.* 2007b), but was earlier compared to reprogramming of neonatal fibroblasts using retroviral vectors, where iPSC colonies were detected on 15 day PTD (Hotta *et al.* 2009). The overall efficiency of colony formation from HUES7-Fib was 0.1±%0.01, consistent with other studies using lentiviral transduction to over-express the four "iPSC factors", and 10 to 100-fold more efficient compared to studies using retroviral transduction (Table 3.2) which is more prone to silencing by the host genome (section 3.1.3.2). An iPSC generation efficiency of 0.1% was at the higher end of the range reported by previous studies who used lentiviral transduction of *OCT4*, *NANOG*, *SOX2* and *LIN28* (Table 3.2), and is consistent with the advantageous use of hESC-derived fibroblasts as an "iPSC parent-line", instead of the more terminally differentiated foetal, neonatal or adult fibroblasts (Park *et al.* 2008c; Laurent *et al.* 2010).

The iPSC-generation method used in this thesis served the purpose it was chosen for, i.e. the efficient derivation of reprogrammed cells that would enable the study of epigenetic changes associated with key pluripotency genes and the transition of cell phenotype from a differentiated to a pluripotent state.

3.3.5 Derivation and characterisation of iPSC-fibroblast lines

HUES7-iPS were successfully differentiated to P4HB positive fibroblasts (Figure 3.32), demonstrating that they could "circle-back" to the same cell-type they were derived from when the same differentiation protocol was applied. This showed that hESCs and iPSCs shared similar differentiation potentials. However, HOGN-Fib differentiation resulted in the generation of P4HB negative cells which lacked the characteristic spindle-like fibroblast morphology. The persistent expression of OCT4 in HOGN-iPS Fib (Figure 3.30) could be responsible for the unexpected morphology of HOGN-iPS Fib. It is likely that HOGN-iPS were differentiated towards endoderm lineages, since *OCT4* over-expression in hESCs has been shown to promote up-regulation of markers indicative of endoderm derivatives (Rodriguez *et al.* 2007). Repression of lentiviral transgene expression is an important characteristic of fully reprogrammed iPSCs (Akitsu Hotta 2008). Even though HOGN-iPS could differentiate to the three embryonic germ layers (Figure 3.23) and expressed all pluripotency-markers analysed (Figure 3.24) their inability to differentiate to the cell-type they were derived from (i.e. to fibroblasts) indicates that HOGN-iPSCs might not have been fully reprogrammed. Despite the karyotype and phenotype abnormalities, cells of the HOGN model system were used in chapter 4 to study the epigenetic mechanisms associated with expression of pluripotency associated genes, in order to determine whether any differences existed between the HOGN and the HUES7 model systems.

4 EXPRESSION AND EPIGENETIC REGULATION OF PLURIPOTENCY GENES IN CELLS OF THE MODEL SYSTEM

4.1 INTRODUCTION

In chapter 3, hESC-fibroblasts, iPSCs and iPSC-fibroblasts were all derived from the same hESC line, generating a model system of cells having the same genotype but different phenotypes. In this chapter, the aim was to link the transcriptional basis associated with the change of cell phenotype from a pluripotent to a fibroblast differentiated state to its regulation by the epigenome. Thus, some of the epigenetic mechanisms associated with key pluripotency-associated genes in cells of the model system, but also during transition between phenotypes, were investigated. The genes involved in this analysis were *OCT4*, *NANOG*, *SOX2* and *LIN28*; used to generate iPSCs, as well as *KLF4*; a TF at the top of the ESC transcriptional hierarchy and necessary for self-renewal in ESCs (section 1.3.2), and *DNMT3B* and *REX1*; two TFs that are dispensable for self-renewal in ESCs but necessary for normal differentiation (Table 1.1).

4.1.1 Transcriptional regulation of pluripotency-associated genes by epigenetic modifications

It is documented that TFs at the top of the transcriptional hierarchy in mouse and human ESCs interact with each other and also with themselves to auto-regulate their expression (sections 1.3.2 & 1.8.2). However, no comprehensive information is available about the epigenetic states of pluripotency associated genes in ESCs or in differentiated cell phenotypes. This section tries to collect the currently available information regarding the epigenetic regulation of pluripotency genes in mouse and human cells.

4.1.1.1 OCT4

Oct4 is the best characterised pluripotency gene in terms of its epigenetic regulation (Table 4.1). The Oct4 promoter is active and unmethylated at the DNA level in mouse and human

ESCs (Deb-Rinker *et al.* 2005a; Brunner *et al.* 2009). Histone de-methylation at H3K9, catalysed by Jmjd1a and Jmjd2c, and methylation at H3R17 & 26, catalysed by CARM1, are also associated with the active *Oct4* promoter in mESCs and are thought to contribute to the maintenance of a euchromatic state at the promoter region (Loh *et al.* 2007; Wu *et al.* 2009a). Silencing of *Oct4* during differentiation (Figure 4.1) has been associated with enriched G9a-mediated H3K9me, which is recruited to the *Oct4* promoter following binding of the germ-cell nuclear factor (GCNF; Feldman *et al.* 2006; Epsztejn-Litman *et al.* 2008). H3K9me also recruits binding of heterochromatin protein 1 (HP1), which is thought to promote heterochromatinisation and repression of the *Oct4* promoter (Gu *et al.* 2006). *Oct4* is believed to then be stably silenced by recruitment of Dnmt3a and 3b which catalyse *de novo* DNA methylation, several days after histone methylation has taken place (Feldman *et al.* 2006; Gu *et al.* 2006; Li *et al.* 2007c). Recruitment of Dnmt3a and 3b is facilitated by binding of the methyl-binding protein 3 (MBP3, core component of the nucleosome remodelling and de-acetylase (NuRD) complex) to the *Oct4* promoter while it is still un-methylated (Xue *et al.* 1998; Gu *et al.* 2006). During differentiation, the pluripotency regulating gene *Oct4* also loses the activating histone marks, H3K9Ac, K3K14Ac and H3K4me (Feldman *et al.* 2006; Gu *et al.* 2006).

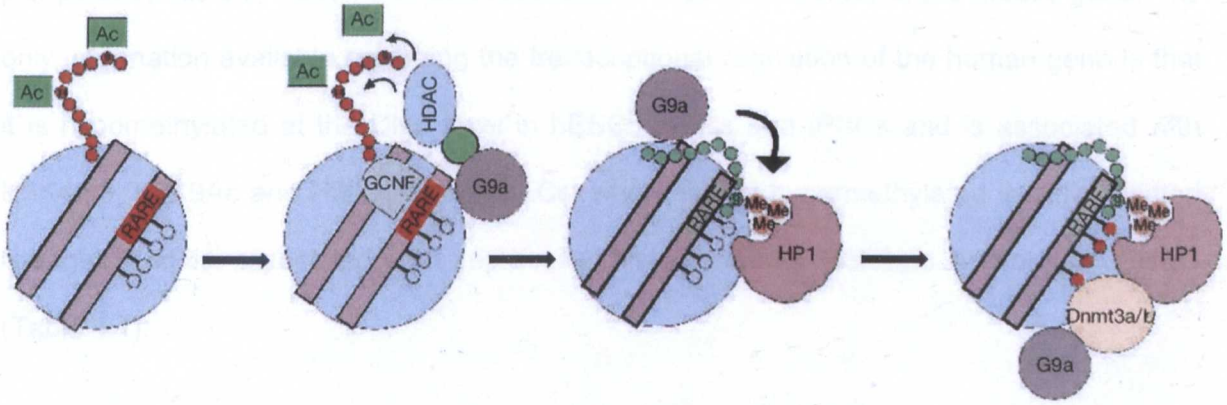

Figure 4.1- Model for *Oct4* heterochromatinisation during differentiation of mESCs
Germ-cell nuclear factor (GCNF) binds the *Oct4* promoter at the retinoic acid receptor element (RARE). This brings about binding of G9a, which catalyses H3K9 methylation, and of histone de-acetylase (HDAC) enzymes, which catalyse removal of H3K4 & K14 acetylation. Heterochromatin protein 1 (HP1) then binds H3K9me residues. Finally, Dnmt3a and 3b are recruited to the *Oct4* promoter to catalyse *de novo* DNA methylation. AC= histone acetylation, Me= histone methylation, open lollipops = un-methylated DNA, red lollipops= methylated DNA (Feldman *et al.* 2006).

Upon reprogramming to iPSCs, *Oct4* becomes de-methylated *via*, thus far, unknown mechanisms (Takahashi *et al.* 2007). H3K9 methylation or association with other histone modifications or histone and chromatin modifying enzymes has not been analysed in the *Oct4* promoter of iPSCs. It is possible that re-activation of Oct4 expression during iPSC formation could be facilitated by protein sumoylation and phosphorylation. These two epigenetic modifications have been shown to affect Oct4 expression in mESCs, with sumoylation promoting Oct4 stability, DNA binding and transcriptional activity (Wei *et al.* 2007), and phosphorylation promoting Oct4 homo- and hetero-dimerisation that in turn support transcriptional activity by auto-regulatory feed-back loops (Saxe *et al.* 2009). In hESCs, expression of OCT4 at the levels required to sustain pluripotency (Niwa *et al.* 2000; Rodriguez *et al.* 2007) is thought to be regulated by the ubiquitin ligase, WWP2, which can directly interact with OCT4, resulting in ubiquitilation and degradation of OCT4 by the 26S proteosome (Xu *et al.* 2009b). Ubiquitilation is also thought to form part of the OCT4 auto-regulatory circuit, perhaps antagonising phosphorylation to maintain OCT4 expression at appropriate levels (Xu *et al.* 2009b).

Even though the epigenetic regulation of *Oct4* has been characterised more than other pluripotency-factors, most information available comes from studies of the mouse gene. The only information available regarding the transcriptional regulation of the human gene is that it is hypomethylated at the DNA level in hESCs, hECs and iPSCs and is associated with H3K4m3, K3K9Ac and H3K36me3 in hECs, whereas it is hypermethylated in differentiated lineages and is associated with repressive histone marks H3K9me and/or H3K79me3 (Table 4.1).

Table 4.1- Epigenetic modifications and enzymes associated with *OCT4*
TSS= Transcription start site, EC= embryonic carcinoma cell, EG= embryonic germ cell, MSC= mesenchymal stem cell, Me= DNA methylation. Histone modifications are on histone 3 (H3), unless otherwise stated. Red= silencing mark, maroon= silencing enzyme, green= activating mark, purple= activating enzyme, black= mark not associated with transcriptional activity, += active transcription, x= inactive transcription (Pan *et al.* 2006; Barrand and Collas 2009; Hemberger *et al.* 2009; Masui 2010; Table 1.3)

OCT4	Cell type	Transcription	Core promote	Proximal enhancer	Distal enhancer
			TSS, No CpG island		OCT/SOX site
Mouse	ICM, ESCs, EGs	+	-	Me	no-Me
	Epiblast, ECs, EpiSCs	+	-	no-Me	Me
	ECs, ESCs	+	de-K9me3 (Jmj1a, Jmjd2C), K4me3 (MLL, Paf1c), R17&26me3 (CARM1), K9&14Ac, Euchromatin (Chd1)		
	Differentiated cells	x	-	Me (Dnmt3a &3b), K9me2&3 (G9a-EHMT1), Heterochromatin (HP1)	
	iPSCs	+	-	de-Me	
Human	ESCs	+	-	no-Me	
	ECs	+	K9Ac, K4me2&3,	-	K4me2&3, K9Ac, K36me3
	Neurons	x	Me		
	Adipose MSCs	x	Me, K9me, K79me3	-	Me, K9me, K79me3, K36me3
	Adult fibroblasts	x	Me, K9me, K79me3	-	Me, K9me, K79me3
	Keratinocytes	x	Me, K9me	-	Me, K9me,
	iPSCs	+	-	de-Me	

4.1.1.2 NANOG

The regulation of *NANOG* expression has not been characterised to the same extent as *OCT4*. Available information from the literature is summarised in Table 4.2. The transcriptional activity of this pluripotency regulator in mouse and human ESCs is associated with an unmethylated promoter at the DNA level (Deb-Rinker *et al.* 2005a; Meissner *et al.* 2008). In hECs, *NANOG* is also associated with the activating histone marks H3K9Ac and H3K36me3 (Barrand and Collas 2009). In differentiated cell types, the *Nanog* promoter becomes associated with increased DNA methylation (especially in the OCT/SOX binding site), possibly through collaboration between Dnmt3a and Dnmt3b in mouse cells (Chen *et al.* 2003; Farthing *et al.* 2008), as well as with H3K9 and K27 methylation, which are believed to promote heterochromatinisation and silencing of this pluripotency gene (Barrand and Collas 2009). However, mechanistic details of how these epigenetic modifications occur are unknown and the human gene is poorly studied.

Table 4.2- Epigenetic modifications and enzymes associated with *NANOG*
Abbreviations and colour coding same as in Table 4.1

NANOG	Cell type	Transcription	Core promote	Proximal enhancer	Distal enhancer
			TSS, No CpG island	OCT/SOX site	
Mouse	ESCs, ECs, EGs	+	de-K9me3 (Jmj1a, Jmjd2C)		
	ESCs	+	K4me3 (Paf1c), R17&26me3 (CARM1), Euchromatin (Chd1)		
	Differentiated cells	x	-	Me (Dnmt3a &3b), K9me2&3 (G9a), HP1, K27me3 (PCR2; Ezh2 Suz12, Eed)	
	iPSCs	+	-	de-Me	
Human	ESCs	+		no-Me	
	ECs	+	-	K4me2&3, K9Ac, K36me3	
	Neurons	x	-	Me	-
	Adipose MSCs, Adult fibroblasts, Keratinocytes	x	-	Me	no-Me
				K9me, K27me3	
	iPSCs	+	-	de-Me	

4.1.1.3 SOX2

Transcriptional activity in *Sox2* has been associated with increased CARM1-catalysed H3R16 and R17 methylation in the mouse, and with increased H3K9Ac in human ECs (Table 4.3). In differentiated cell types, *SOX2* becomes associated with the repressive histone marks H3K27me3 and H3K9 in human cells (Barrand and Collas 2009), and also with DNA methylation in mouse cells; a region 2.7kb upstream from the *Sox2* TSS, containing two POU binding sites, was found to be hyper-methylated in MEFs, brain, kidney and germ cells compared mESCs Imamura *et al.* 2006. Furthermore, a region 3.5kb downstream the *Sox2* TSS, containing an OCT/SOX biding site, was shown to be slightly more methylated in MEFs, brain and kidney than mESCs (Imamura *et al.* 2006). Some *SOX2* hyper-methylation has been observed in human gastric cancer cells (Otsubo *et al.* 2008), but not in healthy human cells.

Table 4.3- Epigenetic modifications and enzymes associated with SOX2
Abbreviations and colour coding same as in Table 4.1

SOX2	Cell type	Transcription	Core promoter	Proximal enhancer	Distal enhancer	Coding region
			TSS CpG island		POU site	OCT/SOX site
Mouse	ESCs	+	no-Me	-	no-Me	no-Me
			R17&26me3 (CARM1), Chd1			-
	Germ cells	x	no-Me	-	Me	no-Me
	MEFs, brain & kidney cells	x	no-Me	-	Me	Me
Human	ECs	+	K4me2&3, K9Ac,		-	K4me2&3, H9Ac, K36me3
	Adipose MSCs, Adult fibroblasts	x	K9me, K27me3, K79me3		-	K9me, K27me3, K79me3
					-	
	Keratinocytes	x	K9me, K27me3		-	K9me, K27me3
	Gastric cancer	x	Me		-	-

4.1.1.4 KLF4

Very little information is available about the epigenetic regulation of *KLF4*. This pluripotency-associated gene was found to be hyper-methylated in cancer cells, in a region located -156 to -39 to the TSS (Wei *et al.* 2006; Yong Gu *et al.* 2007) and more recently, in the CpG island of medulloblastoma cells (Nakahara *et al.* 2010). The *KLF4* TSS is also hypermethylated in hESC-derived fibroblasts and neonatal fibroblasts relative to hESCs, however, the exact region analysed is not well documented (Laurent *et al.* 2010). Even though KLF4 can interact with HAT (e.g. p300) and HDAC (e.g. HDAC5) enzymes (Yoshida *et al.* 2008; Evans *et al.* 2010), association of histone or chromatin modifying enzymes with the *KLF4* promoter has not been characterised to date. At the post-transcriptional level, *KLF4* is negatively regulated by miRNA-145 (Xu *et al.* 2009c).

4.1.1.5 LIN28

LIN28 methylation has been observed in somatic tumour cells (Dansranjavin *et al.* 2009), but not in healthy cells. In fact, down-regulation of *LIN28* upon differentiation of human mesenchymal stem cells (hMSCs) to osteoblasts and adipocytes was shown to occur through a methylation independent pathway (Dansranjavin *et al.* 2009), suggesting that

aberrant DNA methylation could be a cancer-cell specific mechanism for gene inactivation. No other epigenetic modifications have been associated with *LIN28* at the transcriptional level. At the post-transcriptional level, *Lin28* expression is negatively regulated by *miR-125b* (*lin-4*) and *miR-125a*, which interact with the micro-RNA responsive elements miRE0, miRE1 and miRE2 found in the 3' UTR of *Lin28*, and also by miRNAs of the *let-7* family, which are themselves negatively regulated by Lin28 and DNA methylation (Johnson *et al.* 2005; Wu and Belasco 2005; Brueckner *et al.* 2007; Johnson *et al.* 2007; Newman *et al.* 2008; Viswanathan *et al.* 2008; Chang *et al.* 2009b).

4.1.1.6 DNMT3B

DNMT3B has two alternative promoters, both of which lack a TATA-box close to the TSS and contain clusters of binding sites for the TF Sp1, especially at the proximal enhancer region (Yanagisawa *et al.* 2002). Binding of Sp1 and Sp3 TFs to the *DNMT3B* promoter, positively regulates *DNMT3B* transcriptional activity (Jinawath *et al.* 2005). In mouse cells, Dnmt3b associates with several enzymes of the epigenetic machinery (e.g. HP1, Ezh2 and HDAC1) to repress the expression of target genes (reviewed by Hemberger *et al.* 2009). However, other than regulation by the TFs Sp1 and Sp3, mechanisms that have an impact on its own expression have not been characterised.

4.1.1.7 REX1

Rex1 is highly expressed in mESCs, mECs and hESCs (Shi *et al.* 2006; Adewumi *et al.* 2007). Upon differentiation, *Rex1* undergoes similar step-wise silencing to *Oct4* in mESCs, and becomes associated with increased H3K9me and HP1 binding, which promote heterochromatinisation of its promoter (Feldman *et al.* 2006). The *REX1* promoter is also unmethylated in hESCs and iPSCs, but hyper-methylated in human dermal fibroblasts and hECs (Takahashi *et al.* 2007). However, differentiation of hESCs into fibroblasts was not associated with an increase in promoter DNA methylation (Yeo *et al.* 2007).

Overall, the mechanisms that regulate the expression of key pluripotency genes are not well understood, and have mostly been characterised in mouse or cancer cells. Also, most studies suffice in characterising either pluripotent or differentiated cell phenotypes, resulting in poor understanding of how gradual changes occur in gene expression and epigenetic modifications. Therefore, as well as investigating end point phenotypes of cell-types comprising the model system generated in chapter 3, this chapter aimed to analyse several time-points during the transition from pluripotent (hESCs, iPSCs) to fibroblast differentiated phenotypes, and vice-versa from fibroblasts to iPSCs. This chapter focused on analysing the epigenetic modifications most abundantly associated with regulatory regions of pluripotency genes, which were; DNA methylation, H3K9Ac and H3K4me3, H3K9me and H3K27me3.

4.1.2 Chapter Aims and Objectives

The aim of this chapter was to analyse the expression and epigenetic regulation of the pluripotency-associated factors *OCT4*, *NANOG*, *SOX2*, *KLF4*, *LIN28*, *REX1* and *DNMT3B*, in cells of the model system (Figure 1.1, Chapter 3). To achieve this aim, the following objectives had to be met:

* Determine the gene (real-time PCR) and protein (immunofluorescence) expression levels of pluripotency-associated factors, in hESCs, iPSCs and derived fibroblasts
* Analyse DNA methylation and histone modifications in key regulatory regions of pluripotency factors, in hESCs, iPSCs and derived fibroblasts
* Investigate the timing and pattern of pluripotency-gene inactivation during differentiation, and reactivation during reprogramming to iPSCs
* Analyse the timing and pattern of DNA methylation changes and histone modifications associated with pluripotency genes during differentiation, and during reprogramming to iPSCs

4.2 RESULTS

4.2.1 Expression of pluripotency factors in cells of the model system

The first aim of this chapter was to study the expression of the pluripotency-associated factors OCT4, NANOG, SOX2, KLF4, LIN28, REX1 and DNMT3B (sections 1.3.2, 1.3.4 and 4.1.1) in hESCs, iPSCs and derived fibroblasts. As controls, this investigation included the clonal fibroblast line, HUES7-Fib Cl4 (section 3.2.5), the neonatal fibroblast line, BJ, and the adult fibroblast line, SUKE. This would establish whether any differences existed in gene expression between these, potentially, more differentiated fibroblast phenotypes and the heterogeneous hESC-fibroblasts. Expression of the fibroblast-specific marker P4HB (section 3.2.4.2) was also analysed, in order to compare the relationship between expression of pluripotency-associated and lineage commitment genes.

4.2.1.1 Selecting primers for gene expression analysis by real-time PCR

Real-time PCR analysis was performed using TaqMan® assays for *SOX2*, *LIN28*, *KLF4*, *DNMT3B*, *REX1* and *P4HB* (Applied Biosystems, Table 2.5). TaqMan® assays for *SOX2* and *LIN28* specifically amplified the endogenous genes, avoiding detection of lentiviral transgenes. Commercially available TaqMan® assays for *OCT4* and *NANOG* were not able to distinguish between the true genes and their numerous pseudogenes (Takeda *et al.* 1992; Booth and Holland 2004). Therefore, a set of primers for *OCT4* that could distinguish between the true *OCT4* transcript and its pseudogenes, as well as between endogenous *OCT4* and the transgene, were used in this study (Liedtke *et al.* 2007). However, the location and amplicon size of these primers did not permit TaqMan® probe design, leading to the use of SYBR-Green based real-time PCR analysis for *OCT4*. A TaqMan® based assay for *NANOG* was designed in our lab for this experiment, by Mr. Jayson Bispham (Bispham and Young, unpublished data), using Primer Express® software. The primers could distinguish between the true *NANOG* transcript and its eleven pseudogenes

(Appendix III), but it was not possible to also distinguish between the endogenous gene and the transgene.

4.2.1.2 Gene expression analysis by real-time PCR

Real-time PCR analysis was performed with help from Mr. Jayson Bispham and Dr. Roger McGillvray. In the pluripotent cell lines; HUES7, HUES7-iPS, HOGN, and HOGN-iPS, expression of all pluripotency factors was detected, with the exception of *REX1*, which failed to become re-activated in HUES7-iPS (Figure 4.2 and Figure 4.3). HUES7-iPS and HOGN-iPS expressed *OCT4*, *SOX2*, *KLF4, REX1* and *DNMT3B* at lower levels, compared to HUES7 and HOGN, as shown in Table 4.4. *KLF4* was expressed in all samples analysed, and was considerably high in SUKE fibroblasts (RQ= 2.52±0.42) (Figure 4.2 and Figure 4.3). *NANOG* was detected in both HUES7-iPS Fib and HOGN-iPS Fib, but other pluripotency genes were not expressed in fibroblast cells. The fibroblast specific marker *P4HB* showed reduced expression in all pluripotent samples compared to fibroblasts. This was more evident in the HUES7 model system (3 to 5-fold higher expression in fibroblasts, Figure 4.2), whereas in the HOGN system differences were more subtle (<0.5-fold higher expression in fibroblasts, Figure 4.3). The clonal line HUES7-Fib Cl4, showed the highest P4HB expression (RQ= 8.14±0.51).

Table 4.4– Differences in expression of pluripotency factors between hESCs and iPSCs
Expression in hESCs was considered to represent 100% (RQ= 1). Expression in iPSCs is presented relative to hESCs, with "-"depicting lower expression and "+" depicting higher expression.

Gene	HUES7 vs. HUES7-iPS			HOGN vs. HOGN-iPS		
	RQ value	% difference	p-value	RQ value	% difference	p-value
OCT4	0.42±0.11	- 58	0.42	0.28±0.07	- 72	0.02
NANOG	2.19±0.17	+ 119	0.03	0.88±0.18	- 12	0.20
SOX2	0.26±0.01	- 78	0.00	0.38±0.02	- 62	0.00
KLF4	0.36±0.16	- 64	0.00	0.65±0.06	- 35	0.03
LIN28	0.64±0.05	- 36	0.15	0.96±0.06	- 4	0.63
REX1	0.001±0.00	- 100	0.00	0.32±0.06	- 68	0.00
DNMT3B	0.32±0.04	- 68	0.15	0.56±0.01	- 44	0.15
P4HB	0.64±0.01	- 46	0.00	0.71±0.04	- 29	0.63

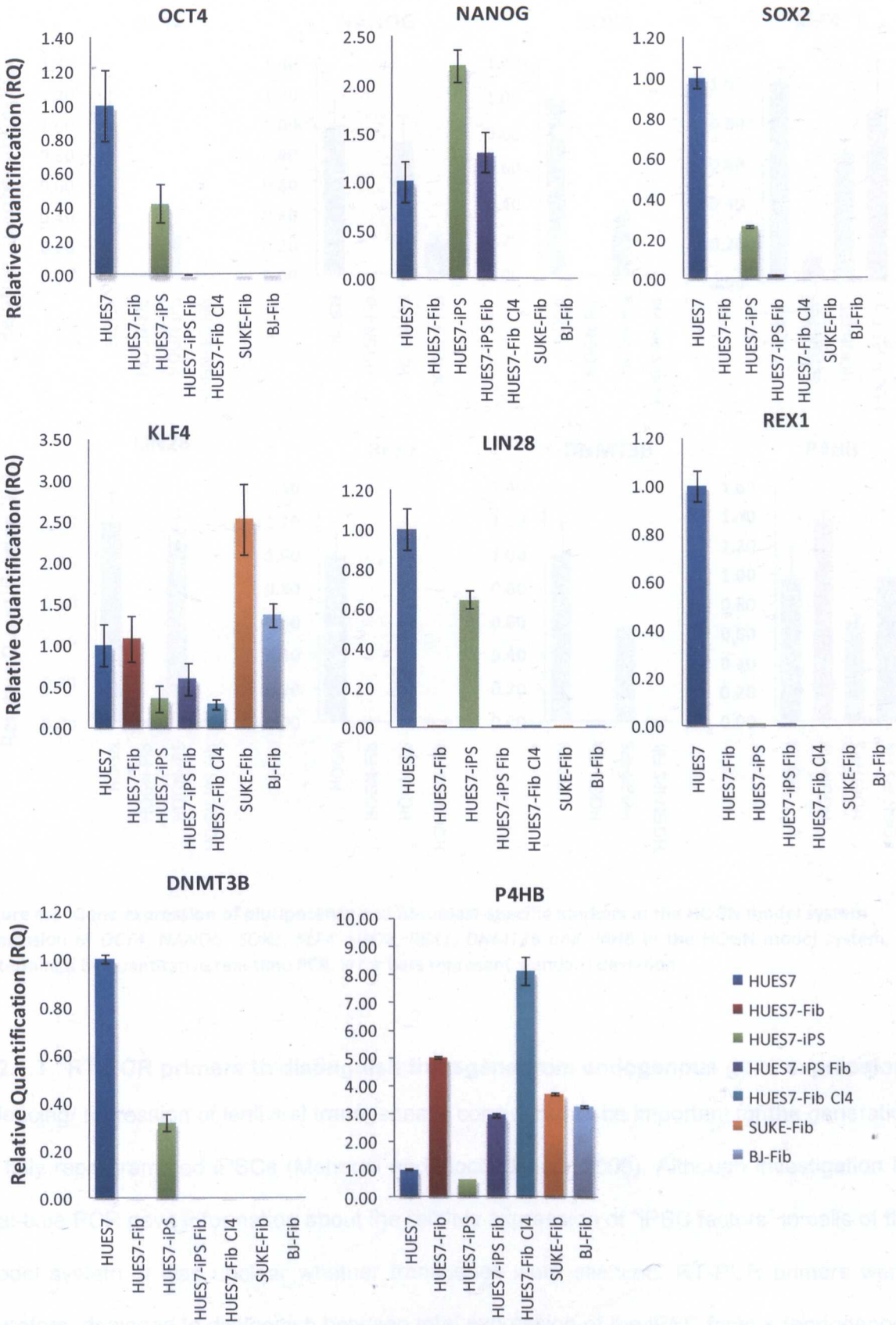

Figure 4.2- Gene expression of pluripotency and fibroblast-specific markers in the HUES7 model system
Expression of *OCT4*, *NANOG*, *SOX2*, *KLF4*, *LIN28*, *REX1*, *DNMT3B and P4HB* in the HUES7 model system and in control fibroblast lines, as determined by quantitative real-time PCR. Error bars represent standard deviation.

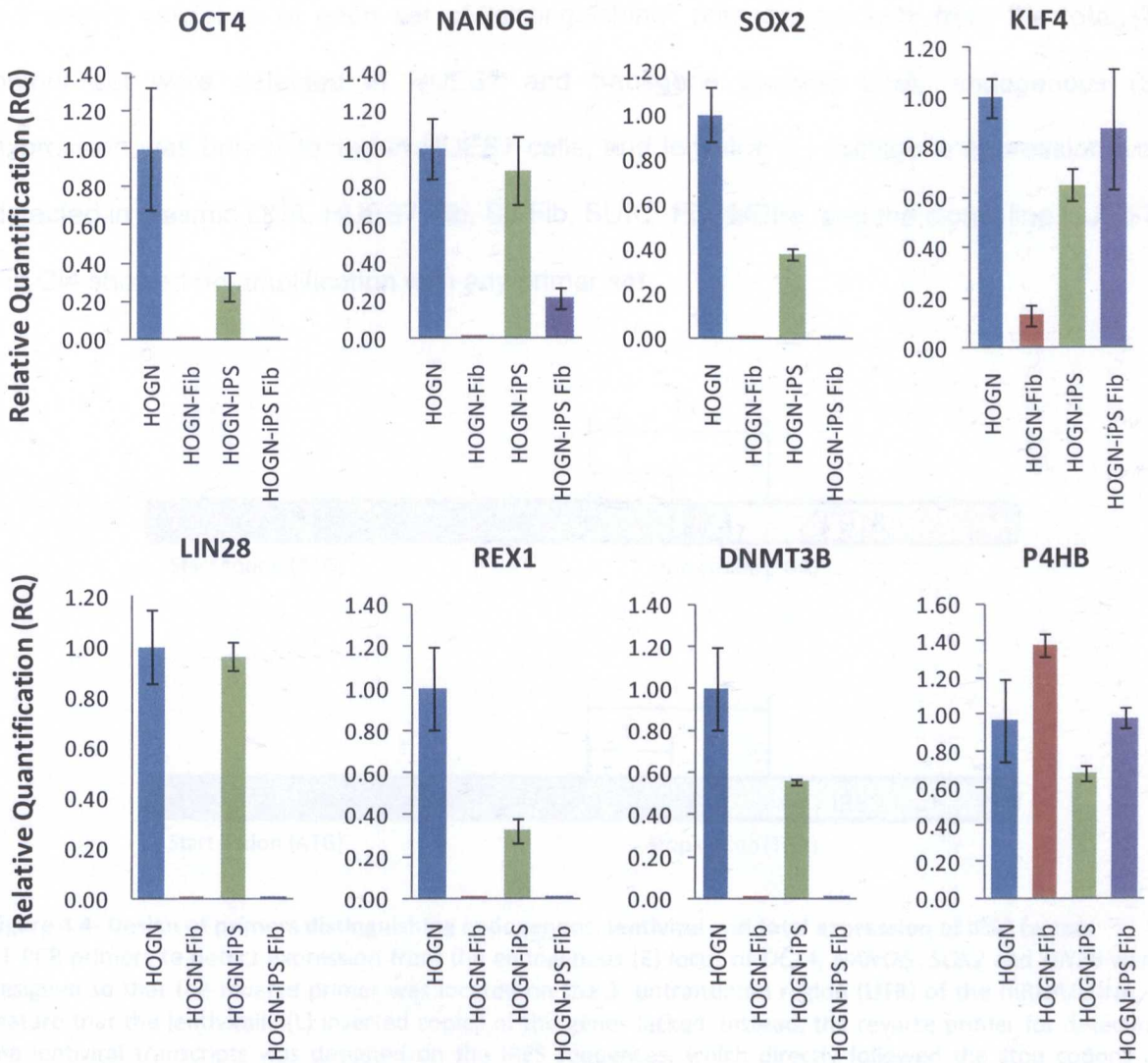

Figure 4.3- Gene expression of pluripotency and fibroblast-specific markers in the HOGN model system
Expression of *OCT4, NANOG, SOX2, KLF4, LIN28, REX1, DNMT3B and P4HB* in the HOGN model system, as determined by quantitative real-time PCR. Error bars represent standard deviation.

4.2.1.3 RT-PCR primers to distinguish transgene from endogenous gene expression

Silencing/ repression of lentiviral transgenes is considered to be important for the generation of fully reprogrammed iPSCs (Maherali and Hochedlinger 2008). Although investigation by real-time PCR gave information about the relative expression of "iPSC factors" in cells of the model system, it was unclear whether transgenes were silenced. RT-PCR primers were, therefore, designed to distinguish between total expression of the iPSC factors (endogenous & lentiviral transgene), from either endogenous or lentiviral expression (Figure 4.4). Figure

4.5 shows validation of each set of "distinguishing" primers; products from the total (T) primer set were detected in HUES7 and transgene plasmid DNA, endogenous (E) expression was only detected in HUES7 cells, and lentiviral (L) transgene expression was detected in plasmid DNA. HUES7-Fib, BJ-Fib, SUKE-Fib, MEFs, and the clonal line HUES7-Fib Cl4 showed no amplification with any primer set.

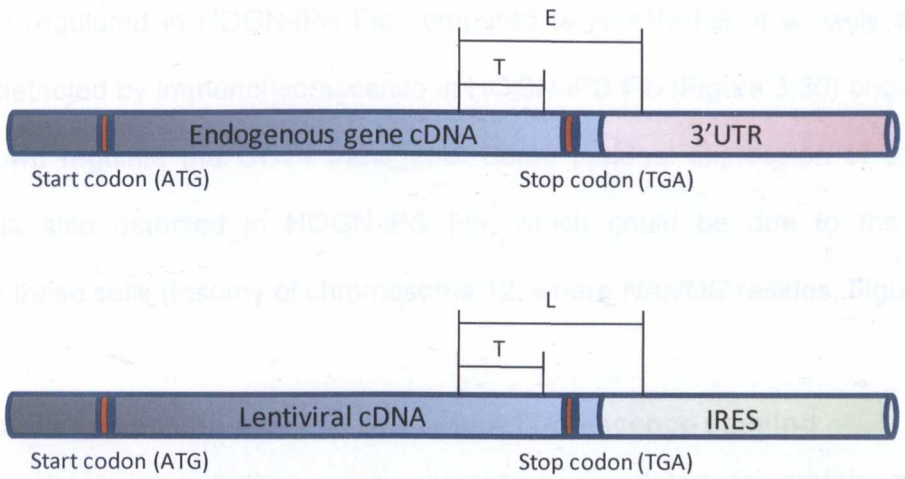

Figure 4.4- Design of primers distinguishing endogenous, lentiviral and total expression of iPSC factors
RT-PCR primers to detect expression from the endogenous (E) locus of *OCT4*, *NANOG*, *SOX2* and *LIN28* were designed so that the reverse primer was located on the 3' untranslated region (UTR) of the mRNA/cDNA, a feature that the lentivirally (L) inserted copies of the genes lacked. Instead, the reverse primer for detecting the lentiviral transcripts was designed on the IRES sequences, which directly followed the stop codons of target genes in the viral inserts. To detect the total (T) expression of target genes, i.e. from both the endogenous and lentiviral loci, the reverse primers were designed in regions 5' to the stop codons, which were present in both transcripts. The forward primers were shared between all reverse primers for each gene.

4.2.1.4 RT-PCR analysis to distinguish transgene from endogenous gene expression

Both HUES7-iPSCs and HOGN-iPSCs showed reactivation of the four iPSC factors from the endogenous loci, as well as silencing of lentiviral transgenes, especially for *SOX2*, *NANOG* and *LIN28* (Figure 4.5). Some residual expression was observed for the *OCT4* transgene in HUES7-iPS, which was however, down regulated upon differentiation to fibroblasts. HUES7-iPS Fib showed down regulation of the four iPSC factors from the endogenous loci. Unexpectedly, PCR with the L primer set in HOGN and HOGN-Fib detected a PCR product. Since neither line was transduced with an *OCT4* lentivirus, it is likely that detection of a PCR

product with the L primer represents expression from the *OCT4*-targeted *IRES-GFP-IRES-Neo* cassette (Figure 3.5.A). Sequence alignment showed that the L primer set would amplify the same product from the *OCT4* transgene and the *OCT4-IRES-GFP-IRES-Neo* locus. HOGN-iPS and HOGN-iPS Fib showed a strong PCR product when amplified with the *OCT4* L primer set, perhaps from accumulation of expression from both the endogenous *OCT4-IRES-GFP-IRES-Neo* and transgene loci. Since endogenous *OCT4* expression was largely down regulated in HOGN-iPS Fib compared to HOGN-iPS, it is likely that protein expression detected by immunofluorescence in HOGN-iPS Fib (Figure 3.30) originated from failure to down regulate the *OCT4* transgene. Some residual expression of endogenous *NANOG* was also detected in HOGN-iPS Fib, which could be due to the aneuploid karyotype of these cells (trisomy of chromosome 12, where *NANOG* resides, Figure 3.4.B).

4.2.1.5 Protein expression analysis by immunofluorescence staining

In order to determine whether gene expression correlated to protein expression, immunofluorescence staining was performed for all the markers analysed by real-time PCR (section 4.2.1.2.). OCT4, NANOG, SOX2, LIN28, REX1 and DNMT3B proteins were detected in the pluripotent lines HUES7, HUES7-iPS, HOGN and HOGN-iPS, with the exception of REX1, which was not detected in HUES7-iPSCs (Figure 4.6-4.9), correlating to TaqMan® PCR data (Figure 4.2 and Figure 4.3). Also, corresponding to the results obtained by real-time PCR, KLF4 protein expression was detected in all samples analysed (Figure 4.7 and Figure 4.9). Pluripotency-associated factors were not detected in fibroblast lines tested (Figure 4.6-4.9), in contrast to P4HB and FSA. As shown before (Figure 3.30), HOGN-iPS Fib were an exception, since they expressed OCT4 and lacked P4HB.

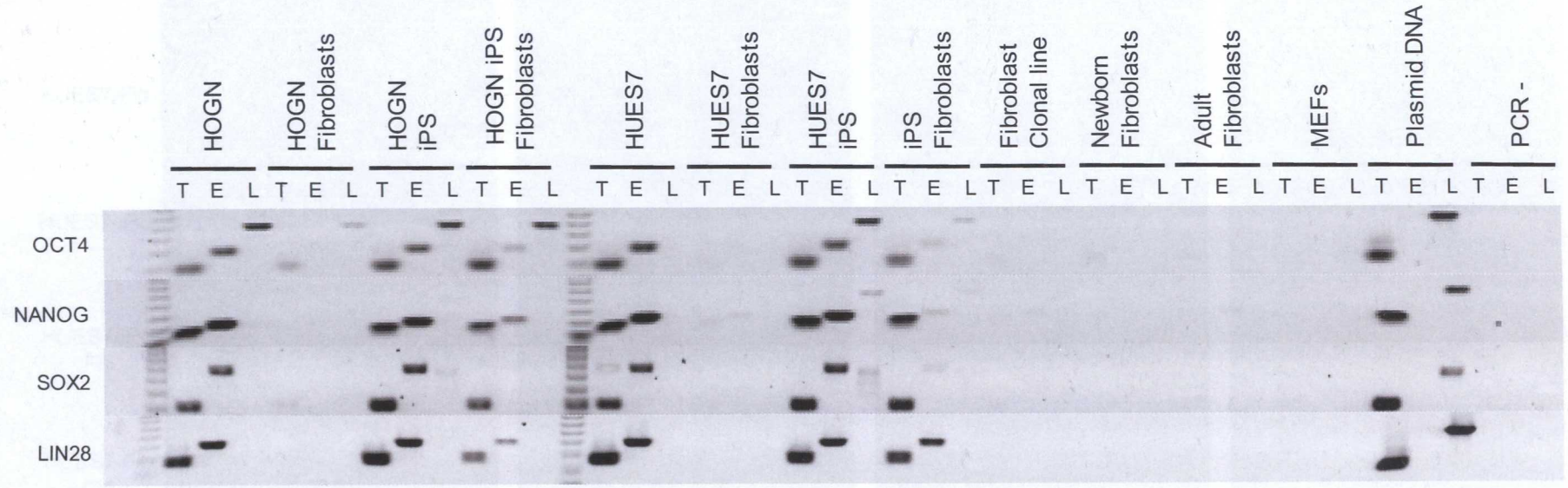

Figure 4.5- Gene expression of endogenous and lentivirally-inserted iPSC factors in the HUES7 and HOGN model systems
RT-PCR analysis showing the expression of total (T), endogenous (E) and lentivirally inserted (L) *OCT4*, *NANOG*, *SOX2* and *LIN28* genes in the HUES7 and HOGN model systems, as well as in control fibroblast lines and native transfer plasmid DNA.

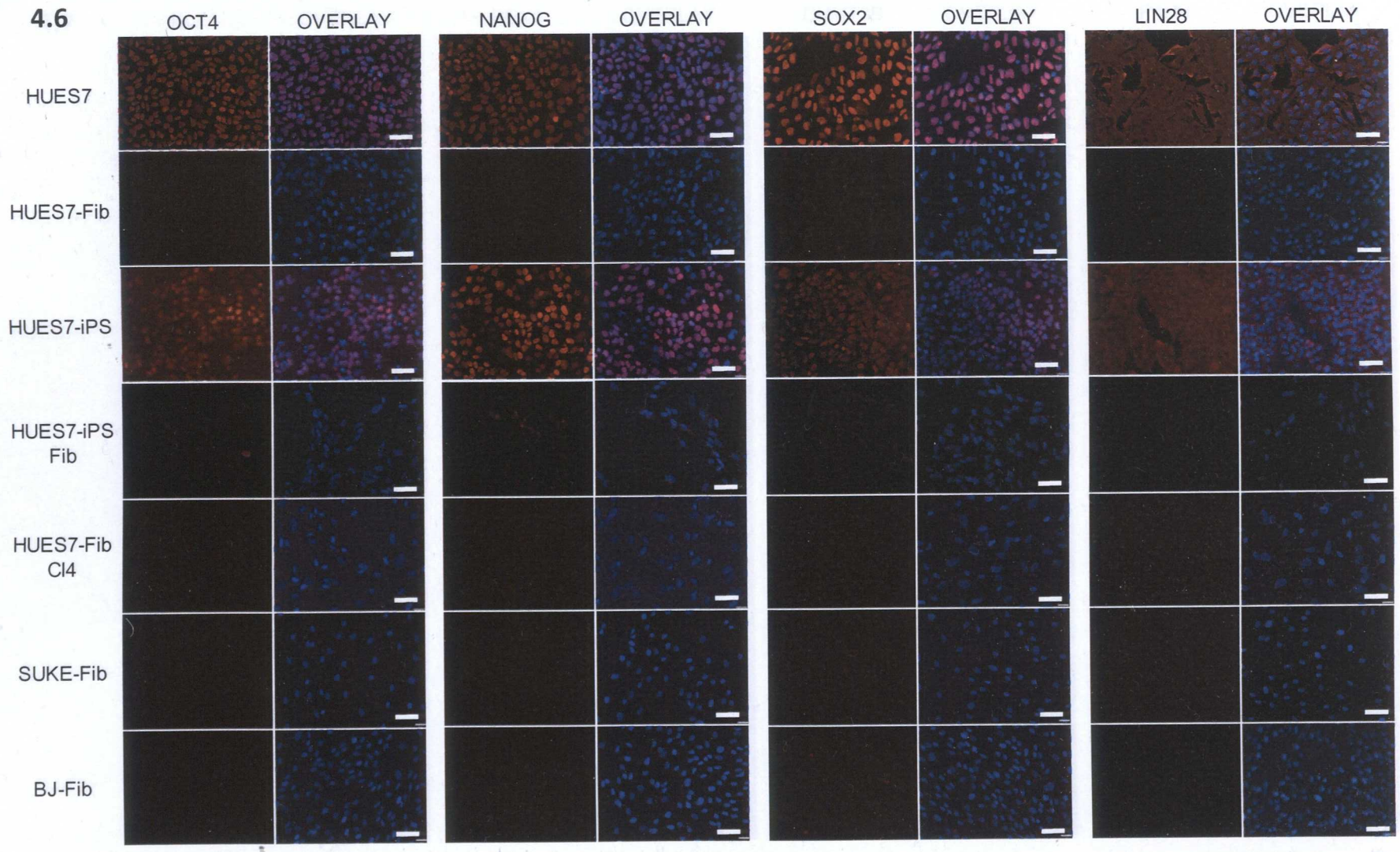
4.6
OCT4
OVERLAY
NANOG
OVERLAY
SOX2
OVERLAY
LIN28
OVERLAY
HUES7
HUES7-Fib
HUES7-iPS
HUES7-iPS Fib
HUES7-Fib Cl4
SUKE-Fib
BJ-Fib

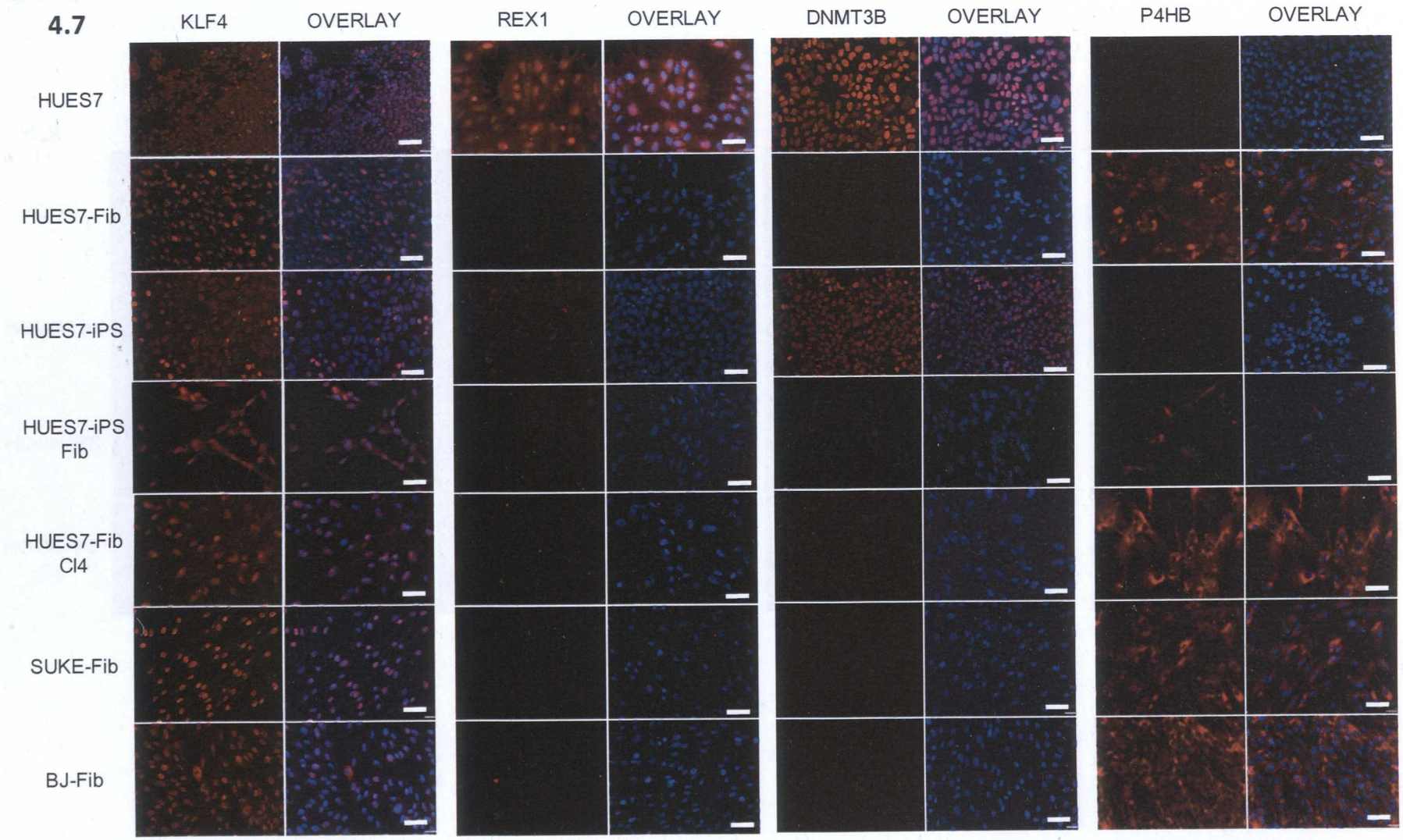
4.7
KLF4
OVERLAY
REX1
OVERLAY
DNMT3B
OVERLAY
P4HB
OVERLAY
HUES7
HUES7-Fib
HUES7-iPS
HUES7-iPS Fib
HUES7-Fib Cl4
SUKE-Fib
BJ-Fib

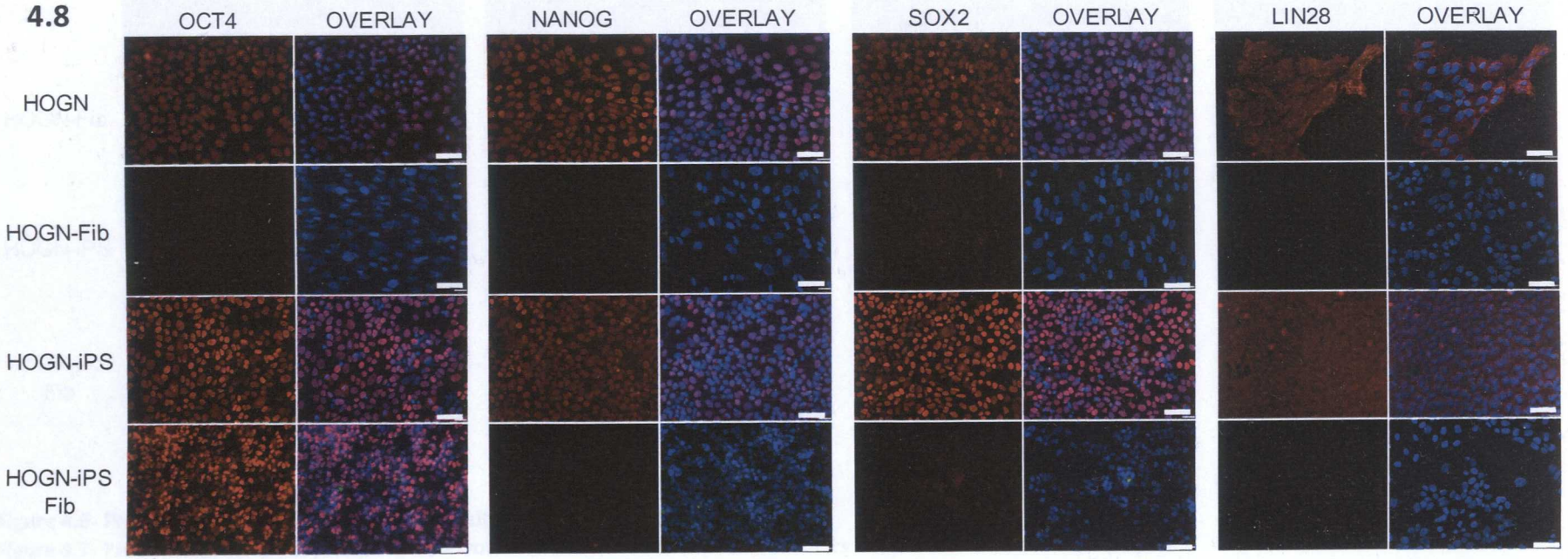
4.8
OCT4
OVERLAY
NANOG
OVERLAY
SOX2
OVERLAY
LIN28
OVERLAY
HOGN
HOGN-Fib
HOGN-iPS
HOGN-iPS Fib

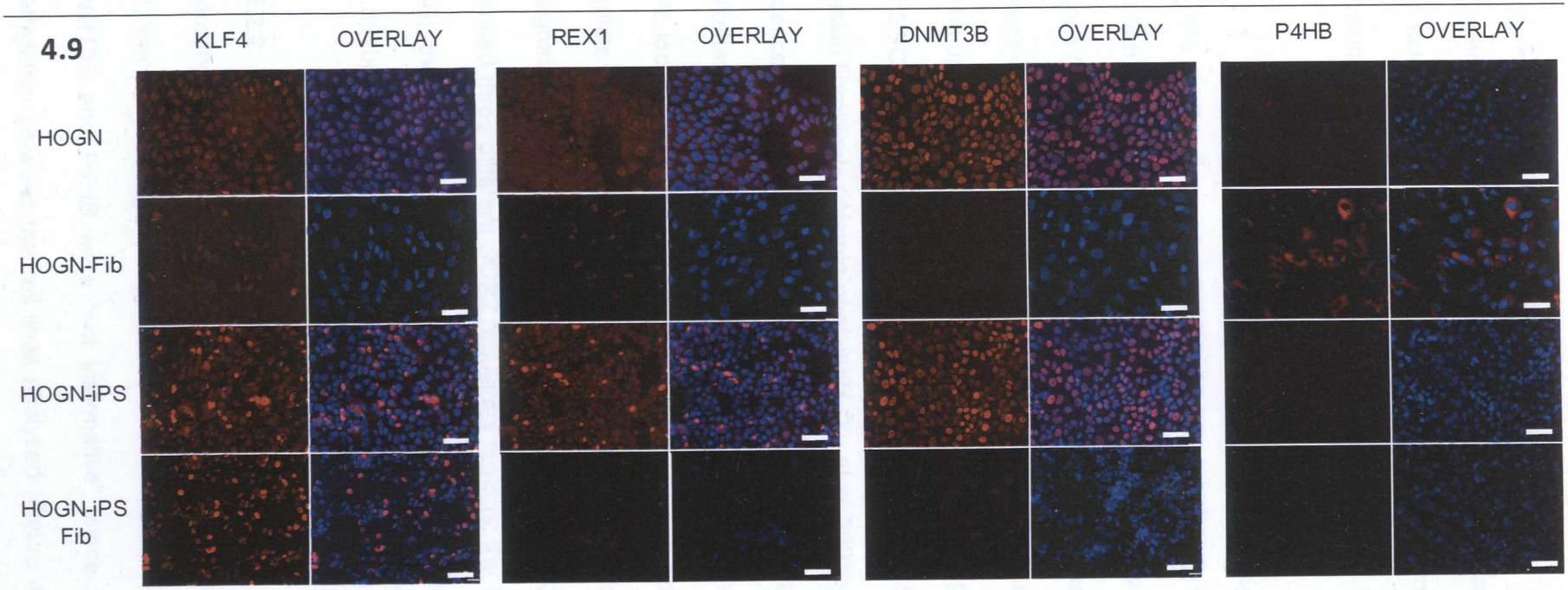

Figure 4.6- Protein expression of iPSC factors in cells of the HUES7 model system
Figure 4.7- Protein expression of pluripotency-associated and fibroblast-specific markers in cells of the HUES7 model system
Figure 4.8- Protein expression of iPSC factors in cells of the HOGN model system
Figure 4.9- Protein expression of pluripotency-associated and fibroblast-specific markers in cells of the HOGN model system
Expression of the pluripotency-associated factors OCT4, NANOG, SOX2, LIN28, KLF4, REX1 and DNMT3B, and the fibroblast specific marker P4HB in the HUES7 and the HOGN model systems, and control fibroblast lines. Protein expression was captured using the Cy3 channel, while the overlay represents a merge of the DAPI (nuclear staining) and Cy3 channels. Scale bars represent 64μm.

4.2.2 DNA methylation analysis in cells of the model system

To determine the epigenetic mechanisms that are associated with pluripotency genes in their active and silenced states, DNA methylation analysis was performed, using direct sequencing of bisulfite PCR products (sections 2.6.1, 2.6.2 and 2.6.3).

4.2.2.1 Selecting primers for DNA methylation analysis by bisulfite PCR

Bisulfite PCR primers for *LIN28*, *KLF4* and *P4HB* were designed within CpG islands (~500bp regions with CG content ≥55%; Takai and Jones 2002), located in their promoter regions (Figure 4.10, Table 2.7). *OCT4* and *NANOG* lack CpG islands in their promoters, so primers were chosen to span their OCT/SOX binding sites (-2,207 to -2,192bp and -336 to -321bp upstream of the transcriptional start site, TSS), previously shown to be unmethylated in hESCs, and hyper-methylated in differentiated hESC-derived fibroblasts and neonatal foreskin fibroblasts (Wernig *et al.* 2007; Yu *et al.* 2007b; Park *et al.* 2008c). Based on similar evidence, *REX1* primers were chosen to span part of the CpG island in its promoter region (Takahashi *et al.* 2007). For *DNMT3B*, primers spanned the 5' end of its CpG island and were located -496 to -839 downstream of Sp1 and Sp3 binding sites, previously shown to regulate *DNMT3B* at the transcriptional level (Jinawath *et al.* 2005). *SOX2* primers were designed based on a study performed in mESCs and germ cells (Imamura *et al.* 2006), and spanned three different *SOX2* regulatory regions; the CpG island (-302 to +153bp from the TSS), the POU binding site (-4,476 to -4,103bp) and the OCT/SOX binding site (+3,548 to +3,891bp).

4.2.2.2 DNA methylation analysis by bisulfite PCR

Following PCR amplification, DNA methylation analysis was performed by bisulfite sequencing, and the results were scored as described in section 2.6.3. *LIN28*, *KLF4*, *DNMT3B* and *P4HB* were "not informative", since they did not show differential DNA methylation between the cell lines analysed (Figure 4.10 and data not shown). The same

was true for the POU binging site and CpG island of *SOX2*. However, the OCT/SOX binding site of *SOX2* was found to be differentially methylated between populations tested; the four CpG sites within this region were unmethylated in the HUES7, HUES7-iPS, HOGN and HOGN-iPS samples, and hypermethylated in all fibroblast samples (Figure 4.11). Similar patterns to *SOX2* were observed in the OCT/SOX binging sites of *OCT4* and *NANOG*, and the CpG island of *REX1* (Figure 4.11). Once more, HOGN-iPS Fib were an exception, since they were hypomethylated in *OCT4* and *SOX2*. HOGN-iPS Fib irregularities could be due to their abnormal karyotype and phenotype (section 3.2.7.7). Also, perhaps not unexpectedly, all CpG dinucleotides of the *REX1* CpG island were heavily methylated in HUES7-iPS, which were previously shown to lack *REX1* expression (Figure 4.2 and Figure 4.6).

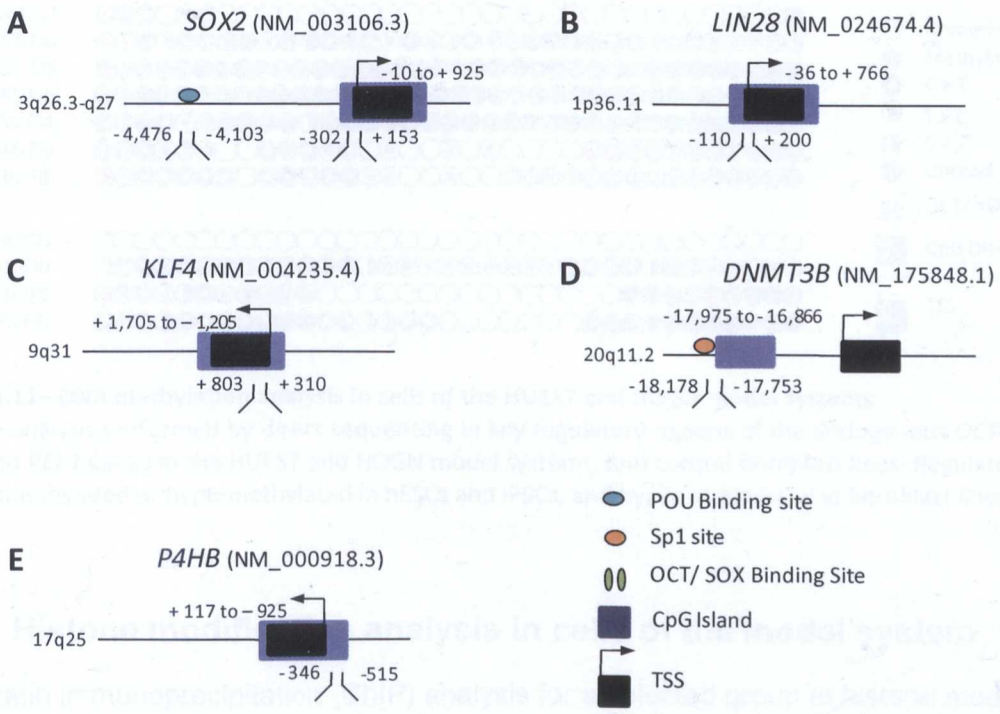

Figure 4.10- Non-informative genes and regions analysed by bisulfite sequencing
The regions shown here were analysed by bisulfite sequencing but were not found to be differentially methylated in hESC, iPSC and fibroblast populations

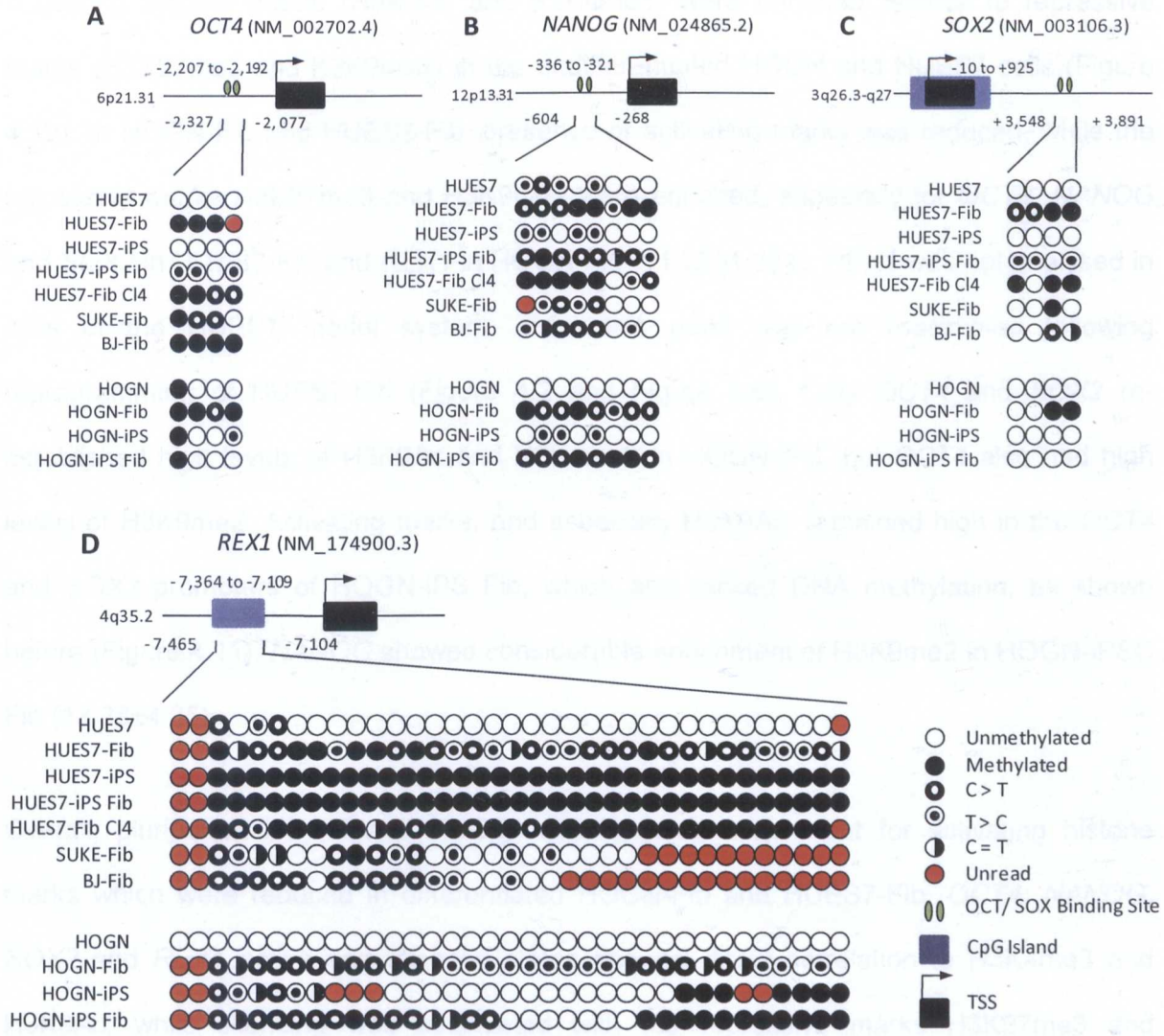

Figure 4.11– DNA methylation analysis in cells of the HUES7 and HOGN model systems
Bisulfite analysis performed by direct sequencing in key regulatory regions of the endogenous *OCT4*, *NANOG*, *SOX2* and *REX1* genes in the HUES7 and HOGN model systems, and control fibroblast lines. Regulatory regions were unmethylated or hypo-methylated in hESCs and iPSCs, and hyper-methylated in fibroblast lines.

4.2.3 Histone modification analysis in cells of the model system

Chromatin immunoprecipitation (ChIP) analysis for a selected group of histone modifications was performed in key regulatory regions of the pluripotency genes *OCT4*, *NANOG*, *SOX2* and *REX1*, which were found to be "informative" for DNA methylation (section 4.2.2.2). Cell pellets were collected in our lab and taken to Birmingham University, where cChIP analysis was performed with the help of Dr. Laura O'Neill. The histone modifications analysed were; H3K27me3, H3K9me2, H3K4me3 and H3K9Ac (section 4.1.1).

Activating histone marks (H3K9Ac and K3H4me3) were enriched relative to repressive marks (H3K27me3 and K3K9me2) in the undifferentiated HOGN and HUES7 cells (Figure 4.12). In HOGN-Fib and HUES7-Fib, presence of activating marks was reduced, while the repressive marks H3K27me3 and H3K9me2 were enriched, especially for *OCT4*, *NANOG* and *SOX2* in HUES7-Fib and *REX1* in HOGN-Fib (11.22±1.321). *REX1* was not analysed in cells of the HUES7 model system, since this gene was not reactivated following reprogramming of HUES7-Fib (Figure 4.2 and Figure 4.6). Only *OCT4* and *SOX2* re-established high levels of H3K9Ac and H3K4me3 in HOGN-iPS, but *OCT4* also had high levels of H3K9me2. Activating marks, and especially H3K9Ac, remained high in the *OCT4* and *SOX2* promoters of HOGN-iPS Fib, which also lacked DNA methylation, as shown before (Figure 4.11). *NANOG* showed considerable enrichment of H3K9me2 in HOGN-iPSC Fib (13.28±4.35).

Overall, pluripotent HOGN and HUES7 cells showed enrichment for activating histone marks which were reduced in differentiated HOGN-Fib and HUES7-Fib. *OCT4*, *NANOG*, *SOX2* and *REX1* active and silenced states showed direct correlation to H3K4me3 and H3K9Ac, while silencing was associated with the repressive marks H3K27me3 and H3K9me2. However, these observations did not correspond to those for HOGN-iPSCs and HOGN-iPS Fib, perhaps due to deregulation of the epigenetic machinery by the reprogramming process, or due to incomplete reprogramming of HOGN-iPSCs. ChIP analysis in HUES7-iPS, HUES7 iPS-Fib and control fibroblast lines, as well as additional pluripotency-genes is continuing in the lab.

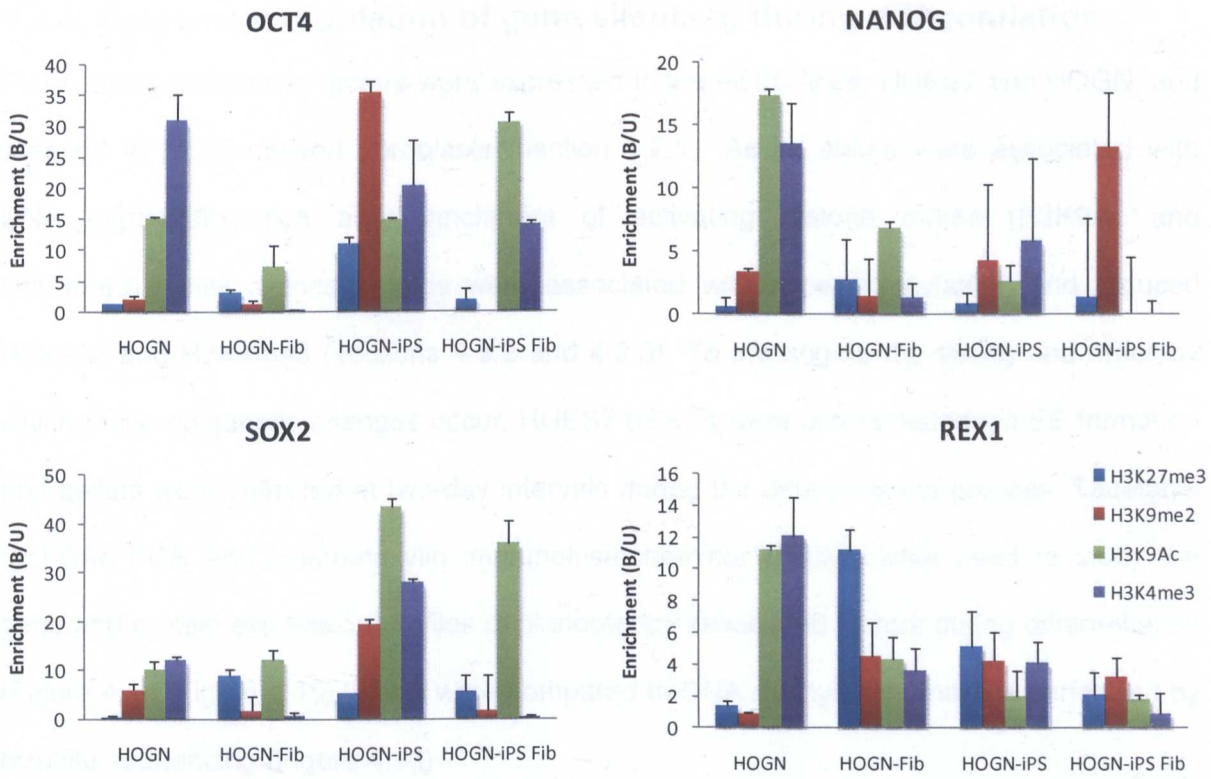

Figure 4.12- cChIP analysis in the HOGN model cell system
cChIP analysis performed with the help of Dr. Laura O'Neill in regions of the endogenous *OCT4*, *NANOG*, *SOX2* and *REX1* genes in the HOGN model system. DNA was immunoprecipitated with anti-H3K27me3, H3K9me2, H3K9Ac and H3K4me3 antibodies, prior to amplification with gene-specific primers using radioactive-PCR. Enrichment of each histone modification was measured by 2D densitometry and was calculated relative to a pre-immune control sample.

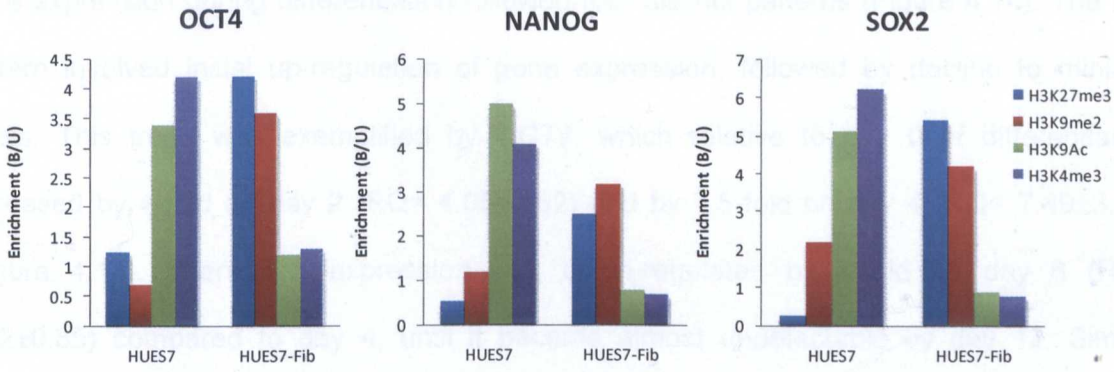

Figure 4.13- cChIP analysis in HUES7 and HUES7-Fib
cChIP analysis performed in regions of the endogenous *OCT4*, *NANOG*, and *SOX2* genes in the HUES7 and HUES7-Fib. DNA was immunoprecipitated with anti-H3K27me3, H3K9me2, H3K9Ac and H3K4me3 antibodies, prior to amplification with gene-specific primers using radioactive-PCR. Enrichment of each histone modification was measured by 2D densitometry and was calculated relative to a pre-immune control sample.

4.2.4 Epigenetic regulation of gene silencing during differentiation

Pluripotency associated factors were expressed in the hESC lines, HUES7 and HOGN, and silenced in hESC-derived fibroblasts (section 4.2.1). Active states were associated with DNA hypo-methylation and enrichment of activating histone marks (H3K9Ac and H3K4me3), while silenced states were associated with hyper-methylation, and reduced H3K9Ac and H3K4me3 (sections 4.2.2 and 4.2.3). To investigate the timing and order by which these epigenetic changes occur, HUES7 hESCs were differentiated *via* EB formation and pellets were collected at two-day intervals during the differentiation process. TaqMan® real-time PCR and Haematoxylin immunohistochemical staining were used to study the gene and protein expression profiles of pluripotency-associated factors during differentiation (Figure 4.14, Figure 4.15), which were compared to DNA methylation analysis performed by bisulfite sequencing (Figure 4.16).

4.2.4.1 Gene expression analysis during differentiation of hESCs

Expression of pluripotency associated and fibroblast-specific genes was investigated in HUES7 cells, from day 0 to day 16 of differentiation. Real-time PCR analysis indicated that gene expression during differentiation followed four distinct patterns (Figure 4.14). The first pattern involved initial up-regulation of gene expression, followed by decline to minimal levels. This trend was exemplified by *OCT4*, which relative to day 0 of differentiation increased by 4-fold on day 2 (RQ= 4.05±2.62) and by 7.5-fold on day 4 (RQ= 7.49±3.61) (Figure 4.14). Thereafter, expression was down-regulated by 4-fold on day 6 (RQ= 1.92±0.85) compared to day 4, until it became almost undetectable by day 12. Similar profiles were seen for *SOX2*, *LIN28*, *REX1* and *DNMT3B,* although some differences were observed in onset and degree of down-regulation (Figure 4.14).

The second trend was characterised by immediate down-regulation of gene expression, as observed for *NANOG* (Figure 4.14). On day 0 and day 2 of differentiation *NANOG*

expression was high (RQ= 1±0.12 and 0.93±0.48, respectively), but was down-regulated by 33% on day 4 (RQ = 0.67±0.11), and by 91% on day 6 (RQ = 0.09±0.005), becoming undetectable by day 12 of differentiation. The third trend was represented by *KLF4*, which showed initial up-regulation between days 0-6 of differentiation (day 6 RQ= 5.9±1.9), followed by decline to sustained levels (Figure 4.14). Between days 8-16, *KLF4* expression was maintained at ~2.5-fold higher levels compared to undifferentiated cells on day 0.

The final trend was that exhibited by the fibroblast-specific marker *P4HB*, whose expression was constant between days 0-6 of differentiation, and was up-regulated from day 8 (RQ = 1.7±0.11). Up-regulation of this fibroblast-specific gene coincided with the down-regulation of pluripotency genes, and especially down-regulation of *REX1* and *LIN28*.

4.2.4.2 Protein expression analysis during differentiation of hESCs

Immunohistochemical analysis using haematoxylin staining was performed with kind help from Miss Maria Barbadillo-Mũnoz in order to detect protein expression of pluripotency-associated factors during differentiation of HUES7-EBs. EBs collected at 2-day intervals were stained with TRA-1-81, OCT4, NANOG, SOX2, KLF4, REX1 and DNMT3B antibodies. Protein expression was reduced from day 14 of differentiation for OCT4, NANOG, SOX2, REX1 and DNMT3B (Figure 4.15). Expression of the hESC-surface marker TRA-1-81 was down-regulated 4 days earlier (day 8 of differentiation), while KLF4 expression appeared constant at all time points analysed (Figure 4.15). Protein down-regulation for OCT4, NANOG, SOX2, REX1 and DNMT3B was delayed by 6-8 days relative to gene down-regulation (Figure 4.14).

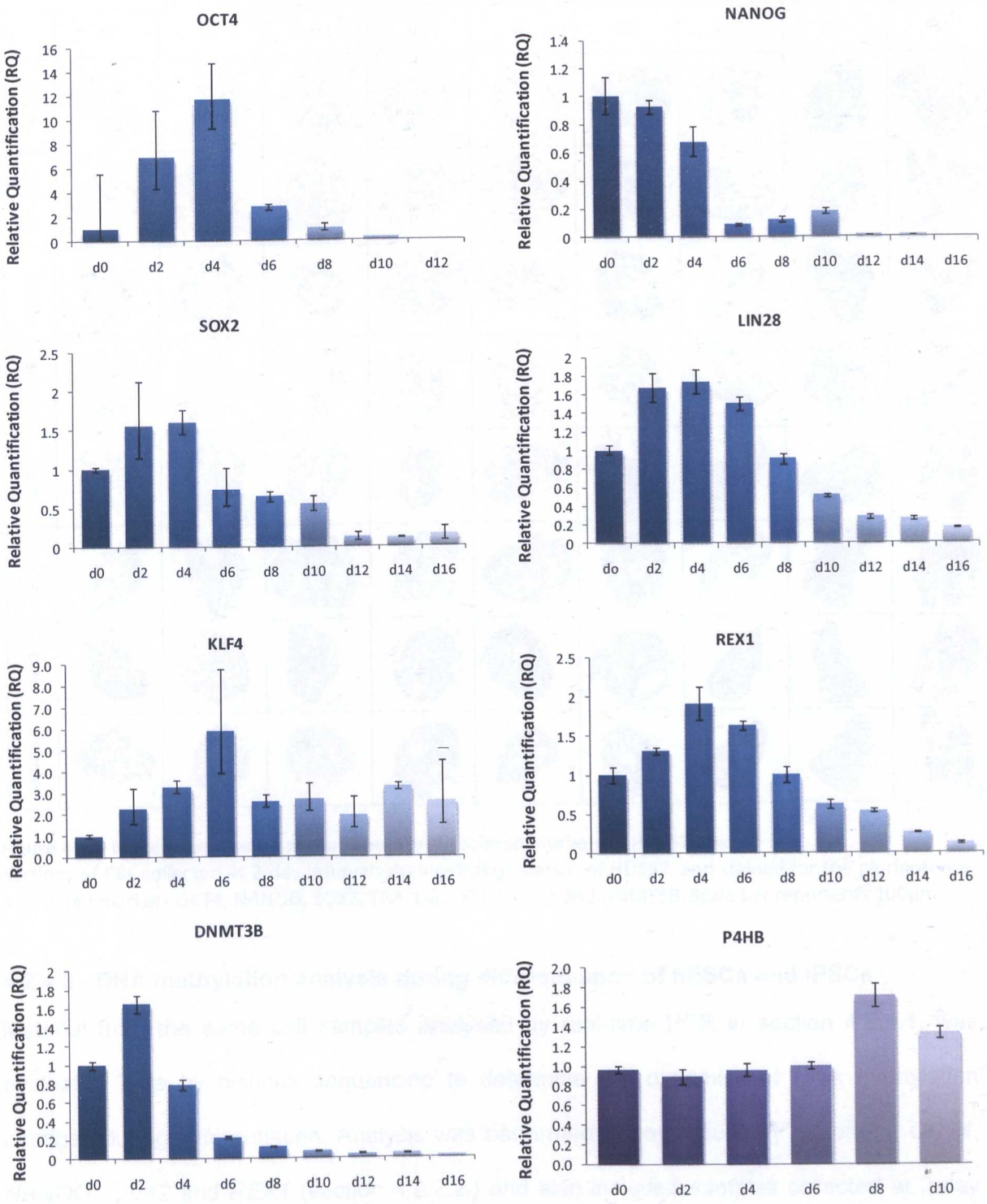

Figure 4.14- Expression of pluripotency-associated and fibroblast markers during differentiation of HUES7
Real-time PCR analysis of *OCT4*, *NANOG*, *SOX2*, *LIN28*, *KLF4*, *REX1*, *DNMT3B* and *P4HB* expression at 2-day intervals during differentiation of HUES7 cells *via* EB formation. Error bars represent standard deviation. Experiments performed in collaboration with Mr. Jayson Bispham and Dr. Roger McGilvray.

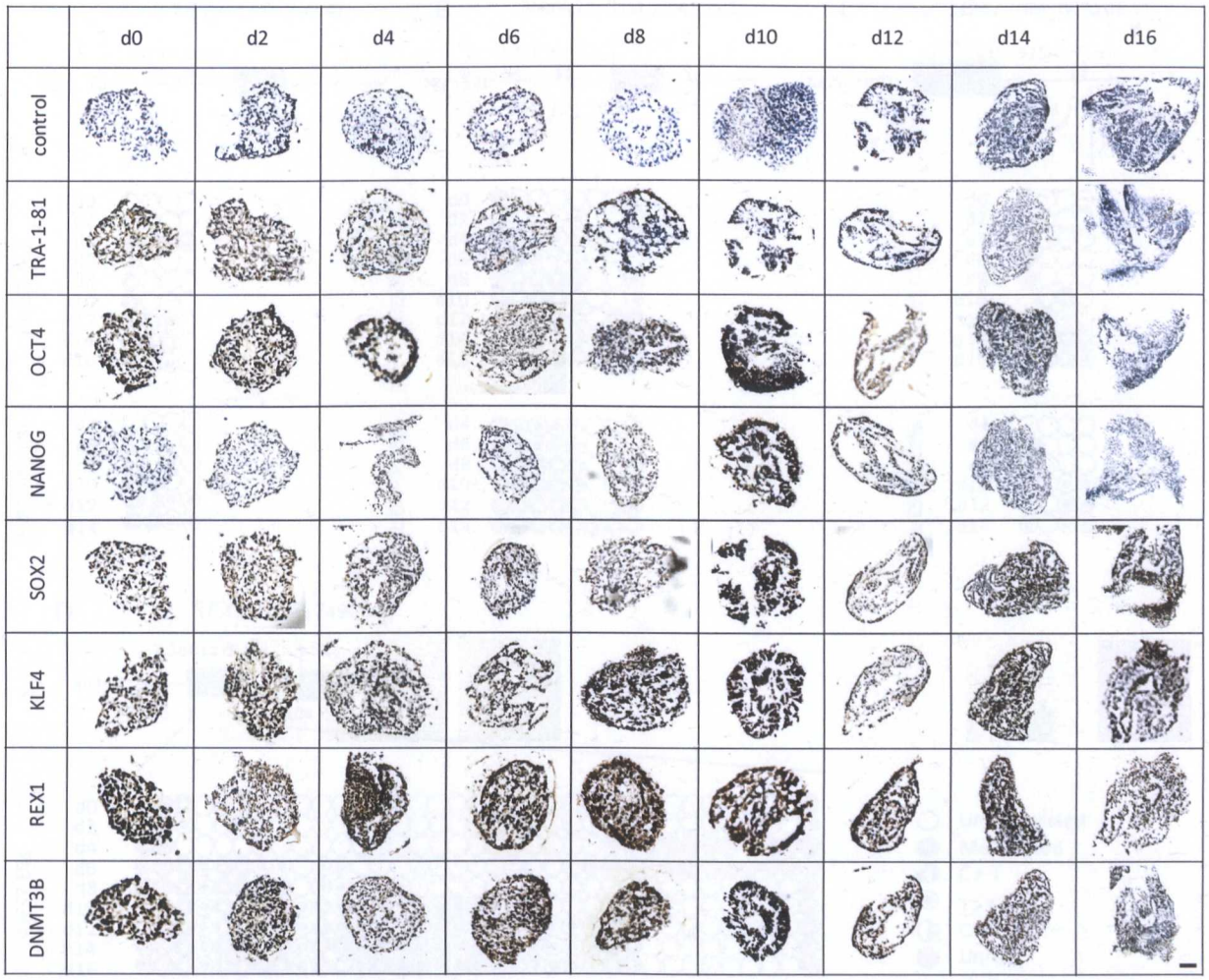

Figure 4.15- Protein expression of pluripotency-associated markers in HUES7-EBs
Sections of EBs collected at 2-day intervals during differentiation of HUES7, and stained for the pluripotency-associated markers OCT4, NANOG, SOX2, TRA-1-81, KLF4, REX1 and DNMT3B. Scale bar represents 100μm

4.2.4.3 DNA methylation analysis during differentiation of hESCs and iPSCs

Material from the same cell samples analysed by real-time PCR in section 4.2.4.1, was evaluated here by bisulfite sequencing to determine the dynamics of DNA methylation changes during differentiation. Analysis was performed in key regulatory regions of *OCT4*, *NANOG*, *SOX2* and *REX1* (section 4.2.2.2.) and also included samples collected at 2-day intervals during differentiation of HUES7-iPSCs.

Methylation in the CpG sites examined increased gradually during differentiation of HUES7 and HUES7-iPSCs, both in terms of the amount of methylation on individual CpGs and the number of CpGs that became hypermethylated (Figure 4.16).

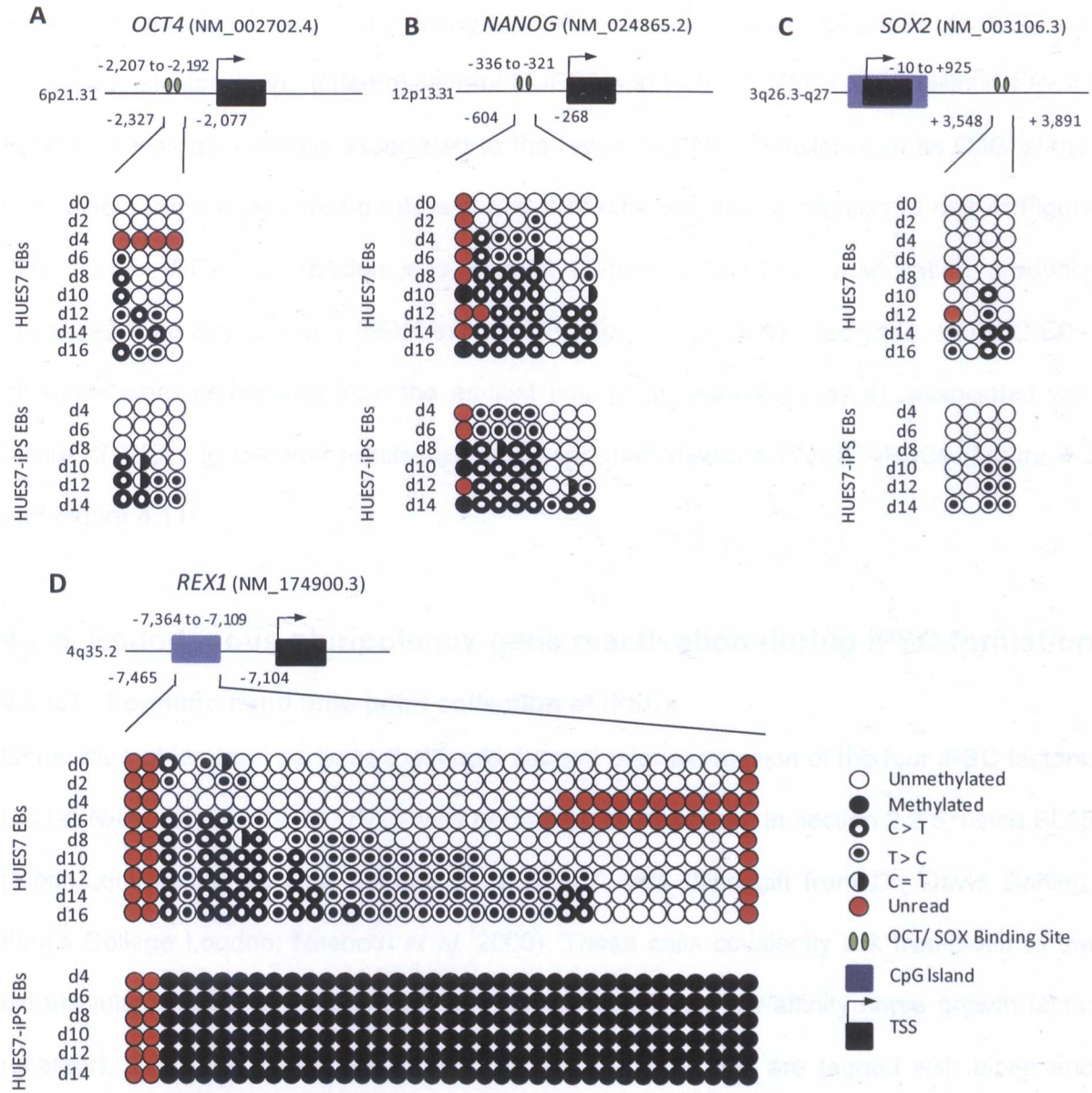

Figure 4.16- Bisulfite analysis in differentiating HUES7 and HUES7-iPSCs
Bisulfite analysis performed by direct sequencing in regions of the endogenous *OCT4*, *NANOG*, *SOX2* and *REX1* genes in differentiating HUES7 and HUES7-iPSCs.

For *OCT4*, increased methylation was observed from day 6 of differentiation, corresponding to the beginning of gene down-regulation (Figure 4.14). For *NANOG*, DNA methylation in HUES7 EBs appeared from day 2 of differentiation, and considerably increased by day 4 (Figure 4.16), which also correlated with timing the gene down-regulation (Figure 4.14). Methylation in *SOX2* was detected from day 10 (Figure 4.16), suggesting that gene down-regulation, evident from day 6 of differentiation (Figure 4.14), was initiated by a mechanism

other than DNA methylation. The timing of DNA methylation events for *OCT4*, *NANOG* and *SOX2* was similar during differentiation of HUES7 and HUES7-iPSCs. Expression of *REX1* in HUES7 was also closely associated to the levels of DNA methylation in its CpG island. CpGs were hypermethylated on days 0 and 2 of differentiation compared to day 4 (Figure 4.16), when *REX1* expression was highest (Figure 4.14). DNA methylation gradually increased from day 6, when *REX1* expression begun to gradually decrease. In iPSC-EBs, all CpGs were methylated from the earliest time-point analysed (day 4), associated with failure of *REX1* to become reactivated and hypo-methylated in HUES7-iPSCs (Figure 4.2 and Figure 4.11).

4.2.5 Endogenous pluripotency-gene reactivation during iPSC formation

4.2.5.1 Formation and time-point collection of iPSCs

Generation of lentiviral particles that could support over-expression of the four iPSC factors; *OCT4*, *NANOG*, *SOX2* and *LIN28*, was performed as described in section 2.2.5, using BL15 (Biotin-Lenti clone 15) cells instead of HEK293T cells (kind gift from Dr. David Darling, King's College London; Nesbeth *et al.* 2006). These cells covalently link free-biotin to the extracellular domain of the cell-surface receptor, ΔLNGFR (low-affinity nerve growth factor receptor). Thus, the envelopes of lentiviral vectors generated are tagged with biotin and have high affinity for streptavidin paramagnetic particles, something that facilitates both the concentration of lentiviral supernatants (by >4500-fold) and the ease of virus production in large scale. The protocol for lentiviral transduction using BL15 cells was generated in our lab in collaboration with Dr. Emily Dick.

HUES7-Fib were induced to form iPSCs by lentiviral transduction with human *OCT4*, *NANOG*, *SOX2* and *LIN28*. Reprogramming was allowed to occur for 18 days, and cell pellets were collected at 2-day intervals. HUES7-Fib started showing morphological changes on day 8 PTD, when incompletely reprogrammed colonies begun to emerge

(Figure 4.17.E&F). Putative iPSC colonies appeared from day 11 PTD, and grew in size number over the following days (Figure 4.17.A-D). Cells transduced with the pLVTHM GFP-control virus did not show a change in morphology (Figure 4.17.G).

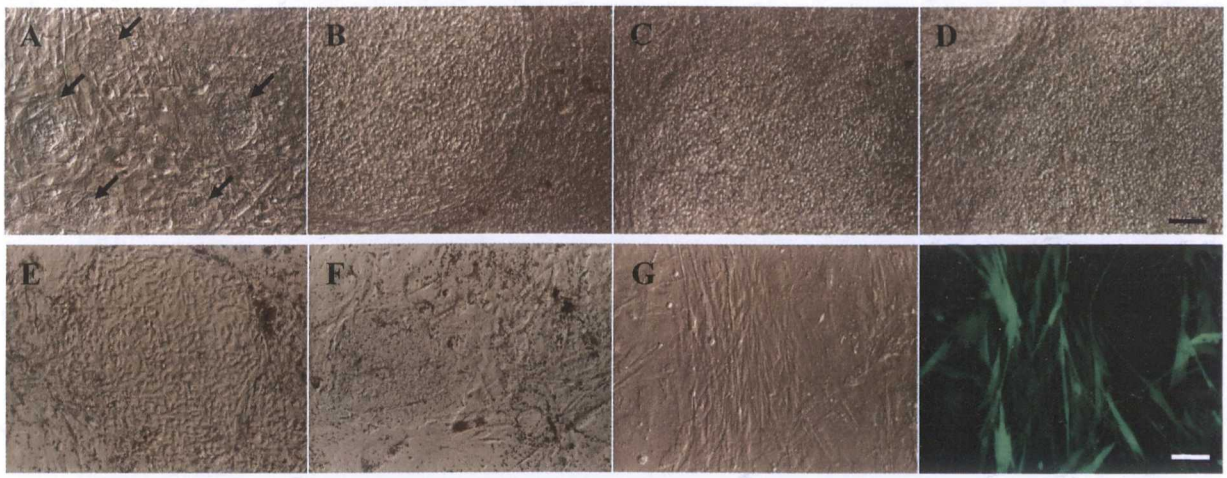

Figure 4.17- Time course collection of HUES7-iPSCs
Bright field images of iPSC colonies on **A.** day 11 **B.** day 14 **C.** day 16 and **D.** day 18 after transduction with lentiviruses over expressing *OCT4, NANOG, SOX2* and *LIN28*. Incompletely reprogrammed colonies of **E.** Type I and **F.** Type II, emerging during induction of hESC-derived fibroblasts to form iPSCs. **G.** Negative control sample, on day 18 of reprogramming. Arrows represent putative iPSC colonies on day 11 of reprogramming. Scale bars represent 100µm.

4.2.5.2 Analysis of endogenous gene reactivation during generation of iPSCs

Using pellets collected in section 4.2.5.1, cDNA was synthesised from 1µg of total RNA, which was diluted to 50µl prior to its use in RT-PCR (modified from section 2.5.3). PCR amplification was performed for 40x cycles. Primers specific to endogenous *OCT4*, *NANOG*, *SOX2* and *LIN28* (Table 2.6; Figure 4.4), were used to detect re-activation of these genes during iPSC generation. Quantification of gene expression was performed by 2D densitometry, using AIDA software (section 2.5.6), and plotted relative to HUES7 cells. Any expression detected in the untreated control (d18 GFP; Figure 4.17) was subtracted from other samples, so that only changes brought about due to transduction with "iPSC factors" would be accounted for.

Endogenous pluripotency genes were reactivated from day 8-10 during iPSC formation (Figure 4.18). In *NANOG* and *SOX2* PCR, non-specific products were detected (arrow-

marked upper bands were true product, lower bands were non-specific). The non-specific *SOX2* bands were due to expression of mouse transcripts from MEF feeders (Figure 4.19) whereas non-specific *NANOG* PCR bands were likely to represent pseudogenes. *OCT4* expression was detected in all samples, either due to residual gene expression or amplification of pseudogenes (Figure 4.18).

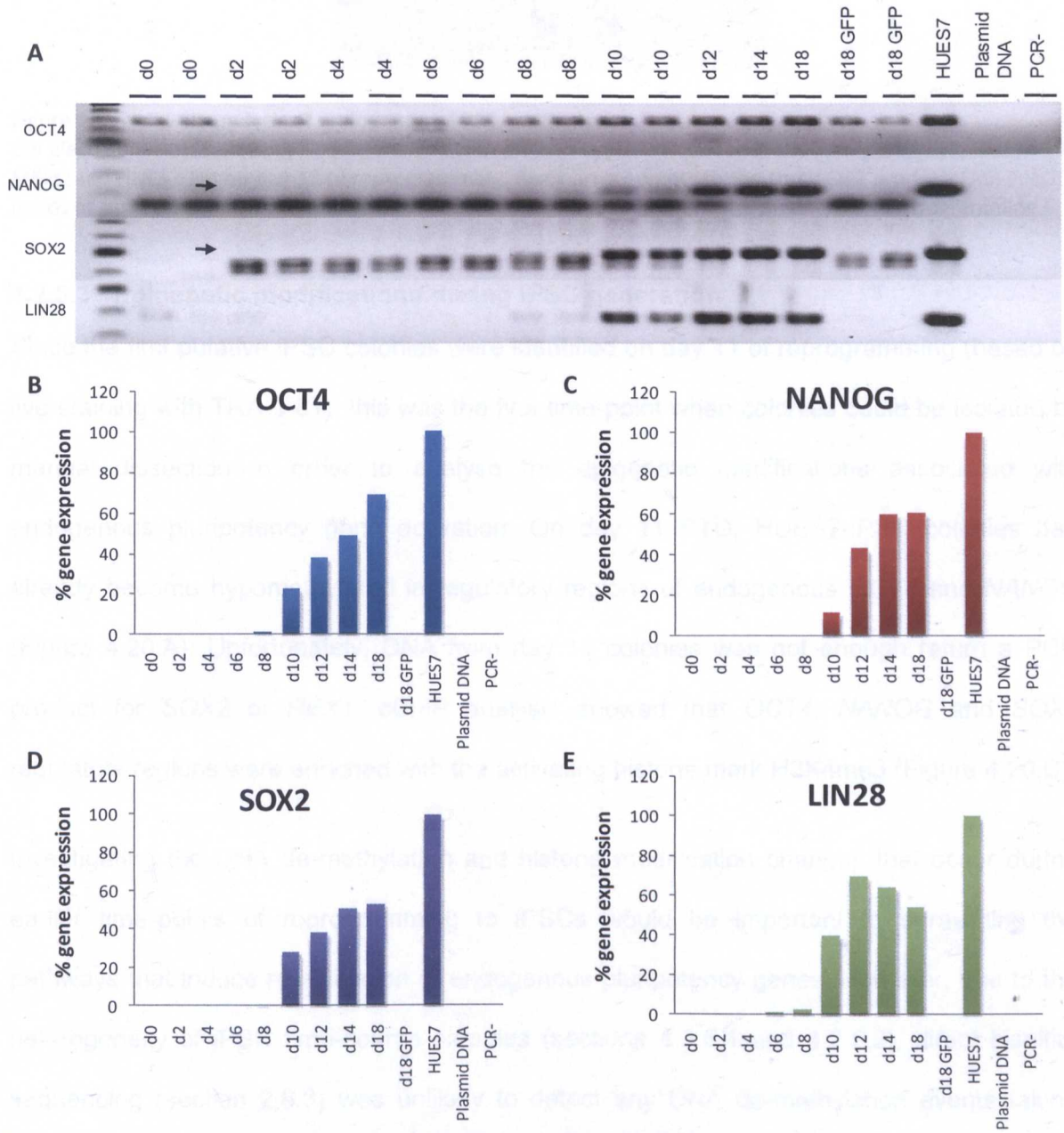

Figure 4.18– Reactivation of endogenous iPSC factors during reprogramming of HUES7-Fib
A. Gel electrophoresis analysis following RT-PCR with primers specific for the endogenous *OCT4*, *NANOG*, *SOX2* and *LIN28* genes, in HUES7-iPS time-course samples. Black arrows represent products of the expected size for *NANOG* and *SOX2*. **B.–E.** Quantification of gene expression by 2D densitometry. Gene expression is presented relative to the HUES7 sample, following subtraction of any expression in the untreated (d18 GFP) control.

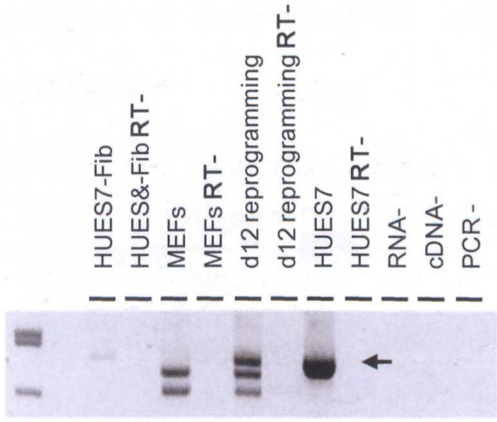

Figure 4.19- RT-PCR analysis of endogenous *SOX2* expression
Gel electrophoresis following RT-PCR analysis with primers specific to endogenous *SOX2*, in HUES7, HUES7-Fib, MEFs, and HUES7-Fib on day 12 of reprogramming. Black arrow points to the true *SOX2* product. Non-specific bands of smaller size than the true *SOX2* product were observed in MEFs and on day 12 of reprogramming.

4.2.5.3 Epigenetic modifications during iPSC generation

Since the first putative iPSC colonies were identified on day 11 of reprogramming (based on live staining with TRA-1-81), this was the first time-point when colonies could be isolated by manual dissection in order to analyse the epigenetic modifications associated with endogenous pluripotency gene activation. On day 11 PTD, HUES7-iPSC colonies had already become hypomethylated in regulatory regions of endogenous *OCT4* and *NANOG* (Figure 4.20.A). Unfortunately, DNA from day 11 colonies was not enough return a PCR product for *SOX2* or *REX1*. cChIP analysis showed that *OCT4*, *NANOG* and *SOX2* regulatory regions were enriched with the activating histone mark H3K4me3 (Figure 4.20.B).

Investigating the DNA de-methylation and histone modification changes that occur during earlier time-points of reprogramming to iPSCs would be important to unravelling the pathways that induce re-activation of endogenous pluripotency genes. However, due to the heterogeneity of iPSC time-course samples (sections 4.2.5.1 and 4.2.5.2), direct bisulfite sequencing (section 2.6.3) was unlikely to detect any DNA de-methylation events taking place. Clonal sequencing (as described in Kim *et al.* 2007) needed to be performed on a large number of clones, in order to calculate the % de-methylation occurring in the

promoters of pluripotency factors at each time-point during reprogramming. These experiments are still ongoing in the lab.

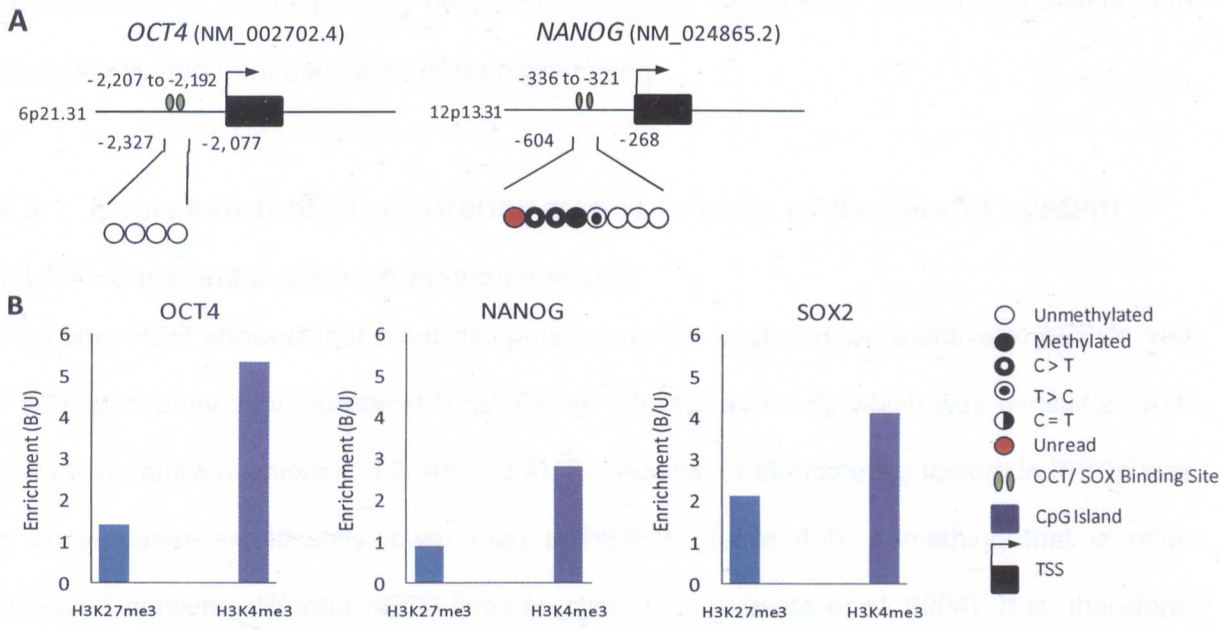

Figure 4.20- Bisulfite sequencing and ChIP analysis in HUES7-iPSC colonies on day 11 of reprogramming
A. Bisulfite sequencing and **B.** cChIP analysis performed in regions of endogenous *OCT4*, *NANOG*, and *SOX2* in HUES7-iPSC colonies, on day 11 during reprogramming. DNA was immunoprecipitated with anti-H3K27me3, and H3K4me3 antibodies, prior to amplification with gene specific enzymes using radioactive-PCR. Enrichment of each histone modification was measured by 2D densitometry and was calculated relative to a pre-immune control sample.

4.3 DISCUSSION

In this chapter, iPSCs generated form HUES7-derived fibroblasts were shown to express the pluripotency associated markers *OCT4*, *NANOG*, *SOX2*, *LIN28*, *REX1* and *DNMT3B*, albeit at lower levels compared to hESCs. iPSCs showed down-regulation of lentiviral transgenes, a trait considered important to complete the reprogramming process. Expression of the master pluripotency regulators *OCT4*, *NANOG* and *SOX2* was inversely related to the levels of DNA methylation found in their OCT/SOX binding sites, while the same was true for DNA methylation in the CpG island of *REX1*. The histone modifications, H3K9Ac and H3K4me3, were directly related to gene expression in hESCs and hESC-Fib. During differentiation of hESCs and iPSCs, DNA methylation in the pluripotency genes analysed was found to increase gradually, both in the number of CpGs that became

methylated and in the amount of methylation on individual CpGs. The timing of DNA methylation events coincided with gene silencing and showed similar dynamics between hESCs and iPSCs. Pluripotency genes were silenced during days 6-8 of differentiation and were reactivated from days 8-10 of reprogramming.

4.3.1 Expression of pluripotency-genes in cells of the model system

4.3.1.1 Gene and protein expression analysis

Real-time PCR showed that most pluripotency genes analysed were active in hESCs and iPSCs, and silenced in fibroblast lines (Figure 4.2, 4.3 and 4.6), which was consistent with current literature (sections 1.3.3 and 1.3.4). Expression of pluripotency factors in iPSCs was in some cases significantly lower than in hESCs (Table 4.4), something that is often observed between different hESC lines (section 1.7.1; Abeyta *et al.* 2004). It is, therefore, plausible that iPSCs acquired a different "pluripotency state" compared to hESCs (Rossant 2008). Importantly, all pluripotency genes analysed were reactivated to a similar level in iPSCs (within 25-60% of their levels in hESC), indicating that the relative and not the absolute expression levels of pluripotency factors might be the determining factor to acquiring a pluripotent state. This also suggests that a minimum threshold level of pluripotency-gene expression could exist, over which cells can acquire an ESC-like phenotype (MacArthur *et al.* 2008). *KLF4* was expressed in all cell lines analysed (Figure 4.2, 4.3 and 4.6), consistent with studies reporting wide-spread tissue specificity for this marker (Garrett-Sinha *et al.* 1996; Shields *et al.* 1996; Aasen *et al.* 2008). Some unexpected results were observed for *REX1*, which failed to become re-activated in HUES7-iPSCs, and for *NANOG*, which was detected in both HOGN- and HUES7-iPSC fibroblasts. These two events are discussed below.

4.3.1.2 NANOG real-time PCR

NANOG expression was unexpectedly detected by real-time PCR in HOGN and HUES7-iPSC fibroblasts, likely due to residual expression from both the endogenous locus and the lentiviral transgene since the *NANOG* real-time PCR assay could not distinguish between them (section 4.2.1.1). Detection from both loci could also account for the increased expression of *NANOG* in HUES7-iPSCs (Figure 4.2). Nevertheless, *NANOG* gene expression in HOGN-iPS Fib was not enough to be detected by immunofluorescence at the protein level (Figure 4.6.C). NANOG protein was also absent in HUES7-iPSC Fib (Figure 4.6.A), despite gene expression levels appearing to be higher than in HUES7 (Figure 4.2). Closer investigation of the real-time PCR raw data revealed that the seemingly increased expression of *NANOG* detected by relative quantification (RQ) using the ΔΔCt method (Yuan *et al.* 2008), was not due to increased expression of *NANOG* mRNA, but due to reduced expression of the reference gene *18S*. The ΔΔCt method of relative quantification assumes that expression of the reference gene is constant in all samples analysed (Livak and Schmittgen 2001), and bases relative quantification on the difference between expression of the target and reference genes, with the target-gene expression being the only variable. Therefore, reduced expression of the reference gene, *18S*, in HUES7-iPS Fib skewed the calculation of RQ values. Quantification of *NANOG* expression using the house-keeping gene *HPRT* had similar results to quantification with *18S*, since *HPRT* was also detected at reduced levels in HUES7-iPS Fib compared to other samples analysed (data not shown).

Reduced expression of reference genes in HUES7-iPS Fib could be due to their slow proliferation rate (section 3.2.7.8), something that has been shown to affect cellular metabolism and, thus, expression of house-keeping genes (Thellin *et al.* 1999; Ullmannova and Haskovec 2003). *18S* and *HPRT* are routinely used as real-time PCR internal controls in our lab and by other groups (reviewed in Bustin 2000; Dheda *et al.* 2004; Huggett *et al.*

2005), but perhaps a more appropriate house-keeping gene for this specific experiment would have been GAPDH, as it exhibits constant expression levels in senescent fibroblasts (Zainuddin *et al.* 2008). Nevertheless, RT-PCR analysis confirmed that endogenous *NANOG* expression was down-regulated in HUES7-iPS Fib (Figure 4.5).

4.3.1.3 REX1 re-activation not required to induce pluripotency

In the HUES7 model cell system, iPSCs expressed a range of pluripotency associated markers, including OCT4, SOX2, NANOG, KLF4, as well as SSEA4, TRA-1-81, DNMT3B and LIN28 (sections 3.3.6.6 and 4.2.1). They had a normal karyotype and were able to exhibit pluripotency by *in vitro* differentiation to cell-types representative of all three germ layers (Figure 3.27). Despite this, they failed to reactivate REX1 (Figure 4.2 and Figure 4.7), a downstream regulator in the pluripotency network (section 1.3.4). Disruption of *Rex1* in mESCs was previously shown to have no effect in cell morphology, self-renewal properties, and *Oct4*, *Sox2* and *Nanog* expression, but did impair differentiation into visceral endoderm (Masui *et al.* 2008). Moreover, knock-out or over-expression of *Rex1* in mESCs were able to enhance or reduce responsiveness to retinoic acid-induced differentiation, respectively (Masui *et al.* 2008; Scotland *et al.* 2009). Based in these observations, Rex1 is believed to play a role in inhibiting differentiation rather than actively maintaining pluripotency in ESCs. ChIP sequencing analysis by Kim *et al.* (2008a) showed that Rex1 targets in mESCs are similar to those of c-Myc, and have a role in cell metabolism rather than developmental processes. Also, Rex1 targets show decreased levels of the repressive histone mark H3K27me3, something that suggests a role of Rex1 in gene activation (Kim *et al.* 2008a). Therefore, Rex1 could be inhibiting differentiation by activating differentiation antagonists. In this thesis, it has been shown that human somatic cells do not require REX1 to induce and maintain pluripotency, challenging the role of this gene as a pluripotency-marker. The exact role of REX1 in the determination of cell phenotype remains poorly understood, and merits further investigation.

4.3.1.4 Transgene silencing

RT-PCR analysis confirmed that lentivirally-inserted transgenes were silenced in iPSCs and iPSC-fibroblasts, both in the HOGN and HUES7 model systems. An exception was the *OCT4* transgene, whose expression was detected in HOGN-iPS and HOGN-iPS Fib, possibly due to accumulation of expression from both the transgene and endogenous *OCT4-IRES-GFP-IRES-Neo* loci (section 4.2.1.4). High expression of iPS transgenes has been shown to ablate iPSC differentiation (Brambrink *et al.* 2008), correlating with the abnormal phenotype of the HOGN-iPS Fib which maintained high expression levels of the *OCT4* transgene (Figure 4.5 and Figure 4.6).

Low levels of residual *OCT4* transgene expression were also observed in HUES7-iPS and HUES7-iPS Fib. This was not dissimilar to previously published data from groups who used the same lentiviral system used here to generate iPSCs (Yu *et al.* 2007b), or from groups using retroviral vectors, which are believed to undergo silencing more easily than lentiviruses (Dimos *et al.* 2008; Park *et al.* 2008b). Residual expression from the *OCT4* transgene did not affect the ability of HUES7-iPSCs to differentiate to the three embryonic germ layers and generate P4HB positive fibroblasts (Figure 3.26 and Figure 3.31), consistent with other studies showing that residual transgene expression did not impair iPSC formation, maintenance and directed differentiation (Papapetrou *et al.* 2009).

4.3.2 DNA methylation analysis in cells of the model system

4.3.2.1 "Non-informative" promoter regions

LIN28, *KLF4*, *DNMT3B* and *P4HB* did not show differential methylation between pluripotent and differentiated cells, even though primers for bisulfite PCR were designed within CpG islands in their promoters (section 4.2.2.2). This indicated these genes were regulated by mechanisms other than DNA methylation, or that their DNA methylation regulatory regions were not the ones analysed. *DNMT3B* primers for bisulfite PCR were originally intended to

span the Sp1 and Sp3 binding sites located in the DNMT3B promoter, which were shown to regulate expression of DNMT3B at the transcriptional level (Jinawath *et al.* 2005). However, bisulphite PCR primers designed to this region were not successful in amplifying a product of the correct size (data not shown). Re-designed primers that could amplify a product of the expected size did not span the Sp binding sites, but were instead located -496 to -839bp downstream, something that could have affected detection of differential DNA methylation for *DNMT3B*.

Lack of differential methylation for *LIN28* was in agreement to current literature, showing that this gene remained unmethylated upon differentiation of hMSCs to osteoblasts and adipocytes, and was down-regulated through a methylation independent pathway (Dansranjavin *et al.* 2009). *KLF4* methylation at the TSS has been shown to increase in hESC-derived fibroblasts compared to undifferentiated hESCs (Laurent *et al.* 2010), an observation that comes in contrast to results from this study, which showed no differential methylation in the *KLF4* CpG island located in close proximity (+310 to +803) to the TSS (Figure 4.10). This difference could be due to analysis of non-overlapping regions within the KLF4 promoter by Laurent *et al.* (2010) and this thesis, or due to the use of alternative methods to derive hESC-fibroblasts (spontaneous monolayer differentiation vs. EB formation), and differences in genotype (WA09 vs. HUES7) and culture conditions (StemPro vs. KSR/bFGF MEF-conditioned medium) between the hESC lines used by Laurent *et al.* (2010) and this thesis. Notably, differences in the method used to differentiate mouse and human ESCs have previously been shown to result in variation of *OCT4* and *NANOG* DNA methylation (Yeo *et al.* 2007), and differential regulation of *Oct4* repression by the NuRD chromatin remodelling complex component; Mbd3 (Kaji *et al.* 2006). The developmental context in which gene regulatory mechanisms are analysed is thus thought to influence the outcome and interpretation of experimental results (Young and Denning 2007).

4.3.2.2 Genes with differentially methylated regulatory regions

Short stretches of CpG sites in the OCT/SOX binding sites of *OCT4* and *NANOG* were previously shown to be unmethylated in pluripotent and differentiated cell lines (sections 4.1.1.1 and 4.1.1.2). These findings were in agreement to the results obtained here, where hESCs and iPSCs were hypomethylated relative to derived fibroblasts, as well as neonatal, adult and clonal fibroblast lines (Figure 4.11). *SOX2* was also differentially methylated between human pluripotent and fibroblast lines (Figure 4.11). This is, to our knowledge, the first report of differential SOX2 methylation between human non-cancerous cell-types. Interestingly, all three master regulators of pluripotency analysed by bisulfite PCR (*OCT4*, *NANOG* and *SOX2*) showed differential methylation in their OCT/SOX binding sites, perhaps unravelling a common regulatory mechanism between them. Methylation of the OCT/SOX binding site could be inhibiting interaction among OCT4, NANOG and SOX2, thus preventing auto-regulatory feedback loops (Chen and Zhong 2008) and serving as a mechanism contributing to gene down regulation during differentiation.

The CpG island of *REX1* showed similar differential methylation to *OCT4*, *NANOG* and *SOX2* (Figure 4.11). This was consistent with observations that *REX1* is hypermethylated in foetal and adult fibroblast cells and hypomethylated hESCs and iPSCs (Takahashi *et al.* 2007). However, it was contradictory to studies showing that this gene was not hypermethylated upon hESC differentiation (Yeo *et al.* 2007). Considering the findings from Takahashi *et al.* (2007) and this study, it is likely that findings from Yeo *et al.* (2007) were due to analysis of a different region within the *REX1* promoter, or due to the methodology used for hESCs culture and differentiation (culture by Yeo *et al.* (2007) was on MEF feeders and differentiation by EB suspension culture in non-adhesive surfaces).

4.3.3 Carrier chromatin immunoprecipitation

Even though details about the epigenetic mechanisms that regulate *Oct4* expression in the mouse have been characterised more extensively than other pluripotency-genes (Feldman *et al.* 2006; Epsztejn-Litman *et al.* 2008), little is known about the precise mechanisms that regulate this gene in human cells. Using chromatin immunoprecipitation analysis, an attempt was made to determine the histone modifications associated with key pluripotency genes in hESCs, hESC-fibroblasts, iPSCs and iPS-fibroblasts. Characterisation was performed in cells of the HOGN model system, as well as in HUES7 and HUES7-Fib (Figure 4.12). HOGN and HUES7 showed high enrichment for the activating marks H3K9Ac and H3K4me3 (especially for *OCT4*, *NANOG* and *REX1*) that were lost when the cells were differentiated into fibroblasts. This was consistent with findings that H3K9Ac associates with *OCT4*, *NANOG* and *SOX2* in mESCs and hECs, and that these genes lose H3K9Ac and H3K4me in differentiated lineages (Barrand and Collas 2009). HOGN-iPSCs and HOGN-iPS Fib did not show the same patterns of histone modifications as HOGN and HOGN-Fib, perhaps due to deregulation of the epigenetic machinery by the reprogramming process, or due to partial reprogramming of HOGN-iPSCs caused by persistent expression of the *OCT4* lentiviral transgene (Figure 3.30).

4.3.4 Epigenetic regulation of gene silencing during differentiation

4.3.4.1 Gene expression analysis during differentiation of hESCs

The pluripotency factors *OCT4*, *NANOG*, *SOX2*, *LIN28*, *DNMT3B*, and *REX1* show high expression levels in ESCs and are usually down-regulated to almost undetectable levels in differentiated cell types (Richards *et al.* 2004; Boyer *et al.* 2005; Adewumi *et al.* 2007; Viswanathan *et al.* 2008). Here, the exact timing and pattern by which these genes are down-regulated was investigated during differentiation of hESCs *via* EB formation. Four patterns of gene expression were observed during differentiation, as shown in Figure 4.14

and Figure 4.21. Initial up-regulation of the pluripotency genes *OCT4*, *SOX2*, *LIN28*, *REX1*, *DNMT3B* and *KLF4* could have been due to a paracrine effect brought about by the forced aggregation of hESCs to form EBs or because the genes are necessary to initiate differentiation towards certain lineages (e.g. OCT4 up-regulation leads to endoderm differentiation; Rodriguez *et al.* 2007, and SOX2 is expressed in neural progenitors; Zappone *et al.* 2000). This effect was also observed by Viswanathan *et al.* (2008), who studied the expression of *LIN28* during hESCs differentiation *via* EB formation. *OCT4* expression in the same study showed immediate decline, but was not analysed prior to day 5 of differentiation.

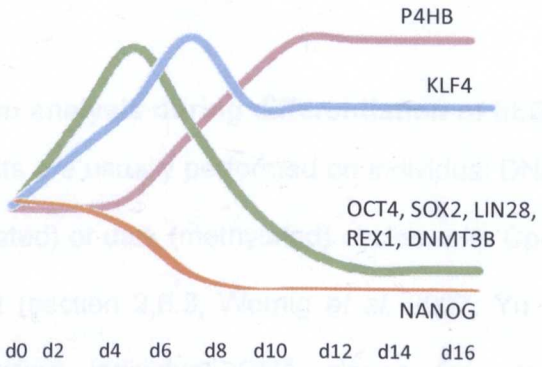

Figure 4.21- Gene expression trends observed during hESCs differentiation
Four expression trends were observed during differentiation of hESCs *via* EB formation. *OCT4*, *SOX2*, *LIN28*, *REX1*, *DNMT3B*; initial up-regulation followed by decline, *NANOG*; immediate decline, *KLF4*; initial up-regulation followed by decline to sustained levels, *P4HB*; up-regulation. Y-axis represents relative expression but is not drawn to scale.

NANOG expression did not show initial up-regulation (Figure 4.14), and together with *DNMT3B*, it was one of the first genes to become down-regulated upon differentiation (Figure 4.22). Down-regulation of *LIN28* and *REX1* was delayed relative to *OCT4*, *NANOG*, *SOX2* and *DNMT3B*, and coincided with up-regulation of the fibroblast marker, *P4HB*. This correlates with the idea that LIN28 and REX1 are downstream regulators of the pluripotency transcription-factor network necessary to suppress the expression of miRNAs and lineage commitment genes that promote differentiation (section 1.3.4). Delayed down-regulation kinetics of *Lin28* relative to *Oct4* and *Nanog* have also been observed by Viswanathan *et al.* (2008).

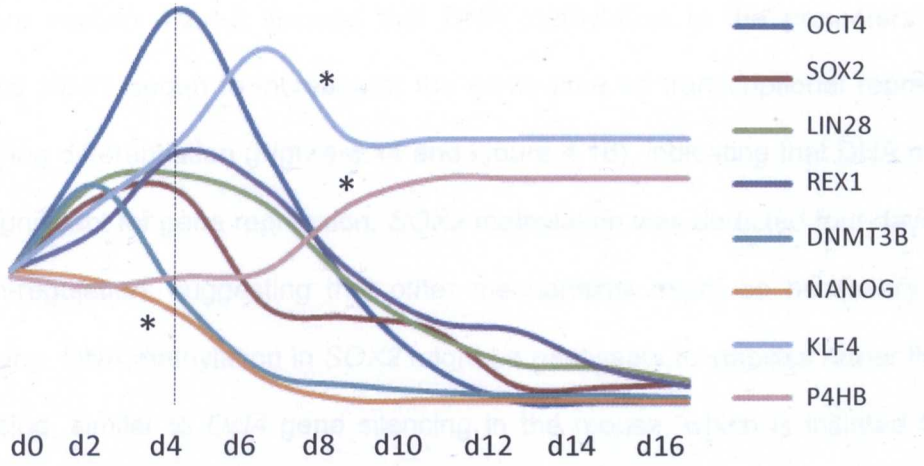

Figure 4.22- Timing of gene repression during hESCs differentiation
NANOG and *DNMT3B* were the first genes to become down-regulated during differentiation of HUES7 hESCs, followed by *SOX2, OCT4, LIN28* and *REX1*. Stars highlight the expression of *NANOG, KLF4* and *P4HB*, which showed different patterns to other genes (Figure 4.21). Y-axis represents relative expression but is not drawn to scale.

4.3.4.2 DNA methylation analysis during differentiation of hESCs and iPSCs

Bisulfite sequencing results are usually performed on individual DNA clones, and are scored by either open (unmethylated) or dark (methylated) circles, with CpGs only considered to be methylated if T is absent (section 2.6.3; Wernig *et al.* 2007; Yu *et al.* 2007b; Park *et al.* 2008c). However, analysing individual DNA clones for several time-points during differentiation, and repeating this for several genes, would be a cumbersome task for this study. Instead, DNA methylation analysis was performed by direct sequencing of whole PCR products, and scoring bisulfite sequencing results with open, dark, half-filled and partially filled circles (section 2.6.3), something that enabled detailed recording of DNA methylation changes during differentiation. This method could discriminate between an increase in the number of CpG sites that became methylated across the whole cell population, and an increase in the proportion of cells that were methylated at each CpG (Figure 4.16, Figure 4.23). A similar 5-category scoring system was recently used in a whole-genome next-generation sequencing study by Laurent *et al.* (2010) to account for DNA methylation differences between hESCs, fibroblast derivatives and neonatal fibroblasts.

Results from section 4.2.4.3 showed that DNA methylation in the promoters of *OCT4*, *NANOG* and *REX1* began to increase at the same time as transcriptional repression was initiated during differentiation (Figure 4.14 and Figure 4.16), indicating that DNA methylation might be significant for gene repression. *SOX2* methylation was detected four days following gene down-regulation, suggesting that other mechanisms might be necessary to initiate gene silencing. DNA methylation in *SOX2* might be necessary to stabilise rather than initiate gene silencing, similar to *Oct4* gene silencing in the mouse, which is initiated by histone modifications and stably repressed by DNA methylation (see section 4.1.1.1). This is to our knowledge the first study correlating the changes in gene expression to DNA methylation during differentiation in non-cancerous cells (Deb-Rinker *et al.* 2005a). *NANOG* was the first pluripotency factor to become down-regulated and methylated during hESC differentiation, suggesting a significant role of this gene in initiating changes in the hESC transcriptional machinery that are necessary for phenotype transition from a pluripotent to a differentiated state.

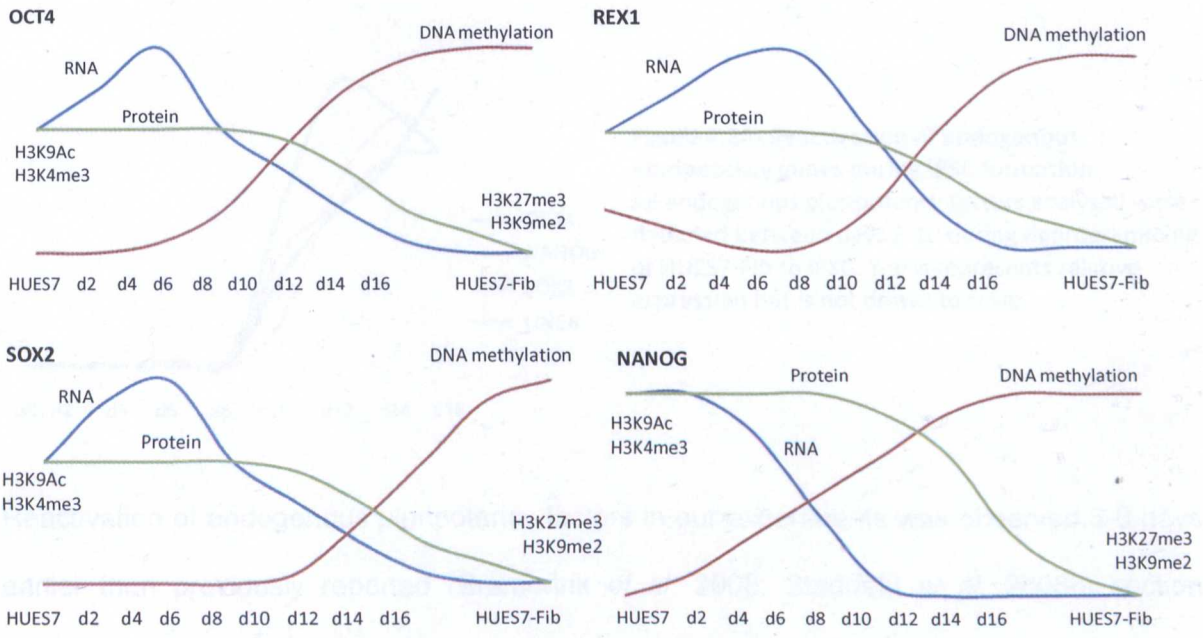

Figure 4.23- Relationship between gene and protein expression to DNA methylation
DNA methylation in *OCT4* and *REX1* was observed after the initial up-regulation in gene expression observed during hESC differentiation, and coincided with the beginning of gene down-regulation. *NANOG*, the only gene to show an immediate decline in gene expression during differentiation, also showed the earliest signs of DNA

methylation in its promoter. *SOX2* transcriptional down-regulation preceded DNA methylation by four days. A change in protein expression was detected several days following gene down-regulation for all pluripotency factors analysed. Y-axis is not drawn to scale.

4.3.5 Reactivation of endogenous pluripotency factors during iPSC formation

Reactivation of the endogenous pluripotency factors, *LIN28*, *NANOG*, *SOX2* and *OCT4*, was observed from days 8-10 PTD, during reprogramming of HUES7-Fib to iPSCs (Figure 4.18 and Figure 4.24). This shows that all four iPSC factors are reactivated with similar kinetics, and are equally necessary for the formation of iPSCs. However, these results should be interpreted with caution since RT-PCR primers for each gene could be amplifying the template cDNA with different efficiencies. Apart from *NANOG*, whose real-time PCR primers did not distinguish between the endogenous gene and the lentiviral transgene, gene expression analysis could be repeated by real-time PCR, where primers work with a similar amplification efficiency (Livak and Schmittgen 2001).

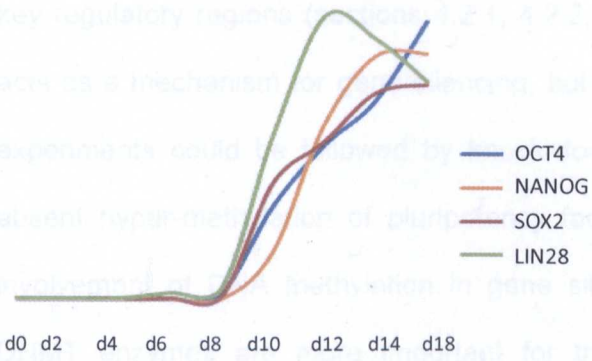

Figure 4.24- Reactivation of endogenous pluripotency genes during iPSC formation
All endogenous pluripotency factors analysed were detected between days 8-10 during deprogramming of HUES7-Fib to iPSC. Y-axis represents relative expression but is not drawn to scale.

Reactivation of endogenous pluripotency factors in our experiments was observed 3-6 days earlier than previously reported (Brambrink *et al.* 2008; Stadtfeld *et al.* 2008b; section 1.8.1.3). However, other studies used flow cytometry to determine protein re-activation, which is likely to be detectable at later stages compared to mRNA expression (Short *et al.* 2005). Considering the population doubling time of HUES7 cells (30-42 hours; Denning *et*

al. 2006) and the appearance of putative iPSC colonies from d11 PTD, which consisted of ~10 cells each (Figure 4.17.A), it was calculated that HUES7-Fib were reprogrammed ~3 days before colony appearance, which would coincide with the timing of endogenous gene re-activation. This suggests that reactivation of endogenous pluripotency genes is what enables a change in phenotype from a differentiated to an ESC-like state.

DNA methylation and histone modification analysis using iPSC colonies on day 11 PTD revealed that repressive epigenetic marks (DNA hyper-methylation and H3K27me3) were removed by this time-point, reinforcing their role in regulating the expression of pluripotency-associated genes. This is the earliest time-point of epigenetic analysis reported to date, during iPSC generation, while analysis of even earlier time-points is continuing in our laboratory.

4.3.6 Future work

Strong inverse relationship was observed between expression of the pluripotency-associated factors *OCT4*, *NANOG*, *SOX2* and *REX1* and the amount of DNA methylation in key regulatory regions (sections 4.2.1, 4.2.2, 4.2.4). This suggested that DNA methylation acts as a mechanism for gene silencing, but in order to establish a more direct link, these experiments could be followed by knock-down studies of DNMTs in hESCs. Delayed or absent hyper-methylation of pluripotency factors during differentiation would confirm the involvement of DNA methylation in gene silencing and provide information about which DNMT enzymes are more important for the process. Similar experiments have been performed in mESCs, but have focused on *Oct4* and *Nanog* expression (Jackson *et al.* 2004; Li *et al.* 2007c), while investigation in hESCs has not been performed.

5 INVESTIGATING THE EFFECT OF DNMT KNOCK-DOWN ON CELL PHENOTYPE AND INDUCED PLURIPOTENCY

5.1 INTRODUCTION

In chapter 4, DNA methylation analysis highlighted that key regulatory-regions of pluripotency factors were unmethylated or hypo-methylated in pluripotent cells and hyper-methylated in differentiated fibroblast cells. DNA methylation was also shown to gradually become enriched as hESCs and iPSCs were differentiated by EB formation. These results suggested that expression of the pluripotency factors under investigation was closely related to DNA methylation. This chapter aimed to investigate whether the timing of pluripotency gene re-activation during reprogramming of differentiated cells, and the overall reprogramming efficiency, could be manipulated by altering the levels of DNA methylation. Considering the abnormal karyotype involved in the HOGN model cell system (Figure 3.4), experiments in this chapter were focused on the HUES7 model system.

5.1.1 Manipulation of DNA methylation through DNMT knock-down

Even though treatment with the chemical 5-aza-cytidine (5-aza) can reduce global DNA methylation and improve the generation of iPSCs from mouse fibroblasts (Huangfu *et al.* 2008a; Mikkelsen *et al.* 2008), this method was not used here as it is highly toxic to hESCs (Allegrucci *et al.* 2007) and shows several side-effects, such as DNA damage and cell cycle arrest in differentiated cells (Liao *et al.* 2009b). In the absence of a DNA de-methylase enzyme in humans (section 1.5.2.4), reduction of DNA methylation in this chapter was performed *via* knock-down of DNA methyltransferase enzymes, using RNA interference (RNAi) technologies. This approach also offered the advantage of identifying which DNMT enzyme had the most profound effect on the efficiency of iPSC generation and the re-activation of endogenous pluripotency factors, thus potentially providing mechanistic details into the regulation of pluripotency-gene expression.

5.1.2 RNA interference

RNA interference (RNAi) is a mechanism for gene silencing that was used here to knock-down the expression of DNA methyltransferase enzymes. RNAi occurs naturally in most eukaryotic organisms as a defence mechanism against viral invasion and transposon expansion, and to mediate post transcriptional regulation (reviewed by Jinek and Doudna 2009). At least 30% of human genes are regulated at the post-transcriptional level by RNAi, reflecting the significance of this mechanism in maintaining genome integrity, and regulating metabolic processes, growth and differentiation (Lewis *et al.* 2005). RNAi has also recently been shown to hold an important role in maintaining pluripotency in hESCs and in reprogramming somatic cells to iPSCs (Ji and Tian 2009; Mallanna and Rizzino 2010).

RNAi is typically initiated in the presence of double-stranded RNAs within cells (Figure 5.1), which promote the RNase III-like enzyme, Dicer, to bind to and cleave the double stranded sequences into non-coding small RNA duplexes of ~20-30bp in length, either in the form of short-interfering RNAs (siRNAs) or micro-RNAs (miRNAs; reviewed by Sontheimer and Carthew 2005). In the cytoplasm, small RNAs form a bond with the RNA-induced Silencing Complex (RISC, composed of enzymes of the Argonaute family), which causes the double stranded small RNAs to unwind and subsequently bind to a homologous endogenous mRNA sequence, causing mRNA degradation, translation inhibition and thus, gene silencing (Figure 5.1; Hutvagner and Simard 2008). Small RNAs of the siRNA family are thought to cause degradation of endogenous mRNAs by endonucleolytic cleavage, while the miRNA family repress mRNA translation by removal/shortening of the mRNA poly(A) tails (process known as de-adenylation) which destabilises mRNAs and causes their degradation (Giraldez *et al.* 2006; Wu *et al.* 2006; McDaneld 2009). Small regulatory siRNAs and miRNAs in eukaryotic organisms can also lead to target gene silencing *via* heterochromatinisation of DNA through DNA methylation and histone modifications (e.g. H3K9 and H3K27; Gonzalez *et al.* 2008; Carthew and Sontheimer 2009).

The efficiency by which RNAi enables degradation of endogenous mRNA is influenced by the accessibility and secondary structure of the mRNA as well as by the length and base-pair complementarity of the functional intermediates, siRNAs or miRNAs, to the endogenous mRNA (Pei and Tuschl 2006; Shao *et al.* 2007). Even though siRNAs associate with target RNAs that contain a perfectly complementary sequence (reviewed by Jinek and Doudna 2009), miRNAs usually base-pair imperfectly with target RNAs (Filipowicz 2005; Jinek and Doudna 2009). The critical region for miRNA target recognition and RISC complex binding is located between 2-8bp from the 5' end ("seed" sequence; Doench and Sharp 2004; Brennecke *et al.* 2005). Due to the short length of the miRNA seed sequence, siRNAs can also sometimes act as miRNAs when base-pairing imperfectly, and can thus potentially cause specific degradation or translational repression of endogenous off-target mRNAs (Saxena *et al.* 2003).

Nevertheless, RNAi is now a well established tool for experimental post transcriptional gene silencing, and its natural occurrence within cells distinguishes it from other nucleic-acid silencing technologies, such as anti-sense oligonucleotides and ribozymes (reviewed by Kurreck 2003). For research purposes, siRNAs can be produced by chemical synthesis, *in vitro* transcription or digestion of dsRNA using recombinant Dicer, and *in vivo* expression of siRNA duplexes as short hairpin RNAs (shRNAs) from plasmids, or viral vectors (Scaringe 2001; Calegari *et al.* 2002; Donze and Picard 2002; Paddison *et al.* 2002; Sui *et al.* 2002). Although chemically synthesized siRNAs are very efficient and readily introduced into most types of cells using cationic-lipid transfection, electroporation or microinjection tools (Menendez *et al.* 2005), they can only produce a transient gene knockdown effect (Vallier *et al.* 2004). *In vitro* transcription or digestion of dsRNA using recombinant Dicer, are cost effective tools for siRNA synthesis, but also present several disadvantages such as low product purity, low specificity, and variable efficiency (reviewed by Whitehead *et al.* 2009). One of the best available tools for RNAi is the expression of shRNAs, from retroviral or

lentiviral vectors (Paddison and Hannon 2003). Several groups have reported long-term gene silencing using these vectors (Szulc *et al.* 2006; Kappel *et al.* 2007).

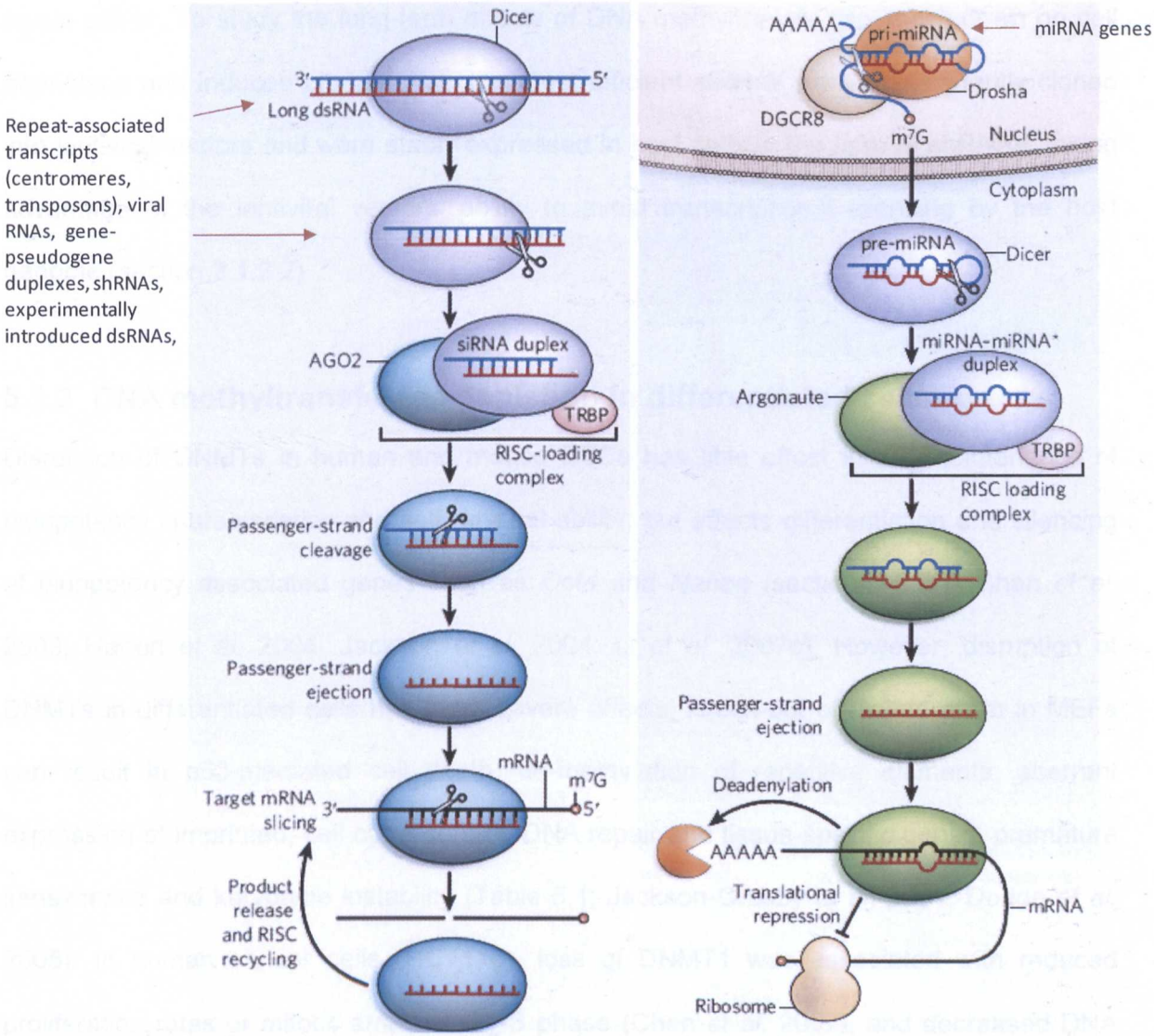

Figure 5.1- The RNA interference (RNAi) pathway
Double stranded RNAs (dsRNA) are processed by Dicer enzyme into 19-30bp long short-interfering RNAs (siRNA, left panel) or micro-RNA (miRNA, right panel). Association with the RNA-induced silencing complex (RISC) unwinds siRNAs or miRNAs into single-stranded molecules and mediates degradation of endogenous mRNA by endonucleolytic cleavage (siRNAs) or removal of the poly-A tails from their 3'UTRs (miRNAs; Jinek and Doudna 2009).

In order to achieve DNA methyltransferase knock-down in this chapter, transient knock-down by lipofection of chemically synthesised siRNAs was initially tested to screen several commercially available siRNAs and select those that best induced knock-down of their target genes. To study the long-term effects of DNA methyltransferase knock-down on cell phenotype and induced pluripotency, the most efficient siRNAs were subsequently cloned into lentiviral vectors and were stably expressed in host cells in the form of shRNAs, taking advantage of the lentiviral vectors' ability to avoid transcriptional silencing by the host genome (section 3.1.3.2)

5.1.3 DNA methyltransferase depletion in differentiated cells

Disruption of DNMTs in human and mouse ESCs has little effect in the maintenance of pluripotency characteristics and self-renewal ability, but affects differentiation and silencing of pluripotency associated genes such as *Oct4* and *Nanog* (section 1.6.2.7; Chen *et al.* 2003; Hattori *et al.* 2004; Jackson *et al.* 2004; Li *et al.* 2007c). However, disruption of DNMTs in differentiated cells has more severe effects; knock-out of *Dnmt1* or *3b* in MEFs can result in p53-mediated cell death, de-methylation of repetitive elements, aberrant expression of imprinted, cell cycle control, DNA repair and tissue-specific genes, premature senescence and karyotype instability (Table 5.1; Jackson-Grusby *et al.* 2001; Dodge *et al.* 2005). In human cancer cells (HCT116), loss of DNMT1 was associated with reduced proliferation rates or mitotic arrest at G1-S phase (Chen *et al.* 2007), and decreased DNA methylation in centromeric regions and tumour suppressor genes (Rhee *et al.* 2000).

These effects were enhanced with combined knock-out of *DNMT1* and *3B,* where a 95% reduction in global DNA methylation was observed (Rhee *et al.* 2002). Single knock-out of *DNMT3B* in human cancer cells had more modest effects than *DNMT1* single knock-out (Table 5.1). Collectively, these data suggest that DNMTs, and especially DNMT1, have a significant role in the proliferation and karyotype stability of differentiated cells. *Dnmt3a*

knock-out was shown to have no effect in the maintenance of global DNA methylation, imprinting stability and expression of tumour suppressor genes in mouse cells (Dodge *et al.* 2005).

Considering data from the literature, the effects of *DNMT1*, but not *DNMT3A*, knock-down on proliferation, cell-cycle progression, global DNA methylation, and DNA methylation at imprinted and tumour suppressor genes were tested in this chapter, prior to the use of fibroblast cells in reprogramming experiments to generate iPSCs.

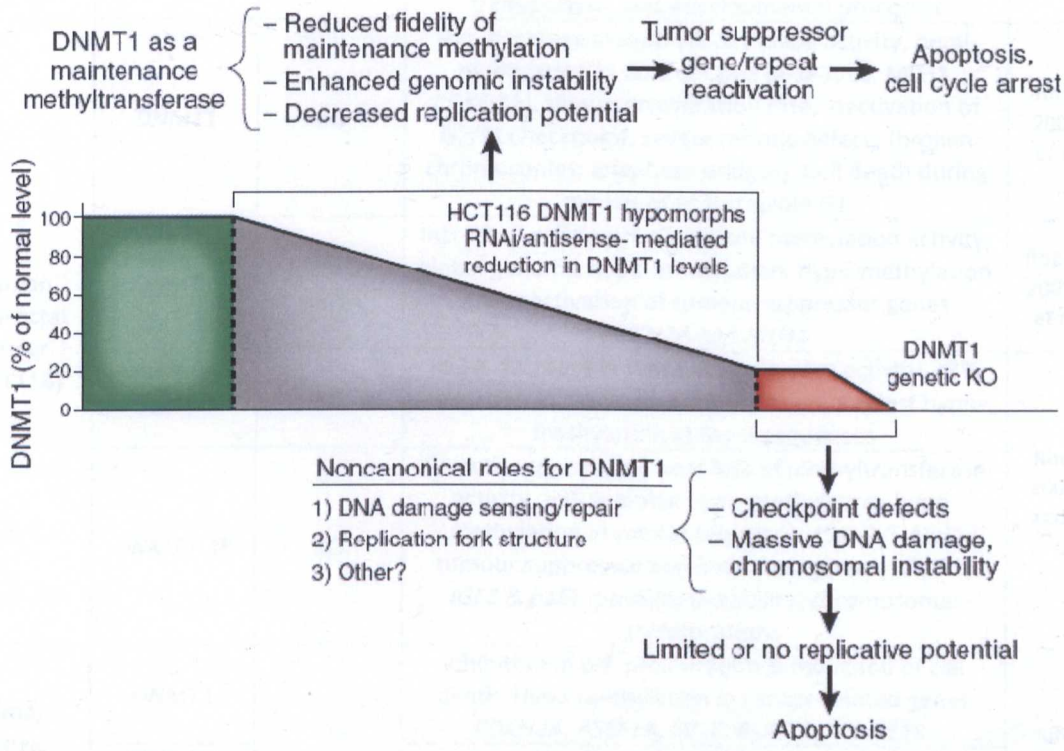

Figure 5.2- Phenotypic effects of DNMT1 manipulation in mammalian cells
Relative levels of DNMT1 expression are shown on the Y-axis, with 100% depicting normal DNMT1 levels and 0% representing DNMT1 knock-out. The severity of reduced DNMT1 expression on cell phenotype increases as the level of down-regulation increases. Outcomes associated with the known DNMT1 role as a maintenance methyltransferase are shown above the graph, whereas non-canonical functions of DNMT1 are shown below the graph (Brown and Robertson 2007).

Table 5.1- Roles of DNA methyltransferase enzymes in differentiated cells
KO= knock-out, DKO= double knock-out

Cell type	Gene	Treatment	Effect	Papers
MEFs	*Dnmt1*	KO	p53 dependent cell death, hypo-methylation of repetitive elements (IAP, L1, G7e), aberrant expression genes involved in imprinting (*Tdag*, *Xist*, *H19*, *Igf2*, *Grb10*, *Peg3*), cell cycle control, DNA repair, lineage specification and mobilisation of retroelements	Jackson-Grusby *et al.* 2001
	Dnmt3a	KO	No effect on processes studied	Dodge *et al.* 2005
	Dnmt3b		p53 dependent cell death, premature senescence, partial loss of global DNA methylation, genome instability (aneuploidy & polyploidy, chromosome breaks and fusions)	
	Dnmt3a-3b	DKO	Same as DNMT3B KO	
Mouse Pituitary Adenoma	*Dnmt1*	RNAi by siRNA	Hypo-methylation of *H19* & *Nnat* promoters & reactivation of *Nnat*. Differential expression of 91 genes involved in induction of apoptosis, signal transduction, and developmental processes	Dudley *et al.* 2008
Human colorectal cancer (HCT116)	*DNMT1*	KO	90% decrease in methyltransferase activity, hemi-methylation in 20% of CpGs (a-SAT, L1, MLH1, CDKN2A), slower proliferation rate, inactivation of G2/M checkpoint, severe mitotic defects (broken chromosomes, anaphase bridges). Cell death during mitosis or at tetraploid G1	Rhee *et al.* 2000; Chen *et al.* 2007
	DNMT1	RNAi by siRNA	Increased cell death, decreased methylation activity, global genomic hypo-methylation, hypo-methylation and reactivation of tumour suppressor genes *CDKN2A* and *MLH1*	Robert *et al.* 2003; Spada *et al.* 2007
	DNMT3B	KO	<13% decrease in methyltransferases activity, <3% reduction in global DNA methylation, modest hypo-methylation at Sat-2 sequences	Rhee *et al.* 2002; Karpf and Matsui 2005
	DNMT1-3B	KO	Growth suppression, near loss of methyltransferase activity, >95 % global hypo-methylation, hypo-methylation at repeat sequences (Sat-2 & Alu), tumour suppressor and imprinted genes (*TIMP-3*, *IGF2 & p16*), genomic instability, chromosomal translocations	
Human gastric cancer	*DNMT1*	RNAi by siRNA	Inhibition of cell proliferation & induction of cell death. Hypo-methylation in cancer-related genes *CDKN2A*, *ASSF1A*, *HTLF*, *RUNX3*, *AKAP12B*.	Jung *et al.* 2007
	DNMT3B		No effect on processes studied	
	DNMT1-3B		No synergistic effect in de-methylation or gene reactivation	
Human lung carcinoma	*DNMT1*		Increased expression of cell-cycle regulating genes *p21* and *BIK*	Milutinovic *et al.* 2004
HEK293				

5.1.4 Chapter Aims and Objectives

This chapter aimed to establish a closer link between the expression of pluripotency-associated genes and DNA methylation by testing whether knock-down of DNMT enzymes would enable easier gene re-activation and/or increased formation of iPSCs during reprogramming. To achieve this aim, the following objectives had to be met:

* Determine the expression levels of each DNMT in hESC-derived fibroblasts
* Use RNAi technologies (siRNAs), to test transient knock-down of the most highly expressed DNMTs in hESC-derived fibroblasts (DNMT1 and 3A) and then induce stable knock-down using lentivirally expressed shRNAs
* Study the effects of *DNMT1* knock-down on pluripotency maintenance and differentiation, population doubling time, cell cycle progression, imprinting stability, and methylation of tumour suppressor genes
* Investigate whether *DNMT1* and/or *3A* knock-down could affect the reactivation of endogenous pluripotency genes during reprogramming and/or result in increased formation of iPSC colonies.

5.2 RESULTS

5.2.1 Expression of DNA methyltransferases in HUES7 and HUES7-Fib

Four DNA methyltransferase enzymes have been detected in human cells (section 1.5.2.2). These are the maintenance methyltransferase DNMT1, and the *de novo* methyltransferases DNMT3A, DNMT3B and DNMT3L. In order to determine which of these enzymes to target for knock-down, their expression levels in hESC-derived fibroblasts were determined by real-time PCR and immunofluorescence staining. Real-time PCR analysis showed that the *de novo* methyltransferases *DNMT3B* and *DNMT3L* were almost undetectable in HUES7-Fib cells (Figure 5.3.A). The same was true for the fibroblast line, BJ-Fib, which was included as a control in this experiment. *DNMT3A* was detected in fibroblast lines, but at lower levels than in HUES7 cells (57% lower in HUES7-Fib, 94% lower in BJ-Fib). The most

abundant DNMT in fibroblast cells was the maintenance methyltransferase *DNMT1*, but was still expressed at 21-25% lower levels than in HUES7. Immunofluorescence staining confirmed the findings of real-time PCR; all DNMTs were expressed at high levels in HUES7 cells (Figure 5.4.A), DNMT3B and DNMT3L were almost undetectable in HUES7-Fib, and DNMT3A was expressed at lower levels compared to HUES7 (Figure 5.4.B). Gene and protein expression analysis suggested that DNMT1 and DNMT3A should be targeted for knock-down in HUES7-Fib.

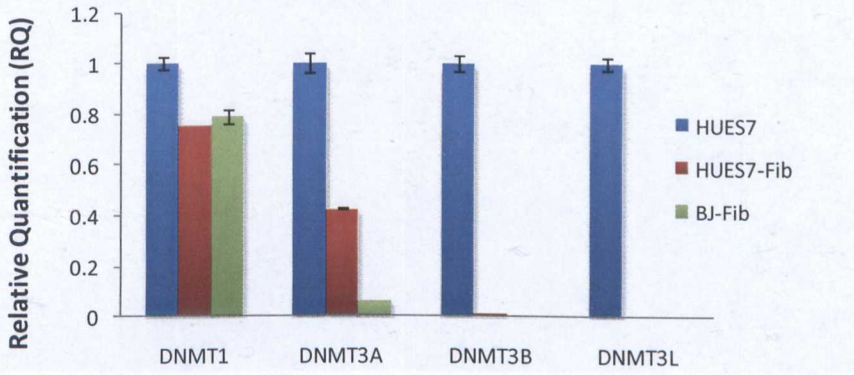

Figure 5.3- Gene expression of DNA methyltransferases in HUES7, HUES7-Fib and BJ-Fib cells
Real-time PCR analysis of *DNMT1, 3A, 3B* and *3L* expression in HUES7, HUES7-Fib and BJ-Fib. Error bars represent standard error.

5.2.2 Knock-down of the DNA methyltransferase DNMT1

5.2.2.1 siRNA-mediated transient knock-down of *DNMT1*

Commercially available siRNAs against human *DNMT1* were tested to determine which one would enable the highest gene knock-down (KD; Figure 5.5). All siRNAs had 100% complementarity to endogenous mRNA and were located within the coding region (siRNA 859; exon 16, siRNA 860; exon 30 and siRNA 861; exon 6). Cells were treated with each siRNA, as well as with combination of all siRNAs together. *DNMT1* expression was assessed by real-time PCR at 24, 48 and 72 hours following transfection with siRNAs. Results were quantified relative to a control sample, treated with the cationic lipid Lipofectamine-2000 but no siRNA (lipid control). Each siRNA was referred to by using the three last digits of its manufacturer's product number (Table 2.3). Tests were performed

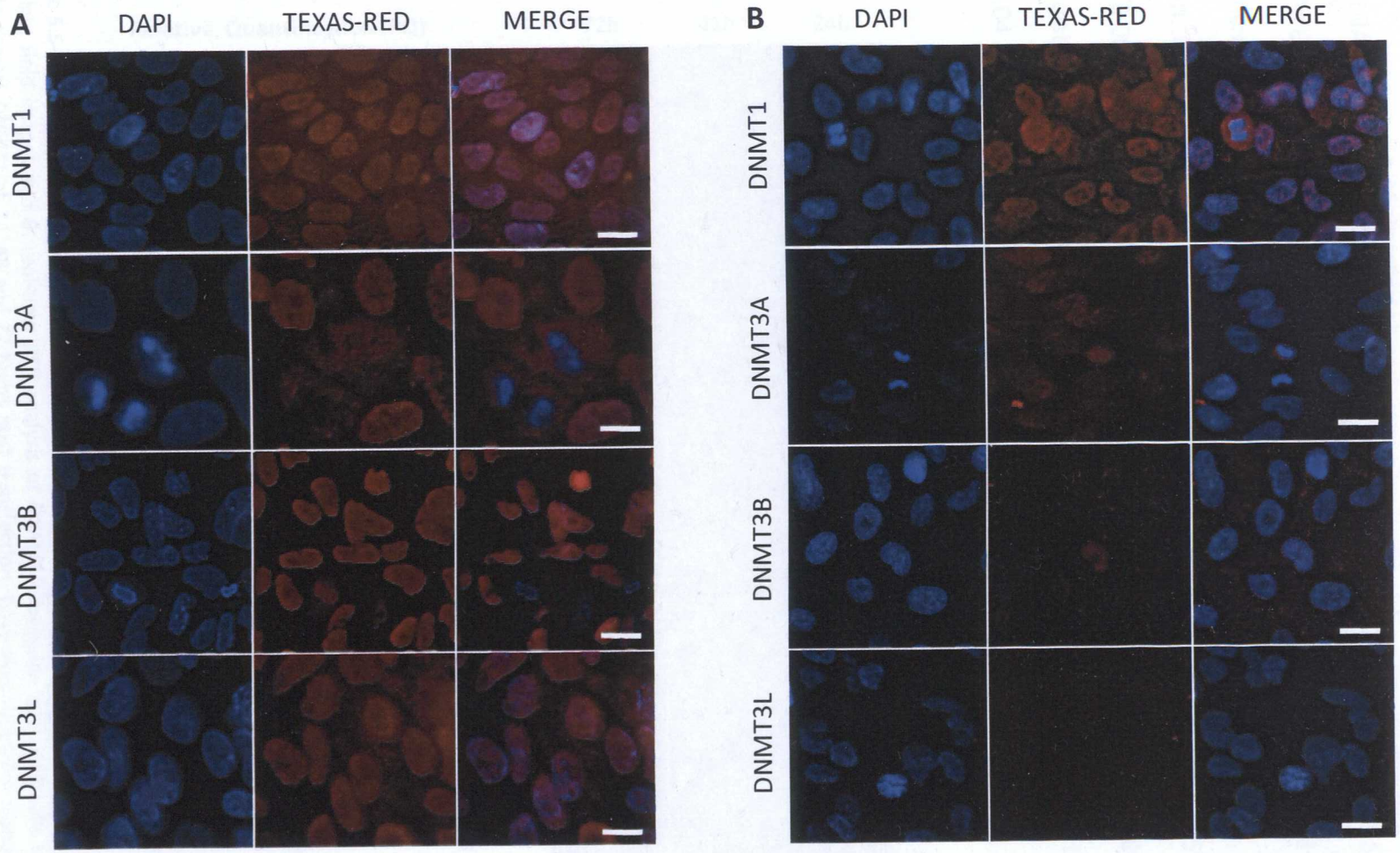

Figure 5.4- Protein expression of DNA methyltransferases in HUES7 and HUES7-Fib
Expression of DNMT1, DNMT3A, 3B and 3L proteins in **A.** HUES7 and **B.** HUES7-Fib cells, as determined by immunofluorescence staining. Protein expression was captured using the Cy3 channel, while the overlay represents a merge of the DAPI (nuclear staining) and Cy3 channels. Scale bars represent 32µm.

using HUES7 cells, since protocols for siRNA transfection of this line were well established in our lab by previous colleagues (section 2.2.2).

All siRNAs tested were able to reduce *DNMT1* expression by 50-85% (Figure 5.5). KD with siRNAs 860, 861, and combination of all siRNAs was at its lowest 24 hours post-transfection and increased at 48 and 72 hours, while siRNA859-mediated KD showed the reverse pattern. Overall, siRNAs 859 and 860 enabled the highest KD for *DNMT1* (85% KD, RQ= 0.15±0.002, p=0.00 and 72% KD, RQ= 0.28±0.013, p=0.00). No statistically significant synergistic effect was observed in the presence of all three siRNAs, relative to siRNA860 (p= 0.04 at 24h, p=0.23 at 48h and p=0.09 at 72h).

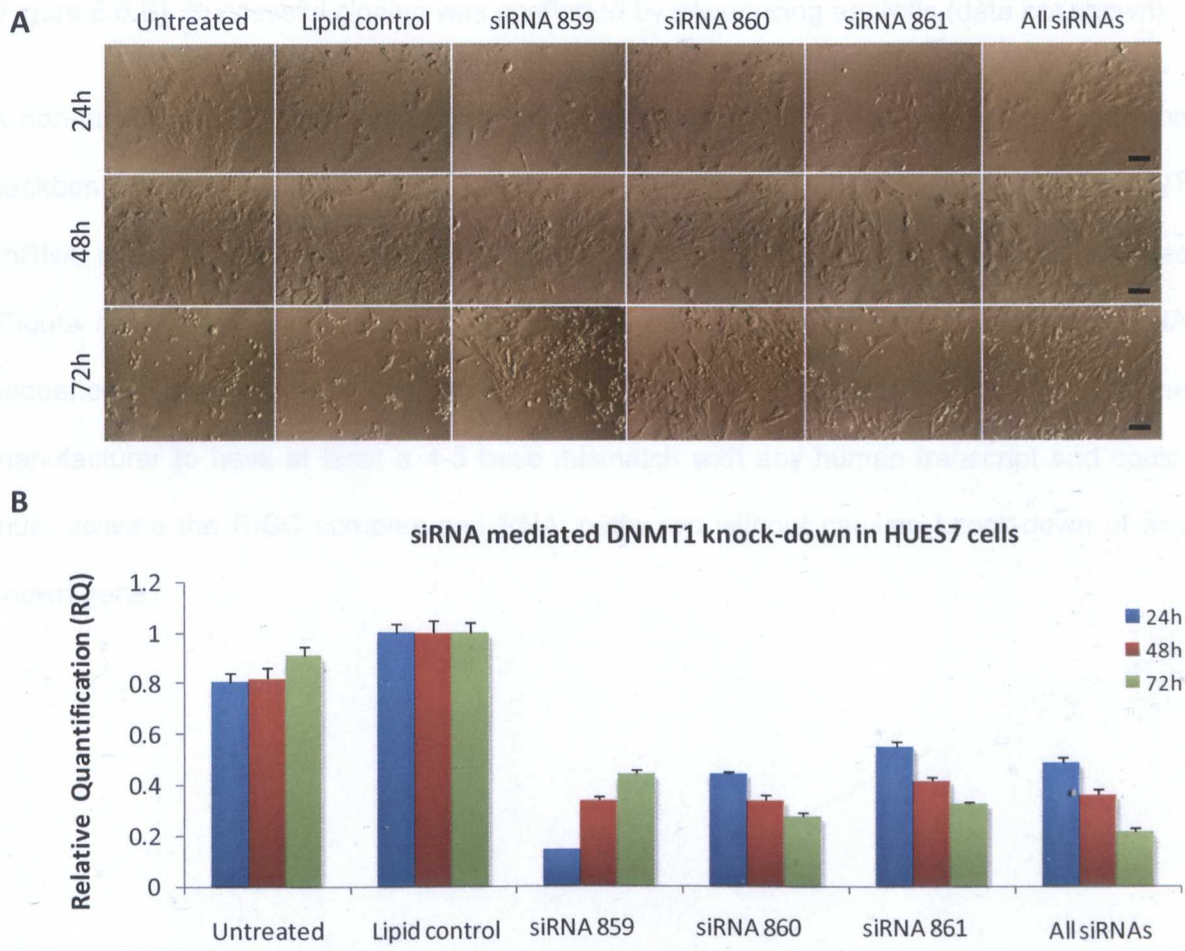

Figure 5.5- siRNA mediated knock-down of *DNMT1* in HUES7 cells
A. Bright field images and **B.** real-time PCR analysis of *DNMT1* expression in HUES7 cells transfected with siRNAs against *DNMT1* at 24, 48 and 72 hours post transfection. Error bars represent standard error. Scale bars represent 100μm.

5.2.2.2 Design of shRNA oligos for stable knock-down of *DNMT1*

Gene knock-down by siRNA mediated pathways has a transient effect on down-regulating expression of target genes (Vallier *et al.* 2004). Stable *DNMT1* KD in HUES7 and HUES7-Fib was introduced by lentiviral delivery of short hairpin RNA (shRNA) oligos. shRNA sequences were based on siRNAs 859 and 860, shown to cause the highest knock-down of *DNMT1* (section 5.2.2.1). shRNAs were designed by synthesising oligos containing two repeats of the siRNA sequences (one 5' to 3' and the other its reverse complement), that were separated by a loop forming sequence (Figure 5.6.A). The loop contained an XbaI restriction site to facilitate screening (Figure 5.6.C), while half-sites for MluI and ClaI were included at the ends of the oligos to enable cloning into the lentiviral plasmid pLVTHM (Figure 5.6.B). Successful cloning was confirmed by sequencing analysis (data not shown).

A non-targeting (NT) shRNA was purchased from SIGMA (SHC002), as an insert into the backbone vector TRC1/1.5 pLKO.1-puro. With help from Dr. David Anderson, the NT shRNA insert was sub-cloned into pLVTHM between its MluI and ClaI restriction sites (Figure 5.6.B), and used as a negative control, instead of scrambled or reverse shRNA sequences (Cortina *et al.* 2007; Wang *et al.* 2008a). The NT shRNA was designed by the manufacturer to have at least a 4-5 base mismatch with any human transcript and could, thus, activate the RISC complex and RNAi pathways without causing knock-down of any known gene.

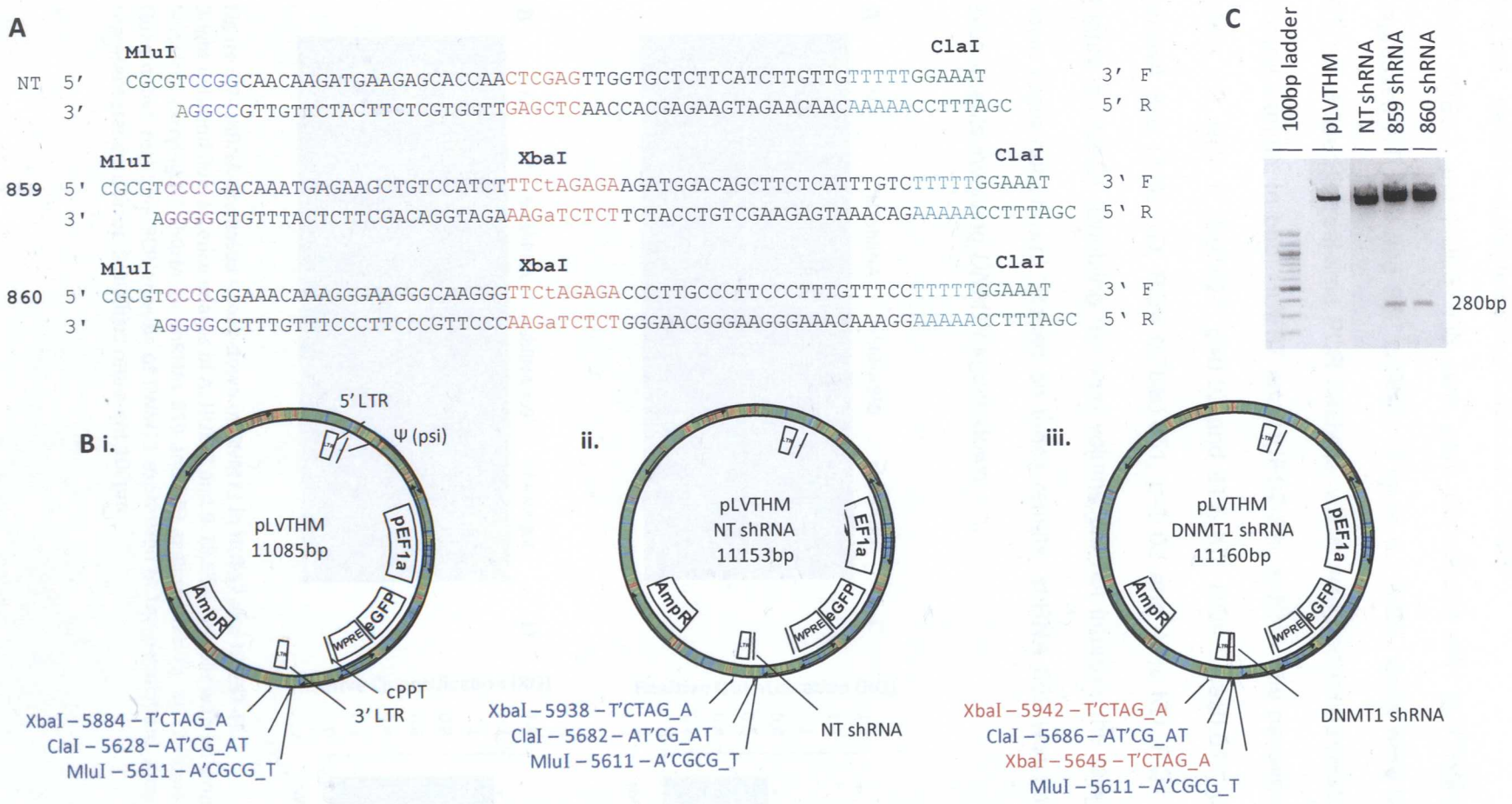

Figure 5.6- Cloning *DNMT1* shRNAs into lentiviral transfer plasmids

A. shRNA sequences specific to human *DNMT1*. Green= restriction enzyme overhangs, black= siRNA sequences, red= loop sequence, purple and light blue= hairpin forming sequences **B.** Map of the lentiviral transfer plasmid pLVTHM **(i)** before and **(ii)** after cloning the NT and **(iii)** *DNMT1* shRNAs between the ClaI and MluI restriction sites. Cloning the *DNMT1* shRNAs into the plasmid created a second XbaI restriction site. **C.** Gel electrophoresis of plasmid DNA following a restriction digest with the enzyme XbaI, used to positively identify clones with the *DNMT1* shRNA inserts.

5.2.2.3 shRNA-mediated knock-down of *DNMT1*

Both HUES7 and HUES7-Fib cells were transduced with pLVTHM-based lentivirus that expressed NT, 859 and 860 shRNAs (Figure 5.7.A&B). Cells were collected at 72 hours PTD and used in real-time PCR analysis, which was performed relative to the NT shRNA control sample. In both HUES7 and HUES7-Fib, shRNA 859 caused a higher *DNMT1* KD (64% KD, RQ= 0.36±0.027, p=0.02 and 81% KD, RQ= 0.19±0.012, p=0.02), compared to shRNA 860 (24% KD, RQ= 0.76±0.051, p=0.02 and 48% KD, RQ= 0.62±0.050, p=0.01; Figure 5.7.C&D). Doubling the viral volume did not improve the levels of *DNMT1* knock-down (data not shown). Based on these results, shRNA 859 was used in all subsequent experiments involving *DNMT1* knock-down.

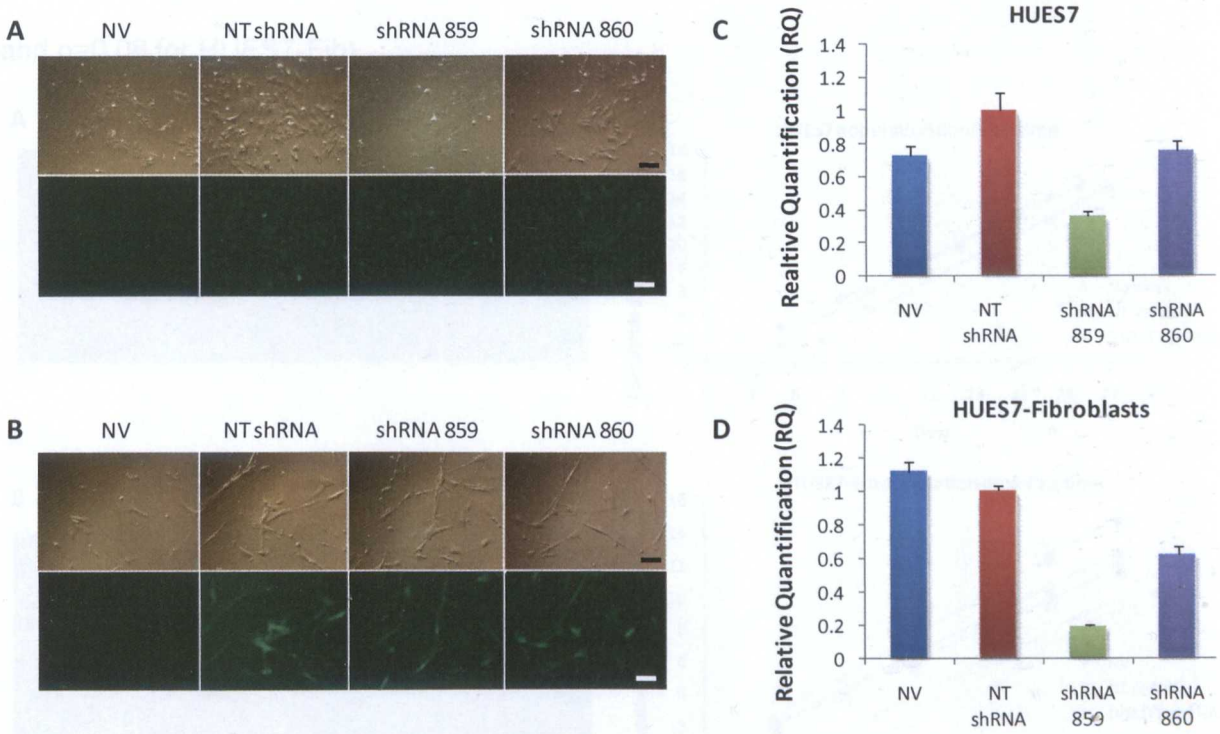

Figure 5.7- shRNA-mediated knock-down of *DNMT1* in HUES7 and HUES7-Fib
Bright field and fluorescence images of **A.** HUES7 and **B.** HUES7-Fib cells with no virus (NV), or transduced with lentivirus carrying NT shRNA, or shRNAs 859 and 860 against *DNMT1*, at 72 hours post transduction. **C.&D.** Quantitative real-time PCR analysis of *DNMT1* expression in the populations shown in A. and B. Error bars represent standard error. Scale bars represent 100μm.

5.2.2.4 Stable-knock-down of *DNMT1*

Following transduction with shRNA-expressing lentivirus, HUES7 and HUES7-Fib cells were cultured in triplicate flasks for five passages. During this time, cell counts were performed at each passage to calculate growth curves, and cell pellets were collected to determine the levels of *DNMT1* mRNA and protein KD. Real-time PCR was performed using all three replicates of each sample, but these were pooled for Western blot analysis in order to provide enough material for protein extraction.

HUES7 and HUES7-Fib lines carrying *DNMT1* KD remained brightly fluorescent for 5 passages (Figure 5.8.A&B), indicating persistent expression of lentiviral genes. They had population doubling (PD) times of 41.22 h/PD and 36.62 h/PD (Figure 5.8.C&D), none of which was significantly different to their respective NT shRNA controls (p=0.63 for HUES7 and p=0.08 for HUES7-Fib).

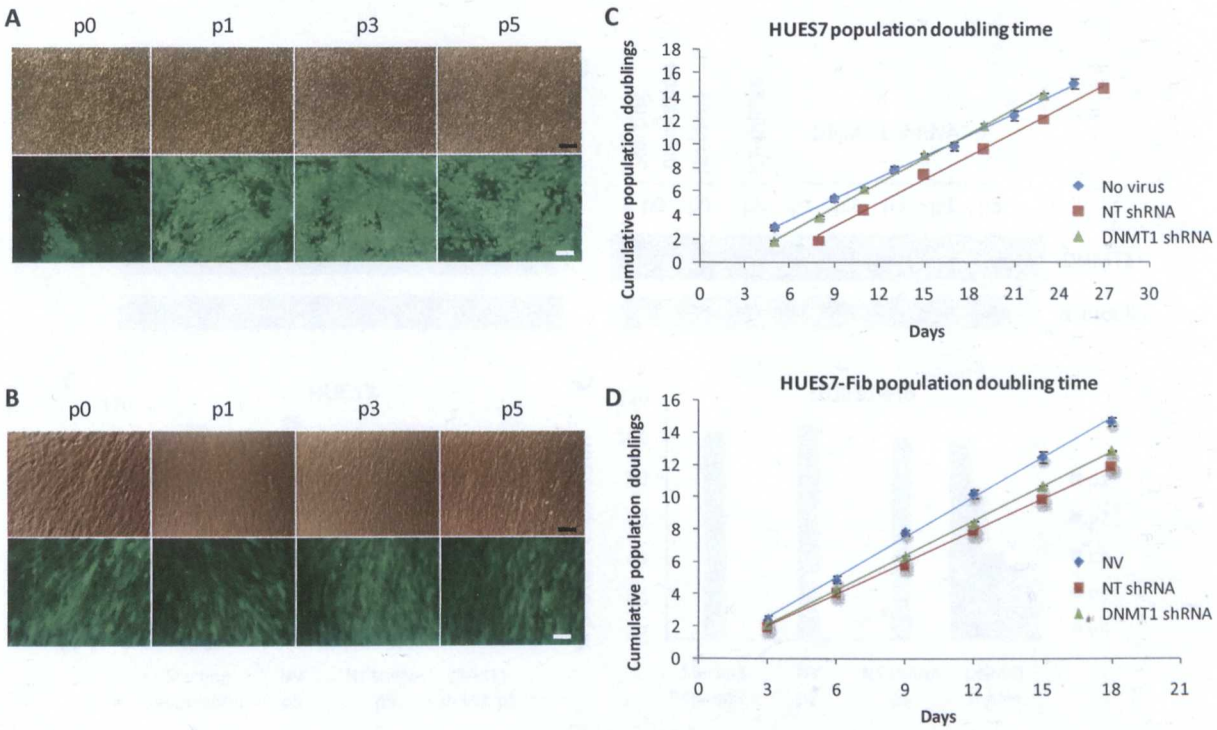

Figure 5.8- Population doubling time in HUES7 and HUES7-Fib cells with stable *DNMT1* knock-down
Bright field and fluorescence images of **A.** HUES7 and **B.** HUES7-Fib cells transduced with lentivirus carrying shRNA859 against *DNMT1*, at passages 0, 1, 3 and 5 after transduction. Dot-plot analysis of the cumulative population doublings between passages 1 and 5, in **C.** HUES7 and **D.** HUES7-Fib cells transduced with no virus, lentivirus carrying NT shRNA or shRNA859 against *DNMT1*. Error bars represent standard error. Scale bars represent 100µm.

Real-time PCR analysis over 5 passages PTD showed that *DNMT1* expression remained 39-51% lower in KD HUES7 and HUES7-Fib lines, compared to the NT shRNA controls at passage 5 ($p<0.05$; Figure 5.9). DNMT1 protein expression was reduced by 28.5-38% in KD lines (Figure 5.10).

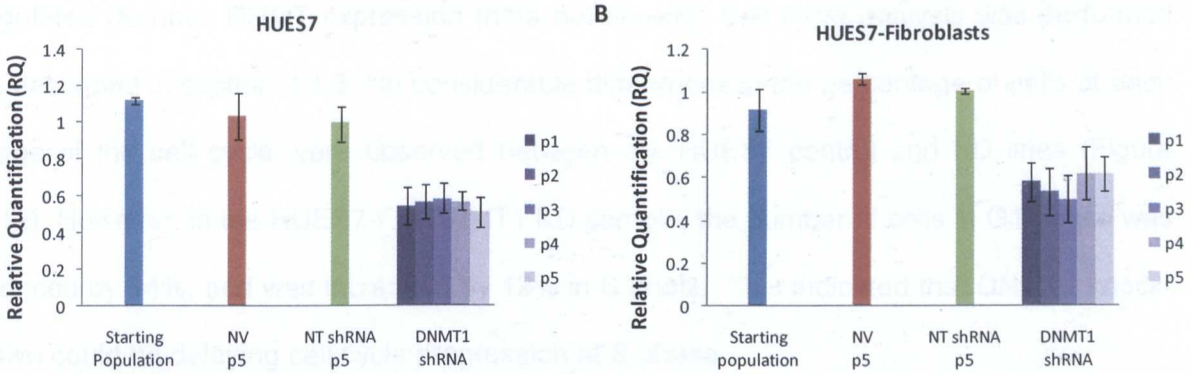

Figure 5.9- *DNMT1* gene expression in HUES7 and HUES7-Fib cells with stable DNMT1 knock-down
Real-time PCR analysis of *DNMT1* expression in cells transduced with lentivirus carrying shRNA859 against *DNMT1* between passages 1 to 5 is shown relative to the starting populations of HUES7 **(A)** and HUES7-Fib **(B)**, cells with no virus (NV) or transduced with lentivirus carrying NT shRNA, for 5 passages. Error bars represent standard error.

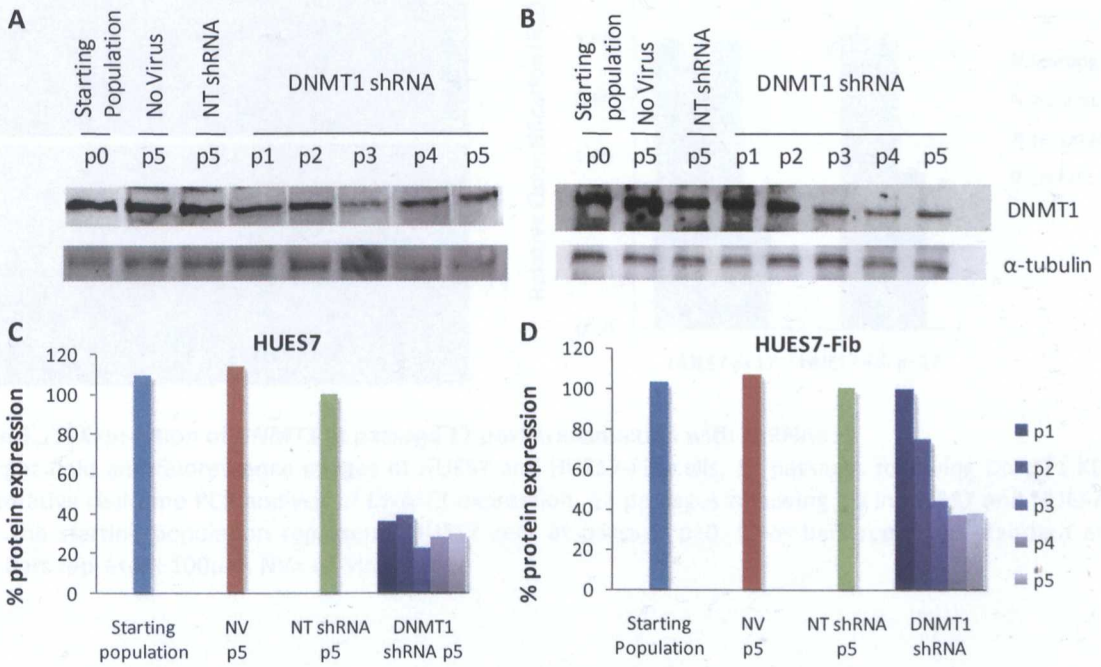

Figure 5.10- DNMT1 protein expression in HUES7 and HUES7-Fib cells with stable DNMT1 knock-down
Western blot analysis of *DNMT1* expression in cells transduced with lentivirus carrying shRNA859 against *DNMT1* between passages 1 to 5 is shown relative to the starting populations of HUES7 **(A)** and HUES7-Fib **(B)**, cells with no virus (NV) or transduced with lentivirus carrying NT shRNA, for 5 passages. **C. D.** Histograms representing the % expression of DNMT1 protein in the samples shown in A. and B. Protein expression was normalised to the NT shRNA sample.

5.2.3 The effect of DNMT1 knock-down on cell cycle progression

HUES7 and HUES7-Fib carrying DNMT1 KD were cultured up to passage 17 PTD, in order to give enough time for the KD to affect DNA methylation (Jackson *et al.* 2004). At passage 17, cells maintained GFP expression and DNMT1 KD (Figure 5.11), while they had not up-regulated *de novo* DNMT expression (data not shown). Cell cycle analysis was performed as described in section 2.4.3. No considerable differences in the percentage of cells at each stage of the cell cycle were observed between the HUES7 control and KD lines (Figure 5.12). However, in the HUES7-Fib DNMT1 KD sample, the number of cells in G1 phase was reduced by 14%, and was increased by 12% in S phase. This indicated that DNMT1 knock-down could be delaying cell cycle progression at S phase.

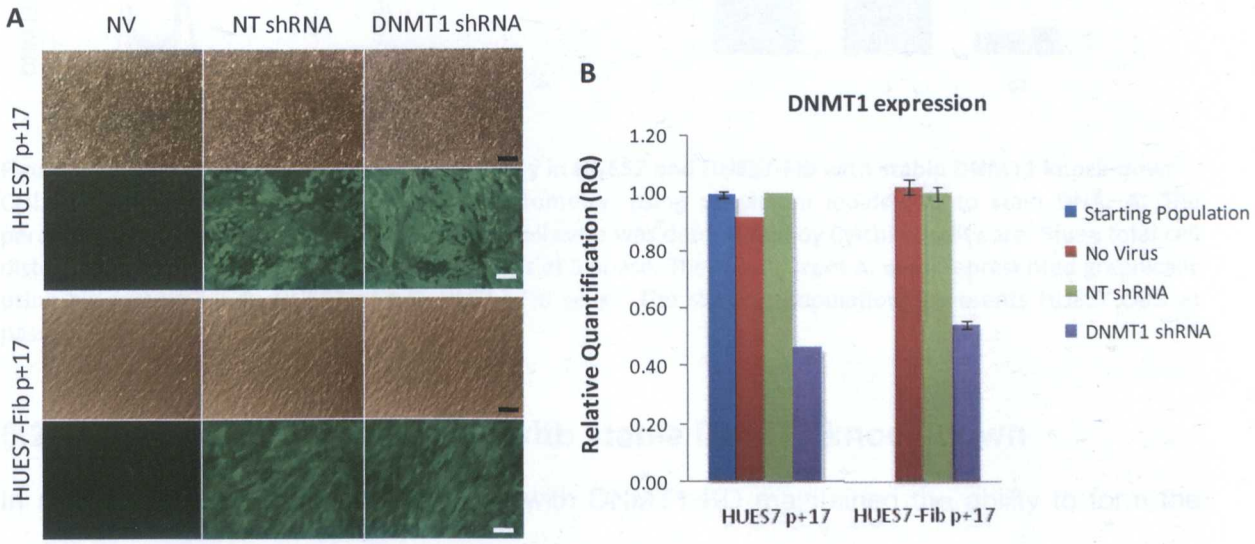

Figure 5.11- Expression of *DNMT1* at passage 17 post-transduction with shRNA859
A. Bright field and fluorescence images of HUES7 and HUES7-Fib cells, 17 passages following DNMT1 KD. **B.** Quantitative real-time PCR analysis of *DNMT1* expression, 17 passages following KD in HUES7 and HUES7-Fib cells. The starting population represents HUES7 cells at passage p+0. Error bars represent standard error. Scale bars represent 100µm. NV= no virus

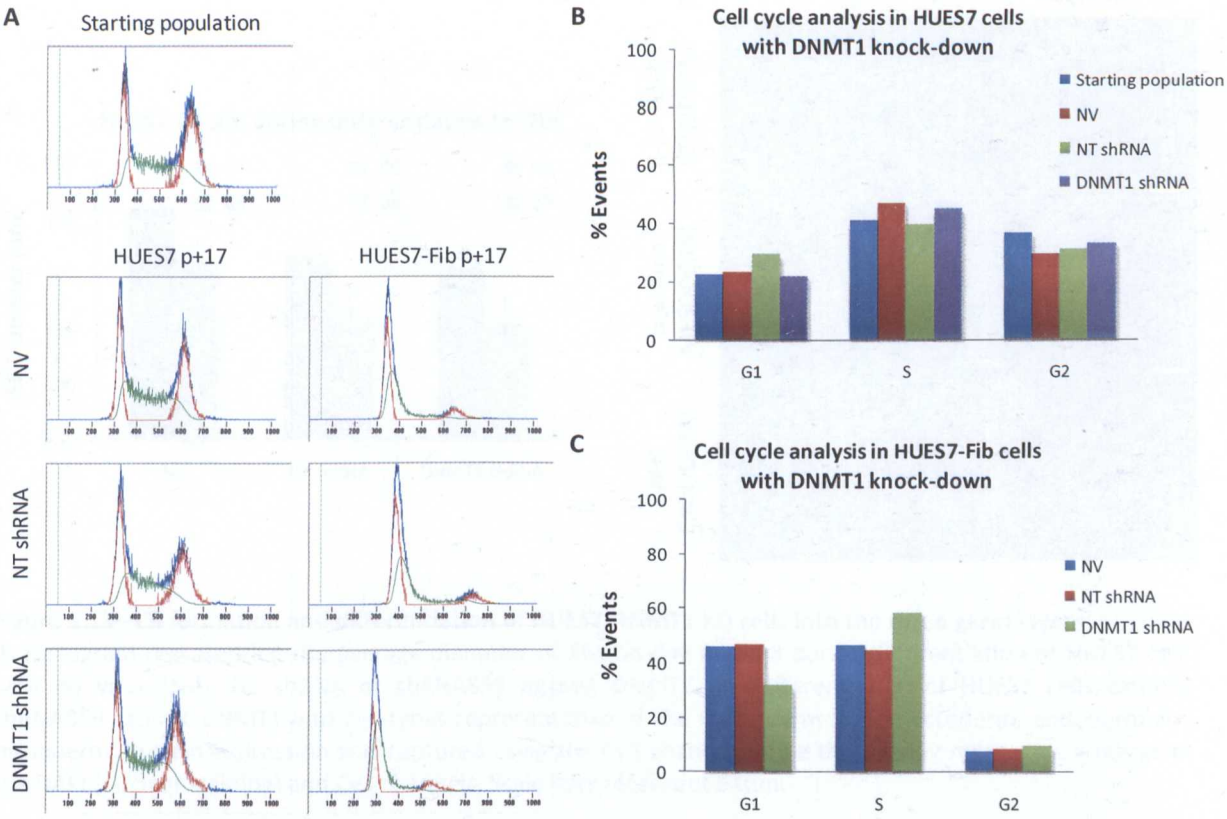

Figure 5.12- Cell cycle analysis by flow cytometry in HUES7 and HUES7-Fib with stable DNMT1 knock-down
Cell cycle analysis was performed by flow cytometry, using propidium iodide (PI) to stain DNA. **A.** The percentage of cells at stages G1, S or G2 of the cell cycle was determined by Cylchred software. Blue= total cell distribution, red= cells at G1 and G2, green= cells at S phase. The results from A. were represented graphically using histograms for **B.** HUES7 and **C.** HUES7-Fib cells. The starting population represents HUES7 cells at passage p+0. NV = no virus.

5.2.4 Differentiation of hESCs with stable DNMT1 knock-down

In order to determine whether HUES7 with DNMT1 KD maintained the ability to form the three embryonic germ layers, cells at passage 17 PTD were differentiated *via* EB formation. Even though EB diameters varied between the NV, NT shRNA and KD samples (Figure 5.13), their differences were not statistically significant (day 4: p=0.09 and day 8: p=0.98). Derivatives of the three embryonic germ layers were identified in the control NV and NT shRNA lines (data not shown), as well as in the DNMT1 KD line (Figure 5.13), demonstrating that DNMT1 KD did not affect pluripotency in HUES7 cells.

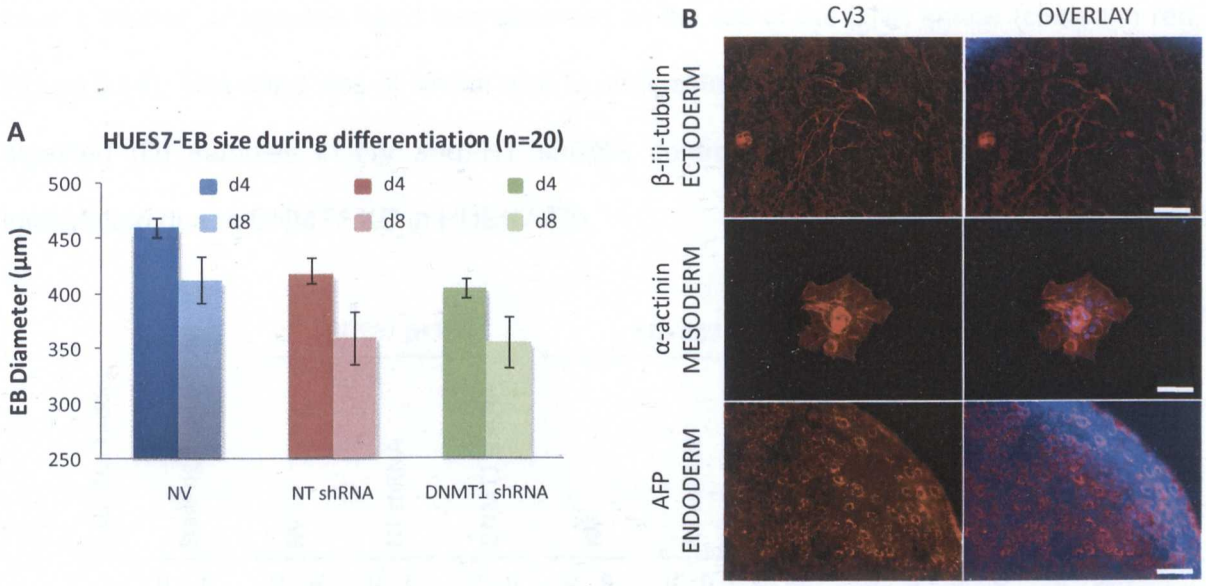

Figure 5.13– EB formation and differentiation of HUES7 DNMT1 KD cells into the three germ layers
A. Histogram representing the average diameter of EBs on day 4 and 8 during differentiation of HUES7 cells with no virus (NV), NT shRNA or shRNA859 against *DNMT1*. **B.** Differentiation of HUES7 cells carrying shRNA859 against DNMT1 into cell-types representative of the three germ layers; ectoderm, endoderm and mesoderm. Protein expression was captured using the Cy3 channel, while the overlay represents a merge of the DAPI (nuclear staining) and Cy3 channels. Scale bars represent 64µm.

5.2.5 DNA methylation analysis in cells with DNMT1 knock-down

HUES7 and HUES7-Fib carrying stable KD of *DNMT1* showed normal population doubling times, while pluripotent HUES7 cells maintained the ability to differentiate to the three embryonic germ layers. KD of *DNMT1* in differentiated HUES7-Fib cells affected progression of the cell cycle at S phase. In this section, the effects of *DNMT1* KD on DNA methylation were investigated.

5.2.5.1 Global methylation of genomic DNA

Global levels of DNA methylation were analysed using restriction digestion with the methylation specific enzyme McrBC (section 2.6.6; Spada *et al.* 2007). This enzyme can only recognise and cut methylated DNA (Sutherland *et al.* 1992; Gowher *et al.* 2000; Zhou *et al.* 2002). Undigested control samples (U), showed thick DNA bands at the top of agarose gels, while digested products (D) formed DNA smears (Figure 5.14). In HUES7 and EBs, DNMT1 KD did not affect global DNA methylation. However, in HUES7-Fib DNMT1 KD

cells, a thicker undigested band was observed at the top of the DNA smear (circled in red, Figure 5.14). This band was of similar size to undigested (U) DNA, and was absent from the digested (D) samples in NV and NT shRNA controls, indicating reduced global DNA methylation due to DNMT1 KD in HUES7-Fib.

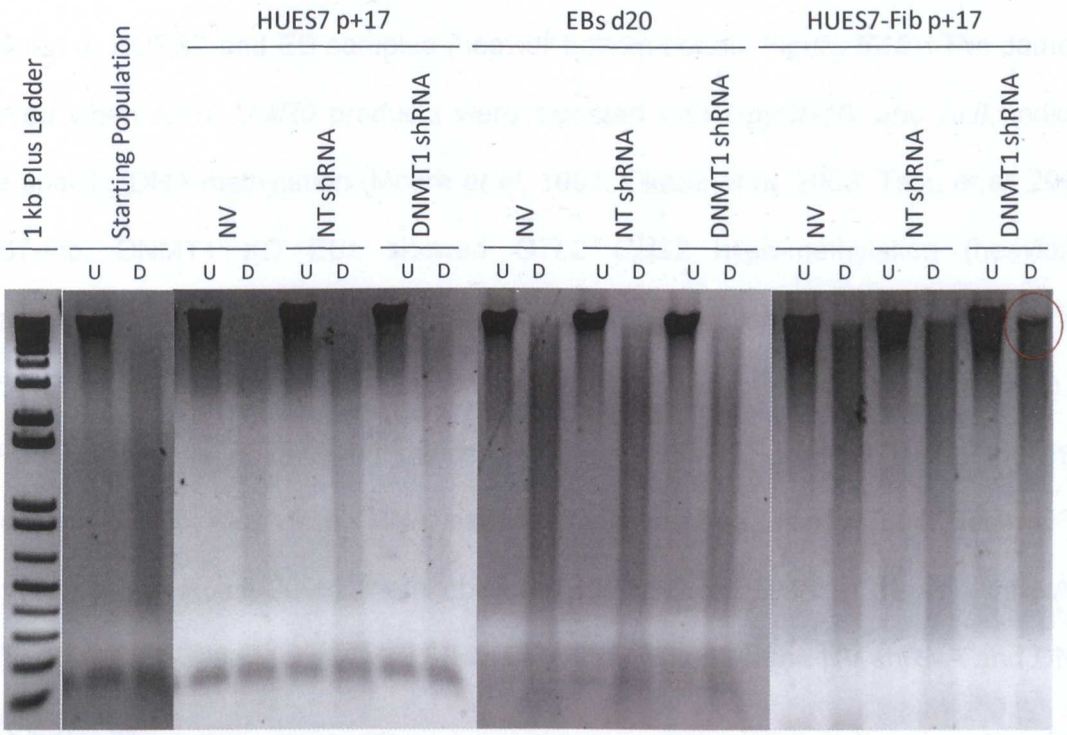

Figure 5.14- Genomic DNA digest with the methylation sensitive enzyme McrBC
Gel electrophoresis of genomic DNA following restriction digest with the enzyme McrBC, which specifically digests methylated DNA. HUES7, EBs and HUES7-Fib cells with a stable DNMT1 knock-down, as well as their respective no virus (NV) and NT shRNA controls, were used for the experiment and were run both undigested (U) and digested (D) with McrBC enzyme. The starting population represents HUES7 cells at passage p+0.

5.2.5.2 DNA methylation in imprinted genes

Genomic DNA digestion with McrBC showed a reduction in global DNA methylation of HUES7-Fib, but gave little information about the genes affected. Considering the role of DNMT1 in imprinting and genome stability (section 5.1.3), the methylation status of imprinted and tumour suppressor and genes were analysed more closely. Since a large number of tumour suppressor and imprinted genes have been identified in the human genome, this study investigated those found to be most unstable in ESC and cancer studies (Esteller and Herman 2002; Kim *et al.* 2007; Rugg-Gunn *et al.* 2007).

DNA methylation analysis of imprinted genes was performed with kind help from Dr. Kee-Pyo Kim, using combined bisulfite restriction analysis (COBRA). PCR products were digested with enzymes that could only cut at their recognition sites if DNA was methylated. Therefore, undigested DNA represented loss of DNA methylation (Figure 5.15). HUES7-Fib PCR products for *PEG10*, digested with the enzyme *BstUI*, showed different band patterns compared to HUES7 and EB samples (heavier bottom bands, Figure 5.15). The same was observed when *IGF2 DMR0* products were digested with *HpyCH4IV* and *AciI*, indicating tissue specific DNA methylation (Moore *et al.* 1997; Okabe *et al.* 2003; Tsou *et al.* 2003) in HUES7-Fib. DNMT1 KD EBs showed *GTL2 CpG2* hypo-methylation (heavier top undigested band with HpyCH4IV digest). Reduced methylation was also observed in the HUES7-Fib DNMT1 KD sample for *GNAS1 XLas* (heavier top undigested band), and *NESP55 DMR* (loss of digested bands). Off-target effects, possibly owing to lentiviral transduction or activation of the RNAi pathway (Jackson and Linsley 2004; Fedorov *et al.* 2006; Morris and Rossi 2006), were observed for *NESP55 DMR* in the NT shRNA and DNMT1 KD HUES7, and for *KvDMR1* (HpyCH4IV digestion) in the NV shRNA and DNMT1 KD HUES7-Fib.

COBRA repeated at passage 30 PTD showed similar results to analysis at passage 17 PTD (data not shown and Figure 5.15). Bisulfite sequencing analysis confirmed the DNMT1 KD-induced hypo-methylation observed by COBRA in *GTL2 CpG2*, *NESP55 DMR* and *GNAS XLas* (data not shown).

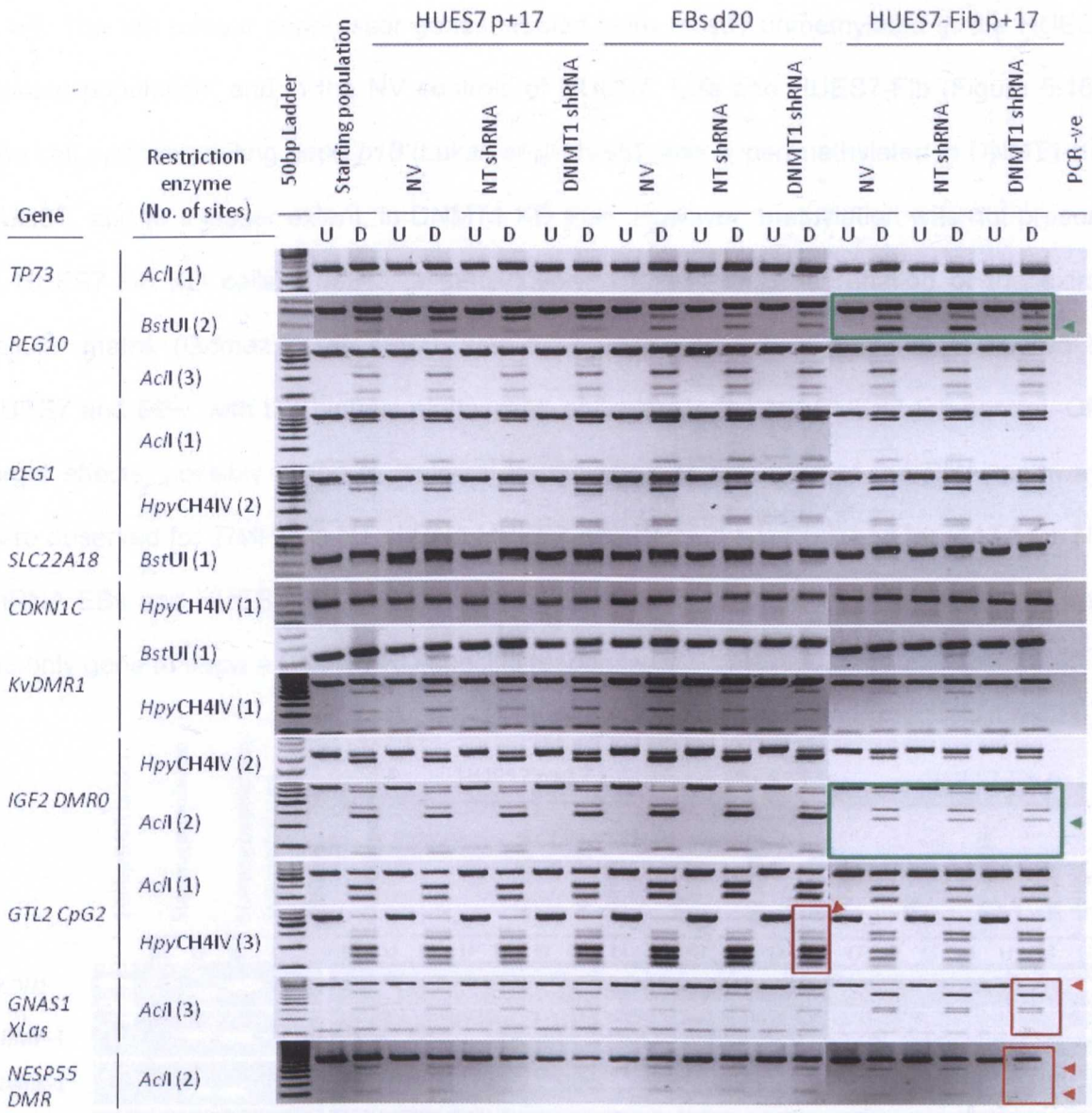

Figure 5.15- COBRA analysis of imprinted genes in cells with DNMT1 knock-down
Gel electrophoresis of PCR products from COBRA. HUES7, EBs and HUES7-Fib cells with a stable DNMT1 knock-down, as well as their respective no virus (NV) and NT shRNA controls, were used for this experiment and were run both undigested (U) and digested (D) with appropriate methylation-dependent restriction enzymes. The starting population represents HUES7 cells at passage p+0. Red boxes/ arrows= samples/bands showing decreased DNA methylation, green boxes/ arrows= samples/bands showing tissue-specific DNA methylation

5.2.5.3 DNA methylation in tumour suppressor genes

Methylation specific PCR (MSP) analysis was performed in ten tumour suppressor genes, with kind help from Dr. Kee-Pyo Kim. In this type of PCR, gene specific primers were designed to detect bisulfite-converted methylated (M) or unmethylated (U) DNA (Table 2.9). *In vitro* methylated HUES7 were included in the investigation, to confirm primer specificity. Products from this sample were only detected with the methylated (M) primer set (Figure

5.16). The ten tumour suppressor genes studied were mostly unmethylated in the HUES7 starting population, and in the NV controls of HUES7, EBs and HUES7-Fib (Figure 5.16). The cell cycle regulating gene *p16* (Lukas *et al.* 1995), was hyper-methylated in DNMT1 KD HUES7, and to a lesser extent, in DNMT1 KD EBs. However, methylation was not present in HUES7-Fib KD cells. *TIMP-3*, a gene involved in inhibiting degradation of the extra-cellular matrix (Gomez *et al.* 1997), was hyper-methylated in HUES7-Fib compared to HUES7 and EBs, with the highest methylation observed in the NV HUES7-Fib control. Off-target effects, possibly owing to lentiviral transduction or activation of the RNAi pathway, were observed for *TIMP-3* in NT shRNA HUES7 and DNMT1 KD EBs, and for *GATA4* in NT shRNA EBs and HUES7-Fib. Overall, very little instability was detected by MSP. *p16* was the only gene to show a DNMT1 KD-specific response.

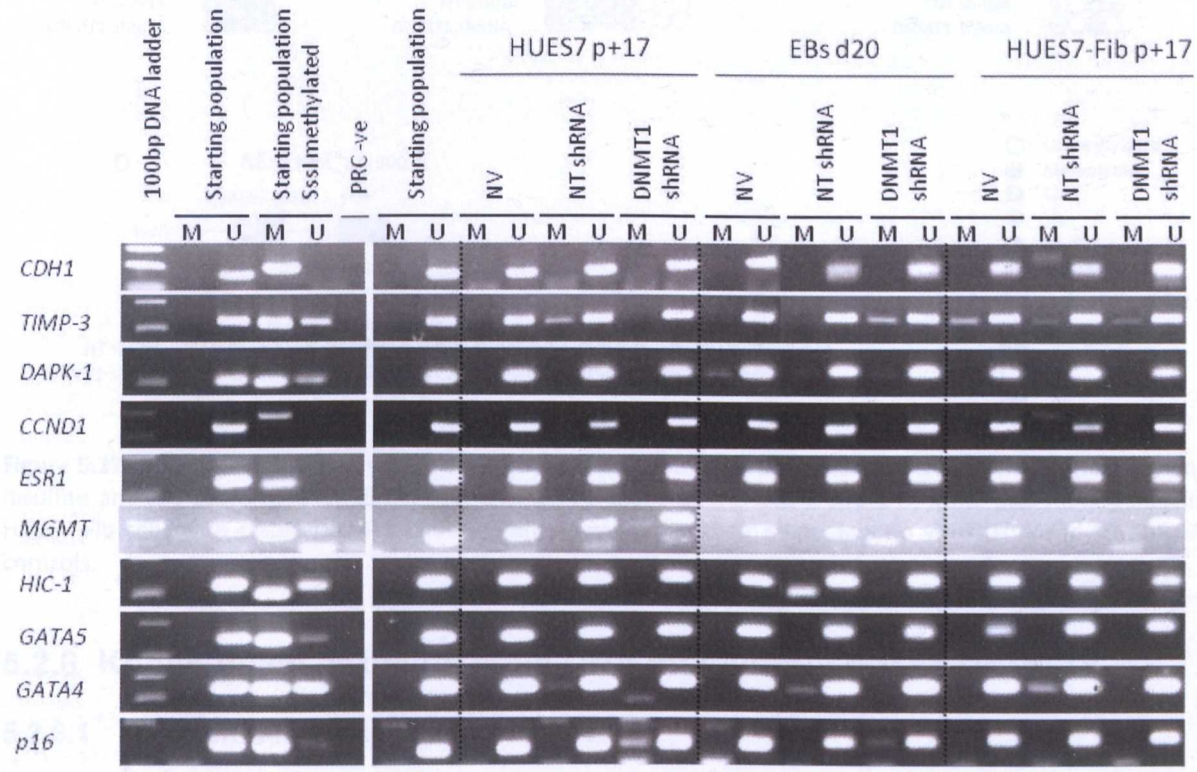

Figure 5.16- MSP analysis of tumour suppressor genes in cells with DNMT1 knock-down
Gel electrophoresis of PCR products from MSP using primers specific for methylated (M) or unmethylated (U) tumour suppressor genes. HUES7, EBs and HUES7-Fib cells with a stable DNMT1 knock-down, as well as their respective no virus (NV) and NT shRNA controls, were used for the experiment. The starting population represents HUES7 cells at passage p+0. As a further control, HUES7 at p+0 were *in vitro* methylated *via* treatment with the SssI methyltransferase and were included in the analysis to conform the specificity of U and M primer sets.

5.2.5.4 DNA methylation in pluripotency genes following DNMT1 knock-down

Bisulfite sequencing analysis was performed in differentiated HUES7-Fib, to determine whether DNMT1 KD had affected DNA methylation in the pluripotency-associated genes *OCT4*, *NANOG*, *SOX2* and *REX1* (section 4.2.2.2). However, bisulfite sequencing showed no differences in DNA methylation between the DNMT1 KD HUES7-Fib and control samples (Figure 5.17). The possibility that DNMT1 could confer an advantage to endogenous gene reactivation when the cells were found in a "reprogramming environment", i.e. upon transduction of with lentiviruses over-expressing the four iPS factors, still existed.

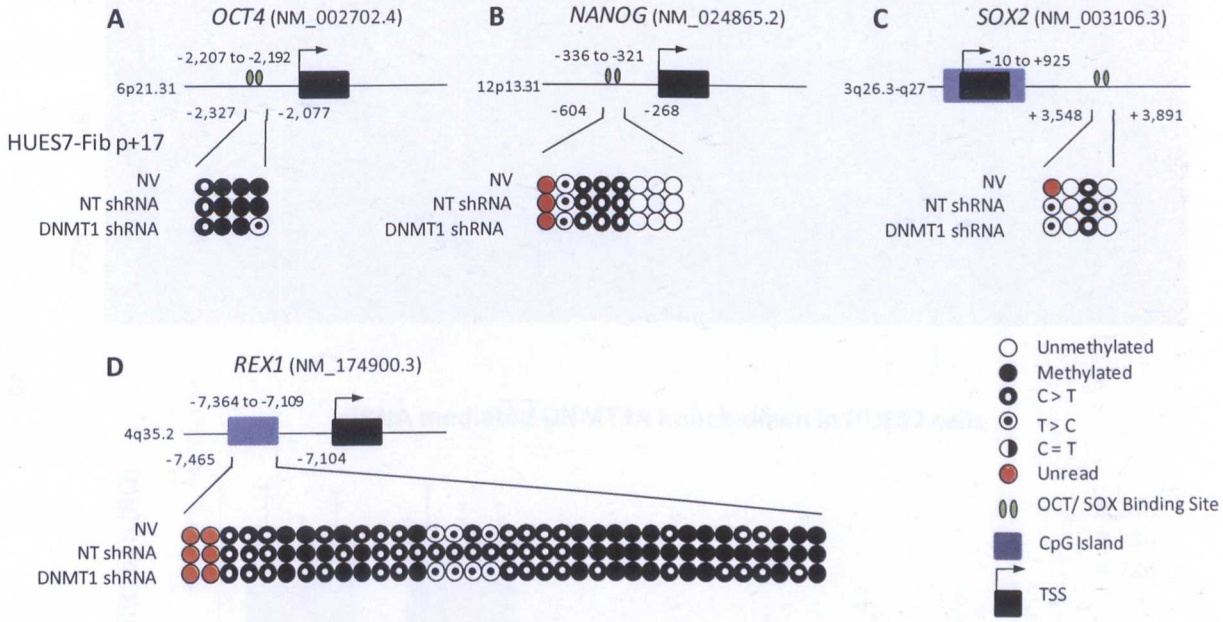

Figure 5.17- Bisulfite sequencing within endogenous iPSC genes in HUES7-Fib cells with DNMT1 knock-down
Bisulfite analysis performed by direct sequencing in regions of the *OCT4*, *NANOG*, *SOX2* and *REX1* genes in HUES7-Fib cells with stable DNMT1 knock-down, as well as in their respective no virus (NV) and NT shRNA controls.

5.2.6 Knock-down of the *de novo* DNA methyltransferase DNMT3A

5.2.6.1 Transient knock-down of DNMT3A

Since HUES7-Fib also expressed the *de novo* DNA methyltransferase, DNMT3A (Figure 5.3 and Figure 5.4), KD of this gene was performed as described in section 5.2.2 for *DNMT1*. A set of three commercially available siRNAs against human *DNMT3A* were tested for their ability to reduce gene expression (Figure 5.18). All siRNAs were had 100% complementarity

to endogenous mRNA and were located within the coding region (siRNA 868; exon 14, siRNA 869; exon 18 and siRNA 870; exon 23). siRNAs 868 and 870 enabled the highest knock-down for *DNMT3A* (81% KD, RQ= 0.19±0.015, p=0.00 and 89% KD, RQ= 0.11±0.012, p=0.00; Figure 5.18). No significant synergistic effect was observed in the presence of all three siRNAs, relative to siRNA 870 (p=0.48 at 24h, p= 0.00 at 48h and p=1.00 at 72h).

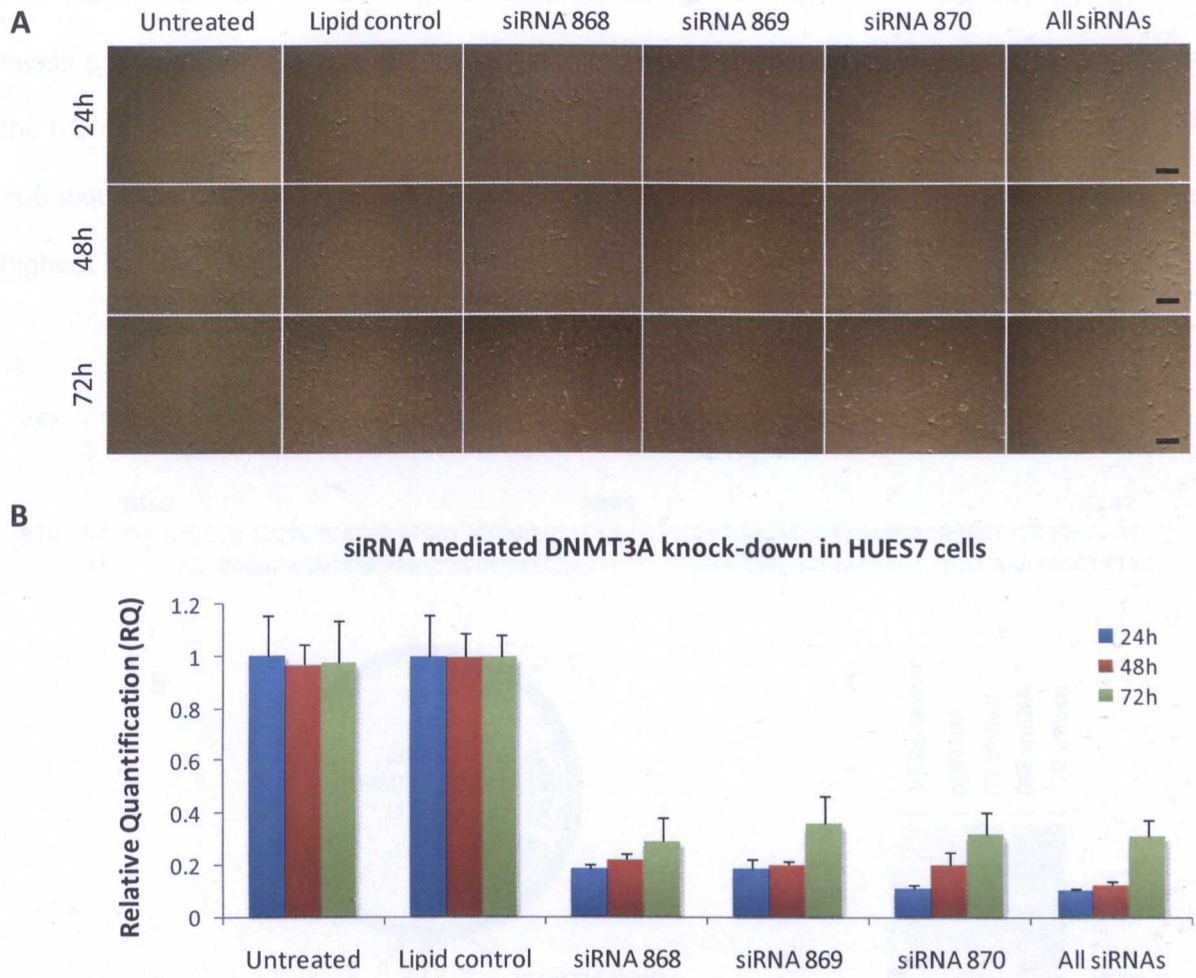

Figure 5.18- siRNA mediated knock-down of *DNMT3A* in HUES7
A. Bright field images and **B.** real-time PCR analysis of *DNMT3A* expression in HUES7 cells transfected with siRNAs against *DNMT3A* at 24, 48 and 72 hours post-transfection. Error bars represent standard error. Scale bars represent 100μm.

5.2.6.2 shRNA-mediated knock-down of DNMT3A

To enable stable *DNMT3A* KD, shRNAs were designed as described in section 5.2.2.2, based on the sequences of siRNAs 868 and 870 (Figure 5.19.A). Oligonucleotide

sequences were cloned into the lentiviral plasmid, pLVTHM (Figure 5.19.B), between its MluI and ClaI restriction sites. Successful cloning was confirmed by digest with the enzyme XbaI and by sequencing (Figure 5.19.C and data not shown). Both HUES7 and HUES7-Fib were transduced with lentivirus carrying shRNAs 868 and 870. Real-time PCR analysis was performed relative to the NT shRNA control, and showed that shRNA 868 caused the highest *DNMT3A* KD (65% KD in HUES7, RQ= 0.45±0.03, p=0.00 and 30% KD in HUES7-Fib, RQ= 0.70±0.02 p=0.34; Figure 5.20). Doubling the viral volume did not improve the levels of *DNMT3A* KD (data not shown). Even though there was no significant difference in the KD caused by shRNAs 868 and 870 in HUES7-Fib (p= 0.27), it was decided that shRNA 868 would be used in all subsequent experiments involving *DNMT3A* KD, as it caused the highest KD in HUES7 cells (p=0.03; Figure 5.20).

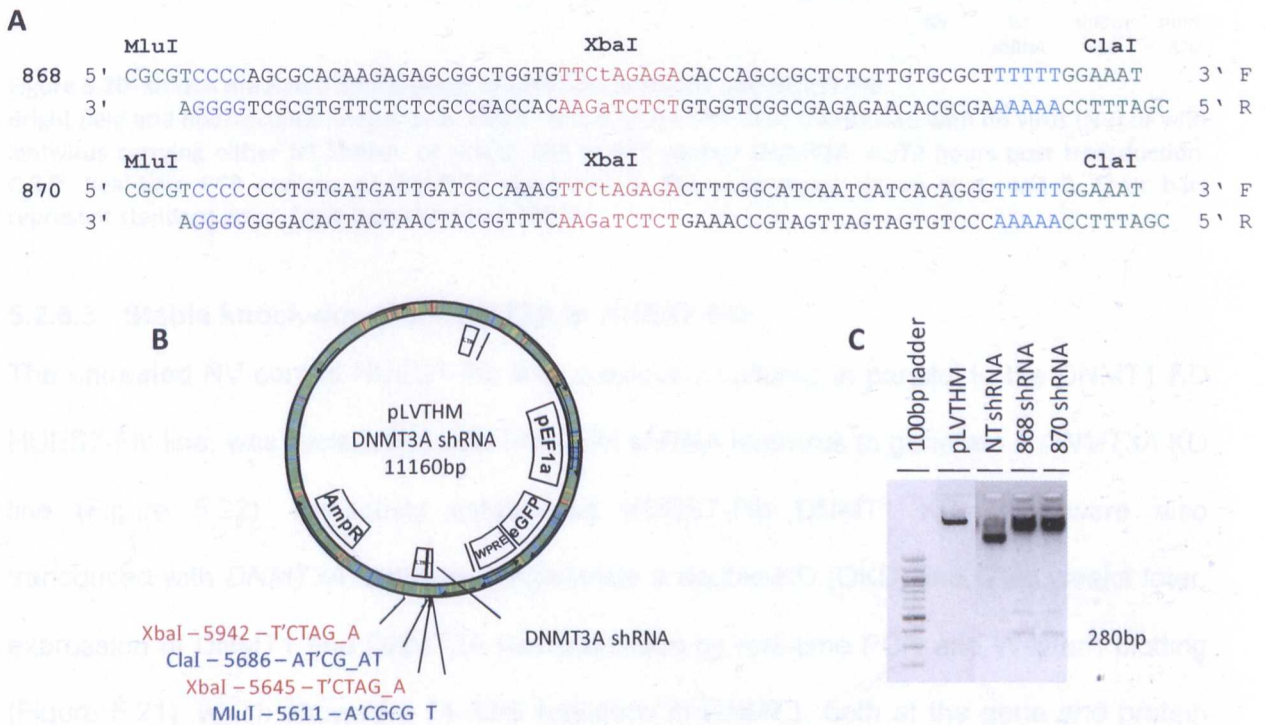

Figure 5.19- Cloning *DNMT3A* shRNAs into lentiviral transfer plasmids

A. shRNA sequences specific to human *DNMT3A*. Green= restriction enzyme overhangs, black= siRNA sequences, red= loop sequence, purple and light blue= hairpin forming sequences **B.** Map of the lentiviral transfer plasmid pLVTHM after cloning *DNMT3A* shRNAs between its ClaI and MluI restriction sites. Cloning the *DNMT3A* shRNAs into the plasmid created a second XbaI restriction site. **C.** Gel electrophoresis of plasmid DNA following a restriction digest with the enzyme XbaI, used to positively identify clones with the *DNMT3A* shRNA inserts.

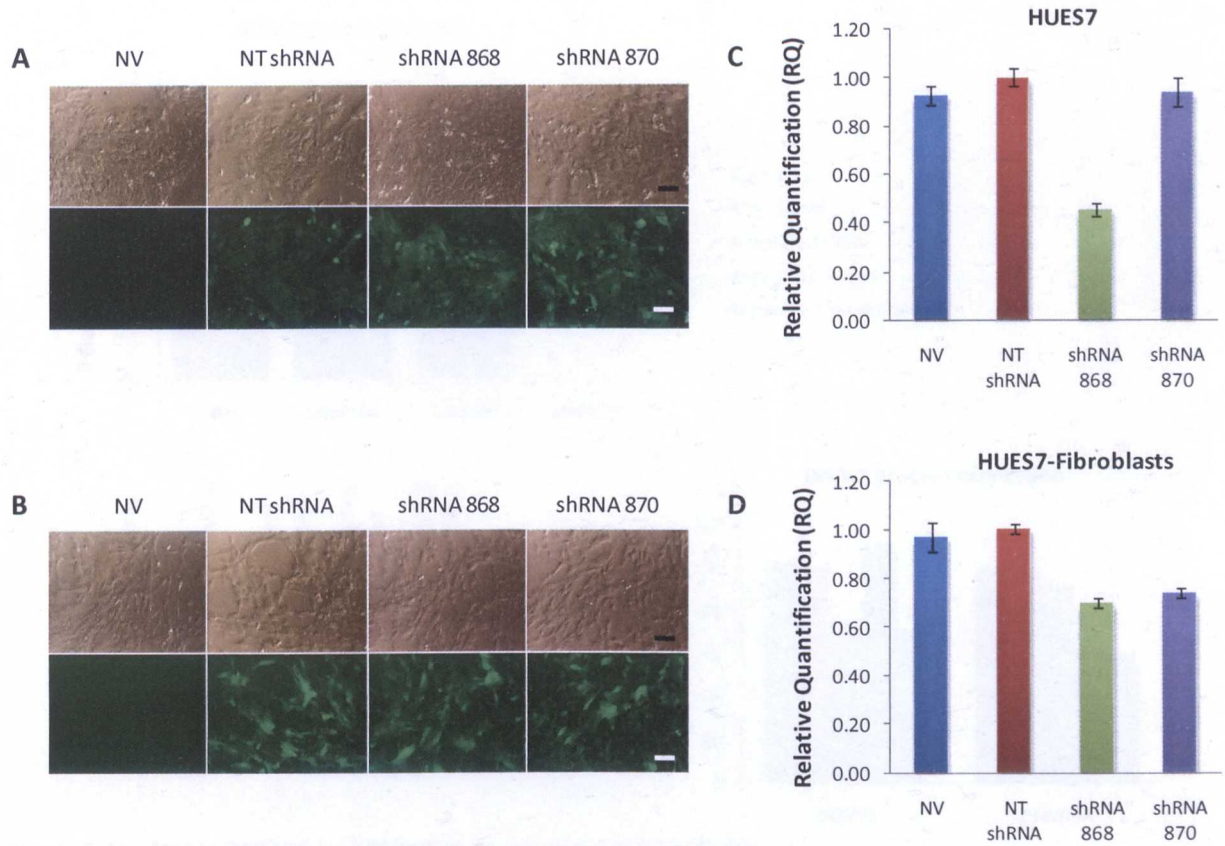

Figure 5.20- shRNA mediated knock-down of *DNMT3A* in HUES7 and HUES7-Fib
Bright field and fluorescence images of **A.** HUES7 and **B.** HUES7-Fib cells transduced with no virus (NV) or with lentivirus carrying either NT shRNA, or shRNA 868 or 870 against *DNMT3A*, at 72 hours post transduction. **C.&D.** Real-time PCR analysis of *DNMT3A* expression in the populations shown in A. and B. Error bars represent standard error. Scale bars represent 100µm.

5.2.6.3 Stable knock-down of DNMT3A in HUES7-Fib

The untreated NV control HUES7-Fib line, previously cultured in parallel to the DNMT1 KD HUES7-Fib line, was transduced with *DNMT3A* shRNA lentivirus to generate a *DNMT3A* KD line (Figure 5.22). Previously established HUES7-Fib DNMT1 KD cells were also transduced with *DNMT3A* lentivirus, to generate a double-KD (DKD) line. Two weeks later, expression of DNMT1 and DNMT3A was assessed by real-time PCR and Western blotting (Figure 5.21), which showed a 24-32% reduction in DNMT1, both at the gene and protein levels, and a 22-40% reduction in DNMT3A gene and protein levels. No up-regulation of the *de novo* DNMTs, DNMT3B and DNMT3L, was observed in response to DNMT1 and DNMT3A KD, but the DKD line showed a 40% reduction in DNMT3B expression (RQ= 0.60±0.008; Figure 5.21.A).

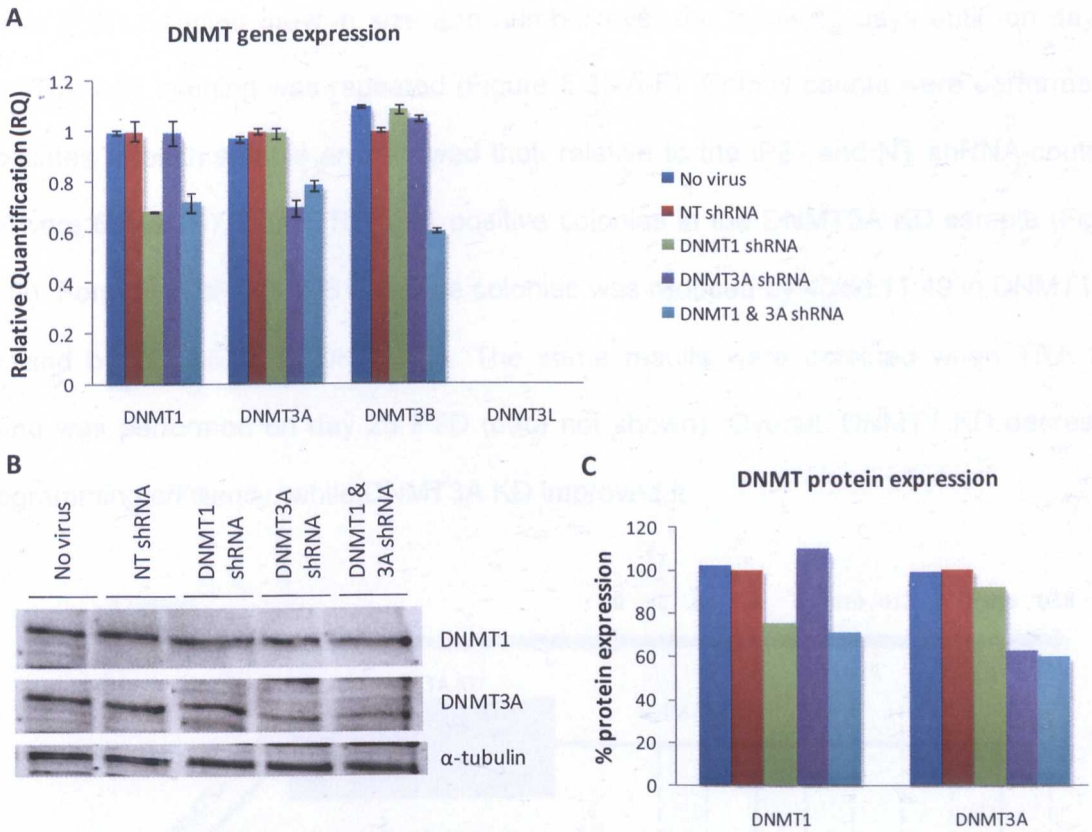

Figure 5.21– Stable DNMT1 and DNMT3A knock-down in HUES7-Fib
A. Real-time PCR and **B.&C.** Western blot analysis of DNMT expression in HUES7-Fib cells carrying knock-down of DNMT1 and/or DNMT3A, as well as in the control HUES7-Fib lines NV and NT shRNA. Protein and gene expression were quantified relative to the NT shRNA control sample.

5.2.7 Generation of iPSCs from hESC-derived fibroblasts carrying DNMT1 and DNMT3A knock-down

DNMT1 and DNMT3A KD HUES7-Fib were induced to form iPSCs by lentiviral transduction with human *OCT4*, *NANOG*, *SOX2* and *LIN28* (section 2.2.7). Reprogramming was allowed to occur for 18 days PTD, with pellets from each sample being collected at 2-day intervals, as outlined in Figure 5.22. Generation of lentiviral particles was performed as described in section 4.2.5.

HUES7-Fib that were transduced with the four iPS factors started showing morphological changes on day 8 PTD, when incompletely reprogrammed colonies begun to emerge (section 4.2.5.1). Live TRA-1-81 staining performed on day 11 PTD allowed detection of potential iPSC colonies in all samples, apart from the DNMT1 KD sample (data not shown).

Putative iPSC colonies grew in size and number over the following days until, on day 18 PTD, TRA-1-81 staining was repeated (Figure 5.23.A-F). Colony counts were performed in 4 replicates of each sample and showed that, relative to the iPS- and NT shRNA-controls, there were 82%±8.97 more TRA-1-81 positive colonies in the DNMT3A KD sample (Figure 5.23.G). Formation of TRA-1-81 positive colonies was reduced by 40%±11.49 in DNMT1 KD cells, and by 22%±5.05 in DKD cells. The same results were obtained when TRA-1-81 staining was performed on day 25 PTD (data not shown). Overall, DNMT1 KD decreased reprogramming efficiency, while DNMT3A KD improved it.

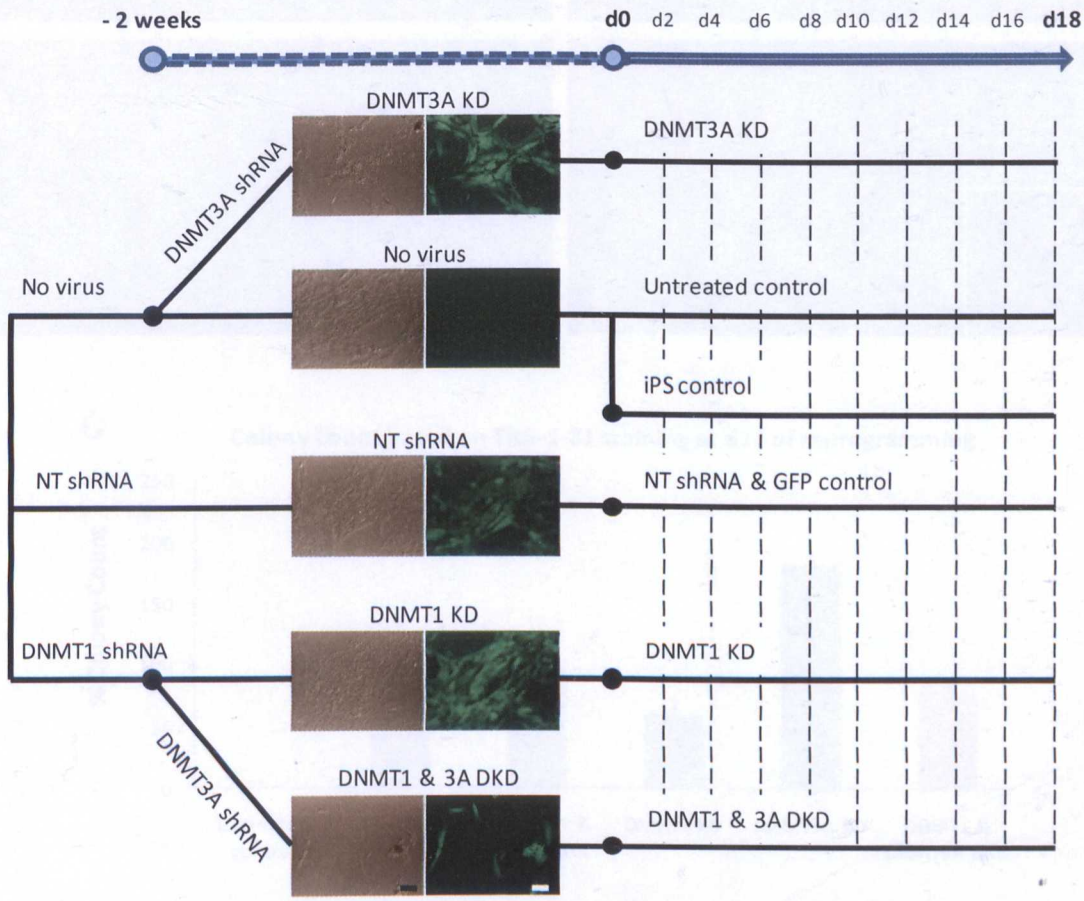

Figure 5.22– Experimental plan for iPSC generation from HUES7-Fib with DNMT1 and DNMT3A knock-down
Previously established HUES7-Fib lines with DNMT1 knock-down were transduced with lentiviral particles expressing shRNAs against *DNMT3A*, to generate a double knock-down fibroblast line. No virus (NV) HUES7-Fib cells were also transduced with the same lentiviral particles. All lines were cultured in parallel for 2 weeks and were then transduced with the four iPS factors (d0). During the reprogramming process, cell pellets from each sample were collected at two day intervals for the following 18 days, in order to be used for molecular analysis. KD = knock-down, DKD = double knock-down. Black circles represent lentiviral transduction. Scale bars represent 100μm.

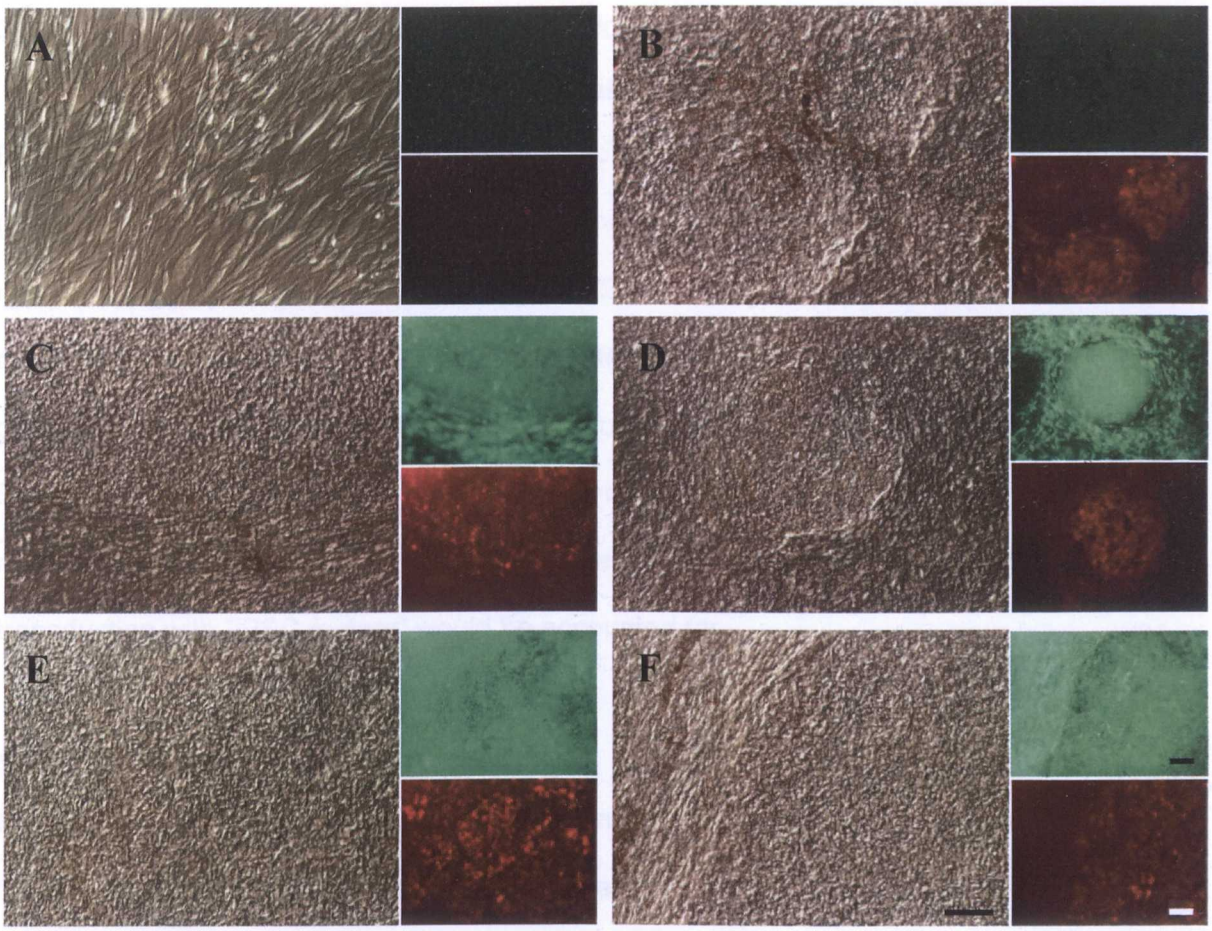

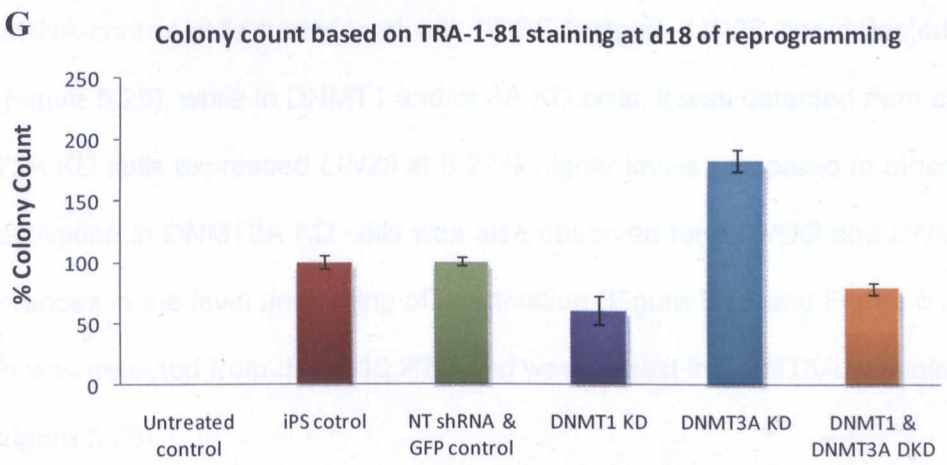

Figure 5.23– Live TRA-1-81 staining on day 18 during iPSC formation
Bright field, GFP fluorescence (green) and Cy3 fluorescence (red) images of **A.** untreated, **B.** iPS and **C.** NT shRNA control samples, as well as **D.** DNMT1, **E.** DNMT3A and **F.** double knock-down samples, on day 18 of reprogramming. Cy3 fluorescence represents live cell staining with a phycoerythrin (PE) conjugated anti-TRA-1-81 antibody. **G.** Histogram representing the % colony counts in each sample, on day 18 of reprogramming. Colonies were counted based on TRA-1-81 expression. Results were normalised to the NT shRNA control sample. NT = non-targeting, KD = knock-down, DKD = double knock-down. Scale bars represent 100µm.

5.2.8 Effect of DNMT1 and DNMT3A knock-down on the reactivation of endogenous pluripotency genes during iPSC generation

RT-PCR analysis was performed using samples collected as described in section 5.2.7. (Figure 5.22). cDNA synthesis was carried out as described in section 4.2.5.2. Primers specific to endogenous *OCT4*, *NANOG*, *SOX2* and *LIN28* (Figure 4.4), and the human *de novo* DNMTs, *DNMT3A*, *3B* and *3L* (Table 2.6), were used to detect re-activation of these genes during iPSC generation. Any expression detected in the untreated control (Figure 5.22) during quantification of gene expression by 2D densitometry, was subtracted from the respective time-point collection of other samples, so that only changes brought about due to transduction with "iPSC factors" would be accounted for.

5.2.8.1 LIN28, NANOG, DNMT3L and SOX2

LIN28 was expressed at residual levels in day 0 fibroblasts, i.e. prior to lentiviral transduction (Figure 5.25), and in days 14 and 18 PTD of the untreated control, when fibroblast cell number increased, depicting residual *LIN28* expression in fibroblasts. In iPS- and NT shRNA-control cells transduced with "iPSC factors", *LIN28* was detected from day 6-8 PTD (Figure 5.25), while in DNMT1 and/or 3A KD cells, it was detected from day 4 PTD, but DNMT3A KD cells expressed *LIN28* at 8-27% higher levels compared to other samples. Earlier reactivation in DNMT3A KD cells was also observed for *NANOG* and *DNMT3L*, with some differences in the level and timing of reactivation (Figure 5.26 and Figure 5.27). *SOX2* expression was detected from day 8-10 PTD and was highest in DNMT3A KD cells from day 10 PTD (Figure 5.28).

5.2.8.2 OCT4, DNMT3B and DNMT3A

PCR products for *OCT4*, *DNMT3B* and *DNMT3A* were observed in all samples analysed. This was expected for *DNMT3A* (Figure 5.3 and Figure 5.4), while for *DNMT3B*, PCR products in day 0 samples and early reprogramming were accounted for by residual *DNMT3B* expression in fibroblasts (Figure 5.24). As mentioned before, to quantify gene

expression changes brought about due to transduction with "iPSC factors", any expression detected in the untreated control was subtracted from the respective time-point collection of other samples. Increased endogenous *OCT4* expression was detected from day 6-10 PTD. In DNMT3A KD cells, *OCT4* showed delayed onset (day 12), but was expressed at 15-40% higher levels compared to other samples by day 18 PTD, (Figure 5.29), while *DNMT3B* was reactivated from day 8-14 PTD, and was expressed at 30-40% higher levels in DNMT3A KD cells by day 18 PTD (Figure 5.30). *DNMT3A* expression showed an overall 30-60% increase during iPSC formation (Figure 5.31). A 12-37% KD was observed in DNMT3A KD cells, on days 0-10 PTD, and in the double knock-down sample, especially on days 2-6 PTD. By day 18 PTD, *DNMT3A* was expressed at 15-50% higher levels in DNMT3A KD cells, perhaps owing to the increased formation of TRA-1-81 positive colonies, which were likely to express *DNMT3A* at higher levels than non-reprogrammed cells (Figure 5.31; Stadtfeld *et al.* 2008b).

Overall, RT-PCR analysis enabled earlier detection (by 2-4 days) of the pluripotency-associated factors *NANOG*, *LIN28* and *DNMT3L* during reprogramming of HUES7-Fib with DNMT3A KD (Figure 5.26, Figure 5.25 and Figure 5.27). *OCT4*, *SOX2*, *DNMT3B* and *DNMT3A* were not detected at earlier time-points in this sample but did show the highest expression levels by day 18 PTD (Figure 5.28-Figure 5.31), possibly owing to the increased formation of iPSC colonies (Figure 5.23).

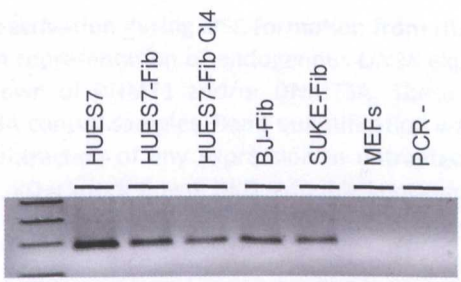

Figure 5.24– RT-PCR analysis of *DNMT3B* expression in fibroblast lines
Gel electrophoresis following RT-PCR analysis with primers specific to human *DNMT3B*, in the fibroblast lines HUES7-Fib, HUES7-Fib Cl4, BJ-Fib, SUKE-Fib and MEFs, and in the hESC line HUES7.

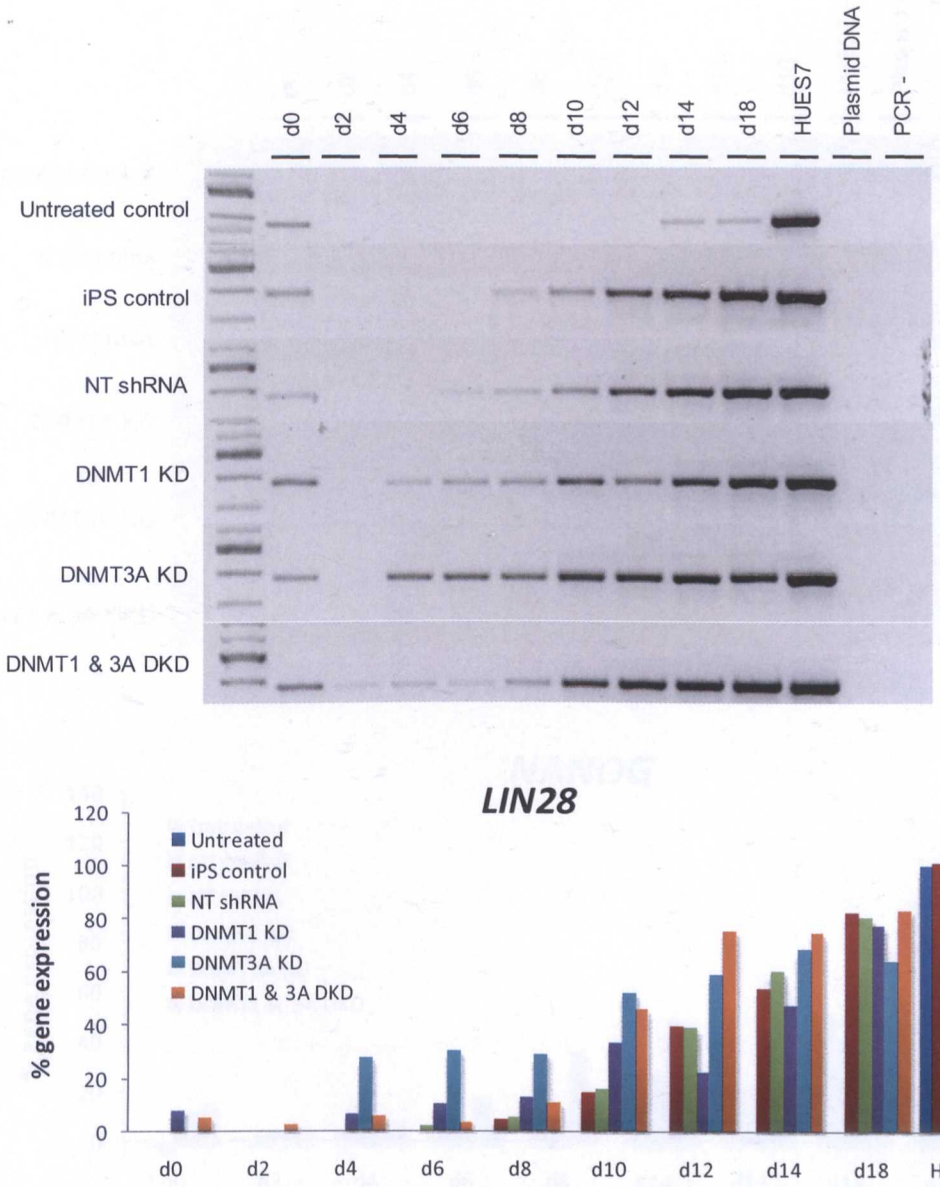

Figure 5.25– Endogenous *LIN28* reactivation during iPSC formation from HUES7-Fib with DNMT1 & 3A KD
Gel electrophoresis and histogram representation of endogenous *LIN28* expression during reprogramming of HUES7-Fib cells carrying knock-down of DNMT1 and/or DNMT3A. These samples were reprogrammed in parallel to untreated and NT shRNA control samples. Band quantification was performed by 2D densitometry, relative to the HUES7 sample. Subtraction of any expression in untreated control was performed prior to quantification. NT = non-targeting, KD = knock-down, DKD = double knock-down

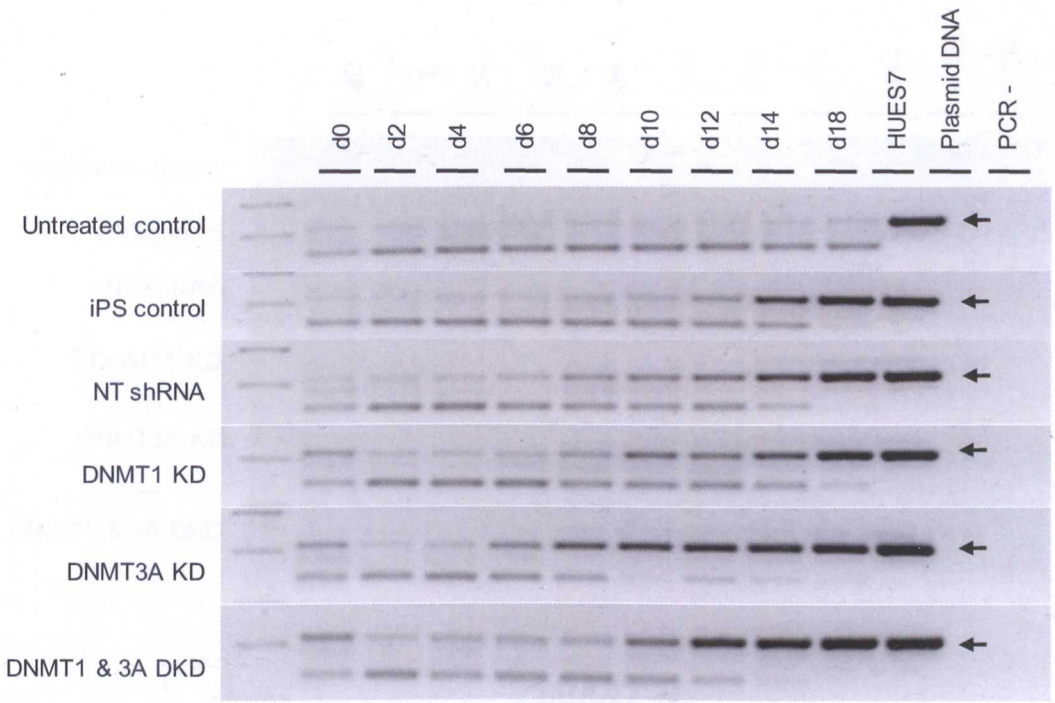

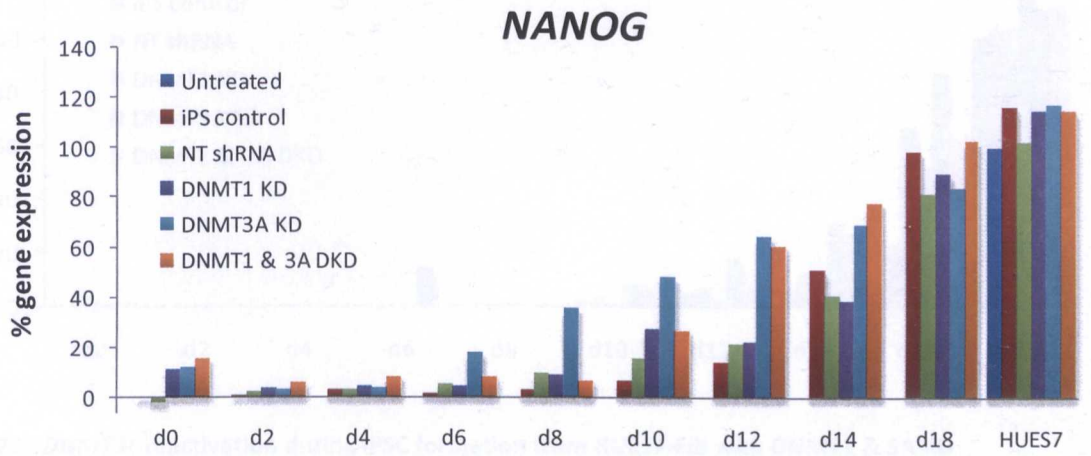

Figure 5.26– Endogenous *NANOG* reactivation during iPSC formation from HUES7-Fib with DNMT1 & 3A KD
Gel electrophoresis and histogram representation of endogenous *NANOG* expression during reprogramming of HUES7-Fib cells carrying knock-down of DNMT1 and/or DNMT3A. These samples were reprogrammed in parallel to untreated and NT shRNA control samples. Black arrows represent PCR products of the expected size. Band quantification was performed by 2D densitometry, relative to the HUES7 sample. Subtraction of any expression in untreated control was performed prior to quantification. NT = non-targeting, KD = knock-down, DKD = double knock-down

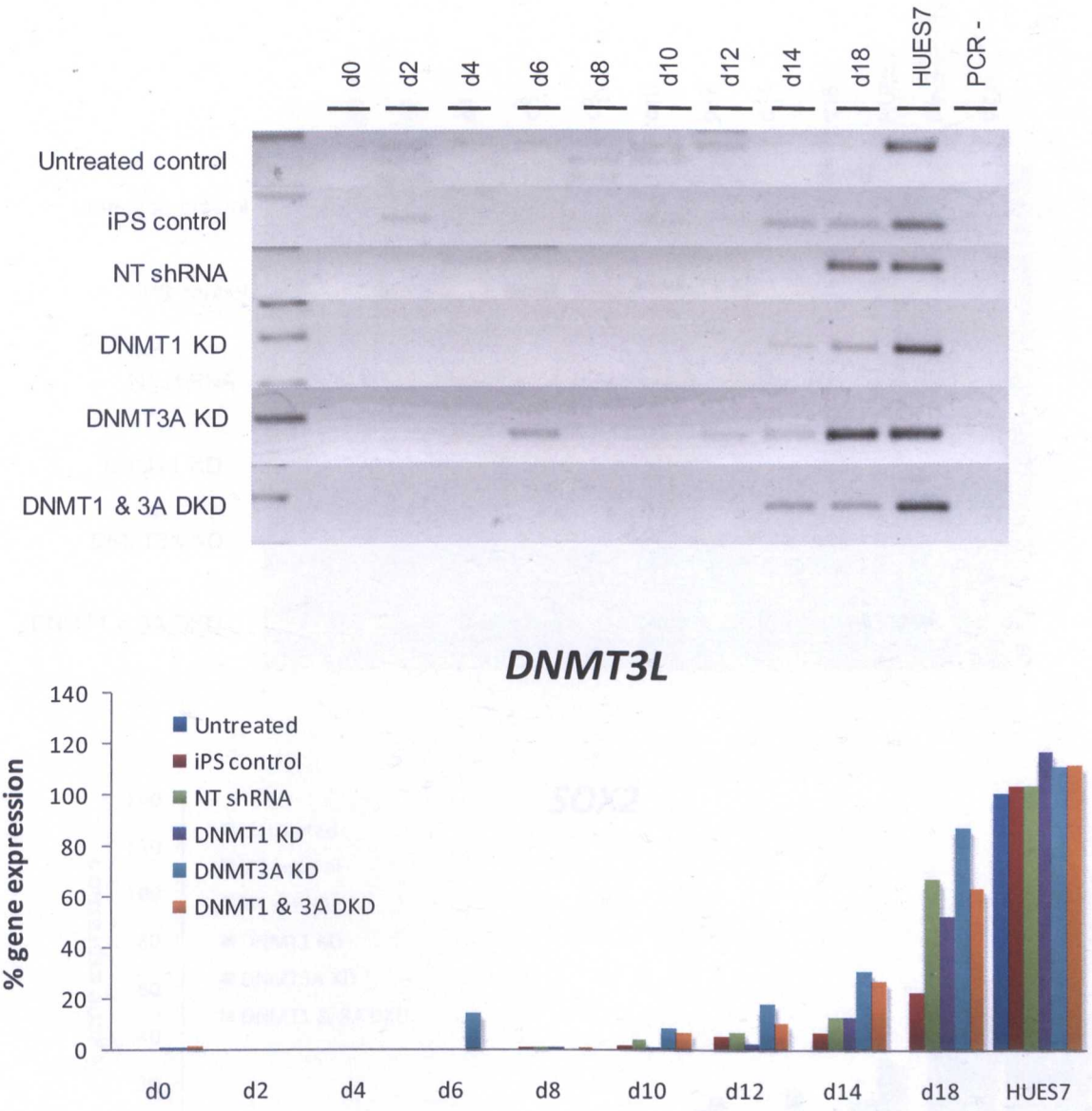

Figure 5.27– *DNMT3L* reactivation during iPSC formation from HUES7-Fib with DNMT1 & 3A KD
Gel electrophoresis and histogram representation of *DNMT3L* expression during reprogramming of HUES7-Fib cells carrying knock-down of DNMT1 and/or DNMT3A. These samples were reprogrammed in parallel to untreated and NT shRNA control samples. Band quantification was performed by 2D densitometry, relative to the HUES7 sample. Subtraction of any expression in untreated control was performed prior to quantification. NT = non-targeting, KD = knock-down, DKD = double knock-down

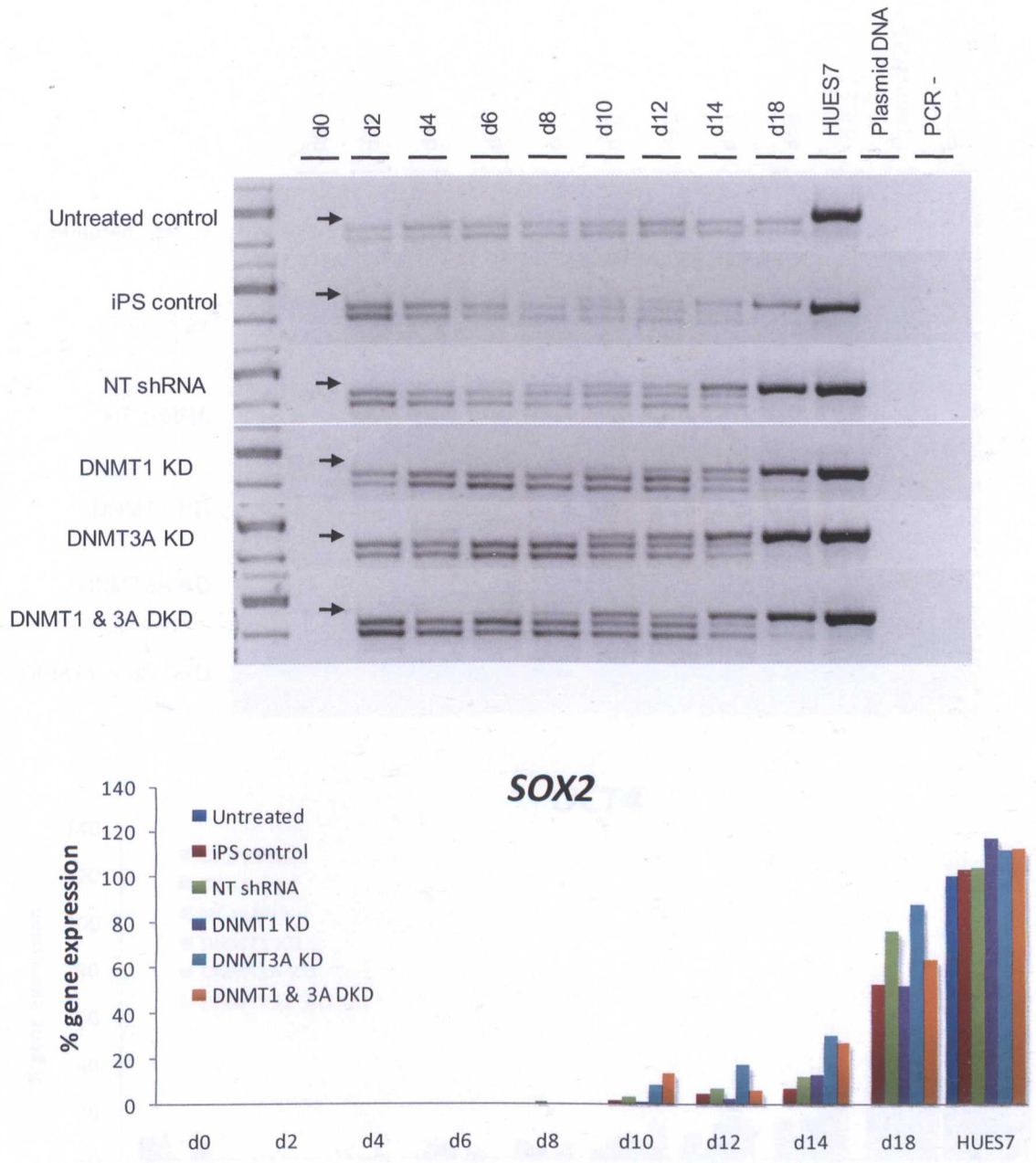

Figure 5.28– Endogenous *SOX2* reactivation during iPSC formation from HUES7-Fib with DNMT1 & 3A KD
Gel electrophoresis and histogram representation of endogenous *SOX2* expression during reprogramming of HUES7-Fib cells carrying knock-down of DNMT1 and/or DNMT3A. These samples were reprogrammed in parallel to untreated and NT shRNA control samples. Black arrows represent PCR products of the expected size. Band quantification was performed by 2D densitometry, relative to the HUES7 sample. Subtraction of any expression in untreated control was performed prior to quantification. NT = non-targeting, KD = knock-down, DKD = double knock-down

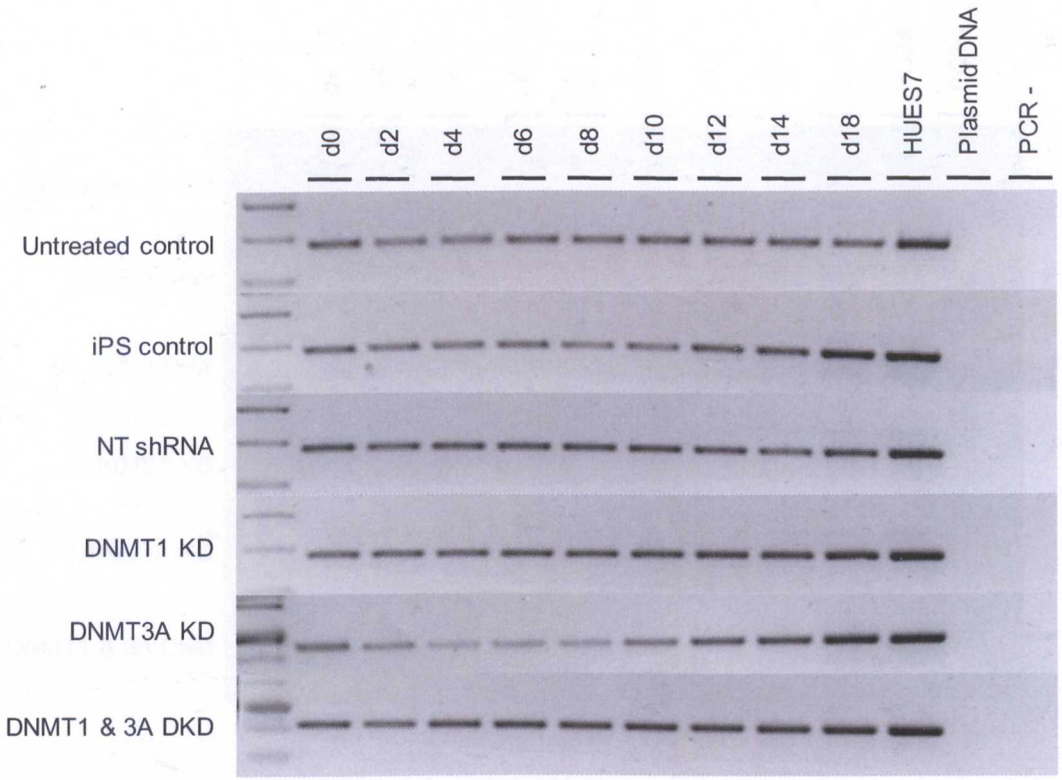

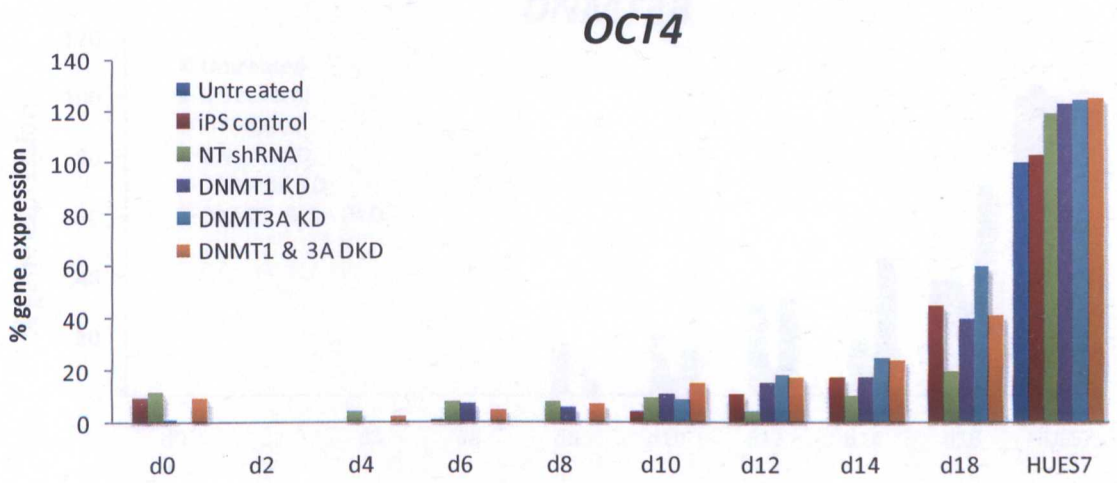

Figure 5.29– Endogenous *OCT4* reactivation during iPSC formation from HUES7-Fib with DNMT1 & 3A KD
Gel electrophoresis and histogram representation of endogenous *OCT4* expression during reprogramming of HUES7-Fib cells carrying knock-down of DNMT1 and/or DNMT3A. These samples were reprogrammed in parallel to untreated and NT shRNA control samples. Band quantification was performed by 2D densitometry, relative to the HUES7 sample. Subtraction of any expression in untreated control was performed prior to quantification. NT = non-targeting, KD = knock-down, DKD = double knock-down

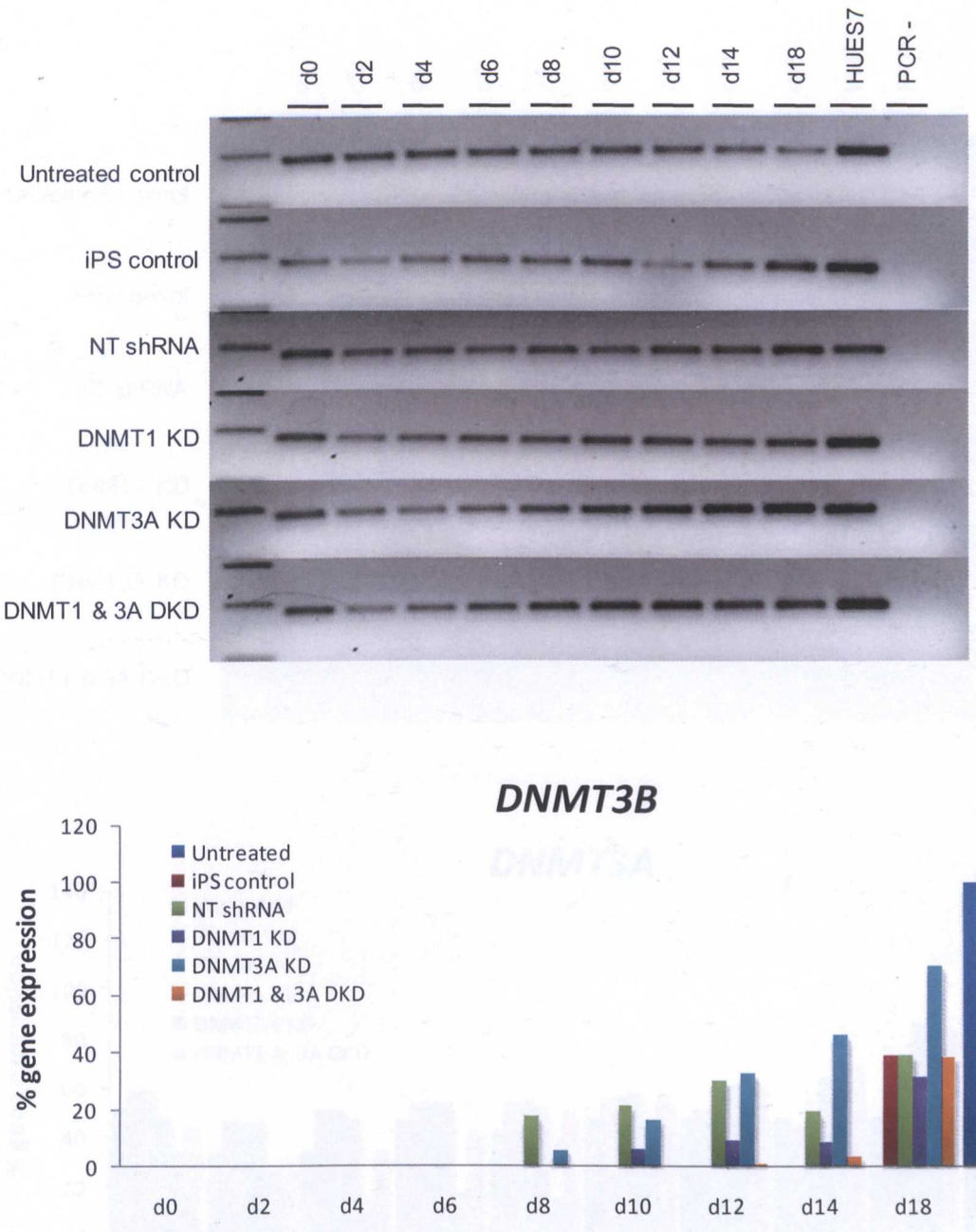

Figure 5.30–DNMT3B reactivation during iPSC formation from HUES7-Fib with DNMT1 & 3A KD
Gel electrophoresis and histogram representation of *DNMT3B* expression during reprogramming of HUES7-Fib cells carrying knock-down of DNMT1 and/or DNMT3A. These samples were reprogrammed in parallel to untreated and NT shRNA control samples. Band quantification was performed by 2D densitometry, relative to the HUES7 sample. Subtraction of any expression in untreated control was performed prior to quantification. NT = non-targeting, KD = knock-down, DKD = double knock-down

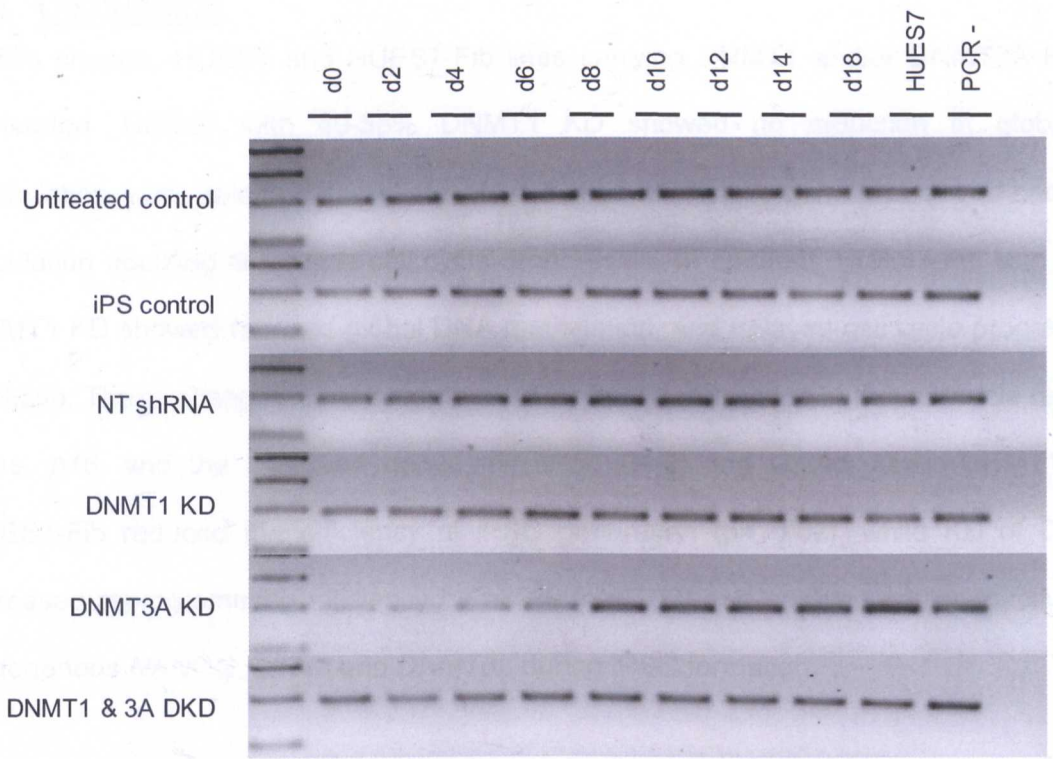

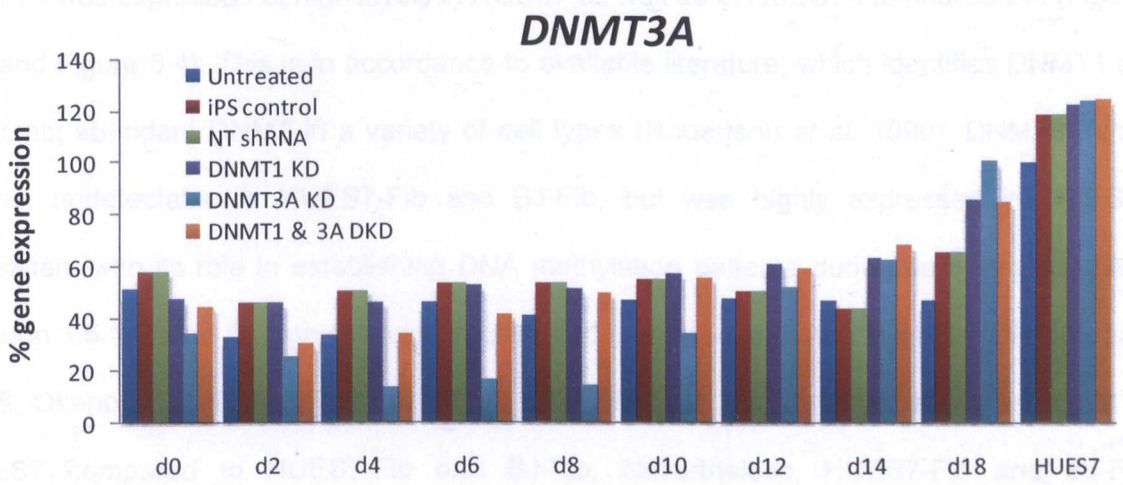

Figure 5.31– *DNMT3A* reactivation during iPSC formation from HUES7-Fib with DNMT1 & 3A KD
Gel electrophoresis and histogram representation of *DNMT3A* expression during reprogramming of HUES7-Fib cells carrying knock-down of DNMT1 and/or DNMT3A. These samples were reprogrammed in parallel to untreated and NT shRNA control samples. Band quantification was performed by 2D densitometry, relative to the HUES7 sample. NT = non-targeting, KD = knock-down, DKD = double knock-down

5.3 DISCUSSION

In this chapter, HUES7 and HUES7-Fib lines carrying DNMT1 and/or DNMT3A KD were generated. HUES7 with 40-55% DNMT1 KD showed no reduction in global DNA methylation, were able to differentiate into the three embryonic germ layers, and had normal population doubling times and cell cycle progression. In contrast, HUES7-Fib with 35-40% DNMT1 KD showed reduced global DNA methylation, and delayed cell cycle progression at S phase. These changes were accompanied by hypo-methylation in the cell cycle regulating gene, *p16*, and the imprinted genes, *NESP55 DMR* and *GNAS XLas*. DNMT1 KD in HUES7-Fib reduced the efficiency of iPSC generation (p= 0.02), while KD of DNMT3A increased reprogramming efficiency by >80% (p= 0.02) and enabled earlier reactivation of endogenous *NANOG*, *LIN28* and *DNMT3L* during iPSC formation.

5.3.1 Expression of DNMTs in hESCs and hESCs-fibroblasts

DNMT1 was expressed at high levels in HUES7 as well as in HUES7-Fib and BJ-Fib (Figure 5.3 and Figure 5.4). This is in accordance to available literature, which identifies DNMT1 as the most abundant DNMT in a variety of cell types (Robertson *et al.* 1999). DNMT3B was almost undetectable in HUES7-Fib and BJ-Fib, but was highly expressed in HUES7, consistent with its role in establishing DNA methylation patterns during early development (section 1.5.1.3) and its high expression observed in human and mouse ESCs (Okano *et al.* 1998; Okano *et al.* 1999; Xie *et al.* 1999). DNMT3A was also detected at higher levels in HUES7 compared to HUES7-Fib and BJ-Fib. Nevertheless, HUES7-Fib and BJ-Fib expressed DNMT3A at higher levels than DNMT3B, in accordance to data supporting that DNMT3A was readily detected in human somatic tissues, while DNMT3B was almost undetectable (Robertson *et al.* 1999). Perhaps due to their more terminal differentiation state (Park *et al.* 2008c) the foetal fibroblasts, BJ, expressed DNMT3A at lower levels compared to the hESCs-derived fibroblasts, HUES7-Fib (Figure 5.3).

5.3.2 Knock-down of DNMT1 in HUES7 and HUES7-Fib cells

Stable *DNMT1* KD was achieved by shRNA-induced RNAi (sections 5.2.2.3 and 5.2.2.4). Real-time PCR analysis at 72 hours PTD, showed a 64% KD of *DNMT1* expression in HUES7 (Figure 5.7), while at later passages, KD was reduced to 40-55% (Figure 5.9 and Figure 5.11). In HUES7-Fib, DNMT1 KD was reduced even more dramatically between 72 hours PTD (81% KD, Figure 5.7) and later passages (35-40% KD, Figure 5.9 and Figure 5.11). Since lentivirally transduced cells remained brightly fluorescent at late passages (Figure 5.11), indicating that the virus was not silenced, it is likely that reduced DNMT1 KD was caused by the death of cells carrying the highest KD levels. This is consistent with data supporting that DNMT1 depletion can lead to increased cell death, and has a more severe effect on differentiated cells compared to pluripotent cells (Jackson-Grusby *et al.* 2001; Jung *et al.* 2007; Spada *et al.* 2007). Residual DNMT1 expression in HUES7-Fib with DNMT1 KD could explain why these cells remained proliferatively active for several passages (section 5.2.2.4), in contrast to differentiated cells carrying knock-out of DNMT1, which have been reported to reach proliferative arrest resulting from complete loss of DNMT1 expression (Brown and Robertson 2007).

5.3.2.1 Differentiation to the three embryonic germ layers

HUES7 cells carrying a stable 40-55% KD of DNMT1 were able to form EBs with similar morphology and size to wild-type cells (Figure 5.13.A) and differentiate into all three embryonic germ layers (Figure 5.13.B). This was in contrast to knock-out studies in mESCs which showed that elimination of DNMT1 resulted in reduced differentiation ability (Jackson *et al.* 2004). Normal differentiation in DNMT1 KD HUES7 could be due to differences in gene regulation between mouse and human ESCs (section 1.6) or complementation of DNMT1 activity by *de novo* DNMTs, which were highly expressed in hESCs (Figure 5.3 and Figure 5.4), and have been shown to co-operate with DNMT1 to maintain DNA methylation at the appropriate levels (section 1.5.2.3). Complementation of DNMT1 activity by *de novo*

methyltransferases in pluripotent cells could also account for the unaltered levels of global DNA methylation (Figure 5.14) and normal cell cycle progression (Figure 5.12) in DNMT1 KD HUES7 cells.

5.3.2.2 Cell cycle progression

DNMT1 KD HUES7-Fib had 12% more cells residing in S phase, compared to controls. DNMT1 enzyme localises to replication foci as cells enter S phase of the cell cycle (Leonhardt *et al.* 1992; Margot *et al.* 2001) in order to catalyse methylation of hemi-methylated DNA (Figure 1.9). Therefore, lack of DNMT1 in HUES7-Fib KD cells could explain their reluctance to progress past S phase of the cell cycle. This is in accordance to studies in human cancer cells, showing defects in cell-cycle check points following DNMT1 down-regulation (Brown and Robertson 2007).

5.3.3 DNA methylation analysis in cells with DNMT1 knock-down

HUES7-Fib DNMT1 KD showed reduced DNA methylation in the imprinted genes *NESP55 DMR* and *GNAS XLas* (Figure 5.15), and the tumour suppressor gene, *p16* (Figure 5.16). *NESP55* and *GNAS XLas* are encoded by the same gene (*GNAS1*) on chromosome 20q13 (Weinstein *et al.* 2001). However, they are oppositely imprinted and do not share a common sequence due to alternative splicing and use of alternative promoters (Hayward *et al.* 1998; Weiss *et al.* 2000; Bastepe *et al.* 2005). The two genes have been involved in endocrine tumour formation, fibrous bone dysplasia and hereditary osteodystrophy (Weinstein *et al.* 2004). In normal tissue, the G protein α sub-unit ($G_s\alpha$) encoded by *GNAS XLas* is involved in stimulating cAMP/ protein kinase A signalling, which inhibits fibroblast proliferation and collagen synthesis (Weinstein *et al.* 2001; Zhang *et al.* 2004). Unfortunately, these two imprinted genes did not carry informative (i.e. heterozygous) allele-specific single nucleotide polymorphisms (SNPs) in HUES7 cells (Kim *et al.* 2007), and thus investigation of a change in their allele-specific expression in response to DNMT1 KD was not possible. Nevertheless, the de-methylation observed in *GNAS XLas,* could have contributed to the delayed S phase

progression seen in DNMT1 KD HUES7-Fib (Figure 5.12), since this gene is involved in fibroblast proliferation. *GTL2 CpG2* hypo-methylation in EBs with DNMT1 KD could indicate some impairment towards differentiation, since *GTL2* has been associated with myogenesis and nervous system development (Schuster-Gossler *et al.* 1998; Fahrenkrug *et al.* 2000).

The tumour suppressor gene, *p16*, is an inhibitor of the cyclin dependent kinase, CDK4, and it is involved in the cell cycle check-point responsible for allowing progression from the G1 to S phase (prevents cells from entering S phase and holds them at G1 phase; Lukas *et al.* 1995). Self renewal in ESCs is supported by a short cell cycle, mostly due to a shortened G1 phase (Becker *et al.* 2006) and, therefore, *p16* methylation observed in DNMT1 KD HUES7 and EBs could have been catalysed by *de novo* DNMTs, in order to repress *p16* and prevent delays in transition from G1-S phase due to DNMT1 KD (Chen *et al.* 2007). Lack of *p16* methylation in DNMT1 KD HUES7-Fib could be due to the low expression of *de novo* DNMTs observed in these cells. Studies in human cancer cells have shown *p16* methylation to be unaffected following DNMT1 KD (Rhee *et al.* 2000), but become hypo-methylated following double knock-out of DNMT1 and 3B (Rhee *et al.* 2002). This supports the observation from DNMT1 KD HUES7-Fib; that both *de novo* and maintenance DNMTs need to be expressed at reduced levels to enable *p16* hypo-methylation. *p16* hypo-methylation could also have contributed to the abnormal cell cycle progression of DNMT1 KD HUES7-Fib (Figure 5.12).

Overall, knock-down of DNMT1 in pluripotent hESCs had no effect on the processes analysed (cell-cycle progression, global DNA methylation, methylation at imprinted and tumour-suppressor genes, and differentiation), whereas in differentiated cells, knock-down caused a more severe change in phenotype. This is consistent with current literature showing that DNMT1 depletion is detrimental to differentiated cells (reviewed by Brown and Robertson 2007). Despite the changes in phenotype, HUES7-Fib with DNMT1 KD were used in reprogramming experiments to address the question of whether DNA methylation

catalysed by DNMT1 was involved in the repression of pluripotency gene expression in fibroblasts.

5.3.4 Knock-down of the *de novo* DNA methyltransferase *DNMT3A*

Real-time PCR analysis showed a 30% reduction in *DNMT3A* expression in HUES7-Fib, at 72 hours PTD (Figure 5.20) and at 2 weeks PTD (Figure 5.21), indicating that prolonged *DNMT3A* KD did not cause increased cell death. This was in agreement to studies showing that *Dnmt3a* knock-out in MEFs did not have an effect on cell death or cell cycle progression (Dodge *et al.* 2005). Surprisingly, combined KD of *DNMT3A* and *DNMT1* in HUES7-Fib, reduced expression of the *de novo* methyltransferase, *DNMT3B* (Figure 5.21). Even though a number of studies have analysed the effects of DNA methyltransferase KD in mouse and human ESCs and differentiated cells (Rhee *et al.* 2002; Hattori *et al.* 2004; Dodge *et al.* 2005; Tsumura *et al.* 2006; Li *et al.* 2007c), none have looked at the combined effect of *DNMT1* and *3A*. Therefore, it is difficult to conclude whether reduction of *DNMT3B* expression occurred stochastically, or was due to reduced DNMT1 and 3A expression, even though interaction between DNMT enzymes (Pradhan and Esteve 2003) suggests that they might be involved in regulating each-other's expression.

5.3.5 Reprogramming of hESC-derived fibroblasts carrying DNMT1 and DNMT3A knock-down

Reprogramming of HUES7-Fib carrying DNMT1 knock-down resulted in a 40% decreased iPSC colony formation (Figure 5.23). This was unexpected, and in contrast to the hypothesis that if DNA methylation associated with pluripotency-gene silencing occurs during early time-points of HUES7 differentiation (section 4.2.4.3) it would only need to be maintained in HUES7-Fib, a reaction likely to be catalysed by the maintenance methyltransferase, DNMT1. It was also in contrast to studies in mouse cells showing that treatment with siRNAs or shRNAs against *DNMT1* could increase the efficiency of iPSC formation by

enabling partially reprogrammed granular colonies, generated from MEFs, to become fully reprogrammed (Mikkelsen *et al.* 2008). The inability of DNMT1 KD to increase the efficiency of iPSC formation in this thesis could reflect further differences between gene regulation in mouse and human ESCs. Alternatively, since the kinetics of iPSC generation were shown to be directly related to the rate of cell division (Hanna *et al.* 2008), it is possible that decreased formation of iPSC colonies from DNMT1 KD HUES7-Fib was due to their delayed progression through S phase of the cell cycle (Figure 5.12).

In contrast to DNMT1 KD, DNMT3A KD enabled increased formation of TRA-1-81 positive colonies by day 18 PTD (Figure 5.23), which suggested that pluripotency gene silencing in differentiated cells was associated with DNMT3A-mediated DNA methylation. Gene expression analysis by RT-PCR supported this hypothesis, since earlier detection of the pluripotency associated factors *NANOG*, *LIN28* and *DNMT3L* was observed during iPSC generation from DNMT3A KD HUES7-Fib (Figure 5.32). *OCT4*, *SOX2* and *DNMT3B* were not detected at earlier time-points in this sample, indicating that DNMT3A-mediated suppression acted in gene-specific mechanisms. Dnmt3a-mediated DNA methylation has previously been shown to regulate *Dnmt3l* expression in mESCs (Hu *et al.* 2008), perhaps explaining the earlier re-activation of *DNMT3L* in HUES7-Fib DNMT3A KD cells (Figure 5.27).

Dnmt3a has also been shown to catalyse methylation of *Nanog* and *Oct4* during differentiation of mESCs (Li *et al.* 2007c), therefore establishing a link between expression of these genes and Dnmt3a-mediated DNA methylation. Lack of *OCT4* detection at earlier time-points in response to DNMT3A KD in this study (Figure 5.29) could be due to differences in regulation of gene expression between mouse and human cells, or due to distortion of PCR results by detection of pseudogene or residual *OCT4* expression in all samples (Figure 5.29). Future experiments analysing *OCT4* expression during reprogramming could be performed by using the *OCT4* real-time PCR primers which are

specific to endogenous *OCT4* and can distinguish between pseudogenes and the real transcript.

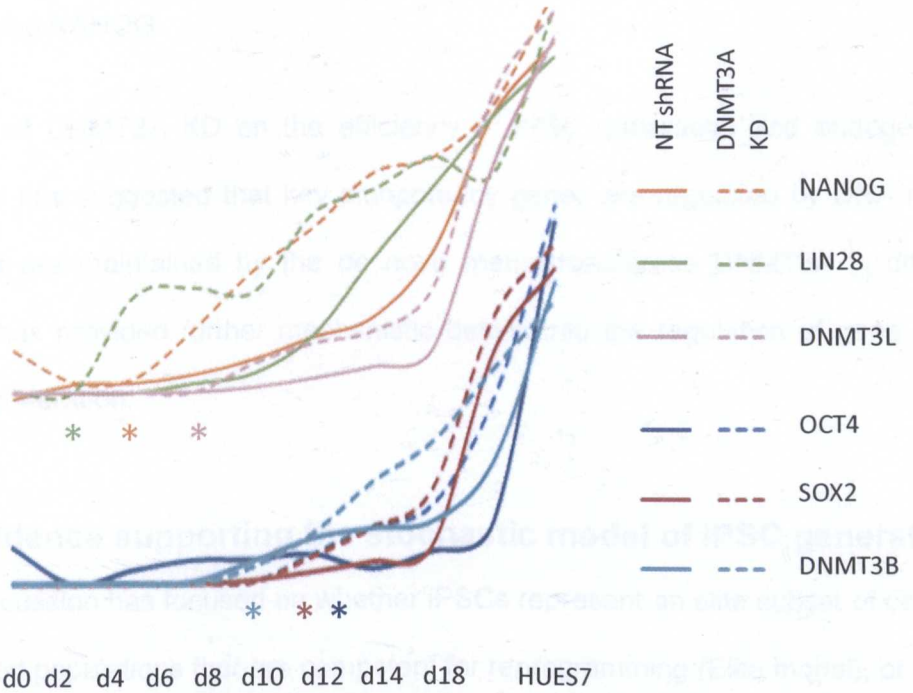

Figure 5.32- Endogenous gene reactivation during reprogramming of HUES7-Fib with DNMT3A KD
Expression of endogenous pluripotency genes during reprogramming of HUES7-Fib with DNMT3A KD (dotted lines) compared to the NT shRNA control sample (solid lines). The pluripotency-associated genes *NANOG*, *LIN28* and *DNMT3L* were detected at earlier time-points in the DNMT3A KD sample, due to earlier reactivation and/or increased overall efficiency of reprogramming to iPSCs. Stars are colour coded and represent the point when gene expression in the DNMT3A KD sample became higher than the control. Y-axis represents relative expression but is not drawn to scale.

Earlier detection of *LIN28* expression in response to DNMT3A KD was perhaps unexpected, since this gene did not show differential methylation between pluripotent and differentiated cells in previous experiments (section 4.2.2.2). RT-PCR results (Figure 5.25) suggested that *LIN28* expression could be regulated by DNA methylation in a different region to the one analysed here, or even by other factors that are themselves regulated by DNA methylation. *Lin28* expression is negatively-regulated at the post-transcriptional level by *miR-125b*, which interacts with three miRNA responsive elements (MREs) found in its 3' UTR, and also by miRNAs of the *let-7* family, which are themselves negatively regulated by Lin28 and DNA methylation (section 4.1.1.5). Nevertheless, neither de-methylation of MREs or *let-7* transcribing genes could explain the earlier detection of *LIN28*, since these were likely to

result in decreased *LIN28* expression. Further investigation is necessary to identify the DNA methylation-dependent *LIN28* regulator, without excluding the possibility that this regulator might even be NANOG.

The effect of DNMT3A KD on the efficiency of iPSC generation and endogenous gene reactivation has suggested that key pluripotency genes are regulated by DNA methylation events that are maintained by the *de novo* methyltransferase DNMT3A in differentiated cells, and has provided further mechanistic details into the regulation of gene expression and iPSC generation.

5.3.6 Evidence supporting the stochastic model of iPSC generation

Current discussion has focused on whether iPSCs represent an elite subset of cells found in differentiated populations that are competent for reprogramming (Elite model), or whether all cells are capable of reprogramming but only a few manage to reach the target phenotype (Stochastic model; Huang 2009; Yamanaka 2009). The Elite model has been somewhat contradicted by the findings of Hanna *et al.* (2008) who were able to generate iPSCs from a clonal population of B lymphocytes that exhibited genetic recombination of the globin locus, characteristic of terminally differentiated cells. This showed that iPSCs could be derived from a pure population of terminally differentiated cells, lacking any precursor of undifferentiated cells that could have formed iPSCs if the elite model held true. Hanna *et al.* (2009) also supported the argument that iPSC generation is a stochastic process by demonstrating that monoclonal transgenic second generation B-cells, expressing all iPS factors at the appropriate levels, could be reprogrammed to iPSCs with 92% efficiency after being maintained in culture for 18 weeks, which indicated that all cells in a differentiated population are capable of reprogramming.

Over-expression of the pluripotency-associated factors, *Esrrb*, *TERT*, or *NANOG* & *LIN28* in combination with the four iPSC factors, *OCT4*, *SOX2*, *KLF4* and *c-MYC* (Liao *et al.* 2008;

Park *et al.* 2008c; Feng *et al.* 2009), as well as treatment of somatic cells with small molecules that are capable of affecting DNA methylation and histone modifications (section 1.8.3.1) were able to improve the formation of iPSC colonies by several-fold, showing that helping somatic cells acquire a transcriptional and epigenetic state more similar to that of hESCs improves the activation of the endogenous machinery necessary for acquiring and maintaining pluripotency, and reinforcing the stochastic model of iPSC generation. DNMT3A knock-down, performed in this study, also helped cells overcome one of the "barriers" towards iPSC generation since it increased iPSC generation efficiency by >80%. This observation strengthened the notion that reprogramming is a stochastic process amenable to acceleration (Hanna *et al.* 2009; Yamanaka 2009), and has laid a foundation for further improving reprogramming efficiency by targeting other epigenetic modifications regulating the expression of key pluripotency genes.

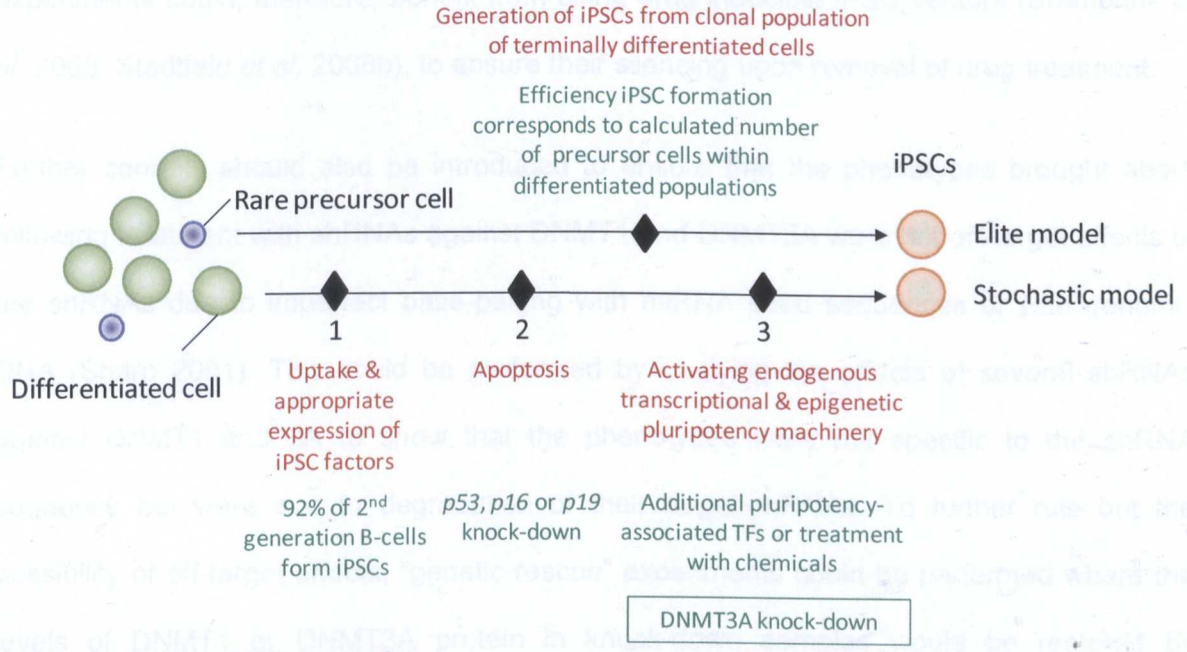

Figure 5.33- Models of iPSC generation
Two models have been proposed for the generation of iPSCs from differentiated cells; one is the Elite model, which supports that only a subset of cells within differentiated populations are capable of reprogramming, and the other is the Stochastic model, which supports that all differentiated cells are capable of reprogramming. The low efficiency of iPSC generation in the Stochastic model is suggested to arise from the inability of some differentiated cells to overcome "barriers" towards iPSC formation. Black diamonds & red writing= "barriers" towards iPSC formation/ evidence disproving Elite model, green writing= treatments used to help cells overcome "barriers"/ evidence supporting Elite model. Improvement of iPSC generation following DNMT3A has supported the hypothesis that reprogramming is a stochastic process, amenable to acceleration (Hong *et al.* 2009; Kawamura *et al.* 2009; Li *et al.* 2009; Marion *et al.* 2009a; Utikal *et al.* 2009).

5.3.7 Future work

DNA methylation catalysed by *de novo* DNMTs has been suggested as a possible mechanism for viral gene silencing (Okano *et al.* 1999; He *et al.* 2005). Also, reactivation of *de novo* DNMTs during iPSC generation was shown to be correlated to the timing of viral transgene silencing (Stadtfeld *et al.* 2008b). It is, thus, possible that increased formation of iPSCs from DNMT3A KD HUES7-Fib was not due to DNA de-methylation of endogenous pluripotency factors, but due to delayed transgene silencing, previously shown to improve the overall formation of iPSCs (Brambrink *et al.* 2008). Unfortunately, studying the inactivation of transgenes by RT-PCR with lentivirus-specific primers (Figure 4.4) did not show a reduction in transgene expression (data not shown), since the time-course iPSC experiments were performed using whole-cell populations (section 5.2.7) which consisted of reprogrammed cells as well as partially reprogrammed and non-reprogrammed ones. Future experiments could, therefore, benefit from using drug-inducible iPSC vectors (Brambrink *et al.* 2008; Stadtfeld *et al.* 2008b), to ensure their silencing upon removal of drug treatment.

Further controls should also be introduced to ensure that the phenotypes brought about following treatment with shRNAs against DNMT1 and DNMT3A were not off-target effects of the shRNAs due to imperfect base-pairing with miRNA seed sequences or with genomic DNA (Sharp 2001). This could be performed by studying the effects of several shRNAs against DNMT1 and 3A to show that the phenotypes were not specific to the shRNA sequence but were due to degradation of their target mRNAs. To further rule out the possibility of off-target effects, "genetic rescue" experiments could be performed where the levels of DNMT1 or DNMT3A protein in knock-down samples would be restored by functional protein, translated form a lentiviral or plasmid-inserted transgene carrying a silent point-mutation that would escape base-pairing with shRNAs. Reversing/rescue of the knock-down phenotype would verify that the effects observed it this thesis following treatment with

shRNAs were specific to down-regulation of DNMT1 or DNMT3A protein and not due to off-target effects of the shRNAs.

Finally, recent analysis of chromosome-wide DNA methylation patterns in iPSCs revealed that although iPSCs and hESCs were clustered together based on their DNA methylation signatures, iPSCs had slightly increased global DNA methylation at CpG sites compared to hESCs (Deng *et al.* 2009). Moreover, imprinted genes such as *H19*, *KCNQ10T1*, *PEG3*, *GTL2* and *IGF2* showed aberrant DNA methylation and allele-specific expression in iPSCs, relative to the differentiated lines they were derived from (Pick *et al.* 2009). It would, therefore, be of interest to investigate the epigenetic stability of iPSCs in the model system generated in this study, to determine whether karyotype or culture-induced effects could account for the differences observed by Deng *et al.* (2009) and Pick *et al.* (2009) or whether reprogramming by defined factors does affect epigenetic stability.

6 GENERAL DISCUSSION

The aim of this thesis was to investigate the precise mechanisms by which key pluripotency-associated transcription factors become activated or repressed in order to enable a change in cell phenotype from a pluripotent to a fibroblast differentiated state, and vice-versa. In this section, key findings from each chapter of this thesis are integrated and discussed in relation to current literature, and new models for the regulation of key pluripotency-genes in human cells are proposed. Also, methods for further investigation of these models are described.

6.1 SINGLE-GENOTYPE HUMAN MODEL CELL SYSTEM

The epigenetic regulation of pluripotency-associated genes is poorly studied in human cells, in contrast to mouse cells, where the mechanisms associated with the regulation of some pluripotency-genes, e.g. *Oct4*, have been characterised in more detail (Figure 4.1; Feldman *et al.* 2006; Epsztejn-Litman *et al.* 2008). However, differences in transcriptional profiles, response to signalling molecules and chemical treatment (section 1.6) have shown that mESCs might represent a different developmental stage to hESCs (Brons *et al.* 2007; Tesar *et al.* 2007). These observations suggested that it was necessary to develop human models for the investigation of gene-expression regulatory mechanisms involved in human development and lineage specification. Also, differences between existing hESC lines, in terms of the levels of pluripotency-gene expression and epigenetic characteristics that are caused by genotype and culture-induced effects (reviewed by Allegrucci and Young 2007), have suggested that these variables should be eliminated in order to avoid false interpretation of experimental results when analysing gene regulatory mechanisms.

To reduce species or genotype and culture-induced variation, chapter 3 of this thesis generated a single-genotype human model cell system, comprising of hESCs, iPSCs and derived-fibroblasts. In this system, hESCs and iPSCs were cultured under similar conditions

(feeder-free culture on Matrigel with MEF-conditioned medium and trypsin passaging; Denning *et al.* 2006), and were differentiated using the standardised forced-aggregation technique (Burridge *et al.* 2007). This approach enabled direct comparison between the epigenetic characteristics of pluripotency-genes in the hESC and iPSC pluripotent states, the hESC- and iPSC-fibroblast differentiated states, and the mechanisms employed by hESCs and iPSCs induce differentiation. This strategy was advantageous to studies comparing the epigenetic profiles of iPSCs, derived from patient fibroblasts, blood or keratinocytes, to existing hESCs that have a different genotype to the iPSCs (Park *et al.* 2008a; Carey *et al.* 2009; Haase *et al.* 2009), and also to studies comparing the profiles of iPSCs to the fibroblast lines they were derived from (Pick *et al.* 2009), without taking into account that characteristics such as genomic imprinting can adopt tissue-specific DNA methylation patterns (Moore *et al.* 1997; Okabe *et al.* 2003; Tsou *et al.* 2003). Through the model cell system derived in this thesis, it emerged that iPSCs and hESCs have similar DNA methylation profiles in key pluripotency-genes (Figure 4.11) and use the same DNA methylation-associated mechanisms to transition to a fibroblast-differentiated state (Figure 4.16). Also, hESC and iPSC-fibroblasts reached similar DNA methylation states (Figure 4.11), showing that iPSCs can "circle" back to the same cell-phenotype they were derived from. Findings from this thesis suggested that iPSCs serve as a good alternative model to hESCs for the investigation of human pluripotency and associated gene-regulatory mechanisms. However, to confirm these findings, further polyclonal or even clonal iPSC lines generated form hESC-derived fibroblasts should be analysed, to ensure that reprogramming consistently yields iPSCs with epigenetic characteristics similar to hESCs.

6.2 PLURIPOTENCY-GENE EXPRESSION AND EPIGENETIC REGULATION

6.2.1 Temporal gene expression during differentiation and iPSC formation

Repression/ silencing of the key pluripotency-associated transcription factors (TFs) can lead to differentiation of pluripotent hESCs (section 1.3.3), while over-expression of the same TFs can reprogram differentiated cells to a pluripotent ESC-like state (section 1.8.1). Nevertheless, the temporal requirements of these transcription factors during differentiation or reprogramming are poorly investigated in mouse or human cells, since most studies focus on analysing gene expression in either the pluripotent or the differentiated cell states (Adewumi *et al.* 2007). Very few studies have performed a time-course analysis of gene expression during differentiation, and have focused on just 2-3 time-points (Dvash *et al.* 2004). To understand how the pluripotent phenotype becomes repressed or re-established in human cells, a 2-day interval time-course analysis over a total of 16 or 18 days during differentiation or iPSC-generation was performed in this thesis (Chapter 4).

Reactivation of the pluripotency-genes *OCT4*, *NANOG*, *SOX2* and *LIN28* was detected at similar time-points (within 8-10 days) during fibroblast reprogramming to iPSCs, perhaps due to the use of RT-PCR primers with dissimilar efficiencies (Figure 4.18). On the other hand, TaqMan real-time PCR analysis during differentiation revealed that pluripotency-genes became repressed at distinct time-points (Figure 4.14). *NANOG* was the first gene to become repressed. Previous studies have shown that Nanog has a role in stabilising pluripotency in mESCs (Chambers *et al.* 2007) and hESCs (Darr *et al.* 2006), therefore supporting the observations from this thesis that *NANOG* down-regulation is important to destabilise the pluripotent state and enable a transition in cell phenotype. Other genes, such as *DNMT3B*, *OCT4*, *SOX2*, *REX1* and *LIN28* showed initial up-regulation during differentiation; either due to a paracrine effect caused by EB formation, or because they

were necessary to initiate differentiation towards certain lineages (Rodriguez *et al.* 2007; Zappone *et al.* 2000). Earlier down-regulation of *DNMT3B* relative to *OCT4* (Figure 4.14) suggests that this *de novo* DNMT might not be involved in *OCT4* methylation during differentiation of hESCs, in contrast to mESCs where *Oct4* repression is associated with Dnmt3b-catalysed DNA methylation (Biniszkiewicz *et al.* 2002; Chen *et al.* 2003). This observation points towards distinct gene-regulatory mechanisms between mouse and human cells. Down-regulation of pluripotency factors during differentiation is proposed to follow a defined hierarchical pattern, based on the requirement of each factor in pluripotency and lineage specification.

6.2.2 Regulation by DNA methylation

The exact mechanisms of how pluripotency-associated transcription factors become activated or repressed are poorly understood, and are scarcely studied in human cells. This thesis aimed at extending our understanding of these mechanisms and providing novel information about how the pluripotent state is activated or repressed in human cells. Chapter 4 of this thesis showed that the master pluripotency regulators *OCT4*, *SOX2* and *NANOG* had differential DNA methylation between pluripotent and fibroblast differentiated cell lines in their OCT/SOX binding regions (Figure 4.11), suggesting a common regulatory mechanism between them. This was also the first report for *SOX2* differential methylation in human non-cancerous cells, since other studies have reported that *SOX2* was unmethylated following hESC differentiation (Yeo *et al.* 2007). OCT/SOX binding sites are found in several developmental-regulators (Sharov and Ko 2009) and are believed to have a significant role in the auto-regulatory circuits of *Oct4* and in the regulation of other pluripotency genes, such as *Fbx15* and *Fgf4* (Okumura-Nakanishi *et al.* 2005). This study has shown that the OCT/SOX binding site might also be involved in *SOX2* auto-regulation. Identification and epigenetic characterisation of this binding motif in further pluripotency-regulators could

reveal further information about the significance of OCT/SOX motifs in developmental processes.

In this thesis, *NANOG*, *OCT4* and *REX1* DNA methylation gradually increased during differentiation of hESCs and iPSCs, and was associated closely with gene down-regulation during differentiation (Figure 4.23). This observation showed that expression of *NANOG*, *OCT4* and *REX1* was initiated by DNA methylation, a finding that comes in contrast to studies from mESCs showing that *Oct4* and *Rex1* down-regulation is initiated by histone modifications that are catalysed by the G9a histone methyltransferase (Feldman *et al.* 2006). Increase in *SOX2* DNA methylation during differentiation was delayed relative to gene down-regulation, suggesting that transcriptional repression was initiated by other mechanisms (e.g. histone modifications or TF binding) and was possibly stabilised by DNA methylation at later time-points, in a manner similar to the regulation of *Oct4* in mESCs (Epsztejn-Litman *et al.* 2008). Therefore, this thesis has highlighted that epigenetic regulation of pluripotency-factors adopts gene-specific patterns in human cells, which are likely to be distinct to the regulatory patterns of each gene in mouse cells.

6.2.3 Proposed model for the transcriptional regulation of pluripotency-associated genes

Through this thesis, *NANOG*, *OCT4* and *REX1* expression has been inversely associated to DNA methylation, which appears to initiate gene down-regulation during differentiation (Figure 4.23). Improved *NANOG* reactivation during reprogramming of HUES7-Fib with DNMT3A KD suggests that DNA methylation is a "dominant" silencing mechanism for this gene, and might act by directly inhibiting TF binding to the NANOG promoter (Vaissiere *et al.* 2008; Figure 1.7.B). Even though histone modifications are associated with the *NANOG* gene (Figure 4.13) these might have a "secondary" role to DNA methylation. *OCT4* down-regulation could be initiated by DNA methylation during differentiation, but this gene showed

no change in reactivation timing during reprogramming of HUES7-Fib with DNMT3A KD. This suggests that *OCT4* is regulated by additional mechanisms, e.g. repressive histone or chromatin modifications that occur after DNA methylation has taken place (Figure 6.1). SOX2 expression also showed no change in reactivation timing in cells with DNMT3A KD, but in contrast to *OCT4*, down-regulation of *SOX2* during differentiation was not initiated by DNA methylation. This suggests that histone modification events (and possibly chromatin remodelling) take place prior to DNA methylation in regulatory regions of this gene. *REX1* showed initial up-regulation during differentiation and transcriptional repression coincided with DNA hyper-methylation, showing that this gene could be regulated by mechanisms similar to *OCT4*. *DNMT3L*, which was detected at earlier time-points during reprogramming of DNMT3A KD HUES7-Fib could be regulated with similar mechanisms to *NANOG*, even though further investigation regarding the methylation of *DNMT3L* during differentiation should be carried out.

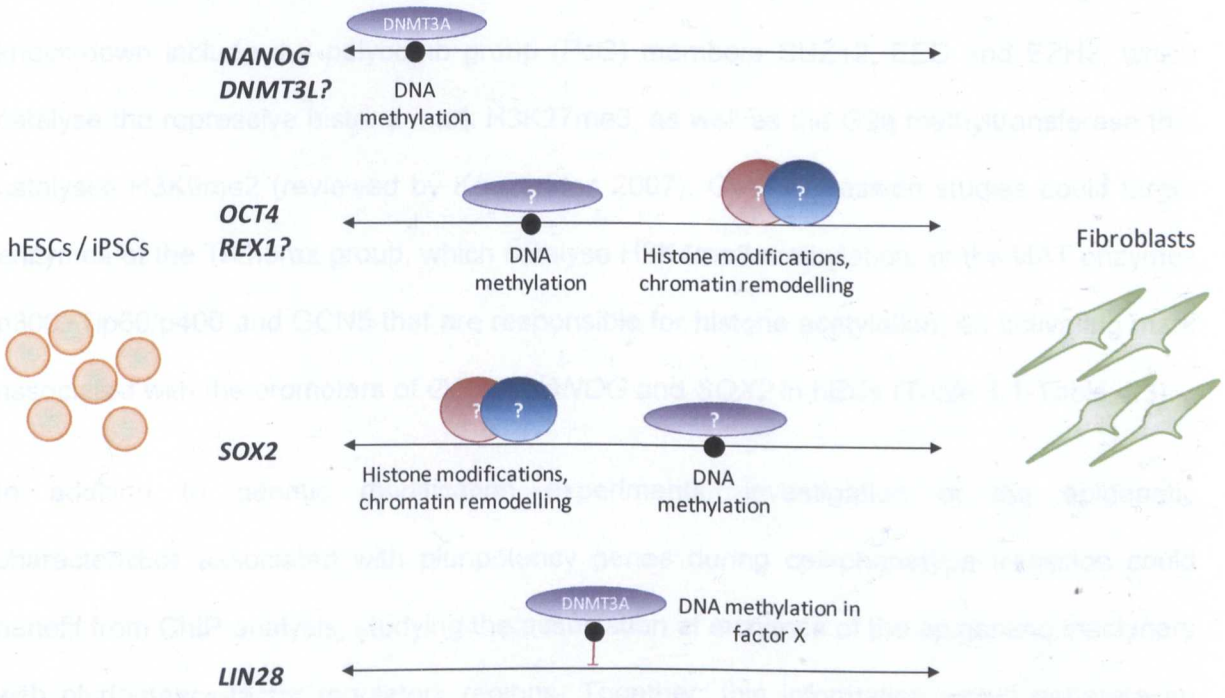

Figure 6.1- Proposed models of the epigenetic regulation of pluripotency-genes in human cells
NANOG repression could be dominantly regulated by DNMT3A-catalysed DNA methylation, whereas OCT4 repression could be initiated by DNA methylation and further stabilised by histone and chromatin modifications. SOX2 repression is likely to be initiated by histone and/or chromatin modifications and stably silenced by DNA methylation. Expression of LIN28 could be responsive to DNA methylation of "secondary" transcription factors that in turn regulate LIN28 expression.

6.2.4 Regulation by histone modifications

In chapter 4, the activating histone marks H3K9Ac and K3K4me3 were associated with transcriptionally active *OCT4*, *NANOG*, *SOX2* and *REX1*, while the silencing histone marks H3K27me3 and H3K9me2 were associated with repressed transcriptional activity, in agreement to data previously available from mouse or hEC studies (Barrand and Collas 2009). However, the timing when these events occurred during differentiation or reprogramming has not been identified so far. Further analysis of histone modifications associated with key pluripotency-genes is in progress and can reveal the precise involvement of H3K9Ac, H3K4me3, H3K9me2 and H3K27me3 in the transition of cell phenotype from a pluripotent to a fibroblast-differentiated state, and vice-versa.

To confirm these findings, enzymes responsible for catalysing these histone modifications could also be targeted for knock-down or over-expression, in order to establish a direct link between histone modifications and gene expression. Enzymes that could be targeted for knock-down include the polycomb group (PcG) members SUZ12, EED and EZH2, which catalyse the repressive histone mark H3K27me3, as well as the G9a methyltransferase that catalyses H3K9me2 (reviewed by Kouzarides 2007). Over-expression studies could target enzymes of the Trithorax group, which catalyse H3K4me3 methylation, or the HAT enzymes p300, Tip60/p400 and GCN5 that are responsible for histone acetylation, an activating mark associated with the promoters of *OCT4*, *NANOG* and *SOX2* in hECs (Table 4.1-Table 4.3).

In addition to genetic modification experiments, investigation of the epigenetic characteristics associated with pluripotency genes during cell-phenotype transition could benefit from ChIP analysis, studying the association of enzymes of the epigenetic machinery with pluripotency-factor regulatory regions. Together, this information would generate an epigenetic "map" of the enzymes and types of modifications associated with pluripotency-gene promoters, and indicate how these modifications affect pluripotency-gene expression and cell phenotype.

6.2.5 Regulation by chromatin remodelling enzymes

Chromatin remodelling (mobilising or displacing of nucleosomes) can also have important consequences on transcriptional activity (see sections 1.5.1), and has been shown to act in concert with histone modifications and TFs to regulate cell phenotype (Bonifer *et al.* 2008). Chromatin remodelling enzymes, such as esBAF and Chd1, associate with *Oct4*, *Sox2* and *Nanog* in mESCs (Chen *et al.* 2008a; Ho *et al.* 2009a) and are thought to be necessary for the maintenance of pluripotency and self-renewal (Gao *et al.* 2008; Yan *et al.* 2008; Ho *et al.* 2009b). Moreover, Chd1 expression was found to be necessary for the formation of iPSCs from MEFs (Gaspar-Maia *et al.* 2009). In effect, chromatin remodelling enzymes could also be targeted for genetic modification, in order to test whether they could enhance the reactivation of endogenous pluripotency genes during reprogramming and improve the efficiency of iPSC generation, but also provide further insight into the precise molecular mechanisms of cell phenotype determination.

6.2.6 Regulation by small molecules

Over-expression of pluripotency-associated TFs for the reprogramming of somatic cells to iPSCs involves genetic modification of target cells, which often introduces the risk of insertional mutagenesis due to integration of vector DNA into the host-genome (section 3.1.3; Scheper and Copray 2009). Other than generating non-integrating or excisable vectors for the over-expression of exogenous TFs (Table 3.2), a number of efforts have been made to completely eliminate the need for transgene over-expression by substituting transgenes with small molecules. High content chemical screening has identified that iPSCs can be generated when *Sox2* and *c-Myc* transgenes are replaced by small molecules that inhibit Tgf-β signalling (Ichida *et al.* 2009; Maherali and Hochedlinger 2009), whereas *Klf4* could be replaced by the small molecule, kenpaullone, which stimulates *Nanog* expression (Lyssiotis *et al.* 2009).

Further investigation into eliminating the need for transgene over-expression to generate iPSCs could focus on the use of small molecules that affect the epigenetic characteristics associated with key pluripotency-genes. Treating differentiated cells with small compounds that alter epigenetic modifications has already been shown to increase the efficiency of iPSC-generation (reviewed by Li and Ding 2009). However, most compounds tested to date have a broad specificity and provide little information about the specific mechanisms of iPSC generation. Future experiments could, therefore, use high content chemical screening to investigate the effect of yet untested small molecules that target specific epigenetic modifications (Table 6.1).

Small molecule screening is now amenable to investigation within our lab which was recently equipped with a new robotic culture system (TECAN; Freedom Evo® 2000) that can accommodate large-scale screening of chemical libraries. A collaboration has been established between our lab and Dr. Tapas Kundu (Jawaharlal Nehru Centre for Advanced Scientific Research, India) whose lab specialises in deriving and derivatising small molecules from natural sources. Some of these molecules have been demonstrated to possess histone modification abilities. For example, Sanguinarine, a plant root extract, has been shown to specifically inhibit H3K4 and R17 methylation *in vivo* (Selvi *et al.* 2009b). Equally, the compound TBBD, can inhibit CARM1-mediated H3R17 methylation (Selvi *et al.* 2009a) which has been detected at elevated levels in the *Oct4* and *Sox2* promoters of mESCs (Wu *et al.* 2009a). Further small compounds that have the potential to affect cell phenotype or iPSC generation are summarised in Table 6.1. Using new technologies and effective collaborations can enable the identification of new small molecules that are able to improve the formation of iPSCs or potentially alleviate the need for lentiviral transgenes altogether, by facilitating activation of endogenous pluripotency-factors for the generation of iPSCs.

Table 6.1– Small molecules that have the potential to improve iPSC generation

Compound	Cell type	Function		References
Anacardic acid	-	p300 HAT & p300-CBP associated factor (PCAF) inhibitor		Balasubramanyam *et al.* 2003
CTBP (Anacardic acid amide derivative)	-	p300 HAT activator		
Garcinol	HeLa cells	p300 HAT & PCAF inhibitor, with preference to p300		Balasubramanyam *et al.* 2004
Curcumin	-	p300-CREB binding protein (CBP) inhibitor	Prevents acetylation of p53	
	Leukaemia cells (MV4-11)		Causes 15-20% global DNA hypo-methylation in MV4-11 cells	Liu *et al.* 2009
LTK-13, 14 & 19 (Garcinol derivatives)	HeLa cells T cells	p300 inhibitors. Induce 70-80% de-acetylation in HeLa cells, and up to 100% de-acetylation when used in combination with TSA or NaBu (HDAC inhibitors), and IG (HAT inhibitor)		Mantelingu *et al.* 2007
TBBD (ellagic acid)	HEK293T	Inhibits CARM1-mediated H3R17 methylation		Selvi *et al.* 2009a
Panobinostat	Human acute leukaemia	HDAC inhibitor, can deplete the histone methyltransferase Ezh2		Fiskus *et al.* 2009
Sanguinarine	Rat liver, HeLa cells	Intercalates with DNA and chromatin, causes chromatin aggregation, inhibits G9a-mediated H3K9me *in vitro*, and histone acetylation, H3K4me and H3R17me *in vivo*		Selvi *et al.* 2009b

6.3 FINAL REMARKS

"Ground-state" pluripotency, i.e. the ability of ESCs to self-renew in an uncommitted state and form all lineages in an adult organism when prompted by developmental signals or cell culture environment (Smith 2009), depends on complex TF networks and epigenetic modifications that are thought to be under transcription-factor regulation (Niwa 2007). Findings from this thesis (summarised in Figure 6.2) have also shown that pluripotency-regulating TFs are themselves controlled by epigenetic modifications, therefore showing that transcription-factor and epigenetic regulation of gene expression are equally significant for the determination of cell-phenotype.

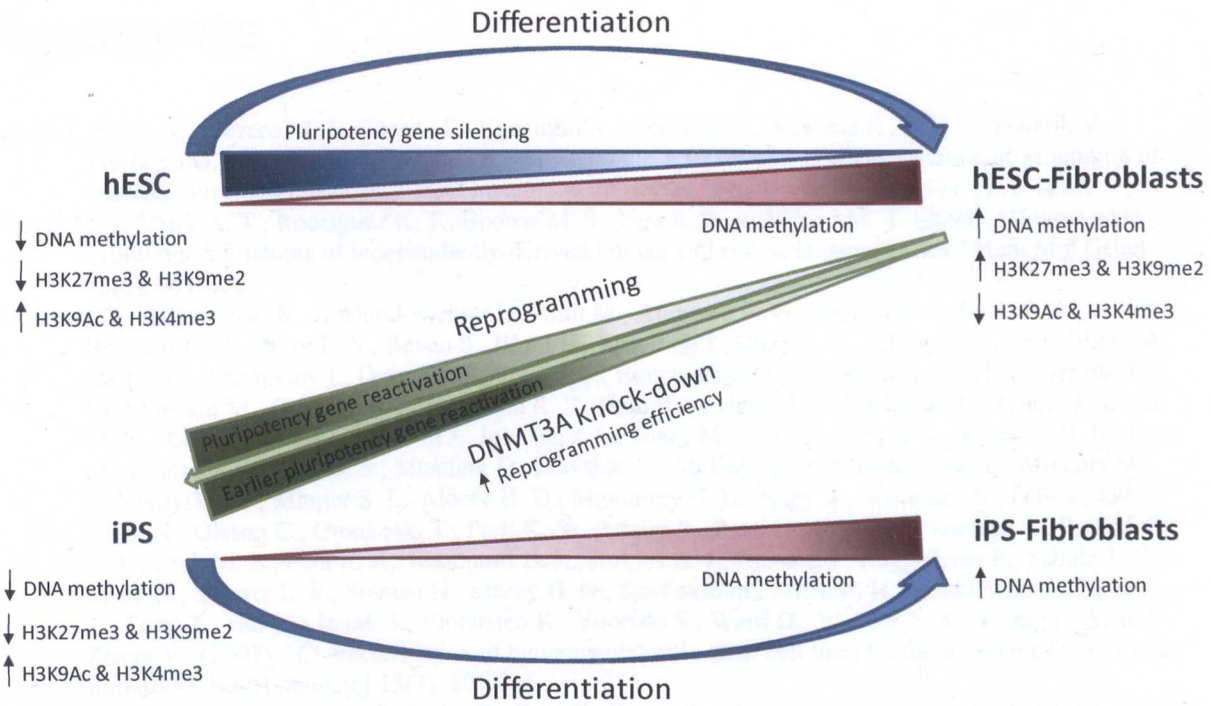

Figure 6.2- Summary of thesis outcomes
Generation of model system comprising of hESCs, iPSCs, and derived fibroblasts, enabled unbiased characterisation of pluripotency gene expression and epigenetic regulation

Studying the intermolecular gene-specific interactions that are at the heart of cell phenotype transitions is important for understanding the complex processes of human development and somatic cell reprogramming. Continued in-depth analysis of individual gene-regulation, investigation of transcription-regulatory trends, as well as the search for new small molecules that can regulate gene expression are all necessary to unravel such interactions. This thesis has investigated the transition of cell phenotype form a pluripotent to a fibroblast differentiated state in human cells, focusing on the epigenetic regulation of transcription factors that enable phenotype changes. Through this investigation, new gene-specific interactions have emerged which increase our understanding of transcriptional gene control and provide the foundation for further improving reprogramming efficiency.

REFERENCES

Aasen T., Raya A., Barrero M. J., Garreta E., Consiglio A., Gonzalez F., Vassena R., Bilic J., Pekarik V., Tiscornia G., Edel M., Boue S. and Izpisua Belmonte J. C. (2008). "Efficient and rapid generation of induced pluripotent stem cells from human keratinocytes." Nat Biotechnol **26**(11): 1276-1284.

Abeyta M. J., Clark A. T., Rodriguez R. T., Bodnar M. S., Pera R. A. and Firpo M. T. (2004). "Unique gene expression signatures of independently-derived human embryonic stem cell lines." Hum Mol Genet **13**(6): 601-608.

Adewumi O., Aflatoonian B., Ahrlund-Richter L., Amit M., Andrews P. W., Beighton G., Bello P. A., Benvenisty N., Berry L. S., Bevan S., Blum B., Brooking J., Chen K. G., Choo A. B., Churchill G. A., Corbel M., Damjanov I., Draper J. S., Dvorak P., Emanuelsson K., Fleck R. A., Ford A., Gertow K., Gertsenstein M., Gokhale P. J., Hamilton R. S., Hampl A., Healy L. E., Hovatta O., Hyllner J., Imreh M. P., Itskovitz-Eldor J., Jackson J., Johnson J. L., Jones M., Kee K., King B. L., Knowles B. B., Lako M., Lebrin F., Mallon B. S., Manning D., Mayshar Y., McKay R. D., Michalska A. E., Mikkola M., Mileikovsky M., Minger S. L., Moore H. D., Mummery C. L., Nagy A., Nakatsuji N., O'Brien C M., Oh S. K., Olsson C., Otonkoski T., Park K. Y., Passier R., Patel H., Patel M., Pedersen R., Pera M. F., Piekarczyk M. S., Pera R. A., Reubinoff B. E., Robins A. J., Rossant J., Rugg-Gunn P., Schulz T. C., Semb H., Sherrer E. S., Siemen H., Stacey G. N., Stojkovic M., Suemori H., Szatkiewicz J., Turetsky T., Tuuri T., van den Brink S., Vintersten K., Vuoristo S., Ward D., Weaver T. A., Young L. A. and Zhang W. (2007). "Characterization of human embryonic stem cell lines by the International Stem Cell Initiative." Nat Biotechnol **25**(7): 803-816.

Agger K., Cloos P. A., Christensen J., Pasini D., Rose S., Rappsilber J., Issaeva I., Canaani E., Salcini A. E. and Helin K. (2007). "UTX and JMJD3 are histone H3K27 demethylases involved in HOX gene regulation and development." Nature **449**(7163): 731-734.

Akitsu Hotta J. E. (2008). "Retroviral vector silencing during iPS cell induction: An epigenetic beacon that signals distinct pluripotent states." Journal of Cellular Biochemistry **105**(4): 940-948.

Akiyama Y., Watkins N., Suzuki H., Jair K. W., van Engeland M., Esteller M., Sakai H., Ren C. Y., Yuasa Y., Herman J. G. and Baylin S. B. (2003). "GATA-4 and GATA-5 transcription factor genes and potential downstream antitumor target genes are epigenetically silenced in colorectal and gastric cancer." Mol Cell Biol **23**(23): 8429-8439.

Alberio R., Campbell K. H. and Johnson A. D. (2006). "Reprogramming somatic cells into stem cells." Reproduction **132**(5): 709-720.

Allegrucci C., Wu Y. Z., Thurston A., Denning C. N., Priddle H., Mummery C. L., Ward-van Oostwaard D., Andrews P. W., Stojkovic M., Smith N., Parkin T., Edmondson Jones M., Warren G., Yu L., Brena R. M., Plass C. and Young L. E. (2007). "Restriction Landmark Genome Scanning identifies culture-induced DNA methylation instability in the human embryonic stem cell epigenome." Hum Mol Genet **16**(10): 1253-1268.

Allegrucci C. and Young L. E. (2007). "Differences between human embryonic stem cell lines." Hum Reprod Update **13**(2): 103-120.

Allsopp R. C. and Harley C. B. (1995). "Evidence for a Critical Telomere Length in Senescent Human Fibroblasts." Exp Cell Res **219**(1): 130-136.

Amabile G. and Meissner A. (2009). "Induced pluripotent stem cells: current progress and potential for regenerative medicine." Trends in Molecular Medicine **15**(2): 59-68.

Amit M., Carpenter M. K., Inokuma M. S., Chiu C. P., Harris C. P., Waknitz M. A., Itskovitz-Eldor J. and Thomson J. A. (2000). "Clonally derived human embryonic stem cell lines maintain pluripotency and proliferative potential for prolonged periods of culture." Dev Biol **227**(2): 271-278.

Amit M., Shariki C., Margulets V. and Itskovitz-Eldor J. (2004). "Feeder layer- and serum-free culture of human embryonic stem cells." Biol Reprod **70**(3): 837-845.

Andrés M. B.-L., Richard L. C. and Todd C. M. (2009). "Engineering the embryoid body microenvironment to direct embryonic stem cell differentiation." Biotechnology Progress **25**(1): 43-51.

Andrews P. W., Banting G., Damjanov I., Arnaud D. and Avner P. (1984). "Three monoclonal antibodies defining distinct differentiation antigens associated with different high molecular weight polypeptides on the surface of human embryonal carcinoma cells." Hybridoma **3**(4): 347-361.

Anke G., Andreas K., Kelley F. and Peter L. (2006). "Current State of Human Embryonic Stem Cell Research: An Overview of Cell Lines and Their Use in Experimental Work." Stem Cells **24**(10): 2187-2191.

Annunen P., Helaakoski T., Myllyharju J., Veijola J., Pihlajaniemi T. and Kivirikko K. I. (1997). "Cloning of the human prolyl 4-hydroxylase alpha subunit isoform alpha(II) and characterization of the type II

enzyme tetramer. The alpha(I) and alpha(II) subunits do not form a mixed alpha(I)alpha(II)beta2 tetramer." J Biol Chem **272**(28): 17342-17348.

Aoi T., Yae K., Nakagawa M., Ichisaka T., Okita K., Takahashi K., Chiba T. and Yamanaka S. (2008). "Generation of Pluripotent Stem Cells from Adult Mouse Liver and Stomach Cells." Science.

Armstrong L., Lako M., Lincoln J., Cairns P. M. and Hole N. (2000). "mTert expression correlates with telomerase activity during the differentiation of murine embryonic stem cells." Mech Dev **97**(1-2): 109-116.

Armstrong L., Saretzki G., Peters H., Wappler I., Evans J., Hole N., von Zglinicki T. and Lako M. (2005). "Overexpression of telomerase confers growth advantage, stress resistance, and enhanced differentiation of ESCs toward the hematopoietic lineage." Stem Cells **23**(4): 516-529.

Avilion A. A., Nicolis S. K., Pevny L. H., Perez L., Vivian N. and Lovell-Badge R. (2003). "Multipotent cell lineages in early mouse development depend on SOX2 function." Genes Dev **17**(1): 126-140.

Ayton P. M. and Cleary M. L. (2001). "Molecular mechanisms of leukemogenesis mediated by MLL fusion proteins." Oncogene **20**(40): 5695-5707.

Azuara V., Perry P., Sauer S., Spivakov M., Jorgensen H. F., John R. M., Gouti M., Casanova M., Warnes G., Merkenschlager M. and Fisher A. G. (2006). "Chromatin signatures of pluripotent cell lines." Nat Cell Biol **8**(5): 532-538.

Babaie Y., Herwig R., Greber B., Brink T. C., Wruck W., Groth D., Lehrach H., Burdon T. and Adjaye J. (2007). "Analysis of Oct4-dependent transcriptional networks regulating self-renewal and pluripotency in human embryonic stem cells." Stem Cells **25**(2): 500-510.

Baharvand H., Jafary H., Massumi M. and Ashtiani S. K. (2006). "Generation of insulin-secreting cells from human embryonic stem cells." Dev Growth Differ **48**(5): 323-332.

Baker D. E. C., Harrison N. J., Maltby E., Smith K., Moore H. D., Shaw P. J., Heath P. R., Holden H. and Andrews P. W. (2007). "Adaptation to culture of human embryonic stem cells and oncogenesis in vivo." Nat Biotech **25**(2): 207-215.

Balasubramanyam K., Altaf M., Varier R. A., Swaminathan V., Ravindran A., Sadhale P. P. and Kundu T. K. (2004). "Polyisoprenylated Benzophenone, Garcinol, a Natural Histone Acetyltransferase Inhibitor, Represses Chromatin Transcription and Alters Global Gene Expression." Journal of Biological Chemistry **279**(32): 33716-33726.

Balasubramanyam K., Swaminathan V., Ranganathan A. and Kundu T. K. (2003). "Small molecule modulators of histone acetyltransferase p300." J Biol Chem **278**(21): 19134-19140.

Ball M. P., Li J. B., Gao Y., Lee J. H., LeProust E. M., Park I. H., Xie B., Daley G. Q. and Church G. M. (2009). "Targeted and genome-scale strategies reveal gene-body methylation signatures in human cells." Nat Biotechnol **27**(4): 361-368.

Barrand S. and Collas P. (2009). "Chromatin states of core pluripotency-associated genes in pluripotent, multipotent and differentiated cells." Biochem Biophys Res Commun **391**(1): 762-767.

Barry E. R., Krueger W., Jakuba C. M., Veilleux E., Ambrosi D. J., Nelson C. E. and Rasmussen T. P. (2009). "ES Cell Cycle Progression and Differentiation Require the Action of the Histone Methyltransferase Dot1L." Stem Cells **27**(7): 1538-1547.

Bartova E., Krejci J., Harnicarova A. and Kozubek S. (2008). "Differentiation of human embryonic stem cells induces condensation of chromosome territories and formation of heterochromatin protein 1 foci." Differentiation **76**(1): 24-32.

Bastepe M., Frohlich L. F., Linglart A., Abu-Zahra H. S., Tojo K., Ward L. M. and Juppner H. (2005). "Deletion of the NESP55 differentially methylated region causes loss of maternal GNAS imprints and pseudohypoparathyroidism type Ib." Nat Genet **37**(1): 25-27.

Becker K. A., Ghule P. N., Therrien J. A., Lian J. B., Stein J. L., van Wijnen A. J. and Stein G. S. (2006). "Self-renewal of human embryonic stem cells is supported by a shortened G1 cell cycle phase." J Cell Physiol **209**(3): 883-893.

Beqqali A., Kloots J., Ward-van Oostwaard D., Mummery C. and Passier R. (2006). "Genome-wide transcriptional profiling of human embryonic stem cells differentiating to cardiomyocytes." Stem Cells **24**(8): 1956-1967.

Berger S. L. (2007). "The complex language of chromatin regulation during transcription." Nature **447**(7143): 407-412.

Bernstein B. E., Mikkelsen T. S., Xie X., Kamal M., Huebert D. J., Cuff J., Fry B., Meissner A., Wernig M., Plath K., Jaenisch R., Wagschal A., Feil R., Schreiber S. L. and Lander E. S. (2006). "A bivalent chromatin structure marks key developmental genes in embryonic stem cells." Cell **125**(2): 315-326.

Beyer W. R., Westphal M., Ostertag W. and von Laer D. (2002). "Oncoretrovirus and lentivirus vectors pseudotyped with lymphocytic choriomeningitis virus glycoprotein: generation, concentration, and broad host range." J Virol **76**(3): 1488-1495.

Bhattacharya S. K., Ramchandani S., Cervoni N. and Szyf M. (1999). "A mammalian protein with specific demethylase activity for mCpG DNA." Nature **397**(6720): 579-583.

Bibikova M., Chudin E., Wu B., Zhou L., Garcia E. W., Liu Y., Shin S., Plaia T. W., Auerbach J. M., Arking D. E., Gonzalez R., Crook J., Davidson B., Schulz T. C., Robins A., Khanna A., Sartipy P., Hyllner J., Vanguri P., Savant-Bhonsale S., Smith A. K., Chakravarti A., Maitra A., Rao M., Barker D. L., Loring J. F. and Fan J. B. (2006). "Human embryonic stem cells have a unique epigenetic signature." Genome Res **16**(9): 1075-1083.

Bigdeli N., Andersson M., Strehl R., Emanuelsson K., Kilmare E., Hyllner J. and Lindahl A. (2008). "Adaptation of human embryonic stem cells to feeder-free and matrix-free culture conditions directly on plastic surfaces." J Biotechnol **133**(1): 146-153.

Biniszkiewicz D., Gribnau J., Ramsahoye B., Gaudet F., Eggan K., Humpherys D., Mastrangelo M. A., Jun Z., Walter J. and Jaenisch R. (2002). "Dnmt1 overexpression causes genomic hypermethylation, loss of imprinting, and embryonic lethality." Mol Cell Biol **22**(7): 2124-2135.

Blesch A. (2004). "Lentiviral and MLV based retroviral vectors for ex vivo and in vivo gene transfer." Methods **33**(2): 164-172.

Boiani M. and Scholer H. R. (2005). "Regulatory networks in embryo-derived pluripotent stem cells." Nat Rev Mol Cell Biol **6**(11): 872-884.

Bonifer C., Hoogenkamp M., Krysinska H. and Tagoh H. (2008). "How transcription factors program chromatin--Lessons from studies of the regulation of myeloid-specific genes." Seminars in Immunology **20**(4): 257-263.

Booth H. A. and Holland P. W. (2004). "Eleven daughters of NANOG." Genomics **84**(2): 229-238.

Bosnali M., Munst B., Thier M. and Edenhofer F. (2009). "Deciphering the stem cell machinery as a basis for understanding the molecular mechanism underlying reprogramming." Cell Mol Life Sci **66**(21): 3403-3420.

Bostick M., Kim J. K., Esteve P. O., Clark A., Pradhan S. and Jacobsen S. E. (2007). "UHRF1 plays a role in maintaining DNA methylation in mammalian cells." Science **317**(5845): 1760-1764.

Boulias K. and Talianidis I. (2004). "Functional role of G9a-induced histone methylation in small heterodimer partner-mediated transcriptional repression." Nucleic Acids Res **32**(20): 6096-6103.

Boyer L. A., Lee T. I., Cole M. F., Johnstone S. E., Levine S. S., Zucker J. P., Guenther M. G., Kumar R. M., Murray H. L., Jenner R. G., Gifford D. K., Melton D. A., Jaenisch R. and Young R. A. (2005). "Core Transcriptional Regulatory Circuitry in Human Embryonic Stem Cells." Cell **122**(6): 947-956.

Boyer L. A., Mathur D. and Jaenisch R. (2006). "Molecular control of pluripotency." Curr Opin Genet Dev **16**(5): 455-462.

Braam S. R., Denning C., Matsa E., Young L. E., Passier R. and Mummery C. L. (2008a). "Feeder-free culture of human embryonic stem cells in conditioned medium for efficient genetic modification." Nat. Protocols **3**(9): 1435-1443.

Braam S. R., Denning C., van den Brink S., Kats P., Hochstenbach R., Passier R. and Mummery C. L. (2008b). "Improved genetic manipulation of human embryonic stem cells." Nat Methods **5**(5): 389-392.

Brambrink T., Foreman R., Welstead G. G., Lengner C. J., Wernig M., Suh H. and Jaenisch R. (2008). "Sequential expression of pluripotency markers during direct reprogramming of mouse somatic cells." Cell Stem Cell **2**(2): 151-159.

Brena R. M., Huang T. H. and Plass C. (2006). "Toward a human epigenome." Nat Genet **38**(12): 1359-1360.

Brennecke J., Stark A., Russell R. B. and Cohen S. M. (2005). "Principles of microRNA-target recognition." PLoS Biol **3**(3): e85.

Brenner C. and Fuks F. (2006). "DNA methyltransferases: facts, clues, mysteries." Curr Top Microbiol Immunol **301**: 45-66.

Brimble S. N., Zeng X., Weiler D. A., Luo Y., Liu Y., Lyons I. G., Freed W. J., Robins A. J., Rao M. S. and Schulz T. C. (2004). "Karyotypic stability, genotyping, differentiation, feeder-free maintenance, and gene expression sampling in three human embryonic stem cell lines derived prior to August 9, 2001." Stem Cells Dev **13**(6): 585-597.

Brons I. G., Smithers L. E., Trotter M. W., Rugg-Gunn P., Sun B., Chuva de Sousa Lopes S. M., Howlett S. K., Clarkson A., Ahrlund-Richter L., Pedersen R. A. and Vallier L. (2007). "Derivation of pluripotent epiblast stem cells from mammalian embryos." Nature **448**(7150): 191-195.

Brown K. D. and Robertson K. D. (2007). "DNMT1 knockout delivers a strong blow to genome stability and cell viability." Nat Genet **39**(3): 289-290.

Brueckner B., Stresemann C., Kuner R., Mund C., Musch T., Meister M., Sultmann H. and Lyko F. (2007). "The human let-7a-3 locus contains an epigenetically regulated microRNA gene with oncogenic function." Cancer Res **67**(4): 1419-1423.

Brunner A. L., Johnson D. S., Kim S. W., Valouev A., Reddy T. E., Neff N. F., Anton E., Medina C., Nguyen L., Chiao E., Oyolu C. B., Schroth G. P., Absher D. M., Baker J. C. and Myers R. M. (2009). "Distinct DNA methylation patterns characterize differentiated human embryonic stem cells and developing human fetal liver." Genome Res **19**(6): 1044-1056.

Buchschacher G. L., Jr. and Wong-Staal F. (2000). "Development of lentiviral vectors for gene therapy for human diseases." Blood **95**(8): 2499-2504.

Buiting K., Lich C., Cottrell S., Barnicoat A. and Horsthemke B. (1999). "A 5-kb imprinting center deletion in a family with Angelman syndrome reduces the shortest region of deletion overlap to 880 bp." Hum Genet **105**(6): 665-666.

Burgold T., Spreafico F., De Santa F., Totaro M. G., Prosperini E., Natoli G. and Testa G. (2008). "The histone H3 lysine 27-specific demethylase Jmjd3 is required for neural commitment." PLoS ONE **3**(8): e3034.

Burns J. C., Friedmann T., Driever W., Burrascano M. and Yee J. K. (1993). "Vesicular stomatitis virus G glycoprotein pseudotyped retroviral vectors: concentration to very high titer and efficient gene transfer into mammalian and nonmammalian cells." Proc Natl Acad Sci U S A **90**(17): 8033-8037.

Burridge P. W., Anderson D., Priddle H., Barbadillo Munoz M. D., Chamberlain S., Allegrucci C., Young L. E. and Denning C. (2007). "Improved human embryonic stem cell embryoid body homogeneity and cardiomyocyte differentiation from a novel V-96 plate aggregation system highlights interline variability." Stem Cells **25**(4): 929-938.

Buschbeck M. and Di Croce L. (2010). "Approaching the molecular and physiological function of macroH2A variants." Epigenetics **5**(2): 118-123.

Bustin S. A. (2000). "Absolute quantification of mRNA using real-time reverse transcription polymerase chain reaction assays." J Mol Endocrinol **25**(2): 169-193.

Cairns B. R. (2005). "Chromatin remodeling complexes: strength in diversity, precision through specialization." Curr Opin Genet Dev **15**(2): 185-190.

Cairns B. R. (2009). "The logic of chromatin architecture and remodelling at promoters." Nature **461**(7261): 193-198.

Calegari F., Haubensak W., Yang D., Huttner W. B. and Buchholz F. (2002). "Tissue-specific RNA interference in postimplantation mouse embryos with endoribonuclease-prepared short interfering RNA." Proc Natl Acad Sci U S A **99**(22): 14236-14240.

Cameron C. M., Hu W. S. and Kaufman D. S. (2006). "Improved development of human embryonic stem cell-derived embryoid bodies by stirred vessel cultivation." Biotechnol Bioeng **94**(5): 938-948.

Carey B. W., Markoulaki S., Hanna J., Saha K., Gao Q., Mitalipova M. and Jaenisch R. (2009). "Reprogramming of murine and human somatic cells using a single polycistronic vector." Proc Natl Acad Sci U S A **106**(1): 157-162.

Carpenter M. K., Rosler E. and Rao M. S. (2003). "Characterization and differentiation of human embryonic stem cells." Cloning Stem Cells **5**(1): 79-88.

Carthew R. W. and Sontheimer E. J. (2009). "Origins and Mechanisms of miRNAs and siRNAs." Cell **136**(4): 642-655.

Cartwright P., McLean C., Sheppard A., Rivett D., Jones K. and Dalton S. (2005). "LIF/STAT3 controls ES cell self-renewal and pluripotency by a Myc-dependent mechanism." Development **132**(5): 885-896.

Cavalli G. (2006). "Chromatin and epigenetics in development: blending cellular memory with cell fate plasticity." Development **133**(11): 2089-2094.

Cervera R. P. and Stojkovic M. (2007). "Human Embryonic Stem Cell Derivation and Nuclear Transfer: Impact on Regenerative Therapeutics and Drug Discovery." Clin Pharmacol Ther **82**(3): 310-315.

Chakraborty C., Hsu C. H., Wen Z. H., Lin C. S. and Agoramoorthy G. (2009). "Zebrafish: a complete animal model for in vivo drug discovery and development." Curr Drug Metab **10**(2): 116-124.

Chambers I. (2004). "The molecular basis of pluripotency in mouse embryonic stem cells." Cloning Stem Cells **6**(4): 386-391.

Chambers I., Silva J., Colby D., Nichols J., Nijmeijer B., Robertson M., Vrana J., Jones K., Grotewold L. and Smith A. (2007). "Nanog safeguards pluripotency and mediates germline development." Nature **450**(7173): 1230-1234.

Chan E. M., Ratanasirintrawoot S., Park I. H., Manos P. D., Loh Y. H., Huo H., Miller J. D., Hartung O., Rho J., Ince T. A., Daley G. Q. and Schlaeger T. M. (2009). "Live cell imaging distinguishes bona fide human iPS cells from partially reprogrammed cells." Nat Biotechnol **27**(11): 1033-1037.

Chang C. W., Lai Y. S., Pawlik K. M., Liu K., Sun C. W., Li C., Schoeb T. R. and Townes T. M. (2009a). "Polycistronic Lentiviral Vector for "Hit and Run" Reprogramming of Adult Skin Fibroblasts to Induced Pluripotent Stem Cells." Stem Cells **27**(5): 1042-1049.

Chang T. C., Zeitels L. R., Hwang H. W., Chivukula R. R., Wentzel E. A., Dews M., Jung J., Gao P., Dang C. V., Beer M. A., Thomas-Tikhonenko A. and Mendell J. T. (2009b). "Lin-28B transactivation is necessary for Myc-mediated let-7 repression and proliferation." Proc Natl Acad Sci U S A **106**(9): 3384-3389.

Changolkar L. N. and Pehrson J. R. (2006). "macroH2A1 histone variants are depleted on active genes but concentrated on the inactive X chromosome." Mol Cell Biol **26**(12): 4410-4420.

Chedin F., Lieber M. R. and Hsieh C. L. (2002). "The DNA methyltransferase-like protein DNMT3L stimulates de novo methylation by Dnmt3a." Proc Natl Acad Sci U S A **99**(26): 16916-16921.

Chen C. C. and Zhong S. (2008). "Inferring gene regulatory networks by thermodynamic modeling." BMC Genomics **9 Suppl 2**: S19.

Chen T., Hevi S., Gay F., Tsujimoto N., He T., Zhang B., Ueda Y. and Li E. (2007). "Complete inactivation of DNMT1 leads to mitotic catastrophe in human cancer cells." Nat Genet **39**(3): 391-396.

Chen T., Ueda Y., Dodge J. E., Wang Z. and Li E. (2003). "Establishment and maintenance of genomic methylation patterns in mouse embryonic stem cells by Dnmt3a and Dnmt3b." Mol Cell Biol **23**(16): 5594-5605.

Chen X., Xu H., Yuan P., Fang F., Huss M., Vega V. B., Wong E., Orlov Y. L., Zhang W., Jiang J., Loh Y.-H., Yeo H. C., Yeo Z. X., Narang V., Govindarajan K. R., Leong B., Shahab A., Ruan Y., Bourque G., Sung W.-K., Clarke N. D., Wei C.-L. and Ng H.-H. (2008a). "Integration of External Signaling Pathways with the Core Transcriptional Network in Embryonic Stem Cells." Cell **133**(6): 1106-1117.

Chen X., Xu H., Yuan P., Fang F., Huss M., Vega V. B., Wong E., Orlov Y. L., Zhang W., Jiang J., Loh Y. H., Yeo H. C., Yeo Z. X., Narang V., Govindarajan K. R., Leong B., Shahab A., Ruan Y., Bourque G., Sung W. K., Clarke N. D., Wei C. L. and Ng H. H. (2008b). "Integration of external signaling pathways with the core transcriptional network in embryonic stem cells." Cell **133**(6): 1106-1117.

Chilton J. M. and Le Doux J. M. (2008). "Quantitative analysis of retroviral and lentiviral gene transfer to murine embryonic stem cells." Journal of Biotechnology **138**(1-2): 42-51.

Chung Y., Klimanskaya I., Becker S., Li T., Maserati M., Lu S. J., Zdravkovic T., Ilic D., Genbacev O., Fisher S., Krtolica A. and Lanza R. (2008). "Human embryonic stem cell lines generated without embryo destruction." Cell Stem Cell **2**(2): 113-117.

Clark A. T., Rodriguez R. T., Bodnar M. S., Abeyta M. J., Cedars M. I., Turek P. J., Firpo M. T. and Reijo Pera R. A. (2004). "Human STELLAR, NANOG, and GDF3 genes are expressed in pluripotent cells and map to chromosome 12p13, a hotspot for teratocarcinoma." Stem Cells **22**(2): 169-179.

Constancia M., Kelsey G. and Reik W. (2004). "Resourceful imprinting." Nature **432**(7013): 53-57.

Corona D. F., Clapier C. R., Becker P. B. and Tamkun J. W. (2002). "Modulation of ISWI function by site-specific histone acetylation." EMBO Rep **3**(3): 242-247.

Cortina C., Palomo-Ponce S., Iglesias M., Fernandez-Masip J. L., Vivancos A., Whissell G., Huma M., Peiro N., Gallego L., Jonkheer S., Davy A., Lloreta J., Sancho E. and Batlle E. (2007). "EphB-ephrin-B interactions suppress colorectal cancer progression by compartmentalizing tumor cells." Nat Genet **39**(11): 1376-1383.

Cosma M. P. (2002). "Ordered recruitment: gene-specific mechanism of transcription activation." Mol Cell **10**(2): 227-236.

Cowan C. A., Klimanskaya I., McMahon J., Atienza J., Witmyer J., Zucker J. P., Wang S., Morton C. C., McMahon A. P., Powers D. and Melton D. A. (2004). "Derivation of embryonic stem-cell lines from human blastocysts." N Engl J Med **350**(13): 1353-1356.

Cutter W. J., Daly E. M., Robertson D. M., Chitnis X. A., van Amelsvoort T. A., Simmons A., Ng V. W., Williams B. S., Shaw P., Conway G. S., Skuse D. H., Collier D. A., Craig M. and Murphy D. G. (2006). "Influence of X chromosome and hormones on human brain development: a magnetic resonance imaging and proton magnetic resonance spectroscopy study of Turner syndrome." Biol Psychiatry **59**(3): 273-283.

Cynthia B. E., Eric C., Yves D., Louis B., Roland W. and Amine K. (2003). "Improving Glucose and Glutamine Metabolism of Human HEK 293 and <I>Trichoplusia</I><I>ni</I> Insect Cells Engineered To Express a Cytosolic Pyruvate Carboxylase Enzyme." Biotechnology Progress **19**(1): 90-97.

D'Costa J., Brown H., Kundra P., Davis-Warren A. and Arya S. (2001). "Human immunodeficiency virus type 2 lentiviral vectors: packaging signal and splice donor in expression and encapsidation." J Gen Virol **82**(Pt 2): 425-434.

Daley G. Q., Lensch M. W., Jaenisch R., Meissner A., Plath K. and Yamanaka S. (2009). "Broader Implications of Defining Standards for the Pluripotency of iPSCs." Cell Stem Cell **4**(3): 200-201.

Dansranjavin T., Krehl S., Mueller T., Mueller L. P., Schmoll H. J. and Dammann R. H. (2009). "The role of promoter CpG methylation in the epigenetic control of stem cell related genes during differentiation." Cell Cycle **8**(6): 916-924.

Darr H. and Benvenisty N. (2009). "Genetic analysis of the role of the reprogramming gene LIN-28 in human embryonic stem cells." Stem Cells **27**(2): 352-362.

Darr H., Mayshar Y. and Benvenisty N. (2006). "Overexpression of NANOG in human ES cells enables feeder-free growth while inducing primitive ectoderm features." Development **133**(6): 1193-1201.

Davies J. and Jimenez A. (1980). "A new selective agent for eukaryotic cloning vectors." Am J Trop Med Hyg **29**(5 Suppl): 1089-1092.

Davis H. E., Morgan J. R. and Yarmush M. L. (2002). "Polybrene increases retrovirus gene transfer efficiency by enhancing receptor-independent virus adsorption on target cell membranes." Biophys Chem **97**(2-3): 159-172.

de Napoles M., Mermoud J. E., Wakao R., Tang Y. A., Endoh M., Appanah R., Nesterova T. B., Silva J., Otte A. P., Vidal M., Koseki H. and Brockdorff N. (2004). "Polycomb group proteins Ring1A/B link ubiquitylation of histone H2A to heritable gene silencing and X inactivation." Dev Cell **7**(5): 663-676.

Deb-Rinker P., Ly D., Jezierski A., Sikorska M. and Walker P. R. (2005a). "Sequential DNA Methylation of the Nanog and Oct-4 Upstream Regions in Human NT2 Cells during Neuronal Differentiation." Journal of Biological Chemistry **280**(8): 6257-6260.

Deb-Rinker P., Ly D., Jezierski A., Sikorska M. and Walker P. R. (2005b). "Sequential DNA methylation of the Nanog and Oct-4 upstream regions in human NT2 cells during neuronal differentiation." J Biol Chem **280**(8): 6257-6260.

Deng J., Shoemaker R., Xie B., Gore A., LeProust E. M., Antosiewicz-Bourget J., Egli D., Maherali N., Park I.-H., Yu J., Daley G. Q., Eggan K., Hochedlinger K., Thomson J., Wang W., Gao Y. and Zhang K. (2009). "Targeted bisulfite sequencing reveals changes in DNA methylation associated with nuclear reprogramming." Nat Biotech **27**(4): 353-360.

Denning C., Allegrucci C., Priddle H., Barbadillo-Munoz M. D., Anderson D., Self T., Smith N. M., Parkin C. T. and Young L. E. (2006). "Common culture conditions for maintenance and cardiomyocyte differentiation of the human embryonic stem cell lines, BG01 and HUES-7." Int J Dev Biol **50**(1): 27-37.

Dennis J. E. and Charbord P. (2002). "Origin and differentiation of human and murine stroma." Stem Cells **20**(3): 205-214.

Detich N., Theberge J. and Szyf M. (2002). "Promoter-specific activation and demethylation by MBD2/demethylase." J Biol Chem **277**(39): 35791-35794.

Dheda K., Huggett J. F., Bustin S. A., Johnson M. A., Rook G. and Zumla A. (2004). "Validation of housekeeping genes for normalizing RNA expression in real-time PCR." Biotechniques **37**(1): 112-114, 116, 118-119.

Dimos J. T., Rodolfa K. T., Niakan K. K., Weisenthal L. M., Mitsumoto H., Chung W., Croft G. F., Saphier G., Leibel R., Goland R., Wichterle H., Henderson C. E. and Eggan K. (2008). "Induced pluripotent stem cells generated from patients with ALS can be differentiated into motor neurons." Science **321**(5893): 1218-1221.

Ding L., Paszkowski-Rogacz M., Nitzsche A., Slabicki M. M., Heninger A.-K., Vries I. d., Kittler R., Junqueira M., Shevchenko A., Schulz H., Hubner N., Doss M. X., Sachinidis A., Hescheler J., Iacone R., Anastassiadis K., Stewart A. F., Pisabarro M. T., Caldarelli A., Poser I., Theis M. and Buchholz F. (2009). "A Genome-Scale RNAi Screen for Oct4 Modulators Defines a Role of the Paf1 Complex for Embryonic Stem Cell Identity."

Dixit R. and Boelsterli U. A. (2007). "Healthy animals and animal models of human disease(s) in safety assessment of human pharmaceuticals, including therapeutic antibodies." Drug Discov Today **12**(7-8): 336-342.

Dodge J. E., Okano M., Dick F., Tsujimoto N., Chen T., Wang S., Ueda Y., Dyson N. and Li E. (2005). "Inactivation of Dnmt3b in mouse embryonic fibroblasts results in DNA hypomethylation, chromosomal instability, and spontaneous immortalization." J Biol Chem **280**(18): 17986-17991.

Doench J. G. and Sharp P. A. (2004). "Specificity of microRNA target selection in translational repression." Genes Dev **18**(5): 504-511.

Doi A., Park I.-H., Wen B., Murakami P., Aryee M. J., Irizarry R., Herb B., Ladd-Acosta C., Rho J., Loewer S., Miller J., Schlaeger T., Daley G. Q. and Feinberg A. P. (2009). "Differential methylation of tissue- and

cancer-specific CpG island shores distinguishes human induced pluripotent stem cells, embryonic stem cells and fibroblasts." Nat Genet **41**(12): 1350 - 1353.

Dong S., Pang J. C., Hu J., Zhou L. F. and Ng H. K. (2002). "Transcriptional inactivation of TP73 expression in oligodendroglial tumors." Int J Cancer **98**(3): 370-375.

Dong S. M., Kim H. S., Rha S. H. and Sidransky D. (2001). "Promoter hypermethylation of multiple genes in carcinoma of the uterine cervix." Clin Cancer Res 7(7): 1982-1986.

Donnelly J. P. (1992). "Describing and comparing in-vitro antimicrobial activity by the box-plot technique." J Antimicrob Chemother **30**(5): 713-719.

Donze O. and Picard D. (2002). "RNA interference in mammalian cells using siRNAs synthesized with T7 RNA polymerase." Nucleic Acids Res **30**(10): e46.

Draper J. S., Smith K., Gokhale P., Moore H. D., Maltby E., Johnson J., Meisner L., Zwaka T. P., Thomson J. A. and Andrews P. W. (2004). "Recurrent gain of chromosomes 17q and 12 in cultured human embryonic stem cells." Nat Biotechnol **22**(1): 53-54.

Dudley K. J., Revill K., Whitby P., Clayton R. N. and Farrell W. E. (2008). "Genome-Wide Analysis in a Murine Dnmt1 Knockdown Model Identifies Epigenetically Silenced Genes in Primary Human Pituitary Tumors." Mol Cancer Res **6**(10): 1567-1574.

Dvash T., Mayshar Y., Darr H., McElhaney M., Barker D., Yanuka O., Kotkow K. J., Rubin L. L., Benvenisty N. and Eiges R. (2004). "Temporal gene expression during differentiation of human embryonic stem cells and embryoid bodies." Hum Reprod **19**(12): 2875-2883.

Ebert A. D., Yu J., Rose F. F., Mattis V. B., Lorson C. L., Thomson J. A. and Svendsen C. N. (2009). "Induced pluripotent stem cells from a spinal muscular atrophy patient." Nature **457**(7227): 277-280.

Efroni S., Duttagupta R., Cheng J., Dehghani H., Hoeppner D. J., Dash C., Bazett-Jones D. P., Le Grice S., McKay R. D., Buetow K. H., Gingeras T. R., Misteli T. and Meshorer E. (2008). "Global transcription in pluripotent embryonic stem cells." Cell Stem Cell **2**(5): 437-447.

Ehrlich M. (2003). "Expression of various genes is controlled by DNA methylation during mammalian development." J Cell Biochem **88**(5): 899-910.

Elias C. B., Carpentier E., Durocher Y., Bisson L., Wagner R. and Kamen A. (2003). "Improving glucose and glutamine metabolism of human HEK 293 and Trichoplusia ni insect cells engineered to express a cytosolic pyruvate carboxylase enzyme." Biotechnol Prog **19**(1): 90-97.

Eminli S., Utikal J., Arnold K., Jaenisch R. and Hochedlinger K. (2008). "Reprogramming of neural progenitor cells into induced pluripotent stem cells in the absence of exogenous Sox2 expression." Stem Cells **26**(10): 2467-2474.

Enseat-Waser R., Santana A., Vicente-Salar N. S., Cigudosa J. C., Roche E., Soria B. and Reig J. A. (2009). "ISOLATION AND CHARACTERIZATION OF RESIDUAL UNDIFFERENTIATED MOUSE EMBRYONIC STEM CELLS FROM EMBRYOID BODY CULTURES BY FLUORESCENCE TRACKING." In Vitro Cellular & Developmental Biology - Animal **42**(5 & 6): 115-123.

Enver T., Soneji S., Joshi C., Brown J., Iborra F., Orntoft T., Thykjaer T., Maltby E., Smith K., Dawud R. A., Jones M., Matin M., Gokhale P., Draper J. and Andrews P. W. (2005). "Cellular differentiation hierarchies in normal and culture-adapted human embryonic stem cells." Hum Mol Genet **14**(21): 3129-3140.

Epsztejn-Litman S., Feldman N., Abu-Remaileh M., Shufaro Y., Gerson A., Ueda J., Deplus R., Fuks F., Shinkai Y., Cedar H. and Bergman Y. (2008). "De novo DNA methylation promoted by G9a prevents reprogramming of embryonically silenced genes." Nat Struct Mol Biol **15**(11): 1176-1183.

Esteban M. A., Peng M., Deli Z., Cai J., Yang J., Xu J., Lai L. and Pei D. (2010). "Porcine induced pluripotent stem cells may bridge the gap between mouse and human iPS." IUBMB Life **62**(4): 277-282.

Esteller M. and Herman J. G. (2002). "Cancer as an epigenetic disease: DNA methylation and chromatin alterations in human tumours." J Pathol **196**(1): 1-7.

Esterre P., Melin M., Serrar M. and Grimaud J. A. (1992). "New specific markers of human and mouse fibroblasts." Cell Mol Biol **38**(3): 297-301.

Evans P. M., Chen X., Zhang W. and Liu C. (2010). "KLF4 interacts with beta-catenin/TCF4 and blocks p300/CBP recruitment by beta-catenin." Mol Cell Biol **30**(2): 372-381.

Evron E., Umbricht C. B., Korz D., Raman V., Loeb D. M., Niranjan B., Buluwela L., Weitzman S. A., Marks J. and Sukumar S. (2001). "Loss of cyclin D2 expression in the majority of breast cancers is associated with promoter hypermethylation." Cancer Res **61**(6): 2782-2787.

Fahrenkrug S. C., Freking B. A., Rexroad C. E., 3rd, Leymaster K. A., Kappes S. M. and Smith T. P. (2000). "Comparative mapping of the ovine clpg locus." Mamm Genome **11**(10): 871-876.

Farthing C. R., Ficz G., Ng R. K., Chan C. F., Andrews S., Dean W., Hemberger M. and Reik W. (2008). "Global mapping of DNA methylation in mouse promoters reveals epigenetic reprogramming of pluripotency genes." PLoS Genet **4**(6): e1000116.

Faust C., Lawson K. A., Schork N. J., Thiel B. and Magnuson T. (1998). "The Polycomb-group gene eed is required for normal morphogenetic movements during gastrulation in the mouse embryo." Development **125**(22): 4495-4506.

Fazzio T. G., Huff J. T. and Panning B. (2008). "An RNAi screen of chromatin proteins identifies Tip60-p400 as a regulator of embryonic stem cell identity." Cell **134**(1): 162-174.

Fazzio T. G. and Tsukiyama T. (2003). "Chromatin remodeling in vivo: evidence for a nucleosome sliding mechanism." Mol Cell **12**(5): 1333-1340.

Fedorov Y., Anderson E. M., Birmingham A., Reynolds A., Karpilow J., Robinson K., Leake D., Marshall W. S. and Khvorova A. (2006). "Off-target effects by siRNA can induce toxic phenotype." RNA **12**(7): 1188-1196.

Feinberg A. P. (2007). "Phenotypic plasticity and the epigenetics of human disease." Nature **447**(7143): 433-440.

Feldman N., Gerson A., Fang J., Li E., Zhang Y., Shinkai Y., Cedar H. and Bergman Y. (2006). "G9a-mediated irreversible epigenetic inactivation of Oct-3/4 during early embryogenesis." Nat Cell Biol **8**(2): 188-194.

Feng B., Ng J. H., Heng J. C. and Ng H. H. (2009). "Molecules that Promote or Enhance Reprogramming of Somatic Cells to Induced Pluripotent Stem Cells." Cell Stem Cell **4**(4): 301-312.

Ferguson-Smith A. C. and Surani M. A. (2001). "Imprinting and the epigenetic asymmetry between parental genomes." Science **293**(5532): 1086-1089.

Ferri A. L., Cavallaro M., Braida D., Di Cristofano A., Canta A., Vezzani A., Ottolenghi S., Pandolfi P. P., Sala M., DeBiasi S. and Nicolis S. K. (2004). "Sox2 deficiency causes neurodegeneration and impaired neurogenesis in the adult mouse brain." Development **131**(15): 3805-3819.

Filipowicz W. (2005). "RNAi: The Nuts and Bolts of the RISC Machine." Cell **122**(1): 17-20.

Fiskus W., Buckley K., Rao R., Mandawat A., Yang Y., Joshi R., Wang Y., Balusu R., Chen J., Koul S., Joshi A., Upadhyay S., Atadja P. and Bhalla K. N. (2009). "Panobinostat treatment depletes EZH2 and DNMT1 levels and enhances decitabine mediated de-repression of JunB and loss of survival of human acute leukemia cells." Cancer Biol Ther **8**(10): 939-950.

Fitzpatrick G. V., Soloway P. D. and Higgins M. J. (2002). "Regional loss of imprinting and growth deficiency in mice with a targeted deletion of KvDMR1." Nat Genet **32**(3): 426-431.

Follenzi A. and Naldini L. (2002). "HIV-based vectors. Preparation and use." Methods Mol Med **69**: 259-274.

Fong H., Hohenstein K. A. and Donovan P. J. (2008). "Regulation of self-renewal and pluripotency by Sox2 in human embryonic stem cells." Stem Cells **26**(8): 1931-1938.

Fournier C., Goto Y., Ballestar E., Delaval K., Hever A. M., Esteller M. and Feil R. (2002). "Allele-specific histone lysine methylation marks regulatory regions at imprinted mouse genes." Embo J **21**(23): 6560-6570.

Fouse S. D., Shen Y., Pellegrini M., Cole S., Meissner A., Van Neste L., Jaenisch R. and Fan G. (2008). "Promoter CpG methylation contributes to ES cell gene regulation in parallel with Oct4/Nanog, PcG complex, and histone H3 K4/K27 trimethylation." Cell Stem Cell **2**(2): 160-169.

Fuda N. J., Ardehali M. B. and Lis J. T. (2009). "Defining mechanisms that regulate RNA polymerase II transcription in vivo." Nature **461**(7261): 186-192.

Fulka H., Mrazek M., Tepla O. and Fulka J., Jr. (2004). "DNA methylation pattern in human zygotes and developing embryos." Reproduction **128**(6): 703-708.

Gai H., Leung E. L., Costantino P. D., Aguila J. R., Nguyen D. M., Fink L. M., Ward D. C. and Ma Y. (2009). "Generation and characterization of functional cardiomyocytes using induced pluripotent stem cells derived from human fibroblasts." Cell Biol Int.

Ganesan S., Richardson A. L., Wang Z. C., Iglehart J. D., Miron A., Feunteun J., Silver D. and Livingston D. M. (2005). "Abnormalities of the inactive X chromosome are a common feature of BRCA1 mutant and sporadic basal-like breast cancer." Cold Spring Harb Symp Quant Biol **70**: 93-97.

Gao X., Tate P., Hu P., Tjian R., Skarnes W. C. and Wang Z. (2008). "ES cell pluripotency and germ-layer formation require the SWI/SNF chromatin remodeling component BAF250a." Proc Natl Acad Sci U S A **105**(18): 6656-6661.

Garrett-Sinha L. A., Eberspaecher H., Seldin M. F. and de Crombrugghe B. (1996). "A gene for a novel zinc-finger protein expressed in differentiated epithelial cells and transiently in certain mesenchymal cells." J Biol Chem **271**(49): 31384-31390.

Garton K. J., Ferri N. and Raines E. W. (2002). "Efficient expression of exogenous genes in primary vascular cells using IRES-based retroviral vectors." Biotechniques **32**(4): 830, 832, 834 passim.

Gaspar-Maia A., Alajem A., Polesso F., Sridharan R., Mason M. J., Heidersbach A., Ramalho-Santos J. o., McManus M. T., Plath K., Meshorer E. and Ramalho-Santos M. (2009). "Chd1 regulates open chromatin and pluripotency of embryonic stem cells." Nature **460**(7257): 863-868.

Genbacev O., Krtolica A., Zdravkovic T., Brunette E., Powell S., Nath A., Caceres E., McMaster M., McDonagh S., Li Y., Mandalam R., Lebkowski J. and Fisher S. J. (2005). "Serum-free derivation of human embryonic stem cell lines on human placental fibroblast feeders." Fertil Steril **83**(5): 1517-1529.

Georgiades P., Cox B., Gertsenstein M., Chawengsaksophak K. and Rossant J. (2007). "Trophoblast-specific gene manipulation using lentivirus-based vectors " BioTechniques.

Geraerts M., Willems S., Baekelandt V., Debyser Z. and Gijsbers R. (2006). "Comparison of lentiviral vector titration methods." BMC Biotechnol **6**: 34.

Ghosh Z., Wilson K. D., Wu Y., Hu S., Quertermous T. and Wu J. C. (2010). "Persistent donor cell gene expression among human induced pluripotent stem cells contributes to differences with human embryonic stem cells." PLoS One **5**(2): e8975.

Gilbert N., Boyle S., Fiegler H., Woodfine K., Carter N. P. and Bickmore W. A. (2004). "Chromatin architecture of the human genome: gene-rich domains are enriched in open chromatin fibers." Cell **118**(5): 555-566.

Giraldez A. J., Mishima Y., Rihel J., Grocock R. J., Van Dongen S., Inoue K., Enright A. J. and Schier A. F. (2006). "Zebrafish MiR-430 promotes deadenylation and clearance of maternal mRNAs." Science **312**(5770): 75-79.

Glasel J. A. (1995). "Validity of nucleic acid purities monitored by 260nm/280nm absorbance ratios." Biotechniques **18**(1): 62-63.

Goldstein S. (1990). "Replicative senescence: the human fibroblast comes of age." Science **249**(4973): 1129-1133.

Gomez D. E., Alonso D. F., Yoshiji H. and Thorgeirsson U. P. (1997). "Tissue inhibitors of metalloproteinases: structure, regulation and biological functions." Eur J Cell Biol **74**(2): 111-122.

Gondor A. and Ohlsson R. (2009). "Replication timing and epigenetic reprogramming of gene expression: a two-way relationship?" Nat Rev Genet **10**(4): 269-276.

Gonzalez F., Barragan Monasterio M., Tiscornia G., Montserrat Pulido N., Vassena R., Batlle Morera L., Rodriguez Piza I. and Izpisua Belmonte J. C. (2009). "Generation of mouse-induced pluripotent stem cells by transient expression of a single nonviral polycistronic vector." Proc Natl Acad Sci U S A **106**(22): 8918-8922.

Gonzalez S., Pisano D. G. and Serrano M. (2008). "Mechanistic principles of chromatin remodeling guided by siRNAs and miRNAs." Cell Cycle **7**(16): 2601-2608.

Gonzalo S., Jaco I., Fraga M. F., Chen T., Li E., Esteller M. and Blasco M. A. (2006). "DNA methyltransferases control telomere length and telomere recombination in mammalian cells." Nat Cell Biol **8**(4): 416-424.

Gopalakrishnan S., Van Emburgh B. O. and Robertson K. D. (2008). "DNA methylation in development and human disease." Mutat Res **647**(1-2): 30-38.

Gowher H., Leismann O. and Jeltsch A. (2000). "DNA of Drosophila melanogaster contains 5-methylcytosine." EMBO J **19**(24): 6918-6923.

Gowher H., Liebert K., Hermann A., Xu G. and Jeltsch A. (2005). "Mechanism of stimulation of catalytic activity of Dnmt3A and Dnmt3B DNA-(cytosine-C5)-methyltransferases by Dnmt3L." J Biol Chem **280**(14): 13341-13348.

Graham F. L., Smiley J., Russell W. C. and Nairn R. (1977). "Characteristics of a human cell line transformed by DNA from human adenovirus type 5." J Gen Virol **36**(1): 59-74.

Graham V., Khudyakov J., Ellis P. and Pevny L. (2003). "SOX2 functions to maintain neural progenitor identity." Neuron **39**(5): 749-765.

Grandela C. and Wolvetang E. (2007). "hESC adaptation, selection and stability." Stem Cell Rev **3**(3): 183-191.

Grandjean V., O'Neill L., Sado T., Turner B. and Ferguson-Smith A. (2001). "Relationship between DNA methylation, histone H4 acetylation and gene expression in the mouse imprinted Igf2-H19 domain." FEBS Lett **488**(3): 165-169.

Gruenbaum Y., Stein R., Cedar H. and Razin A. (1981). "Methylation of CpG sequences in eukaryotic DNA." FEBS Lett **124**(1): 67-71.

Gu P., Le Menuet D., Chung A. C. and Cooney A. J. (2006). "Differential recruitment of methylated CpG binding domains by the orphan receptor GCNF initiates the repression and silencing of Oct4 expression." Mol Cell Biol **26**(24): 9471-9483.

Guelen L., Pagie L., Brasset E., Meuleman W., Faza M. B., Talhout W., Eussen B. H., de Klein A., Wessels L., de Laat W. and van Steensel B. (2008). "Domain organization of human chromosomes revealed by mapping of nuclear lamina interactions." Nature **453**(7197): 948-951.

Haase A., Olmer R., Schwanke K., Wunderlich S., Merkert S., Hess C., Zweigerdt R., Gruh I., Meyer J., Wagner S., Maier L. S., Han D. W., Glage S., Miller K., Fischer P., Scholer H. R. and Martin U. (2009). "Generation of induced pluripotent stem cells from human cord blood." Cell Stem Cell **5**(4): 434-441.

Hake S. B. and Allis C. D. (2006). "Histone H3 variants and their potential role in indexing mammalian genomes: the "H3 barcode hypothesis"." Proc Natl Acad Sci U S A **103**(17): 6428-6435.

Hanna J., Markoulaki S., Schorderet P., Carey B. W., Beard C., Wernig M., Creyghton M. P., Steine E. J., Cassady J. P., Foreman R., Lengner C. J., Dausman J. A. and Jaenisch R. (2008). "Direct reprogramming of terminally differentiated mature B lymphocytes to pluripotency." Cell **133**(2): 250-264.

Hanna J., Saha K., Pando B., van Zon J., Lengner C. J., Creyghton M. P., van Oudenaarden A. and Jaenisch R. (2009). "Direct cell reprogramming is a stochastic process amenable to acceleration." Nature **462**(7273): 595-601.

Hanna J., Wernig M., Markoulaki S., Sun C. W., Meissner A., Cassady J. P., Beard C., Brambrink T., Wu L. C., Townes T. M. and Jaenisch R. (2007). "Treatment of sickle cell anemia mouse model with iPS cells generated from autologous skin." Science **318**(5858): 1920-1923.

Hanna L. A., Foreman R. K., Tarasenko I. A., Kessler D. S. and Labosky P. A. (2002). "Requirement for Foxd3 in maintaining pluripotent cells of the early mouse embryo." Genes Dev **16**(20): 2650-2661.

Hansen R. S., Wijmenga C., Luo P., Stanek A. M., Canfield T. K., Weemaes C. M. and Gartler S. M. (1999). "The DNMT3B DNA methyltransferase gene is mutated in the ICF immunodeficiency syndrome." Proc Natl Acad Sci U S A **96**(25): 14412-14417.

Harrison T., Graham F. and Williams J. (1977). "Host-range mutants of adenovirus type 5 defective for growth in HeLa cells." Virology **77**(1): 319-329.

Hattori N., Abe T., Suzuki M., Matsuyama T., Yoshida S., Li E. and Shiota K. (2004). "Preference of DNA methyltransferases for CpG islands in mouse embryonic stem cells." Genome Res **14**(9): 1733-1740.

Hay D. C., Fletcher J., Payne C., Terrace J. D., Gallagher R. C. J., Snoeys J., Black J. R., Wojtacha D., Samuel K., Hannoun Z., Pryde A., Filippi C., Currie I. S., Forbes S. J., Ross J. A., Newsome P. N. and Iredale J. P. (2008). "Highly efficient differentiation of hESCs to functional hepatic endoderm requires ActivinA and Wnt3a signaling." Proceedings of the National Academy of Sciences **105**(34): 12301-12306.

Hayflick L. and Moorhead P. S. (1961). "The serial cultivation of human diploid cell strains." Exp Cell Res **25**: 585-621.

Hayward B. E., Moran V., Strain L. and Bonthron D. T. (1998). "Bidirectional imprinting of a single gene: GNAS1 encodes maternally, paternally, and biallelically derived proteins." Proc Natl Acad Sci U S A **95**(26): 15475-15480.

He J., Wang Y. and Li Y. L. (2007). "Fibroblast-like cells derived from the gonadal ridges and dorsal mesenteries of human embryos as feeder cells for the culture of human embryonic germ cells." J Biomed Sci **14**(5): 617-628.

He J., Yang Q. and Chang L. J. (2005). "Dynamic DNA methylation and histone modifications contribute to lentiviral transgene silencing in murine embryonic carcinoma cells." J Virol **79**(21): 13497-13508.

Heins N., Englund M. C., Sjoblom C., Dahl U., Tonning A., Bergh C., Lindahl A., Hanson C. and Semb H. (2004). "Derivation, characterization, and differentiation of human embryonic stem cells." Stem Cells **22**(3): 367-376.

Hemberger M., Dean W. and Reik W. (2009). "Epigenetic dynamics of stem cells and cell lineage commitment: digging Waddington's canal." Nat Rev Mol Cell Biol **10**(8): 526-537.

Hendrich B. and Bird A. (1998). "Identification and characterization of a family of mammalian methyl-CpG binding proteins." Mol Cell Biol **18**(11): 6538-6547.

Hendrich B., Guy J., Ramsahoye B., Wilson V. A. and Bird A. (2001). "Closely related proteins MBD2 and MBD3 play distinctive but interacting roles in mouse development." Genes Dev **15**(6): 710-723.

Heng B. C., Liu H., Ge Z. and Cao T. (2007). "Mechanical dissociation of human embryonic stem cell colonies by manual scraping after collagenase treatment is much more detrimental to cellular viability than is trypsinization with gentle pipetting." Biotechnol Appl Biochem **47**(Pt 1): 33-37.

Herman J. G., Graff J. R., Myohanen S., Nelkin B. D. and Baylin S. B. (1996). "Methylation-specific PCR: a novel PCR assay for methylation status of CpG islands." Proc Natl Acad Sci U S A **93**(18): 9821-9826.

Hester M. E., Song S., Miranda C. J., Eagle A., Schwartz P. H. and Kaspar B. K. (2009). "Two factor reprogramming of human neural stem cells into pluripotency." PLoS One **4**(9): e7044.

Hirami Y., Osakada F., Takahashi K., Okita K., Yamanaka S., Ikeda H., Yoshimura N. and Takahashi M. (2009). "Generation of retinal cells from mouse and human induced pluripotent stem cells." Neuroscience Letters **458**(3): 126-131.

Ho L. and Crabtree G. R. (2010). "Chromatin remodelling during development." Nature **463**(7280): 474-484.

Ho L., Jothi R., Ronan J. L., Cui K., Zhao K. and Crabtree G. R. (2009a). "An embryonic stem cell chromatin remodeling complex, esBAF, is an essential component of the core pluripotency transcriptional network." Proc Natl Acad Sci U S A **106**(13): 5187-5191.

Ho L., Ronan J. L., Wu J., Staahl B. T., Chen L., Kuo A., Lessard J., Nesvizhskii A. I., Ranish J. and Crabtree G. R. (2009b). "An embryonic stem cell chromatin remodeling complex, esBAF, is essential for embryonic stem cell self-renewal and pluripotency." Proc Natl Acad Sci U S A **106**(13): 5181-5186.

Hochedlinger K. and Jaenisch R. (2006). "Nuclear reprogramming and pluripotency." Nature **441**(7097): 1061-1067.

Hochedlinger K. and Plath K. (2009). "Epigenetic reprogramming and induced pluripotency." Development **136**(4): 509-523.

Hoffman L. M. and Carpenter M. K. (2005). "Characterization and culture of human embryonic stem cells." Nat Biotechnol **23**(6): 699-708.

Holliday R. (1994). "Epigenetics: an overview." Dev Genet **15**(6): 453-457.

Hong H., Takahashi K., Ichisaka T., Aoi T., Kanagawa O., Nakagawa M., Okita K. and Yamanaka S. (2009). "Suppression of induced pluripotent stem cell generation by the p53-p21 pathway." Nature **460**(7259): 1132-1135.

Hong S., Cho Y. W., Yu L. R., Yu H., Veenstra T. D. and Ge K. (2007). "Identification of JmjC domain-containing UTX and JMJD3 as histone H3 lysine 27 demethylases." Proc Natl Acad Sci U S A **104**(47): 18439-18444.

Hore T. A., Rapkins R. W. and Graves J. A. (2007). "Construction and evolution of imprinted loci in mammals." Trends Genet **23**(9): 440-448.

Hotta A., Cheung A. Y. L., Farra N., Vijayaragavan K., Seguin C. A., Draper J. S., Pasceri P., Maksakova I. A., Mager D. L., Rossant J., Bhatia M. and Ellis J. (2009). "Isolation of human iPS cells using EOS lentiviral vectors to select for pluripotency." Nat Meth **6**(5): 370-376.

Hu J. F., Pham J., Dey I., Li T., Vu T. H. and Hoffman A. R. (2000). "Allele-specific histone acetylation accompanies genomic imprinting of the insulin-like growth factor II receptor gene." Endocrinology **141**(12): 4428-4435.

Hu Y. G., Hirasawa R., Hu J. L., Hata K., Li C. L., Jin Y., Chen T., Li E., Rigolet M., Viegas-Pequignot E., Sasaki H. and Xu G. L. (2008). "Regulation of DNA methylation activity through Dnmt3L promoter methylation by Dnmt3 enzymes in embryonic development." Hum Mol Genet **17**(17): 2654-2664.

Huang S. (2009). "Reprogramming cell fates: reconciling rarity with robustness." Bioessays **31**(5): 546-560.

Huangfu D., Maehr R., Guo W., Eijkelenboom A., Snitow M., Chen A. E. and Melton D. A. (2008a). "Induction of pluripotent stem cells by defined factors is greatly improved by small-molecule compounds." Nat Biotechnol **26**(7): 795-797.

Huangfu D., Osafune K., Maehr R., Guo W., Eijkelenboom A., Chen S., Muhlestein W. and Melton D. A. (2008b). "Induction of pluripotent stem cells from primary human fibroblasts with only Oct4 and Sox2." Nat Biotech **26**(11): 1269-1275.

Huggett J., Dheda K., Bustin S. and Zumla A. (2005). "Real-time RT-PCR normalisation; strategies and considerations." Genes Immun **6**(4): 279-284.

Hutvagner G. and Simard M. J. (2008). "Argonaute proteins: key players in RNA silencing." Nat Rev Mol Cell Biol **9**(1): 22-32.

Hyslop L., Stojkovic M., Armstrong L., Walter T., Stojkovic P., Przyborski S., Herbert M., Murdoch A., Strachan T. and Lako M. (2005). "Downregulation of NANOG induces differentiation of human embryonic stem cells to extraembryonic lineages." Stem Cells **23**(8): 1035-1043.

Ichida J. K., Blanchard J., Lam K., Son E. Y., Chung J. E., Egli D., Loh K. M., Carter A. C., Di Giorgio F. P., Koszka K., Huangfu D., Akutsu H., Liu D. R., Rubin L. L. and Eggan K. (2009). "A small-molecule inhibitor of tgf-Beta signaling replaces sox2 in reprogramming by inducing nanog." Cell Stem Cell **5**(5): 491-503.

Illingworth R., Kerr A., Desousa D., Jorgensen H., Ellis P., Stalker J., Jackson D., Clee C., Plumb R., Rogers J., Humphray S., Cox T., Langford C. and Bird A. (2008). "A novel CpG island set identifies tissue-specific methylation at developmental gene loci." PLoS Biol **6**(1): e22.

Imamura M., Miura K., Iwabuchi K., Ichisaka T., Nakagawa M., Lee J., Kanatsu-Shinohara M., Shinohara T. and Yamanaka S. (2006). "Transcriptional repression and DNA hypermethylation of a small set of ES cell marker genes in male germline stem cells." BMC Dev Biol **6**: 34.

Imura M., Yamashita S., Cai L. Y., Furuta J., Wakabayashi M., Yasugi T. and Ushijima T. (2006). "Methylation and expression analysis of 15 genes and three normally-methylated genes in 13 Ovarian cancer cell lines." Cancer Lett **241**(2): 213-220.

Inzunza J., Gertow K., Stromberg M. A., Matilainen E., Blennow E., Skottman H., Wolbank S., Ahrlund-Richter L. and Hovatta O. (2005). "Derivation of human embryonic stem cell lines in serum replacement medium using postnatal human fibroblasts as feeder cells." Stem Cells **23**(4): 544-549.

Itskovitz-Eldor J., Schuldiner M., Karsenti D., Eden A., Yanuka O., Amit M., Soreq H. and Benvenisty N. (2000). "Differentiation of human embryonic stem cells into embryoid bodies compromising the three embryonic germ layers." Mol Med **6**(2): 88-95.

Ivanova N., Dobrin R., Lu R., Kotenko I., Levorse J., DeCoste C., Schafer X., Lun Y. and Lemischka I. R. (2006). "Dissecting self-renewal in stem cells with RNA interference." Nature **442**(7102): 533-538.

Jacinto F. V., Ballestar E. and Esteller M. (2009). "Impaired recruitment of the histone methyltransferase DOT1L contributes to the incomplete reactivation of tumor suppressor genes upon DNA demethylation." Oncogene.

Jackson-Grusby L., Beard C., Possemato R., Tudor M., Fambrough D., Csankovszki G., Dausman J., Lee P., Wilson C., Lander E. and Jaenisch R. (2001). "Loss of genomic methylation causes p53-dependent apoptosis and epigenetic deregulation." Nat Genet **27**(1): 31-39.

Jackson A. L. and Linsley P. S. (2004). "Noise amidst the silence: off-target effects of siRNAs?" Trends in Genetics **20**(11): 521-524.

Jackson M., Baird J. W., Cambray N., Ansell J. D., Forrester L. M. and Graham G. J. (2002). "Cloning and Characterization of Ehox, a Novel Homeobox Gene Essential for Embryonic Stem Cell Differentiation." Journal of Biological Chemistry **277**(41): 38683-38692.

Jackson M., Krassowska A., Gilbert N., Chevassut T., Forrester L., Ansell J. and Ramsahoye B. (2004). "Severe global DNA hypomethylation blocks differentiation and induces histone hyperacetylation in embryonic stem cells." Mol Cell Biol **24**(20): 8862-8871.

Jaenisch R. and Young R. (2008). "Stem Cells, the Molecular Circuitry of Pluripotency and Nuclear Reprogramming." Cell **132**(4): 567-582.

James D., Levine A. J., Besser D. and Hemmati-Brivanlou A. (2005). "TGFbeta/activin/nodal signaling is necessary for the maintenance of pluripotency in human embryonic stem cells." Development **132**(6): 1273-1282.

Jelinic P. and Shaw P. (2007). "Loss of imprinting and cancer." J Pathol **211**(3): 261-268.

Ji Z. and Tian B. (2009). "Reprogramming of 3' untranslated regions of mRNAs by alternative polyadenylation in generation of pluripotent stem cells from different cell types." PLoS ONE **4**(12): e8419.

Jia F., Wilson K. D., Sun N., Gupta D. M., Huang M., Li Z., Panetta N. J., Chen Z. Y., Robbins R. C., Kay M. A., Longaker M. T. and Wu J. C. (2010). "A nonviral minicircle vector for deriving human iPS cells." Nat Methods 7(3): 197-199.

Jiang J., Chan Y. S., Loh Y. H., Cai J., Tong G. Q., Lim C. A., Robson P., Zhong S. and Ng H. H. (2008). "A core Klf circuitry regulates self-renewal of embryonic stem cells." Nat Cell Biol **10**(3): 353-360.

Jin B., Tao Q., Peng J., Soo H. M., Wu W., Ying J., Fields C. R., Delmas A. L., Liu X., Qiu J. and Robertson K. D. (2008). "DNA methyltransferase 3B (DNMT3B) mutations in ICF syndrome lead to altered epigenetic modifications and aberrant expression of genes regulating development, neurogenesis and immune function." Hum Mol Genet **17**(5): 690-709.

Jinawath A., Miyake S., Yanagisawa Y., Akiyama Y. and Yuasa Y. (2005). "Transcriptional regulation of the human DNA methyltransferase 3A and 3B genes by Sp3 and Sp1 zinc finger proteins." Biochem J **385**(Pt 2): 557-564.

Jinek M. and Doudna J. A. (2009). "A three-dimensional view of the molecular machinery of RNA interference." Nature **457**(7228): 405-412.

Johnson C. D., Esquela-Kerscher A., Stefani G., Byrom M., Kelnar K., Ovcharenko D., Wilson M., Wang X., Shelton J., Shingara J., Chin L., Brown D. and Slack F. J. (2007). "The let-7 microRNA represses cell proliferation pathways in human cells." Cancer Res **67**(16): 7713-7722.

Johnson S. M., Grosshans H., Shingara J., Byrom M., Jarvis R., Cheng A., Labourier E., Reinert K. L., Brown D. and Slack F. J. (2005). "RAS is regulated by the let-7 microRNA family." Cell **120**(5): 635-647.

Jones P. A. and Liang G. (2009). "Rethinking how DNA methylation patterns are maintained." Nat Rev Genet **10**(11): 805-811.

Judson H., Hayward B. E., Sheridan E. and Bonthron D. T. (2002). "A global disorder of imprinting in the human female germ line." Nature **416**(6880): 539-542.

Jung Y., Park J., Kim T. Y., Park J. H., Jong H. S., Im S. A., Robertson K. D. and Bang Y. J. (2007). "Potential advantages of DNA methyltransferase 1 (DNMT1)-targeted inhibition for cancer therapy." J Mol Med **85**(10): 1137-1148.

Kaji K., Caballero I. M., MacLeod R., Nichols J., Wilson V. A. and Hendrich B. (2006). "The NuRD component Mbd3 is required for pluripotency of embryonic stem cells." Nat Cell Biol **8**(3): 285-292.

Kaji K., Norrby K., Paca A., Mileikovsky M., Mohseni P. and Woltjen K. (2009). "Virus-free induction of pluripotency and subsequent excision of reprogramming factors." Nature **458**(7239): 771-775.

Kalluri R. and Neilson E. G. (2003). "Epithelial-mesenchymal transition and its implications for fibrosis." J Clin Invest **112**(12): 1776-1784.

Kaneda M., Okano M., Hata K., Sado T., Tsujimoto N., Li E. and Sasaki H. (2004). "Essential role for de novo DNA methyltransferase Dnmt3a in paternal and maternal imprinting." Nature **429**(6994): 900-903.

Kangaspeska S., Stride B., Metivier R., Polycarpou-Schwarz M., Ibberson D., Carmouche R. P., Benes V., Gannon F. and Reid G. (2008). "Transient cyclical methylation of promoter DNA." Nature **452**(7183): 112-115.

Kannagi R., Cochran N. A., Ishigami F., Hakomori S., Andrews P. W., Knowles B. B. and Solter D. (1983). "Stage-specific embryonic antigens (SSEA-3 and -4) are epitopes of a unique globo-series ganglioside isolated from human teratocarcinoma cells." EMBO J **2**(12): 2355-2361.

Kappel S., Matthess Y., Kaufmann M. and Strebhardt K. (2007). "Silencing of mammalian genes by tetracycline-inducible shRNA expression." Nat Protoc **2**(12): 3257-3269.

Karpf A. R. and Matsui S. (2005). "Genetic disruption of cytosine DNA methyltransferase enzymes induces chromosomal instability in human cancer cells." Cancer Res **65**(19): 8635-8639.

Katsuhisa T., Mitsuru I., Kenji K., Fuminori S., Koichi Y., Takao H. and Hiroyuki M. (2009). "Efficient Adipocyte and Osteoblast Differentiation From Mouse Induced Pluripotent Stem Cells By Adenoviral Transduction." Stem Cells **27**(8): 1802 - 1811.

Kawakami T., Chano T., Minami K., Okabe H., Okada Y. and Okamoto K. (2006). "Imprinted DLK1 is a putative tumor suppressor gene and inactivated by epimutation at the region upstream of GTL2 in human renal cell carcinoma." Hum Mol Genet **15**(6): 821-830.

Kawamura T., Suzuki J., Wang Y. V., Menendez S., Morera L. B., Raya A., Wahl G. M. and Belmonte J. C. (2009). "Linking the p53 tumour suppressor pathway to somatic cell reprogramming." Nature **460**(7259): 1140-1144.

Kehat I., Kenyagin-Karsenti D., Snir M., Segev H., Amit M., Gepstein A., Livne E., Binah O., Itskovitz-Eldor J. and Gepstein L. (2001). "Human embryonic stem cells can differentiate into myocytes with structural and functional properties of cardiomyocytes." J Clin Invest **108**(3): 407-414.

Kerjean A., Dupont J. M., Vasseur C., Le Tessier D., Cuisset L., Paldi A., Jouannet P. and Jeanpierre M. (2000). "Establishment of the paternal methylation imprint of the human H19 and MEST/PEG1 genes during spermatogenesis." Hum Mol Genet **9**(14): 2183-2187.

Kim D., Kim C.-H., Moon J.-I., Chung Y.-G., Chang M.-Y., Han B.-S., Ko S., Yang E., Cha K. Y., Lanza R. and Kim K.-S. (2009a). "Generation of Human Induced Pluripotent Stem Cells by Direct Delivery of Reprogramming Proteins." Cell Stem Cell **4**(6): 472-476.

Kim J., Chu J., Shen X., Wang J. and Orkin S. H. (2008a). "An extended transcriptional network for pluripotency of embryonic stem cells." Cell **132**(6): 1049-1061.

Kim J. B., Greber B., Arauzo-Bravo M. J., Meyer J., Park K. I., Zaehres H. and Scholer H. R. (2009b). "Direct reprogramming of human neural stem cells by OCT4." Nature **461**(7264): 649-643.

Kim J. B., Sebastiano V., Wu G., Araúzo-Bravo M. J., Sasse P., Gentile L., Ko K., Ruau D., Ehrich M., van den Boom D., Meyer J., Hübner K., Bernemann C., Ortmeier C., Zenke M., Fleischmann B. K., Zaehres H. and Schöler H. R. (2009c). "Oct4-Induced Pluripotency in Adult Neural Stem Cells." Cell **136**(3): 411-419.

Kim J. B., Zaehres H., Wu G., Gentile L., Ko K., Sebastiano V., Arauzo-Bravo M. J., Ruau D., Han D. W., Zenke M. and Scholer H. R. (2008b). "Pluripotent stem cells induced from adult neural stem cells by reprogramming with two factors." Nature **454**(7204): 646-650.

Kim K. P., Thurston A., Mummery C., Ward-van Oostwaard D., Priddle H., Allegrucci C., Denning C. and Young L. (2007). "Gene-specific vulnerability to imprinting variability in human embryonic stem cell lines." Genome Res **17**(12): 1731-1742.

Kim V. N., Han J. and Siomi M. C. (2009d). "Biogenesis of small RNAs in animals." Nat Rev Mol Cell Biol **10**(2): 126-139.

Kivirikko K. I., Myllyla R. and Pihlajaniemi T. (1989). "Protein hydroxylation: prolyl 4-hydroxylase, an enzyme with four cosubstrates and a multifunctional subunit." FASEB J **3**(5): 1609-1617.

Klein R., Ruttkowski B., Knapp E., Salmons B., Gunzburg W. H. and Hohenadl C. (2006). "WPRE-mediated enhancement of gene expression is promoter and cell line specific." Gene **372**: 153-161.

Kleinman H. K. and Martin G. R. (2005). "Matrigel: basement membrane matrix with biological activity." Semin Cancer Biol **15**(5): 378-386.

Klimanskaya I., Chung Y., Becker S., Lu S. J. and Lanza R. (2006). "Human embryonic stem cell lines derived from single blastomeres." Nature **444**(7118): 481-485.

Koestenbauer S., Zech N. H., Juch H., Vanderzwalmen P., Schoonjans L. and Dohr G. (2006). "Embryonic stem cells: similarities and differences between human and murine embryonic stem cells." Am J Reprod Immunol **55**(3): 169-180.

Koivisto H., Hyvarinen M., Stromberg A. M., Inzunza J., Matilainen E., Mikkola M., Hovatta O. and Teerijoki H. (2004). "Cultures of human embryonic stem cells: serum replacement medium or serum-containing media and the effect of basic fibroblast growth factor." Reprod Biomed Online **9**(3): 330-337.

Kouzarides T. (2007). "Chromatin Modifications and Their Function." Cell **128**(4): 693-705.

Kubicek S., O'Sullivan R. J., August E. M., Hickey E. R., Zhang Q., Teodoro M. L., Rea S., Mechtler K., Kowalski J. A., Homon C. A., Kelly T. A. and Jenuwein T. (2007). "Reversal of H3K9me2 by a small-molecule inhibitor for the G9a histone methyltransferase." Mol Cell **25**(3): 473-481.

Kumar M. S., Lu J., Mercer K. L., Golub T. R. and Jacks T. (2007). "Impaired microRNA processing enhances cellular transformation and tumorigenesis." Nat Genet **39**(5): 673-677.

Kurdistani S. K. and Grunstein M. (2003). "Histone acetylation and deacetylation in yeast." Nat Rev Mol Cell Biol **4**(4): 276-284.

Kurreck J. (2003). "Antisense technologies. Improvement through novel chemical modifications." Eur J Biochem **270**(8): 1628-1644.

Kutner R. H., Zhang X. Y. and Reiser J. (2009). "Production, concentration and titration of pseudotyped HIV-1-based lentiviral vectors." Nat Protoc **4**(4): 495-505.

Laflamme M. A., Chen K. Y., Naumova A. V., Muskheli V., Fugate J. A., Dupras S. K., Reinecke H., Xu C., Hassanipour M., Police S., O'Sullivan C., Collins L., Chen Y., Minami E., Gill E. A., Ueno S., Yuan C., Gold J. and Murry C. E. (2007). "Cardiomyocytes derived from human embryonic stem cells in pro-survival factors enhance function of infarcted rat hearts." Nat Biotechnol **25**(9): 1015-1024.

Lagarkova M. A., Shutova M. V., Bogomazova A. N., Vassina E. M., Glazov E. A., Zhang P., Rizvanov A. A., Chestkov I. V. and Kiselev S. L. (2010). "Induction of pluripotency in human endothelial cells resets epigenetic profile on genome scale." Cell Cycle **9**(5): 937-946.

Lan F., Bayliss P. E., Rinn J. L., Whetstine J. R., Wang J. K., Chen S., Iwase S., Alpatov R., Issaeva I., Canaani E., Roberts T. M., Chang H. Y. and Shi Y. (2007). "A histone H3 lysine 27 demethylase regulates animal posterior development." Nature **449**(7163): 689-694.

Lanctot C., Cheutin T., Cremer M., Cavalli G. and Cremer T. (2007a). "Dynamic genome architecture in the nuclear space: regulation of gene expression in three dimensions." Nat Rev Genet **8**(2): 104-115.

Lanctot P. M., Gage F. H. and Varki A. P. (2007b). "The glycans of stem cells." Curr Opin Chem Biol **11**(4): 373-380.

Laslett A. L., Filipczyk A. A. and Pera M. F. (2003). "Characterization and culture of human embryonic stem cells." Trends Cardiovasc Med **13**(7): 295-301.

Laurent L., Wong E., Li G., Huynh T., Tsirigos A., Ong C. T., Low H. M., Kin Sung K. W., Rigoutsos I., Loring J. and Wei C. L. (2010). "Dynamic changes in the human methylome during differentiation." Genome Res **20**(3): 320-331.

Law J. A. and Jacobsen S. E. (2010). "Establishing, maintaining and modifying DNA methylation patterns in plants and animals." Nat Rev Genet **11**(3): 204-220.

Lebkowski J. S., Gold J., Xu C., Funk W., Chiu C. P. and Carpenter M. K. (2001). "Human embryonic stem cells: culture, differentiation, and genetic modification for regenerative medicine applications." Cancer J **7 Suppl 2**: S83-93.

Lee M. G., Villa R., Trojer P., Norman J., Yan K. P., Reinberg D., Di Croce L. and Shiekhattar R. (2007). "Demethylation of H3K27 regulates polycomb recruitment and H2A ubiquitination." Science **318**(5849): 447-450.

Lehnertz B., Ueda Y., Derijck A. A., Braunschweig U., Perez-Burgos L., Kubicek S., Chen T., Li E., Jenuwein T. and Peters A. H. (2003). "Suv39h-mediated histone H3 lysine 9 methylation directs DNA methylation to major satellite repeats at pericentric heterochromatin." Curr Biol **13**(14): 1192-1200.

Leonhardt H., Page A. W., Weier H. U. and Bestor T. H. (1992). "A targeting sequence directs DNA methyltransferase to sites of DNA replication in mammalian nuclei." Cell **71**(5): 865-873.

Lewis A., Mitsuya K., Umlauf D., Smith P., Dean W., Walter J., Higgins M., Feil R. and Reik W. (2004). "Imprinting on distal chromosome 7 in the placenta involves repressive histone methylation independent of DNA methylation." Nat Genet **36**(12): 1291-1295.

Lewis B. P., Burge C. B. and Bartel D. P. (2005). "Conserved seed pairing, often flanked by adenosines, indicates that thousands of human genes are microRNA targets." Cell **120**(1): 15-20.

Li (2002). "Chromatin modification and epigenetic reprogramming in mammalian development." Nat Rev Genet **3**(9): 662-673.

Li H., Collado M., Villasante A., Strati K., Ortega S., Canamero M., Blasco M. A. and Serrano M. (2009). "The Ink4/Arf locus is a barrier for iPS cell reprogramming." Nature **460**(7259): 1136-1139.

Li J., Pan G., Cui K., Liu Y., Xu S. and Pei D. (2007a). "A dominant-negative form of mouse SOX2 induces trophectoderm differentiation and progressive polyploidy in mouse embryonic stem cells." J Biol Chem **282**(27): 19481-19492.

Li J., Wang G., Wang C., Zhao Y., Zhang H., Tan Z., Song Z., Ding M. and Deng H. (2007b). "MEK/ERK signaling contributes to the maintenance of human embryonic stem cell self-renewal." Differentiation **75**(4): 299-307.

Li J. Y., Pu M. T., Hirasawa R., Li B. Z., Huang Y. N., Zeng R., Jing N. H., Chen T., Li E., Sasaki H. and Xu G. L. (2007c). "Synergistic function of DNA methyltransferases Dnmt3a and Dnmt3b in the methylation of Oct4 and Nanog." Mol Cell Biol **27**(24): 8748-8759.

Li L. C. and Dahiya R. (2002). "MethPrimer: designing primers for methylation PCRs." Bioinformatics **18**(11): 1427-1431.

Li W. and Ding S. (2009). "Small molecules that modulate embryonic stem cell fate and somatic cell reprogramming." Trends in Pharmacological Sciences **31**(1): 36-45.

Li Y., McClintick J., Zhong L., Edenberg H. J., Yoder M. C. and Chan R. J. (2005). "Murine embryonic stem cell differentiation is promoted by SOCS-3 and inhibited by the zinc finger transcription factor Klf4." Blood **105**(2): 635-637.

Liang G., Chan M. F., Tomigahara Y., Tsai Y. C., Gonzales F. A., Li E., Laird P. W. and Jones P. A. (2002). "Cooperativity between DNA methyltransferases in the maintenance methylation of repetitive elements." Mol Cell Biol **22**(2): 480-491.

Liang J., Wan M., Zhang Y., Gu P., Xin H., Jung S. Y., Qin J., Wong J., Cooney A. J., Liu D. and Songyang Z. (2008). "Nanog and Oct4 associate with unique transcriptional repression complexes in embryonic stem cells." Nat Cell Biol **10**(6): 731-739.

Liao J., Cui C., Chen S., Ren J., Chen J., Gao Y., Li H., Jia N., Cheng L., Xiao H. and Xiao L. (2009a). "Generation of induced pluripotent stem cell lines from adult rat cells." Cell Stem Cell **4**(1): 11-15.

Liao J., Wu Z., Wang Y., Cheng L., Cui C., Gao Y., Chen T., Rao L., Chen S., Jia N., Dai H., Xin S., Kang J., Pei G. and Xiao L. (2008). "Enhanced efficiency of generating induced pluripotent stem (iPS) cells from human somatic cells by a combination of six transcription factors." Cell Res **18**(5): 600-603.

Liao W., McNutt M. A. and Zhu W.-G. (2009b). "The comet assay: A sensitive method for detecting DNA damage in individual cells." Methods **48**(1): 46-53.

Liedtke S., Enczmann J., Waclawczyk S., Wernet P. and Kogler G. (2007). "Oct4 and its pseudogenes confuse stem cell research." Cell Stem Cell **1**(4): 364-366.

Lim D. A., Huang Y. C., Swigut T., Mirick A. L., Garcia-Verdugo J. M., Wysocka J., Ernst P. and Alvarez-Buylla A. (2009). "Chromatin remodelling factor Mll1 is essential for neurogenesis from postnatal neural stem cells." Nature **458**(7237): 529-533.

Lin S. P., Youngson N., Takada S., Seitz H., Reik W., Paulsen M., Cavaille J. and Ferguson-Smith A. C. (2003). "Asymmetric regulation of imprinting on the maternal and paternal chromosomes at the Dlk1-Gtl2 imprinted cluster on mouse chromosome 12." Nat Genet **35**(1): 97-102.

Liu H., Zhu F., Yong J., Zhang P., Hou P., Li H., Jiang W., Cai J., Liu M., Cui K., Qu X., Xiang T., Lu D., Chi X., Gao G., Ji W., Ding M. and Deng H. (2008a). "Generation of Induced Pluripotent Stem Cells from Adult Rhesus Monkey Fibroblasts." Cell Stem Cell **3**(6): 587-590.

Liu X., Huang J., Chen T., Wang Y., Xin S., Li J., Pei G. and Kang J. (2008b). "Yamanaka factors critically regulate the developmental signaling network in mouse embryonic stem cells." Cell Res **18**(12): 1177-1189.

Liu Z., Xie Z., Jones W., Pavlovicz R. E., Liu S., Yu J., Li P.-k., Lin J., Fuchs J. R., Marcucci G., Li C. and Chan K. K. (2009). "Curcumin is a potent DNA hypomethylation agent." Bioorganic & Medicinal Chemistry Letters **19**(3): 706-709.

Livak K. J. and Schmittgen T. D. (2001). "Analysis of relative gene expression data using real-time quantitative PCR and the 2(-Delta Delta C(T)) Method." Methods **25**(4): 402-408.

Loh X. J., Gong J., Sakuragi M., Kitajima T., Liu M., Li J. and Ito Y. (2009). "Surface Coating with a Thermoresponsive Copolymer for the Culture and Non-Enzymatic Recovery of Mouse Embryonic Stem Cells." Macromol Biosci.

Loh Y. H., Wu Q., Chew J. L., Vega V. B., Zhang W., Chen X., Bourque G., George J., Leong B., Liu J., Wong K. Y., Sung K. W., Lee C. W., Zhao X. D., Chiu K. P., Lipovich L., Kuznetsov V. A., Robson P., Stanton L. W., Wei C. L., Ruan Y., Lim B. and Ng H. H. (2006). "The Oct4 and Nanog transcription network regulates pluripotency in mouse embryonic stem cells." Nat Genet **38**(4): 431-440.

Loh Y. H., Zhang W., Chen X., George J. and Ng H. H. (2007). "Jmjd1a and Jmjd2c histone H3 Lys 9 demethylases regulate self-renewal in embryonic stem cells." Genes Dev **21**(20): 2545-2557.

Lopez-Bigas N., Kisiel T. A., Dewaal D. C., Holmes K. B., Volkert T. L., Gupta S., Love J., Murray H. L., Young R. A. and Benevolenskaya E. V. (2008). "Genome-wide analysis of the H3K4 histone demethylase RBP2 reveals a transcriptional program controlling differentiation." Mol Cell **31**(4): 520-530.

Lowry W. E., Richter L., Yachechko R., Pyle A. D., Tchieu J., Sridharan R., Clark A. T. and Plath K. (2008). "Generation of human induced pluripotent stem cells from dermal fibroblasts." Proc Natl Acad Sci U S A **105**(8): 2883-2888.

Ludwig T. E., Bergendahl V., Levenstein M. E., Yu J., Probasco M. D. and Thomson J. A. (2006a). "Feeder-independent culture of human embryonic stem cells." Nat Methods **3**(8): 637-646.

Ludwig T. E., Levenstein M. E., Jones J. M., Berggren W. T., Mitchen E. R., Frane J. L., Crandall L. J., Daigh C. A., Conard K. R., Piekarczyk M. S., Llanas R. A. and Thomson J. A. (2006b). "Derivation of human embryonic stem cells in defined conditions." Nat Biotechnol **24**(2): 185-187.

Luger K. (2003). "Structure and dynamic behavior of nucleosomes." Curr Opin Genet Dev **13**(2): 127-135.

Lukas J., Parry D., Aagaard L., Mann D. J., Bartkova J., Strauss M., Peters G. and Bartek J. (1995). "Retinoblastoma-protein-dependent cell-cycle inhibition by the tumour suppressor p16." Nature **375**(6531): 503-506.

Lynch K. W. (2004). "Consequences of regulated pre-mRNA splicing in the immune system." Nat Rev Immunol **4**(12): 931-940.

Lyssiotis C. A., Foreman R. K., Staerk J., Garcia M., Mathur D., Markoulaki S., Hanna J., Lairson L. L., Charette B. D., Bouchez L. C., Bollong M., Kunick C., Brinker A., Cho C. Y., Schultz P. G. and Jaenisch R. (2009). "Reprogramming of murine fibroblasts to induced pluripotent stem cells with chemical complementation of Klf4." Proceedings of the National Academy of Sciences **106**(22): 8912-8917.

Ma D. and Wells J. W. (2004). "Mathematical basis for the optimization of single cell-line screening on multi-well plates." Biotechnol Lett **26**(18): 1441-1446.

Ma F., Wang D., Hanada S., Ebihara Y., Kawasaki H., Zaike Y., Heike T., Nakahata T. and Tsuji K. (2007). "Novel method for efficient production of multipotential hematopoietic progenitors from human embryonic stem cells." Int J Hematol **85**(5): 371-379.

Ma P. and Schultz R. M. (2008). "Histone deacetylase 1 (HDAC1) regulates histone acetylation, development, and gene expression in preimplantation mouse embryos." Dev Biol **319**(1): 110-120.

MacArthur B. D., Please C. P. and Oreffo R. O. (2008). "Stochasticity and the molecular mechanisms of induced pluripotency." PLoS One **3**(8): e3086.

Madan V., Madan B., Brykczynska U., Zilbermann F., Hogeveen K., Dohner K., Dohner H., Weber O., Blum C., Rodewald H. R., Sassone-Corsi P., Peters A. H. and Fehling H. J. (2009). "Impaired function of primitive hematopoietic cells in mice lacking the Mixed-Lineage-Leukemia homolog MLL5." Blood **113**(7): 1444-1454.

Maherali N. and Hochedlinger K. (2008). "Guidelines and techniques for the generation of induced pluripotent stem cells." Cell Stem Cell **3**(6): 595-605.

Maherali N. and Hochedlinger K. (2009). "Tgfbeta signal inhibition cooperates in the induction of iPSCs and replaces Sox2 and cMyc." Curr Biol **19**(20): 1718-1723.

Maherali N., Shridheran R., Xie W., Utikal J., Eminli S., Arnold K., Stadfeld M., Yachechko R., Tchieu J., Jaenisch R., Plath K. and Hochedlinger K. (2007). "Directly Reprogrammed Fibroblasts Show Global Epigenetic Remodelling and Widespread Tissue Contribution." Cell Stem Cell **doi:10.1016/j.stem.2007.05.014**

Mahlstedt M. M., Anderson D., Sharp J. S., McGilvray R., Barbadillo Munoz M. D., Buttery L. D., Alexander M. R., Rose F. R. and Denning C. (2009). "Maintenance of pluripotency in human embryonic stem cells cultured on a synthetic substrate in conditioned medium." Biotechnol Bioeng.

Mahlstedt M. M., Anderson D., Sharp J. S., McGilvray R., Barbadillo Munoz M. D., Buttery L. D., Alexander M. R., Rose F. R. and Denning C. (2010). "Maintenance of pluripotency in human embryonic stem cells cultured on a synthetic substrate in conditioned medium." Biotechnol Bioeng **105**(1): 130-140.

Maitra A., Arking D. E., Shivapurkar N., Ikeda M., Stastny V., Kassauei K., Sui G., Cutler D. J., Liu Y., Brimble S. N., Noaksson K., Hyllner J., Schulz T. C., Zeng X., Freed W. J., Crook J., Abraham S., Colman A., Sartipy P., Matsui S., Carpenter M., Gazdar A. F., Rao M. and Chakravarti A. (2005). "Genomic alterations in cultured human embryonic stem cells." Nat Genet **37**(10): 1099-1103.

Mallanna S. K. and Rizzino A. (2010). "Emerging roles of microRNAs in the control of embryonic stem cells and the generation of induced pluripotent stem cells." Dev Biol.

Mantelingu K., Reddy B. A., Swaminathan V., Kishore A. H., Siddappa N. B., Kumar G. V., Nagashankar G., Natesh N., Roy S., Sadhale P. P., Ranga U., Narayana C. and Kundu T. K. (2007). "Specific inhibition of p300-HAT alters global gene expression and represses HIV replication." Chem Biol **14**(6): 645-657.

Margot J. B., Cardoso M. C. and Leonhardt H. (2001). "Mammalian DNA methyltransferases show different subnuclear distributions." J Cell Biochem **83**(3): 373-379.

Margueron R., Trojer P. and Reinberg D. (2005). "The key to development: interpreting the histone code?" Curr Opin Genet Dev **15**(2): 163-176.

Marino-Ramirez L., Spouge J. L., Kanga G. C. and Landsman D. (2004). "Statistical analysis of over-represented words in human promoter sequences." Nucleic Acids Res **32**(3): 949-958.

Marion R. M., Strati K., Li H., Murga M., Blanco R., Ortega S., Fernandez-Capetillo O., Serrano M. and Blasco M. A. (2009a). "A p53-mediated DNA damage response limits reprogramming to ensure iPS cell genomic integrity." Nature **460**(7259): 1149-1153.

Marion R. M., Strati K., Li H., Tejera A., Schoeftner S., Ortega S., Serrano M. and Blasco M. A. (2009b). "Telomeres acquire embryonic stem cell characteristics in induced pluripotent stem cells." Cell Stem Cell **4**(2): 141-154.

Martin C. and Zhang Y. (2005). "The diverse functions of histone lysine methylation." Nat Rev Mol Cell Biol **6**(11): 838-849.

Martin M. J., Muotri A., Gage F. and Varki A. (2005). "Human embryonic stem cells express an immunogenic nonhuman sialic acid." Nat Med **11**(2): 228-232.

Masui S. (2010). "Pluripotency maintenance mechanism of embryonic stem cells and reprogramming." Int J Hematol **91**(3): 360-372.

Masui S., Nakatake Y., Toyooka Y., Shimosato D., Yagi R., Takahashi K., Okochi H., Okuda A., Matoba R., Sharov A. A., Ko M. S. and Niwa H. (2007). "Pluripotency governed by Sox2 via regulation of Oct3/4 expression in mouse embryonic stem cells." Nat Cell Biol **9**(6): 625-635.

Masui S., Ohtsuka S., Yagi R., Takahashi K., Ko M. S. and Niwa H. (2008). "Rex1/Zfp42 is dispensable for pluripotency in mouse ES cells." BMC Dev Biol **8**: 45.

McDaneld T. G. (2009). "MicroRNA: mechanism of gene regulation and application to livestock." J Anim Sci **87**(14 Suppl): E21-28.

McKittrick E., Gafken P. R., Ahmad K. and Henikoff S. (2004). "Histone H3.3 is enriched in covalent modifications associated with active chromatin." Proc Natl Acad Sci U S A **101**(6): 1525-1530.

Meissner A., Mikkelsen T. S., Gu H., Wernig M., Hanna J., Sivachenko A., Zhang X., Bernstein B. E., Nusbaum C., Jaffe D. B., Gnirke A., Jaenisch R. and Lander E. S. (2008). "Genome-scale DNA methylation maps of pluripotent and differentiated cells." Nature **454**(7205): 766-770.

Meissner A., Wernig M. and Jaenisch R. (2007). "Direct reprogramming of genetically unmodified fibroblasts into pluripotent stem cells." Nat Biotechnol **25**(10): 1177-1181.

Menendez P., Wang L. and Bhatia M. (2005). "Genetic manipulation of human embryonic stem cells: a system to study early human development and potential therapeutic applications." Curr Gene Ther **5**(4): 375-385.

Merten O. W. (2004). "State-of-the-art of the production of retroviral vectors." J Gene Med **6 Suppl 1**: S105-124.

Meshorer E. and Misteli T. (2006). "Chromatin in pluripotent embryonic stem cells and differentiation." Nat Rev Mol Cell Biol **7**(7): 540-546.

Metivier R., Gallais R., Tiffoche C., Le Peron C., Jurkowska R. Z., Carmouche R. P., Ibberson D., Barath P., Demay F., Reid G., Benes V., Jeltsch A., Gannon F. and Salbert G. (2008). "Cyclical DNA methylation of a transcriptionally active promoter." Nature **452**(7183): 45-50.

Mikkelsen T. S., Hanna J., Zhang X., Ku M., Wernig M., Schorderet P., Bernstein B. E., Jaenisch R., Lander E. S. and Meissner A. (2008). "Dissecting direct reprogramming through integrative genomic analysis." Nature **454**(7200): 49-55.

Mikkelsen T. S., Ku M., Jaffe D. B., Issac B., Lieberman E., Giannoukos G., Alvarez P., Brockman W., Kim T. K., Koche R. P., Lee W., Mendenhall E., O'Donovan A., Presser A., Russ C., Xie X., Meissner A., Wernig M., Jaenisch R., Nusbaum C., Lander E. S. and Bernstein B. E. (2007). "Genome-wide maps of chromatin state in pluripotent and lineage-committed cells." Nature **448**(7153): 553-560.

Milutinovic S., Brown S. E., Zhuang Q. and Szyf M. (2004). "DNA methyltransferase 1 knock down induces gene expression by a mechanism independent of DNA methylation and histone deacetylation." J Biol Chem **279**(27): 27915-27927.

Minard M. E., Jain A. K. and Barton M. C. (2009). "Analysis of epigenetic alterations to chromatin during development." Genesis **47**(8): 559-572.

Mitsui K., Tokuzawa Y., Itoh H., Segawa K., Murakami M., Takahashi K., Maruyama M., Maeda M. and Yamanaka S. (2003). "The homeoprotein Nanog is required for maintenance of pluripotency in mouse epiblast and ES cells." Cell **113**(5): 631-642.

Miura K., Okada Y., Aoi T., Okada A., Takahashi K., Okita K., Nakagawa M., Koyanagi M., Tanabe K., Ohnuki M., Ogawa D., Ikeda E., Okano H. and Yamanaka S. (2009). "Variation in the safety of induced pluripotent stem cell lines." Nat Biotechnol **27**(8): 743-745.

Miyagi S., Nishimoto M., Saito T., Ninomiya M., Sawamoto K., Okano H., Muramatsu M., Oguro H., Iwama A. and Okuda A. (2006). "The Sox2 regulatory region 2 functions as a neural stem cell-specific enhancer in the telencephalon." J Biol Chem **281**(19): 13374-13381.

Miyagi S., Saito T., Mizutani K., Masuyama N., Gotoh Y., Iwama A., Nakauchi H., Masui S., Niwa H., Nishimoto M., Muramatsu M. and Okuda A. (2004). "The Sox-2 regulatory regions display their activities in two distinct types of multipotent stem cells." Mol Cell Biol **24**(10): 4207-4220.

Mohn F., Weber M., Rebhan M., Roloff T. C., Richter J., Stadler M. B., Bibel M. and Schubeler D. (2008). "Lineage-specific polycomb targets and de novo DNA methylation define restriction and potential of neuronal progenitors." Mol Cell **30**(6): 755-766.

Moll R., Franke W. W., Schiller D. L., Geiger B. and Krepler R. (1982). "The catalog of human cytokeratins: patterns of expression in normal epithelia, tumors and cultured cells." Cell **31**(1): 11-24.

Monk D., Arnaud P., Apostolidou S., Hills F. A., Kelsey G., Stanier P., Feil R. and Moore G. E. (2006a). "Limited evolutionary conservation of imprinting in the human placenta." Proc Natl Acad Sci U S A **103**(17): 6623-6628.

Monk D., Sanches R., Arnaud P., Apostolidou S., Hills F. A., Abu-Amero S., Murrell A., Friess H., Reik W., Stanier P., Constancia M. and Moore G. E. (2006b). "Imprinting of IGF2 P0 transcript and novel alternatively spliced INS-IGF2 isoforms show differences between mouse and human." Hum Mol Genet **15**(8): 1259-1269.

Monk M. and Harper M. I. (1979). "Sequential X chromosome inactivation coupled with cellular differentiation in early mouse embryos." Nature **281**(5729): 311-313.

Moore T., Constancia M., Zubair M., Bailleul B., Feil R., Sasaki H. and Reik W. (1997). "Multiple imprinted sense and antisense transcripts, differential methylation and tandem repeats in a putative imprinting control region upstream of mouse Igf2." Proc Natl Acad Sci U S A **94**(23): 12509-12514.

Morison I. M., Ramsay J. P. and Spencer H. G. (2005). "A census of mammalian imprinting." Trends Genet **21**(8): 457-465.

Morris K. V. and Rossi J. J. (2006). "Lentiviral-mediated delivery of siRNAs for antiviral therapy." Gene Ther **13**(6): 553-558.

Mummery C., Ward-van Oostwaard D., Doevendans P., Spijker R., van den Brink S., Hassink R., van der Heyden M., Opthof T., Pera M., de la Riviere A. B., Passier R. and Tertoolen L. (2003). "Differentiation of human embryonic stem cells to cardiomyocytes: role of coculture with visceral endoderm-like cells." Circulation **107**(21): 2733-2740.

Nakagawa M., Koyanagi M., Tanabe K., Takahashi K., Ichisaka T., Aoi T., Okita K., Mochiduki Y., Takizawa N. and Yamanaka S. (2008). "Generation of induced pluripotent stem cells without Myc from mouse and human fibroblasts." Nat Biotechnol **26**(1): 101-106.

Nakahara Y., Northcott P. A., Li M., Kongkham P. N., Smith C., Yan H., Croul S., Ra Y. S., Eberhart C., Huang A., Bigner D., Grajkowska W., Van Meter T., Rutka J. T. and Taylor M. D. (2010). "Genetic and epigenetic inactivation of Kruppel-like factor 4 in medulloblastoma." Neoplasia **12**(1): 20-27.

Nakatake Y., Fukui N., Iwamatsu Y., Masui S., Takahashi K., Yagi R., Yagi K., Miyazaki J., Matoba R., Ko M. S. and Niwa H. (2006). "Klf4 cooperates with Oct3/4 and Sox2 to activate the Lefty1 core promoter in embryonic stem cells." Mol Cell Biol **26**(20): 7772-7782.

Naldini L., Blomer U., Gage F. H., Trono D. and Verma I. M. (1996). "Efficient transfer, integration, and sustained long-term expression of the transgene in adult rat brains injected with a lentiviral vector." Proc Natl Acad Sci U S A **93**(21): 11382-11388.

Nesbeth D., Williams S. L., Chan L., Brain T., Slater N. K., Farzaneh F. and Darling D. (2006). "Metabolic biotinylation of lentiviral pseudotypes for scalable paramagnetic microparticle-dependent manipulation." Mol Ther **13**(4): 814-822.

Newman M. A., Thomson J. M. and Hammond S. M. (2008). "Lin-28 interaction with the Let-7 precursor loop mediates regulated microRNA processing." RNA **14**(8): 1539-1549.

Ng E. S., Davis R. P., Azzola L., Stanley E. G. and Elefanty A. G. (2005a). "Forced aggregation of defined numbers of human embryonic stem cells into embryoid bodies fosters robust, reproducible hematopoietic differentiation." Blood **106**(5): 1601-1603.

Ng E. S., Davis R. P., Azzola L., Stanley E. G. and Elefanty A. G. (2005b). "Forced aggregation of defined numbers of human embryonic stem cells into embryoid bodies fosters robust, reproducible hematopoietic differentiation." Blood **106**(5): 1601-1603.

Nichols J., Zevnik B., Anastassiadis K., Niwa H., Klewe-Nebenius D., Chambers I., Scholer H. and Smith A. (1998). "Formation of pluripotent stem cells in the mammalian embryo depends on the POU transcription factor Oct4." Cell **95**(3): 379-391.

Nimura K., Ishida C., Koriyama H., Hata K., Yamanaka S., Li E., Ura K. and Kaneda Y. (2006). "Dnmt3a2 targets endogenous Dnmt3L to ES cell chromatin and induces regional DNA methylation." Genes Cells **11**(10): 1225-1237.

Nishimoto M., Miyagi S., Yamagishi T., Sakaguchi T., Niwa H., Muramatsu M. and Okuda A. (2005). "Oct-3/4 maintains the proliferative embryonic stem cell state via specific binding to a variant octamer sequence in the regulatory region of the UTF1 locus." Mol Cell Biol **25**(12): 5084-5094.

Nisole S. and Saib A. (2004). "Early steps of retrovirus replicative cycle." Retrovirology **1**(1): 9.

Niwa H. (2007). "How is pluripotency determined and maintained?" Development **134**(4): 635-646.

Niwa H., Miyazaki J. and Smith A. G. (2000). "Quantitative expression of Oct-3/4 defines differentiation, dedifferentiation or self-renewal of ES cells." Nat Genet **24**(4): 372-376.

Niwa H., Toyooka Y., Shimosato D., Strumpf D., Takahashi K., Yagi R. and Rossant J. (2005). "Interaction between Oct3/4 and Cdx2 determines trophectoderm differentiation." Cell **123**(5): 917-929.

O'Carroll D., Erhardt S., Pagani M., Barton S. C., Surani M. A. and Jenuwein T. (2001). "The polycomb-group gene Ezh2 is required for early mouse development." Mol Cell Biol **21**(13): 4330-4336.

O'Neill L P., Vermilyea M. D. and Turner B. M. (2006). "Epigenetic characterization of the early embryo with a chromatin immunoprecipitation protocol applicable to small cell populations." Nat Genet **38**(7): 835-841.

Odorico J. S., Kaufman D. S. and Thomson J. A. (2001). "Multilineage differentiation from human embryonic stem cell lines." Stem Cells **19**(3): 193-204.

Oh J. E., Krapfenbauer K. and Lubec G. (2004). "Proteomic identification of collagens and related proteins in human fibroblasts." Amino Acids **27**(3-4): 305-311.

Okabe H., Satoh S., Furukawa Y., Kato T., Hasegawa S., Nakajima Y., Yamaoka Y. and Nakamura Y. (2003). "Involvement of PEG10 in human hepatocellular carcinogenesis through interaction with SIAH1." Cancer Res **63**(12): 3043-3048.

Okano M., Bell D. W., Haber D. A. and Li E. (1999). "DNA methyltransferases Dnmt3a and Dnmt3b are essential for de novo methylation and mammalian development." Cell **99**(3): 247-257.

Okano M., Xie S. and Li E. (1998). "Cloning and characterization of a family of novel mammalian DNA (cytosine-5) methyltransferases." Nat Genet **19**(3): 219-220.

Okita K., Hong H., Takahashi K. and Yamanaka S. (2010). "Generation of mouse-induced pluripotent stem cells with plasmid vectors." Nat. Protocols **5**(3): 418-428.

Okita K., Ichisaka T. and Yamanaka S. (2007). "Generation of germline-competent induced pluripotent stem cells." Nature **448**(7151): 313-317.

Okita K., Nakagawa M., Hyenjong H., Ichisaka T. and Yamanaka S. (2008). "Generation of mouse induced pluripotent stem cells without viral vectors." Science **322**(5903): 949-953.

Okuda A., Fukushima A., Nishimoto M., Orimo A., Yamagishi T., Nabeshima Y., Kuro-o M., Boon K., Keaveney M., Stunnenberg H. G. and Muramatsu M. (1998). "UTF1, a novel transcriptional coactivator expressed in pluripotent embryonic stem cells and extra-embryonic cells." EMBO J **17**(7): 2019-2032.

Okumura-Nakanishi S., Saito M., Niwa H. and Ishikawa F. (2005). "Oct-3/4 and Sox2 regulate Oct-3/4 gene in embryonic stem cells." J Biol Chem **280**(7): 5307-5317.

Olson H., Betton G., Robinson D., Thomas K., Monro A., Kolaja G., Lilly P., Sanders J., Sipes G., Bracken W., Dorato M., Van Deun K., Smith P., Berger B. and Heller A. (2000). "Concordance of the toxicity of pharmaceuticals in humans and in animals." Regul Toxicol Pharmacol **32**(1): 56-67.

Ooi S. K. and Bestor T. H. (2008). "The colorful history of active DNA demethylation." Cell **133**(7): 1145-1148.

Orkin S. H. (2005). "Chipping away at the embryonic stem cell network." Cell **122**(6): 828-830.

Osafune K., Caron L., Borowiak M., Martinez R. J., Fitz-Gerald C. S., Sato Y., Cowan C. A., Chien K. R. and Melton D. A. (2008). "Marked differences in differentiation propensity among human embryonic stem cell lines." Nat Biotech **26**(3): 313-315.

Oswald J., Engemann S., Lane N., Mayer W., Olek A., Fundele R., Dean W., Reik W. and Walter J. (2000). "Active demethylation of the paternal genome in the mouse zygote." Curr Biol **10**(8): 475-478.

Otsubo T., Akiyama Y., Yanagihara K. and Yuasa Y. (2008). "SOX2 is frequently downregulated in gastric cancers and inhibits cell growth through cell-cycle arrest and apoptosis." Br J Cancer **98**(4): 824-831.

Paddison P. J., Caudy A. A., Bernstein E., Hannon G. J. and Conklin D. S. (2002). "Short hairpin RNAs (shRNAs) induce sequence-specific silencing in mammalian cells." Genes Dev **16**(8): 948-958.

Paddison P. J. and Hannon G. J. (2003). "siRNAs and shRNAs: skeleton keys to the human genome." Curr Opin Mol Ther **5**(3): 217-224.

Pal R. and Khanna A. (2007). "Similar pattern in cardiac differentiation of human embryonic stem cell lines, BG01V and ReliCellhES1, under low serum concentration supplemented with bone morphogenetic protein-2." Differentiation **75**(2): 112-122.

Pan G., Li J., Zhou Y., Zheng H. and Pei D. (2006). "A negative feedback loop of transcription factors that controls stem cell pluripotency and self-renewal." FASEB J **20**(10): 1730-1732.

Pan G., Tian S., Nie J., Yang C., Ruotti V., Wei H., Jonsdottir G. A., Stewart R. and Thomson J. A. (2007). "Whole-genome analysis of histone H3 lysine 4 and lysine 27 methylation in human embryonic stem cells." Cell Stem Cell **1**(3): 299-312.

Papapetrou E. P., Tomishima M. J., Chambers S. M., Mica Y., Reed E., Menon J., Tabar V., Mo Q., Studer L. and Sadelain M. (2009). "Stoichiometric and temporal requirements of Oct4, Sox2, Klf4, and c-Myc expression for efficient human iPSC induction and differentiation." Proceedings of the National Academy of Sciences **106**(13): 12759-12764.

Park F. (2007). "Lentiviral vectors: are they the future of animal transgenesis?" Physiol Genomics **31**(2): 159-173.

Park I. H., Arora N., Huo H., Maherali N., Ahfeldt T., Shimamura A., Lensch M. W., Cowan C., Hochedlinger K. and Daley G. Q. (2008a). "Disease-Specific Induced Pluripotent Stem Cells." Cell.

Park I. H., Lerou P. H., Zhao R., Huo H. and Daley G. Q. (2008b). "Generation of human-induced pluripotent stem cells." Nat Protoc **3**(7): 1180-1186.

Park I. H., Zhao R., West J. A., Yabuuchi A., Huo H., Ince T. A., Lerou P. H., Lensch M. W. and Daley G. Q. (2008c). "Reprogramming of human somatic cells to pluripotency with defined factors." Nature **451**(7175): 141-146.

Pasini D., Bracken A. P., Hansen J. B., Capillo M. and Helin K. (2007). "The polycomb group protein Suz12 is required for embryonic stem cell differentiation." Mol Cell Biol **27**(10): 3769-3779.

Passier R., Oostwaard D. W., Snapper J., Kloots J., Hassink R. J., Kuijk E., Roelen B., de la Riviere A. B. and Mummery C. (2005). "Increased cardiomyocyte differentiation from human embryonic stem cells in serum-free cultures." Stem Cells **23**(6): 772-780.

Patil S. D., Rhodes D. G. and Burgess D. J. (2005). "DNA-based therapeutics and DNA delivery systems: a comprehensive review." AAPS J 7(1): E61-77.

Pei Y. and Tuschl T. (2006). "On the art of identifying effective and specific siRNAs." Nat Methods **3**(9): 670-676.

Pera M. F., Reubinoff B. and Trounson A. (2000). "Human embryonic stem cells." J Cell Sci **113 (Pt 1)**: 5-10.

Pick M., Stelzer Y., Bar-Nur O., Mayshar Y., Eden A. and Benvenisty N. (2009). "Clone and Gene Specific Aberrations of Parental Imprinting in Human Induced Pluripotent Stem Cells." Stem Cells **27**(11): 2686-2690.

Pittenger M. F., Mackay A. M., Beck S. C., Jaiswal R. K., Douglas R., Mosca J. D., Moorman M. A., Simonetti D. W., Craig S. and Marshak D. R. (1999). "Multilineage potential of adult human mesenchymal stem cells." Science **284**(5411): 143-147.

Pound P., Ebrahim S., Sandercock P., Bracken M. B. and Roberts I. (2004). "Where is the evidence that animal research benefits humans?" BMJ **328**(7438): 514-517.

Pradhan S., Bacolla A., Wells R. D. and Roberts R. J. (1999). "Recombinant human DNA (cytosine-5) methyltransferase. I. Expression, purification, and comparison of de novo and maintenance methylation." J Biol Chem **274**(46): 33002-33010.

Pradhan S. and Esteve P. O. (2003). "Mammalian DNA (cytosine-5) methyltransferases and their expression." Clin Immunol **109**(1): 6-16.

Ptashne M. and Gann A. (1997). "Transcriptional activation by recruitment." Nature **386**(6625): 569-577.
Qiu C., Ma Y., Wang J., Peng S. and Huang Y. (2009). "Lin28-mediated post-transcriptional regulation of Oct4 expression in human embryonic stem cells." Nucleic Acids Res **38**(4): 1240-1248.
Ramchandani S., Bhattacharya S. K., Cervoni N. and Szyf M. (1999). "DNA methylation is a reversible biological signal." Proc Natl Acad Sci U S A **96**(11): 6107-6112.
Rao M. (2004). "Conserved and divergent paths that regulate self-renewal in mouse and human embryonic stem cells." Dev Biol **275**(2): 269-286.
Rege T. A. and Hagood J. S. (2006). "Thy-1, a versatile modulator of signaling affecting cellular adhesion, proliferation, survival, and cytokine/growth factor responses." Biochim Biophys Acta **1763**(10): 991-999.
Reid J., Evans K., Dyer N., Wernisch L. and Ott S. (2010). "Variable structure motifs for transcription factor binding sites." BMC Genomics **11**(1): 30.
Reik W. and Walter J. (2001). "Genomic imprinting: parental influence on the genome." Nat Rev Genet **2**(1): 21-32.
Reubinoff B. E., Pera M. F., Fong C. Y., Trounson A. and Bongso A. (2000). "Embryonic stem cell lines from human blastocysts: somatic differentiation in vitro." Nat Biotechnol **18**(4): 399-404.
Rhee I., Bachman K. E., Park B. H., Jair K. W., Yen R. W., Schuebel K. E., Cui H., Feinberg A. P., Lengauer C., Kinzler K. W., Baylin S. B. and Vogelstein B. (2002). "DNMT1 and DNMT3b cooperate to silence genes in human cancer cells." Nature **416**(6880): 552-556.
Rhee I., Jair K. W., Yen R. W., Lengauer C., Herman J. G., Kinzler K. W., Vogelstein B., Baylin S. B. and Schuebel K. E. (2000). "CpG methylation is maintained in human cancer cells lacking DNMT1." Nature **404**(6781): 1003-1007.
Rho J. Y., Yu K., Han J. S., Chae J. I., Koo D. B., Yoon H. S., Moon S. Y., Lee K. K. and Han Y. M. (2006). "Transcriptional profiling of the developmentally important signalling pathways in human embryonic stem cells." Hum Reprod **21**(2): 405-412.
Richards M., Fong C. Y., Chan W. K., Wong P. C. and Bongso A. (2002). "Human feeders support prolonged undifferentiated growth of human inner cell masses and embryonic stem cells." Nat Biotechnol **20**(9): 933-936.
Richards M., Tan S., Fong C. Y., Biswas A., Chan W. K. and Bongso A. (2003). "Comparative evaluation of various human feeders for prolonged undifferentiated growth of human embryonic stem cells." Stem Cells **21**(5): 546-556.
Richards M., Tan S. P., Tan J. H., Chan W. K. and Bongso A. (2004). "The transcriptome profile of human embryonic stem cells as defined by SAGE." Stem Cells **22**(1): 51-64.
Rittie L. and Fisher G. J. (2005). "Isolation and culture of skin fibroblasts." Methods Mol Med **117**: 83-98.
Robert M. F., Morin S., Beaulieu N., Gauthier F., Chute I. C., Barsalou A. and MacLeod A. R. (2003). "DNMT1 is required to maintain CpG methylation and aberrant gene silencing in human cancer cells." Nat Genet **33**(1): 61-65.
Roberts R. M., Telugu B. P. and Ezashi T. (2009). "Induced pluripotent stem cells from swine (Sus scrofa): why they may prove to be important." Cell Cycle **8**(19): 3078-3081.
Robertson K. D. (2005). "DNA methylation and human disease." Nat Rev Genet **6**(8): 597-610.
Robertson K. D., Uzvolgyi E., Liang G., Talmadge C., Sumegi J., Gonzales F. A. and Jones P. A. (1999). "The human DNA methyltransferases (DNMTs) 1, 3a and 3b: coordinate mRNA expression in normal tissues and overexpression in tumors." Nucleic Acids Res **27**(11): 2291-2298.
Rodda D. J., Chew J. L., Lim L. H., Loh Y. H., Wang B., Ng H. H. and Robson P. (2005). "Transcriptional regulation of nanog by OCT4 and SOX2." J Biol Chem **280**(26): 24731-24737.
Rodriguez R. T., Velkey J. M., Lutzko C., Seerke R., Kohn D. B., O'Shea K. S. and Firpo M. T. (2007). "Manipulation of OCT4 levels in human embryonic stem cells results in induction of differential cell types." Exp Biol Med (Maywood) **232**(10): 1368-1380.
Rossant J. (2008). "Stem cells and early lineage development." Cell **132**(4): 527-531.
Rugg-Gunn P. J., Ferguson-Smith A. C. and Pedersen R. A. (2007). "Status of genomic imprinting in human embryonic stem cells as revealed by a large cohort of independently derived and maintained lines." Hum Mol Genet **16 Spec No. 2**: R243-251.
Saalbach A., Aneregg U., Bruns M., Schnabel E., Herrmann K. and Haustein U. F. (1996). "Novel fibroblast-specific monoclonal antibodies: properties and specificities." J Invest Dermatol **106**(6): 1314-1319.
Saalbach A., Aust G., Haustein U. F., Herrmann K. and Anderegg U. (1997). "The fibroblast-specific MAb AS02: a novel tool for detection and elimination of human fibroblasts." Cell Tissue Res **290**(3): 593-599.

Saalbach A., Kraft R., Herrmann K., Haustein U. F. and Anderegg U. (1998). "The monoclonal antibody AS02 recognizes a protein on human fibroblasts being highly homologous to Thy-1." Arch Dermatol Res **290**(7): 360-366.

Sadhana A., Katherine L. H. and Robert L. (2008). "Efficient Differentiation of Functional Hepatocytes from Human Embryonic Stem Cells." Stem Cells **26**(5): 1117-1127.

Sato N., Sanjuan I. M., Heke M., Uchida M., Naef F. and Brivanlou A. H. (2003). "Molecular signature of human embryonic stem cells and its comparison with the mouse." Dev Biol **260**(2): 404-413.

Saxe J. P., Tomilin A., Scholer H. R., Plath K. and Huang J. (2009). "Post-translational regulation of Oct4 transcriptional activity." PLoS One **4**(2): e4467.

Saxena S., Jónsson Z. O. and Dutta A. (2003). "Small RNAs with Imperfect Match to Endogenous mRNA Repress Translation." Journal of Biological Chemistry **278**(45): 44312-44319.

Saxonov S., Berg P. and Brutlag D. L. (2006). "A genome-wide analysis of CpG dinucleotides in the human genome distinguishes two distinct classes of promoters." Proc Natl Acad Sci U S A **103**(5): 1412-1417.

Scaringe S. A. (2001). "RNA oligonucleotide synthesis via 5'-silyl-2'-orthoester chemistry." Methods **23**(3): 206-217.

Scheper W. and Copray S. (2009). "The molecular mechanism of induced pluripotency: a two-stage switch." Stem Cell Rev **5**(3): 204-223.

Schroeder M., Niebruegge S., Werner A., Willbold E., Burg M., Ruediger M., Field L. J., Lehmann J. and Zweigerdt R. (2005). "Differentiation and lineage selection of mouse embryonic stem cells in a stirred bench scale bioreactor with automated process control." Biotechnol Bioeng **92**(7): 920-933.

Schuster-Gossler K., Bilinski P., Sado T., Ferguson-Smith A. and Gossler A. (1998). "The mouse Gtl2 gene is differentially expressed during embryonic development, encodes multiple alternatively spliced transcripts, and may act as an RNA." Dev Dyn **212**(2): 214-228.

Scotland K. B., Chen S., Sylvester R. and Gudas L. J. (2009). "Analysis of Rex1 (zfp42) function in embryonic stem cell differentiation." Dev Dyn **238**(8): 1863-1877.

Selvi B. R., Batta K., Kishore A. H., Mantelingu K., Varier R. A., Balasubramanyam K., Pradhan S. K., Dasgupta D., Sriram S., Agrawal S. and Kundu T. K. (2009a). "Identification of a novel inhibitor of CARM1-mediated methylation of histone H3R17." J Biol Chem **285**(10): 7143-7152.

Selvi B. R., Pradhan S. K., Shandilya J., Das C., Sailaja B. S., Shankar G. N., Gadad S. S., Reddy A., Dasgupta D. and Kundu T. K. (2009b). "Sanguinarine interacts with chromatin, modulates epigenetic modifications, and transcription in the context of chromatin." Chem Biol **16**(2): 203-216.

Sen G. L., Webster D. E., Barragan D. I., Chang H. Y. and Khavari P. A. (2008). "Control of differentiation in a self-renewing mammalian tissue by the histone demethylase JMJD3." Genes Dev **22**(14): 1865-1870.

Sena-Esteves M., Tebbets J. C., Steffens S., Crombleholme T. and Flake A. W. (2004). "Optimized large-scale production of high titer lentivirus vector pseudotypes." J Virol Methods **122**(2): 131-139.

Senner C. E. and Brockdorff N. (2009). "Xist gene regulation at the onset of X inactivation." Curr Opin Genet Dev **19**(2): 122-126.

Shamblott M. J., Axelman J., Wang S., Bugg E. M., Littlefield J. W., Donovan P. J., Blumenthal P. D., Huggins G. R. and Gearhart J. D. (1998). "Derivation of pluripotent stem cells from cultured human primordial germ cells." Proc Natl Acad Sci U S A **95**(23): 13726-13731.

Shanks N., Greek R. and Greek J. (2009). "Are animal models predictive for humans?" Philos Ethics Humanit Med **4**(1): 2.

Shao L., Feng W., Sun Y., Bai H., Liu J., Currie C., Kim J., Gama R., Wang Z., Qian Z., Liaw L. and Wu W.-S. (2009). "Generation of iPS cells using defined factors linked via the self-cleaving 2A sequences in a single open reading frame." Cell Res **19**(3): 296-306.

Shao Y., Chan C. Y., Maliyekkel A., Lawrence C. E., Roninson I. B. and Ding Y. (2007). "Effect of target secondary structure on RNAi efficiency." RNA **13**(10): 1631-1640.

Sharov A. A. and Ko M. S. H. (2009). "Exhaustive Search for Over-represented DNA Sequence Motifs with CisFinder." DNA Res **16**(5): 261-273.

Shen X., Kim W., Fujiwara Y., Simon M. D., Liu Y., Mysliwiec M. R., Yuan G.-C., Lee Y. and Orkin S. H. (2009). "Jumonji Modulates Polycomb Activity and Self-Renewal versus Differentiation of Stem Cells." Cell **139**(7): 1303-1314.

Shen Y., Chow J., Wang Z. and Fan G. (2006). "Abnormal CpG island methylation occurs during in vitro differentiation of human embryonic stem cells." Hum. Mol. Genet. **15**(17): 2623-2635.

Shi W., Wang H., Pan G., Geng Y., Guo Y. and Pei D. (2006). "Regulation of the Pluripotency Marker Rex-1 by Nanog and Sox2." J. Biol. Chem. **281**(33): 23319-23325.

Shi Y., Desponts C., Do J. T., Hahm H. S., Scholer H. R. and Ding S. (2008). "Induction of pluripotent stem cells from mouse embryonic fibroblasts by Oct4 and Klf4 with small-molecule compounds." Cell Stem Cell **3**(5): 568-574.

Shields J. M., Christy R. J. and Yang V. W. (1996). "Identification and characterization of a gene encoding a gut-enriched Kruppel-like factor expressed during growth arrest." J Biol Chem **271**(33): 20009-20017.

Shilatifard A. (2008). "Molecular implementation and physiological roles for histone H3 lysine 4 (H3K4) methylation." Curr Opin Cell Biol **20**(3): 341-348.

Shively C. A. and Clarkson T. B. (2009). "The unique value of primate models in translational research. Nonhuman primate models of women's health: introduction and overview." Am J Primatol **71**(9): 715-721.

Short K. R., Vittone J. L., Bigelow M. L., Proctor D. N., Coenen-Schimke J. M., Rys P. and Nair K. S. (2005). "Changes in myosin heavy chain mRNA and protein expression in human skeletal muscle with age and endurance exercise training." J Appl Physiol **99**(1): 95-102.

Silva S. S., Rowntree R. K., Mekhoubad S. and Lee J. T. (2008). "X-chromosome inactivation and epigenetic fluidity in human embryonic stem cells." Proc Natl Acad Sci U S A **105**(12): 4820-4825.

Sims R. J., 3rd, Millhouse S., Chen C. F., Lewis B. A., Erdjument-Bromage H., Tempst P., Manley J. L. and Reinberg D. (2007). "Recognition of trimethylated histone H3 lysine 4 facilitates the recruitment of transcription postinitiation factors and pre-mRNA splicing." Mol Cell **28**(4): 665-676.

Singer K. H., Scearce R. M., Tuck D. T., Whichard L. P., Denning S. M. and Haynes B. F. (1989). "Removal of fibroblasts from human epithelial cell cultures with use of a complement fixing monoclonal antibody reactive with human fibroblasts and monocytes/macrophages." J Invest Dermatol **92**(2): 166-170.

Sjogren-Jansson E., Zetterstrom M., Moya K., Lindqvist J., Strehl R. and Eriksson P. S. (2005). "Large-scale propagation of four undifferentiated human embryonic stem cell lines in a feeder-free culture system." Dev Dyn **233**(4): 1304-1314.

Skottman H. and Hovatta O. (2006). "Culture conditions for human embryonic stem cells." Reproduction **132**(5): 691-698.

Skottman H., Mikkola M., Lundin K., Olsson C., Stromberg A. M., Tuuri T., Otonkoski T., Hovatta O. and Lahesmaa R. (2005). "Gene expression signatures of seven individual human embryonic stem cell lines." Stem Cells **23**(9): 1343-1356.

Skottman H., Stromberg A. M., Matilainen E., Inzunza J., Hovatta O. and Lahesmaa R. (2006). "Unique gene expression signature by human embryonic stem cells cultured under serum-free conditions correlates with their enhanced and prolonged growth in an undifferentiated stage." Stem Cells **24**(1): 151-167.

Skuse D. H. (2005). "X-linked genes and mental functioning." Hum Mol Genet **14 Spec No 1**: R27-32.

Smith A. (2009). "Design principles of pluripotency." EMBO Mol Med **1**(5): 251-254.

Smith A. G. (2001). "Embryo-derived stem cells: of mice and men." Annu Rev Cell Dev Biol **17**: 435-462.

Soldner F., Hockemeyer D., Beard C., Gao Q., Bell G. W., Cook E. G., Hargus G., Blak A., Cooper O., Mitalipova M., Isacson O. and Jaenisch R. (2009). "Parkinson's disease patient-derived induced pluripotent stem cells free of viral reprogramming factors." Cell **136**(5): 964-977.

Somia N. and Verma I. M. (2000). "Gene therapy: trials and tribulations." Nat Rev Genet **1**(2): 91-99.

Song Z., Cai J., Liu Y., Zhao D., Yong J., Duo S., Song X., Guo Y., Zhao Y., Qin H., Yin X., Wu C., Che J., Lu S., Ding M. and Deng H. (2009). "Efficient generation of hepatocyte-like cells from human induced pluripotent stem cells." Cell Res.

Sontheimer E. J. and Carthew R. W. (2005). "Silence from within: Endogenous siRNAs and miRNAs." Cell **122**(1): 9-12.

Spada F., Haemmer A., Kuch D., Rothbauer U., Schermelleh L., Kremmer E., Carell T., Langst G. and Leonhardt H. (2007). "DNMT1 but not its interaction with the replication machinery is required for maintenance of DNA methylation in human cells." J Cell Biol **176**(5): 565-571.

Sparmann A. and van Lohuizen M. (2006). "Polycomb silencers control cell fate, development and cancer." Nat Rev Cancer **6**(11): 846-856.

Spits C., Mateizel I., Geens M., Mertzanidou A., Staessen C., Vandeskelde Y., Van der Elst J., Liebaers I. and Sermon K. (2008). "Recurrent chromosomal abnormalities in human embryonic stem cells." Nat Biotechnol **26**(12): 1361-1363.

Spivakov M. and Fisher A. G. (2007). "Epigenetic signatures of stem-cell identity." Nat Rev Genet **8**(4): 263-271.

Sridharan R., Tchieu J., Mason M. J., Yachechko R., Kuoy E., Horvath S., Zhou Q. and Plath K. (2009). "Role of the Murine Reprogramming Factors in the Induction of Pluripotency." **136**(2): 364-377.

Stadtfeld M., Brennand K. and Hochedlinger K. (2008a). "Reprogramming of pancreatic beta cells into induced pluripotent stem cells." Curr Biol **18**(12): 890-894.

Stadtfeld M., Maherali N., Breault D. T. and Hochedlinger K. (2008b). "Defining molecular cornerstones during fibroblast to iPS cell reprogramming in mouse." Cell Stem Cell **2**(3): 230-240.

Stadtfeld M., Nagaya M., Utikal J., Weir G. and Hochedlinger K. (2008c). "Induced pluripotent stem cells generated without viral integration." Science **322**(5903): 945-949.

Stock J. K., Giadrossi S., Casanova M., Brookes E., Vidal M., Koseki H., Brockdorff N., Fisher A. G. and Pombo A. (2007). "Ring1-mediated ubiquitination of H2A restrains poised RNA polymerase II at bivalent genes in mouse ES cells." Nat Cell Biol **9**(12): 1428-1435.

Stojkovic P., Lako M., Stewart R., Przyborski S., Armstrong L., Evans J., Murdoch A., Strachan T. and Stojkovic M. (2005). "An autogeneic feeder cell system that efficiently supports growth of undifferentiated human embryonic stem cells." Stem Cells **23**(3): 306-314.

Subramanyam D. and Blelloch R. (2009). "Watching reprogramming in real time." Nat Biotech **27**(11): 997-998.

Suetake I., Shinozaki F., Miyagawa J., Takeshima H. and Tajima S. (2004). "DNMT3L stimulates the DNA methylation activity of Dnmt3a and Dnmt3b through a direct interaction." J Biol Chem **279**(26): 27816-27823.

Sui G., Soohoo C., Affar el B., Gay F., Shi Y., Forrester W. C. and Shi Y. (2002). "A DNA vector-based RNAi technology to suppress gene expression in mammalian cells." Proc Natl Acad Sci U S A **99**(8): 5515-5520.

Sun B. W., Yang A. C., Feng Y., Sun Y. J., Zhu Y., Zhang Y., Jiang H., Li C. L., Gao F. R., Zhang Z. H., Wang W. C., Kong X. Y., Jin G., Fu S. J. and Jin Y. (2006). "Temporal and parental-specific expression of imprinted genes in a newly derived Chinese human embryonic stem cell line and embryoid bodies." Hum Mol Genet **15**(1): 65-75.

Sun Y., Li H., Liu Y., Shin S., Mattson M. P., Rao M. S. and Zhan M. (2007). "Cross-species transcriptional profiles establish a functional portrait of embryonic stem cells." Genomics **89**(1): 22-35.

Surani M. A. (2001). "Reprogramming of genome function through epigenetic inheritance." Nature **414**(6859): 122-128.

Suter D. M., Cartier L., Bettiol E., Tirefort D., Jaconi M. E., Dubois-Dauphin M. and Krause K. H. (2006). "Rapid generation of stable transgenic embryonic stem cell lines using modular lentivectors." Stem Cells **24**(3): 615-623.

Sutherland E., Coe L. and Raleigh E. A. (1992). "McrBC: a multisubunit GTP-dependent restriction endonuclease." J Mol Biol **225**(2): 327-348.

Swistowski A., Peng J., Han Y., Swistowska A. M., Rao M. S. and Zeng X. (2009). "Xeno-free defined conditions for culture of human embryonic stem cells, neural stem cells and dopaminergic neurons derived from them." PLoS One **4**(7): e6233.

Szulc J., Wiznerowicz M., Sauvain M. O., Trono D. and Aebischer P. (2006). "A versatile tool for conditional gene expression and knockdown." Nat Methods **3**(2): 109-116.

Szyf M. (2003). "Targeting DNA methylation in cancer." Ageing Res Rev **2**(3): 299-328.

Tachibana M., Sugimoto K., Fukushima T. and Shinkai Y. (2001). "Set domain-containing protein, G9a, is a novel lysine-preferring mammalian histone methyltransferase with hyperactivity and specific selectivity to lysines 9 and 27 of histone H3." J Biol Chem **276**(27): 25309-25317.

Tachibana M., Sugimoto K., Nozaki M., Ueda J., Ohta T., Ohki M., Fukuda M., Takeda N., Niida H., Kato H. and Shinkai Y. (2002). "G9a histone methyltransferase plays a dominant role in euchromatic histone H3 lysine 9 methylation and is essential for early embryogenesis." Genes Dev **16**(14): 1779-1791.

Takahashi K., Tanabe K., Ohnuki M., Narita M., Ichisaka T., Tomoda K. and Yamanaka S. (2007). "Induction of pluripotent stem cells from adult human fibroblasts by defined factors." Cell **131**(5): 861-872.

Takahashi K. and Yamanaka S. (2006). "Induction of pluripotent stem cells from mouse embryonic and adult fibroblast cultures by defined factors." Cell **126**(4): 663-676.

Takai D. and Jones P. A. (2002). "Comprehensive analysis of CpG islands in human chromosomes 21 and 22." Proc Natl Acad Sci U S A **99**(6): 3740-3745.

Takeda J., Seino S. and Bell G. I. (1992). "Human Oct3 gene family: cDNA sequences, alternative splicing, gene organization, chromosomal location, and expression at low levels in adult tissues." Nucleic Acids Res **20**(17): 4613-4620.

Taura D., Sone M., Homma K., Oyamada N., Takahashi K., Tamura N., Yamanaka S. and Nakao K. (2009). "Induction and Isolation of Vascular Cells From Human-Induced Pluripotent Stem Cells." Arterioscler Thromb Vasc Biol **29**(7): 1100-1103.

Terstegge S., Rath B. H., Laufenberg I., Limbach N., Buchstaller A., Schütze K. and Brüstle O. (2009). "Laser-assisted selection and passaging of human pluripotent stem cell colonies." Journal of Biotechnology **143**(3): 224-230.

Tesar P. J., Chenoweth J. G., Brook F. A., Davies T. J., Evans E. P., Mack D. L., Gardner R. L. and McKay R. D. (2007). "New cell lines from mouse epiblast share defining features with human embryonic stem cells." Nature **448**(7150): 196-199.

Thellin O., Zorzi W., Lakaye B., De Borman B., Coumans B., Hennen G., Grisar T., Igout A. and Heinen E. (1999). "Housekeeping genes as internal standards: use and limits." J Biotechnol **75**(2-3): 291-295.

Thomas P. and Smart T. G. (2005). "HEK293 cell line: a vehicle for the expression of recombinant proteins." J Pharmacol Toxicol Methods **51**(3): 187-200.

Thompson J. R. and Gudas L. J. (2002). "Retinoic acid induces parietal endoderm but not primitive endoderm and visceral endoderm differentiation in F9 teratocarcinoma stem cells with a targeted deletion of the Rex-1 (Zfp-42) gene." Mol Cell Endocrinol **195**(1-2): 119-133.

Thomson J. A., Itskovitz-Eldor J., Shapiro S. S., Waknitz M. A., Swiergiel J. J., Marshall V. S. and Jones J. M. (1998). "Embryonic stem cell lines derived from human blastocysts." Science **282**(5391): 1145-1147.

Thorvaldsen J. L., Duran K. L. and Bartolomei M. S. (1998). "Deletion of the H19 differentially methylated domain results in loss of imprinted expression of H19 and Igf2." Genes Dev **12**(23): 3693-3702.

Ting A. H., Jair K. W., Suzuki H., Yen R. W., Baylin S. B. and Schuebel K. E. (2004). "Mammalian DNA methyltransferase 1: inspiration for new directions." Cell Cycle **3**(8): 1024-1026.

Tiscornia G., Singer O. and Verma I. M. (2006). "Production and purification of lentiviral vectors." Nat Protoc **1**(1): 241-245.

Tokuzawa Y., Kaiho E., Maruyama M., Takahashi K., Mitsui K., Maeda M., Niwa H. and Yamanaka S. (2003). "Fbx15 is a novel target of Oct3/4 but is dispensable for embryonic stem cell self-renewal and mouse development." Mol Cell Biol **23**(8): 2699-2708.

Tomkins D. J., McDonald H. L., Farrell S. A. and Brown C. J. (2002). "Lack of expression of XIST from a small ring X chromosome containing the XIST locus in a girl with short stature, facial dysmorphism and developmental delay." Eur J Hum Genet **10**(1): 44-51.

Torres-Padilla M.-E., Parfitt D.-E., Kouzarides T. and Zernicka-Goetz M. (2007). "Histone arginine methylation regulates pluripotency in the early mouse embryo." Nature **445**(7124): 214-218.

Tsou A. P., Chuang Y. C., Su J. Y., Yang C. W., Liao Y. L., Liu W. K., Chiu J. H. and Chou C. K. (2003). "Overexpression of a novel imprinted gene, PEG10, in human hepatocellular carcinoma and in regenerating mouse livers." J Biomed Sci **10**(6 Pt 1): 625-635.

Tsumura A., Hayakawa T., Kumaki Y., Takebayashi S., Sakaue M., Matsuoka C., Shimotohno K., Ishikawa F., Li E., Ueda H. R., Nakayama J. and Okano M. (2006). "Maintenance of self-renewal ability of mouse embryonic stem cells in the absence of DNA methyltransferases Dnmt1, Dnmt3a and Dnmt3b." Genes Cells **11**(7): 805-814.

Turek-Plewa J. and Jagodzinski P. P. (2005). "The role of mammalian DNA methyltransferases in the regulation of gene expression." Cell Mol Biol Lett **10**(4): 631-647.

Ueda Y., Okano M., Williams C., Chen T., Georgopoulos K. and Li E. (2006). "Roles for Dnmt3b in mammalian development: a mouse model for the ICF syndrome." Development **133**(6): 1183-1192.

Ullmannova V. and Haskovec C. (2003). "The use of housekeeping genes (HKG) as an internal control for the detection of gene expression by quantitative real-time RT-PCR." Folia Biol (Praha) **49**(6): 211-216.

Unger C., Skottman H., Blomberg P., Dilber M. S. and Hovatta O. (2008). "Good manufacturing practice and clinical-grade human embryonic stem cell lines." Hum Mol Genet **17**(R1): R48-53.

Ungrin M. D., Joshi C., Nica A., Bauwens C. and Zandstra P. W. (2008). "Reproducible, ultra high-throughput formation of multicellular organization from single cell suspension-derived human embryonic stem cell aggregates." PLoS One **3**(2): e1565.

Unterberger A., Andrews S. D., Weaver I. C. and Szyf M. (2006). "DNA methyltransferase 1 knockdown activates a replication stress checkpoint." Mol Cell Biol **26**(20): 7575-7586.

Utikal J., Polo J. M., Stadtfeld M., Maherali N., Kulalert W., Walsh R. M., Khalil A., Rheinwald J. G. and Hochedlinger K. (2009). "Immortalization eliminates a roadblock during cellular reprogramming into iPS cells." Nature **460**(7259): 1145-1148.

Vaissiere T., Sawan C. and Herceg Z. (2008). "Epigenetic interplay between histone modifications and DNA methylation in gene silencing." Mutat Res **659**(1-2): 40-48.

Valencia-Sanchez M. A., Liu J., Hannon G. J. and Parker R. (2006). "Control of translation and mRNA degradation by miRNAs and siRNAs." Genes Dev **20**(5): 515-524.

Vallier L., Alexander M. and Pedersen R. A. (2005). "Activin/Nodal and FGF pathways cooperate to maintain pluripotency of human embryonic stem cells." J Cell Sci **118**(Pt 19): 4495-4509.

Vallier L., Mendjan S., Brown S., Chng Z., Teo A., Smithers L. E., Trotter M. W., Cho C. H., Martinez A., Rugg-Gunn P., Brons G. and Pedersen R. A. (2009a). "Activin/Nodal signalling maintains pluripotency by controlling Nanog expression." Development **136**(8): 1339-1349.

Vallier L., Rugg-Gunn P. J., Bouhon I. A., Andersson F. K., Sadler A. J. and Pedersen R. A. (2004). "Enhancing and diminishing gene function in human embryonic stem cells." Stem Cells **22**(1): 2-11.

Vallier L., Touboul T., Brown S., Cho C., Bilican B., Alexander M., Cedervall J., Chandran S., Ahrlund-Richter L., Weber A. and Pedersen R. A. (2009b). "Signalling pathways controlling pluripotency and early cell fate decisions of human induced pluripotent stem cells." Stem Cells **27**(11): 2655-2666.

Vallier L., Touboul T., Chng Z., Brimpari M., Hannan N., Millan E., Smithers L. E., Trotter M., Rugg-Gunn P., Weber A. and Pedersen R. A. (2009c). "Early cell fate decisions of human embryonic stem cells and mouse epiblast stem cells are controlled by the same signalling pathways." PLoS One **4**(6): e6082.

van der Stoop P., Boutsma E. A., Hulsman D., Noback S., Heimerikx M., Kerkhoven R. M., Voncken J. W., Wessels L. F. and van Lohuizen M. (2008). "Ubiquitin E3 ligase Ring1b/Rnf2 of polycomb repressive complex 1 contributes to stable maintenance of mouse embryonic stem cells." PLoS ONE **3**(5): e2235.

Vertino P. M., Yen R. W., Gao J. and Baylin S. B. (1996). "De novo methylation of CpG island sequences in human fibroblasts overexpressing DNA (cytosine-5-)-methyltransferase." Mol Cell Biol **16**(8): 4555-4565.

Vidricaire G., Jardine K. and McBurney M. W. (1994). "Expression of the Brachyury gene during mesoderm development in differentiating embryonal carcinoma cell cultures." Development **120**(1): 115-122.

Visel A., Blow M. J., Li Z., Zhang T., Akiyama J. A., Holt A., Plajzer-Frick I., Shoukry M., Wright C., Chen F., Afzal V., Ren B., Rubin E. M. and Pennacchio L. A. (2009). "ChIP-seq accurately predicts tissue-specific activity of enhancers." Nature **457**(7231): 854-858.

Viswanathan S. R., Daley G. Q. and Gregory R. I. (2008). "Selective blockade of microRNA processing by Lin28." Science **320**(5872): 97-100.

Voss A. K., Thomas T., Petrou P., Anastassiadis K., Scholer H. and Gruss P. (2000). "Taube nuss is a novel gene essential for the survival of pluripotent cells of early mouse embryos." Development **127**(24): 5449-5461.

Wang J., Rao S., Chu J., Shen X., Levasseur D. N., Theunissen T. W. and Orkin S. H. (2006). "A protein interaction network for pluripotency of embryonic stem cells." Nature **444**(7117): 364-368.

Wang J., Wang H., Li Z., Wu Q., Lathia J. D., McLendon R. E., Hjelmeland A. B. and Rich J. N. (2008a). "c-Myc is required for maintenance of glioma cancer stem cells." PLoS One **3**(11): e3769.

Wang L., Schulz T. C., Sherrer E. S., Dauphin D. S., Shin S., Nelson A. M., Ware C. B., Zhan M., Song C. Z., Chen X., Brimble S. N., McLean A., Galeano M. J., Uhl E. W., D'Amour K. A., Chesnut J. D., Rao M. S., Blau C. A. and Robins A. J. (2007). "Self-renewal of human embryonic stem cells requires insulin-like growth factor-1 receptor and ERBB2 receptor signaling." Blood **110**(12): 4111-4119.

Wang Q., Fang Z. F., Jin F., Lu Y., Gai H. and Sheng H. Z. (2005). "Derivation and growing human embryonic stem cells on feeders derived from themselves." Stem Cells **23**(9): 1221-1227.

Wang Y., Baskerville S., Shenoy A., Babiarz J. E., Baehner L. and Blelloch R. (2008b). "Embryonic stem cell-specific microRNAs regulate the G1-S transition and promote rapid proliferation." Nat Genet **40**(12): 1478-1483.

Weake V. M. and Workman J. L. (2008). "Histone Ubiquitination: Triggering Gene Activity." **29**(6): 653-663.

Wei C. L., Miura T., Robson P., Lim S. K., Xu X. Q., Lee M. Y., Gupta S., Stanton L., Luo Y., Schmitt J., Thies S., Wang W., Khrebtukova I., Zhou D., Liu E. T., Ruan Y. J., Rao M. and Lim B. (2005). "Transcriptome profiling of human and murine ESCs identifies divergent paths required to maintain the stem cell state." Stem Cells **23**(2): 166-185.

Wei D., Kanai M., Huang S. and Xie K. (2006). "Emerging role of KLF4 in human gastrointestinal cancer." Carcinogenesis **27**(1): 23-31.

Wei F., Scholer H. R. and Atchison M. L. (2007). "Sumoylation of Oct4 enhances its stability, DNA binding, and transactivation." J Biol Chem **282**(29): 21551-21560.

Wei Z., Yang Y., Zhang P., Andrianakos R., Hasegawa K., Lyu J., Chen X., Bai G., Liu C., Pera M. and Lu W. (2009). "Klf4 interacts directly with Oct4 and Sox2 to promote reprogramming." Stem Cells **27**(12): 2969-2978.

Weichert W., Roske A., Gekeler V., Beckers T., Stephan C., Jung K., Fritzsche F. R., Niesporek S., Denkert C., Dietel M. and Kristiansen G. (2008). "Histone deacetylases 1, 2 and 3 are highly expressed in prostate cancer and HDAC2 expression is associated with shorter PSA relapse time after radical prostatectomy." Br J Cancer **98**(3): 604-610.

Weinstein L. S., Liu J., Sakamoto A., Xie T. and Chen M. (2004). "Minireview: GNAS: normal and abnormal functions." Endocrinology **145**(12): 5459-5464.

Weinstein L. S., Yu S., Warner D. R. and Liu J. (2001). "Endocrine manifestations of stimulatory G protein alpha-subunit mutations and the role of genomic imprinting." Endocr Rev **22**(5): 675-705.

Weiss U., Ischia R., Eder S., Lovisetti-Scamihorn P., Bauer R. and Fischer-Colbrie R. (2000). "Neuroendocrine secretory protein 55 (NESP55): alternative splicing onto transcripts of the GNAS gene and posttranslational processing of a maternally expressed protein." Neuroendocrinology **71**(3): 177-186.

Weitzer G. (2006). "Embryonic stem cell-derived embryoid bodies: an in vitro model of eutherian pregastrulation development and early gastrulation." Handb Exp Pharmacol(174): 21-51.

Wernig M., Meissner A., Cassady J. P. and Jaenisch R. (2008a). "c-Myc is dispensable for direct reprogramming of mouse fibroblasts." Cell Stem Cell **2**(1): 10-12.

Wernig M., Meissner A., Foreman R., Brambrink T., Ku M., Hochedlinger K., Bernstein B. E. and Jaenisch R. (2007). "In vitro reprogramming of fibroblasts into a pluripotent ES-cell-like state." Nature **448**(7151): 318-324.

Wernig M., Zhao J. P., Pruszak J., Hedlund E., Fu D., Soldner F., Broccoli V., Constantine-Paton M., Isacson O. and Jaenisch R. (2008b). "Neurons derived from reprogrammed fibroblasts functionally integrate into the fetal brain and improve symptoms of rats with Parkinson's disease." Proc Natl Acad Sci U S A **105**(15): 5856-5861.

Whitehead K. A., Langer R. and Anderson D. G. (2009). "Knocking down barriers: advances in siRNA delivery." Nat Rev Drug Discov **8**(2): 129-138.

Williamson C. M., Ball S. T., Nottingham W. T., Skinner J. A., Plagge A., Turner M. D., Powles N., Hough T., Papworth D., Fraser W. D., Maconochie M. and Peters J. (2004). "A cis-acting control region is required exclusively for the tissue-specific imprinting of Gnas." Nat Genet **36**(8): 894-899.

Williamson C. M., Turner M. D., Ball S. T., Nottingham W. T., Glenister P., Fray M., Tymowska-Lalanne Z., Plagge A., Powles-Glover N., Kelsey G., Maconochie M. and Peters J. (2006). "Identification of an imprinting control region affecting the expression of all transcripts in the Gnas cluster." Nat Genet **38**(3): 350-355.

Williamson D. F., Parker R. A. and Kendrick J. S. (1989). "The box plot: a simple visual method to interpret data." Ann Intern Med **110**(11): 916-921.

Wilson A. S., Power B. E. and Molloy P. L. (2007). "DNA hypomethylation and human diseases." Biochim Biophys Acta **1775**(1): 138-162.

Woltjen K., Michael I. P., Mohseni P., Desai R., Mileikovsky M., Hamalainen R., Cowling R., Wang W., Liu P., Gertsenstein M., Kaji K., Sung H. K. and Nagy A. (2009). "piggyBac transposition reprograms fibroblasts to induced pluripotent stem cells." Nature **458**(7239): 766-770.

Woodcock C. L. and Dimitrov S. (2001). "Higher-order structure of chromatin and chromosomes." Curr Opin Genet Dev **11**(2): 130-135.

Wu L. and Belasco J. G. (2005). "Micro-RNA regulation of the mammalian lin-28 gene during neuronal differentiation of embryonal carcinoma cells." Mol Cell Biol **25**(21): 9198-9208.

Wu L., Fan J. and Belasco J. G. (2006). "MicroRNAs direct rapid deadenylation of mRNA." Proc Natl Acad Sci U S A **103**(11): 4034-4039.

Wu Q., Bruce A. W., Jedrusik A., Ellis P. D., Andrews R. M., Langford C. F., Glover D. M. and Zernicka-Goetz M. (2009a). "CARM1 is Required in ES Cells to Maintain Pluripotency and Resist Differentiation." Stem Cells **27**(11): 2637 - 2645.

Wu Z., Chen J., Ren J., Bao L., Liao J., Cui C., Rao L., Li H., Gu Y., Dai H., Zhu H., Teng X., Cheng L. and Xiao L. (2009b). "Generation of pig induced pluripotent stem cells with a drug-inducible system." J Mol Cell Biol **1**(1): 46-54.

Xia X., Ayala M., Thiede B. R. and Zhang S. C. (2008). "In vitro- and in vivo-induced transgene expression in human embryonic stem cells and derivatives." Stem Cells **26**(2): 525-533.

Xiang Y., Zhu Z., Han G., Lin H., Xu L. and Chen C. D. (2007). "JMJD3 is a histone H3K27 demethylase." Cell Res **17**(10): 850-857.

Xie S., Wang Z., Okano M., Nogami M., Li Y., He W. W., Okumura K. and Li E. (1999). "Cloning, expression and chromosome locations of the human DNMT3 gene family." Gene **236**(1): 87-95.

Xiong Z. and Laird P. W. (1997). "COBRA: a sensitive and quantitative DNA methylation assay." Nucleic Acids Res **25**(12): 2532-2534.

Xu B. and Huang Y. (2009). "Histone H2a mRNA interacts with Lin28 and contains a Lin28-dependent posttranscriptional regulatory element." Nucleic Acids Res **37**(13): 4256-4263.

Xu B., Zhang K. and Huang Y. (2009a). "Lin28 modulates cell growth and associates with a subset of cell cycle regulator mRNAs in mouse embryonic stem cells." RNA **15**(3): 357-361.

Xu C., Inokuma M. S., Denham J., Golds K., Kundu P., Gold J. D. and Carpenter M. K. (2001). "Feeder-free growth of undifferentiated human embryonic stem cells." Nat Biotechnol **19**(10): 971-974.

Xu C., Jiang J., Sottile V., McWhir J., Lebkowski J. and Carpenter M. K. (2004). "Immortalized fibroblast-like cells derived from human embryonic stem cells support undifferentiated cell growth." Stem Cells **22**(6): 972-980.

Xu H., Wang W., Li C., Yu H., Yang A., Wang B. and Jin Y. (2009b). "WWP2 promotes degradation of transcription factor OCT4 in human embryonic stem cells." Cell Res **19**(5): 561-573.

Xu N., Papagiannakopoulos T., Pan G., Thomson J. A. and Kosik K. S. (2009c). "MicroRNA-145 Regulates OCT4, SOX2, and KLF4 and Represses Pluripotency in Human Embryonic Stem Cells." Cell **137**(4): 647-658.

Xu R. H., Peck R. M., Li D. S., Feng X., Ludwig T. and Thomson J. A. (2005). "Basic FGF and suppression of BMP signaling sustain undifferentiated proliferation of human ES cells." Nat Methods **2**(3): 185-190.

Xue Y., Wong J., Moreno G. T., Young M. K., Cote J. and Wang W. (1998). "NURD, a novel complex with both ATP-dependent chromatin-remodeling and histone deacetylase activities." Mol Cell **2**(6): 851-861.

Yamanaka S. (2009). "Elite and stochastic models for induced pluripotent stem cell generation." Nature **460**(7251): 49-52.

Yan Z., Wang Z., Sharova L., Sharov A. A., Ling C., Piao Y., Aiba K., Matoba R., Wang W. and Ko M. S. (2008). "BAF250B-associated SWI/SNF chromatin-remodeling complex is required to maintain undifferentiated mouse embryonic stem cells." Stem Cells **26**(5): 1155-1165.

Yanagisawa Y., Ito E., Yuasa Y. and Maruyama K. (2002). "The human DNA methyltransferases DNMT3A and DNMT3B have two types of promoters with different CpG contents." Biochim Biophys Acta **1577**(3): 457-465.

Yang H. H., Hu N., Wang C., Ding T., Dunn B. K., Goldstein A. M., Taylor P. R. and Lee M. P. "Influence of genetic background and tissue types on global DNA methylation patterns." PLoS One **5**(2): e9355.

Yang J., Yang S., Beaujean N., Niu Y., He X., Xie Y., Tang X., Wang L., Zhou Q. and Ji W. (2007). "Epigenetic marks in cloned rhesus monkey embryos: comparison with counterparts produced in vitro." Biol Reprod **76**(1): 36-42.

Yang T., Adamson T. E., Resnick J. L., Leff S., Wevrick R., Francke U., Jenkins N. A., Copeland N. G. and Brannan C. I. (1998). "A mouse model for Prader-Willi syndrome imprinting-centre mutations." Nat Genet **19**(1): 25-31.

Yao S., Chen S., Clark J., Hao E., Beattie G. M., Hayek A. and Ding S. (2006). "Long-term self-renewal and directed differentiation of human embryonic stem cells in chemically defined conditions." Proc Natl Acad Sci U S A **103**(18): 6907-6912.

Yen Z. C., Meyer I. M., Karalic S. and Brown C. J. (2007). "A cross-species comparison of X-chromosome inactivation in Eutheria." Genomics **90**(4): 453-463.

Yeo S., Jeong S., Kim J., Han J. S., Han Y. M. and Kang Y. K. (2007). "Characterization of DNA methylation change in stem cell marker genes during differentiation of human embryonic stem cells." Biochem Biophys Res Commun **359**(3): 536-542.

Yokoo N., Baba S., Kaichi S., Niwa A., Mima T., Doi H., Yamanaka S., Nakahata T. and Heike T. (2009). "The effects of cardioactive drugs on cardiomyocytes derived from human induced pluripotent stem cells." Biochemical and Biophysical Research Communications **387**(3): 482-488.

Yong Gu C. H. O., Jae Hwi S., Chang Jae K. I. M., Suk Woo N. A. M., Nam Jin Y. O. O., Jung Young L. E. E. and Won Sang P. (2007). "Genetic and epigenetic analysis of the KLF4 gene in gastric cancer." Apmis **115**(7): 802-808.

Yoon B. S., Yoo S. J., Lee J. E., You S., Lee H. T. and Yoon H. S. (2006). "Enhanced differentiation of human embryonic stem cells into cardiomyocytes by combining hanging drop culture and 5-azacytidine treatment." Differentiation **74**(4): 149-159.

Yoshida T., Gan Q. and Owens G. K. (2008). "Kruppel-like factor 4, Elk-1, and histone deacetylases cooperatively suppress smooth muscle cell differentiation markers in response to oxidized , phospholipids." Am J Physiol Cell Physiol **295**(5): C1175-1182.

Young L. E. and Beaujean N. (2004). "DNA methylation in the preimplantation embryo: the differing stories of the mouse and sheep." Anim Reprod Sci **82-83**: 61-78.

Young L. E. and Denning C. (2007). "Oct4 during the pluripotency differentiation transition: who is regulating the regulator." Regen Med **2**(2): 211-215.

Yu F., Yao H., Zhu P., Zhang X., Pan Q., Gong C., Huang Y., Hu X., Su F., Lieberman J. and Song E. (2007a). "let-7 regulates self renewal and tumorigenicity of breast cancer cells." Cell **131**(6): 1109-1123.

Yu J., Hu K., Smuga-Otto K., Tian S., Stewart R., Slukvin I. I. and Thomson J. A. (2009). "Human Induced Pluripotent Stem Cells Free of Vector and Transgene Sequences." Science **324**(5928): 797-801.

Yu J., Vodyanik M. A., Smuga-Otto K., Antosiewicz-Bourget J., Frane J. L., Tian S., Nie J., Jonsdottir G. A., Ruotti V., Stewart R., Slukvin, II and Thomson J. A. (2007b). "Induced pluripotent stem cell lines derived from human somatic cells." Science **318**(5858): 1917-1920.

Yuan J. S., Wang D. and Stewart C. N., Jr. (2008). "Statistical methods for efficiency adjusted real-time PCR quantification." Biotechnol J **3**(1): 112-123.

Yusa K., Rad R., Takeda J. and Bradley A. (2009). "Generation of transgene-free induced pluripotent mouse stem cells by the piggyBac transposon." Nat Methods **6**(5): 363-369.

Zainuddin A., Makpol S., Chua K. H., Abdul Rahim N., Yusof Y. A. and Ngah W. Z. (2008). "GAPDH as housekeeping gene for human skin fibroblast senescent model." Med J Malaysia **63 Suppl A**: 73-74.

Zappone M. V., Galli R., Catena R., Meani N., De Biasi S., Mattei E., Tiveron C., Vescovi A. L., Lovell-Badge R., Ottolenghi S. and Nicolis S. K. (2000). "Sox2 regulatory sequences direct expression of a (beta)-geo transgene to telencephalic neural stem cells and precursors of the mouse embryo, revealing regionalization of gene expression in CNS stem cells." Development **127**(11): 2367-2382.

Zeng X., Miura T., Luo Y., Bhattacharya B., Condie B., Chen J., Ginis I., Lyons I., Mejido J., Puri R. K., Rao M. S. and Freed W. J. (2004). "Properties of pluripotent human embryonic stem cells BG01 and BG02." Stem Cells **22**(3): 292-312.

Zhang, Stojkovic P., Przyborski S., Cooke M., Armstrong L., Lako M. and Stojkovic M. (2006). "Derivation of human embryonic stem cells from developing and arrested embryos." Stem Cells **24**(12): 2669-2676.

Zhang H., Roberts D. N. and Cairns B. R. (2005). "Genome-wide dynamics of Htz1, a histone H2A variant that poises repressed/basal promoters for activation through histone loss." Cell **123**(2): 219-231.

Zhang X., Zhang J., Wang T., Esteban M. A. and Pei D. (2008). "Esrrb activates Oct4 transcription and sustains self-renewal and pluripotency in embryonic stem cells." J Biol Chem **283**(51): 35825-35833.

Zhang X. F., Guo S. Z., Lu K. H., Li H. Y., Li X. D., Zhang L. X. and Yang L. (2004). "Different roles of PKC and PKA in effect of interferon-gamma on proliferation and collagen synthesis of fibroblasts." Acta Pharmacol Sin **25**(10): 1320-1326.

Zhao Z. and Zhang F. (2006). "Sequence context analysis in the mouse genome: single nucleotide polymorphisms and CpG island sequences." Genomics **87**(1): 68-74.

Zhou H., Wu S., Joo J. Y., Zhu S., Han D. W., Lin T., Trauger S., Bien G., Yao S., Zhu Y., Siuzdak G., Schöler H. R., Duan L. and Ding S. (2009). "Generation of Induced Pluripotent Stem Cells Using Recombinant Proteins." Differentiation **4**(5): 381-384.

Zhou X., Cui Y., Huang X., Yu Z., Thomas A. M., Ye Z., Pardoll D. M., Jaffee E. M. and Cheng L. (2003). "Lentivirus-mediated gene transfer and expression in established human tumor antigen-specific cytotoxic T cells and primary unstimulated T cells." Hum Gene Ther **14**(11): 1089-1105.

Zhou Y., Bui T., Auckland L. D. and Williams C. G. (2002). "Undermethylated DNA as a source of microsatellites from a conifer genome." Genome **45**(1): 91-99.

Zhu B., Zheng Y., Hess D., Angliker H., Schwarz S., Siegmann M., Thiry S. and Jost J. P. (2000). "5-methylcytosine-DNA glycosylase activity is present in a cloned G/T mismatch DNA glycosylase associated with the chicken embryo DNA demethylation complex." Proc Natl Acad Sci U S A **97**(10): 5135-5139.

Zochbauer-Muller S., Fong K. M., Virmani A. K., Geradts J., Gazdar A. F. and Minna J. D. (2001). "Aberrant promoter methylation of multiple genes in non-small cell lung cancers." Cancer Res **61**(1): 249-255.

APPENDIX I - PUBLICATION DOCUMENTS

6.4 ARTICLES

Braam SR, Denning C. Matsa E, Young LE, Passier R and Mummery CL (2008). "Feeder-free culture of human embryonic stem cells in conditioned medium for efficient genetic modification." Nat. Protocols **3**(9): 1435-1443.

6.5 BOOK CHAPTERS

Lucas ES, Matsa E and Young LE (2010). "Epigenetic consequences of *in vitro* embryo and stem cell manipulation." Springer Epigenetics and Human Reproduction. In press.

Bispham J, Matsa E, Thurston A and Young LE (2010). "Real-time PCR to detect expression of the pluripotency factor *NANOG* in human embryonic stem cells". In writing.

6.6 CONFERENCE ABSTRACTS

Matsa E, O'Neil L, Bispham J, Barbadillo Muñoz MD, Thurston A, McGilvray R, Denning C, Young LE (2009) "Epigenetic regulation of pluripotency in hESCs." Rank Prize Funds Symposium, Cumbria, UK. May 2009. – Paper awarded first prize among participating young scientists

Matsa E, O'Neil L, Thurston A, Bispham J, Barbadillo Muñoz MD, Dick EP, Denning C, Young LE (2009) "Epigenetic insights into the formation of human iPS cells." Annual meeting of the International Society for Stem Cell Research (ISSCR), Barcelona, Spain. July 2009.

APPENDIX II - LIST OF COMPANY DETAILS

Company Name	Website
Abcam, Plc.	http://www.abcam.com
Addgene, Inc.	http://www.addgene.org
Alpha Laboratories (UK)	http://www.alphalabs.co.uk
Amersham Pharmacia Biotech UK Ltd	http.//www.apbiotech.com
Applied Biosystems	http://www.appliedbiosystems.com
Axygen Scientific, Inc.	http://www.axygen.com
BD Biosciences, UK	http://www.bdbiosciences.com
BDH, C/O VWR International (UK), Ltd.	http://uk.vwr.com
Beckman Coulter (UK), Ltd.	http://www.beckmancoulter.co.uk
Bioline Ltd	http://www.bioline.com
Biological Industries (Israel), Ltd.	http://www.bioind.com
Cell Signalling Technology, Inc.	http://www.cellsignal.com
Charles River Laboratories, Inc.	http://www.criver.com
Chemicon Europe, Ltd.	http://www.chemicon.com
Clontech-Takara Bio Europe	http://www.clontech.com
Eppendorf (UK), Ltd.	http://www.eppendorf.co.uk
Fisher Scientific (UK), Ltd.	http://www.fisher.co.uk
FUJIFILM (UK), Ltd.	http://www.fujifilm.co.uk
GE Healthcare	http://www.gehealthcare.com
Grant Instruments (UK), Ltd.	http://www.grant.co.uk
Hyclone	http://www.hyclone.com
Improvision	http://www.improvision.com
Invitrogen, Ltd.	http://www.invitrogen.com
Jackson Immunoresearch Laboratories, Inc.	http://www.jacksonimmuno.com
Menzel-Glaser	http://www.menzel.de
Merck Biosciences / Novagen (UK), Ltd.	http://www.merckbiosciences.co.uk
Millipore (UK.) Ltd.	http://www.millipore.com
Nalge Nunc International	http://www.nuncbrand.com
NanoDrop Technologies	http://www.nanodrop.com
New England Biolabs (UK), Ltd.	http://www.neb.uk.com
Nikon Ltd.	http://www.europe-nikon.com
Promega UK Ltd	http://www.promega.com
Qiagen, Ltd.	http://www.qiagen.com
R & D Systems, Inc.	http://www.rndsystems.com
Raytek Scientific (UK), Ltd.	http://www.raytek.co.uk
Roche Diagnostics Ltd.	http://www.rocheuk.com
Santa Cruz Biotechnology, Inc.	http://www.scbt.com
Sarstedt Ltd	http://www.sarstedt.com
Sartorius (UK), Ltd.	http://www.sartorius.co.uk
Scientific Laboratory Supplies, Ltd.	http://www.scientificlabs.eu
Sigma-Aldrich / Sigma-Genosys Ltd.	http://www.sigmaaldrich.com
Thermo Electron Corporation	http://www.thermo.com
Vector Laboratories, Ltd.	http://www.vectorlabs.com

APPENDIX III - *NANOG* TAQMAN ASSAY DESIGN

Design of *NANOG* TaqMan Assay was based on a single nucleotide polymorphism (SNP) to distinguish between the true NANOG gene and its pseudogenes

APPENDIX IV - STATISTICAL ANALYSIS

Statistical analysis of non-parametric independent variables
H_0= Samples are drawn from independent populations with equal medians
H_a= Samples are drawn from independent populations with non-equal medians
Significance level = 0.05

CHAPTER 4
Gene expression analysis by real-time PCR in the HUES7 and HOGN model systems

OCT4

Grouping Variable	Sample	Median	Mean	Standard error	Probability value (p)	H_0
HUES7 Median= 9.287 Mean= 8.9678 St. error= 0.78481	HUES7-Fib	25.9094	25.9094	1.35933	0.045500	Reject
	HUES7-iPS	9.485979	9.400016	0.95263	0.423340	Accept
	HUES7-iPS Fib	18.39372	18.35008	0.78882	0.003948	Reject
	HUES7-Fib Cl4	-	-	-	0.002093	Reject
	SUKE-Fib	28.8497	29.29636	1.052333	0.020137	Reject
	BJ-Fib	27.06157	27.07187	0.639558	0.003948	Reject
HOGN Median= 6.9618 Mean= 7.5049 St. error= 0.2772	HOGN-Fib	24.37291	24.36013	0.2772017	0.003579	Reject
	HOGN-iPS	9.058858	8.923901	0.289626	0.023471	Reject
	HOGN-iPS Fib	16.91208	17.21931	0.3117006	0.003579	Reject

NANOG

Grouping Variable	Sample	Median	Mean	Standard error	Probability value (p)	H_0
HUES7 Median= 15.453 Mean= 15.4249 St. error= 0.37365	HUES7-Fib	27.34122	27.02458	0.3736502	0.003948	Reject
	HUES7-iPS	14.23995	14.185	0.2848353	0.037373	Reject
	HUES7-iPS Fib	15.01702	14.96467	0.2811683	0.200185	Accept
	HUES7-Fib Cl4	27.23021	27.09966	0.3639324	0.003948	Reject
	SUKE-Fib	25.42235	25.60737	0.2999439	0.003948	Reject
	BJ-Fib	24.44486	24.23281	0.35131	0.003948	Reject
HOGN Median= 15.921 Mean= 15.893 St. error= 0.33884	HOGN-Fib	26.29628	26.61872	0.3388385	0.003948	Reject
	HOGN-iPS	16.40458	16.33193	0.3335624	0.200185	Accept
	HOGN-iPS Fib	18.03669	18.15962	0.2882671	0.003948	Reject

SOX2

Grouping Variable	Sample	Median	Mean	Standard error	Probability value (p)	H_0
HUES7 Median= 11.34035 Mean= 11.38277 St. error= 0.32859	HUES7-Fib	24.24765	24.07612	0.3285909	0.003948	Reject
	HUES7-iPS	13.2709	13.29087	0.2064237	0.003948	Reject
	HUES7-iPS Fib	17.14607	17.17515	0.171713	0.003948	Reject
	HUES7-Fib Cl4	24.86983	24.67653	0.3663152	0.003948	Reject
	SUKE-Fib	22.61161	22.72109	0.4417535	0.003948	Reject
	BJ-Fib	22.14886	22.08077	0.2706956	0.003948	Reject
HOGN Median= 11.2691 Mean= 11.19226 St. error= 0.25398	HOGN-Fib	21.55057	21.68957	0.2539824	0.003948	Reject
	HOGN-iPS	12.35315	12.39261	0.1923115	0.003948	Reject
	HOGN-iPS Fib	19.32827	19.47639	0.1847141	0.003948	Reject

LIN28

Grouping Variable	Sample	Median	Mean	Standard error	Probability value (p)	H_0
HUES7 Median= 10.19753 Mean= 10.18498 St. error= 0.436475	HUES7-Fib	25.37381	24.71629	0.4781346	0.006170	Reject
	HUES7-iPS	10.79433	10.81079	0.4113156	0.149541	Accept
	HUES7-iPS Fib	18.48386	18.78631	0.4103148	0.003948	Reject
	HUES7-Fib Cl4	24.97948	24.81719	0.4049484	0.003948	Reject
	SUKE-Fib	22.24881	22.40644	0.5156769	0.003948	Reject
	BJ-Fib	22.11683	22.1397	0.3208649	0.003948	Reject
HOGN Median=10.41708 Mean=10.41699 St. error= 0.478122	HOGN-Fib	24.07357	24.0327	0.478122	0.003948	Reject
	HOGN-iPS	10.36568	10.34997	0.3806755	0.630954	Accept
	HOGN-iPS Fib	18.00882	17.96105	0.3451578	0.003948	Reject

KLF4

Grouping Variable	Sample	Median	Mean	Standard error	Probability value (p)	H_0
HUES7 Median=24.8657 Mean=24.86371 St. error= 0.168128	HUES7-Fib	24.43035	24.4866	0.1681287	0.149541	Accept
	HUES7-iPS	26.18638	26.29413	0.0098057	0.003948	Reject
	HUES7-iPS Fib	25.7019	25.7652	0.0087272	0.003948	Reject
	HUES7-Fib Cl4	26.71874	26.74418	0.0069024	0.003948	Reject
	SUKE-Fib	24.27029	24.25252	0.2276703	0.262332	Accept
	BJ-Fib	23.36864	23.61779	0.2175693	0.003948	Reject
HOGN Median=25.47297 Mean=25.36978 St. error= 0.1287607	HOGN-Fib	28.42579	28.4423	0.1200987	0.003948	Reject
	HOGN-iPS	26.02183	25.98255	0.1579745	0.037373	Reject
	HOGN-iPS Fib	25.56286	25.62783	0.1314173	0.336668	Accept

REX1

Grouping Variable	Sample	Median	Mean	Standard error	Probability value (p)	H_0
HUES7 Median=13.54009 Mean=13.56946 St. error= 0.1287607	HUES7-Fib	27.61343	27.61343	0.1586892	0.045500	Reject
	HUES7-iPS	23.54689	23.55304	0.139509	0.003948	Reject
	HUES7-iPS Fib	26.11933	25.98291	0.3496676	0.006170	Reject
	HUES7-Fib Cl4	-	-	-	0.002093	Reject
	SUKE-Fib	-	-	-	0.002093	Reject
	BJ-Fib	-	-	-	0.002093	Reject
HOGN Median=13.18482 Mean=13.22766 St. error= 0.122745	HOGN-Fib	22.26485	22.37518	0.1227456	0.003948	Reject
	HOGN-iPS	14.81171	14.83772	0.0971701	0.003948	Reject
	HOGN-iPS Fib	23.31185	23.5101	0.2267205	0.003948	Reject

DNMT3B

Grouping Variable	Sample	Median	Mean	Standard error	Probability value (p)	H_0
HUES7 Median=15.4259 Mean=15.41022 St. error= 0.770171	HUES7-Fib	23.85983	23.71037	0.7701713	0.003948	Reject
	HUES7-iPS	16.97787	17.00202	0.8062362	0.149541	Accept
	HUES7-iPS Fib	23.94463	23.94288	0.7421852	0.003948	Reject
	HUES7-Fib Cl4	25.13584	25.19358	0.7318104	0.003948	Reject
	SUKE-Fib	24.92129	24.91646	0.8540214	0.003948	Reject
	BJ-Fib	25.23142	25.25573	0.8369006	0.003948	Reject
HOGN Median=14.92297 Mean=14.81762 St. error=0.1287607	HOGN-Fib	24.93937	24.94041	0.1287607	0.003948	Reject
	HOGN-iPS	15.88525	16.00218	0.7013581	0.149541	Accept
	HOGN-iPS Fib	21.70299	21.9302	0.7164029	0.003948	Reject

P4HB

Grouping Variable	Sample	Median	Mean	Standard error	Probability value (p)	H_0
HUES7 Median=19.061 Mean=19.09332 St. error=0.1532458	HUES7-Fib	16.80164	16.98019	0.1532458	0.003948	Reject
	HUES7-iPS	19.63215	19.63598	0.0087511	0.006485	Reject
	HUES7-iPS Fib	17.52477	17.55824	0.1036741	0.003948	Reject
	HUES7-Fib Cl4	16.68957	16.64437	0.1662038	0.003948	Reject
	SUKE-Fib	17.38194	17.36285	0.0080103	0.003948	Reject
	BJ-Fib	17.13778	17.10863	0.144398	0.003948	Reject
HOGN Median=17.65896 Mean=17.95032 St. error=0.243551	HOGN-Fib	16.56254	16.53767	0.2435509	0.003948	Reject
	HOGN-iPS	17.95757	17.92071	0.1983235	0.630954	Accept
	HOGN-iPS Fib	17.2525	17.43817	0.2352213	0.037373	Reject

Box plots

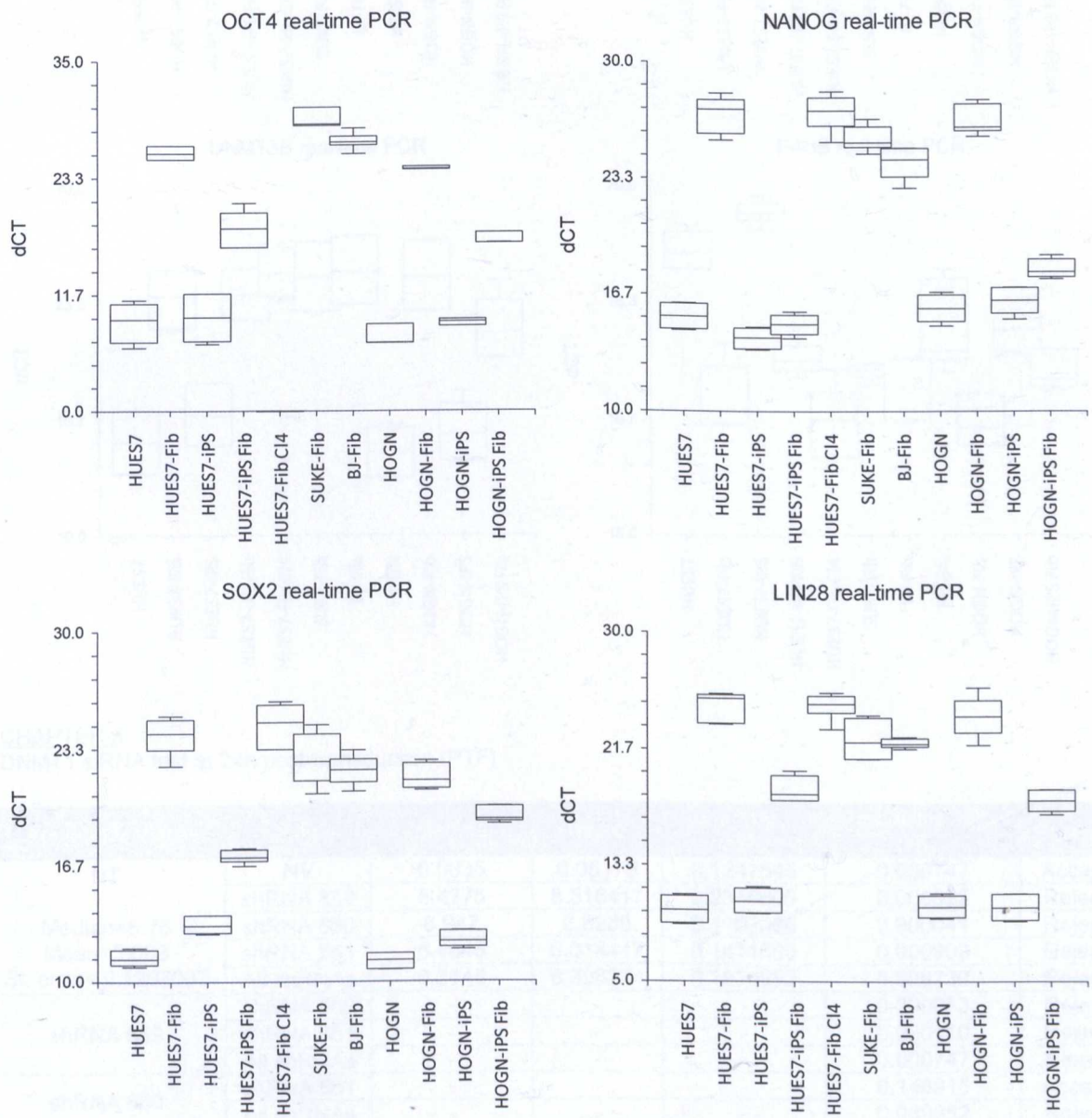

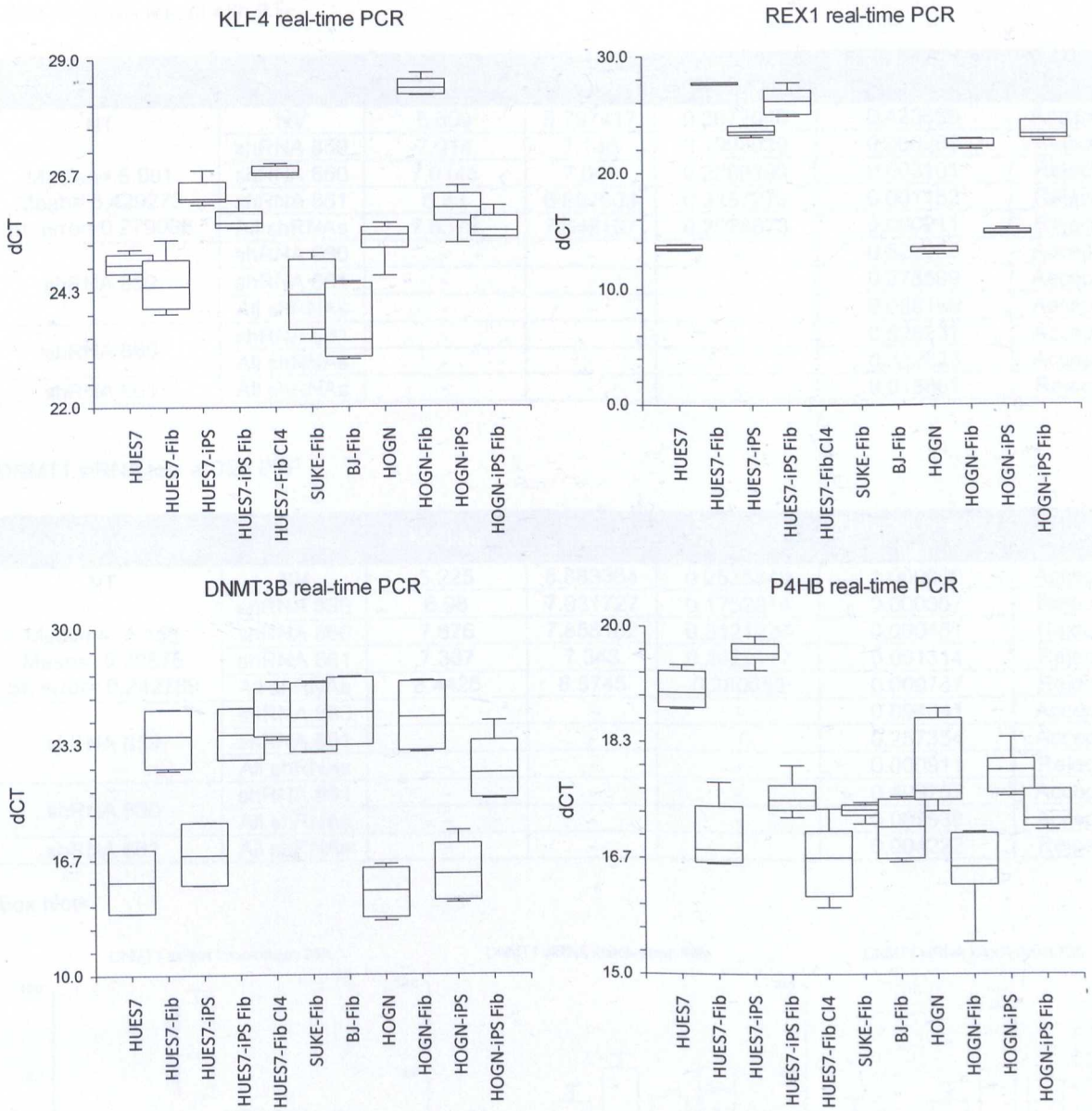

CHAPTER 5

DNMT1 siRNA test at 24h post-transduction (PTF)

Grouping Variable	Sample	Median	Mean	Standard error	Probability value (p)	H_0
NT Median=5.76 Mean=5.693 St. error= 0.1287607	NV	6.0635	6.05175	0.1247545	0.056747	Accept
	shRNA 859	8.4775	8.516417	0.2346606	0.000032	Reject
	shRNA 860	6.947	6.8985	0.1102086	0.000041	Reject
	shRNA 861	6.4645	6.614417	0.1471693	0.000999	Reject
	All shRNAs	6.2145	6.398334	0.1820952	0.008730	Reject
shRNA 859	shRNA 860	-	-	-	0.000053	Reject
	shRNA 861	-	-	-	0.000110	Reject
	All shRNAs	-	-	-	0.000747	Reject
shRNA 860	shRNA 861	-	-	-	0.148915	Accept
	All shRNAs	-	-	-	0.039352	Reject
shRNA 861	All shRNAs	-	-	-	0.453695	Accept

DNMT1 siRNA test at 48h PTF

Grouping Variable	Sample	Median	Mean	Standard error	Probability value (p)	H_0
NT Median= 5.091 Mean= 5.429273 St. error=0.279086	NV	5.609	5.797417	0.2672046	0.423656	Accept
	shRNA 859	7.014	7.146	0.1998039	0.000268	Reject
	shRNA 860	7.0145	7.048	0.2889399	0.003101	Reject
	shRNA 861	6.83	6.807909	0.2187273	0.001152	Reject
	All shRNAs	7.6375	7.649167	0.2928873	0.000911	Reject
shRNA 859	shRNA 860	-	-	-	0.622065	Accept
	shRNA 861	-	-	-	0.278599	Accept
	All shRNAs	-	-	-	0.056188	Accept
shRNA 860	shRNA 861	-	-	-	0.526237	Accept
	All shRNAs	-	-	-	0.232823	Accept
shRNA 861	All shRNAs	-	-	-	0.015861	Reject

DNMT1 siRNA test at 72h PTF

Grouping Variable	Sample	Median	Mean	Standard error	Probability value (p)	H_0
NT Median= 5.758 Mean= 5.79875 St. error= 0.242789	NV	5.225	5.883364	0.2535849	1.000000	Accept
	shRNA 859	6.98	7.031727	0.1752014	0.000357	Reject
	shRNA 860	7.676	7.858182	0.3121224	0.000451	Reject
	shRNA 861	7.367	7.343	0.2422117	0.001314	Reject
	All shRNAs	8.4425	8.5745	0.280653	0.000747	Reject
shRNA 859	shRNA 860	-	-	-	0.094041	Accept
	shRNA 861	-	-	-	0.257354	Accept
	All shRNAs	-	-	-	0.000911	Reject
shRNA 860	shRNA 861	-	-	-	0.496757	Accept
	All shRNAs	-	-	-	0.087532	Accept
shRNA 861	All shRNAs	-	-	-	0.004222	Reject

Box plots

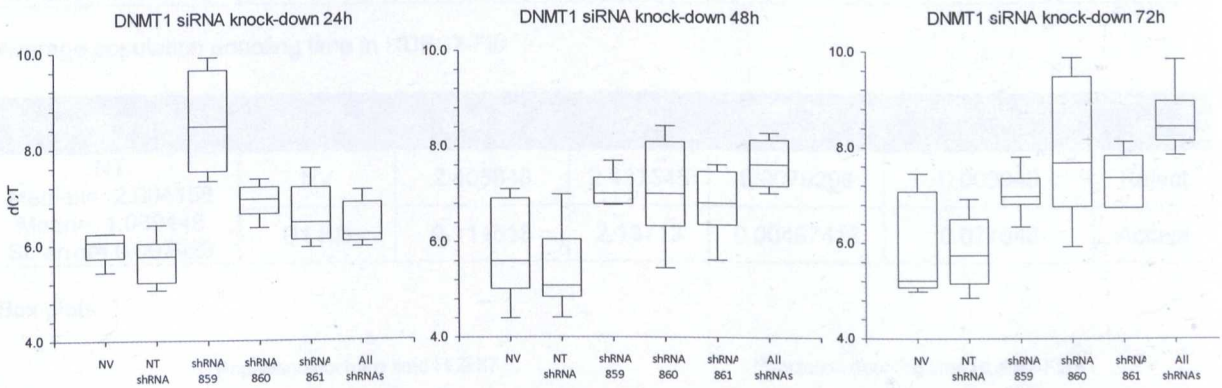

DNMT1 shRNA test in HUES7

Grouping Variable	Sample	Median	Mean	Standard error	Probability value (p)	H_0
NT Median= 0.9905 Mean= 0.9485 St. error= 0.0072842	NV	1.376	1.402333	0.0841117	0.033895	Reject
	shRNA 859	2.276	2.3185	0.0087617	0.020921	Reject
	shRNA 860	1.3255	1.34075	0.00677808	0.020921	Reject
shRNA 859	shRNA 860	-	-	-	0.019419	Reject

DNMT1 shRNA test in HUES7-Fib

Grouping Variable	Sample	Median	Mean	Standard error	Probability value (p)	H_0
NT Median= 1.931 Mean= 1.89525 St. error=0.005547	NV	1.7005	1.737	0.0055471	0.083265	Accept
	shRNA 859	4.1895	4.2745	0.1335636	0.020921	Reject
	shRNA 860	2.626	2.5864	0.103667	0.014306	Reject
shRNA 859	shRNA 860	-	-	-	0.014306	Reject

Box plots

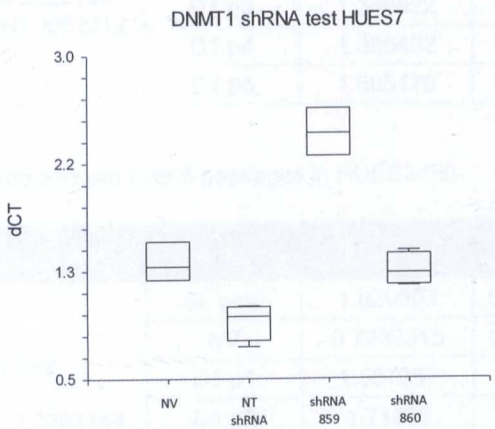

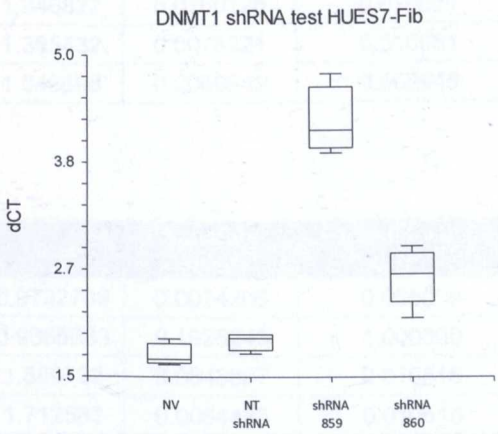

Average population doubling time in HUES7

Grouping Variable	Sample	Median	Mean	Standard error	Probability value (p)	H_0
NT Median= 410 Mean= 418 St. error= 0.038016	NV	2.489505	2.511947	0.1520136	1.000000	Accept
	D1 KD	2.428959	2.339822	0.1646778	0.630954	Accept

Average population doubling time in HUES7-Fib

Grouping Variable	Sample	Median	Mean	Standard error	Probability value (p)	H_0
NT Median= 2.004158 Mean= 1.969445 St. error= 0.007929	NV	2.405848	2.437545	0.0079298	0.003948	Reject
	D1 KD	2.111518	2.13713	0.00497418	0.077648	Accept

Box plots

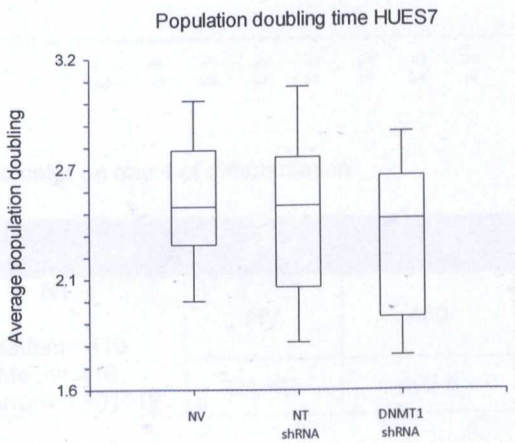

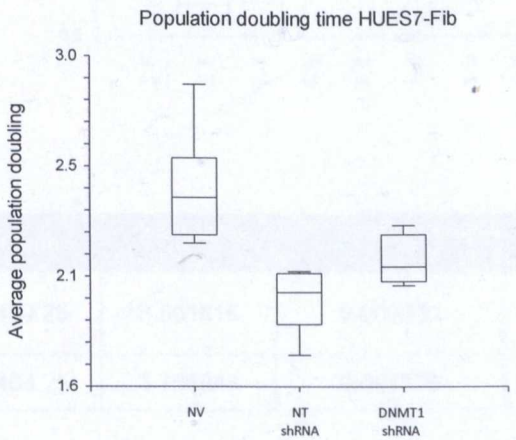

DNMT1 knock-down over 5 passages in HUES7

Grouping Variable	Sample	Median	Mean	Standard error	Probability value (p)	H_0
NT 2ml Median= 0.9775534 Mean= 0.9025109 St. error= 0.0065212	St. pop.	0.7524986	0.7269503	0.1127842	0.297107	Accept
	NV	0.5061256	0.5117769	0.0807753	0.052197	Accept
	D1 p1	1.443258	1.377888	0.00897538	0.010515	Reject
	D1 p2	1.398708	1.394572	0.0079868	0.010515	Reject
	D1 p3	1.346822	1.346822	0.0760126	0.010051	Reject
	D1 p4	1.385432	1.385432	0.0075321	0.010051	Reject
	D1 p5	1.565179	1.546698	0.0069649	0.003948	Reject

DNMT1 knock-down over 5 passages in HUES7-Fib

Grouping Variable	Sample	Median	Mean	Standard error	Probability value (p)	H_0
NT 2ml Median= 0.7381144 Mean= 0.7241271 St. error= 0.006059	St. pop.	1.029093	0.9792709	0.0074206	0.055009	Accept
	NV	0.7233315	0.9655633	0.1925243	1.000000	Accept
	D1 p1	1.567257	1.589732	0.0648887	0.010515	Reject
	D1 p2	1.71836	1.712582	0.0064423	0.010515	Reject
	D1 p3	1.615713	1.812445	0.1687236	0.010515	Reject
	D1 p4	1.465883	1.502467	0.108835	0.010515	Reject
	D1 p5	1.445227	1.505657	0.008432	0.020137	Reject

Box plots

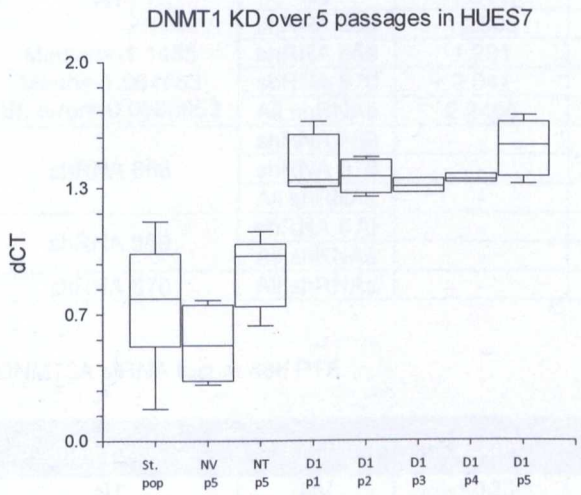

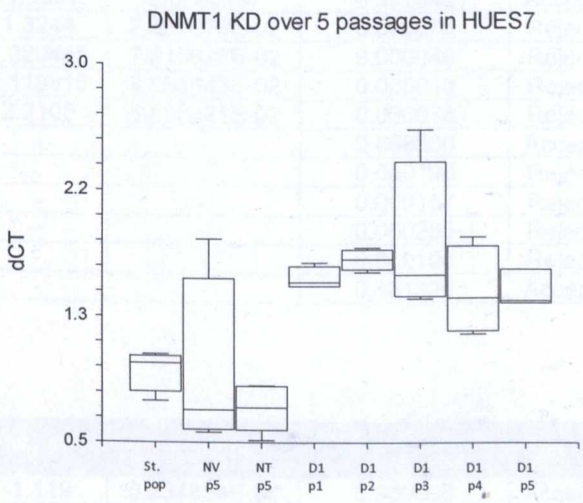

EB diameter on day 4 of differentiation

Grouping Variable	Sample	Median	Mean	Standard error	Probability value (p)	H_0
NT Median= 410 Mean= 418 St. error= 3.801618	NV	460	459.25	3.801618	0.000000	Reject
	D1 KD	402.5	404.25	3.766848	0.091576	Accept

EB diameter on day 8 of differentiation

Grouping Variable	Sample	Median	Mean	Standard error	Probability value (p)	H_0
NT Median= 350 Mean= 359 St. error= 7.062107	NV	410	412.25	7.062107	0.000023	Reject
	D1 KD	357.5	355	7.387756	0.978155	Accept

Box plots

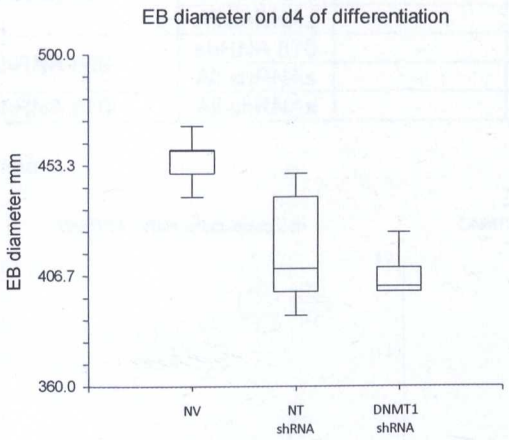

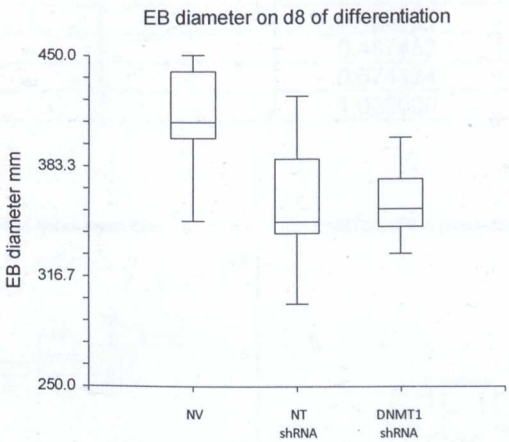

DNMT3A siRNA test at 24h PTF

Grouping Variable	Sample	Median	Mean	Standard error	Probability value (p)	H_0
NT Median=-1.1485 Mean=-1.064583 St. error= 0.0680853	NV	-1.0115	-1.0521	0.0745837	0.597843	Accept
	shRNA 868	1.2505	1.3244	7.421379E-02	0.000076	Reject
	shRNA 869	1.291	1.329455	7.810625E-02	0.000049	Reject
	shRNA 870	2.041	2.118818	8.583843E-02	0.000049	Reject
	All shRNAs	2.2465	2.2105	6.620421E-02	0.000076	Reject
shRNA 868	shRNA 869	-	-	-	0.888000	Accept
	shRNA 870	-	-	-	0.000190	Reject
	All shRNAs	-	-	-	0.000157	Reject
shRNA 869	shRNA 870	-	-	-	0.000268	Reject
	All shRNAs	-	-	-	0.000108	Reject
shRNA 870	All shRNAs	-	-	-	0.481321	Accept

DNMT3A siRNA test at 48h PTF

Grouping Variable	Sample	Median	Mean	Standard error	Probability value (p)	H_0
NT Median= -1.088 Mean= -1.160364 St. error= 0.004.7349	NV	-1.133	-1.119	5.234634E-02	0.969698	Accept
	shRNA 868	0.957	1.012727	4.870956E-02	0.000071	Reject
	shRNA 869	1.302	1.260333	9.760004E-02	0.000169	Reject
	shRNA 870	0.981	1.152182	9.840492E-02	0.000071	Reject
	All shRNAs	1.667	1.792556	9.189751E-02	0.000169	Reject
shRNA 868	shRNA 869	-	-	-	0.119361	Accept
	shRNA 870	-	-	-	0.669509	Accept
	All shRNAs	-	-	-	0.000169	Reject
shRNA 869	shRNA 870	-	-	-	0.425031	Accept
	All shRNAs	-	-	-	0.019283	Reject
shRNA 870	All shRNAs	-	-	-	0.004385	Reject

DNMT3A siRNA test at 72h PTF

Grouping Variable	Sample	Median	Mean	Standard error	Probability value (p)	H_0
NT	NV	-0.985	-1.1177	0.1468274	0.858955	Accept
	shRNA 868	0.617	0.5790909	0.1171494	0.000280	Reject
Median= -1.1035	shRNA 869	0.3635	0.337875	0.1686702	0.000778	Reject
Mean= -1.2195	shRNA 870	0.642	0.479	0.1655051	0.001194	Reject
St. error= 0.164158	All shRNAs	0.417	0.44975	0.834625	0.000778	Reject
shRNA 868	shRNA 869	-	-	-	0.247676	Accept
	shRNA 870	-	-	-	0.683604	Accept
	All shRNAs	-	-	-	0.408961	Accept
shRNA 869	shRNA 870	-	-	-	0.487453	Accept
	All shRNAs	-	-	-	0.674424	Accept
shRNA 870	All shRNAs	-	-	-	1.000000	Accept

Box Plots

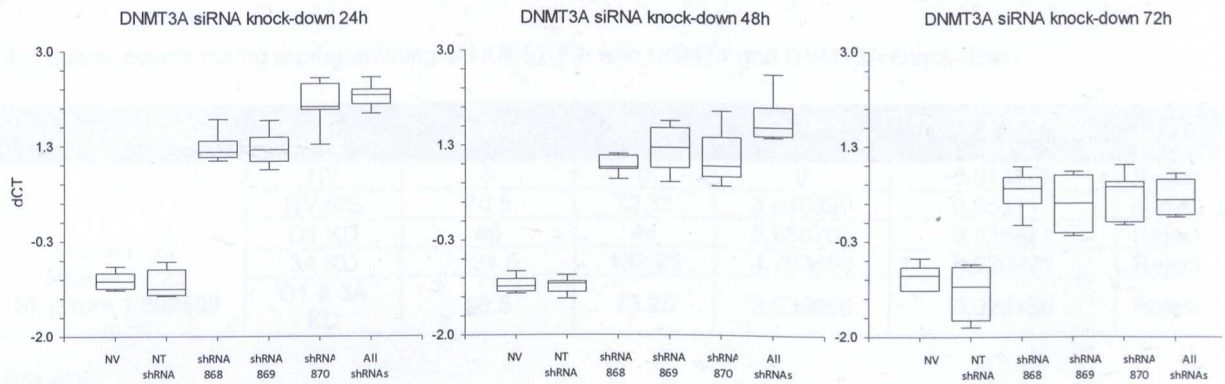

DNMT3A shRNA test HUES7

Grouping Variable	Sample	Median	Mean	Standard error	Probability value (p)	H_0
NT	NV	-1.175342	-1.206225	0.0030582	0.067264	Accept
Median= -1.304644	shRNA 868	-0.1801643	-0.176369	0.0194891	0.006054	Reject
Mean= -1.318359	shRNA 870	-1.214071	-1.22894	0.0044583	0.220671	Accept
St. error= 0.003350						
shRNA 868	shRNA 870	-	-	-	0.033895	Reject

DNMT3A shRNA test HUES7-Fib

Grouping Variable	Sample	Median	Mean	Standard error	Probability value (p)	H_0
NT	NV	1.759946	1.747541	0.0057709	0.563703	Accept
Median= 1.686086	shRNA 868	2.250748	2.219598	0.0371056	0.033895	Reject
Mean= 1.703564	shRNA 870	2.156113	2.138145	0.0037232	0.033895	Reject
St. error= 0.0321344						
shRNA 868	shRNA 870	-	-	-	0.275234	Accept

Box plots

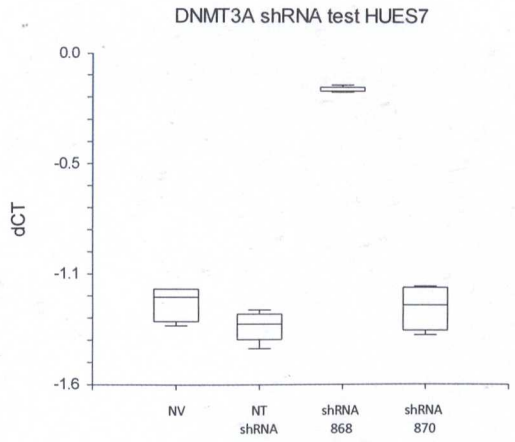

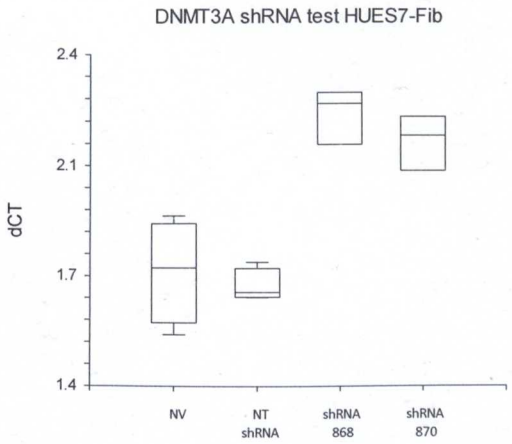

iPS colony counts during reprogramming of HUES7-Fib with DNMT1 and DNMT3A knock-down

Grouping Variable	Sample	Median	Mean	Standard error	Probability value (p)	H_0
NT Median= 72 Mean= 73.25 St. error= 1.692508	NV	0	0	0	0.013874	Reject
	NV-iPS	70.5	72.75	3.010399	0.663117	Accept
	D1 KD	46	44	5.988705	0.020921	Reject
	3A KD	134.5	133.25	4.793659	0.020921	Reject
	D1 & 3A KD	55.5	73.25	3.039668	0.020165	Reject

Box plot